Phosphate Tether-Mediated Metathesis Studies and Application Towards Natural Product Synthesis

By

Soma Maitra

Submitted to the graduate degree program in the Department of Chemistry and the Graduate Faculty of the University of Kansas in partial fulfillment of the requirements of the degree of Doctor of Philosophy

Paul R. Hanson, chair

Jon A.Tunge

Thomas E. Prisinzano

Helena C. Malinakova

Michael D. Clift

June 11th, 2015
Date Defended

The Dissertation Committee for Soma Maitra certifies that this is

the approved version of the following dissertation:

Phosphate Tether-Mediated Metathesis Studies and

Application Towards Natural Product Synthesis

_____

Paul R. Hanson, chair

June 11th, 2015
Date Approved

Abstract

Soma Maitra

Department of Chemistry

University of Kansas, June 11th, 2015

Over the past decade, work in our lab has focused on phosphate tether-mediated desymmetrization of C_2-symmetric 1,3-*anti*-dienediol via ring-closing metathesis (RCM) to afford *P*-stereogenic bicyclo[4.3.1]phosphates. However, efforts in this direction relied solely on phosphate tether-mediated coupling of allylic alcohol cross partners with 1,3-*anti*-dienediol synthons leading to the formation of simple bicyclo[4.3.1]phosphates and their applications in natural product synthesis. The objective of this dissertation work is to advance the phosphate tether-mediated methods to include the construction of complex bicyclo[n.3.1]phosphates via ring-closing metathesis (RCM). The RCM study, discussed in detail in Chapter 2, highlights the synthetic potential of phosphates as a temporary tethers in facilitating the coupling of complex fragments to produce novel *P*-stereogenic bicyclic phosphate scaffolds. Chapter 3 describes the development of phosphate tether-mediated one-pot and two-pot sequential metathesis/reduction protocols towards the stereodivergent synthesis of complex polyols. The potential application of phosphate tether-mediated reactions en route to the synthesis of the C9–C25 fragment of spirastrellolide B is discussed in Chapter 4.

To my family

Acknowledgments

I would first like to acknowledge my family members – my father, my mother and my brother, Sourav for their continuous support and love during past years. It has not only been hard for me to stay so far away from my family but also for them. But whenever I get a chance to talk to my brother, all I hear is – you focus on your work, we are fine here – and I can't express my gratitude in words towards them for being there for me always. I would like to thank my husband Gurpreet for loving me, caring for me and helping me stay focused. It has been extremely challenging experience to go through graduate school together – but I believe it has only made our bond stronger. I would also like to acknowledge my extended family members, my uncle Debashish, my cousin sister Upanita and brother Samit for their love and encouragement. They took care of my parents and made it possible for me to stay focused here. Without all of you, I could have never come so far and get opportunity to work in such a wonderful environment.

After coming to US, I have had opportunity to meet some wonderful people-who became lifetime friends. I would like to thank Lindsay, Radha, Bharat, Amrita, Susanthi, Rohan, Suzi and Ramu for being such a nice friend. With you all, I felt at home here. And even though you all are far away, I know that you are only a phone call away from me and I can always rely on you.

I would like to acknowledge my advisor Paul R. Hanson for his support and patience. Paul, it has been crazy working with you, with all the yelling and super-long group meetings, "pow-wows (which have no idea about!)", listening "this is good for you" at least 100 times a day- but at the end of the day I am privileged to get an opportunity to work with you. Thank you for teaching me not to give up under any circumstances and believing in me. I am very grateful for all that you have done for me. I would also like to thank Yumi for being very supportive throughout these years.

I would like to thank all of the former and present Hanson members for their support. A special thanks to Susanthi, Naeem, Moon, Joanna and Jana for being such a wonderful friend and helping me all the time. I would like to thank Jessica, a present post doc in Hanson lab and Jana for their help and useful feedbacks while writing this dissertation. I also appreciate the help of former postdocs including Ram and Thiwanka for their advice.

I would like to acknowledge all of my committee members, Professors Tunge, Malinakova, Clift and Prisinzano for their help and guidance. I would also like to thank other research groups in Malott Hall, including all of the Tunge, Clift, Blagg and Prisinzano group members.

Lastly, a special thanks to Justin and Sarah for their help in NMR experiments and data interpretation and Vicor for providing X-ray data for many of my compounds. I

would like to acknowledge our front office staffs, Susan, Beth, Beverly, Ruben, Dan and Donnie for their help.

Phosphate Tether-Mediated Metathesis Studies and

Application Towards Natural Product Synthesis

CONTENTS Page #

Title Page i

Acceptance Page ii

Abstract iii

Acknowledgments iv

Table of Contents viii

Abbreviations xiii

Chapter 1: Tether-mediated ring-closing metathesis 1

1.1 Introduction 2

1.2 Background and significance 8

1.2.1 Silicon tether-mediated ring-closing metathesis 8

1.2.2 Ketal tether-mediated ring-closing metathesis 17

1.2.3 Additional tether-mediated ring-closing metathesis studies 24

1.2.3.1 γ-lactone tether-mediated ring-closing metathesis 24

1.2.3.2: Carboxylate tether-mediated ring-closing metathesis 25

1.3 Use of *P*-tethers in synthesis 26

1.4 Conclusion 31

1.5 References cited 32

Chapter 2: Phosphate tether-mediated ring-closing metathesis studies 39
2.1 Introduction 40
2.2 Results and discussion 40
2.2.1 Substrate design 43
2.2.2 Synthesis of *P*-stereogenic bicyclo[4.3.1]phosphates 44
2.2.3.1 Synthesis of *P*-stereogenic bicyclo[5.3.1]phosphates 47
2.2.3.2 Synthesis of bicyclo[5.3.1]phosphates with C5-methyl substitution 48
2.2.3.3 Synthesis of bicyclo[5.3.1]phosphates with homoallylic alcohol partners containing allylic methyl substituents 50
2.2.3.4 Synthesis of bicyclo[5.3.1]phosphates derived from homologated diene diol 54
2.2.4 Synthesis of *P*-stereogenic bicyclo[6.3.1]phosphates 56
2.2.5 Synthesis of *P*-stereogenic bicyclo[7.3.1]phosphates 61
2.2.6: Synthesis of *P*-stereogenic bicyclo[8.3.1]phosphates 63
2.3: Conclusion 64
2.4: References cited 65

Chapter 3: A Modular phosphate tether-mediated divergent strategy to complex polyols **71**
3.1 Introduction 72
3.2 Generation of stereodiverse small molecule libraries 73
3.3 Results and discussion 78
3.3.1 Rational design 80
3.3.2 Synthesis of the first set of 5 polyols 82
3.3.3 Synthesis of the second set of 5 polyols 87
3.4 Conclusion 91
3.5 References cited 91

Chapter 4: Phosphate tether-mediated approach towards the synthesis of the C9–C25 Fragment of spirastrellolide B **97**
4.1 Introduction 98
4.1.1 Overview of the spirastrellolides family 98
4.1.2 Spirastrellolides and other PP2A inhibitors 100
4.2 Synthetic efforts towards spirastrellolides 104
4.2.1 Paterson's group synthesis of the C1–C25 fragment of spirastrellolide A 104
4.2.2 The Fürstner group synthesis of the C1–C24 fragments of spirastrellolide F and spirastrellolide A 107
4.2.3 The Phillips group synthesis of the C1–C23 fragment of spirastrellolide B 112
4.2.4 The Smith group synthesis of the C1–C25 fragments of spirastrellolide A, B and the C1–C24 fragment of spirastrellolide E 114

4.2.5 The Hsung group synthesis of the C1–C23 fragment of spirastrellolide A 120

4.2.6 The Brabander group synthesis of the C1–C22 fragment of spirastrellolide A 124

4.2.7 The Chandrasekhar group synthesis of the C9–C25 fragment of spirastrellolide B 125

4.2.8 Yadav group synthesis of the C1–C25 fragment of spirastrellolide B and F 126

4.3 Results and discussion 127

4.3.1 Proposed retrosynthetic analysis of the C9–C25 fragment of spirastrellolide B 128

4.3.2 Model studies towards the synthesis of the C9–C23 fragment of spirastrellolide B 130

4.3.2.1 Synthesis of the C9–C16 fragment and the C17–C23 fragment: model studies towards the synthesis of C9–C23 fragment of spirastrellolide B 131

4.3.2.2 Efforts towards the synthesis of the model C9–C23 fragment via Suzuki-Miyuara coupling 133

4.3.3 Synthesis of the C17–C25 fragment 137

4.3.4 Progress towards the C9–C23 fragment 138

4.4 Future direction 140

4.5: References cited 142

Chapter 5: Experimental data and spectra for chapters 2–4 153

Abbreviations

RCM	ring-closing metathesis
$LiAlH_4$	lithium aluminum hydride
G-II	Grubbs' second generation catalyst
G-I	Grubbs' first generation catalyst $[(PCy_3)_2(Cl)_2Ru{=}CHPh]$
HG-II	Hoveyda-Grubbs second generation catalyst
CM	cross metathesis
o-NBSH	*o*-nitrobenzene sulfonyl hydrazine
CH_2Cl_2	dichloromethane
DCE	1,2-Dichloroethane
2,2-DMP	dimethoxypropane
PPTS	pyridinium *p*-toluenesulfonate
Et_3N	triethylamine
MeCN	acetonitrile
LLS	longest linear sequence
TSC	total step count
NBS	N-bromosuccinimide
$NaHCO_3$	sodium bicarbonate
$NaOAc{\bullet}3H_2O$	sodium acetate trihydrate
NaHMDS	sodium bis(trimethylsilyl)amide
Ac_2O	acetic anhydride
BOPCl	bis(2-oxo-3-oxazolidinyl)phosphonic chloride
TIPS	triisopropylsilyl-
Me_2SO_4	dimethylsulfate
LiDBB	lithium di-tert-butyl biphenylide
NMO	N-methylmorpholine-N-oxide
DMSO	dimethyl sulfoxide
DMAP	4-dimethylaminopyridine

TBAF	tetra-n-butylammonium fluoride
DDQ	2,3-dichloro-5,6-dicyano-1,4-benzoquinone
TBSCl	tert-butyldimethylsilyl chloride
TES	triethylsilyl
9-BBN	9-Borabicyclo(3.3.1)nonane
PMB	para-methoxybenzyl-
MOM	Methoxymethyl-
Bn	benzyl
BnBr	benzyl bromide
Ag_2O	silver oxide
Boc	*tert*-butyloxycarbonyl
t-BuOH	*t*-Butanol
H_2O	water
$(DHQ)_2PHAL$	hydroquinine 1,4-phthalazinediyl diether
$CHCl_3$	chloroform
CuCN	copper cyanide
Me_2Zn	dimethylzinc
cat.	catalytic
PhH	benzene
Et_2O	diethyl ether
DIPEA	*N*,*N*'-Diisopropylethylamine
DMF	dimethylformamide
DOS	diversity oriented synthesis
Eq.	equivalent
Et	ethyl
EtOAc	ethyl acetate
HCl	hydrochloric acid
HF	hydrofluoric acid
HPLC	high performance liquid chromatography

HMPA	hexamethylphosphoramide
Hz	hertz
IR	infrared radiation
IC_{50}	inhibitory concentration at 50%
*n*BuLi	n-butyllithium
*i*Pr	isopropyl
LiOH	Lithium hydroxide
MeOH	Methanol
MeI	methyl iodide
MsCl	methanesulfonyl chloride
NMR	nuclear magnetic resonance
OMe	methoxy
ppm	parts per million
Ph	phenyl
PTSA	*p*-toluenesulfonic Acid
K_2CO_3	potassium carbonate
K_3PO_4	potassium phosphate
Bpin	pinacolborane
PK	protein kinase
PP1	protein phosphatase 1
PP2A	protein phosphatase 2A
rt	room temperature
Sat'd	saturated
Si	silicon
NaHMDS	sodium hexamethyldisilazide
SM	starting material
SAR	structure-activity-relationship
TBAF	tetrabutyl ammonium fluoride
TFA	trifluoroacetic acid

PPh_3	triphenylphosphine
PCy_3	tricyclohexylphosphine
TLC	thin layer chromatography
$P(2\text{-fur})_3$	tri(2-furyl)phosphine
*t*Bu	*tert*-butyl
THF	tetrahydrofuran
TOS	target oriented synthesis

Chapter 1

Tether-mediated ring-closing metathesis

1.1: Introduction

The development of new atom-,[1] step-,[2] and redox-economical[3] methods to access complex subunits common to a variety of bioactive natural products stands at the forefront of modern-day synthesis and drug discovery. In particular, tether-mediated transformations that couple both simple and complex molecular fragments to access highly functionalized core intermediates represent some of the most facile and convergent pathways to accomplish this goal.[4] Historically, silicon has been the most exploited and well-studied tether, owing to its stability, ease of synthesis and advantage of late-stage removal.[5] These attributes of silicon tethers have served as a cornerstone for a number of elegant applications in total synthesis.[5] In contrast, the prospect of phosphate tethers were largely unexplored until 2005 and were only limited to two literature examples.[6] This is surprising due to the number of salient features of phosphate tethers, including: (i) tripodal coupling characteristics, (ii) serving as a protecting group and leaving group, (iii) acting as a functional handle for transition metal-mediated transformations, and (iv) having the ability to possess asymmetry at phosphorus (*P*-chirality).[7]

In this regard, efforts in our group since 1997 have focused on investigating phosphorus-based transformations, including tethers since 2000, with the ultimate aim of generating diverse *P*-heterocycles with biological and synthetic utility (Figure 1.1).[8,6b] Towards this goal, we have utilized ring-closing metathesis (RCM) to synthesize phosphonamides, phosphonates and phostones (*P*-sugars).[8] In addition, generation of *P*-stereogenic phosphonamides and phosphonates were achieved via desymmetrization of pseudo C_2-symmetric *P*-template via RCM and intramolecular cyclopropanation (ICP).[9]

Our investigation on the use of phosphate-based tethers was initiated in 2005 with the report of phosphate tether-mediated desymmetrizations of a C_2-symmetric diene diol via RCM en route to the synthesis of *P*-stereogenic bicyclo[4.3.1]phosphates.[10]

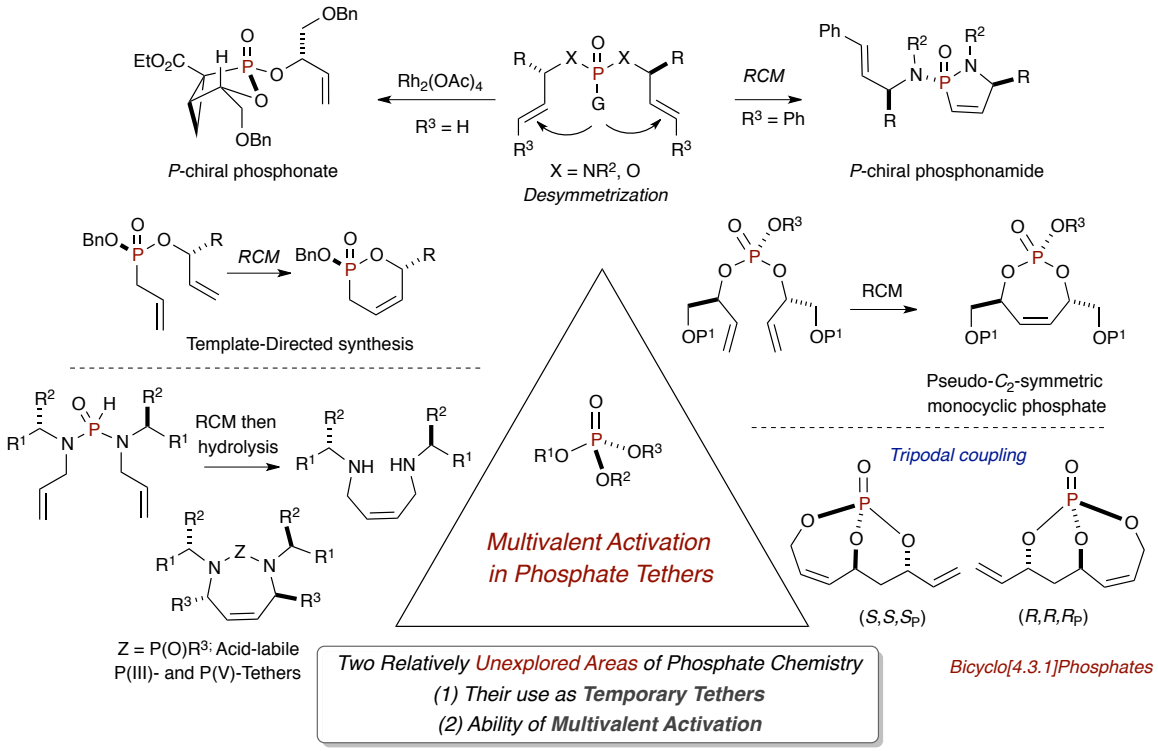

Figure 1.1. *Summary of our work towards exploring phosphorous-based tether and template-directed synthesis of diverse P-chiral heterocycles.*

Our attention was next directed towards exploring the synthetic utility of bicyclo[4.3.1]phosphates. Taking advantage of the steric and stereoelectronic differentiation present in the bicyclic framework of bicyclo[4.3.1]phosphate, a number of regio- and chemoselective reactions were developed (Figure 1.2).[11] The synthetic potential of phosphate tether-mediated reactions was further demonstrated towards the synthesis of 1,3-diol containing natural products (Figure 1.3).[12] In addition current efforts are focused towards the development of the phosphate tether-mediated one-pot

sequential synthetic strategies, which would further expedite the total synthesis projects and provide opportunity for library synthesis.

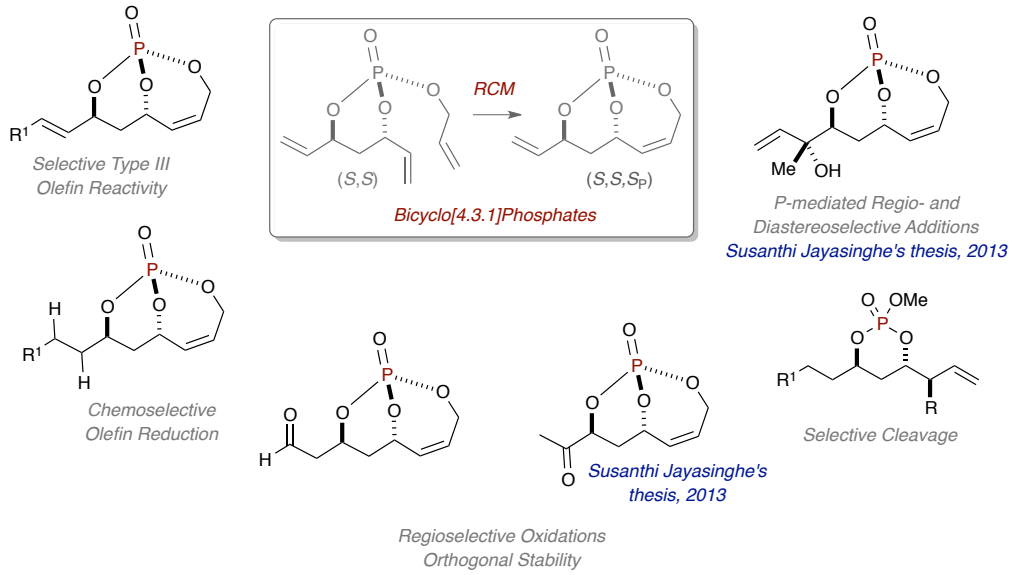

Figure 1.2. *Synthetic utility of bicyclo[4.3.1]phosphates.*

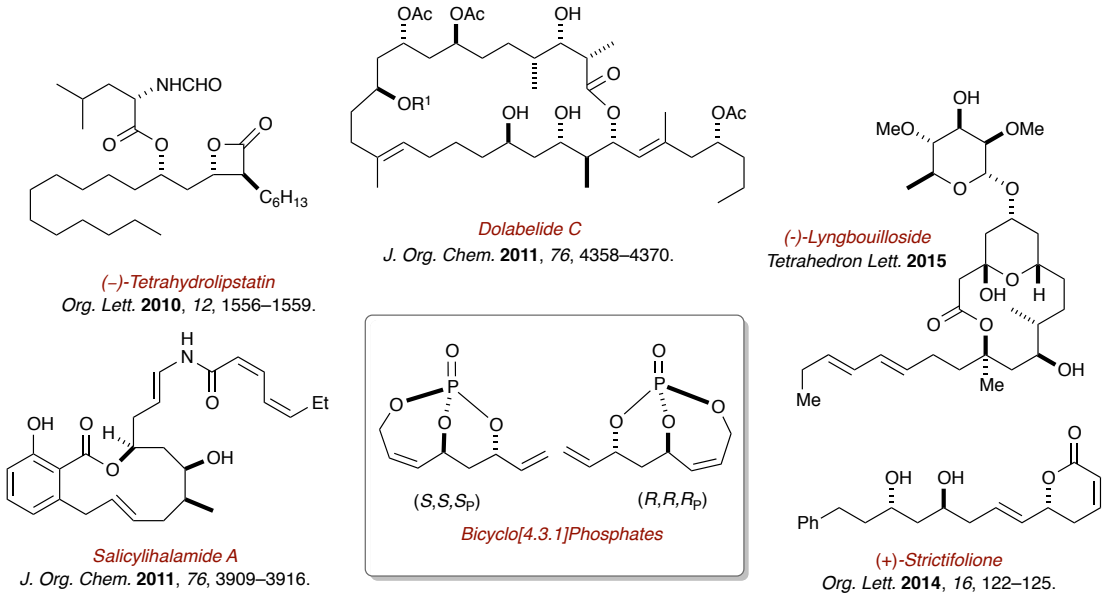

Figure 1.3. *1,3-diol containing natural product synthesis starting from bicyclo[4.3.1]phosphates.*

Aligned with our goal of studying phosphate tether-mediated processes and their

applications to complex natural product synthesis, we have initiated a thorough study of phosphate tether-mediated RCM reactions during the period of this dissertation work. The purpose of this dissertation is to advance the phosphate-tether method further towards the construction of complex bicyclo[n.3.1]phosphates via RCM. Before this study, all of our previous reports were focused on the synthesis and utility of bicyclo[4.3.1]phosphates derived from phosphate tether-mediated coupling of simple, unsubstituted, allylic alcohol cross partners. However, to expand the utility of phosphate tether in terms of accessing more stereochemically complex fragments, we deemed it important to have a more thorough understanding of the behavior of phosphate tethers during RCM across a wide range of complex substrates.

With respect to the literature report for tether-mediated RCM studies, it should be noted that the lack of literature precedence for phosphate tether-mediated RCM study also stands in contrast to the large volume of work devoted to study silicon tethers during RCM. In this regard, two seminal work by the research groups of Evans,[13] Kobayashi,[14] and many others[5] have provided insight on the behavior of silicon tethers in the RCM of a variety of substrates and the stereochemical outcome of such studies have been strategically utilized in many total synthesis projects. The aim of the current chapter is to provide a brief account of the literature reports on the use of other tethers including silicon tether in RCM processes and their applications towards natural product synthesis.

Chapter 2 of this dissertation describes phosphate tether-mediated RCM studies towards the construction of novel bicyclo[n.3.1]phosphate scaffolds.[15] The focus of this study was to explore the effect of ring-size, stereochemistry and substitutions of both of the coupling partners in the RCM reaction. This study highlighted the utility of

phosphate-tether in generating complex systems and provided insight into the factors governing RCM in such complex systems.

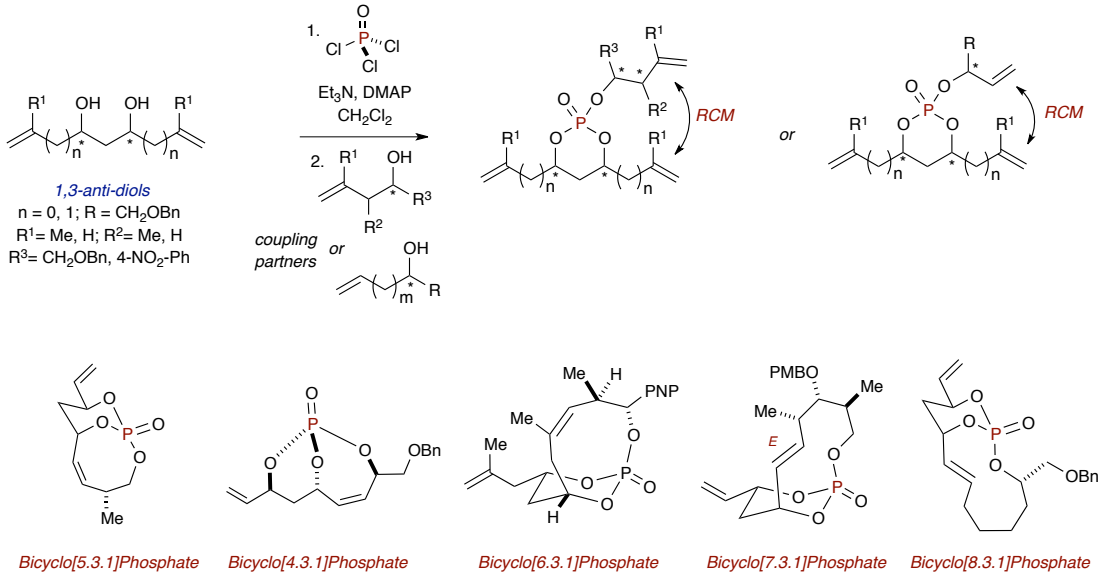

Figure 1.4. *Chapter 2 describes phosphate tether-mediated RCM studies towards the generation of novel bicyclo[n.3.1]phosphate scaffolds.*

The application of phosphate tether-mediated one-, two-pot sequential processes towards the stereodivergent synthesis of complex polyols is discussed in chapter 3.[16] A modular 3-component coupling strategy was developed in this regard to synthesize stereo-enriched polyols. The divergent aspect of the method was introduced by simple switching of the olefinic partners in the subsequent CM reaction to afford five differentiated polyols starting from three coupling partners.

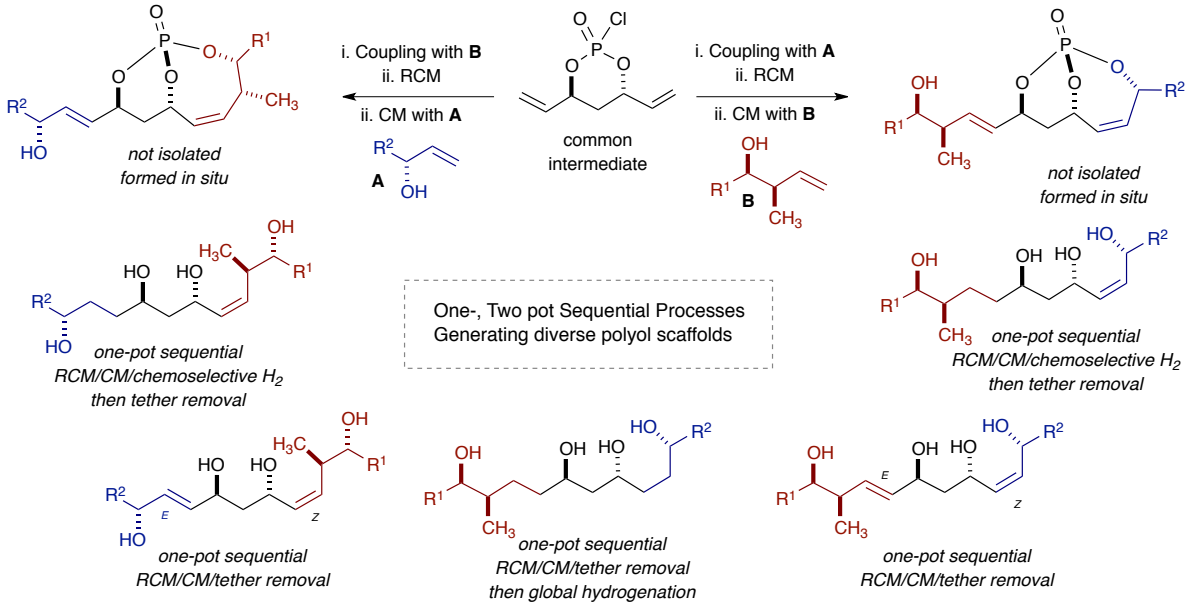

Figure 1.5. *Chapter 3 is focused on the stereodivergent synthesis of polyols by utilizing phosphate tether-mediated one- and two-pot sequential protocols.*

Chapter 4 describes the application of phosphate tether-mediated reactions to synthesize the C9–C25 fragment of spirastrellolide B. Originally isolated in 2007,[17] spirastrellolide B and its congeners possess interesting biological activity and feature a

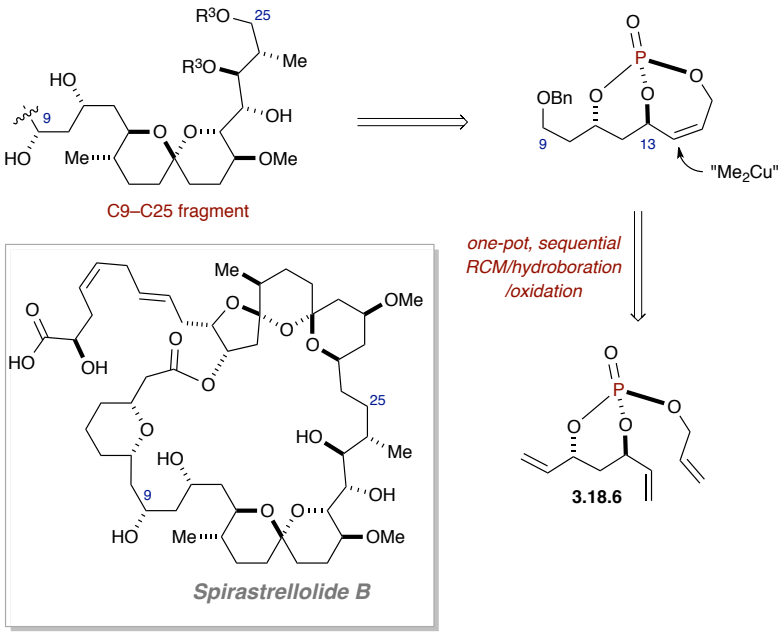

Figure 1.6. *A phosphate tether-mediated route to the C9–C25 fragment of spirastrelloide*

B is discussed in chapter 4.

challenging framework including a 38-membered macrolactone, a bicyclic and a tricyclic spiroacetal subunit. A strategy aimed at developing phosphate tether-mediated regio- and chemoselective reactions to facilitate the synthesis of the C9–C25 fragment in an efficient manner will be discussed in this chapter.

1.2: Background and significance

Tether-mediated RCM strategies have been utilized towards the synthesis of a various natural products. Many groups have investigated the use of tethers in RCM including the stereochemical outcome of such tether-mediated RCM reactions. A brief account of the literature reports on the use of other tethers including silicon in RCM processes and their applications towards natural product synthesis is discussed below.

1.2.1: Silicon tether-mediated ring-closing metathesis

Silicon is one of the most exploited tethers used in RCM.[5] It offers several advantages such as ease of coupling often under mild basic condition, tolerance for a range of functionalities that makes it attractive choice for natural product synthesis and mild reaction conditions are required for removal. In 1992, Grubbs and Fu first reported temporary *Si*-tethered (TST) RCM to synthesize 7-membered cyclic silyl ether, which was next treated with nBu$_4$NF to provide 1,4-diols (Scheme 1.1).[18] In 1997, Grubbs and coworkers illustrated the first example of RCM of vinylsilyl dienes in the presence of the **G-I** or the **[Mo]-I** catalyst (Scheme 1.1).[19] Various 6- to 10-membered cyclic silyl ethers (**1.1.5a–d**) were generated via the RCM of *Si*-tethered dienes (**1.1.4**) in excellent yields.

Subsequent Tamao oxidation[20] of cyclic silyl ethers produced (*Z*)-configured olefinic polyhydroxy compounds (**1.1.6a–b**, Scheme 1.1). In 1997, Cossy and coworkers reported *Si*-tethered RCM to generate 6–8-membered allylsiloxanes (**1.1.8a–d**), which were subjected to modified Sakurai conditions to generate substituted tetrahydrofurans or tetrahydropyrans (**1.1.9**, Scheme 1.1).[21] Notably, the formation of 7-membered allylsiloxane (**1.1.8c**) was found to be sensitive to the presence of allylic substituents presumably because of unfavorable steric interactions between the C2 substituent (allylic methyl group) and ruthenium catalyst.

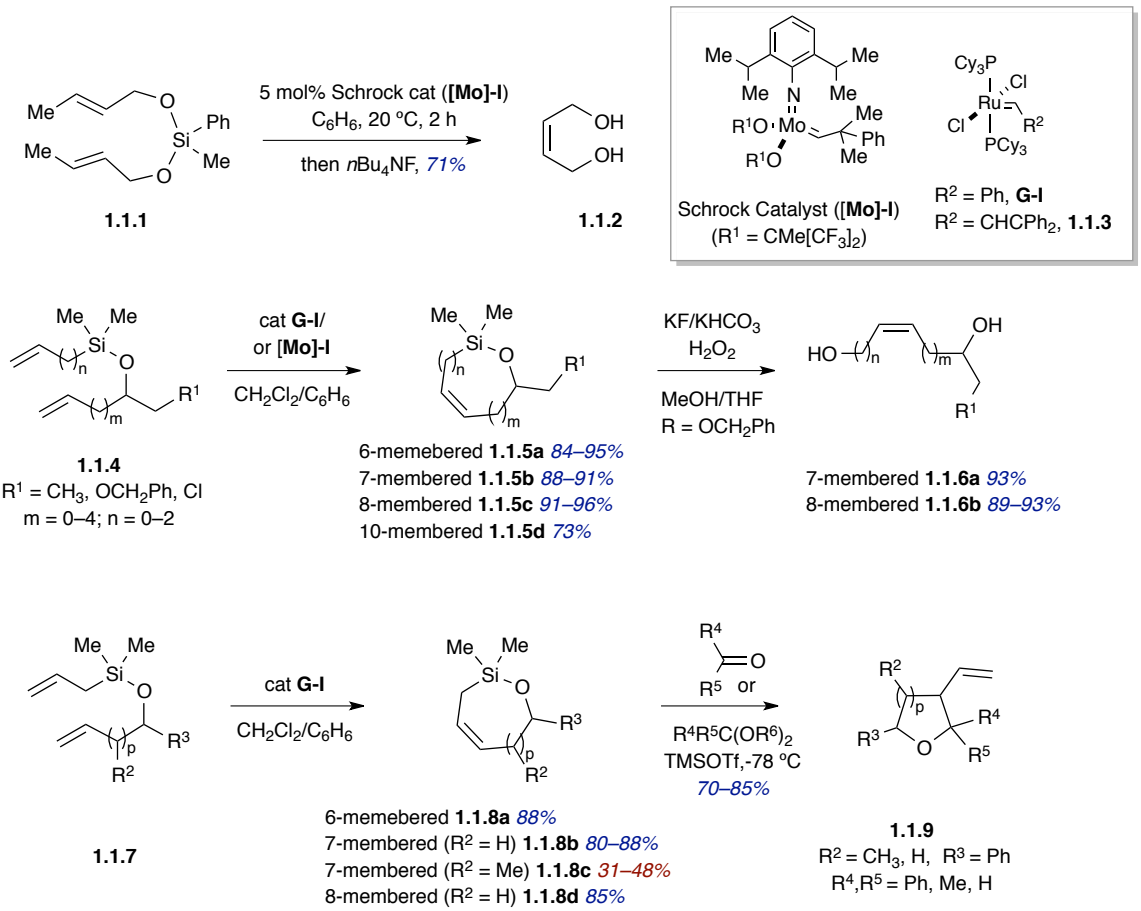

Scheme 1.1. *Cyclic silyl ether formation via temporary Si-tethered (TST) RCM.*

In 1998, Evans and coworkers reported the synthesis of protected C_2-symmetric,

chiral 1,4-diols (**1.2.3**) via a temporary silicon-tethered ring-closing metathesis (TST RCM) strategy involving the coupling of chiral, non-racemic allylic alcohols (Scheme 1.2.). This method was further exploited towards the asymmetric synthesis of *D*-altriol (**1.2.5**, Scheme 1.2).[22]

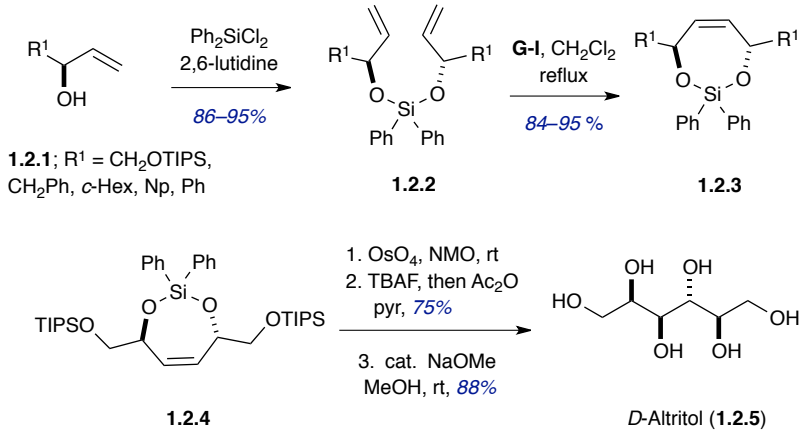

Scheme 1.2. *Evan's group TST strategy to synthesize C_2-symmetric, chiral 1,4-diols.*

Use of silicon tether towards the construction of large ring systems is also well documented. In 1999, Hoye and coworkers demonstrated that TST RCM could be extended further to the self- and cross coupling of various alkenol partners leading to 7-, 9- and 11-membered cyclic silaketals (**1.3.3**–**1.3.5**) with excellent *Z*/*E* selectivity (Scheme 1.3).[23] It was noted that slow addition of the catalyst was required for the effective RCM process leading to 9- and 11-membered ring systems. For the 7-membered silaketal ring formation, both yield and the duration of the RCM process were dependent on allylic and olefinic substituents.

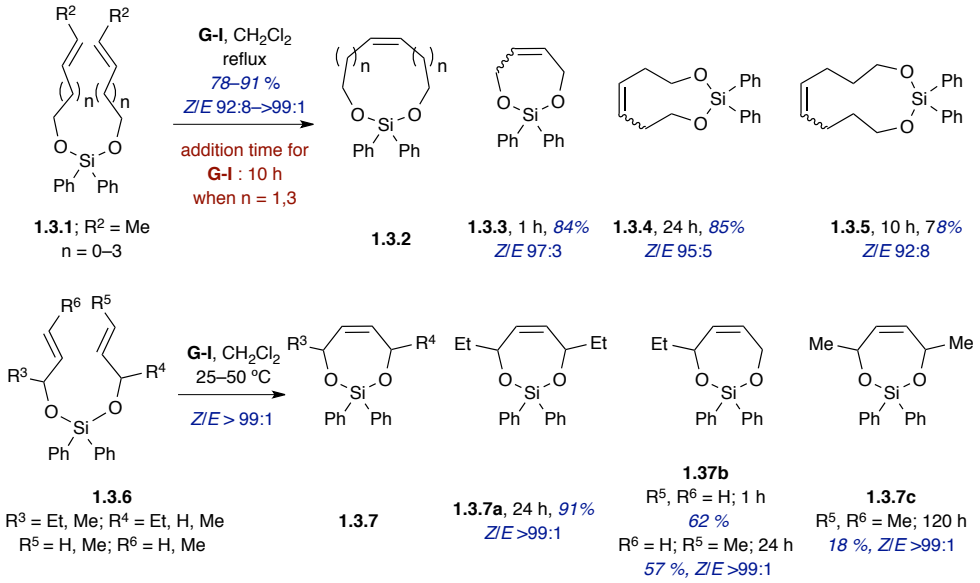

Scheme 1.3. *Si-tethered RCM towards the generation of 7-, 9- and 11-membered cyclic silaketals.*

Silicon tethers have been effectively utilized in diastereoselective RCM reactions and the stereochemical outcome of such reactions has been thoroughly studied. One of such elegant studies reported by the Evans group in 2003 documented the use of TST RCM strategy for the long-range asymmetric induction leading to the diastereoselective synthesis of (*Z*)-configured, 7–11-membered siloxane rings (**1.4.4**, Scheme 1.4).[13] Trienes were synthesized by silylating prochiral, substituted divinyl alcohol and then coupling with different alcohol partners. An exclusive *cis*-selectivity was observed for 7-membered siloxane ring formation whereas moderate to excellent *trans*-selectivity was observed for 8–11-membered rings. The observed selectivity was rationalized by the formation of the favored TS state **1.4.5A**, in which the propenyl group occupies a pseudoequitorial position to avoid non-bonding interactions with the isopropyl substituents of silicon. Additional studies indicated that the diastereoselectivity of both the 7- and 8-membered rings were dependent on the duration of the reaction and therefore

could be optimized.

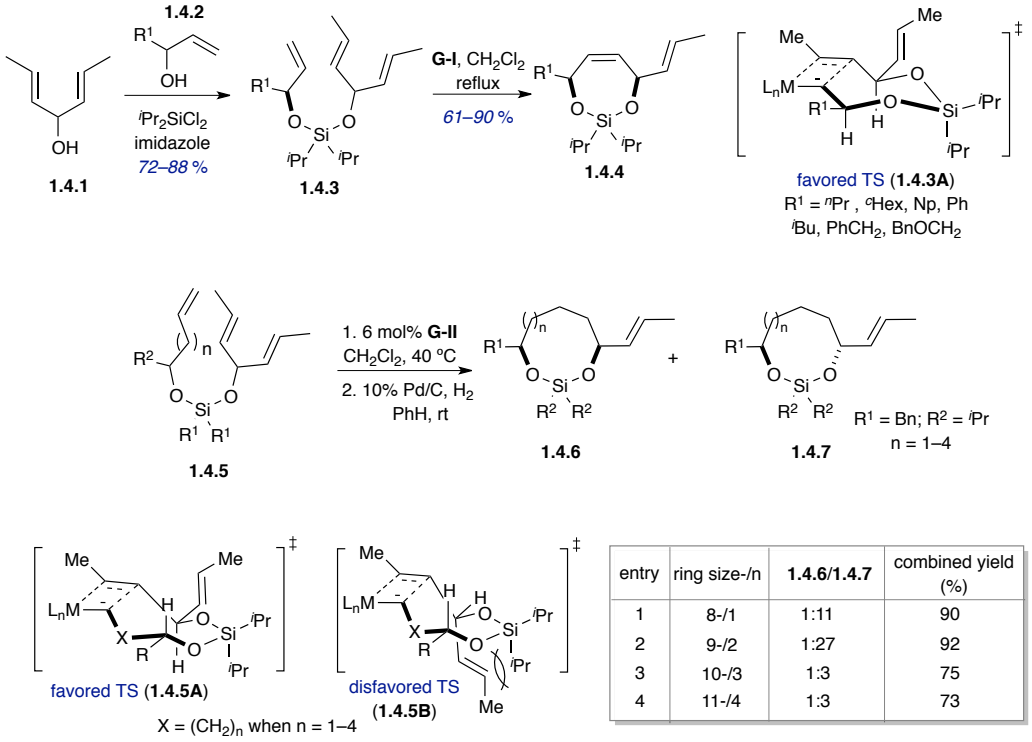

entry	ring size-/n	1.4.6/1.4.7	combined yield (%)
1	8-/1	1:11	90
2	9-/2	1:27	92
3	10-/3	1:3	75
4	11-/4	1:3	73

Scheme 1.4. *Diastereoselective TST RCM of prochiral alcohols towards the synthesis of 7–11-membered siloxane rings.*

In 2003, Evans and coworkers reported the first application of the *Si*-tethered RCM cross-coupling reaction towards an efficient and convergent total synthesis of mucocin, a potent antitumor agent (**1.5.4**, Scheme 1.5).[24] Allylic alcohol **1.5.1** was silylated and coupled with tetrahydrofuran-containing allylic alcohol partner **1.5.2** to generate the diene intermediate, which was next subjected to TST RCM in the presence of a stoichiometric amount of the **G-I** in refluxing 1,2-DCE. A stoichiometric amount of catalyst was required to avoid the inherent *cis*-selectivity observed for 1,4-disubstituted 7-membered siloxane systems.[13] In 2008, Harvey and coworkers utilized TST-RCM in the kinetic resolution of diene **1.5.5** to achieve the diastereoselective synthesis of the

C12–C24 fragment **1.5.6** of peloruside A, a potent cytotoxic agent (**1.5.7**, Scheme 1.5).[25] Diene **1.5.5** was subjected to the RCM reaction in the presence of the **G-II** catalyst [$(ImesH_2)(PCy_3)(Cl)_2Ru{=}CHPh$] [26] in refluxing CH_2Cl_2 to generate the single diastereoisomer **1.5.6** in 35% overall yield.

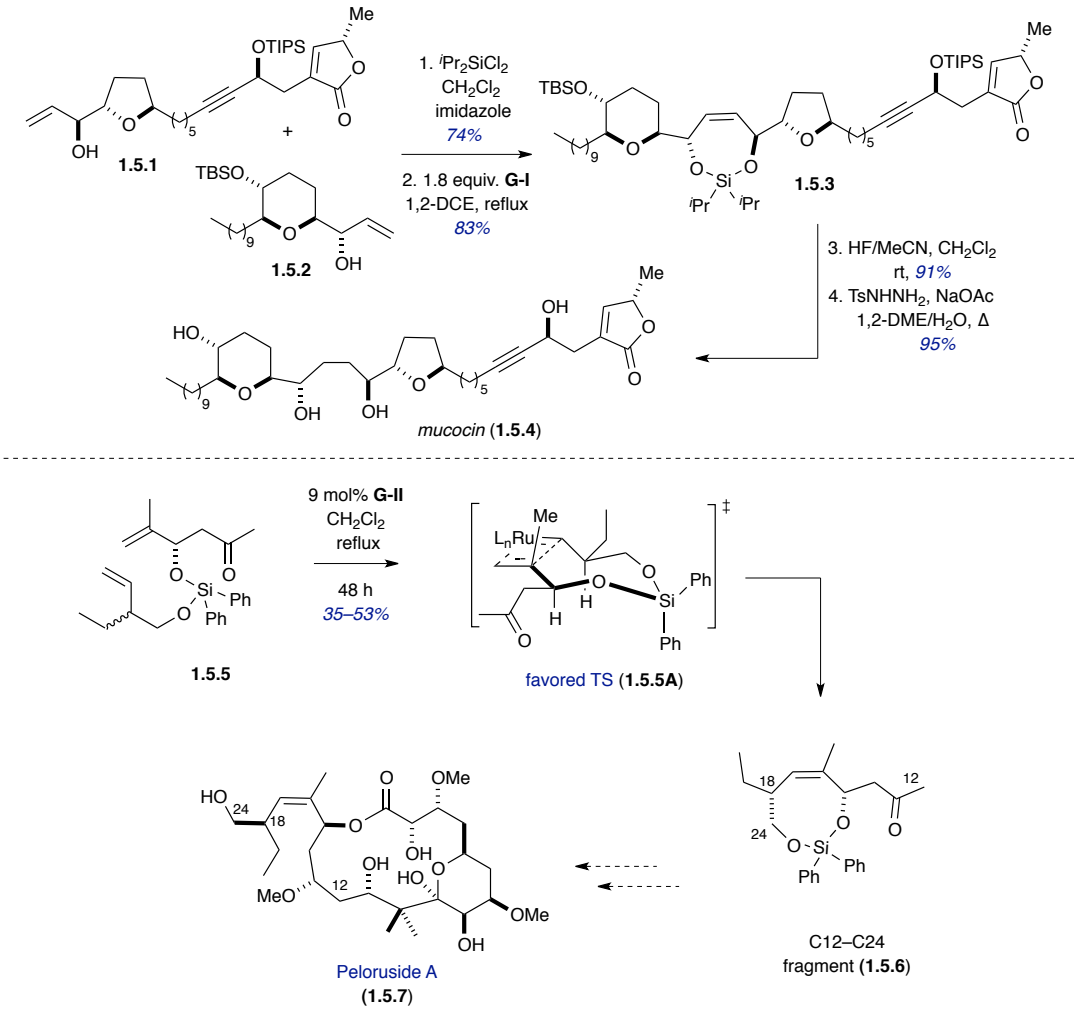

Scheme 1.5. *Application of Si-tether-mediated RCM towards the synthesis of mucocin and peloruside A.*

The synthetic utility of TST RCM strategy was further demonstrated in 2001 by Verdine and coworkers towards the goal of generating stereo-diversified ligand libraries

of *cis*-1,5-enediols (Scheme 1.6).[27] Starting with substituted allylic alcohol **1.6.1**, silylation, followed by addition of homoallylic alcohol **1.6.2**, generated 16-stereoisomers of *Si*-tethered dienes **1.6.4**. The RCM of stereoisomeric dienes **1.6.3** were performed in the presence of the **G-II** catalyst in toluene at 95 ºC to provide 16-stereoisomers of **1.6.4** in excellent yields. Interestingly, comparable yields were seen in both TST RCM processes leading to *cis*- and *trans*-ring substitution patterns.

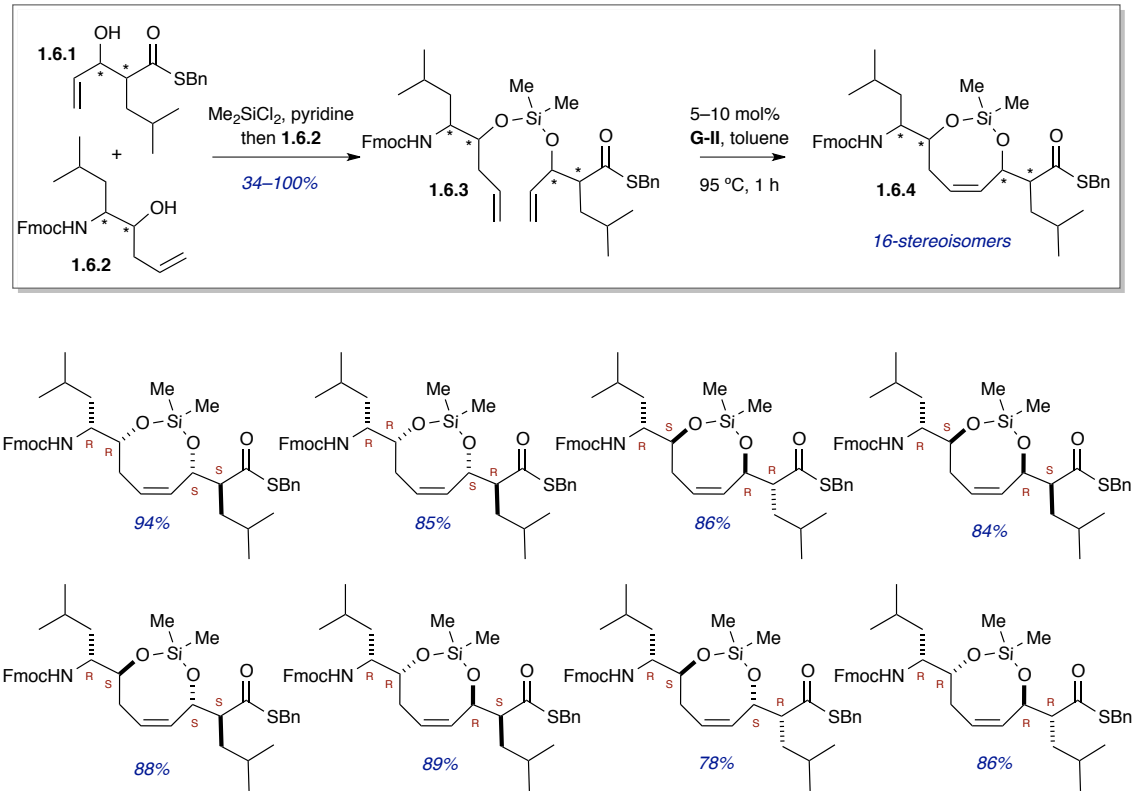

Scheme 1.6. *Synthesis of stereodiversified library of cis-1,5-enediols via TST RCM.*

In 2010, Kobayashi and coworkers published an extensive study of *Si*-tether mediated RCM towards the formation of 8-membered dioxasilane rings with regards to the olefinic geometry of the newly formed C=C bond (Scheme 1.7).[14] *Si*-tethered dienes

1.7.3 were synthesized *via* silylation of homoallylic alcohol **1.7.1**, followed by the coupling with substituted allylic alcohol partner **1.7.2**. Dienes **1.7.3** were subjected to the RCM reaction in the presence of the **HG-II** catalyst in refluxing xylene. It was observed that the stereochemistry and substituents on both alcohol coupling partners play a pivotal role in determining the geometry of the newly formed C=C bond. While the *cis* relationship of R^1 and R^2 substituents, and the presence of C2'-Me and *anti*-crotyl groups in diene **1.7.3** led to the formation of (*E*)-configured dioxasilacyclooctene, the RCM of silicon tethered triene **1.7.6**—prepared via the coupling of homoallylic alcohol and prochiral alcohol, generated (*Z*)-configured dioxasilacyclooctene exclusively revealing the inherent tendency of the system to be (*Z*)-configured. This data was consistent with the finding by the Evans and Harvey groups.[13,25]

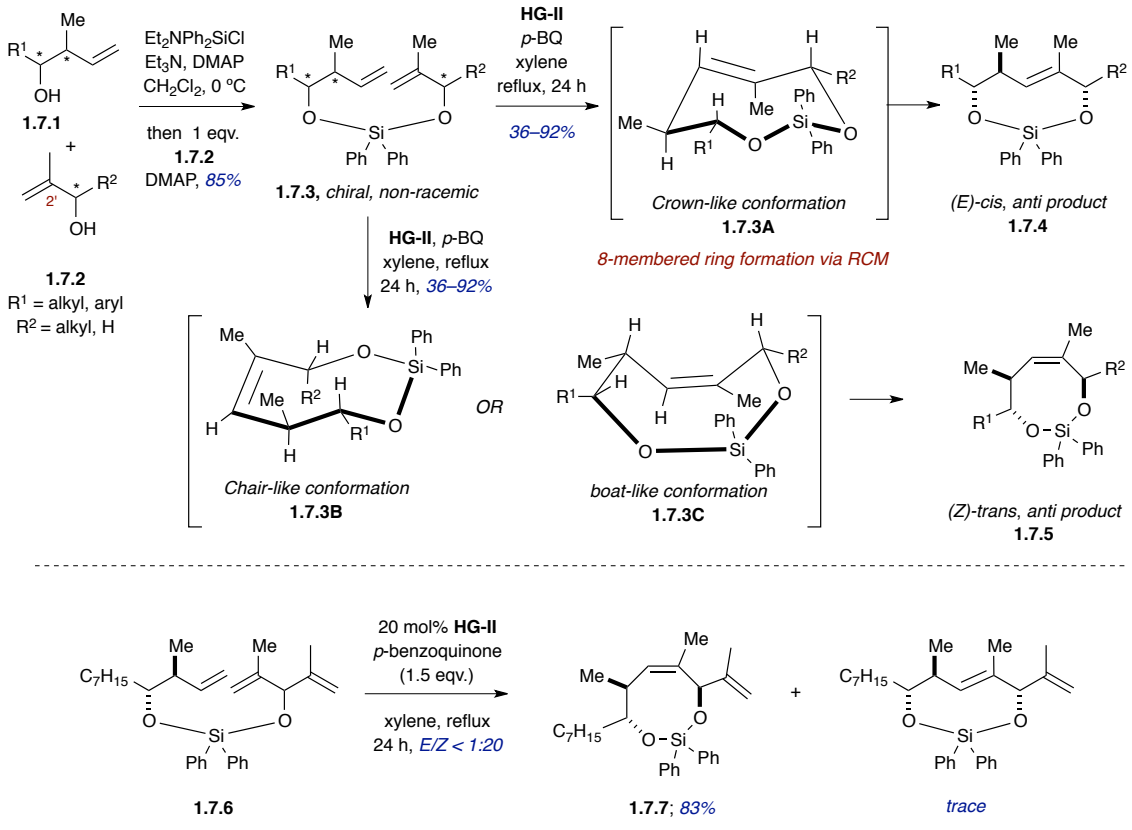

Scheme 1.7. *Study of Si-tether-mediated RCM towards the formation of (E)-selective 8-membered dioxasilane rings.*

In 2011, Kobayashi and coworkers further demonstrated the utility of the above mentioned *Si*-tether mediated (*E*)-selective RCM reaction towards the total synthesis of (+)-TMC-151C, possessing significant cytotoxicity against a wide range of tumor cell lines, including HCT-116, B16, and HeLa cells (Scheme 1.8).[28]

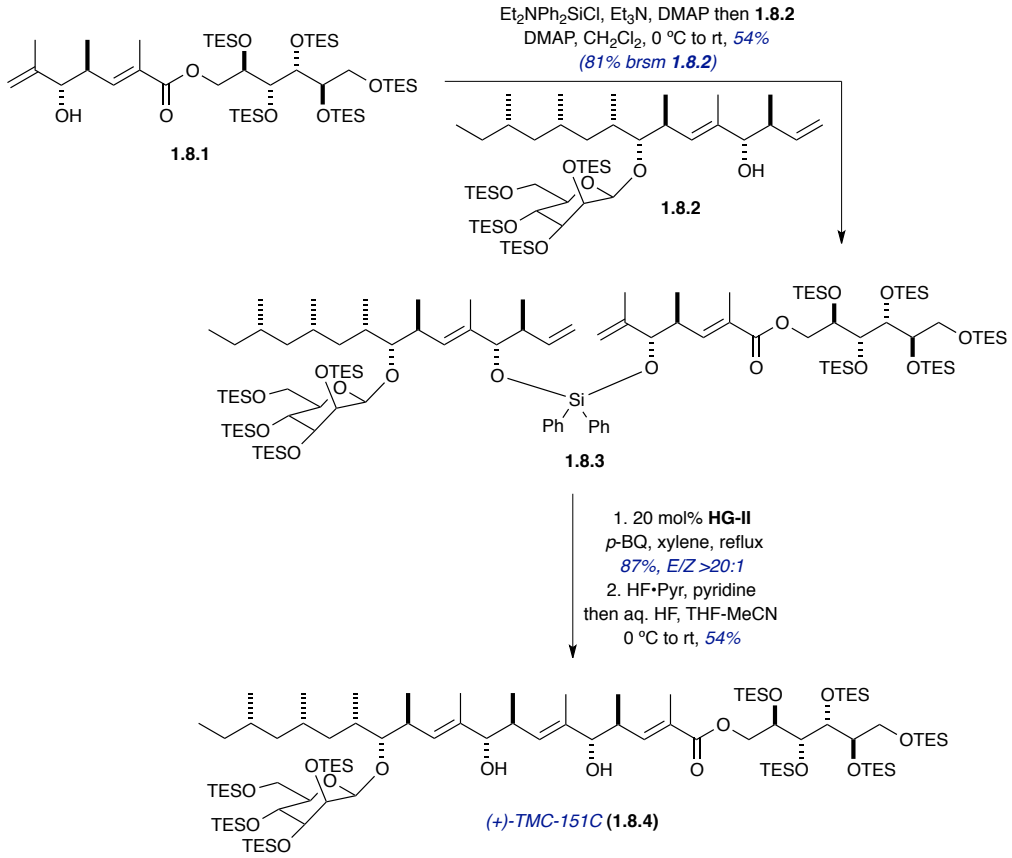

Scheme 1.8. *Application of Si-tether-mediated (E)-selective RCM strategy towards the total synthesis of (+)-TMC-151C.*

The synthesis featured a vinylogous Mukaiyama aldol[29] strategy to construct the key advanced intermediates **1.8.1** and **1.8.2** followed by a late-stage (*E*)-selective RCM mediated by *Si*-tether. The RCM precursor was synthesized conveniently by first

silylation of substituted allylic alcohol partner **1.8.1** and subsequent addition of homoallylic alcohol partner **1.8.2**. When subjected to RCM in the presence of 20 mol% of the **HG-II** catalyst, the 8-membered dioxasilane ring (not shown in the Scheme **1.8**) was generated with exclusive (*E*)-selectivity in excellent yield. Treatment of the RCM product with aqueous HF•pyr produced the natural product in 54% yield.

1.2.2: Ketal tether-mediated ring-closing metathesis

The use of ketals as tether systems in RCM reaction can be divided into four categories (Scheme 1.9). Type A and B represent the most common use of ketal/acetal, but these are mostly viewed as protecting groups for ketones and diols and have little consideration as tethers. Type C and D are relatively rare and can be viewed as the best representation for a ketal tethered-RCM process. In 1999, Grubbs and coworkers reported an example of type C ketal-tethered RCM strategy in which bridged oxabicycles **1.9.2** were generated *via* the RCM of 5-membered ketals **1.9.1** (Scheme 1.9).[30] The RCM of an equimolar mixture of *syn* and *anti*-diastereomers (~1:1 ratio) of ketal **1.9.1**, was performed efficiently in the presence of the **G-I** catalyst in CH_2Cl_2 at room temperature to provide bridged oxabicycle **1.9.2** in 45% yield along with unreacted *anti*-cyclic ketal **1.9.3**. Interestingly, the unreacted *anti*-isomer **1.9.3** did not dimerize during the RCM reaction (0.01M) and was conveniently converted to a mixture of *syn*- and *anti*-diastereoisomers by subsequent treatment with an acidic resin.

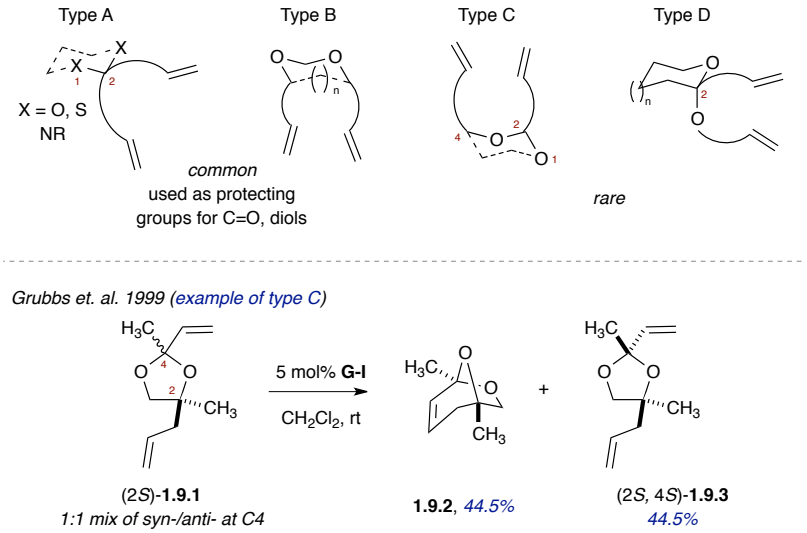

Scheme 1.9. *Ketal tether-mediated RCM.*

In 1999, Burke and coworkers reported a unique type C ketal tethered-RCM strategy for substrate desymmetrization *en route* to the synthesis of (+)-*exo*- and *endo*-brevicomin (**1.10.5** and **1.10.10**, Scheme 1.10).[31] The pseudo-C_2-symmetric triene **1.10.3** was synthesized from the C_2 symmetric substrate (3*S*,4*S*)-3,4-dihydroxy-1,5-hexadiene (**1.10.1**) via coupling with ketone **1.10.2**, followed by E2-elimination of the alkyl chloride, to provide the corresponding olefin. Ring-closing metathesis of triene **1.10.3** produced **1.10.4** in 86% yield as a single diastereomer. Subsequent hydrogenation generated (+)-*exo*-brevicomin (**1.10.5**) in 82% yield. Starting with a mixture of *meso* and (±)-diol **1.10.6**, ketalization with ketone **1.10.7** generated a mixture of diastereoisomers. *Meso*-ketal **1.10.8** was further subjected to the RCM reaction followed by hydrogenation to provide racemic *endo*-brevicomin (**1.10.10**). Later, this strategy was successfully applied in the synthesis of sialic acids, KDN and Neu5Ac.[32,33]

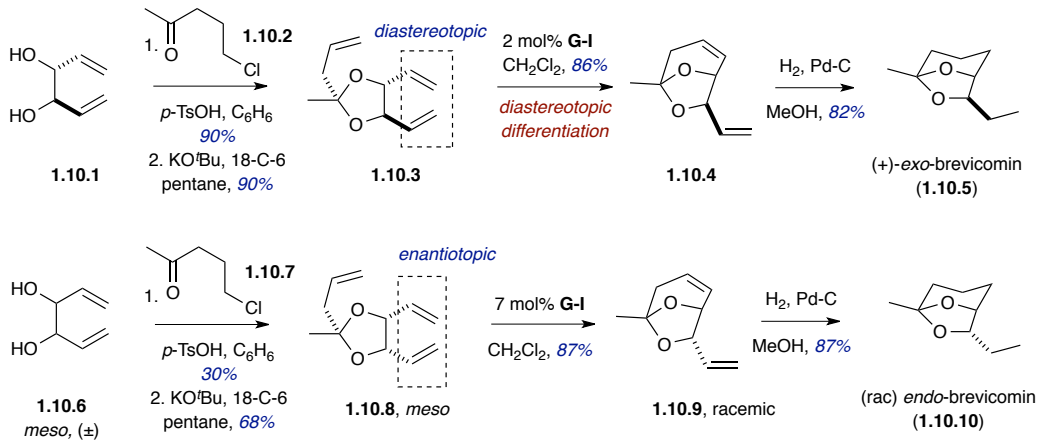

Scheme 1.10. *Synthesis of (+)-exo- and endo-brevicomin via ketal tethered-RCM strategy*.

In 1998, van Boom and coworkers exploited a ketal tether-mediated RCM strategy towards the synthesis of pyranose spiroacetal derivatives (**1.11.2**, Scheme 1.11). RCM of pyranose derivatives **1.11.1** was performed in the presence of the **G-I** catalyst in toluene at 60 ºC to construct [5,4]-, [5,5]-, [5,6]- and [5,7]-spiroacetals.[34] In 1999, Harrity and coworkers reported ketal tether-mediated, tandem metathesis reactions to generate spiroacetals (Scheme 1.11).[35] Tetraolefinic ether **1.11.3** was subjected to tandem RCM reaction in the presence of the **G-I** catalyst in CH_2Cl_2 to provide [4,4]-spiroacetal **1.11.4** in excellent yield. Interestingly, the [4,4]-spiroacetal **1.11.4** was found to decompose in the presence of catalytic amount of TsOH to furan, which further emphasized the importance of ketal-tethered, tandem RCM reactions to construct such

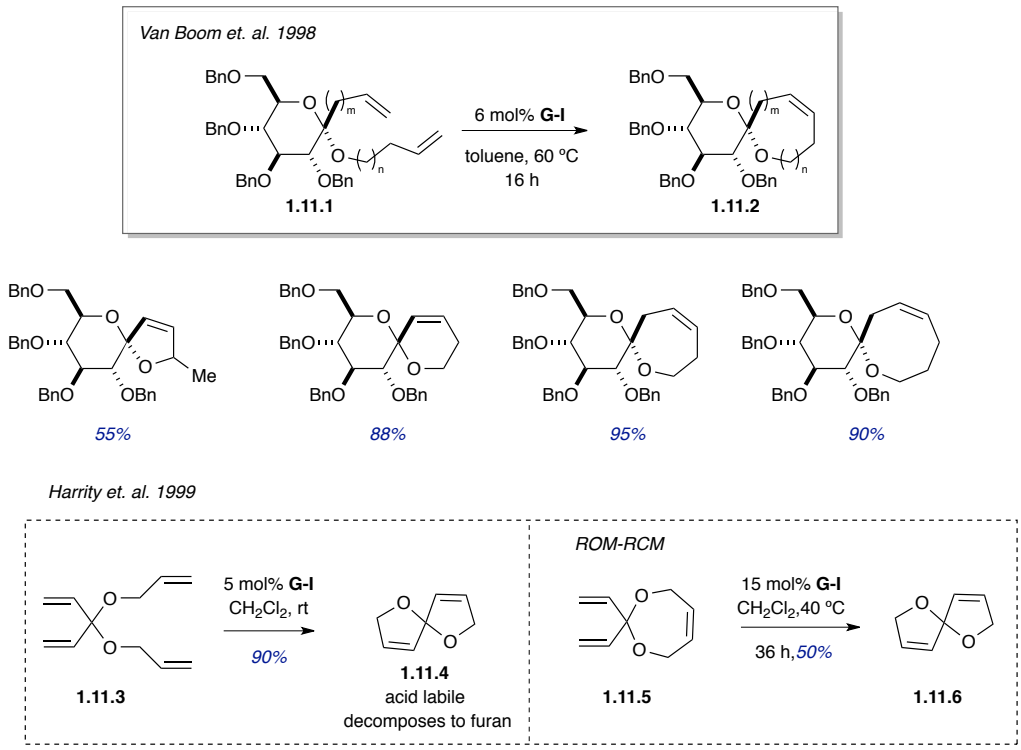

Scheme 1.11. *Ketal tether-mediated RCM to synthesize pyranose spiroacetal derivatives.*

systems over an acid catalyzed spiroketalization method. Notably, ROM-RCM (ring-opening-ring-closing metathesis) strategy was also employed to construct [4,4]-spiroacetal **1.11.6** in 50% yield (Scheme 1.11). All these reactions represent early examples of type D ketal-tethered RCM strategy.

In 2004, Hsung and coworkers reported the use of ketal-tethered RCM reactions *en route* to the synthesis of various spiroketals (Scheme 1.12).[36] In this method, 1,2-*syn* and *anti* diastereoisomers of cyclic ketals **1.12.1** were treated with the **G-I**/**G-II** catalysts at room temperature in CH_2Cl_2/PhH to yield 1,2-*syn* and 1,2-*anti*- isomer of spiroketals **1.12.2** of various sizes. Ring-closing metathesis proceeded smoothly with differently

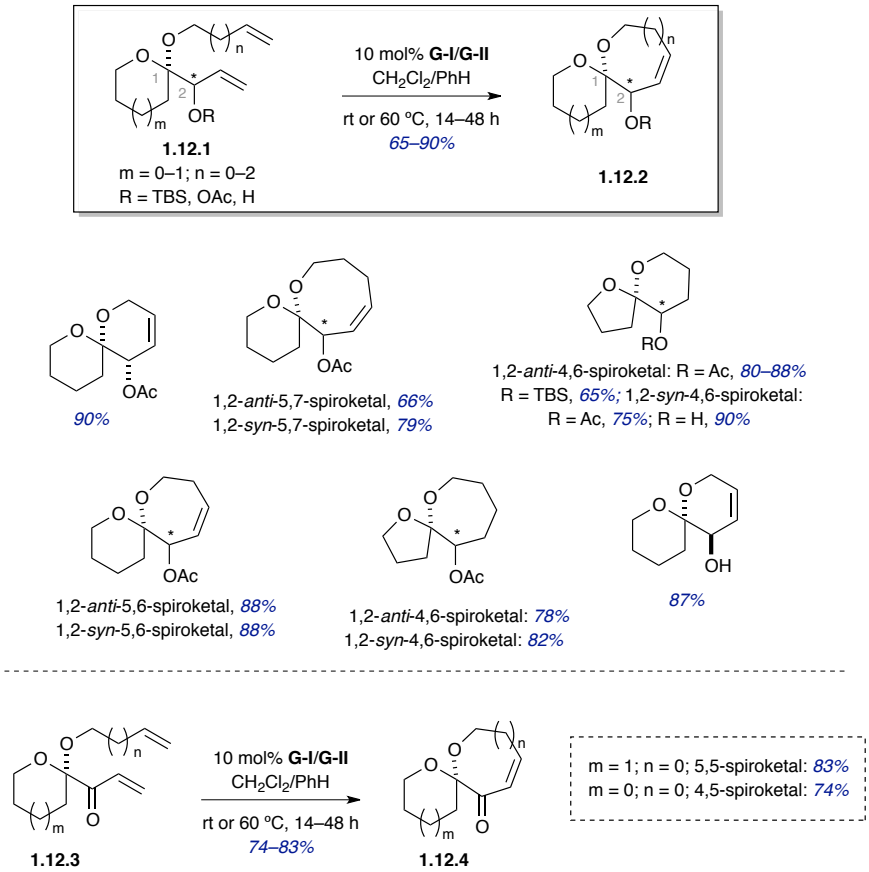

Scheme 1.12. *Ketal-tethered RCM reactions towards the synthesis of spiroketals.*

protected allylic alcohols (R = TBS and Ac), as well as a free hydroxyl group and carbonyl functionality at C-2 (**1.12.3**, Scheme 1.12). For larger rings formation of 5,7-, 6,7- and 6,8-spiroketals, RCM products were obtained under higher dilution and in the presence of the **G-II** catalyst in PhH.

In 2004, Hsung applied ketal tether-mediated RCM towards the synthesis of bee pheromone **1.13.4** to further demonstrate the utility of this powerful strategy (Scheme 1.13).[36] Lithiation of substituted tetrahydropyran **1.13.1**, followed by addition of crotyl bromide and subsequent ketalization with allylic alcohol in the presence of PPTS, generated cyclic ketal **1.13.2** in 30% overall yield with 4:1 diastereoselectivity. RCM of

cyclic ketal **1.13.2** provided 5,5-spiroacetal **1.13.3**, which upon hydrogenation afforded bee pheromone **1.13.4** in good overall yield.

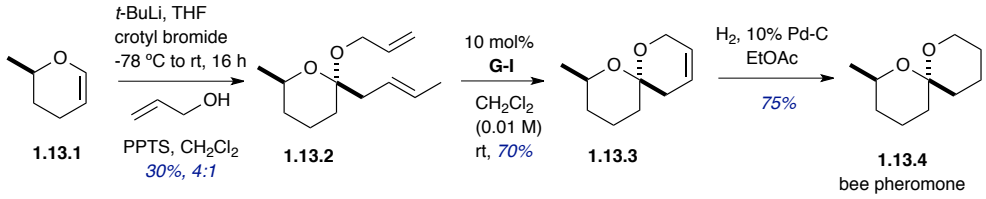

Scheme 1.13. *Ketal-tethered RCM reactions towards the synthesis of bee pheromone.*

Later in 2005, Hsung and coworkers employed the ketal-tethered RCM strategy for the synthesis of C11–C23 fragment of spirastrellolide A (**1.14.4**, Scheme 1.14).[37] The C11–C16 fragment was installed *via* ketalization of lactol **1.14.1**, derived from *D*-glucose, in the presence of 1 equivalent of the Brønsted acid, Tf_2NH, to produce cyclic ketal **1.14.3** in 89% yield as a single diastereomer. Ring-closing metathesis of the cyclic ketal in the presence of the **G-I** catalyst in PhH provided the C11–C23 fragment **1.14.4** of spirastrellolide A in 50% yield.

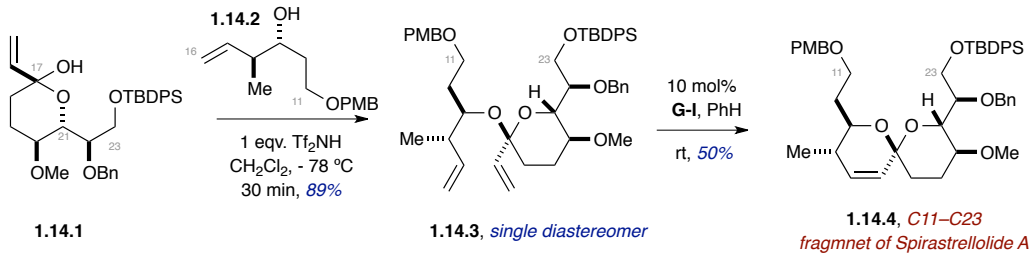

Scheme 1.14. *Application of ketal-tethered RCM approach towards the synthesis of the C11–C23 fragment of spirastrellolide A.*

In 2006, Hsung and coworkers expanded the scope of ketal-tethered RCM strategy for the construction of spiroaminal **1.15.3** (Scheme 1.15).[38] RCM precursors

1.15.2 (1,2-*syn* and 1,2-*anti*-isomers) were prepared by allylation of **1.15.1**. Subsequent RCM generated 1,2-*syn*- and 1,2-*anti*-isomers of spiroaminals **1.15.3** in excellent yields.

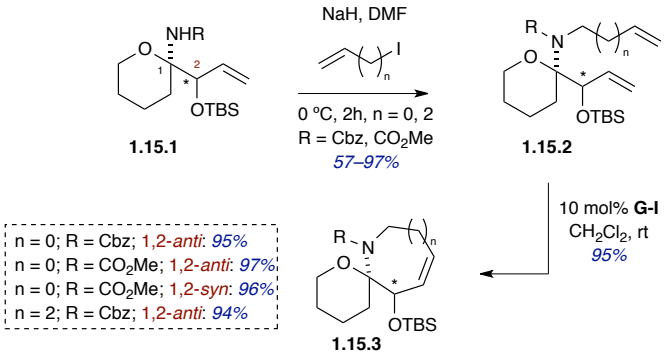

Scheme 1.15. *Ketal-tethered RCM approach to spiroaminals.*

In 2007, Hsung and coworkers again demonstrated the utility of a ketal-tethered RCM strategy en route to the total synthesis of (+)-aigialospirol (**1.16.5**, Scheme 1.16).[39] Addition of homoallylic alcohol **1.16.2** to lactol **1.16.1** from the equatorial face of the corresponding oxo-carbenium, generated in the presence of stoichiometric amount of Tf_2NH (Brønsted acid), allowed for the formation of cyclic ketal **1.16.3** as a single diastereomer in 76% yield. Subsequent RCM provided spiroketal **1.16.4** in 86% yield. This spiroketal was then converted to (+)-aigialospirol (**1.16.5**) over a few steps.

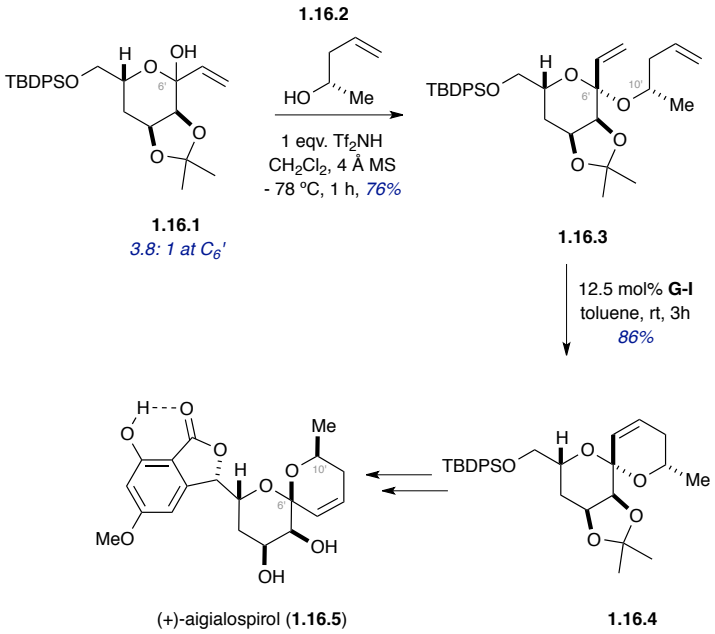

Scheme 1.16. *Application of ketal-tethered RCM strategy towards the total synthesis of (+)-aigialospirol.*

1.2.3: Additional tether-mediated ring-closing metathesis studies

1.2.3.1: γ-lactone tether-mediated ring-closing metathesis

In 2004, Martin and coworkers reported the synthesis of α,β-fused γ-lactone carbocycles and cyclic ethers via a γ-lactone tethered-RCM strategy (**1.17.3**, Scheme 1.17).[40] Ring-closing metathesis reactions of γ-lactones **1.17.2**, derived from chiral, 2,3-epoxy alcohol **1.17.1**, were performed in the presence of the **G-II** catalyst to generate cyclic ethers and carbocycles of various sizes in moderate to excellent yields.

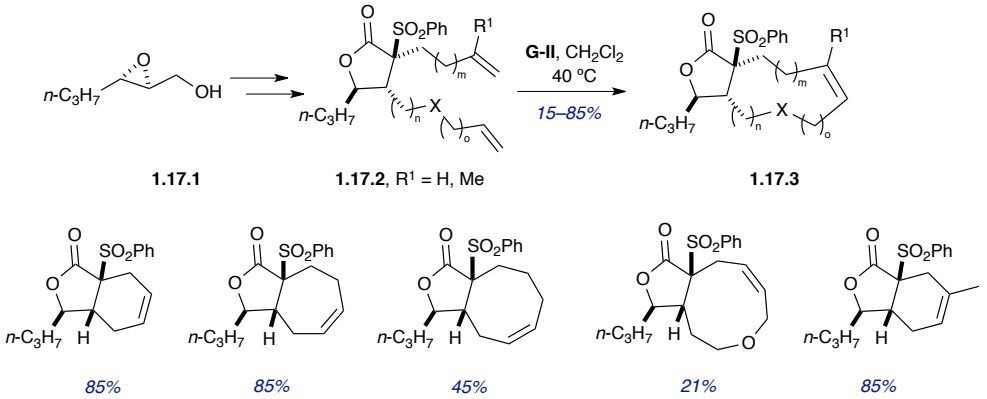

Scheme 1.17. *Example of Lactone-tethered RCM.*

1.2.3.2: Carboxylate tether-mediated ring-closing metathesis

In 2012, Schmidt and coworkers reported the stereoselective synthesis of 2*Z*,4*E*-configured dienoic acids *via* a one-flask RCM/base-mediated ring-opening of carboxylate tethered dienes (Scheme 1.18).[41] Butenoates **1.18.2**, synthesized from the coupling of allylic alcohol **1.18.1** with vinyl acetic acid, was subjected to RCM in the presence of the **G-II** catalyst in toluene in 65 ºC. Subsequent ring-opening, mediated by NaH, produced a variety of 2*Z*,4*E*-configured dienoic acids **1.18.3** in good to excellent yields. Later, this method was successfully applied towards the synthesis of **1.18.6**, a macrolactonization precursor of the fungal metabolite fusanolide A.[41] Towards this end, butenoate **1.18.4** was subjected to RCM in the presence of the **G-II** catalyst in toluene at 80 ºC, followed by NaH, to facilitate ring-opening and generate dienoic acid **1.18.5**. Subsequent deprotection of the silyl group provided **1.18.6** in 96% yield.

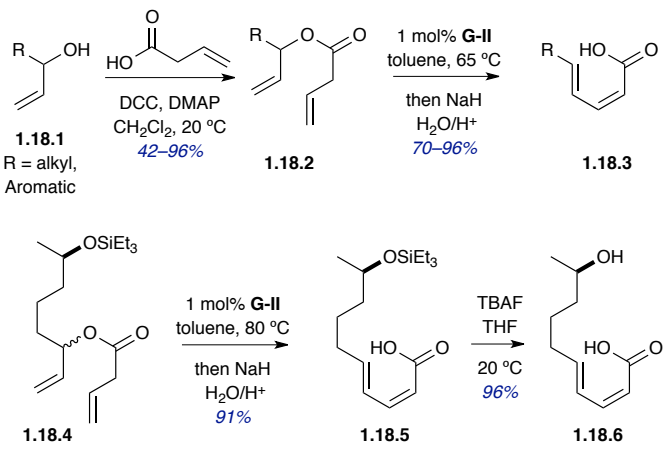

Scheme 1.18. *Application of carboxylate tether-mediated RCM towards the synthesis of advanced intermediate en route to fusanolide A.*

1.3: Use of *P*-tethers in synthesis

As opposed to the large body of work published on silicon tethers, literature reports on the use of phosphorous-based tethers is limited. A brief account of our previous work will be discussed in this section, which has served as a prelude to the work on complex phosphate-tether method discussed in next chapter.

One of the earliest examples of the use of phosphoramido tether was reported in 1997 by Sinay and coworkers towards the synthesis of *C*-disaccharide and its β-anomer via radical cyclization (Scheme 1.19).[6a] The coupling of two pyranose subunits was mediated by phosphoramido tether. The removal of this tether was performed by using a 2-step procedure of cleaving P-N bond by using methanolic•HCl followed by P-O bond cleavage under basic condition.

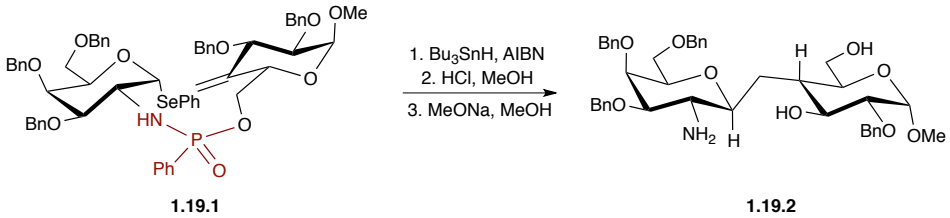

1.19.1 **1.19.2**

Scheme 1.19. *Use of phosphoramido tether towards the synthesis of C-disaccharide and its β-anomer via radical cyclization.*

Our group began exploring phosphorous as a temporary tether [both P(III) and P(V)] in 2001 with the synthesis of C_2-symmetric and unsymmetric, non-racemic 1,4-diamines **1.20.3** and **1.20.7** (Scheme 1.20).[6b] Homocoupling of α-branched secondary allylamine **1.20.1** was performed in the presence of PCl_3. Subsequent hydrolysis and RCM in the presence of the **G-II** catalyst generated 1,3,2-diazaphosphepine 2-oxide **1.20.2** in excellent yield. The C_2-symmetric, 1,4-diamine **1.20.3** was then generated by hydrolysis in a one-pot protocol combined with RCM. Interestingly, efforts to facilitate this coupling/RCM sequence by utilizing other temporary tethers, including *Si*-tether, were not successful. The synthesis of unsymmetrical, non-racemic, 1,4-diamine **1.20.7** started with the heterocoupling of amine **1.20.4** and **1.20.5** that generated the RCM precursor **1.20.6** in excellent yield with good diastereoselectivity. Subsequent one-pot RCM/hydrolysis sequence to cleave the P(V)-tether produced the desired 1,4-diamine **1.20.7**.

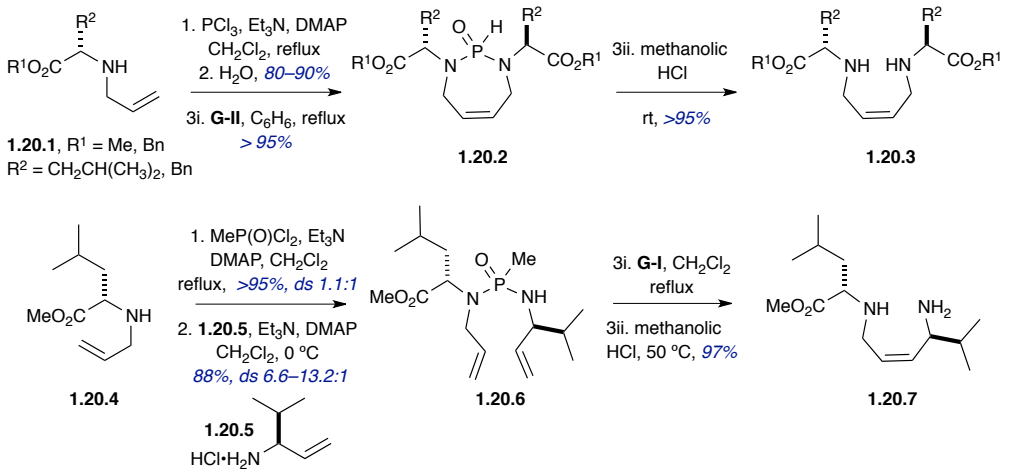

Scheme 1.20. *Use of temporary Phosphorous tether-mediated RCM in the synthesis of functinalized 1,4-diamines.*

The study towards the synthesis of monocyclic phosphates was reported in 2006 in which the phosphate ester played a dual role as a tether and as a leaving group in subsequent cuprate displacement reaction (Scheme 1.21).[42,11b] In this process, the homo-coupling of substituted allylic alcohol **1.21.1** was mediated by a phosphate triester tether to obtain the pseudo-C_2-symmetric monocyclic phosphate scaffold (*S*,*S*)-**1.21.2** in excellent yield. The C_2-symmetric (*Z*)-configured 1,4-diol **1.21.3** was produced in excellent yields after reductive removal of phosphate. In a similar fashion, the corresponding saturated analogue **1.21.6** was produced by adding a hydrogenation step before tether removal. Finally, a key symmetry breaking operation involved a highly diastereoselective allylic cuprate displacement reaction to generate the phosphoric acid intermediate, which upon tether removal delivered the homoallylic alcohol fragment **1.21.4**.

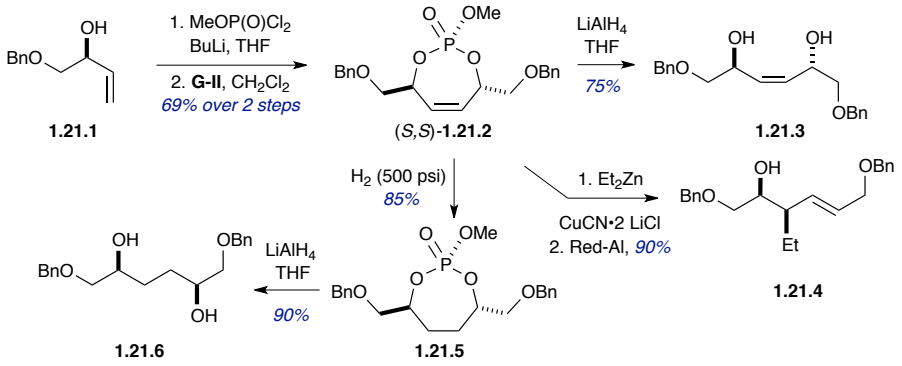

Scheme 1.21. *Synthesis of monocyclic phosphate and its synthetic utility.*

In 2005, the utility of phosphate tethers was further demonstrated towards the desymmetrization of C_2-symmetric diene diol (*S*,*S*)-**1.22.1** via RCM (Scheme 1.22).[10] The homotopic olefinic groups present in the C_2-symmetric 1,3-*anti*-diol diene (*S*,*S*)-**1.22.1** were differentiated and rendered diastereotopic in the process of generating the pseudo-C_2-symmetric phosphate triester intermediate (*S*,*S*)-**1.22.2** with the installation of phosphate tether. This RCM precursor (*S*,*S*)-**1.22.2** contained a chirotopic, non-stereogenic phosphorus atom, which after diastereoselective RCM between the two *cis*-substituted olefins, in the presence of the **G-II** catalyst, enabled the formation of *P*-stereogenic bicyclo[4.3.1]phosphate (S,S,S_P)-**1.22.3** in good yield. The overall process had been previously described by Schreiber and others as terminus differentiation or diastereotopic differentiation of pseudo-C_2-symmetric substrates.[43]

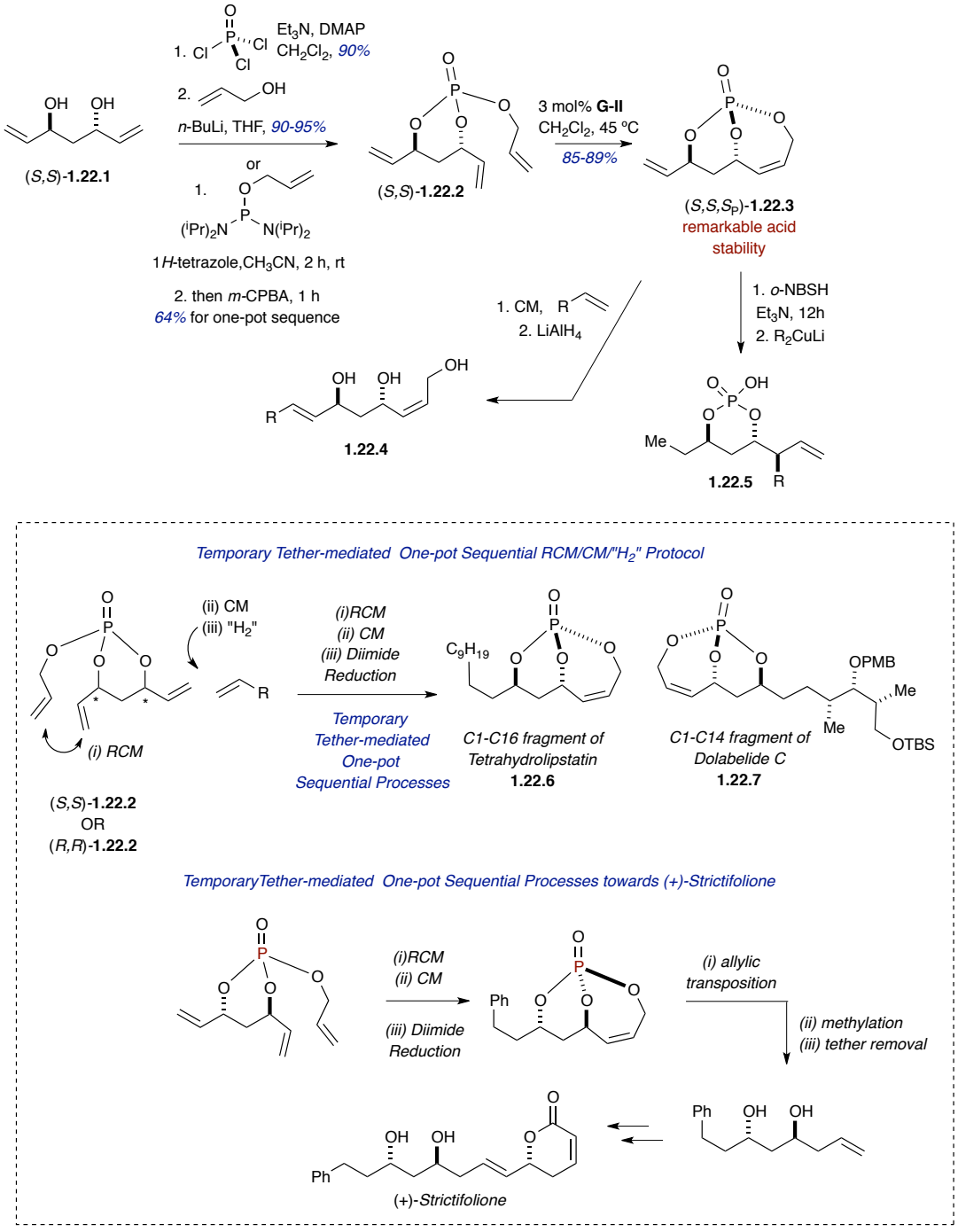

Scheme 1.22. *Synthesis of bicyclo[4.3.1]phosphate and its synthetic utility.*

A series of synthetically useful transformations were further developed centered on this bicyclic phosphate template (S,S,S_P)-**1.22.3**, [or its enantiomeric (R,R,R_P)-

counterpart].[10,11a,b] A sequence of selective CM reactions of the external olefinic group of bicyclo[4.3.1]phosphate (*S,S,S*$_P$)-**1.22.3**, followed by reductive tether-removal using $LiAlH_4$, produced polyol intermediate **1.22.4**.[11a] Utilizing the leaving group ability of phosphate, a diastereselective cuprate displacement protocol was developed after subsequent hydrogenation of the external olefin to generate polyketide-like intermediate **1.22.5**.[10] In addition, a multi-step, one-pot, sequential RCM/CM/H_2 process was developed starting from trienes **1.22.2** to generate complex intermediates such as **1.22.6** and **1.22.7** in a facile manner.[11c] The chemo- and regioselective hydrogenation was made possible by the stereoelectronic properties inherent to phosphate tethers. Most importantly, this tandem RCM/CM/H_2 process preserved the stereochemical integrity of the bicyclic phosphate, which is critical for the success of later transformations. Later in 2014, the utility of phosphate tether-mediated one-pot sequential protocols was further demonstrated towards the efficient synthesis of (+)-strictifolione (Scheme 1.22).[12d] This modular synthetic route featured two consecutive phosphate tether-mediated one-pot sequential protocols followed by a final cross-metathesis reaction to yield the natural product in a streamlined 3-pot processes starting from triene.

1.4: Conclusion

In general, tether mediated RCM strategies have been well-studied and utilized towards the construction of important building blocks en route to total synthesis of bioactive natural products. Our group has aimed at efforts towards the use of phosphorous-based tethers in RCM and their synthetic utility. The synthetic potential of phosphate tether in multivalent activation of carbinol centers, serving as a protecting

group and as a leaving group as well as their use in desymmetrization of homotopic olefinic groups present in 1,3-*anti*-diene diol substrates warrants further investigation of the phosphate tether in mediating coupling of complex subunits. In addition, RCM studies of complex phosphate-tethered system would facilitate our understanding of the underlying factors governing RCM for such complex systems, which in turn, would also increase the applicability of phosphate tether-mediated RCM reactions towards the synthesis of complex advanced fragments *en route* to bioactive natural products. The focus of this dissertation has been exploring the use of phosphate tethers in combining complex subunits, investigation of RCM of such complex phosphate-tethered system and utilizing bicyclo[n.3.1] as building blocks to synthesize stereoenriched polyols. In addition, potential application of phosphate tether-mediated reactions towards the synthesis of the C9–C25 fragments of spirastrellolide B will also be discussed.

1.5: References cited:

[1] (a) Trost, B. M. The atom economy: a search for synthetic efficiency. *Science* **1991**, *254*, 1471–1477; (b) Trost, B. M. Atom economy - a challenge for organic synthesis: homogeneous catalysis leads the way. *Angew. Chem., Int. Ed. Engl.* **1995**, *34*, 259–281.

[2] Wender, P. A.; Verma, V. A.; Paxton, T. J.; Pillow, T. H. Function-Oriented Synthesis, Step Economy, and Drug Design. *Acc. Chem. Res.* **2008**, *41*, 40–49.

[3] (a) Young, I. S.; Baran, P. S. Protecting-group-free synthesis as an opportunity for invention. *Nat. Chem.* **2009**, *1*, 193–205; (b) Hoffmann, R. W. Protecting-group-free synthesis. *Synthesis* **2006**, 3531–3541.

[4] For a review on disposable tethers in organic synthesis see: Gauthier, D. R., Jr.; Zandi, K. S.; Shea, K. J. Disposable tethers in synthetic organic chemistry.

Tetrahedron **1998**, *54*, 2289–2338.

[5] (a) Čusak, A. Temporary Silicon-Tethered Ring-Closing Metathesis: Recent Advances in Methodology Development and Natural Product Synthesis. *Chem. Eur. J.* **2012**, *18*, 5800–5824; (b) Bracegirdle, S.; Anderson, E. A. Recent advances in the use of temporary silicon tethers in metal-mediated reactions. *Chem. Soc. Rev.* **2010**, *39*, 4114–4129.

[6] (a) Rubinstenn, G.; Esnault, J.; Mallet, J.-M.; Sinay, P. Radical mediated synthesis of N-acetyl-D-galactosamine containing C-disaccharides via a temporary phosphoramidic connection. *Tetrahedron Asymmetry* **1997**, *8*, 1327–1336; (b) Sprott, K. T.; McReynolds, M. D.; Hanson, P. R. A Temporary Phosphorus Tether/Ring-Closing Metathesis Strategy to Functionalized 1,4-Diamines. *Org. Lett.* **2001**, *3*, 3939–3942.

[7] (a) Hoveyda, A. H.; Murphy, K. E. Enantioselective synthesis of α-alkyl-β,γ-unsaturated esters through efficient Cu-catalyzed allylic alkylations. *J Am Chem Soc*. **2003**, *125*, 4690–4691; (b) Morin, M. D.; Rychnovsky, S. D. Reductive spiroannulation of nitriles with secondary electrophiles. *Org Lett*. **2005**, *7*, 2051–2053; (c) Bartlett, P. A.; Jernstedt, K. K. A stereocontrolled synthesis of the methyl ester of (±)-nonactic acid. *Tetrahedron Lett.* **1980**, *21*, 1607–1610; (d) Nicolaou, K. C.; Shi, G-Q.; Gunzner, J. L.; Gärtner, P.; Yang, Z. Palladium-Catalyzed Functionalization of Lactones via Their Cyclic Ketene Acetal Phosphates. Efficient New Synthetic Technology for the Construction of Medium and Large Cyclic Ethers. *J. Am. Chem. Soc.* **1997**, *119*, 5467–5468; (e) Yanagisawa, A.; Noritake, Y.; Nomura, N.; Yamamoto, H. Superiority of Phosphate Ester as Leaving Group for Organocopper Reactions. Highly S_N2'-, (*E*)-, and Antiselective Alkylation of Allylic Alcohol Derivatives. *Synlett*. **1991**, 251–253.

[8] (a) Hanson, P. R.; Stoianova, D. S. Ring closing metathesis reactions on a phosphonate template. *Tetrahedron Lett.* **1998**, *39*, 3939–3942; (b) Hanson, P. R.; Stoianova, D. S. Ring-closing metathesis strategy to P-heterocycles. *Tetrahedron*

Lett. **1999**, *40*, 3297–3300; (c) Sprott, K. T.; Hanson, P. R. The Synthesis of P-Chiral Amino Acid-Derived Phosphonamidic Anhydrides. *J. Org. Chem.* **2000**, *65*, 4721–4728; (d) Sprott, K. T.; Hanson, P. R. The Synthesis of Sterically Demanding Amino Acid-Derived Cyclic Phosphonamides. *J. Org. Chem.* **2000**, *65*, 7913–7918; (e) Sprott, K. T.; McReynolds, M. D.; Hanson, P. R. Ring-closing metathesis strategies to amino acid-derived P-heterocycles. *Synthesis* **2001**, 612–620; (f) Stoianova, D. S.; Hanson, P. R. A Ring-Closing Metathesis Strategy to Phosphonosugars. *Org. Lett.* **2001**, *3*, 3285–3288.

[9] (a) Stoianova, D. S.; Hanson, P. R. Diastereotopic Differentiation on Phosphorus Templates via the Ring-Closing Metathesis Reaction. *Org. Lett.* **2000**, *2*, 1769–1772; (b) Moore, J. D.; Hanson, P. R. Substituent effects in the double diastereotopic differentiation of α-diazophosphonates via intramolecular cyclopropanation. *Tetrahedron: Asymmetry* **2003**, *14*, 873–880.

[10] Whitehead, A.; McReynolds, M. D.; Moore, J. D.; Hanson, P. R. Multivalent Activation in Temporary Phosphate Tethers: A New Tether for Small Molecule Synthesis. *Org. Lett.* **2005**, *7*, 3375–3378.

[11] (a) Waetzig, J. D.; Hanson, P. R. Temporary Phosphate Tethers: A Metathesis Strategy to Differentiated Polyol Subunits. *Org. Lett.* **2006**, *8*, 1673–1676; (b) Thomas, C. D.; McParland, J. P.; Hanson, P. R. Divalent and Multivalent Activation in Phosphate Triesters: A Versatile Method for the Synthesis of Advanced Polyol Synthons. *Eur. J. Org. Chem.* **2009**, 5487–5500; (c) Venukadasula, P. K. M.; Chegondi, R.; Suryn, G. M.; Hanson, P. R. A Phosphate Tether-Mediated, One-Pot, Sequential Ring-Closing Metathesis/Cross-Metathesis/Chemoselective Hydrogenation Protocol. *Org. Lett.* **2012**, *14*, 2634–2637; (d) For a comprehensive review on our tether work, see: Hanson, P. R.; Jayasinghe, S.; Maitra, S.; Markley, J. L. Phosphate tethers in natural product synthesis. *Top Curr Chem* **2015**, *361*, 253–271.

[12] (a) Venukadasula, P. K. M.; Chegondi, R.; Maitra, S.; Hanson, P. R. A Concise, Phosphate-Mediated Approach to the Total Synthesis of (–)-Tetrahydrolipstatin.

Org. Lett. **2010**, *12*, 1556–1559; (b) Hanson, P. R.; Chegondi, R.; Nguyen, J.; Thomas, C. D.; Waetzig, J. D.; Whitehead, A. Total synthesis of dolabelide C: A phosphate-mediated approach. *J. Org. Chem.* **2011**, *76*, 4358–4370; (c) Chegondi, R.; Tan, M. M. L.; Hanson, P. R. Phosphate tether-mediated approach to the formal total synthesis of (–)-salicylihalamides A and B. *J. Org. Chem.* **2011**, *76*, 3909–3916; (d) Jayasinghe, S.; Venukadasula, P. K. M.; Hanson, P. R. An Efficient, Modular Approach for the Synthesis of (+)-Strictifolione and a Related Natural Product. *Org. Lett.* **2014**, *16*, 122–125; (e) Chegondi, R.; Hanson, P. R. Synthetic studies to lyngbouilloside: a phosphate tether-mediated synthesis of the macrolactone core. *Tetrahedron Lett.* **2015**, Ahead of Print.

[13] Evans, P. A.; Cui, J.; Buffone, G. P. Diastereoselective temporary silicon-tethered ring-closing-metathesis reactions with prochiral alcohols: A new approach to long-range asymmetric induction. *Angew. Chem., Int. Ed.* **2003**, *42*, 1734–1737.

[14] Matsui, R.; Seto, K.; Fujita, K.; Suzuki, T.; Nakazaki, A.; Kobayashi, S. Unusual E-selective ring-closing metathesis to form eight-membered rings. *Angew. Chem., Int. Ed.* **2010**, *49*, 10068–10073.

[15] (a) Chegondi, R.; Maitra, S.; Markley, J. L.; Hanson, P. R. Phosphate-Tether-Mediated Ring-Closing Metathesis for the Preparation of Complex 1,3-anti-Diol-Containing Subunits. *Chem. - Eur. J.* **2013**, *19*, 8088–8093; (b) Maitra, S.; Markley, J. L.; Chegondi, R.; Hanson, P. R. Phosphate Tether-Mediated Ring-Closing Metathesis for the Generation of Medium to LargeBicyclo[n.3.1]phosphates *Tetrahedron* **2015**, *ASAP*.

[16] Hanson, P. R.; Jayasinghe, S.; Maitra, S.; Ndi, C. N.; Chegondi, R. A modular phosphate tether-mediated divergent strategy to complex polyols. *Beilstein J. Org. Chem.* **2014**, *10*, 2332–2337.

[17] Warabi, K.; Williams, D. E.; Patrick, B. O.; Roberge, M.; Andersen, R. J. Spirastrellolide B Reveals the Absolute Configuration of the Spirastrellolide Macrolide Core. *J. Am. Chem. Soc.* **2007**, *129*, 508–509.

[18] Fu, G. C.; Grubbs, R. H. The application of catalytic ring-closing olefin

metathesis to the synthesis of unsaturated oxygen heterocycles. *J. Am. Chem. Soc.* **1992**, *114*, 5426–5427.

[19] Chang, S.; Grubbs, R. H. A simple method to polyhydroxylated olefinic molecules using ring-closing olefin metathesis. *Tetrahedron Lett.* **1997**, *38*, 4757–4760.

[20] Tamao, K.; Ishida, N.; Ito, Y.; Kumada, M. Nucleophilic hydroxymethylation of carbonyl compounds: 1-(hydroxymethyl)cyclohexanol. *Org. Synth.* **1990**, *69*, 96–105.

[21] Meyer, C.; Cossy, J. Synthesis of oxygenated heterocycles from cyclic allylsiloxanes using ring-closing olefin metathesis. *Tetrahedron Lett.* **1997**, *38*, 7861–7864.

[22] Evans, P. A.; Murthy, V. S. Temporary Silicon-Tethered Ring-Closing Metathesis Approach to C2-Symmetrical 1,4-Diols: Asymmetric Synthesis of D-Altritol. *J. Org. Chem.* **1998**, *63*, 6768–6769.

[23] Hoye, T. R.; Promo, M. A. Silicon tethered ring-closing metathesis reactions for self- and cross-coupling of alkenols. *Tetrahedron Lett.* **1999**, *40*, 1429–1432.

[24] Evans, P. A.; Cui, J.; Gharpure, S. J.; Polosukhin, A.; Zhang, H.-R. Enantioselective Total Synthesis of the Potent Antitumor Agent (-)-Mucocin Using a Temporary Silicon-Tethered Ring-Closing Metathesis Cross-Coupling Reaction. *J. Am. Chem. Soc.* **2003**, *125*, 14702–14703.

[25] Casey, E. M.; Teesdale-Spittle, P.; Harvey, J. E. Synthesis of the C12-C24 fragment of peloruside A by silyl-tethered diastereomer-discriminating RCM. *Tetrahedron Lett.* **2008**, *49*, 7021–7023.

[26] Scholl, M.; Ding, S.; Lee, C. W.; Grubbs, R. H. Synthesis and Activity of a New Generation of Ruthenium-Based Olefin Metathesis Catalysts Coordinated with 1,3-Dimesityl-4,5-dihydroimidazol-2-ylidene Ligands. *Org. Lett.* **1999**, *1*, 953–956.

[27] Harrison, B. A.; Verdine, G. L. The Synthesis of an Exhaustively

Stereodiversified Library of cis-1,5 Enediols by Silyl-Tethered Ring-Closing Metathesis. *Org. Lett.* **2001**, *3*, 2157–2159.

[28] Matsui, R.; Seto, K.; Sato, Y.; Suzuki, T.; Nakazaki, A.; Kobayashi, S. Convergent Total Synthesis of (+)-TMC-151C by a Vinylogous Mukaiyama Aldol Reaction and Ring-Closing Metathesis. *Angew. Chem., Int. Ed.* **2011**, *50*, 680–683.

[29] (a) Shirokawa, S.; Kamiyama, M.; Nakamura, T.; Okada, M.; Nakazaki, A.; Hosokawa, S.; Kobayashi, S. Remote Asymmetric Induction with Vinylketene Silyl N,O-Acetal. *J. Am. Chem. Soc.* **2004**, *126*, 13604–13605; (b) Shinoyama, M.; Shirokawa, S.-i.; Nakazaki, A.; Kobayashi, S. A Switch of Facial Selectivities Using α-Heteroatom-Substituted Aldehydes in the Vinylogous Mukaiyama Aldol Reaction. *Org. Lett.* **2009**, *11*, 1277–1280; (c) Yamaoka, M.; Nakazaki, A.; Kobayashi, S. Rate enhancement by water in a TiCl4-mediated stereoselective vinylogous Mukaiyama aldol reaction. *Tetrahedron Lett.* **2010**, *51*, 287–289.

[30] Scholl, M.; Grubbs, R. H. Total synthesis of (–)- and (±)-frontalin via ring-closing metathesis. *Tetrahedron Lett.* **1999**, *40*, 1425–1428.

[31] Burke, S. D.; Mueller, N.; Beaudry, C. M. Desymmetrization by Ring-Closing Metathesis Leading to 6,8-Dioxabicyclo[3.2.1]octanes: A New Route for the Synthesis of (+)-exo- and endo-Brevicomin. *Org. Lett.* **1999**, *1*, 1827–1829.

[32] Burke, S. D.; Voight, E. A. Formal Synthesis of (+)-3-Deoxy-D-glycero-D-galacto-2-nonulosonic Acid (KDN) via Desymmetrization by Ring-Closing Metathesis. *Org. Lett.* **2001**, *3*, 237–240.

[33] Voight, E. A.; Rein, C.; Burke, S. D. Synthesis of Sialic Acids via Desymmetrization by Ring-Closing Metathesis. *J. Org. Chem.* **2002**, *67*, 8489–8499.

[34] Van Hooft, P. A. V.; Leeuwenburgh, M. A.; Overkleeft, H. S.; Van Der Marel, G. A.; Van Boeckel, C. A. A.; Van Boom, J. H. A novel and flexible synthesis of pyranose spiroacetal derivatives. *Tetrahedron Lett.* **1998**, *39*, 6061–6064.

[35] Bassindale, M. J.; Hamley, P.; Leitner, A.; Harrity, J. P. A. Spirocycle assembly through selective tandem ring closing metathesis reactions. *Tetrahedron Lett.* **1999**, *40*, 3247–3250.

[36] Ghosh, S. K.; Hsung, R. P.; Wang, J. Ketal-tethered ring-closing metathesis. An unconventional approach to constructing spiroketals and total synthesis of an insect pheromone. *Tetrahedron Lett.* **2004**, *45*, 5505–5510.

[37] Liu, J.; Hsung, R. P. Synthesis of the C11–C23 Fragment of Spirastrellolide A. A Ketal-Tethered RCM Approach to the Construction of Spiroketals. *Org. Lett.* **2005**, *7*, 2273–2276.

[38] Ghosh, S. K.; Ko, C.; Liu, J.; Wang, J.; Hsung, R. P. A ketal-tethered RCM strategy toward the synthesis of spiroketal related natural products. *Tetrahedron* **2006**, *62*, 10485–10496.

[39] Figueroa, R.; Hsung, R. P.; Guevarra, C. C. An Enantioselective Total Synthesis of (+)-Aigialospirol. *Org. Lett.* **2007**, *9*, 4857–4859.

[40] Rodriguez, C. M.; Ravelo, J. L.; Martin, V. S. γ-Lactone-Tethered Ring-Closing Metathesis. A Route to Enantiomerically Enriched γ-Lactones α,β-Fused to Medium-Sized Rings. *Org. Lett.* **2004**, *6*, 4787–4789.

[41] Schmidt, B.; Kunz, O. One-flask tethered ring closing metathesis-electrocyclic ring opening for the highly stereoselective synthesis of conjugated Z/E-dienes. *Eur. J. Org. Chem.* **2012**, *2012*, 1008–1018.

[42] Whitehead, A.; McParland, J. P.; Hanson, P. R. Divalent Activation in Temporary Phosphate Tethers: Highly Selective Cuprate Displacement Reactions. *Org. Lett.* **2006**, *8*, 5025–5028.

[43] (a) Poss, C. S.; Schreiber, S. L. Two-directional chain synthesis and terminus differentiation. *Acc. Chem. Res.* **1994**, *27*, 9–17; (b) For a review of both diastereotopic and enantiotopic differentiation, see: Magnuson, S. R. Two-directional synthesis and its use in natural product synthesis. *Tetrahedron* **1995**, *51*, 2167–2213.

Chapter 2

Phosphate tether-mediated ring-closing metathesis studies

2.1: Introduction

The development of new convergent strategies that allow for the stereoselective formation of C–C double bonds are fundamentally important in the field of organic synthesis. In this regard, olefin metathesis is one of the most powerful and important carbon-carbon bond forming reactions in modern synthetic organic chemistry.[1] In particular, ring-closing metathesis (RCM) has continued to be a broadly utilized metathesis reaction in terms of the synthesis of small molecule and bioactive natural products.[2,3,4] The emergence of tether-mediated RCM strategies towards the goal of developing atom,[5] redox[6] and step[7] economical synthetic routes for complex fragments is discussed in detail in the previous chapter. In this respect, the most commonly used tethers such as silicon,[8,9,10] ketal[11] and carboxylate,[12] etc. have provided an elegant solution to the coupling of complex tether-partners, under mild reaction conditions, to provide small, medium, and large rings. This chapter will provide a detailed investigation of our phosphate tether-mediated RCM studies leading to the formation of complex *P*-stereogenic bicyclo[n.3.1]phosphates.

2.2: Results and discussion

In 2005, we reported phosphate tether-mediated desymmetrization of C_2-symmetric diene diol via RCM *en route* to the diastereoselective synthesis of bicyclo[4.3.1]phosphates (this process is mentioned in detail in chapter 1, Scheme 1.22).[13] Various chemo- and regioselective reactions were developed by utilizing the stereoelectronic properties inherent to bicyclo[4.3.1]phosphate.[14] The synthetic utility of phosphate tethers was further established towards the synthesis of 1,3-diol containing

bioactive natural products.[15] During the course of this study, our ongoing efforts towards the synthesis of 1,3-*anti*-diol containing natural products by using phosphate tether-mediated selective reactions, led to its application for dictyostatin (**2.1A**), a marine macrolide with promising antitumor and anticancer activities (Figure 2.1).[16] Retrosynthetic analysis of fragment **2.1B** revealed that **2.1B** could, in theory, be constructed through a phosphate-tether-mediated tripodal coupling of $POCl_3$, C_2-symmetric dienediol (*S*,*S*)-**2.1D**, and olefin partner **2.1E**, followed by RCM to yield the bicyclo[5.3.1]phosphate **2.1C**.

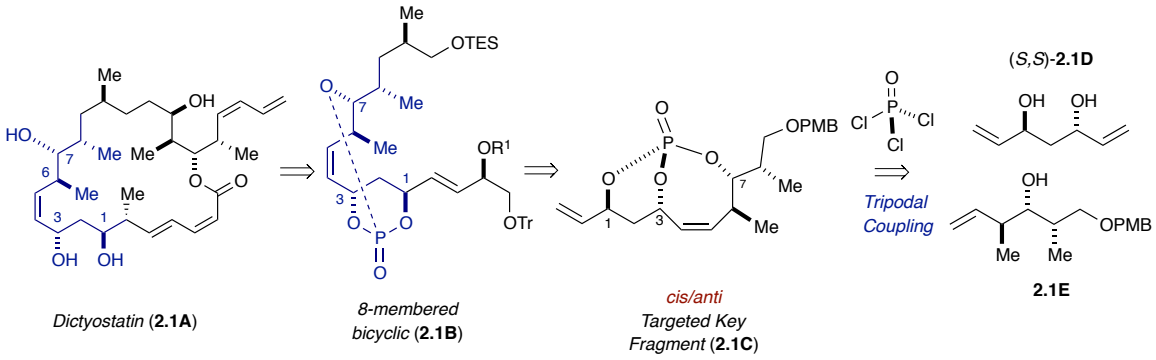

Figure 2.1. *Proposed retrosynthesis of dictyostatin involving phosphate tether-mediated RCM strategy.*

Initial studies focused on the synthesis of the C1–C8 fragment of dictyostatin through formation of the (*Z*)-configured bicyclo[5.3.1]phosphate **2.1.5** from triene **2.1.3** (Scheme 2.1). The triene **2.1.3** was conveniently synthesized via the coupling of monochlorophosphate (*S*,*S*)-**2.1.2** with homoallylic alcohol cross partner **2.1.1**,[17] derived from (*S*)-Roche ester (Scheme 2.1). However, the desired product, **2.1.5**, was not observed. Interestingly, coupling of (*R*,*R*)-**2.1.2** with **2.1.1** generated triene **2.1.4**, which

upon RCM provided bicyclic phosphate *trans,anti*-**2.1.6** (dictyostatin diastereomeric subunit) in 65% yield. The *trans,anti*- descriptors used in compound *trans,anti*-**2.1.6** referred to the relative stereochemistry between the substituents at C3 and C4 in the bicyclo[5.3.1]phosphates This result demonstrated that unforeseen factors were operative for the 8-membered ring formation leading to bicyclo[5.3.1]phosphate **2.1.5**, thus prompting efforts to carry out a detailed investigation with an analogous alcohol partner.

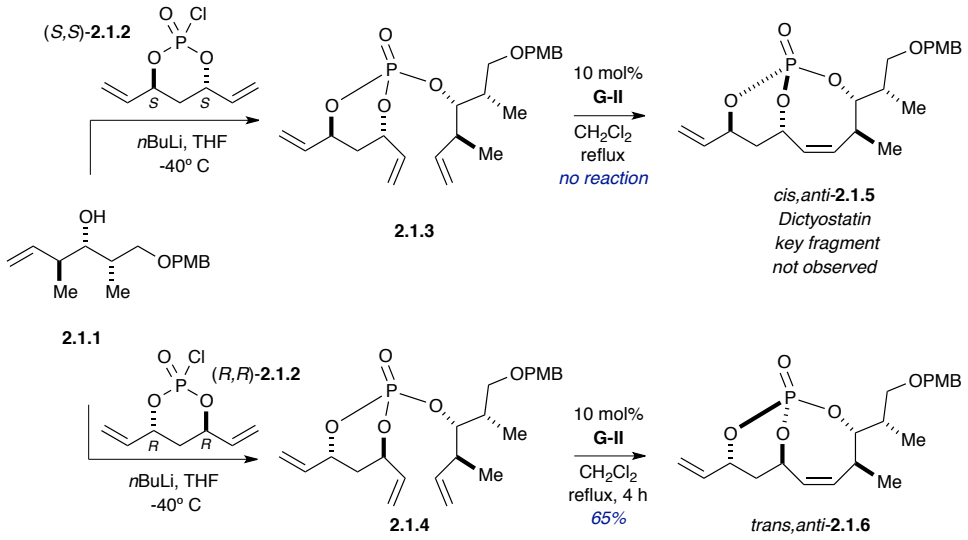

Scheme 2.1. *Synthesis of bicyclo[5.3.1]phosphate en route to the key fragment of dictyostatin.*

The surprising outcome of the RCM reaction en route to dictyostatin and the lack of any literature precedence for phosphate tether-mediated RCM study have served as a motivation to initiate the current RCM study discussed in this chapter. Before this study, all our efforts were focused on generating simple bicyclic phosphate scaffolds by utilizing unsubstituted allylic alcohol cross partners. The goal of this RCM study is to

gain insight into the mechanistic detail of phosphate tether-mediated RCM study across the wide range of substrates, which in turn would also expand the utility of phosphate tether to access, more stereochemically complex fragments. It should be noted that the lack of literature precedence for phosphate tether-mediated RCM study stands in contrast to seminal work by many research groups[8,9,10] on the behavior of silicon tethers in the RCM of a variety of substrates and is mentioned briefly in the previous chapter. The objective of the current study was to probe the effect of various parameters including ring-size and substitutions of both of the coupling partners in the RCM reaction.

2.2.1: Substrate design

To facilitate our understanding of phosphate-tether-mediated RCM reaction, we designed substrate trienes by incorporating different olefin types and varying the stereochemistry of the alcohol cross partner (Figure 2.2). The requisite trienes **2.2D–E** were generated *via* the tripodal coupling of phosphorous oxy-chloride with C_2-symmetric 1,3-*anti*-diols **2.2A** and substituted allylic, homoallylic and higher homologated alcohols (**2.2B**–**C**). All the required alcohols were synthesized following literature procedures.[18]

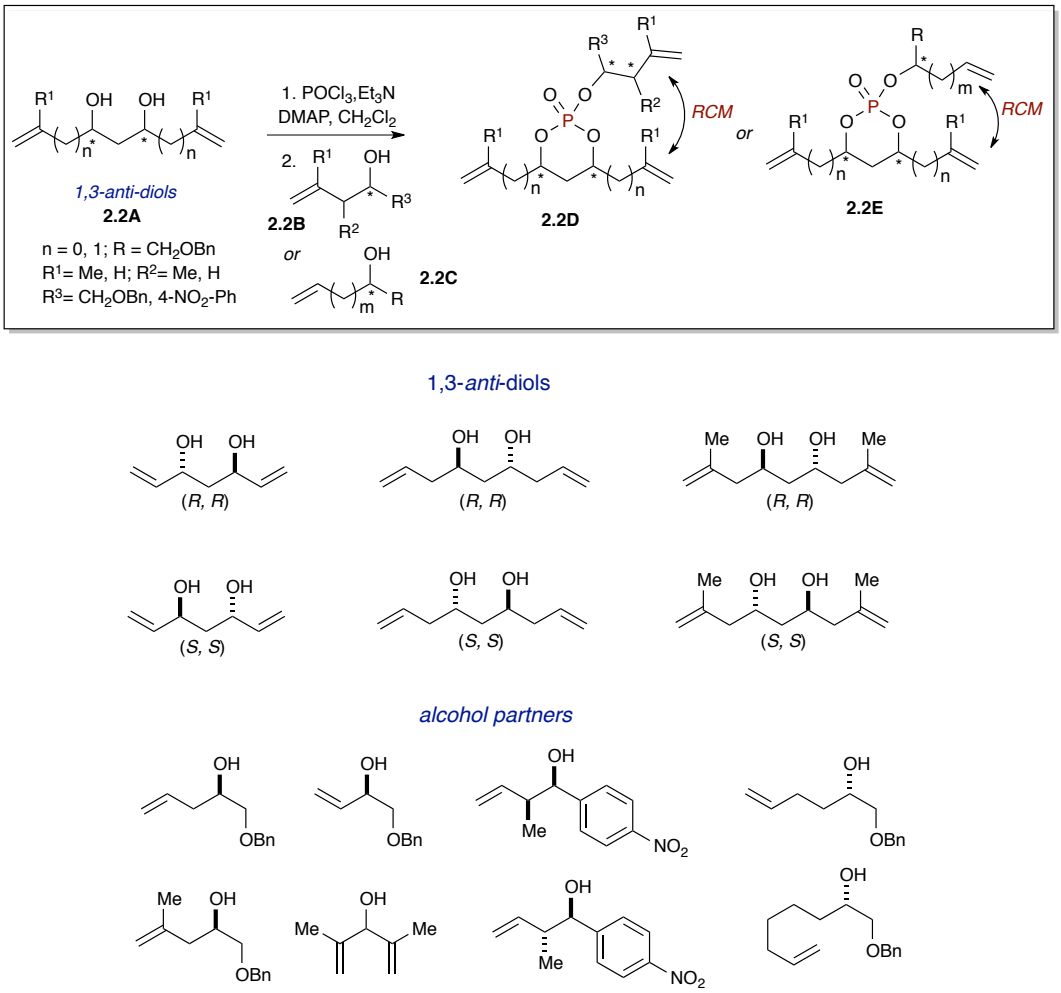

Figure 2.2. *Substrate design for the RCM study.*

2.2.2: Synthesis of *P*-stereogenic bicyclo[4.3.1]phosphates

The RCM study was initiated with the synthesis of 7-membered ring starting from trienes **2.2.2** and **2.2.3** (Scheme 2.2). Both of the trienes were prepared from the coupling of enantiomeric pseudo-C_2-symmetric monocyclic phosphoryl chlorides (*S,S*)-**2.1.2** and (*R,R*)-**2.1.2** with allylic alcohol (*S*)-**2.2.1**. When subjected to the **G-II** catalyst[19] in refluxing dichloromethane, bicyclo[4.3.1]phosphates *trans*-**2.2.4** and *cis*-**2.2.5** were

generated from triene **2.2.2** and **2.2.3** in 54% and 72% yield respectively (Scheme 2.2). The *cis*-/*trans*- descriptors in *cis*-**2.2.5** and *trans*-**2.2.4** refer to the relative stereochemistry between the substituents at C3 and C6 in the bicyclo[4.3.1]phosphates. It should be noted here that the elegant studies by Evans and coworkers indicated that 7-membered rings formation of *Si*-tethered systems was highly diastereoselective where only *cis*-substituted 7-membered-ring products were observed.[10] In contrast to the their observations, RCM of phosphate trienes **2.2.2** and **2.2.3** yielded both 7-membered-ring products *trans*-**2.2.4** and *cis*-**2.2.5**, albeit with different reaction rates and catalyst loadings of the **G-II** catalyst (Scheme 2.2). In addition, it was observed that the *cis*-diastereomer reacted at a much faster rate (within 30 minutes as compared to the *trans* isomer that took 6 hours for completion) and with better yields.

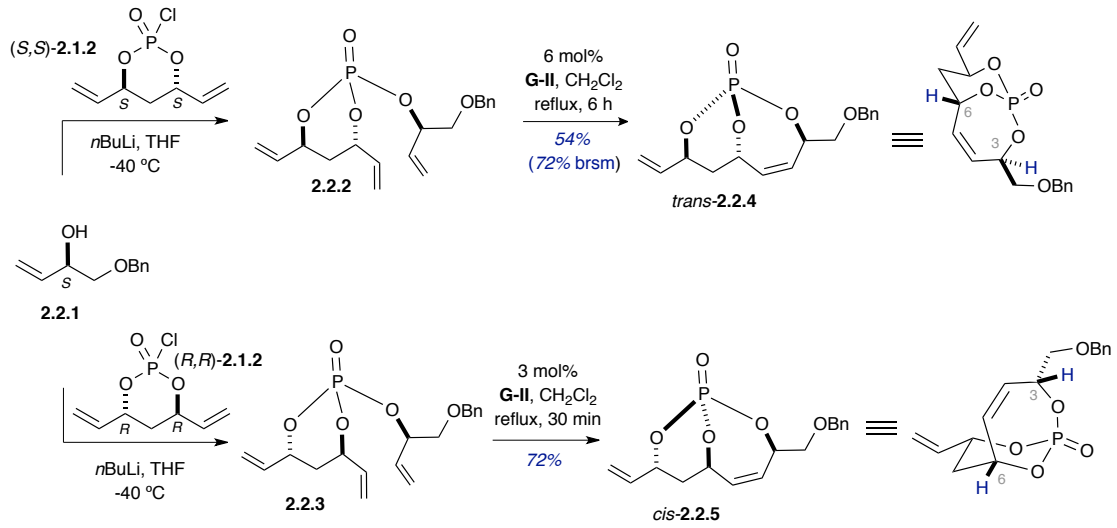

Scheme 2.2. *Synthesis of bicyclo[4.3.1]phosphates.*

To explain, the outcome of this differential reactivity, we looked into the high-

energy intermediates leading to the formation of *cis*-**2.2.5** and *trans*-**2.2.4** (Figure 2.3). Presumably, a detrimental 1,2-steric interaction between the CH_2OBn group and the metallocyclobutane in intermediate *trans*-**2.2.4A**, outlined in Figure 2.3, is operative, thus slowing RCM for *trans*-**2.2.4**.

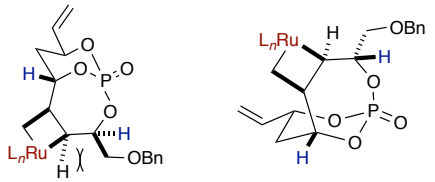

Figure 2.3. *Proposed metallocyclobutane intermediate towards the formation of bicyclo[4.3.1]phosphates.*

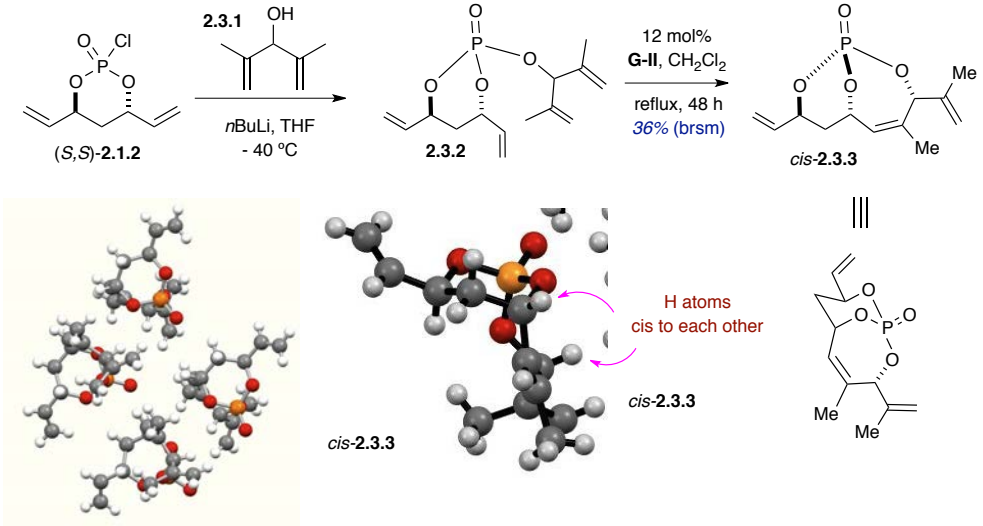

Scheme 2.3. *Double diastereotopic differentiation towards the formation of bicyclo[4.3.1]phosphate cis-2.3.3.*

To ascertain additional information regarding the aforementioned 1,2-interaction,

a double diastereotopic differentiation investigation of triene **2.3.2** was initiated (Scheme 2.3). RCM of triene **2.3.2**, which was derived from the coupling of monochlorophosphate (*S*,*S*)-**2.1.2** with 2,4-dimethylpenta-1,4-dien-3-ol (**2.3.1**), exclusively produced the kinetically favored *cis*-substituted bicyclo[4.3.1]phosphate **2.3.3**. This outcome presumably resulted via an intermediate analogous to *cis*-**2.2.5A**, which lacks an unfavorable 1,2-interaction. X-ray crystallographic data confirmed the structure of *cis*-**2.3.3**.

2.2.3.1: Synthesis of *P*-stereogenic bicyclo[5.3.1]phosphates

Studies were next directed to the 8-membered-ring-forming RCM reactions of trienes **2.4.2** and **2.4.3**, which were derived from the coupling of alcohol (*R*)-**2.4.1** with monochlorophosphates (*S,S*)-**2.1.2** and (*R,R*)-**2.1.2** respectively. Gratifyingly, both 8-membered bicyclo[5.3.1]phosphates, *trans*-**2.4.4** and *cis*-**2.4.5**, were formed with good yields (Scheme 2.4). The *cis*-/*trans*- descriptors in *cis*-**2.4.5** and *trans*-**2.4.4** refer to the relative stereochemistry between the substituents at C3 and C7 in the bicyclo[5.3.1]phosphates. In the case of *trans*-**2.4.4** formation, the difference in yield (60% as compared to the *cis*-diastereomer **2.4.5**, which was formed in 72% yield) could be rationalized based on the unfavorable 1,3-interaction present in the high energy intermediate *trans*-**2.4.4A** between the metallocyclobutane formed on the *exo* face and the C3 substituents of homoallylic alcohol (*R*)-**2.4.1**.

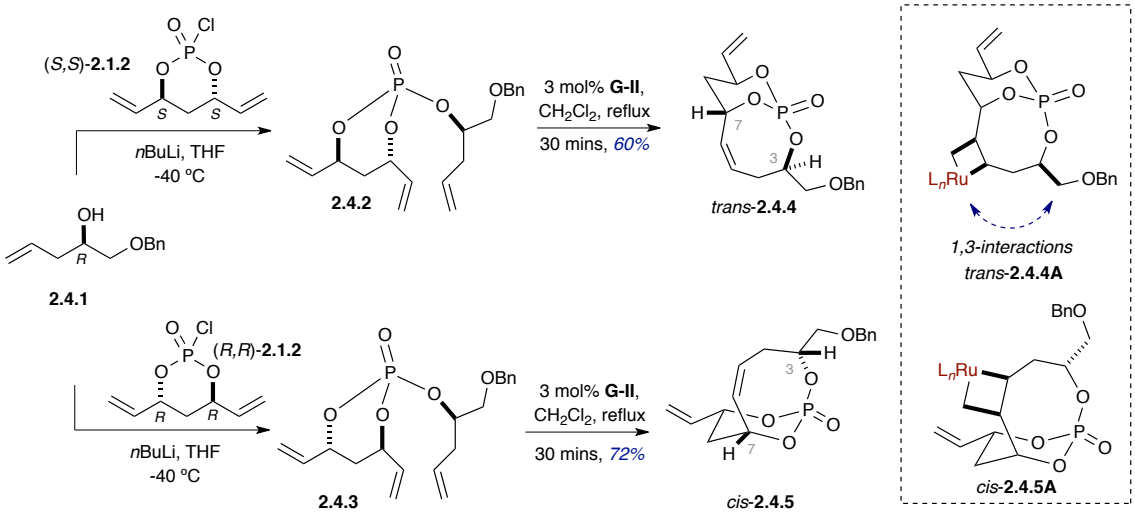

Scheme 2.4. *Synthesis of bicyclo[5.3.1]phosphates.*

2.2.3.2: Synthesis of bicyclo[5.3.1]phosphates with C5-methyl substitution

To probe the effect of the unfavorable 1,3-interaction observed during the formation of *trans*-**2.4.4A**, next we introduced a methyl substituent at the C5 position of the homoallylic alcohol cross partner (*R*)-**2.5.1** (Scheme 2.5). The desired trienes **2.5.2** and **2.5.3** were synthesized from the coupling of methyl-substituted alcohol (*R*)-**2.5.1** with monochlorophosphates (*S*,*S*)-**2.1.2** and (*R*,*R*)-**2.1.2**, respectively. Subjection to the RCM reaction, only lead to *trans*-**2.5.4**, albeit in a modest 32% yield, while *cis*-**2.5.5** was not observed and this outcome further consolidated our previous assumption about unfavorable 1,3-interactions. Based on these results, we have concluded that the unfavorable 1,3-interaction between the vinylic methyl and CH_2OBn groups in *cis*-**2.5.5A**, impedes RCM, while in *trans*-**2.5.4A**, no such interaction exists, allowing for the RCM to proceed.

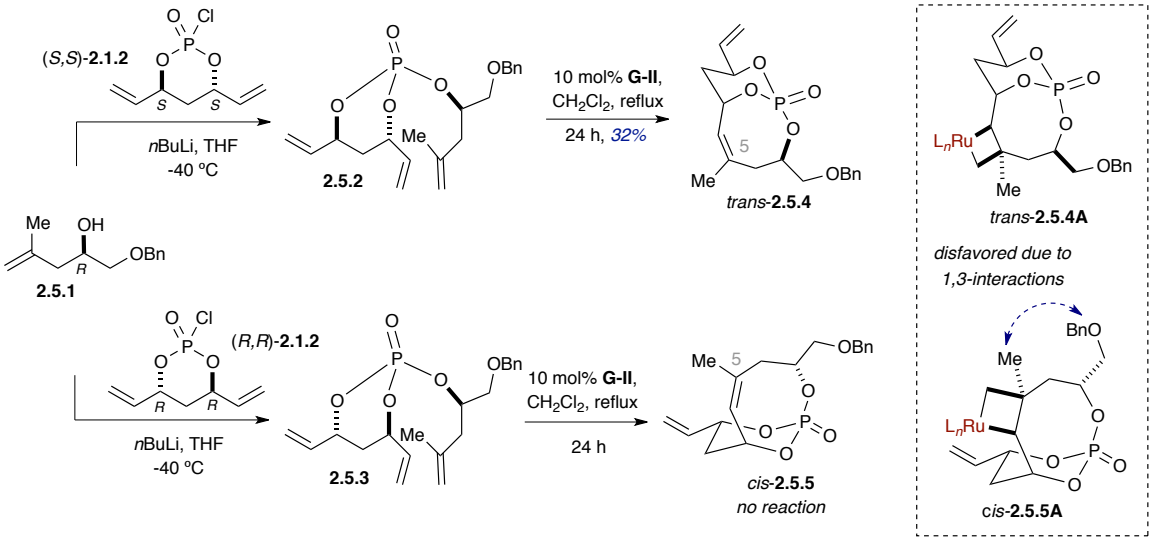

Scheme 2.5. *Effect of the substitution at C5 of homoallyl alcohol towards the synthesis of bicyclo[5.3.1]-phosphates.*

In 2011, Sorensen and coworkers reported similar observations en route to the synthesis of pleuromutilin, a prototype class of antibiotics, which inhibit bacterial protein synthesis (Scheme 2.6).[20] Towards the aim of developing a streamlined and convenient synthesis of pleuromutilin, both diastereomeric RCM precursors **2.6.3** and **2.6.5** were generated. When **2.6.3** and **2.6.5** were separately subjected to RCM in the presence of the **HG-II** catalyst[21] in refluxing CH_2Cl_2, only one of the diastereomers (**2.6.3**) yielded the RCM product. The product formation was rationalized based on the high-energy metallocyclobutane intermediate **2.6.3A** in which the steric hindrance between the hydroxyl-derived group at C14 and methyl group at C12 prevented the formation of the RCM product. However no such steric interactions were present for the diasteremeric RCM product **2.6.6**. This fact was further confirmed by the observed rate enhancement of RCM on increasing the steric bulk at C14.

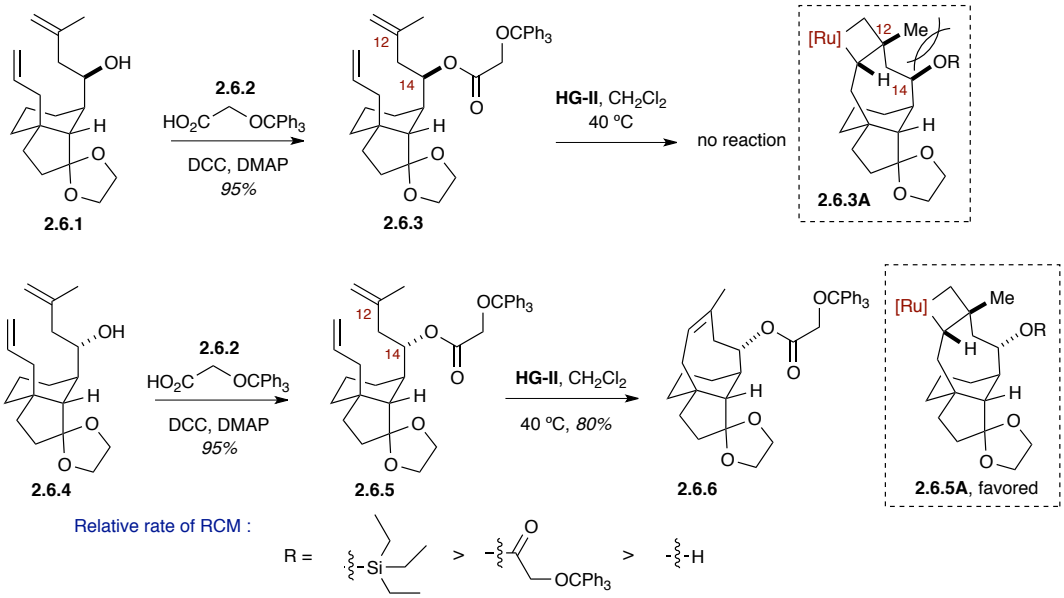

Scheme 2.6. *Proposed conformational bias during RCM en route to the synthesis of pleuromutilin.*

2.2.3.3: Synthesis of bicyclo[5.3.1]phosphates with homoallylic alcohol partners containing allylic methyl substituents

As mentioned previously, the current RCM study was initiated due to our inability to access the key fragment *cis*,*anti*-**2.1.5** via phosphate tether-mediated RCM en route to the synthesis of dictyostatin (Scheme 2.1). Structural comparison of trienes **2.4.2** and **2.4.3**, lacking the allylic methyl substituents, which readily underwent RCM (Scheme 2.4), to trienes **2.1.3** and **2.1.4** (Scheme 2.1) allowed us to conclude that the stereochemistry at the allylic position determines whether the RCM is successful.

To investigate the effect of the allylic methyl group further we synthesized trienes that are structurally similar to trienes **2.1.3** and **2.1.4** containing allylic methyl substituents. The allylic methyl group in the triene was introduced via *syn*- and *anti*-crotylation of *para*-nitrobenzaldehyde generating substituted homoallylic alcohols

(1*R*,2*S*)-2-methyl-1-(4-nitrophenyl)but-3-en-1-ol (**2.7.1**) and (1*R*,2*R*)-2-methyl-1-(4-nitrophenyl)but-3-en-1-ol (**2.8.1**). Next the requisite trienes **2.7.2** and **2.7.3** were synthesized from the coupling of homoallylic alcohol (*R*)-*syn*-**2.7.1** with monochlorophosphates (*S*,*S*)-**2.1.2** and (*R*,*R*)-**2.1.2** respectively. When subjected to RCM, product was only observed with *cis*,*syn*-stereochemistry leading to the *cis*,*syn*-**2.7.4** in 65% yield. The *cis*,*syn*- descriptors used in compound *cis*,*syn*-**2.7.4** referred to the relative stereochemistry between the substituents at C3 and C4 (*syn*) and at C3 and C7 (*cis*) in the bicyclo[5.3.1]phosphates.

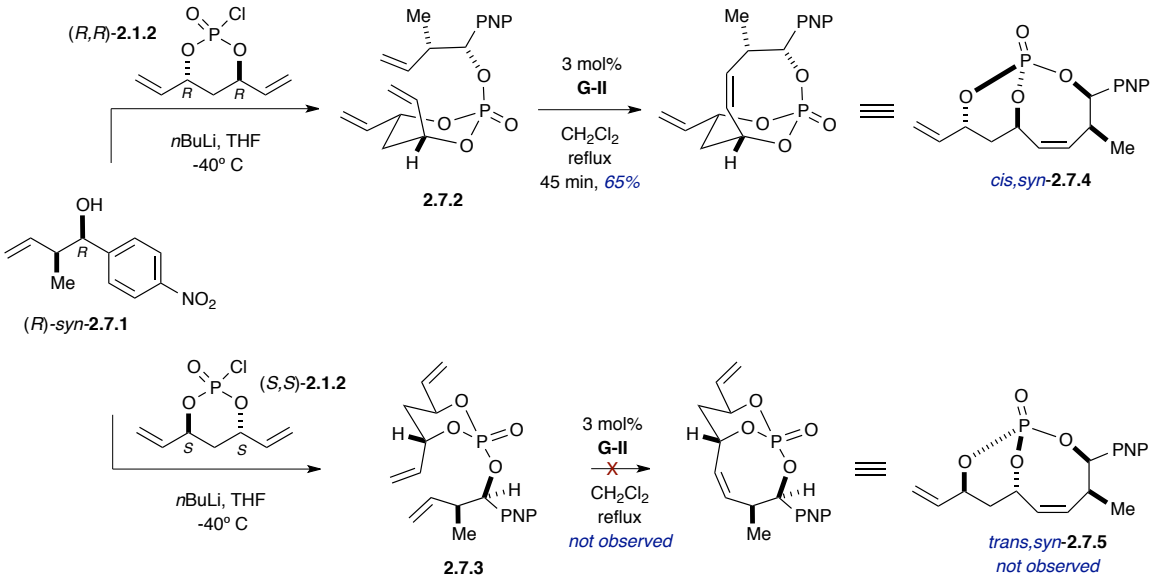

Scheme 2.7. *Effect of substitution at C2 of homoallyl alcohol towards the synthesis of bicyclo[5.3.1]phosphates.*

Additional studies were conducted for the RCM reactions of trienes derived from monochlorophosphates (*R*,*R*)-**2.1.2** and (*S*,*S*)-**2.1.2** and substituted homoallyl alcohol (*R*)-*anti*-**2.8.1** (Scheme **2.8**). Product was observed only for *trans*,*anti*-**2.8.5**, both of these

results are consistent with the previously mentioned preliminary results for dictyostatin.

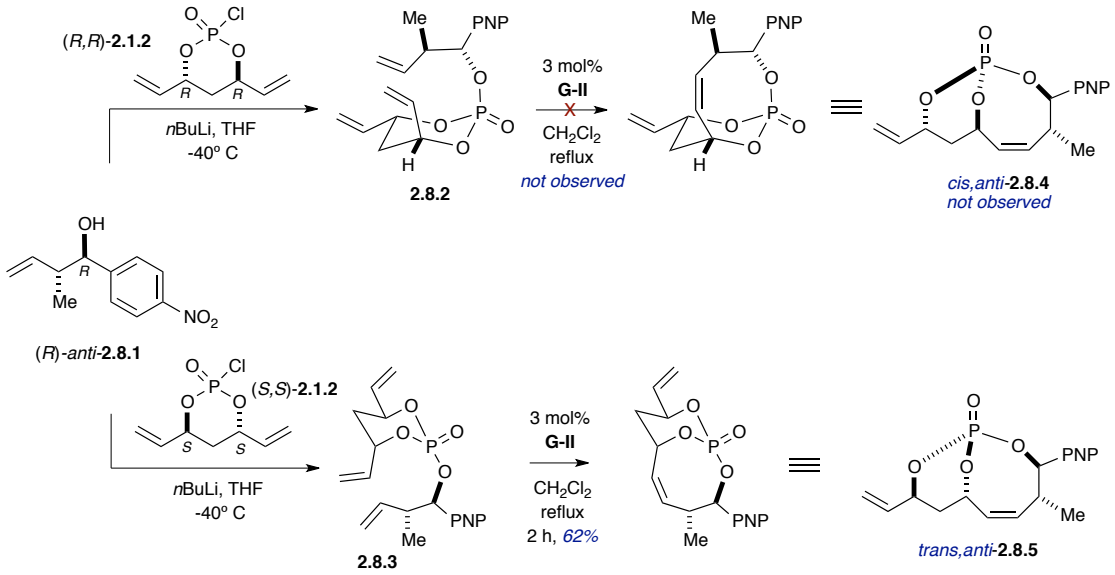

Scheme 2.8. *Effect of substitution at C2 of homoallyl alcohol towards the synthesis of bicyclo[5.3.1]-phosphates.*

A plausible model was developed to provide insight into the observed stereochemical outcomes for the bicyclo[5.3.1]phosphate cases, in which the stereochemistry of the allylic position is the critical factor (Figure 2.4). When considering the metallocyclobutane intermediates, the previous assumption that metallocyclobutane formation occurs on the exocyclic face eliminates the involvement of intermediates, *endo,endo*-**2.4A** and *endo,exo*-**2.4B**. Inspection of the remaining two intermediates, *exo,exo*-**2.4C**and *exo,endo*-**2.4D**, reveals an unfavorable steric interaction between the *exo* Me group and the required *exo* metallocyclobutane for the case of *exo,exo*-**2.4C**, an interaction that impedes the formation of the resultant bicyclic phosphate. Thus, only when the allylic Me group is *endo* and the formed

metallocyclobutane is *exo* is the intermediate energetically accessible such that the reaction can proceed to completion. This analysis, therefore, accounts for the selectivity.

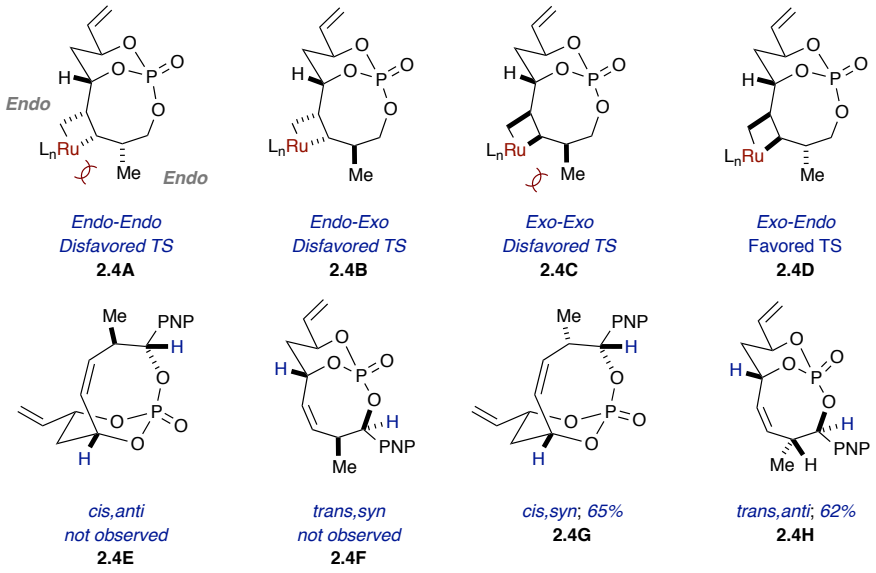

Figure 2.4. *Proposed metallocyclobutane intermediate towards the formation of bicyclo[5.3.1]phosphates.*

For experimental confirmation of the proposed intermediates in Figure 2.4, we synthesized triene **2.9.2** from (±)-2-methylbut-3-en-1-ol (**2.9.1**) and the monochlorophosphate (*S*,*S*)-**2.1.2** to perform a double diastereotopic differentiation experiment (Scheme 2.9). Subsequent RCM reaction exclusively generated bicyclo[5.3.1]phosphate diastereomer **2.9.4**, which was confirmed by X-ray crystallography, along with unreacted diastereomeric triene **2.9.3**. Similar diastereotopic differentiation studies were performed by Harvey and corworkers en route to the synthesis of C12–C24 fragment of peloruside A (discussed in chapter 1).[22] X-ray crystallography analysis confirmed the *endo* orientation of the allylic methyl group in the

bicyclic phosphate **2.9.4**, thus supporting our proposed favored intermediate *exo,endo*-**2.4D**, as shown in Figure 2.4.

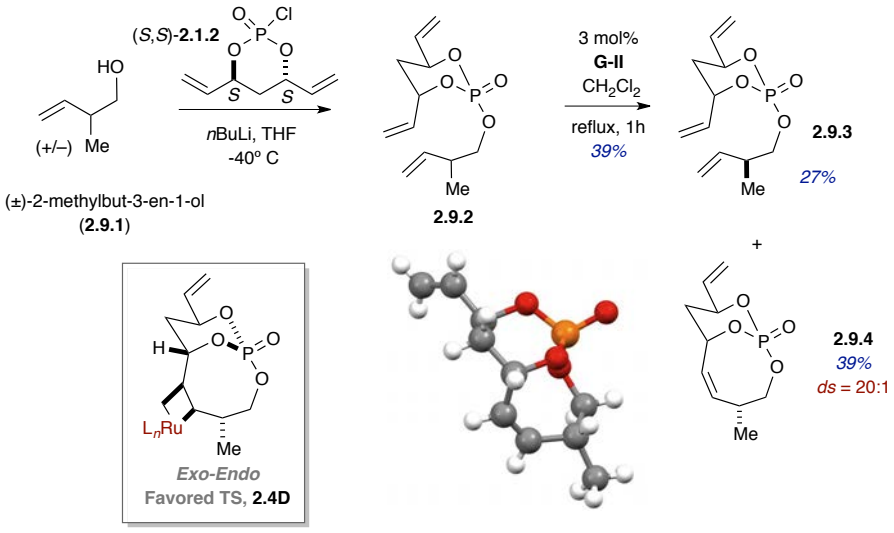

Scheme 2.9. *Double diastereotopic differentiation towards the formation of bicyclo[5.3.1]phosphate 2.9.4.*

2.2.3.4: Synthesis of bicyclo[5.3.1]phosphates derived from homologated diene diol

Next, we extended our study of 8-membered-ring-forming RCM reactions to include coupling of each of the homologated monochlorophosphates, (*R*,*R*)-**2.10.2** and (*S*,*S*)-**2.10.2** with allylic alcohol (*R*)-**2.10.1** (Scheme 2.10). Trienes **2.10.3** and **2.10.4** participated in the RCM reaction, although the yield of *trans*-substituted bicyclo[5.3.1]phosphate **2.10.5** was notably less than that of *cis*-substituted bicyclo[5.3.1]phosphate **2.10.6**. The lower yield of *trans*-**2.10.5** was presumably due to an unfavorable 1,2-interaction between the metallocyclobutane and the CH_2OBn group in

intermediate *trans*-**2.10.5A**.

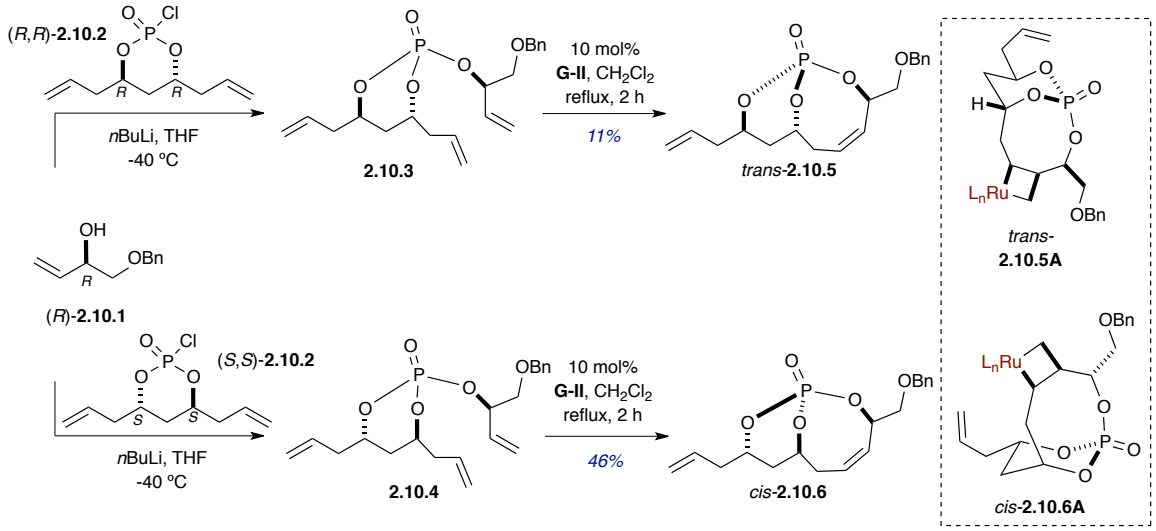

Scheme 2.10. *Synthesis of bicyclo[5.3.1]phosphates derived from homologated diene diol.*

In the cases of methyl-substituted homologated trienes **2.11.3** and **2.11.4**, which were synthesized by the coupling of the methyl-substituted homologated monochlorophosphates, (*R*,*R*)-**2.11.2** and (*S*,*S*)-**2.11.2**, with allylic alcohol (*R*)-**2.11.1**, no *cis* RCM product **2.11.6** was observed owing to a highly unfavorable 1,3-interaction (*syn*-pentane) between the CH_3 and CH_2OBn groups in intermediate *cis*-**2.11.6A** (Scheme 2.11). In the case of the trans product formation, no such unfavorable 1,3-interaction was present although the lower yield observed might be rationalized based on the existing 1,2-steric interaction between the metallocyclobutane and CH_2OBn. Notably, this observation was consistent with our previous observations towards the formation of *trans*-substituted bicyclo[4.3.1]phosphate **2.4.4** (Scheme 2.4) where the detrimental 1,2-steric interaction between the CH_2OBn group and the metallocyclobutane lowered the

reaction yield.

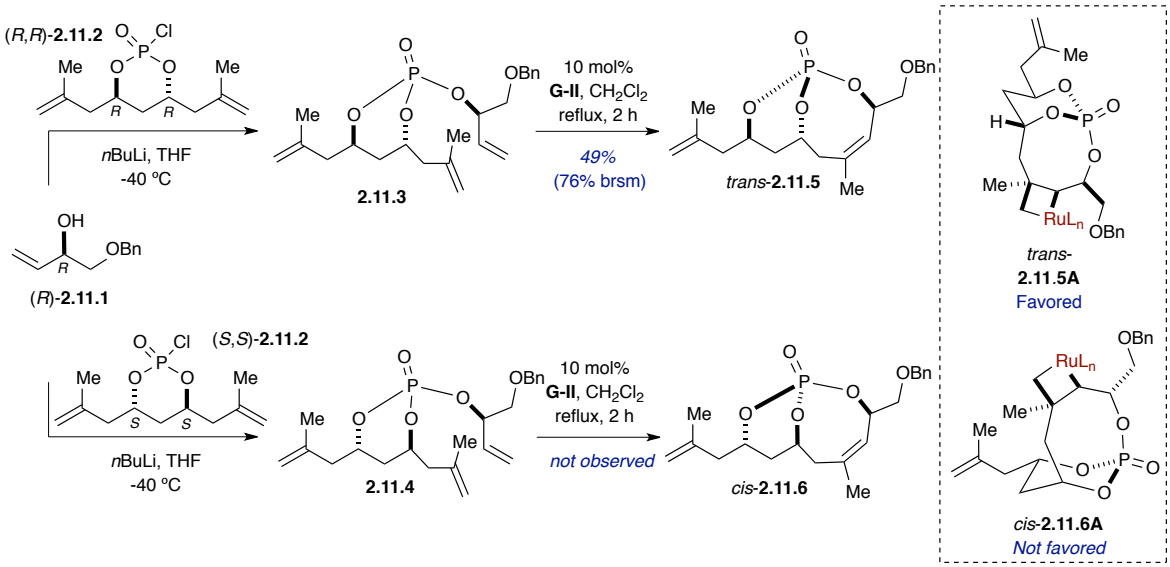

Scheme 2.11. *Synthesis of bicyclo[5.3.1]phosphates derived from methyl-substituted homologated diene diol.*

2.2.4: Synthesis of *P*-stereogenic bicyclo[6.3.1]phosphates

Investigations towards the medium size ring formations commenced with the study of RCM reactions involved in the formation of bicyclo[6.3.1]phosphates, which requires the generation of a 9-membered ring (Scheme 2.12). Trienes **2.12.2** and **2.12.3** were derived from the coupling of alcohol (*S*)-**2.12.1** with monochlorophosphates (*S,S*)-**2.1.2** and (*R,R*)-**2.1.2**, respectively. Upon treatment with the **G-II** catalyst in refluxing dichloromethane, both 9-membered bicyclo[6.3.1]phosphates *cis*-**2.12.4** and *trans*-**2.12.5** were formed in good yields (Scheme 2.12). These examples suggest that like in the formation of bicyclo[5.3.1]phosphates (8-membered ring formation) stereochemistry at the C3-position of the tether-partner doesn't affect the efficiency of the phosphate tether-

mediated RCM reaction to bicyclo[6.3.1]phosphates.

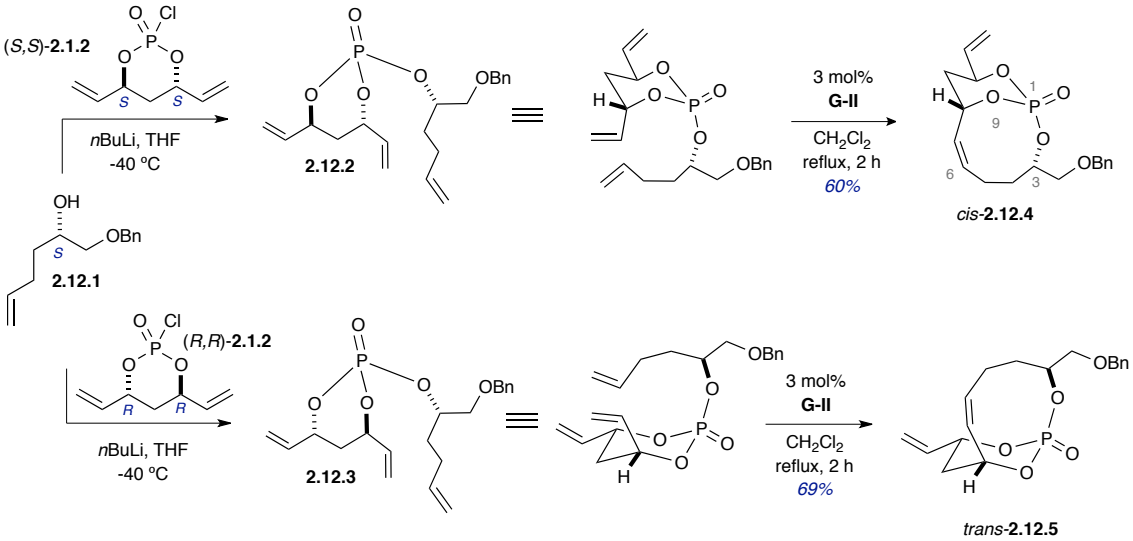

Scheme 2.12. *Synthesis of bicyclo[6.3.1]phosphates.*

To further probe substrate scope of the 9-membered ring formation, we extended the method to include tether-partners with greater stereochemical complexity. Thus, methyl-substituted homologated monochlorophosphate (*S,S*)-**2.11.2** was coupled with homoallyl alcohol (*R*)-**2.4.1** to generate triene **2.13.1** (Scheme 2.13). Upon treatment with the **G-II** catalyst (3 mol %, single addition), successful RCM provided bicyclo[6.3.1]phosphate *cis*-**2.13.2** in modest yield with exclusive *Z*-selectivity. In addition, the effect of the allylic methyl substituent in the corresponding alcohol tether-partner on the success of RCM was studied. For this purpose, methyl-substituted homologated monochlorophosphate (*S,S*)-**2.11.2** was coupled with *anti*- and *syn*-crotylated alcohols **2.8.1** and **2.7.1** to generate trienes **2.13.3** and **2.13.4**, respectively (Scheme 2.13).

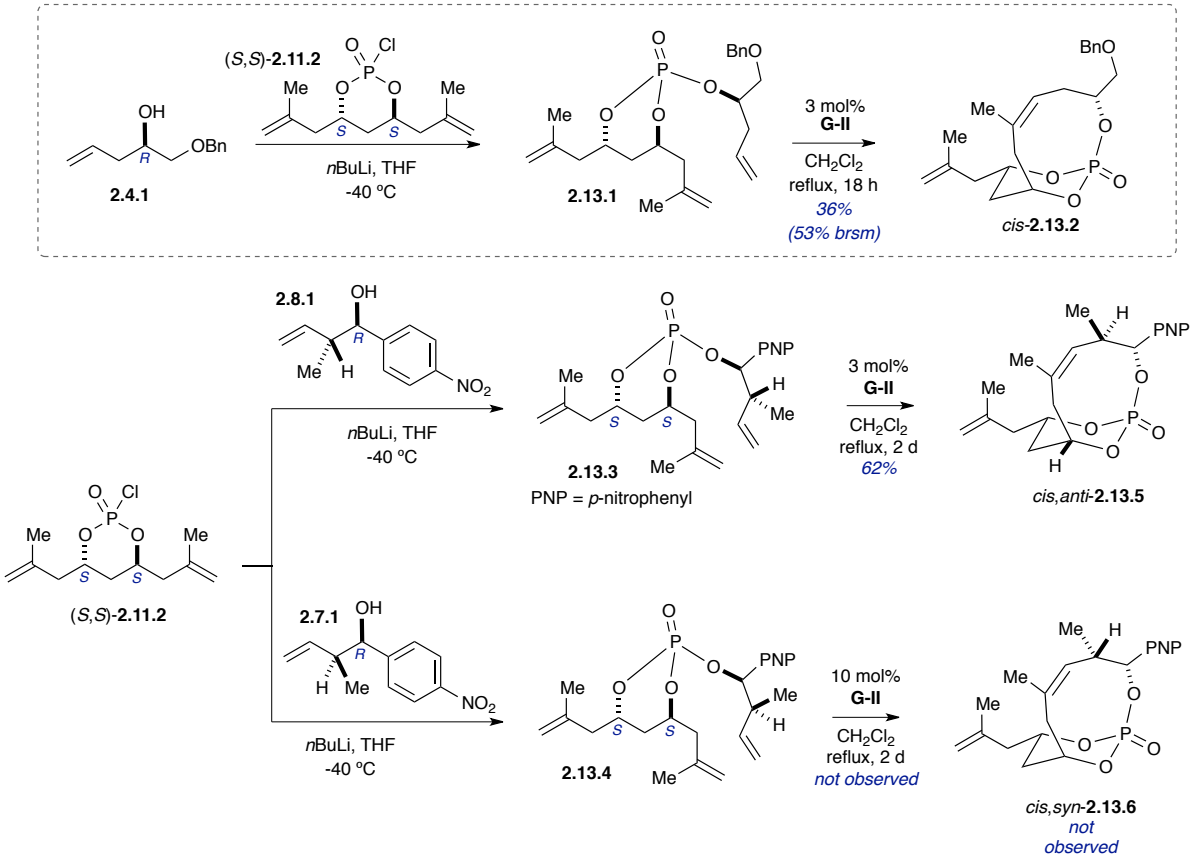

Scheme 2.13. *Synthesis of bicyclo[6.3.1]phosphates starting from methyl-substituted homologated diene diol.*

When subjected to the **G-II** catalyst (3 mol % in one portion), triene **2.13.3** underwent RCM to provide the corresponding product *cis,anti*-**2.13.5** in 62% yield. However, the bicyclo[6.3.1]phosphate *cis,syn*-**2.13.6**, resulting from the RCM of triene **2.13.4** was not observed. It should be noted that this reactivity was unexpected, as the RCM reactions of homologous systems (with identical crotylated alcohol tether partners) to form bicyclo[5.3.1]phosphates provided selective *cis,syn*-product formation (**2.7.4** in Scheme 2.7); the corresponding *cis,anti*-product (**2.8.4** in Scheme 2.8) was not observed.

To rationalize this unexpected reactivity, we developed plausible structures for

high-energy Ru-metallocyclobutane intermediates based upon X-ray crystallographic analysis of the observed products *cis*-**2.13.2** and *cis,anti*-**2.13.5** (Figures 2.5).[23] As shown in the second depiction of the X-ray structures in Figure 2.5, the conformation of bicyclo[6.3.1]phosphates *cis*-**2.13.2** and *cis,anti*-**2.13.5** is such that the Ru-metallocyclobutane would presumably form on the more sterically accessible *endo*-face of the forming olefin. While unfavorable 1,3-steric interactions are present in both proposed intermediates (*cis*-**2.13.2** and *cis,anti*-**2.13.5**), the successful formation of products implies that this interaction is not insurmountable, though longer reaction times were required to generate product.

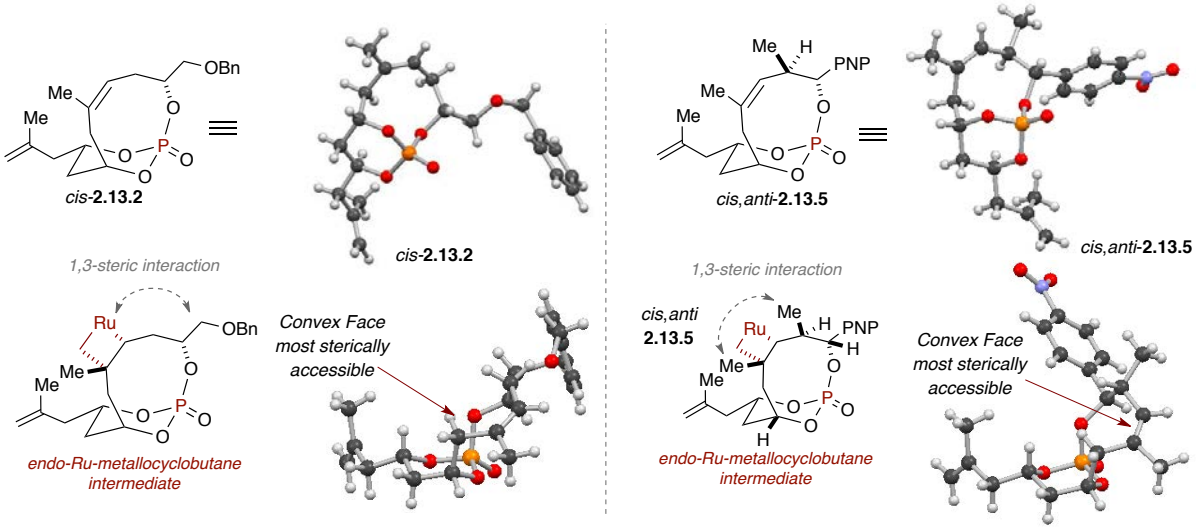

Figure 2.5. *X-ray crystal structures of bicyclo[6.3.1]phosphates and plausible Ru-metallocyclobutane intermediates in the formation of cis*-**2.4** and *cis,anti*-**2.13.5**.

Taken collectively, these results—in combination with observations gathered from the studies involving the formation of bicyclo[5.3.1]phosphates have led to the proposed mechanistic rationale shown in Figure 2.6. In the case of

bicyclo[5.3.1]phosphate formation, the concave nature of the bicyclic phosphate would suggest that Ru-metallocyclobutane formation is only energetically feasible when the Ru-metallocycle forms on the *exo*-face of the bicyclic phosphate (e.g. successful formation of *cis,syn*-**2.7.4** via high energy intermediate *cis,syn*-**2.4G**, Figure 2.6) Based upon this assumption, bicyclic phosphate formation is impeded in *cis,anti*-**2.8.4** where an unfavorable 1,2-steric interaction is present (e.g. *cis,anti*-**2.4E**), as well as in *cis*-**2.5.5** where an unfavorable 1,3-steric interaction is present (e.g. *cis*-**2.5.5A**) between the *exo*-intermediate Ru-metallocyclobutane and substituents on the olefinic tether-partner. Likewise, in the case of *cis,syn*-**2.7.4**, an unfavorable 1,2-steric interaction is present (e.g. *cis,syn*-**2.4G**) between the *endo*-Ru-metallocyclobutane and the C4-methyl substituent of the olefinic tether-partner preventing the formation of product. However, subtle differences in the ring dynamics of the 9-membered ring (i.e. bicyclo[6.3.1]phosphate) versus the 8-membered ring (i.e. bicyclo[5.3.1]phosphate) may be responsible for the successful formation of *cis,anti*-**2.13.5** (via *cis,anti*-**2.13.5A**), even in the presence of an unfavorable 1,3-steric interaction between the *exo*-methyl substituent on the Ru-metallocyclobutane and the C4-methyl substituent of the alcohol tether-partner.

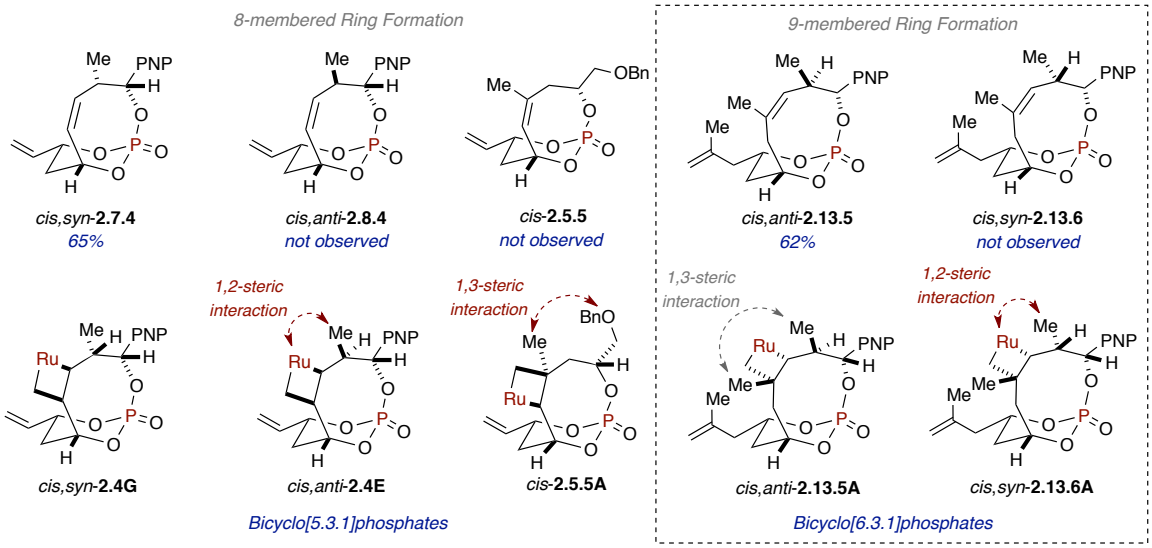

Figure 2.6. *Comparison and Plausible mechanistic rationale for the formation of bicyclo[5.3.1]- and bicyclo[6.3.1]phosphates.*

2.2.5: Synthesis of *P*-stereogenic bicyclo[7.3.1]phosphates

Studies towards the formation of 10-memberd rings via RCM started with our interest in synthesizing dictyostatin via alternative approach of targeting a larger ring size as compared to the 8-membered ring as discussed before. Our retrosynthetic analysis revealed that the C1–C9 fragment **2.1A** of dictyostatin could be obtained via phosphate tether-mediated RCM. Interestingly, this target fragment **2.7A** contained an internal (*Z*)-olefin. As such, it was unclear what selectivity would be observed in the context of bicyclo[7.3.1]phosphate generation prior to experimental confirmation. In this respect, to check the feasibility of our proposal, we decided to synthesize a simplified analogue of the 10-membered ring required to synthesize dictyostatin. Studies were therefore focused on the preparation of the (*Z*)-configured, 10-membered ring-containing subunit **2.7B** (Figure 2.7) through RCM with substrates bearing requisite "dictyostatin-like" olefin

tether partners (Figure 2.7).

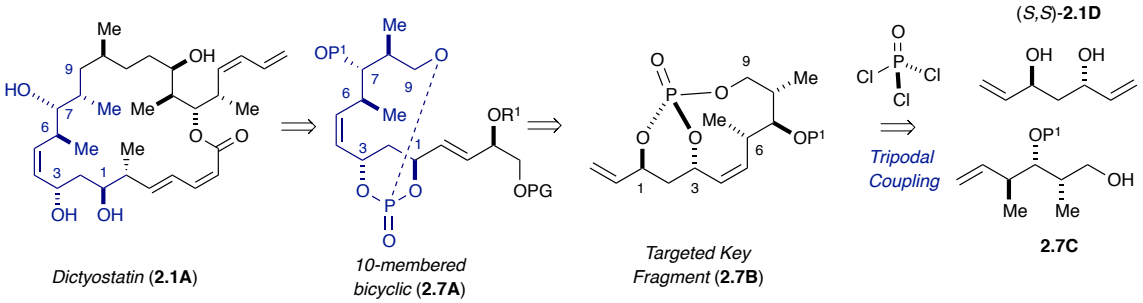

Figure 2.7. *Proposed retrosynthetic strategy en route to dictyostatin via phosphate tether-mediated RCM to obtain (Z)-selective 10-membered key fragment 2.7A.*

For this study, trienes **2.14.2a–b** and **2.14.3**, possessing various substitutions at the C3 carbinol (P^1=H, TBS, and PMB), were synthesized to investigate if differently protected homoallylic hydroxyl group at C4 would have any effect on the selectivity of the resulting internal olefin (Scheme 2.14). Subsequent RCM of **2.14.2a–b** afforded excellent yields of (*E*)-configured 62icycle[7.3.1]phosphates **2.14.4a–b**. In addition, the diastereomeric triene **2.14.3**, which was derived from (*R,R*)-**2.1.2**, also produced the RCM product **2.14.5** in good yield and with exclusive (*E)*-selectivity. Although this result was not encouraging in terms of the synthesis of dictyostatin, we believe that use of (*Z*)-selective catalyst as reported by Grubbs and coworkers[24] and/or introduction of silyl substituents on the double bond of the coupling partner as reported by Schreiber and coworkers[25] might provide the required (*Z*)-selectivity. More studies on the 10-membered ring formation and the selectivity of the resulting olefin are in progress in our lab.

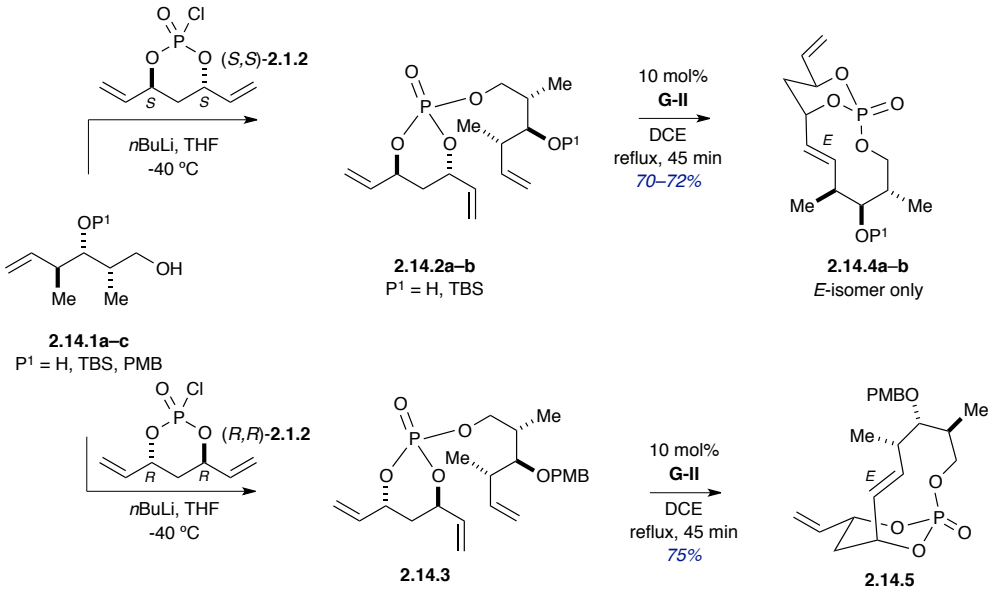

Scheme 2.14. *Formation of bicyclo[7.3.1]phosphates bearing requisite "dictyostatin-like" substituents.*

2.2.6: Synthesis of *P*-stereogenic bicyclo[8.3.1]phosphates

Studies were then extended to include RCM of 11-membered rings to generate bicyclo[8.3.1]phosphates (Scheme 2.15). In a similar fashion, diastereomeric trienes **2.15.2** and **2.15.3** were formed via the coupling of alcohol (*S*)-**2.15.1** with monochlorophosphates (*S*,*S*)-**2.1.2** and (*R*,*R*)-**2.1.2**. While RCM of triene **2.15.2** proceeded smoothly in the presence of the **G-II** catalyst to provide bicyclo[8.3.1]phosphate *cis*-**2.15.4** in 69% yield, the corresponding RCM of **2.15.3** did not provide the desired product. Though the source of this observed reactivity is still under investigation, the complex ring dynamics of these larger ring systems within the

context of the bicyclic phosphate framework may be responsible for stark differences in reactivity with respect to stereochemistry at the C3-position of the alcohol tether-partner.

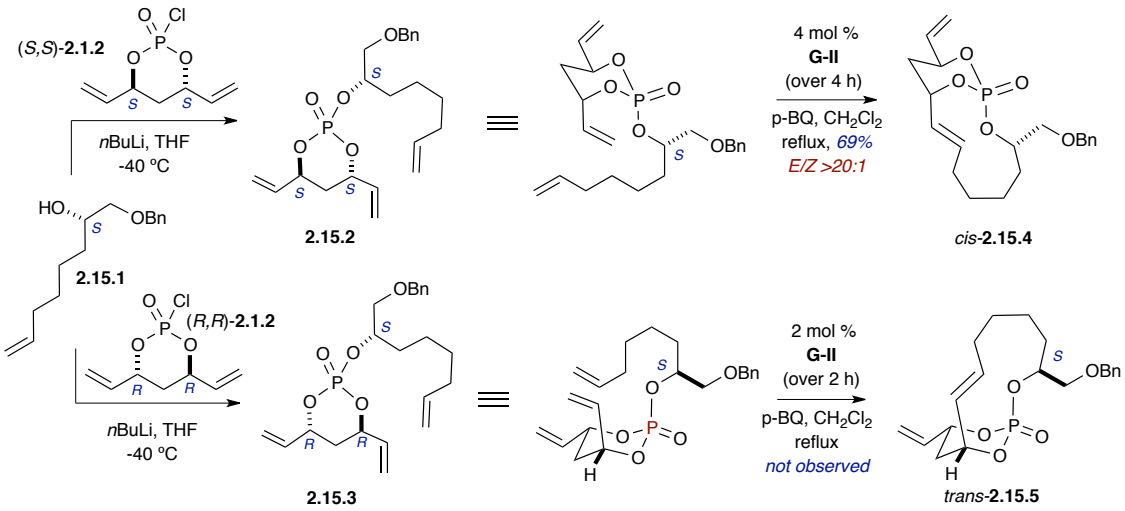

Scheme 2.15. *Synthesis of bicyclo[8.3.1]phosphates.*

2.3: Conclusion

In conclusion, we have investigated the phosphate-tether mediated diastereotopic differentiation of C_2-symmetric dienediol subunits via RCM for complex substrates. This transformation was dependent on parameters such as the concave nature of the bicyclic phosphate, the stereochemistry within each coupling partner, and the ring size. Plausible metallocyclobutane-containing intermediates for RCM reactions that give *P*-stereogenic bicyclo[4.3.1]phosphates, bicyclo[5.3.1]phosphates and bicyclo[6.3.1]phosphates were proposed to rationalize observed experimental outcomes. The notable outcome of these studies were: (i) the *trans* product formation in the bicyclo[4.3.1]phosphate series; (ii) exclusive (*E*)-selectivity observed in the bicyclo[7.3.1]phosphate series; (iii) the crucial role of the allylic methyl group in the coupling partner in determining the observed

selectivity in the bicyclo[5.3.1]phosphate series and (iv) the different reactivity pattern observed in the case of bicyclo[6.3.1]phosphate series as opposed to the bicyclo[5.3.1]phosphate series. Further applications in the synthesis of polyketide natural products, along with studies on RCM reactions that give other bicyclo[n.3.1] phosphates are currently being pursued in our lab.

2.4: References cited:

[1] (a) Deiters, A.; Martin, S. F. Synthesis of oxygen- and nitrogen-containing heterocycles by ring-closing metathesis. *Chem. Rev.* **2004**, *104*, 2199–2238; (b) McReynolds, M. D.; Dougherty, J. M.; Hanson, P. R. Synthesis of Phosphorus and Sulfur Heterocycles via Ring-Closing Olefin Metathesis. *Chem. Rev.* **2004**, *104*, 2239–2258; (c) Nicolaou, K. C.; Bulger, P. G.; Sarlah, D. Metathesis reactions in total synthesis. *Angew. Chem., Int. Ed.* **2005**, *44*, 4490–4527; (d) Gradillas, A.; Perez-Castells, J. Macrocyclization by ring-closing metathesis in the total synthesis of natural products: reaction conditions and limitations. *Angew. Chem., Int. Ed.* **2006**, *45*, 6086–6101; (e) Hoveyda, A. H.; Zhugralin, A. R. The remarkable metal-catalysed olefin metathesis reaction. *Nature* **2007**, *450*, 243–251; (f) Kotha, S.; Lahiri, K. Synthesis of diverse polycyclic compounds via catalytic metathesis. *Synlett* **2007**, 2767–2784; (g) van Otterlo, W. A. L.; de Koning, C. B. Metathesis in the synthesis of aromatic compounds. *Chem. Rev.* **2009**, *109*, 3743–3782; (h) Nolan, S. P.; Clavier, H. Chemoselective olefin metathesis transformations mediated by ruthenium complexes. *Chem. Soc. Rev.* **2010**, *39*, 3305–3316; (i) Monfette, S.; Fogg, D. E. Equilibrium Ring-Closing Metathesis. *Chem. Rev.* **2009**, *109*, 3783–3816; (j) Prunet, J. Progress in Metathesis Through Natural Product Synthesis. *Eur. J. Org. Chem.* **2011**, *2011*, 3634–3647.

[2] For an excellent secondary source/collection of reviews, see: *Metathesis in Natural Product Synthesis: Strategies, Substrates and Catalysts*; Cossy, J.; Areniyadis, S.; Meyer, C., Eds.; Wiley-VCH, Weinheim, Germany, **2010**.

[3] For an exceptional collection of reviews on current advances in olefin metathesis, see: *Handbook of Metathesis*, 2nd ed.; Grubbs, R. H. and O'Leary, D. J., Eds.; Wiley-VCH: Weinheim, Germany, **2015**; Vol. 2.

[4] Schmidt, B.; Hauke, S.; Krehl, S.; Kunz, O. Ring-closing metathesis. Comprehensive Organic Synthesis (2nd Ed.). Elsevier B.V.: **2014**; Vol. 5, p 1400–1482.

[5] (a) Trost, B. M. The atom economy: a search for synthetic efficiency. *Science* **1991**, *254*, 1471-1477; (b) Trost, B. M. Atom economy - a challenge for organic synthesis: homogeneous catalysis leads the way. *Angew. Chem., Int. Ed. Engl.* **1995**, *34*, 259–281.

[6] Wender, P. A.; Verma, V. A.; Paxton, T. J.; Pillow, T. H. Function-Oriented Synthesis, Step Economy, and Drug Design. *Acc. Chem. Res.* **2008**, *41*, 40–49.

[7] a) Young, I. S.; Baran, P. S. Protecting-group-free synthesis as an opportunity for invention. *Nat. Chem.* **2009**, *1*, 193–205; (b) Hoffmann, R. W. Protecting-group-free synthesis. *Synthesis* **2006**, 3531–3541.

[8] (a) Evans, P. A. Temporary Silicon-Tethered Ring-Closing Metathesis Reactions in Natural Product Synthesis. In *Metathesis in Natural Product Synthesis*. Cossy, J.; Areniyadis, S.; Meyer, C., Eds.; Wiley-VCH,Weinheim, Germany, **2010**, p. 225–259; (b) Čusak, A. Temporary Silicon-Tethered Ring-Closing Metathesis: Recent Advances in Methodology Development and Natural Product Synthesis. *Chem. - Eur. J.* **2012**, *18*, 5800–5824; (c) Bracegirdle, S.; Anderson, E. A. Recent advances in the use of temporary silicon tethers in metal-mediated reactions. *Chem. Soc. Rev.* **2010**, *39*, 4114–4129.

[9] Hoye, T. R.; Promo, M. A. *Tetrahedron Lett.* **1999**, *40*, 1429–1432.

[10] (a) Evans, P. A.; Cui, J.; Buffone, G. P. *Angew. Chem., Int. Ed.* **2003**, *42*, 1734–1737. (b) Matsui, R.; Seto, K.; Fujita, K.; Suzuki, T.; Nakazaki, A.; Kobayashi, S. *Angew. Chem., Int. Ed.* **2010**, *49*, 10068–10073.

[11] (a) Burke, S. D.; Mueller, N.; Beaudry, C. M. *Org. Lett.* **1999**, *1*, 1827–1829; (b) Burke, S. D.; Voight, E. A. *Org. Lett.* **2001**, *3*, 237–240; (c) Voight, E. A.; Rein, C.; Burke, S. D. *J. Org. Chem.* **2002**, *67*, 8489–8499; (d) Van Hooft, P. A. V.; Leeuwenburgh, M. A.; Overkleeft, H. S.; Van Der Marel, G. A.; Van Boeckel, C. A. A.; Van Boom, J. H. *Lett.* **1998**, *39*, 6061–6064; (e) Scholl, M.; Grubbs, R. H. *Tetrahedron Lett.* **1999**, *40*, 1425–1428; (f) Ghosh, S. K.; Hsung, R. P.; Wang, J. *Tetrahedron Lett.* **2004**, *45*, 5505–5510; (g) Ghosh, S. K.; Ko, C.; Liu, J.; Wang, J.; Hsung, R. P. *Tetrahedron* **2006**, *62*, 10485–10496.

[12] Schmidt, B.; Kunz, O. One-flask tethered ring closing metathesis-electrocyclic ring opening for the highly stereoselective synthesis of conjugated Z/E-dienes. *Eur. J. Org. Chem.* **2012**, *2012*, 1008–1018.

[13] Whitehead, A.; McReynolds, M. D.; Moore, J. D.; Hanson, P. R. Multivalent Activation in Temporary Phosphate Tethers: A New Tether for Small Molecule Synthesis. *Org. Lett.* **2005**, *7*, 3375–3378.

[14] (a) Waetzig, J. D.; Hanson, P. R. Temporary Phosphate Tethers: A Metathesis Strategy to Differentiated Polyol Subunits. *Org. Lett.* **2006**, *8*, 1673–1676; (b) Thomas, C. D.; McParland, J. P.; Hanson, P. R. Divalent and Multivalent Activation in Phosphate Triesters: A Versatile Method for the Synthesis of Advanced Polyol Synthons. *Eur. J. Org. Chem.* **2009**, 5487–5500; (c) Venukadasula, P. K. M.; Chegondi, R.; Suryn, G. M.; Hanson, P. R. A Phosphate Tether-Mediated, One-Pot, Sequential Ring-Closing Metathesis/Cross-Metathesis/Chemoselective Hydrogenation Protocol. *Org. Lett.* **2012**, *14*, 2634–2637.

[15] (a) Venukadasula, P. K. M.; Chegondi, R.; Maitra, S.; Hanson, P. R. A Concise, Phosphate-Mediated Approach to the Total Synthesis of (–)-Tetrahydrolipstatin. *Org. Lett.* **2010**, *12*, 1556–1559; (b) Hanson, P. R.; Chegondi, R.; Nguyen, J.; Thomas, C. D.; Waetzig, J. D.; Whitehead, A. Total synthesis of dolabelide C: A phosphate-mediated approach. *J. Org. Chem.* **2011**, *76*, 4358–4370; (c) Chegondi, R.; Tan, M. M. L.; Hanson, P. R. Phosphate tether-mediated approach to the formal total synthesis of (–)-salicylihalamides A and B. *J. Org. Chem.* **2011**, *76*, 3909–3916; (d) Jayasinghe, S.; Venukadasula, P. K. M.; Hanson, P. R. An Efficient, Modular Approach for the Synthesis of (+)-Strictifolione and a Related Natural Product. *Org. Lett.* **2014**, *16*, 122–125; (e) Chegondi, R.; Hanson, P. R. Synthetic studies to lyngbouilloside: a phosphate tether-mediated synthesis of the macrolactone core. *Tetrahedron Lett.* **2015**, Ahead of Print.

[16] a) Pettit, G. R.; Cichacz, Z. A.; Gao, F.; Boyd, M. R.; Schmidt, J. M. Isolation and structure of the cancer cell growth inhibitor dictyostatin 1. *J. Chem. Soc., Chem. Commun.* **1994**, 1111–1112; b) Paterson, I.; Britton, R.; Delgado, O.; Gardner, N. M.; Meyer, A.; Naylor, G. J.; Poullennec, K. G. Total synthesis of (–)-dictyostatin, a microtubule-stabilizing anticancer macrolide of marine sponge origin. *Tetrahedron* **2010**, *66*, 6534–6545; c) Shin, Y.; Fournier, J.-H.; Fukui, Y.; Brueckner, A. M.; Curran, D. P. Total synthesis of (–)-dictyostatin: Confirmation of relative and absolute configurations. *Angew. Chem., Int. Ed.* **2004**, *43*, 4634–4637; d) Zhu, W.; Jimenez, M.; Jung, W.-H.; Camarco, D. P.; Balachandran, R.; Vogt, A.; Day, B. W.; Curran, D. P. Streamlined Syntheses of (–)-Dictyostatin, 16-Desmethyl-25,26-dihydrodictyostatin, and 6-epi-16-Desmethyl-25,26-dihydrodictyostatin. *J. Am. Chem. Soc.* **2010**, *132*, 9175–9187; e) O'Neil, G. W.; Phillips, A. J. Total Synthesis of (–)-Dictyostatin. *J. Am. Chem. Soc.* **2006**, *128*, 5340–5341; f) Ramachandran, P. V.; Srivastava, A.; Hazra, D. Total Synthesis of Potential Antitumor Agent, (–)-Dictyostatin. *Org. Lett.* **2007**, *9*, 157–160; g) Jogalekar, A. S.; Damodaran, K.; Kriel, F. H.; Jung, W.-H.; Alcaraz, A. A.;

Zhong, S.; Curran, D. P.; Snyder, J. P. Dictyostatin Flexibility Bridges Conformations in Solution and in the *b*-Tubulin Taxane Binding Site. *J. Am. Chem. Soc.* **2011**, *133*, 2427-2436; h) Gallon, J.; Esteban, J.; Bouzbouz, S.; Campbell, M.; Reymond, S.; Cossy, J. Formal Synthesis of Dictyostatin and Synthesis of Two Dictyostatin Analogues. *Chem. - Eur. J.* **2012**, *18*, 11788–11797 and references cited therein.

[17] Ying, M.; Roush, W. R. Studies on the synthesis of reidispongiolide A: stereoselective synthesis of the C(22)-C(36) fragment. *Tetrahedron* **2011**, *67*, 10274–10280.

[18] a) Tullis, J. S.; Vares, L.; Kann, N.; Norrby, P.-O.; Rein, T. Reagent Control of Geometric Selectivity and Enantiotopic Group Preference in Asymmetric Horner-Wadsworth-Emmons Reactions with meso-Dialdehydes. *J. Org. Chem.* **1998**, *63*, 8284–8294; b) Rychnovsky, S. D.; Yang, G.; Hu, Y.; Khire, U. R. Prins Desymmetrization of a C2-Symmetric Diol: Application to the Synthesis of 17-Deoxyroflamycoin. *J. Org. Chem.* **1997**, *62*, 3022–3023; c) Rychnovsky, S. D.; Griesgraber, G.; Zeller, S.; Skalitzky, D. J. Optically pure 1,3-diols from (2*R*,4*R*)- and (2*S*,4*S*)-1,2:4,5-diepoxypentane. *J. Org. Chem.* **1991**, *56*, 5161–5169.

[19] Scholl, M.; Grubbs, R. H. Total synthesis of (–)- and (±)-frontalin via ring-closing metathesis. *Tetrahedron Lett.* **1999**, *40*, 1425–1428.

[20] Liu, J.; Lotesta, S. D.; Sorensen, E. J. A concise synthesis of the molecular framework of pleuromutilin. *Chem. Commun.* **2011**, *47*, 1500–1502.

[21] (a) Kingsbury, J. S.; Harrity, J. P. A.; Bonitatebus, P. J., Jr.; Hoveyda, A. H. A Recyclable Ru-Based Metathesis Catalyst. *J. Am. Chem. Soc.* **1999**, *121*, 791–799; (b) Garber, S. B.; Kingsbury, J. S.; Gray, B. L.; Hoveyda, A. H. Efficient and Recyclable Monomeric and Dendritic Ru-Based Metathesis Catalysts. *J. Am. Chem. Soc.* **2000**, *122*, 8168–8179; (c) Gessler, S.; Randl, S.; Blechert, S. Synthesis and metathesis reactions of a phosphine-free dihydroimidazole carbene

ruthenium complex. *Tetrahedron Lett.* **2000**, *41*, 9973–9976.

[22] Casey, E. M.; Teesdale-Spittle, P.; Harvey, J. E. Synthesis of the C12-C24 fragment of peloruside A by silyl-tethered diastereomer-discriminating RCM. *Tetrahedron Lett.* **2008**, *49*, 7021–7023.

[23] As molecular modeling and subsequent energy calculations for potential conformations of high-energy Ru-metallocyclobutane intermediates are challenging, we propose potential intermediate structures based upon observed product structures (confirmed by X-ray crystallography). For examples where this rationale is applied to describe a similar observation made in all carbon-based RCM, see ref [20] Liu, J.; Lotesta, S. D.; Sorensen, E. J. *Chem. Commun.* **2011**, *47*, 1500–1502.

[24] Marx, V. M.; Herbert, M. B.; Keitz, B. K.; Grubbs, R. H. Stereoselective Access to Z and E Macrocycles by Ruthenium-Catalyzed Z-Selective Ring-Closing Metathesis and Ethenolysis. *J. Am. Chem. Soc.* **2013**, *135*, 94–97.

[25] Wang, Y.; Jimenez, M.; Hansen, A. S.; Raiber, E.-A.; Schreiber, S. L.; Young, D. W. Control of Olefin Geometry in Macrocyclic Ring-Closing Metathesis Using a Removable Silyl Group. *J. Am. Chem. Soc.* **2011**, *133*, 9196–9199.

Chapter 3

A Modular phosphate tether-mediated divergent strategy to complex polyols

3.1: Introduction

The central components of several polyketides that exhibit a wealth of medicinally important activities, including antibiotic, anticancer, antifungal, antiparasitic and immunosuppressive properties are 1,3-*anti*-diol subunits (Figure 3.1).[1] The structural diversity and biological importance of 1,3-*anti*-diol containing natural products has led to the development of various synthetic methods for their construction.[2] Some representative examples of polyol-containing natural products are shown below in Figure 3.1.

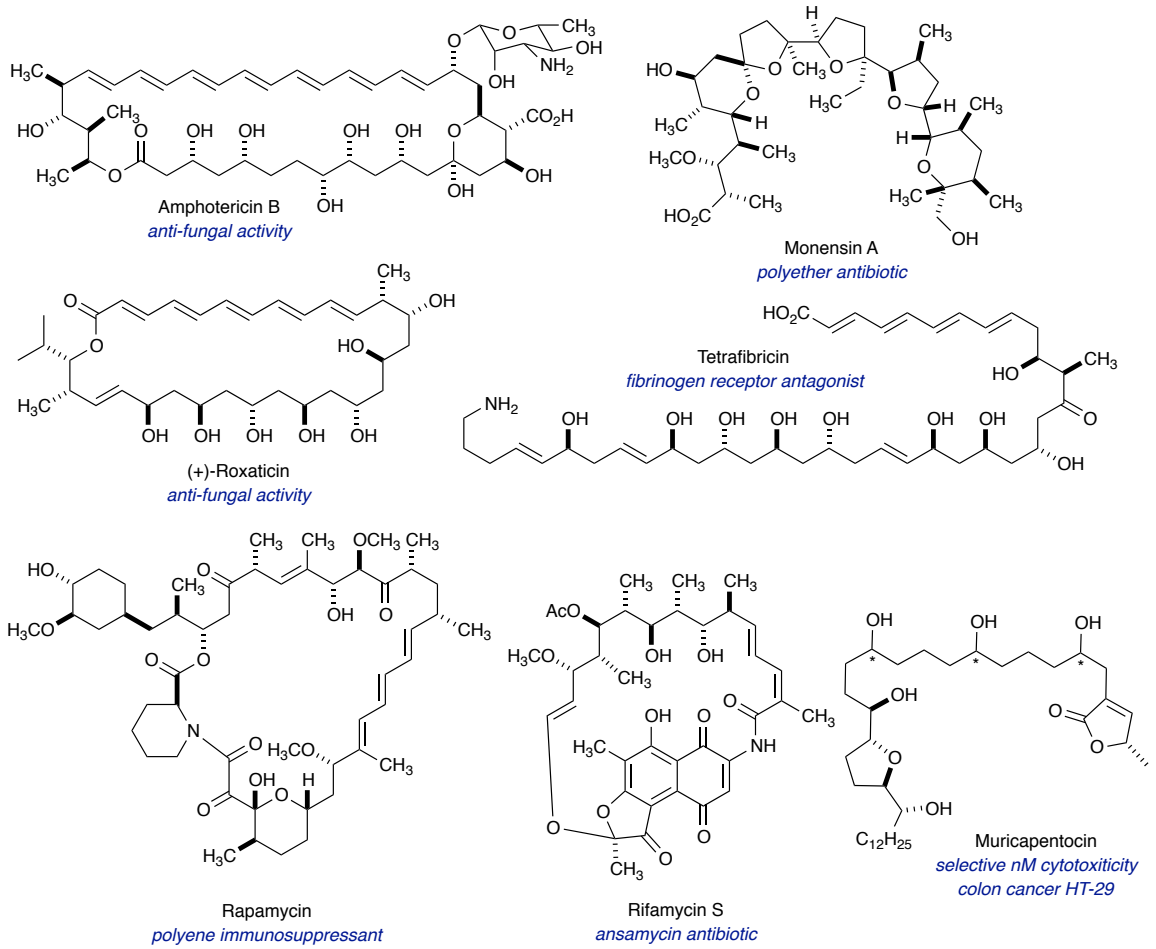

Figure 3.1. *Some representative examples of polyol-containing bioactive natural products.*

Divergent strategies to access functionalized core scaffolds of these bioactive small molecules are ideal for analog generation, which in turn enhance the quality of screening decks in early phase drug discovery.[3] In this regard, one-pot, sequential processes,[4] which form multiple bonds and stereocenters, while invoking step,[5] atom,[6] green,[7] and pot economy,[8] are well suited to address the challenge of generating diverse compounds in an efficient manner. This chapter provides a brief description of phosphate tether-mediated, one-pot, sequential RCM/CM/reduction processes towards the synthesis of diverse polyol-containing subunits. Other divergent approaches towards accessing small libraries of polyol-containing compounds will also be discussed.

3.2: Generation of stereodiverse small molecule libraries

The goal of diversity-oriented synthesis (DOS) is to identify therapeutic protein targets and their small-molecule regulators simultaneously by generating a collection of compounds having structural complexity and diversity.[9] One such DOS approach includes utilizing different building blocks to couple with a common intermediate producing multiple scaffolds. The complementary DOS approach utilizes stereochemistry to introduce diversity among constitutionally identical, stereoisomeric products.[10] Unlike target-oriented synthesis (TOS), DOS strategies focus on the generation of diverse collections of molecules, and therefore, the incorporation of easily derivatizable functional group handles and the development of modular strategies to expedite the synthesis are crucial to the success of DOS approaches. In this respect, hydroxyl-containing compounds such as polyol/polyketide fragments are abundant in many potent biologically active natural products and, therefore, are attractive choices to

be incorporated in small molecule libraries.[11] In addition, from a synthetic point of view, incorporation of hydroxyl groups in the design of library compounds is desirable as they can be easily be derivatized and utilized in hydroxyl-directed reactions for further diversification. Similarly, a synthetic DOS strategy should be carefully chosen to expedite the process of library generation; these strategies must install stereochemical and structural diversity while, at the same time, tolerate a number of functional groups. In this respect, metathesis approaches are excellent choices since metathesis reactions are mostly run under neutral reaction conditions and exhibit a high functional group tolerance. In 2009, Schreiber and coworkers demonstrated the utility of RCM reactions in generating a 2070-member library of 12–14-membered macrocycles.[12] The screening of the library compounds led to the discovery of Robotnikinin (**3.2A**), an inhibitor of the Sonic Hedgehog (Shh) signaling pathway (Figure 3.2).[13]

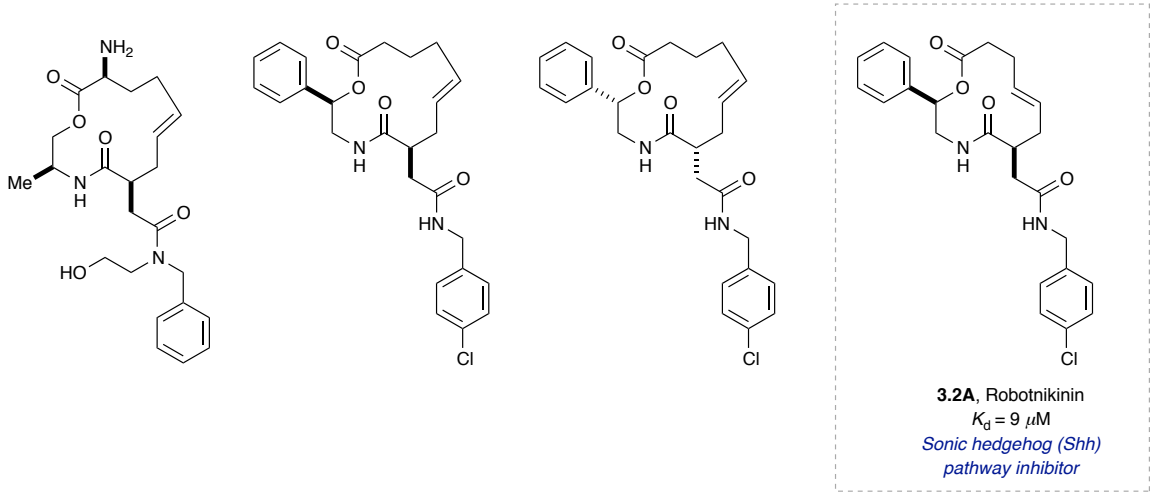

Figure 3.2 *Some representative members of a 2070-member library of 12–14-membered macrocycles by Schreiber and coworkers.*

Tether-mediated metathesis approaches have also been reported for the generation of small molecule libraries. In 2009, Nelson and coworkers reported the synthesis of 80-

distinct natural product-like scaffolds such as **3.1.5**, **3.1.8** and **3.1.11** via the use of metathesis/tether-mediated metathesis as the key reaction (Scheme 3.1).[14] In this example, the fluorous tag attached to the linkers **3.1.1** (X = OH, NHNs) aided in the purification process, as well as in the release of metathesis product. Their strategy involved the use of silicon as a temporary tether for a majority of the products, and a range of skeletally diverse compounds were synthesized by varying the linkages between the building blocks.

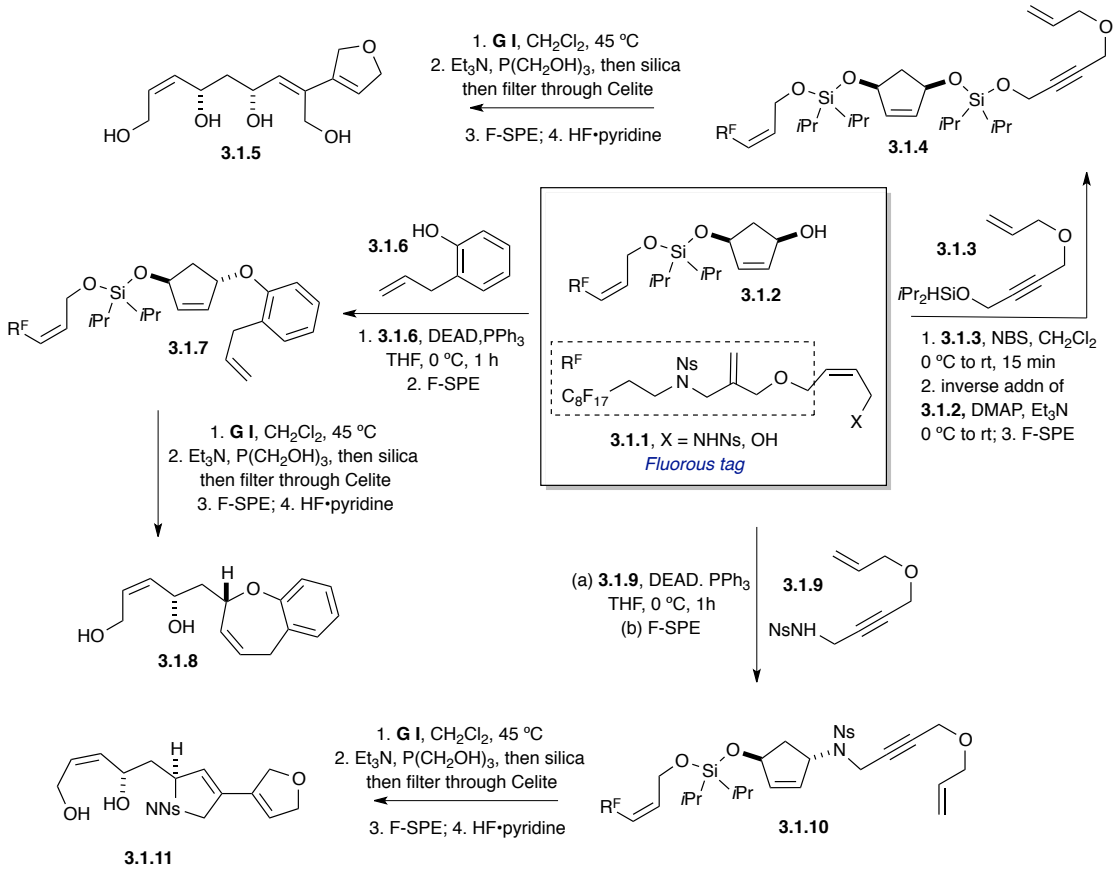

Scheme 3.1 *Selected examples of metathesis cascade leading to skeletally diverse products by Nelson and coworkers.*

In 2000, Verdine and coworkers reported a modular strategy towards the synthesis of 16-stereoisomers of *cis*-1,4-enediols (Scheme 3.2).[15] The core structure of the library members, *cis*-1,4-enediols, was carefully chosen to incorporate a number of properties including semi-rigidity of the acyclic framework, the presence of variable substituents that could be easily generated over few steps and the presence of hydrogen bonding functionalities. In this process, two differently substituted allylic alcohols were coupled in the presence of $MeSiCl_2$ and pyridine to generate the hetero-tethered product **3.2.3** in good to excellent yields. Ring-closing metathesis of the hetero-tethered product **3.2.3** in the presence of the **G-II** catalyst produced the 7-membered cyclic silyl ether **3.2.4** in excellent yields (Scheme 3.2). Subsequent tether removal generated 16-stereoisomers of *cis*-1,4-enediols **3.2.5**. Further functionalization on both ends of *cis*-1,4-dieneol scaffold produced an ensemble of stereodiversified chimerae **3.2.6**. Interestingly, the hydrophobicities of these chimeric products were significantly different, which indicated that stereochemical variation is essential to optimize affinity and also to tune the pharmacological properties of small molecule ligands.

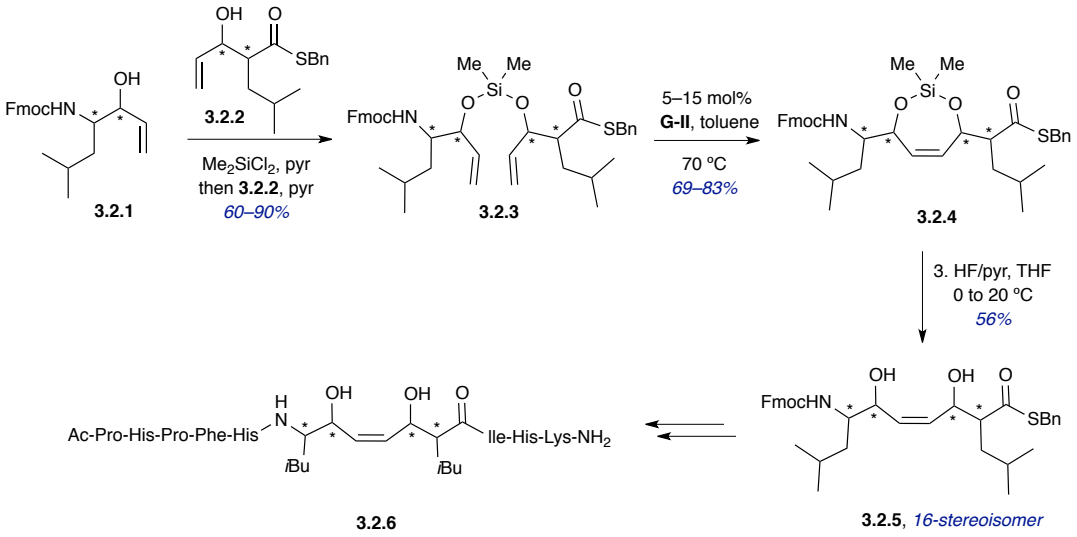

Scheme 3.2 *A modular approach towards stereodiversified ligand libraries of cis-1,4-*

enediol by Verdine and coworkers.

In 2001, Verdine and coworkers reported the synthesis of 16-stereoisomers of *cis*-1,5-enediol intermediates *en route* to discovery of stereodiversified ligands (Scheme 3.3).[16] The rational design of core scaffold *cis*-1,5-enediol **3.3.5** was guided by a structural comparison of *cis*-1,5-enediol **3.3.5** with isoatomic tripeptide **3.3.6** scaffold and previously synthesized *cis*-1,4-enediol scaffold **3.3.7**. The *cis*-1,5-enediol possesses more structural flexibility due to the presence of an unsubstituted allylic position in comparison to tripeptide **3.3.6** and *cis*-1,4-enediol scaffold **3.3.7**, which was proposed to be advantageous to access the biologically active confirmation not available to *cis*-1,4-enediol scaffold **3.3.7**. In addition, the two hydroxyl groups present in *cis*-1,5-enediol **3.3.5** are chemically differentiated, which allows for further hydroxyl-directed derivatization. For the synthesis of the library compounds, substituted allylic alcohols **3.3.1** and homoallylic alcohol fragments **3.3.2** were initially coupled in the presence of $MeSiCl_2$ and pyridine to produce hetero-tethered product **3.3.3** in good to moderate yields. Ring-closing methathesis was performed in the presence of the **G-II** catalyst in toluene at 95 ºC to obtain 8-membered siloxane **3.3.4** in excellent yields. Subsequent tether removal under HF/pyridine condition generated 16-stereoisomers of *cis*-1,5-enediol **3.3.5**. Screening of these compounds for affinity towards the mu opioid receptor (MOR) identified several active stereoisomers, which in turn led to the generation of a secondary library containing *trans*-1,4-enediol compounds[17] Screening of this secondary library compounds helped in identifying multiple potent and selective partial agonist of MOR. These outcomes demonstrated the need for the synthesis of stereo-enriched small molecule libraries.

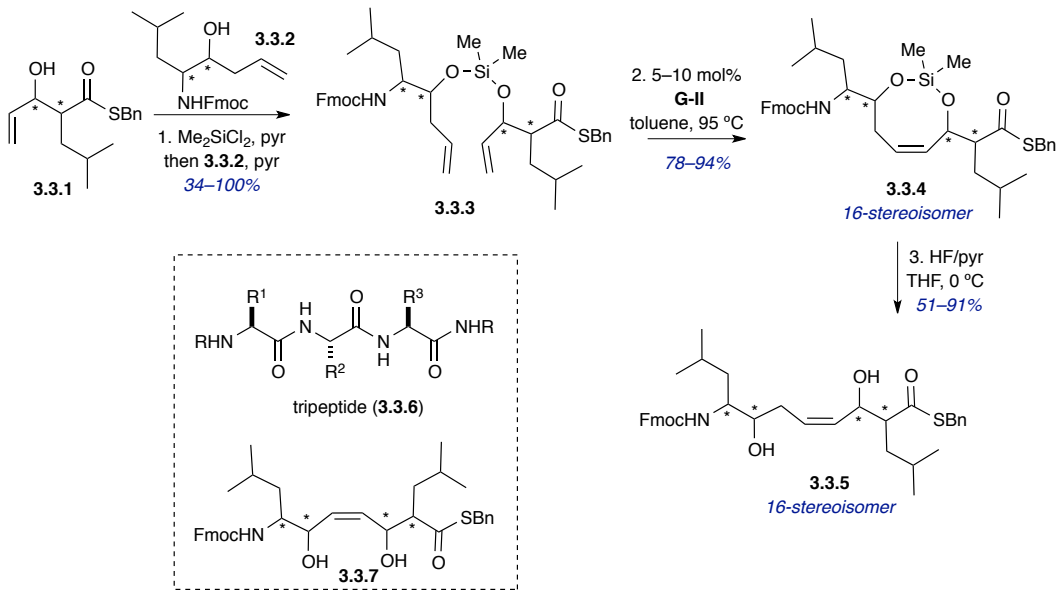

Scheme 3.3 *Synthesis of stereodiversified ligand libraries of cis-1,5-enediol by Verdine and coworkers.*

3.3: Results and discussion

In 2005, we reported the synthesis of the bicyclo[4.3.1]phosphate by utilizing a phosphate tether-mediated desymmetrization of 1,3-*anti*-diol substrate (this method was discussed in detail in chapter 1 and also mentioned in chapter 2).[18] Diverse bicyclic phosphate intermediates containing additional functional handles were generated via phosphate tether-mediated selective cross-metathesis reactions of the external olefinic group.[19] In addition, efforts were directed toward developing orthogonal reaction patterns en route to the synthesis of 1,3-*anti*-diol containing natural products.[20] In 2012, we have reported a one-pot sequential protocol involving RCM/CM/chemoselective hydrogenation (RCM/CM/"H_2") to produce advanced phosphate intermediates **3.4.3**, starting from triene (*R*,*R*)-**3.4.1** (Scheme 3.4).[21] The selective cross-metathesis and chemo- and regioselective hydrogenation in this one-pot sequence were achieved by taking advantage of stereoelectronic properties inherent to phosphate tethers. Most

importantly, this tandem RCM/CM/H_2 process preserved the chemical integrity for the bicyclic phosphate for further transformation. In particular, this one-pot sequential RCM/CM/"H_2" protocol is a powerful strategy not only in terms of streamlining the synthesis of advanced polyol fragments, but also in the efficient generation of library of polyol-containing scaffolds.

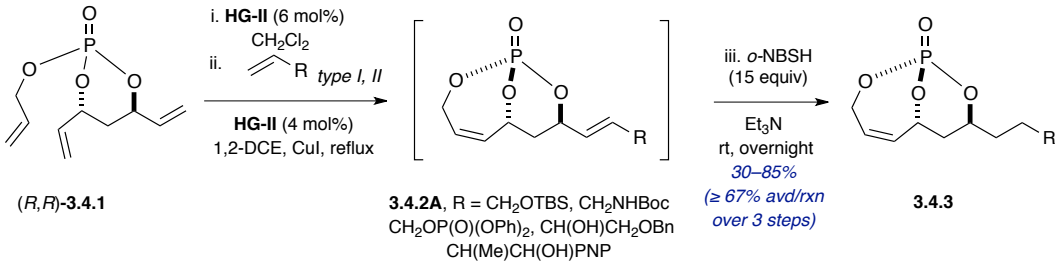

Scheme 3.4 *Phosphate tether-mediated one-pot sequential protocol involving ring-closing metathesis/cross metathesis/chemoselective hydrogenation.protocol.*

In 2013, we continued our studies of phosphate-tether mediated processes with the synthesis of complex bicyclo[n.3.1]phosphate intermediates of different ring sizes utilizing phosphate tether-mediated diastereoselective RCM reactions (figure 3.3, also discussed in chapter 1).[22]

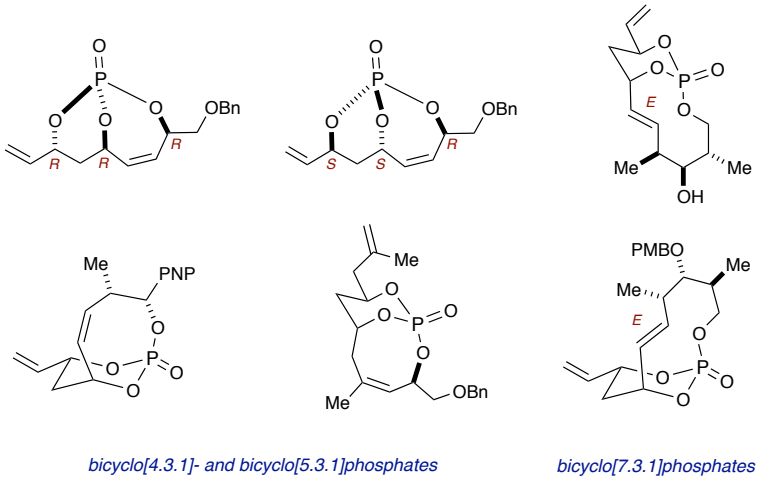

Figure 3.3 *Synthesis of bicyclo[4.3.1]-, bicyclo[5.3.1]- and bicyclo[7.3.1]phosphates.*

3.3.1: Rational design

To further demonstrate the utility of phosphate tethers towards the efficient synthesis of a small collection of compounds containing stereochemically-enriched polyols, we designed a divergent strategy in which changing the order of addition of coupling partners could produce differently substituted polyol scaffolds (Figure 3.4). Coupling of the pseudo-C_2-symmetric phosphoryl chloride (*S*,*S*)-**3.4.1**, generated over one step from 1,3-*anti*-diene diol, with two different alcohols **3.4.2** and **3.4.3** separately would generate two different trienes. Upon completion of the RCM, the coupling partners could be switched and introduced as CM partners to obtain two different bicyclic phosphate intermediates. From these two intermediates, five differently-substituted polyol scaffolds can be generated efficiently by further functional group modification. Taken collectively, we realized that this modular, divergent 3-component coupling strategy would produce five polyol fragments, bearing differential *Z*- and *E*- olefins, from a pair of olefinic-alcohol components **3.4.2** and **3.4.3** and a pseudo-C_2-symmetric phosphoryl chloride (*S*,*S*)-**3.4.1**. Moreover, the method relied on simple "order of addition" of components for the phosphoryl coupling, RCM and CM steps of the process as outlined in Figure 3.4. In addition, our previous development of the one-pot sequential RCM/CM/"H_2" protocol would further facilitate in streamlining the synthesis of polyols. We also aimed to develop a new one-pot sequential protocol of RCM/CM/tether removal to expedite the synthesis of (*E*),(*Z*)-substituted polyols. This synthesis would further highlight the utility of phosphate tether mediated desymmetrization of C_2-symmetric 1,3-

anti diene-diol subunit to generate polyol scaffolds with high diastereoselectivities, which would otherwise be difficult to produce via (*Z*)- selective and (*E*)- selective CM of 1,3-*anti* diene-diol subunits with olefinic-alcohol components.

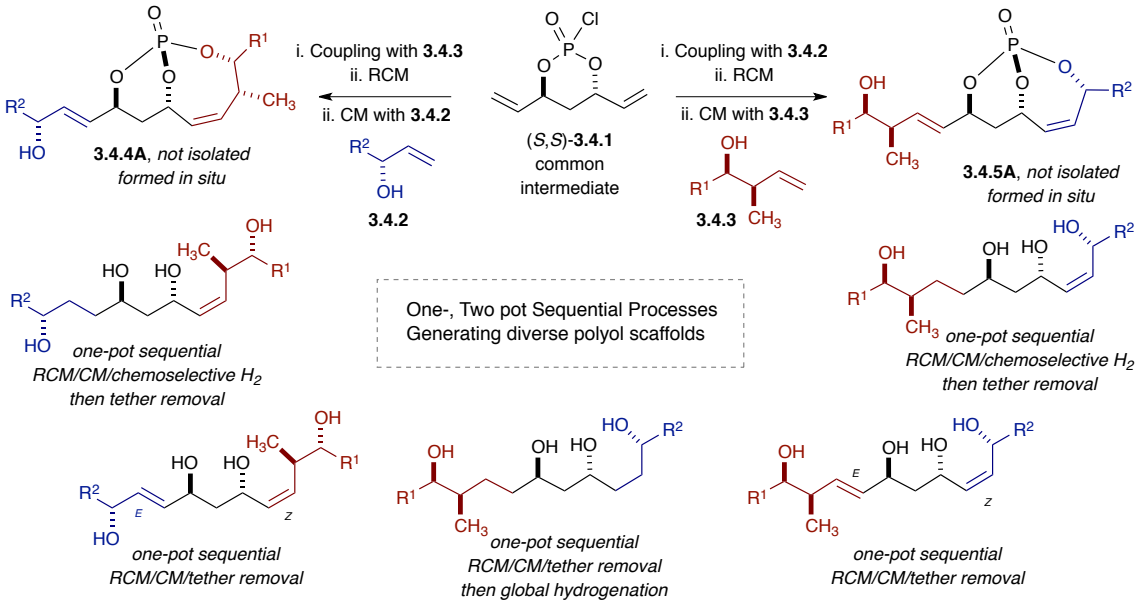

Figure 3.4 *Rational design for the synthesis of stereodiverse polyols via phosphate tether-mediated one-, two-pot sequential RCM/CM/reduction protocol.*

The requisite trienes **3.5.4**–**3.5.6** for this study were generated *via* our previously reported coupling of the pseudo-C_2-symmetric phosphoryl chloride (*S,S*)-**3.4.1** with the olefinic alcohol components **3.5.1**–**3.5.3** (Scheme 3.5).[18] The alcohol substrates were carefully chosen to incorporate *exo*-allylic methyl groups since previous RCM studies[22] (discussed in chapter 1) showed that the productive RCM for 8-membered ring formation was observed only for the (*S,S*)-configured trienes in the presence of an *exo*-methyl group at the allylic position.

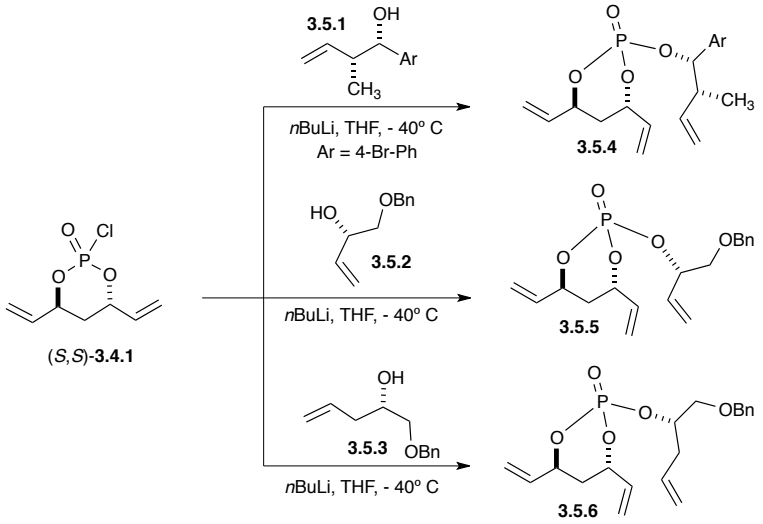

Scheme 3.5 *Synthesis of trienes.*

3.3.2: Synthesis of the first set of 5 polyols

Initial attempts were focused on generating the first set of five polyols from trienes **3.5.4** and **3.5.5** in a two-pot operation (Scheme 3.6). The first operation entailed a one-pot, sequential RCM/CM/chemoselective hydrogenation protocol,[21] yielding two bicyclo[n.3.1] phosphate intermediates **3.6.1** and **3.6.3**, and a second pot $LiAlH_4$ reduction to provide the (*Z*)-configured tetraol subunits **3.6.2** and **3.6.4**. Trienes **3.5.4** and **3.5.5** were generated via coupling with alcohol partners **3.5.1** and **3.5.2**, respectively, and the divergent aspect of the method was introduced by simple switching of the olefinic partners in the subsequent CM reaction to afford five differentiated polyols starting from three coupling partners.

In this regard, triene **3.5.4** was first subjected to RCM in the presence of the Hoveyda-Grubbs II (**HG-II**) catalyst[23] in refluxing CH_2Cl_2, followed by solvent concentration and CM with allylic alcohol **3.5.2** in refluxing CH_2Cl_2 for two hours. It was observed that the use of CH_2Cl_2 was critical for the successful CM reactions in order

to avoid the formation of isomerized ketone by-products. Subsequent chemoselective diimide reduction with *o*-nitrobenzenesulfonyl hydrazine (*o*-NBSH)[24] in CH_2Cl_2 at room temperature afforded bicyclo[5.3.1]phosphate **3.6.1** in 33% overall yield, representing a 70% average yield/reaction in the one-pot, sequential protocol (Scheme 3.6). Subsequent treatment of **3.6.1** with $LiAlH_4$ furnished the tetraol **3.6.2** in 24% overall yield over the course of four reactions carried out in two pots, representing a 70% average yield per reaction.

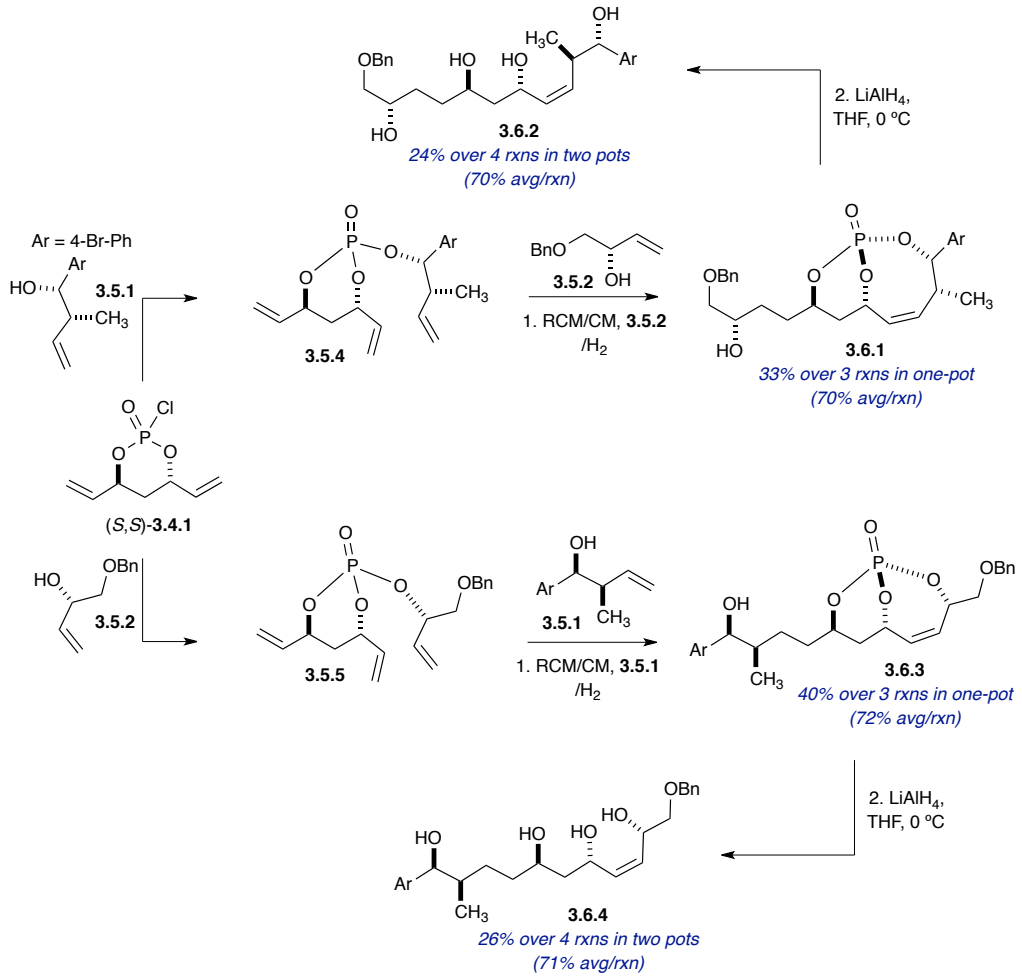

Scheme 3.6 *Phosphate tether-mediated two-pot protocol consisting of RCM/CM/H_2 and subsequent LAH reduction: Reaction Conditions: RCM -* ***HG-II*** *(3 mol%), 1,2-DCE/CH_2Cl_2, 2 h; CM -* ***HG-II*** *(3 mol%), CH_2Cl_2, CM partner (3–5 equiv.); H_2 - o-NBSH (12 equiv.), CH_2Cl_2, Et_3N, overnight.*

Similarly, starting with the triene **3.5.5**, a one-pot RCM/CM/chemoselective H_2 was performed to obtain the bicyclo[4.3.1]phosphate **3.6.3** in 40% yield over 3 reactions in a one-pot operation (72% avg/rxn). In this example, the RCM reaction was performed in dicholoroethane (DCE) at 70ºC for 2 h, since lower reactivity was observed in CH_2Cl_2. Subsequently, phosphate **3.6.3** was treated with $LiAlH_4$ to generate tetraol **3.6.4** in 26% overall yield in the four reactions carried out in two pots, representing a 71% average yield per reaction (Scheme 3.6).

Next, a one-pot RCM/CM/LAH protocol was established to obtain two additional tetraol subunits possessing both (*E*)- and (*Z*)-olefinic geometries. Triene **3.5.4** was subjected to an RCM reaction, followed by a CM reaction with allylic alcohol **3.5.2**. After removing solvent, the CM product was treated with $LiAlH_4$ in THF at 0 ºC for 2 hours to produce tetraol **3.7.1** in 38% yield over three reactions in the one-pot, sequential process (73% avg/rxn) (Scheme 3.7).

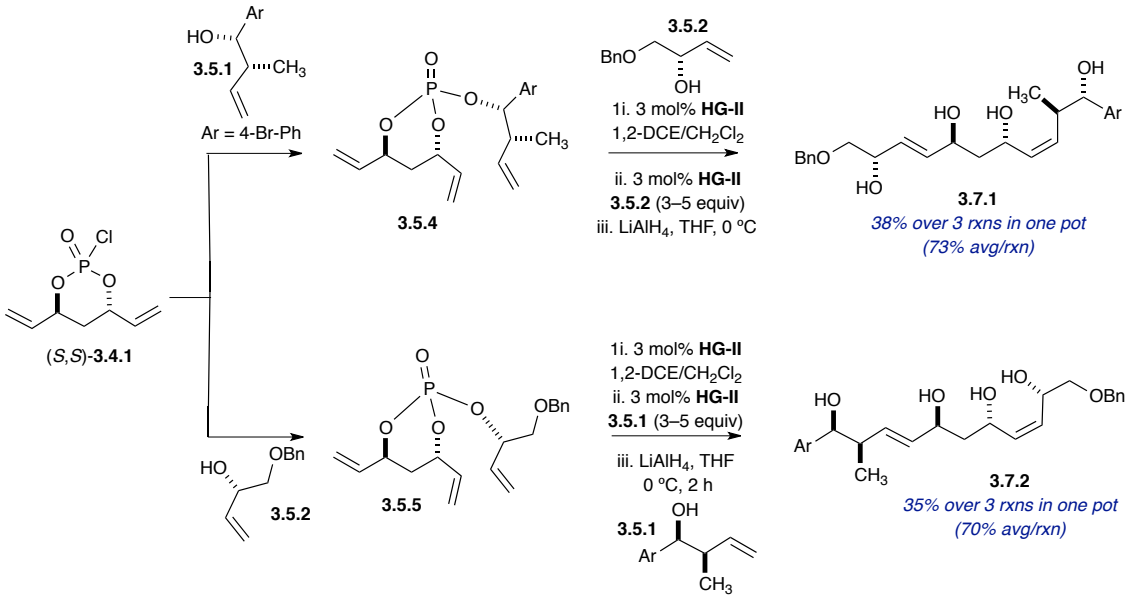

Scheme 3.7 *Phosphate tether-mediated one-pot RCM/CM/LAH protocol towards polyols containing (E)- and (Z)-substituted internal olefins.*

Similarly, triene **3.5.5** was subjected to an RCM reaction, followed by CM with homoallylic alcohol **3.5.1**, and subsequent treatment with $LiAlH_4$ to afford tetraol **3.7.2** in 35% yield over the three reactions, representing a 70% avg/rxn in the one-pot, sequential method (Scheme 3.7).

The previously described one-pot sequential RCM/CM/LAH procedure was further merged with global hydrogenation to generated saturated polyol scaffold. The resulting tetraols **3.7.1** and **3.7.2**, obtained after one-pot, sequential RCM/CM/LAH protocol, were separately treated with *o*-NBSH to obtain tetraol **3.8.1** in 26% yield over the four reactions in a two-pot operation starting from triene **3.6.1** (72% avg/rxn, Scheme 3.8).

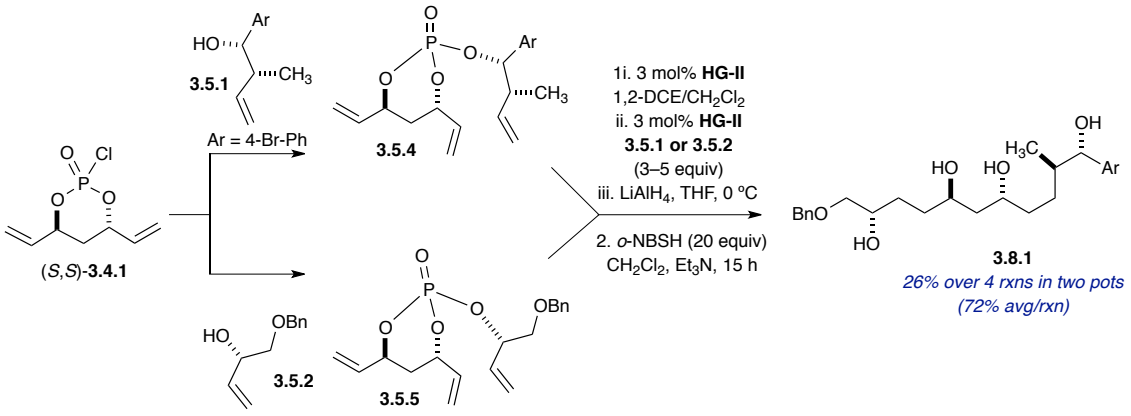

Scheme 3.8 *Phosphate tether-mediated two-pot RCM/CM/LAH and global reduction protocol towards the generation of saturated polyol.*

Utilizing this two-pot sequential protocol, the same tetraol **3.8.1** was obtained starting from two different trienes (**3.5.4** and **3.5.5**) and reacting with two different CM partners (Scheme 3.8). It should be noted, that after phosphate tether removal, treatment of tetraol with *o*-NBSH (10 eq) resulted in the global reduction of both (*E*)- and (*Z*)-

configured olefins in very good yields; in contrast, diimide reduction in the presence of phosphate intermediates did not hydrogenate the *endo*-cyclic olefin even when large excesses of diimide reagent were employed (30 eq). This empirical result further substantiates the protecting group ability of the phosphate tether for the endocyclic (*Z*) olefin.

Overall, 5 diverse polyol scaffolds were generated starting from three coupling partners by simply altering the order of addition for the coupling and in the cross-metathesis reaction (Scheme 3.9). The development of phosphate tether-mediated one- and two-pot sequential reactions facilitated the synthesis of these polyols.

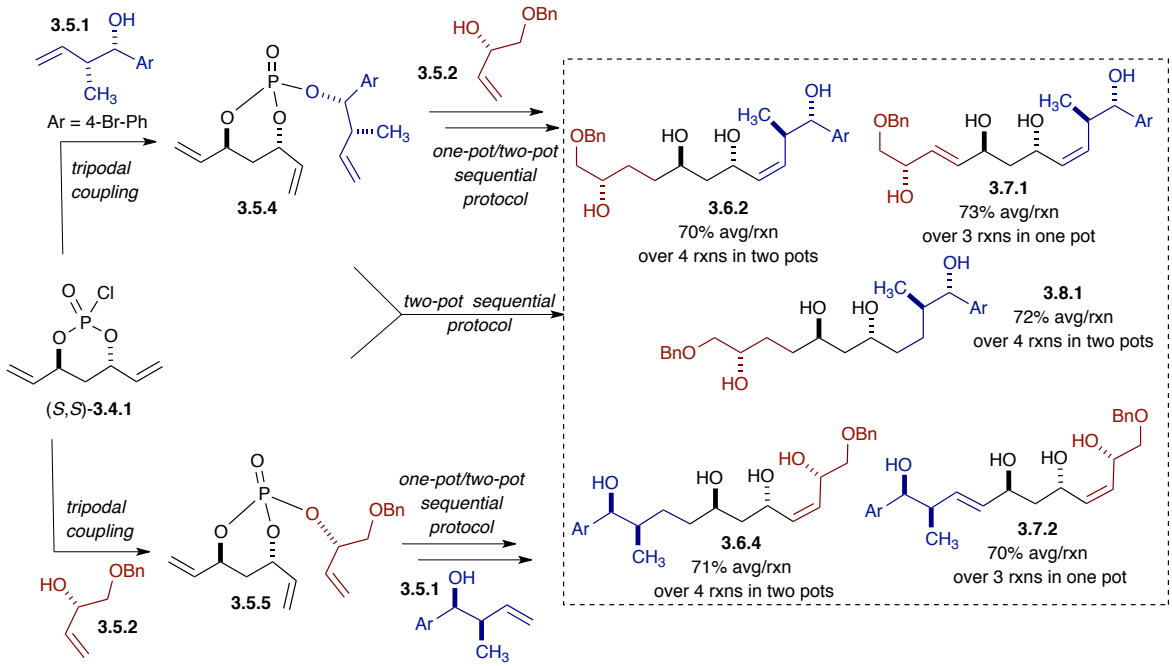

Scheme 3.9 *Synthesis of 5-diverse polyols via phosphate tether-mediated one-pot, two-pot sequential protocols.*

3.3.3: Synthesis of the second set of 5 polyols

Next, our attempts were focused on generating the second set of five polyols starting from trienes **3.5.6** and **3.5.5**. Utilizing the aforementioned strategy detailed in Scheme 3.6, triene **3.5.6** was subjected to the one-pot, sequential RCM/CM/ chemoselective H_2 procedure and subsequent LAH reduction to generate tetraol **3.10.2** in 24% yield over 4 reactions in a two-pot operation (70% avg/rxn, Scheme 3.10). Further, starting with same triene **3.5.5**, which was previously used in Scheme 3.6, but utilizing a different cross-metathesis partner (homoallylic alcohol **3.5.3**), a different tetraol **3.10.4** was generated in 23% yield over the four reactions in a two-pot operation (69% avg/rxn) (Scheme 3.10).

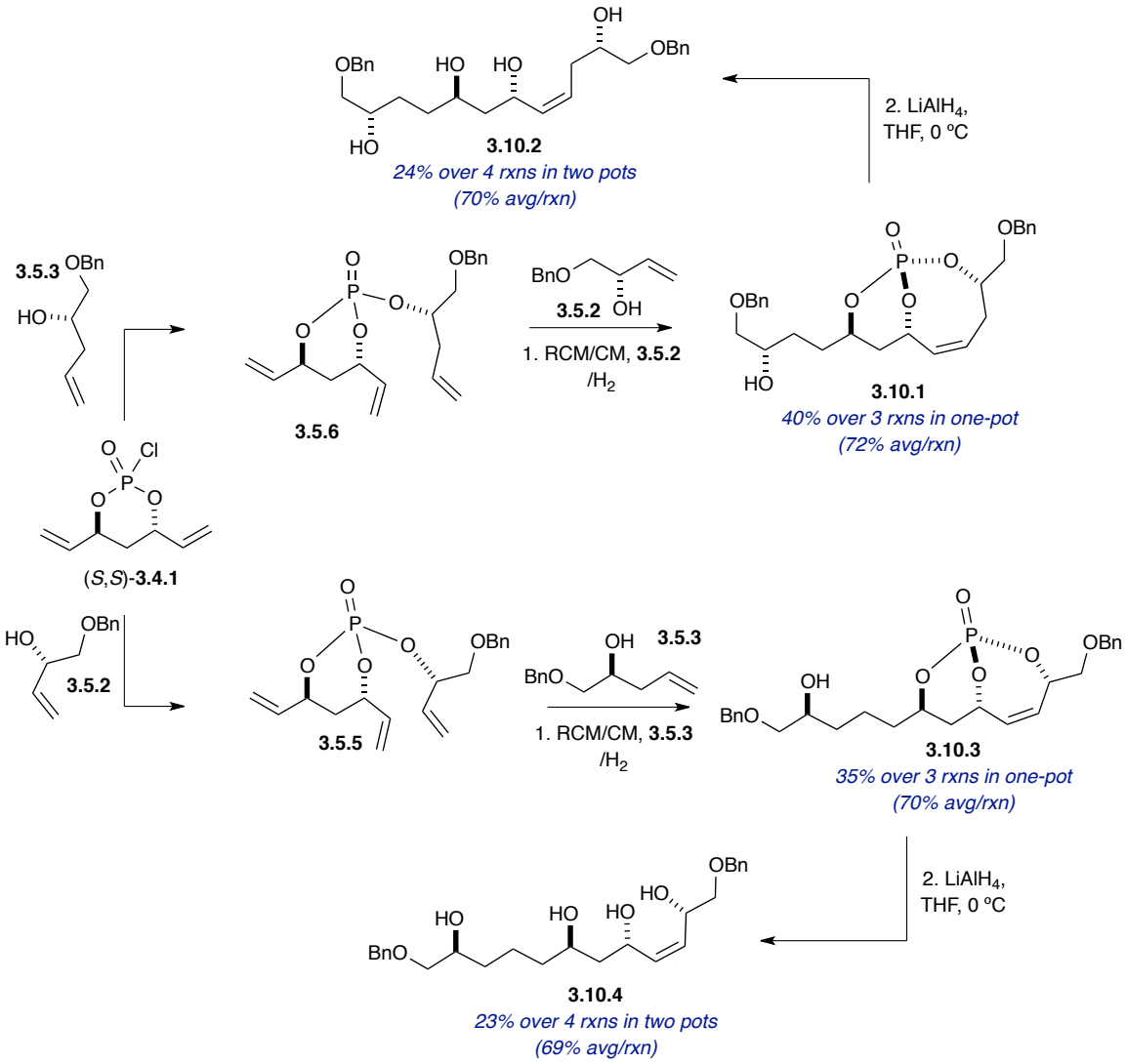

Scheme 3.10 *Phosphate tether-mediated two-pot protocol consisting of RCM/CM/H_2 and subsequent LAH reduction: Reaction Conditions: RCM -* ***HG-II*** *(3 mol%), 1,2-DCE/CH_2Cl_2, 2 h; CM -* ***HG-II*** *(3 mol%), CH_2Cl_2, CM partner (3–5 equiv.); H_2 - o-NBSH (12 equiv.), CH_2Cl_2, Et_3N, overnight.*

In a similar manner as described above in Scheme 3.7, starting with triene **3.5.6**, RCM and subsequent CM with allylic alcohol **3.5.2** were performed, followed by tether removal with $LiAlH_4$, to obtain tetraol **3.11.1** in 42% yield over three reactions in the one-pot, sequential operation (75% avg/rxn, Scheme 3.11). Triene **3.5.5** was next

subjected to RCM, followed by CM with homoallylic alcohol **3.5.3** and $LiAlH_4$ reduction, to furnish tetraol **3.11.2** in an overall 40% yield over three reactions in a one-pot operation (72% avg/rxn).

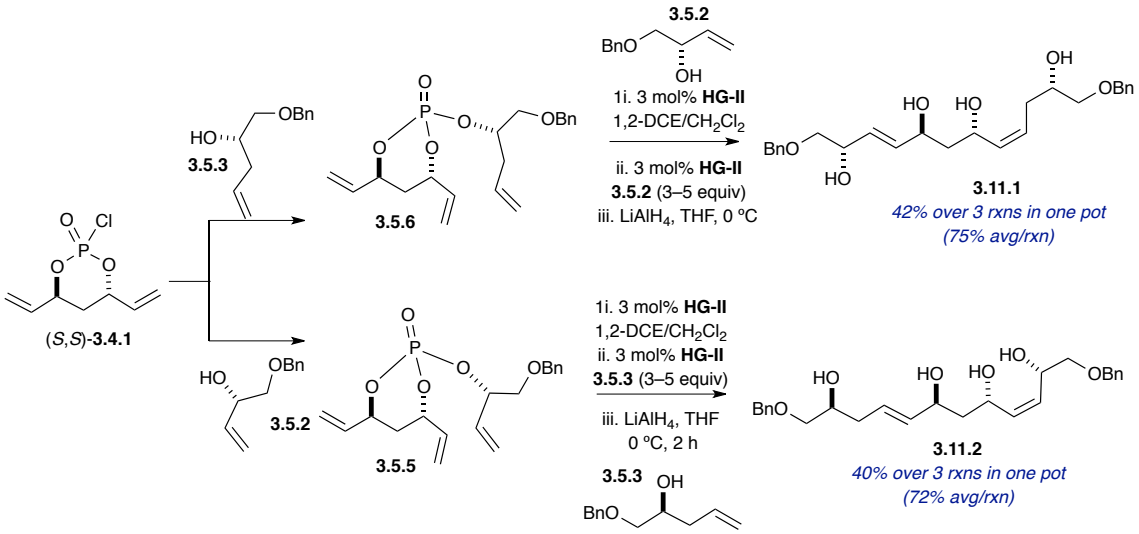

Scheme 3.11 *Phosphate tether-mediated one-pot RCM/CM/LAH protocol towards polyols containing (E)- and (Z)-substituted internal olefins.*

Tetraols **3.11.1** and **3.11.2** obtained from trienes **3.5.6** and **3.5.5** respectively, were separately subjected to a global hydrogenation using *o*-NBSH to afford tetraol **3.12.1** (Scheme 3.12) in 34% yield over four reactions in a two-pot operation starting from triene **3.5.5** (77% avg/rxn).

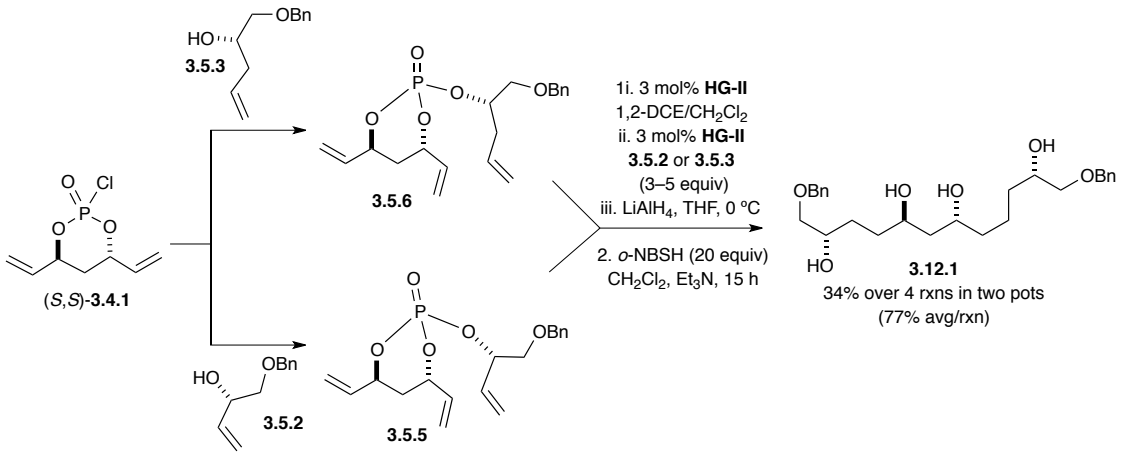

Scheme 3.12 *Phosphate tether-mediated two-pot RCM/CM/LAH and global reduction protocol towards the generation of saturated polyol.*

Overall, 5 polyol diverse scaffolds were generated starting from three coupling partners by simple alteration of the order of addition for the coupling and in the cross-metathesis reactions (Scheme 3.13).

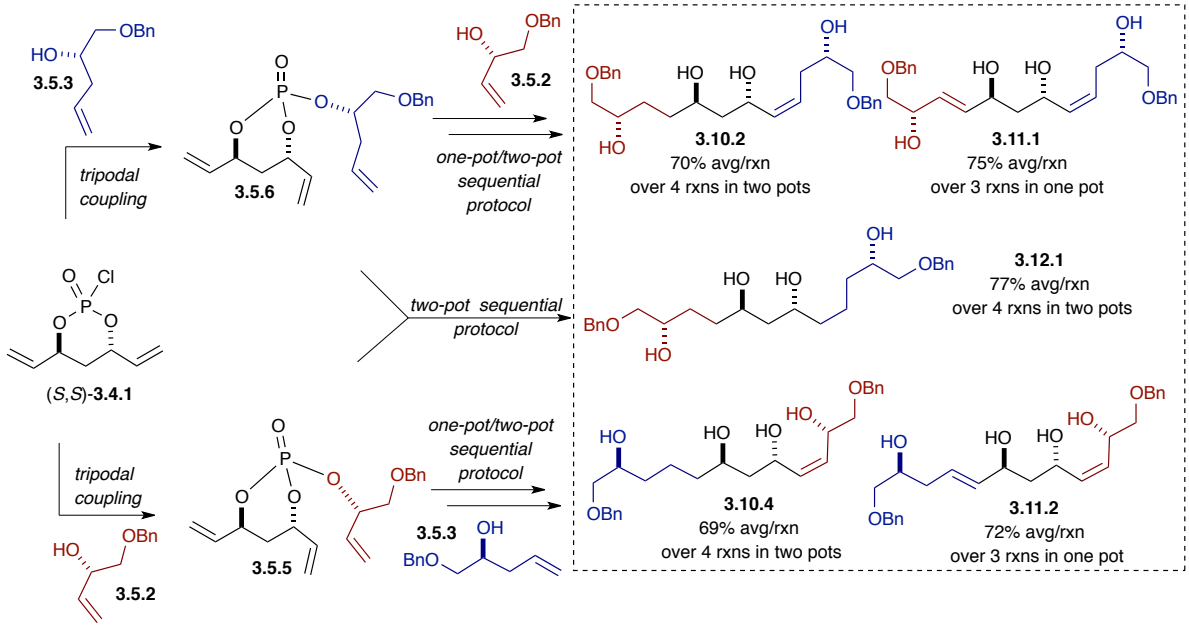

Scheme 3.13 *Synthesis of 5-diverse polyols via phosphate tether-mediated one-pot, two-pot sequential protocols.*

3.4: Conclusion

In conclusion, diverse polyol scaffolds, bearing a central 1,3-*anti*-diol subunit with differential olefinic geometries at the periphery, were generated efficiently via a phosphate tether mediated 3-component coupling and subsequent one-pot, two-pot sequential metathesis/reduction reactions. The polyols were synthesized by utilizing the following properties of phosphate triester including (i) the ability to serve as a temporary tether, (ii) protecting group properties, (iii) the ability to mediate tripodal coupling and facilitate sequential metathesis/reduction protocols. The divergent nature of this strategy was developed by altering the "order of addition" of a pair of olefinic-alcohol components to a pseudo-C_2-symmetric phosphoryl chloride. Future directions will focus on further diversification of the scaffolds by utilizing hydroxyl-directed transformations.

3.5: References cited:

[1] (a) Katz, L. Manipulation of Modular Polyketide Synthases. *Chem. Rev.* **1997**, *97*, 2557–2575; (b) Staunton, J.; Weissman, K. J. Polyketide biosynthesis: A millennium review. *Nat. Prod. Rep.* **2001**, *18*, 380–416; (c) Gupta, P.; Mahajan, N.; Taneja, S. C. Recent advances in the stereoselective synthesis of 1,3-diols using biocatalysts. *Catal. Sci. Technol.* **2013**, *3*, 2462–2480.

[2] (a) For a review on polyol synthesis, see: Bode, S. E.; Wolberg, M.; Mueller, M. Stereoselective synthesis of 1,3-diols. *Synthesis* **2006**, 557–588; (b) For a review on oxopolyene macrolide antibiotics, see: Rychnovsky, S. D. Oxo Polyene Macrolide Antibiotics. *Chem. Rev.* **1995**, *95*, 2021–2040.

[3] (a) Mori, Y.; Suzuki, M. Stereodivergent synthesis of 1,3-polyols. *Tetrahedron Lett.* **1989**, *30*, 4387–4388; (b) Zacuto, M. J.; Leighton, J. L. Divergent Synthesis of Complex Polyketide-Like Macrolides from a Simple Polyol Fragment. *Org.*

Lett. **2005**, *7*, 5525–5527; (c) Burke, M. D.; Schreiber, S. L. A planning strategy for diversity-oriented synthesis. *Angew. Chem., Int. Ed.* **2004**, *43*, 46–58.

[4] (a) Louie, J.; Bielawski, C. W.; Grubbs, R. H. Tandem Catalysis: The Sequential Mediation of Olefin Metathesis, Hydrogenation, and Hydrogen Transfer with Single-Component Ru Complexes. *J. Am. Chem. Soc.* **2001**, *123*, 11312–11313; (b) Scholte, A. A.; An, M. H.; Snapper, M. L. Ruthenium-Catalyzed Tandem Olefin Metathesis-Oxidations. *Org. Lett.* **2006**, *8*, 4759–4762; (c) Seigal, B. A.; Fajardo, C.; Snapper, M. L. Tandem Catalysis: Generating Multiple Contiguous Carbon-Carbon Bonds through a Ruthenium-Catalyzed Ring-Closing Metathesis/Kharasch Addition. *J. Am. Chem. Soc.* **2005**, *127*, 16329–16332; (d) Ferrie, L.; Bouzbouz, S.; Cossy, J. Acryloyl chloride: an excellent substrate for cross-metathesis. a one-pot sequence for the synthesis of substituted α,β-unsaturated carbonyl derivatives. *Org. Lett.* **2009**, *11*, 5446–5448.

[5] Wender, P. A.; Verma, V. A.; Paxton, T. J.; Pillow, T. H. Function-Oriented Synthesis, Step Economy, and Drug Design. *Acc. Chem. Res.* **2008**, *41*, 40–49.

[6] (a) Trost, B. M. Atom economy - a challenge for organic synthesis: homogeneous catalysis leads the way. *Angew. Chem., Int. Ed. Engl.* **1995**, *34*, 259–281; (b) Trost, B. M. The atom economy: a search for synthetic efficiency. *Science* **1991**, *254*, 1471–1477; (c) Young, I. S.; Baran, P. S. Protecting-group-free synthesis as an opportunity for invention. *Nat. Chem.* **2009**, *1*, 193–205.

[7] (a) Lipshutz, B. H.; Huang, S.; Leong, W. W. Y.; Isley, N. A. C-C Bond Formation via Copper-Catalyzed Conjugate Addition Reactions to Enones in Water at Room Temperature. *J. Am. Chem. Soc.* **2012**, *134*, 19985–19988; (b) Sheldon, R. A.; Arends, I. W. C. E.; Hanefeld, U. *Green Chemistry and Catalysis*; Wiley-VCH: Weinheim, **2007**, 1–47.

[8] (a) Ishikawa, H.; Suzuki, T.; Hayashi, Y. High-yielding synthesis of the anti-influenza neuramidase inhibitor (-)-oseltamivir by three "one-pot" operations. *Angew. Chem., Int. Ed.* **2009**, *48*, 1304–1307; (b) Ishikawa, H.; Honma, M.;

Hayashi, Y. One-Pot High-Yielding Synthesis of the DPP4-Selective Inhibitor ABT-341 by a Four-Component Coupling Mediated by a Diphenylprolinol Silyl Ether. *Angew. Chem., Int. Ed.* **2011**, *50*, 2824–2827; (c) Hayashi, Y.; Umemiya, S. Pot Economy in the Synthesis of Prostaglandin A1 and E1 Methyl Esters. *Angew. Chem., Int. Ed.* **2013**, *52*, 3450–3452.

[9] Schreiber, S. L. Target-oriented and diversity-oriented organic synthesis in drug discovery. *Science* **2000**, *287*, 1964–1969.

[10] (a) Paterson, I.; Scott, J. P. Laboratory emulation of polyketide biosynthesis: an iterative, aldol-based, synthetic entry to polyketide libraries using (R)- and (S)-1-(benzyloxy)-2-methylpentan-3-one, conformational aspects of extended polypropionates. *J. Chem. Soc., Perkin Trans. 1* **1999**, 1003–1014; (b) Feng, Y.; Pattarawarapan, M.; Wang, Z.; Burgess, K. Stereochemical Implications on Diversity in β-Turn Peptidomimetic Libraries. *J. Org. Chem.* **1999**, *64*, 9175–9177; (c) Wermuth, J.; Goodman, S. L.; Jonczyk, A.; Kessler, H. Stereoisomerism and Biological Activity of the Selective and Superactive $\alpha_v\beta_3$ Integrin Inhibitor cyclo(RGDfV) and Its Retro-Inverso Peptide. *J. Am. Chem. Soc.* **1997**, *119*, 1328–1335.

[11] (a) Reggelin, M.; Brenig, V. Towards polyketide libraries: iterative, asymmetric aldol reactions on a solid support. *Tetrahedron Lett.* **1996**, *37*, 6851–6852; (b) Patterson, I.; Scott, J. P. Polyketide library synthesis: iterative assembly of extended polypropionates using (R)- and (S)-1-(benzyloxy)-2-methylpentan-3-one. *Tetrahedron Lett.* **1997**, *38*, 7441–7444; (c) Paterson, I.; Temal-Laieb, T. Toward the Combinatorial Synthesis of Polyketide Libraries: Asymmetric Aldol Reactions with α-Chiral Aldehydes on Solid Support. *Org. Lett.* **2002**, *4*, 2473–2476; (d) Paterson, I.; Scott, J. P. Polyketide library synthesis: conformational control in extended polypropionates. *Tetrahedron Lett.* **1997**, *38*, 7445–7448.

[12] Peng, L. F.; Stanton, B. Z.; Maloof, N.; Wang, X.; Schreiber, S. L. Syntheses of aminoalcohol-derived macrocycles leading to a small-molecule binder to and inhibitor of Sonic Hedgehog. *Bioorg. Med. Chem. Lett.* **2009**, *19*, 6319–6325.

[13] Stanton, B. Z.; Peng, L. F.; Maloof, N.; Nakai, K.; Wang, X.; Duffner, J. L.; Taveras, K. M.; Hyman, J. M.; Lee, S. W.; Koehler, A. N.; Chen, J. K.; Fox, J. L.; Mandinova, A.; Schreiber, S. L. A small molecule that binds Hedgehog and blocks its signaling in human cells. *Nat. Chem. Biol.* **2009**, *5*, 154–156.

[14] Morton, D.; Leach, S.; Cordier, C.; Warriner, S.; Nelson, A. Synthesis of natural-product-like molecules with over eighty distinct scaffolds. *Angew. Chem., Int. Ed.* **2009**, *48*, 104–109.

[15] Gierasch, T. M.; Chytil, M.; Didiuk, M. T.; Park, J. Y.; Urban, J. J.; Nolan, S. P.; Verdine, G. L. A Modular Synthetic Approach toward Exhaustively Stereodiversified Ligand Libraries. *Org. Lett.* **2000**, *2*, 3999–4002.

[16] Harrison, B. A.; Verdine, G. L. The Synthesis of an Exhaustively Stereodiversified Library of cis-1,5 Enediols by Silyl-Tethered Ring-Closing Metathesis. *Org. Lett.* **2001**, *3*, 2157–2159.

[17] Shi, Z.; Harrison, B. A.; Verdine, G. L. Unpredictable Stereochemical Preferences for Mu Opioid Receptor Activity in an Exhaustively Stereodiversified Library of 1,4-Enediols. *Org. Lett.* **2003**, *5*, 633–636.

[18] (a) Whitehead, A.; McReynolds, M. D.; Moore, J. D.; Hanson, P. R. Multivalent Activation in Temporary Phosphate Tethers: A New Tether for Small Molecule Synthesis. *Org. Lett.* **2005**, *7*, 3375–3378; (b) Thomas, C. D.; McParland, J. P.; Hanson, P. R. Divalent and Multivalent Activation in Phosphate Triesters: A Versatile Method for the Synthesis of Advanced Polyol Synthons. *Eur. J. Org. Chem.* **2009**, 5487–5500.

[19] Waetzig, J. D.; Hanson, P. R. Temporary Phosphate Tethers: A Metathesis Strategy to Differentiated Polyol Subunits. *Org. Lett.* **2006**, *8*, 1673–1676.

[20] (a) Venukadasula, P. K. M.; Chegondi, R.; Maitra, S.; Hanson, P. R. A Concise, Phosphate-Mediated Approach to the Total Synthesis of (–)-Tetrahydrolipstatin. *Org. Lett.* **2010**, *12*, 1556–1559; (b) Chegondi, R.; Tan, M. M. L.; Hanson, P. R. Phosphate tether-mediated approach to the formal total synthesis of (–)-salicylihalamides A and B. *J. Org. Chem.* **2011**, *76*, 3909–3916; (c) Hanson, P. R.; Chegondi, R.; Nguyen, J.; Thomas, C. D.; Waetzig, J. D.; Whitehead, A. Total synthesis of dolabelide C:A phosphate-mediated approach. *J. Org. Chem.* **2011**, *76*, 4358–4370; (d) Jayasinghe, S.; Venukadasula, P. K. M.; Hanson, P. R. An Efficient, Modular Approach for the Synthesis of (+)-Strictifolione and a Related Natural Product. *Org. Lett.* **2014**, *16*, 122–125.

[21] Venukadasula, P. K. M.; Chegondi, R.; Suryn, G. M.; Hanson, P. R. A Phosphate Tether-Mediated, One-Pot, Sequential Ring-Closing Metathesis/Cross-Metathesis/Chemoselective Hydrogenation Protocol. *Org. Lett.* **2012**, *14*, 2634–2637.

[22] (a) Chegondi, R.; Maitra, S.; Markley, J. L.; Hanson, P. R. Phosphate-Tether-Mediated Ring-Closing Metathesis for the Preparation of Complex 1,3-anti-Diol-Containing Subunits. *Chem. - Eur. J.* **2013**, *19*, 8088–8093; (b) Maitra, S.; Markley, J. L.; Chegondi, R.; Hanson, P. R. Phosphate Tether-Mediated Ring-Closing Metathesis for the Generation of Medium to LargeBicyclo[n.3.1]phosphates *Tetrahedron* **2015**, *ASAP*.

[23] (a) Kingsbury, J. S.; Harrity, J. P. A.; Bonitatebus, P. J., Jr.; Hoveyda, A. H. A Recyclable Ru-Based Metathesis Catalyst. *J. Am. Chem. Soc.* **1999**, *121*, 791–799; (b) Garber, S. B.; Kingsbury, J. S.; Gray, B. L.; Hoveyda, A. H. Efficient and Recyclable Monomeric and Dendritic Ru-Based Metathesis Catalysts. *J. Am. Chem. Soc.* **2000**, *122*, 8168–8179; (c) Gessler, S.; Randl, S.; Blechert, S. Synthesis and metathesis reactions of a phosphine-free dihydroimidazole carbene ruthenium complex. *Tetrahedron Lett.* **2000**, *41*, 9973–9976.

[24] (a) Myers, A. G.; Zheng, B.; Movassaghi, M. Preparation of the Reagent o-Nitrobenzenesulfonohydrazide. *J. Org. Chem.* **1997**, *62*, 7507; (b) Buszek, K. R.;

Brown, N. Improved Method for the Diimide Reduction of Multiple Bonds on Solid-Supported Substrates. *J. Org. Chem.* **2007**, *72*, 3125–3128; (c) Haukaas, M. H.; O'Doherty, G. A. Enantioselective Synthesis of 2-Deoxy- and 2,3-Dideoxyhexoses. *Org. Lett.* **2002**, *4*, 1771–1774.

Chapter 4

Phosphate tether-mediated approach towards
the synthesis of the C9–C25 fragment of spirastrellolide B

4.1: Introduction

Marine invertebrates are excellent sources of antimitotic secondary metabolites that contain a range of structural diversity such as found in polyketides, cycle peptides, terpenoids and cyclic ketones. Some representative examples of such antimitotic secondary metabolites are discodermolide, dolastatin-10, laulimalide, eleutherobin, halichondrin B, peloruside, vitilevuamide, spongistatin, and hemiasterlin.[1,2] The use of antimitotic drugs that are based on natural products, such as the taxane (paclitaxel and docetaxel) and Vinca alkaloid (vincristine, vinblastine, vinorelbine) families in cancer treatment, has inspired the search for additional natural products that show similar antimitotic activities. The spirastrellolides are a class of such secondary metabolites that show potent activity in a cell-based antimitotic assay.[3] Interest in the development of methods towards polyketide natural products has inspired efforts towards this goal. This chapter provides our initial efforts towards the synthesis of the C9–C25 fragment of spirastrellolide B.

4.1.1: Overview of the spirastrellolides family

Spirastrellolide A is the first member of the family and was isolated in 2003 by Anderson and coworkers from the extracts of the Caribbean marine sponge *Spirastrella coccinea* (Figure 4.1).[4] The key structural features of the macrolide include a 47-carbon linear polyketide backbone, a highly functionalized 38-membered lactone that contains a tetrahydropyran, and two spiro-bispyran substructures embedded in the macrocycle, as well as a side chain-containing carboxylic acid. In terms of biological activity, spirastrellolide A methyl ester **4.1.1A** exhibited potent activity (IC_{50} 100 ng/mL) in a

cell-based (human carcinoma MCF-7 cells) antimitotic assay.[3] Typically, antimitotic macrolides act by preventing tubulin polymerization (formation of microtubules), a necessary element for cell division.[5] However, the antimitotic activity of spirastrellolide A is not caused by interference with tubulin polymerization, but rather has been found to be a potent inhibitor of protein phosphatase 2A (IC_{50} = 1*n*M).[6] In addition, spirastrellolide A has been shown to accelerate the premature entry of cells into mitosis.[6]

In 2007, Anderson and coworkers isolated spirastrellolide B from the same extract, and confirmed the absolute configuration of the macrocyclic core of the spirastrellolides using X-ray crystallographic data of the degradation product of spirastrellolide B.[7] Additional family members, methylspirastrellolides C–G, were isolated from a *S. coccinea* extract in 2007, and among them, methylspirastrellolide C–E were tested in a cell-based assay for premature mitosis.[8] The IC_{50} values were found to be 0.4, 0.7, and 0.7 μM, respectively, which are comparable to that of methylspirastrellolide A (IC_{50} = 0.4 μM).[8] In addition, the absolute stereochemistry of C46 was unambiguously determined based on chiral GC analysis of methylspirastrellolide D.[8]

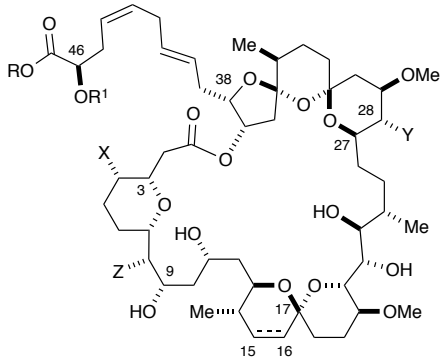

Figure 4.1. *Spirastrellolides A–G.*

4.1.2: Spirastrellolides and other PP2A inhibitors

The reversible phosphorylation of proteins containing hydroxyl group bearing amino acids such as serine, threonine and tyrosine represents one of the fundamental mechanisms by which crucial cellular processes are regulated.[9] The mechanism can involve changes in protein conformation, protein-protein interaction, protein-ligand interaction, membrane permeability and solute gradients among others.[9] The phosphorylation process is catalyzed by protein kinases (PKs), and the reverse process of dephosphorylation is catalyzed by protein phosphatases (PPs) (Figure 4.2). There are different classes/types of phosphatases known to be present on eukaryotic cells, based on the substrate specificity, metal-ion dependency, and biochemical assay categorizations.[10] Irregularities in protein phosphorylation is known to contribute to many human diseases such as cancer and diabetes.[11] Therefore it is imperative to identify inhibitors of phosphatases in order to understand their role in such biological problems and aid in detecting potential drug targets.

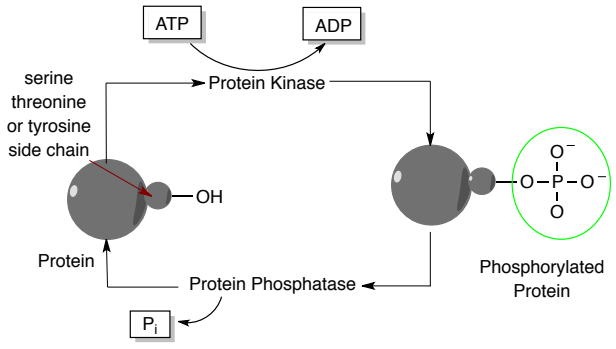

Figure 4.2. *Reversible Phosphorylation of Phosphatases and Kinases.*

In 2001, Wipf and coworkers designed a library of protein Serine/Threonine phosphatase (PSTPase) inhibitors based on the structure-activity-relationship studies for the natural-product inhibitors and a pharmacophore model was proposed to summarize the important features of such inhibitors (Figure 4.3).[12] According to this model, the presence of a carboxylate or a phosphate group, a hydrophobic backbone, and H-bond donors and acceptors in an appropriate array, are crucial for strong and selective binding.

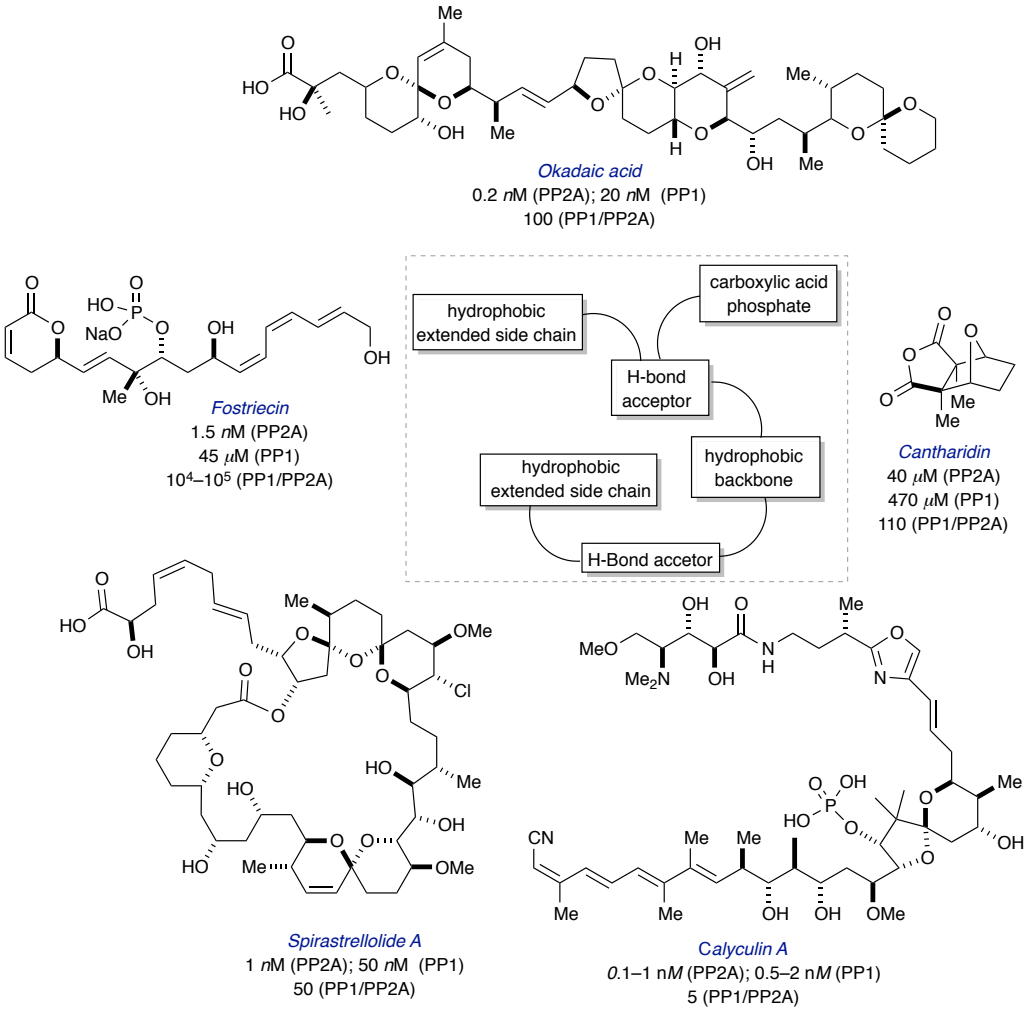

Figure 4.3. *Phamacophore model developed by Wipf and coworkers for PP1 and PP2A inhibitors: Ser/Thr protein phosphatase inhibitor natural products.*

There are many selective small molecule natural product inhibitors reported in the literature that are promising targets because of their ability to mimic and/or complement small areas of the protein-protein interaction while avoiding problems faced by common peptide inhibitors (high molecular weight, poor permeability, hydrolytic instability and isolation issues). Some representative examples of small molecule inhibitors of PP1 or PP2A, are the Fostriecin, Spirastrellolide A, Calyculin A and Okadaic classes of inhibitors, as shown in Figure 4.3. Structually, all of naturals products shown in the Figure 4.3 belong to polyketide-class of phosphatase inhibitor— except for Cantharidin, which is a terpenoid class of natural product inhibitors.[13]

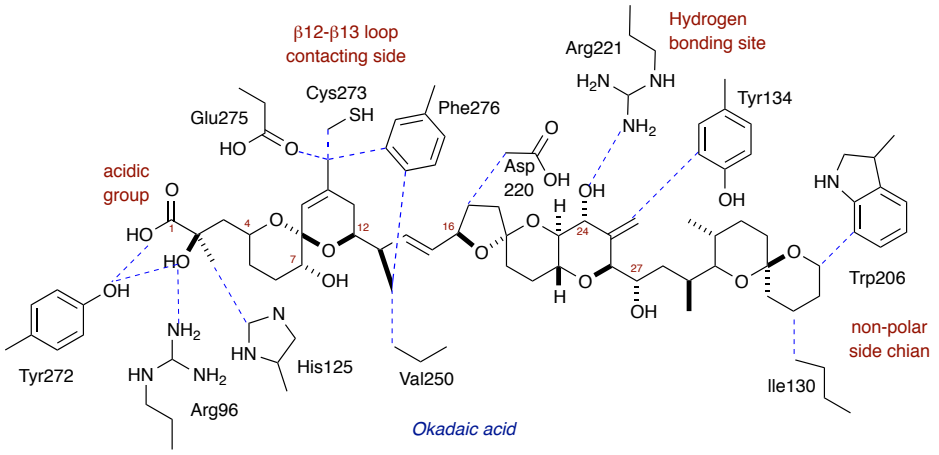

Figure 4.4. *Active site of PP1•OA complex.*

Okadaic acid (OA), isolated from marine sponges *Halichondria okadai* and *Halichondria melanodocia*, was one of the first small molecules to be isolated among the protein phosphatase inhibitors and studied extensively.[14] In 2001, Holmes and coworkers reported the crystal structure of OA bound to protein phosphatase-1 (Figure 4.4).[15] The

crystal structure revealed that the acidic group present in OA resided in a hydrophobic groove adjacent to the active site of the protein and interacts with the basic residues within the active site. In addition, it was also observed that OA existed as pseudo-cyclic shape in which the C24 hydroxyl group has hydrogen bonding with the C1 carboxylic acid group. For spirastrellolide A, no correlation of structure and biological activity (PP2A inhibition activity) has been reported yet. But a crude comparison of spirastrellolide A with okadaic acid (OA)[16] reveals the presence of similar functionalities in both molecules (Figure 4.5). It should be noted that the structural comparison alone, might be an oversimplification in terms of identifying the pharmacophore present in spirastrellolide A. However, synthetic studies towards the spirastrellolide family, in which subtle manipulation of functionalities could be incorporated to provide SAR, would generate useful information regarding the PP2A inhibition mechanism involving spirastrellolide A.

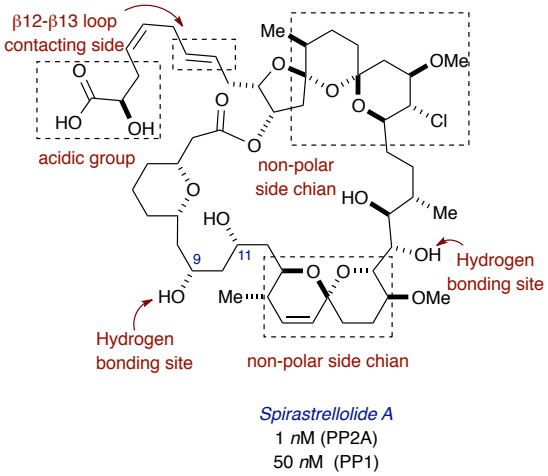

Figure 4.5. *Spirastrellolide A*.

Spirastrelloide B, isolated in 2007, contains a challenging framework including a

38-membered macrolactone and a bicyclic and a tricyclic spiroacetal unit.[17] In 2012, both of the family members, spirastrellolides A and B, were reisolated as free acids from a marine sponge *Epipolasis sp.* and tested against *HeLa* cancer cell lines. The IC_{50} values of the free acids of spirastrellolides A and B were found to be 20 and 40 *n*M respectively, comparable to the corresponding methyl ester of spirastrellolide A and B which exhibited IC_{50} values of 30 *n*M and 70 *n*M, respectively.[18]

4.2: Synthetic efforts towards spirastrellolides

The interesting biological activity and novel structural features of spirastrellolides has inspired many synthetic efforts towards spirastrellolides A, B, E and F.[19] The total synthesis of spirastrellolide A was accomplished by both the Fürstner and the Paterson groups.[20,21,22] For the purpose of this chapter, only the key features of the synthetic studies towards the southern hemisphere fragments will be discussed.

4.2.1: Paterson group's synthesis of the C1–C25 fragment of spirastrellolide A

Due to the lack of X-ray crystal data, the stereocenters at C3, C7, C9–C24, C27–C38 and C-46 of methylspirastrellolide A were not unambiguously assigned until the isolation of spirastrellolide B in 2007.[7] Therefore, synthetic studies before 2007 were focused on generating all possible stereoisomers. The Paterson group demonstrated a monumental effort towards this challenge by producing diastereomers of the southern fragments through the development efficient and convergent synthetic strategies (Figure 4.6).[20a,b,c] All of the syntheses from the Paterson group included elegant boron-mediated

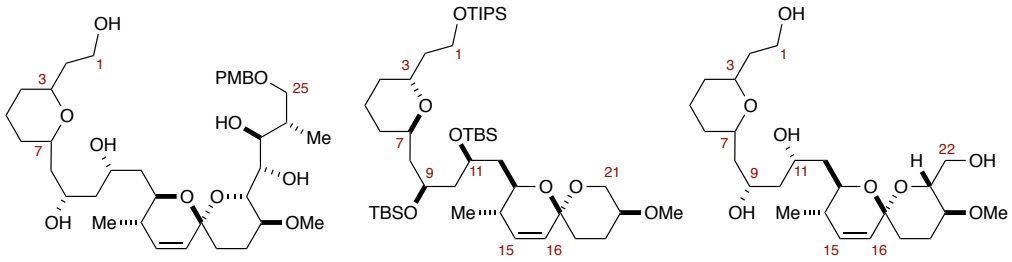

C1–C25 diastereomers (containing C3, C7-*cis*-disubstituted teterahedropyran) of methylspirastrelolide A
Org. Lett. **2005**, *7*, 4125–4128.

C1-C21 of methylspirastrelolide A
Synthesis **2005**, 3225–3228.

C1–C22 diastereomers (containing C3, C7-*cis*-disubstituted teterahedropyran) of methylspirastrelolide A
Chem. Commun. **2007**, 1852–1854.

Figure 4.6. *Diastereomeric fragments of the southern hemisphere of methylspirastrellolide A synthesized by Paterson and coworkers.*

asymmetric aldol and allylation strategies to construct key fragments. Since similar strategies have been utilized for the fragments, as well as the total synthesis, only one of the full reports on the synthesis of the southern hemisphere by the Paterson group is described herein.

In 2005, Paterson and coworkers reported the synthesis of two diastereomeric C1–C25 fragments of spirastrellolide A (Scheme 4.1–4.2).[20b] A late stage union of two key fragments, the C1–C16 alkyne fragment and the C17–C25 aldehyde fragment, was established to access the open chain precursor prior to spirocyclization. Both of the fragments were efficiently synthesized utilizing boron-mediated asymmetric allylation and aldol methods.

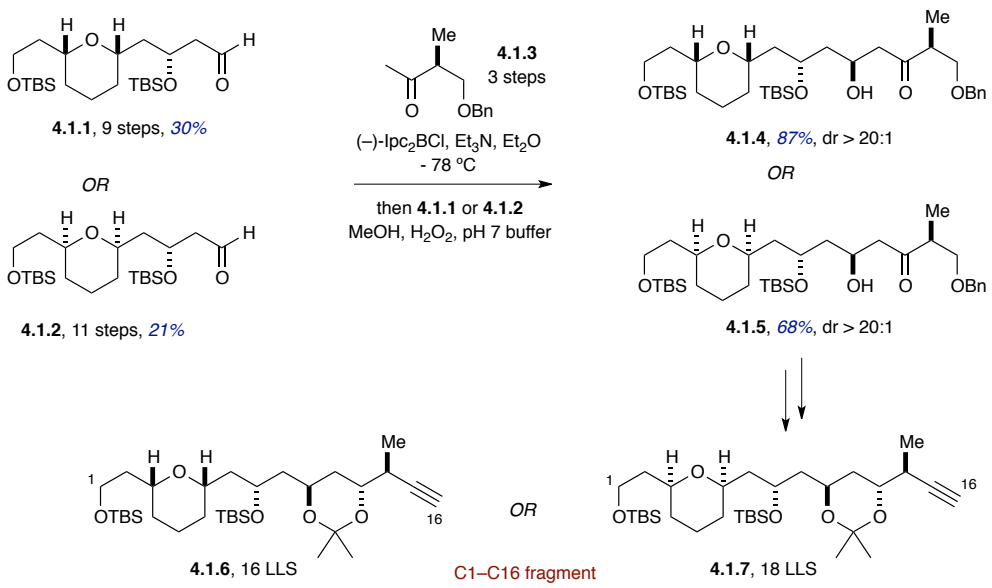

Scheme 4.1. *Paterson's synthesis of the C1–C16 fragment of spirastrellolide A.*

A boron-mediated aldol reaction of ethyl ketone **4.1.3** separately with aldehyde **4.1.1** or **4.1.2** was employed to generate β-hydroxy keto products **4.1.4** and **4.1.5** in excellent yields and diastereoselectivities (Scheme 4.1).[23] The aldol products **4.1.4** and **4.1.5** were later converted to diastereomeric alkyne fragments **4.1.6** and **4.1.7** over a few steps.

The synthesis of the C17–C25 fragment commenced with Brown allylation[24] of aldehyde **4.2.1,** followed by methylation, desilylation and oxidation to obtain aldehyde **4.2.2** (Scheme 4.2). Subsequent boron-mediated aldol reaction[23] provided keto compound **4.24,** which was further functionalized to generate the C17–C25 fragment **4.25** in 14 linear steps overall. The late stage coupling of two key intermediates, the C1–C16 alkyne fragment and the C17–C25 aldehyde fragment was achieved via lithiation of alkyne **4.1.6** or **4.1.7**, followed by addition to aldehyde **4.25,** providing the coupled

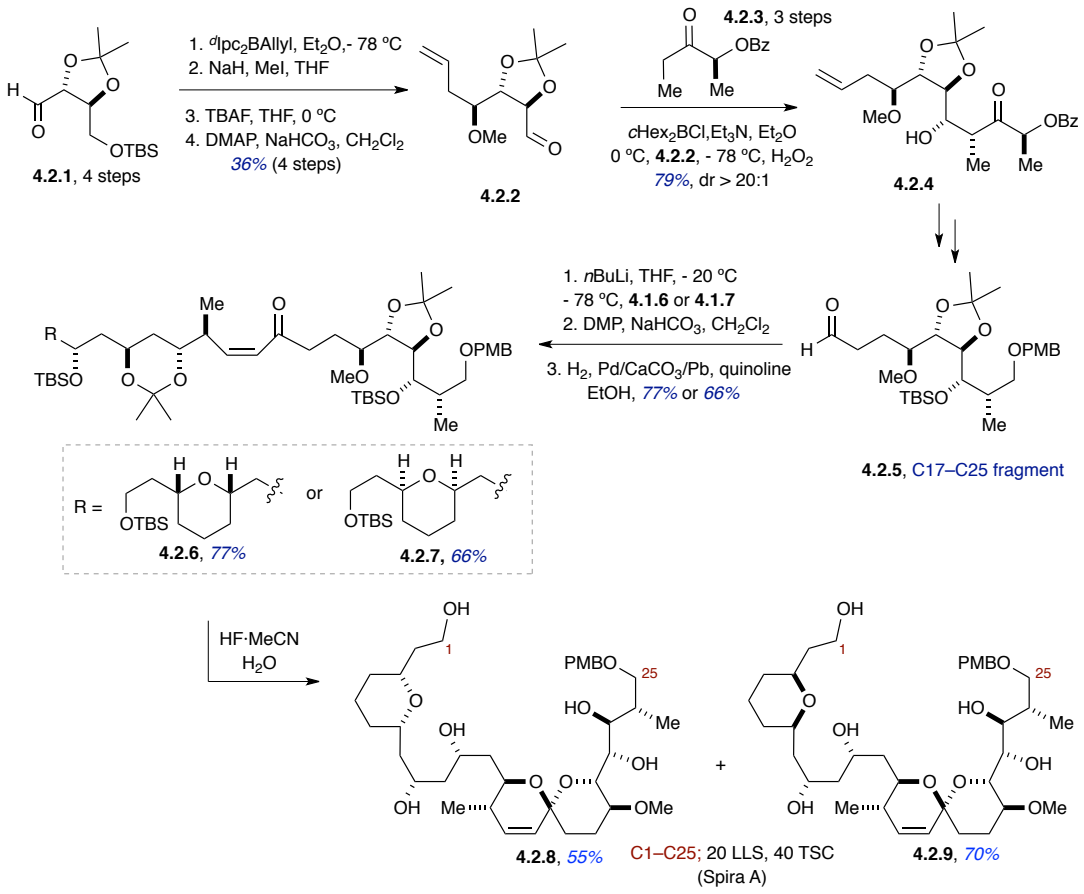

Scheme 4.2. *Paterson's synthesis of the two diastrereomeric C1–C25 fragments of spirastrellolide A.*

product in a 1:1 diastereomeric mixture at C17. Subsequent oxidation and Lindlar hydrogenation furnished (*Z*)-enones **4.26** and **4.27** in 77% and 66% yields, respectively, over 3 steps. The open-chain precursors **4.26** and **4.27** were then treated with HF•MeCN, which led to acetonide deprotection and desilylation, followed by spirocyclization, to provide a single diastereomer of spiroacetal **4.28** and **4.29**.

4.2.2: The Fürstner group synthesis of the C1–C24 fragments of spirastrellolide F and spirastrellolide A

The synthesis campaign by the Fürstner group towards spirostrellolides was first

reported in 2006.[25] As in the original approaches published by Paterson (*vide supra*), initial efforts by the Fürstner group were also focused on generating diastereomer of the southern fragments due to the ambiguity in assigning the absolute stereochemistry of the natural product. In 2006, Fürstner and coworkers reported the synthesis of two possible diastereomers of the C1–C25 fragment of spirastrellolide A (Figure 4.7). [25]

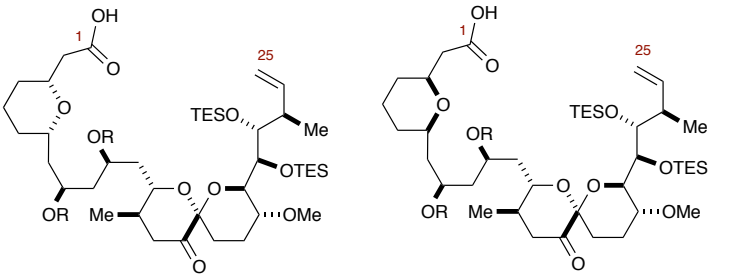

Figure 4.7. *Fürstner's synthesis of two diastereomeric C1–C25 fragments of methylspirastrellolide A.*

However, their first attempt at the total synthesis of spirastrellolide A was unsuccessful, and included the union of the southern fragment and the northern fragment via ring-closing metathesis (RCM).[26] The synthetic route was therefore revised, which required significant changes in the strategy for the construction of the southern fragment en route to the synthesis of southern hemisphere of spirastrellolide F, as described below in Scheme 4.3–4.4. [27]

The construction of the C1–C16 started with the modified Mukaiyama aldol reaction[28] of C11–C16 fragment **4.3.1** with silyl enol ether intermediate of the C1–C10 fragment **4.3.2** to provide the *β*-hydroxy keto product **4.3.3** in good yield and as a single

diastereomer. Further manipulations included 1,3-*anti* reduction following the Evans-Tischenko protocol,[29] the reduction of the ester (at C1), C-Si bond cleavage and persilylation to deliver the C1–C16 fragment **4.3.4** over 13 longest linear steps and overall 22 steps (Scheme 4.3).

The 2,3-*anti*-3,4-*syn* stereocenters of C17–C24 fragment **4.3.9** was established *via* a highly diastereoselctive glycolate aldol reaction[30] of aldehyde **4.3.5** with silyl ketene acetal **4.3.6** (Scheme 4.3).[31] Subsequent desilylation, protection of vicinal alcohols and

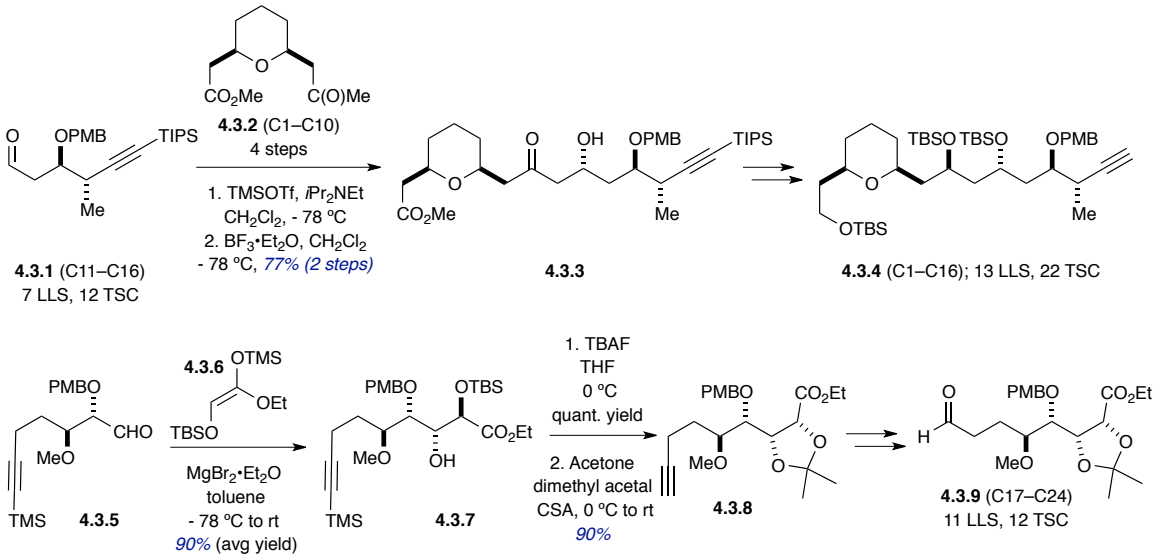

Scheme 4.3. *Fürstner synthesis of C1–C16 and C17–C24 fragments of spirastrellolide F.*

conversion of the alkyne terminus to the carbonyl group, produced C17–C24 fragment **4.3.9** efficiently over 11 longest linear steps and 12 total steps overall (Scheme 4.3).

The endgame towards the completion of the C1–C24 fragment included the lithiation of alkyne **4.3.4** and subsequent addition to aldehyde **4.3.9** to provide the key intermediate **4.4.1** in excellent yield (Scheme 4.4). Oxidation of the resultant alcohol in **4.4.1** produced the open chain precursor of the spirocycle **4.4.2**. Perhydrogenation of the

internal alkyne, PMB deprotection and subsequent spirocyclization were achieved in one single step by using $Pd(OH)_2$ in EtOAc. It should be noted that $Pd(OH)_2$ in EtOAc was found to be the only catalyst effective for this whole transformation in which the solvent EtOAc was believed to be the source of the trace amount of acid required for spirocyclization.

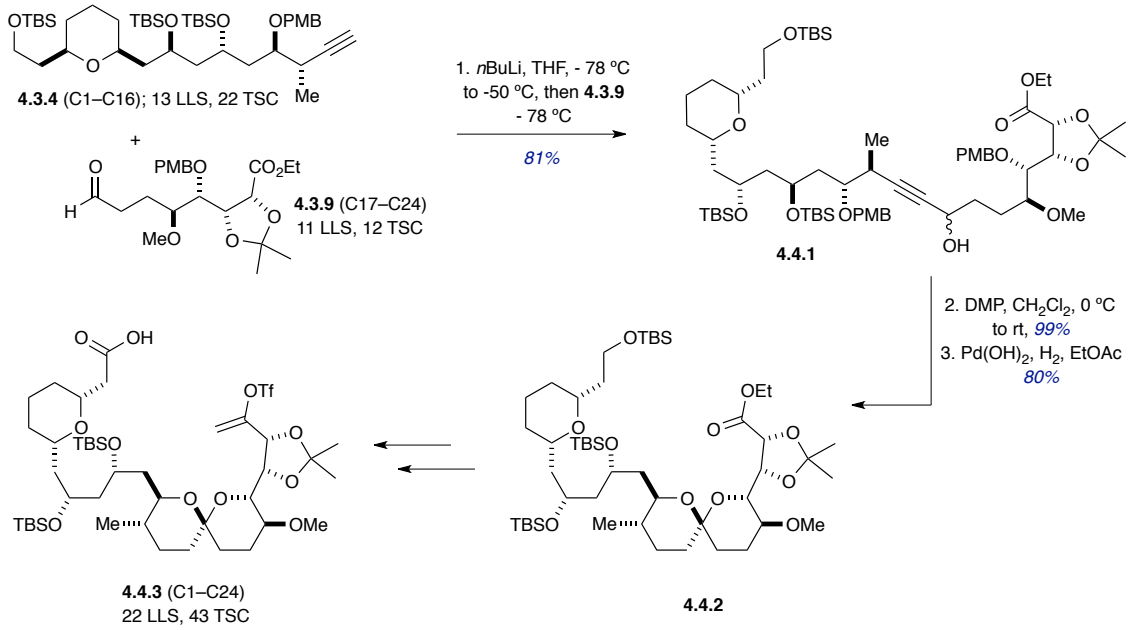

Scheme 4.4. *Endgame towards the synthesis of the C1–C24 fragment of spirastrellolide F by Fürstner and coworkers*.

In 2013, Fürstner and coworkers reported the total synthesis of spirastrellolide A methyl ester which encompassed a similar synthetic strategy to access the southern hemisphere, namely the C1–C24 fragment (Scheme 4.5).[32] The synthesis started with the union of methyl ketone **4.3.2**, the C1–C10 fragment and the aldehyde **4.5.1**, the C11–C16 fragment, *via* modified Mukaiyama aldol reaction.[28] This key bond formation was quite similar to the synthetic route for spirastrellolide F (described above); however, the aldehyde **4.5.1**, utilized in this strategy, contained a dithiane functional group, which served the dual purpose of being a functional handle to couple advanced fragments and also as a masked carbonyl that was revealed at a later stage of the synthesis to form the double bond in between C15 and C16. The southern fragment was further elaborated via the addition of dithiane **4.5.2** to the aldehyde **4.5.3**, the C17–C24 fragment, in the presence of a mixed metallic reagent to obtain the extended C1–C24 fragment **4.5.4** in excellent yield. Subsequent oxidation and PMB deprotection yielded the spirocyclic precursor, which upon the treatment with PPTS produced the spirocyclic intermediate albeit in modest yield mainly due to primary TBS deprotection (at C1). After reprotecting the primary alcohol at C1 in the presence of TBSOTf, the secondary alcohol at C24 was converted to enol triflate present in **4.5.6**. The endgame included deprotection of dithiane to reveal the carbonyl at C16 and subsequent oxidation of the primary alcohol (at C1) to carboxylic acid in a 2-step DMP/Pinnick oxidation protocol[33] to provide the C1–C24 fragment **4.5.7** over 26 linear steps.

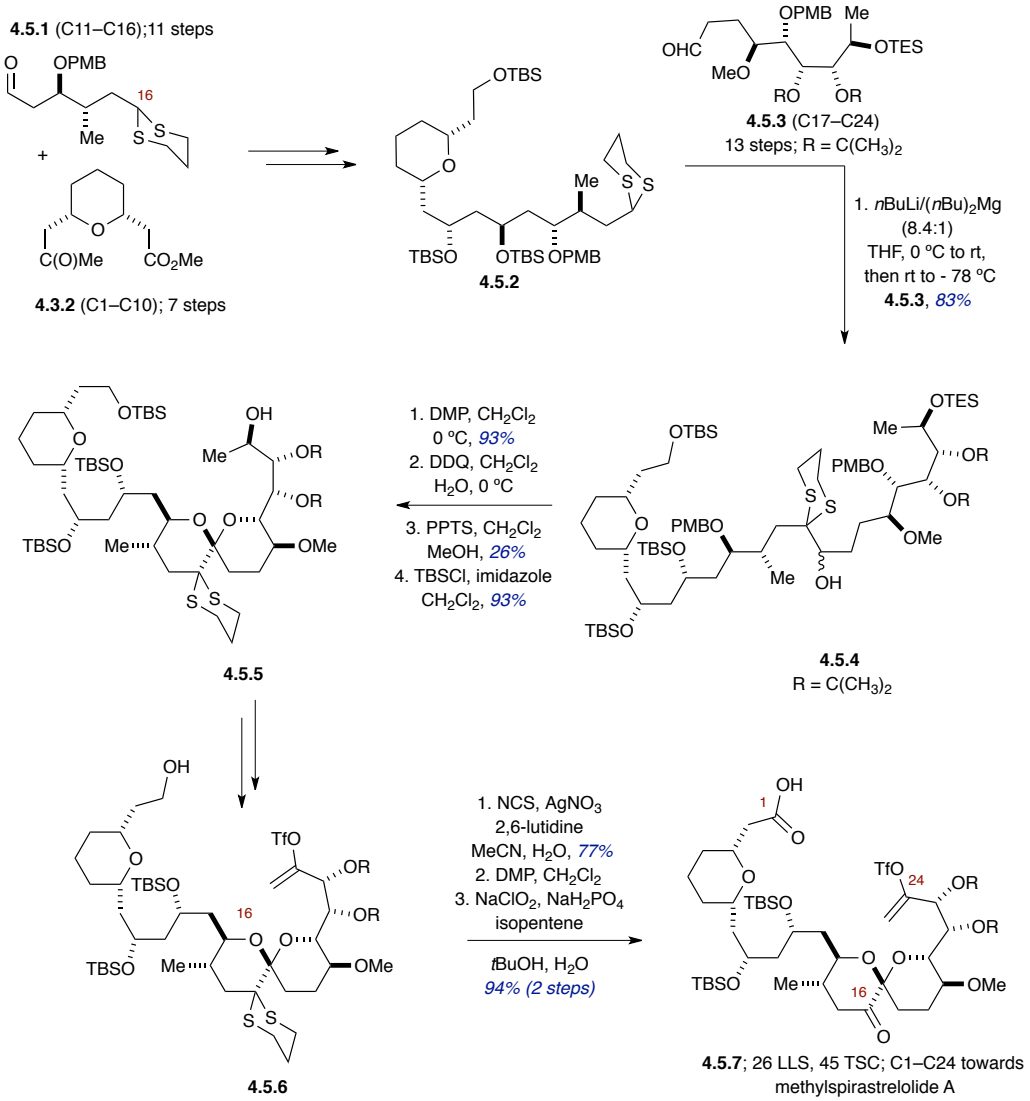

Scheme 4.5. *Fürstner's group synthesis of the C1–C24 fragment of methylspirastrellolide A.*

4.2.3: The Phillips group synthesis of the C1–C23 fragment of spirastrellolide B

In 2008, Phillips and coworkers reported the synthesis of the C1–C23 fragment of spirastrellolide B utilizing Kulinkovich-cyclopropanol ring-opening strategy[34] twice for the key bond forming reactions (Scheme 4.6–4.7).[35] The desired cyclopropanol intermediate was generated from TBS-protected alcohol **4.6.1** by treating with cyclohexylmagnesium bromide in the presence of Ti(O*i*Pr)$_4$ (Scheme 4.6). The first Kulinkovich-cyclopropanol ring-opening,[34] was next performed by treating with NCS in

the presence of $Fe(NO_3)_2$ and DBU to produce the corresponding enone, which was cyclized to pyran **4.6.2** over five steps. Mukaiyama aldol reaction between pyran **4.6.2** and aldehyde **4.6.3**, synthesized over six steps, yielded a β-hydroxyketo intermediate, which was diastereoselectively reduced in the presence of Li(*t*BuO)$_3$AlH. Subsequent TBS protection of the resulting alcohol generated the C1–C16 fragment **4.6.5**.

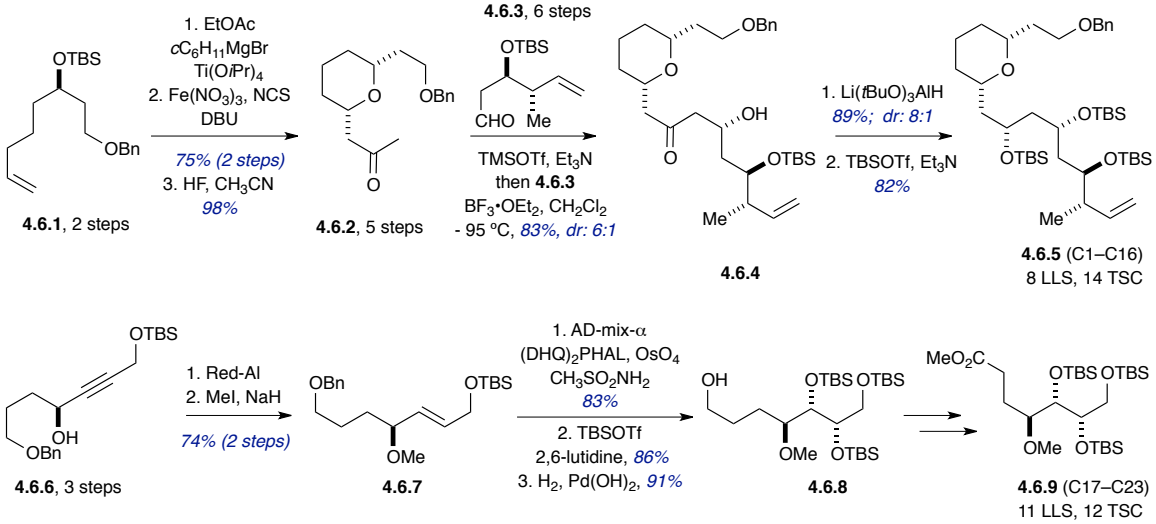

Scheme 4.6. *Philip's synthesis of the C1–C16 and C17–C24 fragments of spirastrellolide B.*

The synthesis of the C17–C23 fragment **4.6.9** started with the reduction and protection of propargylic alcohol **4.6.6** to generate the protected (*E*)-substituted allylic alcohol **4.6.7** in 74% yield (Scheme 4.6). Subsequent Sharpless asymmetric dihyroxylation, silylation and hydrogenolysis of the benzyl group generated the primary alcohol intermediate **4.6.8**. Further oxidation and methylation produced the desired methyl ester substrate **4.6.9**, the C17–C23 fragment over 11 longest linear steps.

The two key fragments were next united by utilizing a second Kulinkovich-cyclopropanol ring-opening strategy; for this purpose, ester **4.6.9** and alkene **4.6.5** were

subjected to Ti(*i*OPr)$_4$ and cyclohexylmagnesium bromide to generate the advanced cyclopropanol intermediate **4.7.1** in 90% yield (Scheme 4.7). Subsequent ring-opening in the presence of $Fe(NO_3)_2$ and Bu_3SnH to produce ketone **4.7.2** in 71% yield. Desilylation, along with spirocyclization in the presence of HF in MeCN and reprotection, delivered the spirocyclized product **4.7.3**, the C1–C23 fragment over 15 longest linear steps.

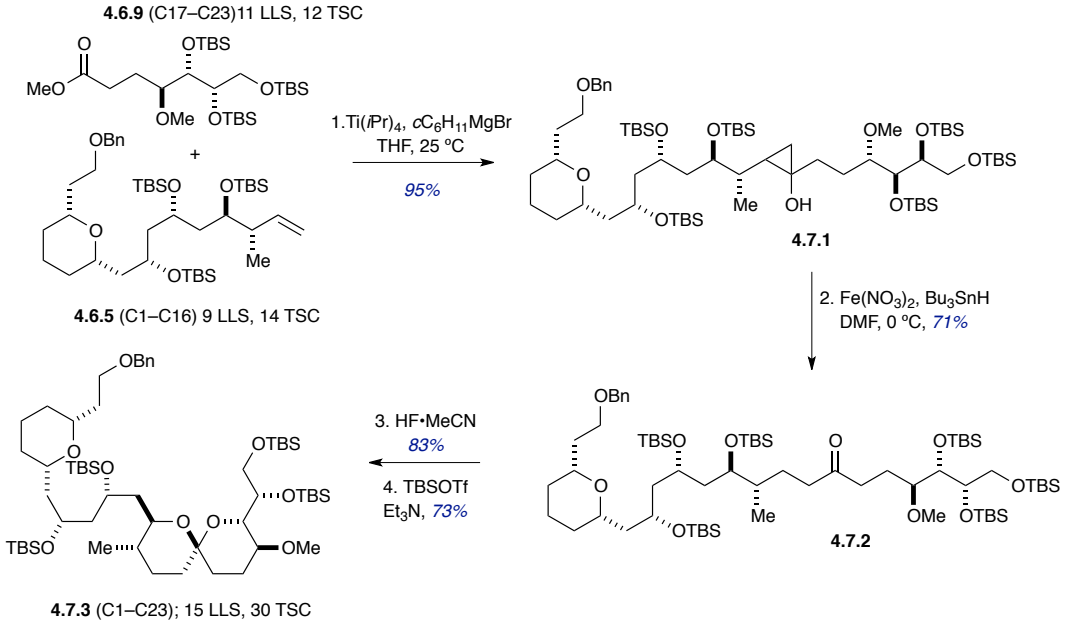

Scheme 4.7. *Endgame for the C1–C23 fragment of spirastrellolide B by Philips et. al.*

4.2.4: The Smith group synthesis of the C1–C25 fragments of spirastrellolide A, B and the C1–C24 fragment of spirastrellolide E

In 2007, Smith and coworkers reported the synthesis of the C1–C25 fragment of spirastrellolide A and later, in 2010, expanded the method to access the southern hemispheres of both A and B.[36] Both of the syntheses featured the elegant anion relay chemistry (ARC) developed by Smith and coworkers[37] to construct key building blocks

en route to the spirastrellolide family as described below in Scheme 4.8–4.9.

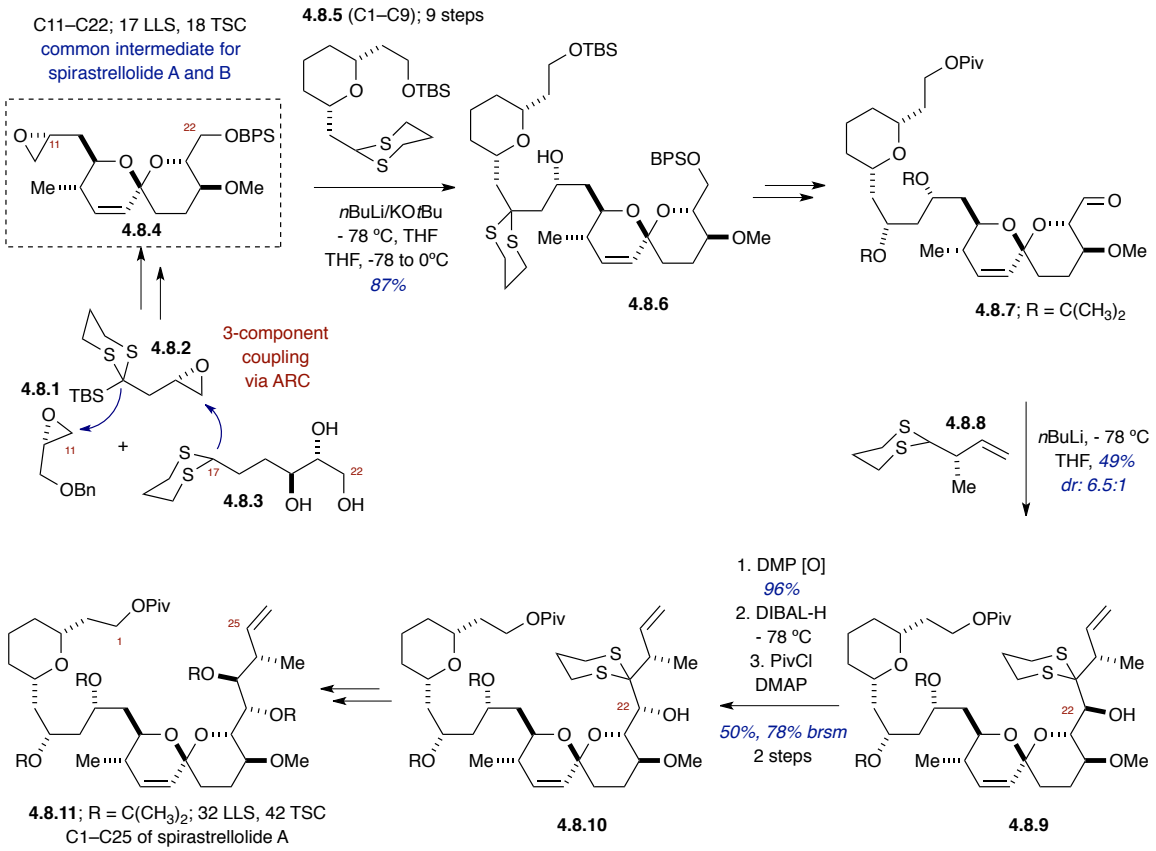

Scheme 4.8. *Synthesis of the C1–C25 fragment of spirastrellolide A by Smith and coworkers.*

The spirocycle–containing C11–C22 fragment **4.8.4** was synthesized by employing the ARC strategy to couple 3 synthons, epoxide **4.8.1**, dithiane-containing subunits **4.8.2** and **4.8.3** (Scheme 4.8). Subsequent treatment of dithiane **4.8.5** with the Schlosser base[38] and concomitant addition of epoxy-spirocycle intermediate **4.8.4** revealed the C1–C22 fragment **4.8.6** in 87% yield. This fragment was further converted the aldehyde **4.8.7** containing the C1–C22 framework. Next, the 4-carbon fragment **4.8.8**, the dithiane-containing C23–C26 fragment, was installed by treating **4.8.8** with *n*BuLi and subsequent addition to aldehyde **4.8.7** as per Honda's protocol.[39] However,

the major diastereomer **4.8.9** obtained from this reaction turned out to be the C22 epimer of the desired alcohol. The alcohol was then oxidized and reduced in the presence of DiBAL-H to produce a single diastereomer of the required alcohol via chelation controlled addition of hydride, and subsequent protection of the resultant alcohol furnished pivaloyl protected **4.8.10**, which was converted to the desired C1–C25 fragment **4.8.11** (Scheme 4.8). The synthetic sequence consisted of 33 longest linear steps and 43 overall steps.

In 2010, Smith and coworkers exploited a similar strategy to access the C1–C25 fragment of spirastrellolide B (Scheme 4.9).[36b] The synthetic sequence, consisting of 32 longest linear steps, involved similar bond disconnections, and heavily relied on ARC strategy to couple simple building blocks in an efficient manner to construct the key fragments. The only structural difference of the C1–C25 fragments of spirastrellolide A and B is the absence of internal double bond in the B ring of spiroacetal of spirastrellolide B. This factor was addressed earlier in the synthesis to investigate if the conformational change of the reduced spirocyclic product could be beneficial for improving the selectivity of desired alcohol formed by dithiane addition. Accordingly, the spiroacetal **4.9.1** was chemoselectively reduced in the presence of PtO_2. Subsequent introduction of the dithiane group **4.8.8** following Honda's protocol[39] furnished alcohol **4.9.3**, though as separable 1:1 diastereomeric mixture. This protocol was an improvement considering that the analogous unsaturated (at C15–C16) spirocyclic aldehyde **4.8.7** (Scheme 4.8), towards the synthesis of C1–C25 fragment of spirastrellolide A, provided the undesired isomer **4.8.9** in 6.5:1 ratio when subjected to the same reaction (Scheme 4.8). Subsequent oxidation-reduction sequence, dithiane removal, followed by chelation-

controlled 1,2-reduction revealed the eastern half of the fragment. Further, removal of benzyl groups and the use of Fraser-Reid tactic[40] generated epoxide **4.9.4**, which was then subjected to the addition of dithiane **4.9.5** to obtain fully functionalized, dithiane-containing C1–C25 fragment **4.9.6**. Removal of dithiane followed by reduction and subsequent protection generated the C1–C25 fragment **4.9.7** of spirostrellolide B.

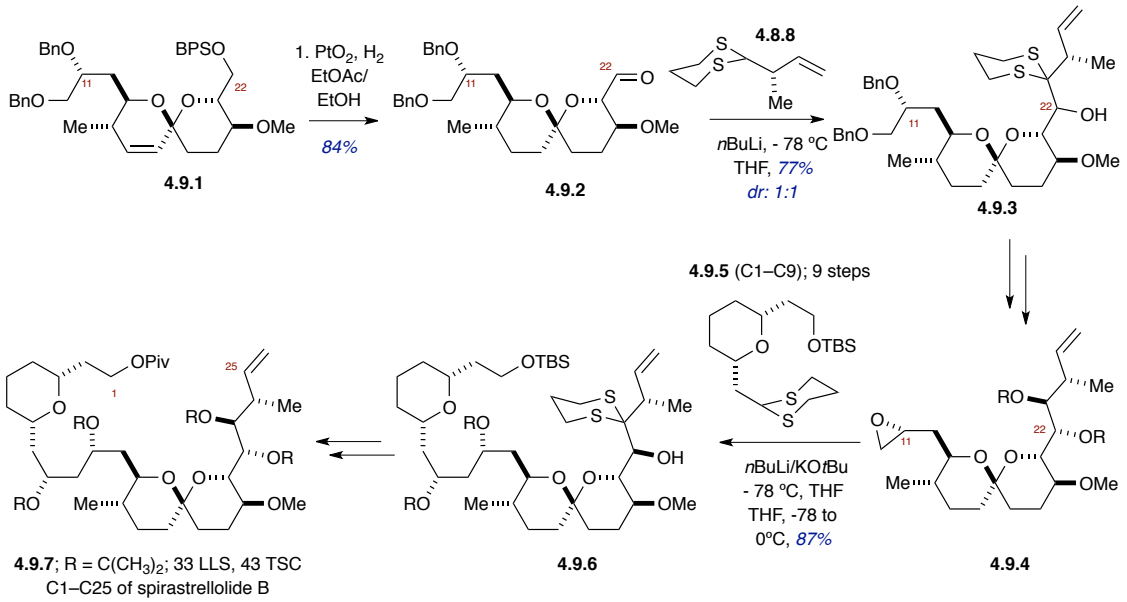

Scheme 4.9. *Synthesis of the C1–C25 fragment of spirastrellolide B by Smith and coworkers*.

In 2015, Smith and coworkers reported the synthesis of the C1–C24 fragment of spirastrellolide E by utilizing ARC strategy in conjunction with directed, regioselective gold-catalyzed alkyne functionalization (Scheme 4.10).[41] Lithiation of TBS-dithiane **4.10.1** and subsequent addition of epoxide **4.10.2** led to the generation of the intermediate lithium alkoxide, which underwent solvent-mediated Brook rearrangement in the presence of HMPA and epoxide **4.10.3** to furnish the 3-component adduct **4.10.4** in an impressive 68% yield.

Further manipulation generated aldehyde **4.10.5** over a few steps, which was then

subjected to addition of alkyne **4.10.6** in the presence of LDA to produce alcohol **4.10.7** in excellent yield (85%) as a mixture of diastereomers at C15 (Scheme 4.10).

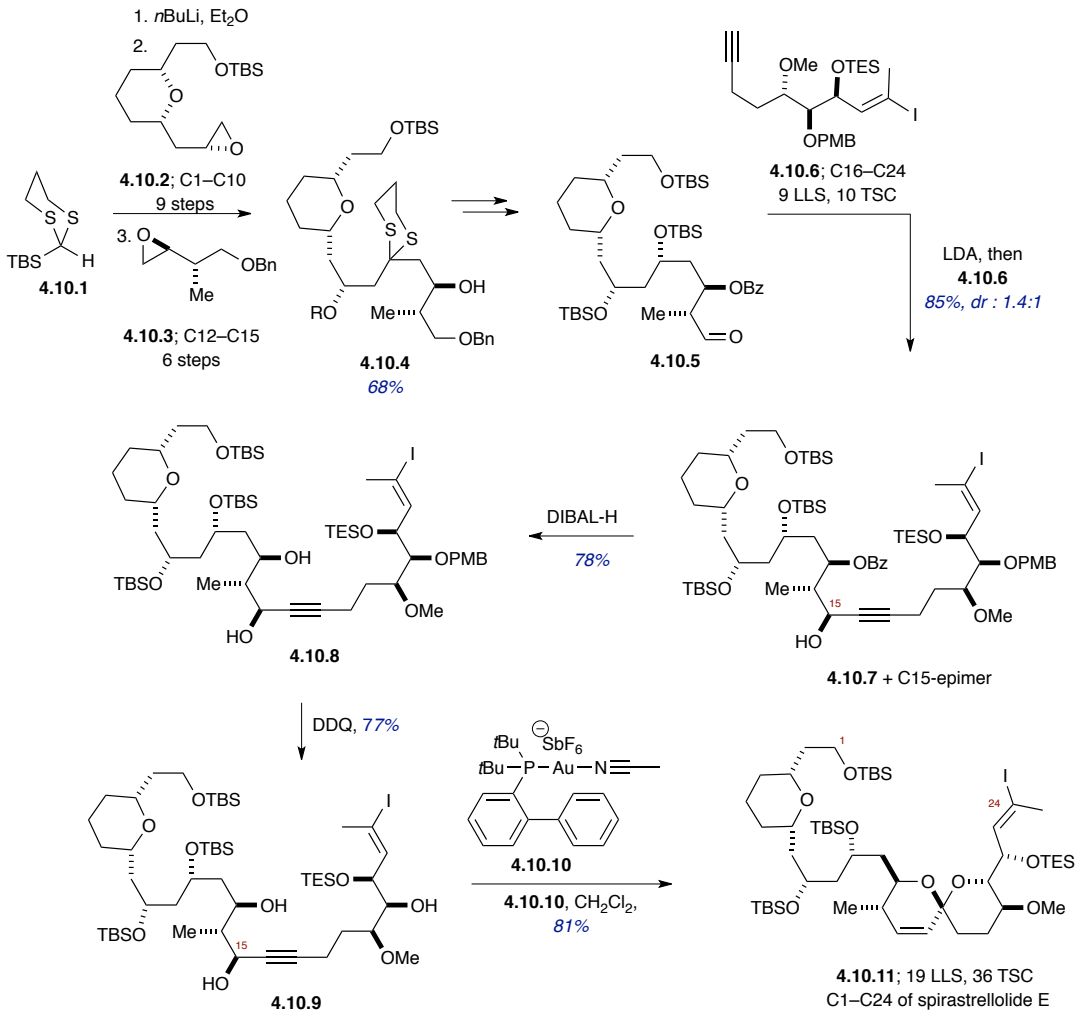

Scheme 4.10. *Synthesis of the C1–C24 fragment of spirastrellolide E by Smith and coworkers.*

The diastereomers were separated and treated with DIBAL-H and DDQ to remove the benzoyl and PMB groups, respectively to obtain triol **4.10.9**. When separately treated in the presence of the cationic gold reagent **4.10.10**, first developed by Echavarren and coworkers,[42] the *anti*-isomer (the stereochemistry referred to the relative orientation of the C13 and C15 hydroxyl group) underwent spirocyclization to produce

the desired C1–C24 fragment **4.10.11** of spirastrellolide E. Interestingly, the *cis*-isomer (C15-epimer of **4.10.9**) did not furnish the desired product. Overall, this second generation synthesis, consisting of 19 longest linear steps, provides a scalable, streamlined and modular route to access the advanced C1–C24 fragment of spirastrellolide E.

Shortly after this publication, Smith and coworkers reported a similar strategy towards the construction of the C1–C23 fragment of spirastrellolide E, in which mechanistic aspect of the gold-catalyzed, spirocyclization step was studied in detail (Scheme 4.11).[43] Following same synthetic strategy as discussed before, the addition of the lithiated C16–C23 fragment **4.11.1** to the aldehyde **4.10.5** generated alcohol **4.11.2** in 89% combined yield. Removal of benzoyl group followed by PMB deprotection produced the spirocyclization precursor triol **4.11.3** in excellent yield. The *anti*-isomer **4.11.3a** was subjected to spirocyclization in the presence of the cationic gold reagent **4.10.10** to generate the C1–C23 fragment **4.11.4** as reported before by Smith and coworkers towards the synthesis of the C1–C24 fragment of spirostrellolide E (Scheme 4.10).[41] Unlike the previous report, in which the *syn*-isomer did not furnish the desired spirocycle, the study of the crucial Au-catalyzed cyclization step, in this case facilitated the conversion of the *syn*-isomer to the desired spirocyclic product. The spirocyclization of the syn-isomer **4.11.3b** was achieved first by protecting both of hydroxyl group at C13 and C15 as acetonide and then by treating with AuCl and K_2CO_3 to obtain the spirocycle present in the C1–C23 fragment in 24% yield over 2 steps.

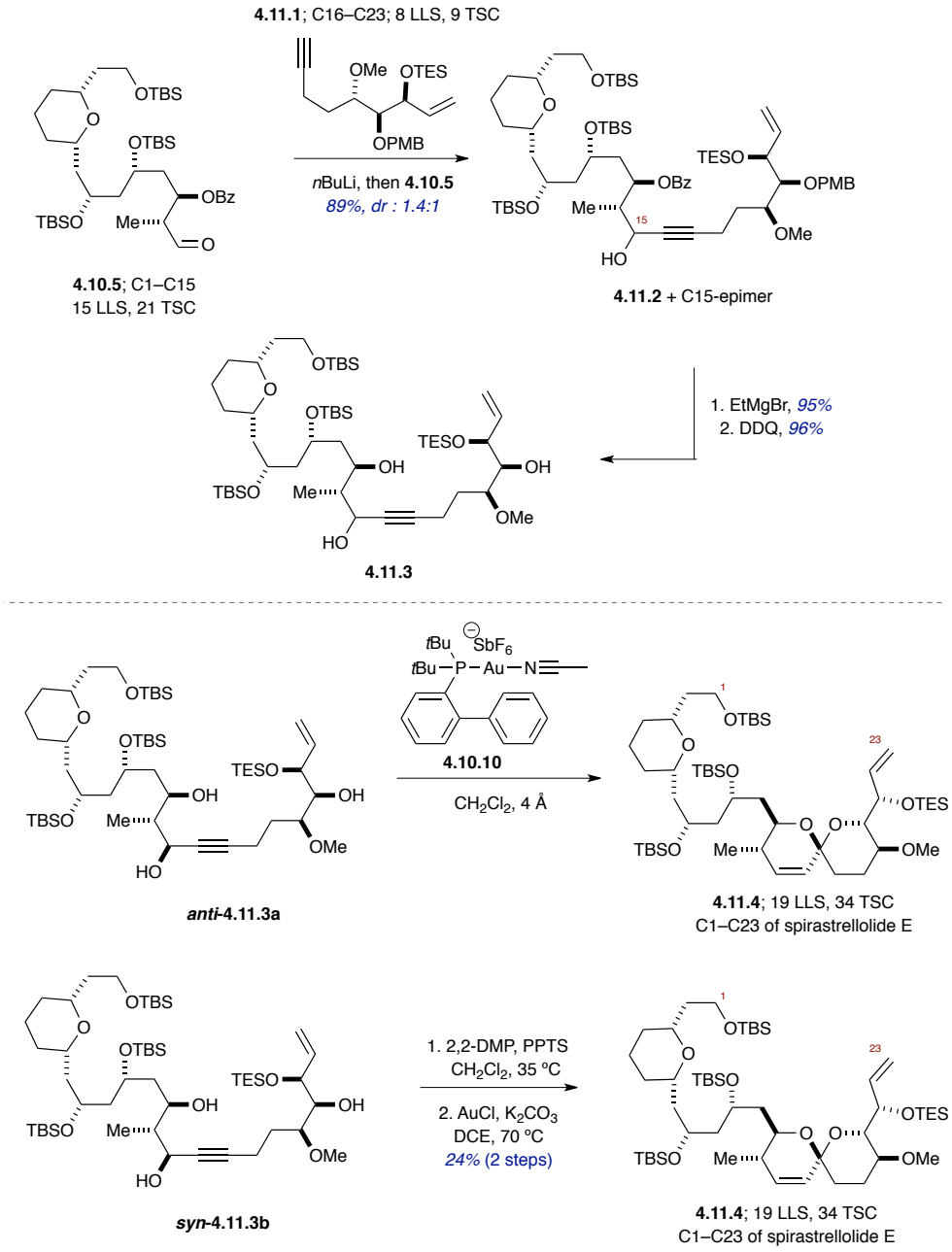

Scheme 4.11. *Study of gold-catalyzed spirocyclization en route to the C1–C23 fragment of spirastrellolide E by Smith and coworkers*.

4.2.5: The Hsung group synthesis of the C1–C23 fragment of spirastrellolide A

In 2006, Hsung and coworkers reported the synthesis of the C1–C16 fragment of spirastrellolide A (Scheme 4.12).[44] The epoxyalcohol **4.12.1**, synthesized over five steps

from 1,5-pentanediol, was subjected to directed reductive ring-opening, acetonide protection of the diol, debenzylation and Parikh-Doering oxidation (modified Moffat protocol)[45] to produce aldehyde **4.12.2**. The aldehyde was next converted to pyran **4.12.3** in excellent yield via Wittig olefination and subsequent deprotection followed by intramolecular *O*-1,4-addition. Pivaloyl protection of the primary alcohol present in pyran **4.12.3** followed by coupling with aldehyde **4.12.4** under Mukaiyama's condition[46] produced the C1–C16 fragments **4.12.5** and **4.12.6** in moderate yields and selectivity.

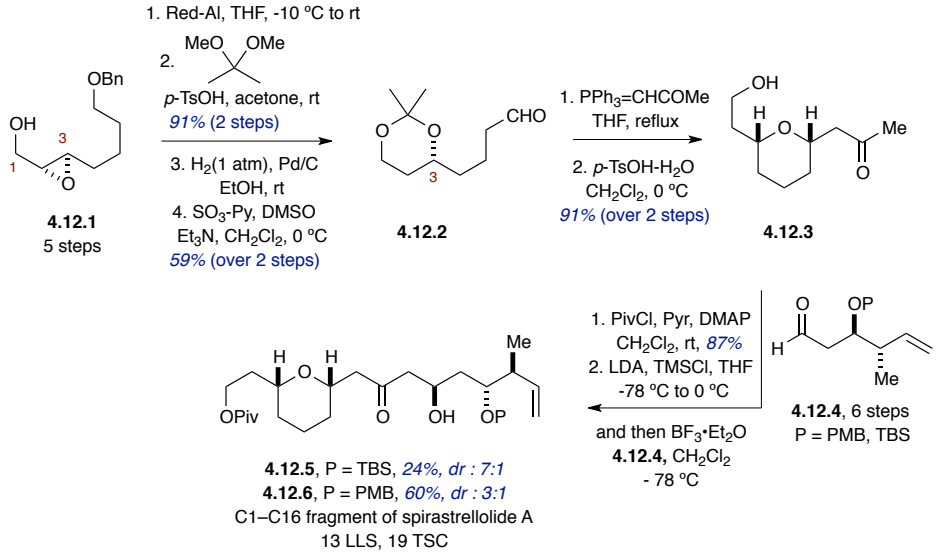

Scheme 4.12. *Hsung's synthesis of the C1–C16 fragment of spirastrellolide A.*

In 2005, Hsung and coworkers reported the synthesis of the C22 epimer of the C11–C23 fragment **4.13.6** of spirastrellolide A employing a ketal-tethered RCM strategy to construct the spirocycle (Scheme 4.13, also mentioned briefly in chapter 1).[47] Starting with substituted allylic alcohol **4.13.1**, synthesized from *D*-glucose over 8 steps, a linear strategy was followed to construct the key RCM precursor **4.13.5**. Protection of the secondary alcohol followed by deprotection of both TBS groups generated the corresponding diol, which was subjected to selective TBS protection of the primary

alcohol. Subsequent hydroboration-oxidation revealed diol **4.13.2** in 78% yield (over 3 steps). The generation of intermediate lactone (not shown in the scheme below) was performed by TEMPO oxidation followed by deprotection-protection of the C23 hydroxyl group as TBDPS ether. The later step was required, as the C23 TBS group did not survive the subsequent cyclic ketalization step. Addition of vinylmagnesium bromide to the lactone produced lactol **4.13.3** as single diastereomer in 73% yield. The key RCM precursor **4.13.5** was generated by the ketalization of lactol **4.13.3** with homoallylic alcohol **4.13.4** in the presence of the Bronsted acid Tf_2NH as a single isomer. When subjected to the **G-I** catalyst, **4.13.5** underwent RCM to produce the C22 epimer of the C11–C23 fragment **4.13.6** in 50% overall yield over two steps. Overall, the synthetic route, consisting of 18 longest linear steps and 21 total steps, demonstrated the utility of ketal tether-mediated RCM strategy to build complex spirocyclic core such as **4.13.6** (Scheme 4.13).

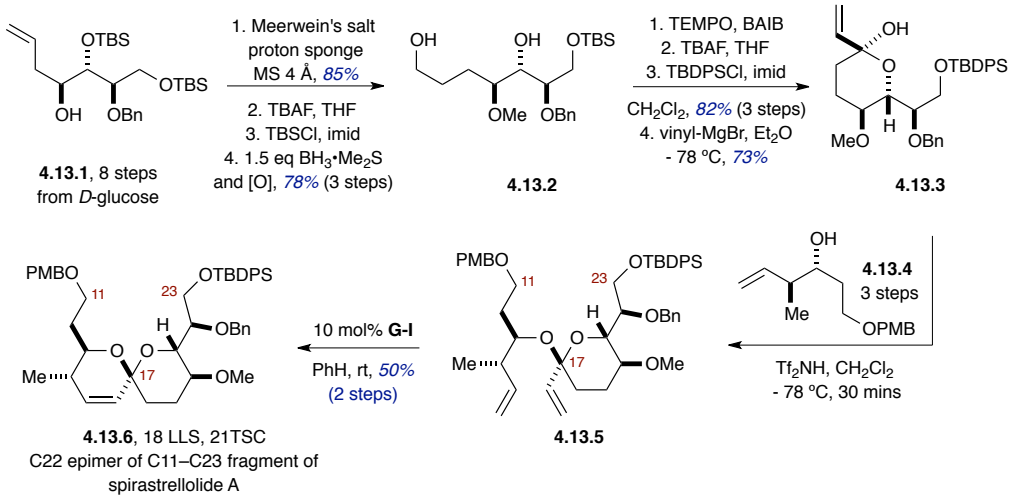

Scheme 4.13. *Hsung's synthesis of the C22 epimer of C11–C23 fragment of spirastrellolide A.*

In 2008, Hsung and coworkers reported the synthesis of the C1–C23 fragment **4.14.6**, which involved ketal tethered-RCM strategy to construct the spirocyclic key intermediate **4.14.2** and then a late-stage union of two key fragments **4.14.4** (C1–C10 fragment) and **4.14.3** (C11–C23) via Mukaiyama aldol reaction (Scheme 4.14).[48] This synthesis featured a streamlined and concise synthesis of the C11–C23 fragment **4.14.2** starting from (+)-2,3-(*O*)-iso-propylidene-L-threitol (**4.14.1**) as compared to the previously discussed synthesis reported in 2005.[47] Further deprotection of PMB group followed by Parikh-Doering oxidation[45] of **4.14.2** produced the coupling partner aldehyde **4.14.3** in 79% overall yield. Subsequent Mukaiyama aldol[46] reaction of aldehyde **4.14.3** and methyl ketone **4.14.4**,[44] synthesized over 12 steps, in the presence of stoichiometric amount of BF_3•Et_2O generated solely C11, C13-*anti*-diastereomer **4.14.5** in 62% yield. Directed reduction of **4.14.5** revealed diol in 68% yield with 3:1 *anti*/*syn* (C9 and C11) ratio. Acetonide protection of resulting diol generated the C1–C23 fragment **4.14.6** in overall 17 longest linear steps and 29 total steps.

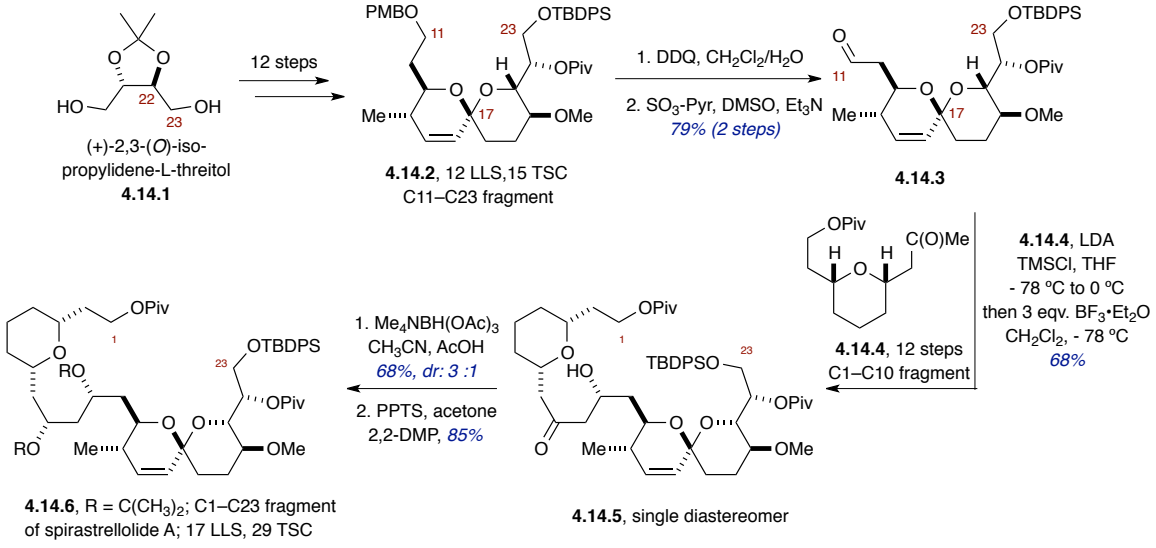

Scheme 4.14. *Hsung's synthesis of the C1–C23 fragment of spirastrellolide A.*

4.2.6: The Brabander group synthesis of the C1–C22 fragment of spirastrellolide A

In 2006, Brabander and coworkers reported the synthesis of two diastereomers of C1–C22 fragment of spirastrellolide A utilizing a late-stage, substrate-controlled, 1,3-*anti*-Mukaiyama aldol reaction[49] to couple two key fragments **4.15.5** and **4.15.6** (Scheme 4.15).[50] Initial efforts to construct spirocyclic intermediate **4.15.4** started with lithiation of alkyene **4.15.1** and subsequent addition of amide **4.15.2** to produce the coupling product **4.15.3** in 82% yield. Reduction of alkyne to the (*Z*)-alkene intermediate and acid-catalyzed spirocyclization in the presence of *p*-TsOH generated spirocyclic intermediate **4.15.4**. Aldehyde **4.15.5**, generated after Swern oxidation, was then subjected to substrate-controlled, 1,3-*anti*-Mukaiyama aldol reaction[49] with enantiomeric methyl ketones **4.15.6** and *ent*-**4.15.6**, separately, in the presence of TMSOTf and 2,6-lutidine to produce two diastereomers of β-hydroxy ketone **4.15.7**. Subsequent reduction to obtain 1,3-*anti*-diols[51] and PMB deprotection delivered the diastereomers of the C1–C22 fragment **4.15.8** of spirostrellolide A efficiently over 13-longest linear steps.

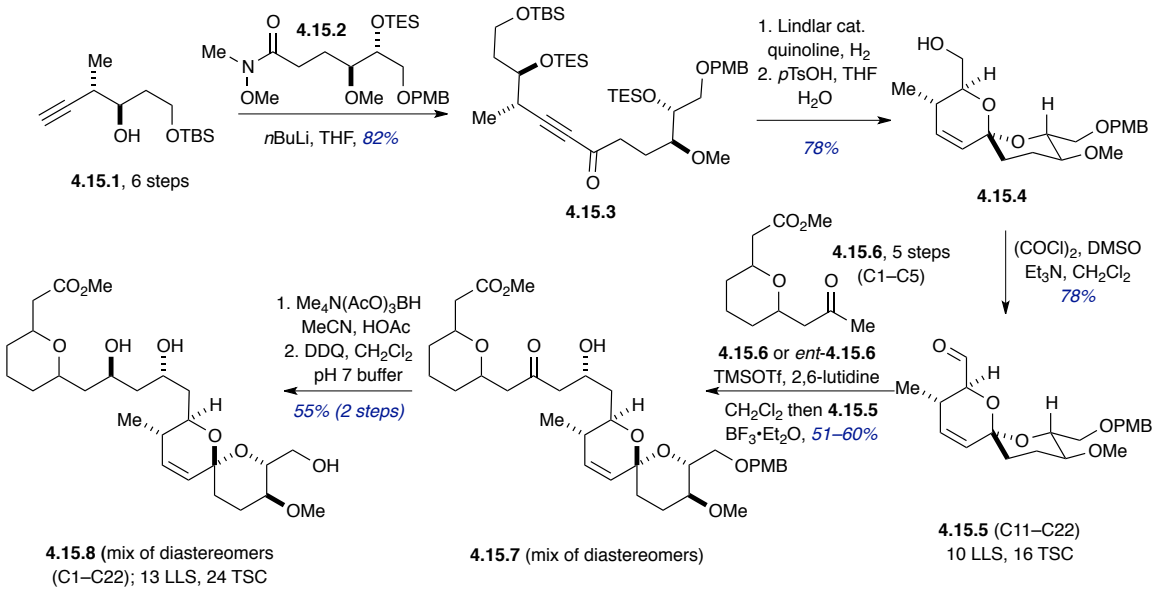

Scheme 4.15. *Brabander's synthesis of the diastreomeric fragments containing C1–C22 framework of spirastrellolide A.*

4.2.7: The Chandrasekhar group synthesis of the C9–C25 fragment of spirastrellolide B

In 2008, Chandrasekhar and coworkers reported the synthesis of the C9–C25 fragment by utilizing a combination of "chiron"[52] and asymmetric approaches (Scheme 4.16).[53] The C9–C16 fragment was derived from known epoxide **4.16.1** over 11 steps, that included a Sharpless asymmetric epoxidation[54] to introduce C13 stereogenecity and then a diastrereoselective and regioselctive cuprate[55] reaction to generate C14-Me center.

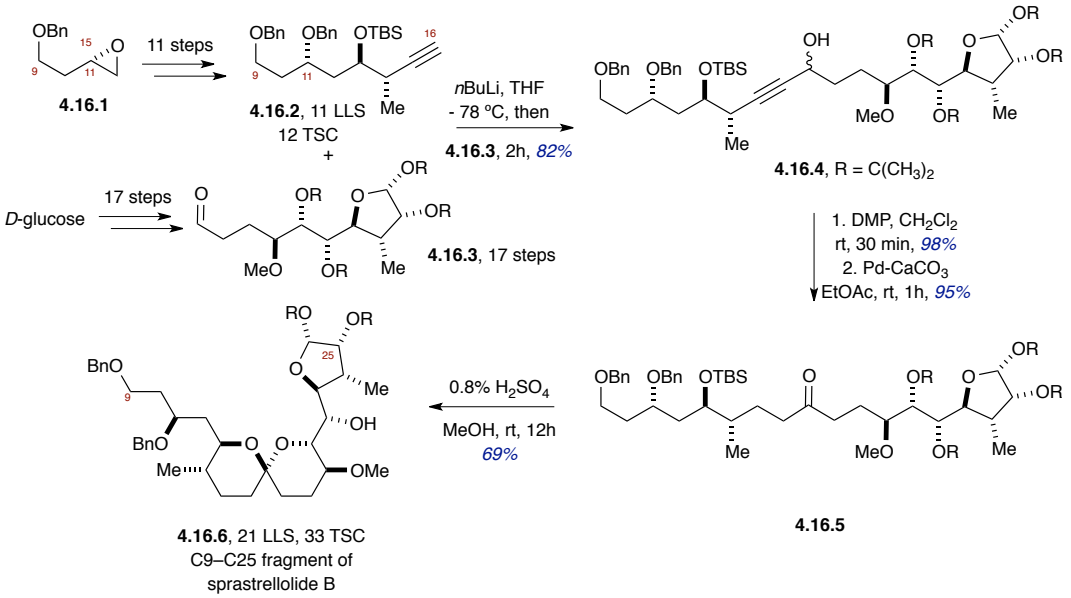

Scheme 4.16. *Chandrasekhar's synthesis of the C9–C25 fragment of spirastrellolide B.*

The other key fragment **4.16.3**, the C17–C25 was synthesized from *D*-glucose following a chiron approach that involved utilizing the stereocenters of the substrate (usually a carbohydrate or amino acid) to access elaborated advanced fragments.[52] The late-stage union of the key fragments **4.16.2** and **4.16.3** was established by lithiation of **4.16.2** and subsequent addition to aldehyde **4.16.3** to obtain the desired coupling product

4.16.4 in excellent yield as a mixture of diastereomers. The newly formed hydroxyl group of **4.16.4** was then oxidized and the internal triple bond was reduced using the Lindlar catalyst to generate the spirocyclization precursor **4.16.5**. Finally, spirocyclcization in the presence of .8% H_2SO_4 produced the C9–C25 fragment **4.16.6** of spirastrellolide B in a 21-longest linear step and 33 overall total steps synthetic sequence.

4.2.8: Yadav group synthesis of the C1–C25 fragment of spirastrellolide B and F

In 2013, Yadav and coworkers reported the synthesis of the C1–C25 fragment of spirastrellolide B and F employing a late-stage union of two advanced fragments via Horner–Wadsworth–Emmons (HWE)[56] coupling strategy (Scheme 4.17).[57] The coupling partners required for the HWE coupling, namely the aldehyde **4.17.1** and the β-keto-phosphonate intermediate **4.17.2** were synthesized in 35 and 17 steps respectively.

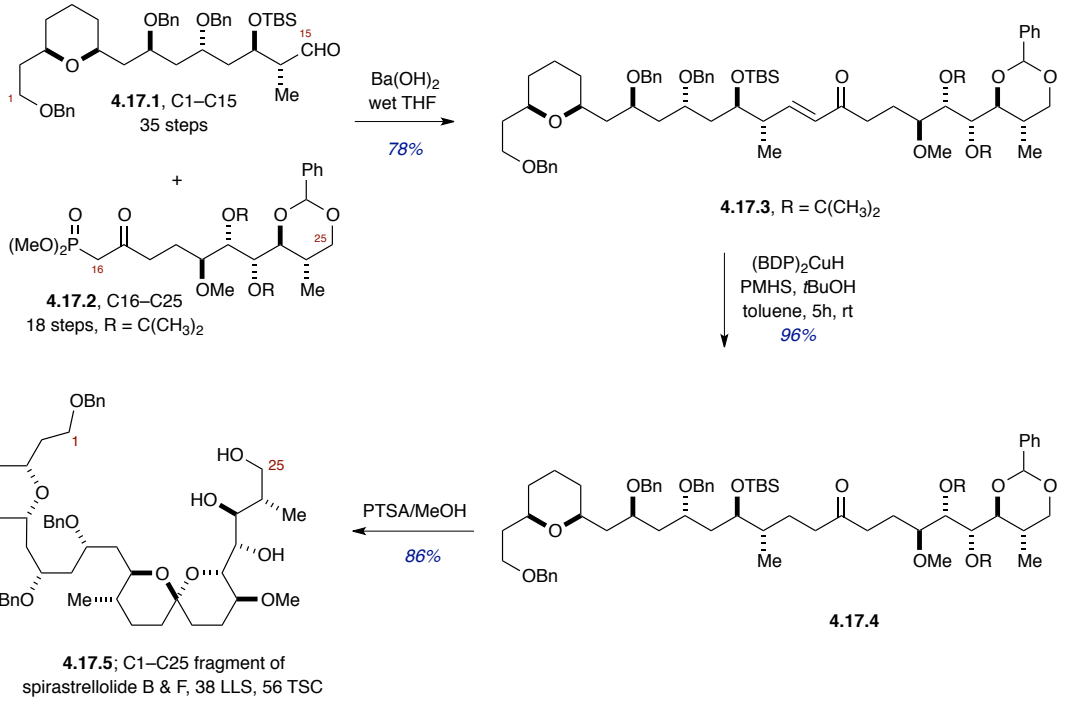

Scheme 4.17. *Yadav's synthesis of the C1–C25 fragment of spirastrellolide B.*

For the final coupling, aldehyde **4.17.1** was subjected to HWE coupling with phosphonate **4.17.2** in the presence of $Ba(OH)_2$[56] to produce the enone **4.17.3** in good yield. Subsequent reduction of enone with $(BDP)_2CuH$ [58] generated ketone **4.17.4** in excellent yield, which was then treated with PTSA/MeOH to produce the C1–C25 fragment **4.17.5** in excellent yield.

4.3: Results and discussion

Our group has concentrated efforts aimed at developing efficient synthetic strategies utilizing phosphate tether-mediated desymmetrization of C_2-symmetric 1,3-diene diols en route to 1,3-*anti*-diol group containing bioactive natural products.[59] Aligned with this goal, we were interested in the total synthesis of spirastrellolide B, possessing a challenging framework of a 38-membered macrolactone, and a bicyclic and tricyclic spiroacetal unit buried within the framework. Even though there are elegant reports from the Paterson and the Fürstner group regarding the total synthesis of spirastrellolide A and/or F, the total synthesis of its congener, spirastrellolide B has not been reported to date. In addition, despite having striking structural similarities, spirastrellolide A is known to be a potent inhibitor of PP2A while spirastrellolide B has not been tested/or reported to be a phosphatase inhibitor. In fact, there were no biological activities reported for spirastrellolide B until 2012. In 2012, both of the family members, A and B were re-isolated as free acids and tested against *HeLa* cancer cell lines. As discussed earlier in this chapter, the IC_{50} values of the free acids of spirastrellolide A and B were found to be 20 and 40 *n*M, respectively, comparable to the corresponding methyl ester of spirastrellolide A and B which exhibited IC_{50} values of 30 *n*M and 70 *n*M, respectively. However, unlike spirastrellolide A, the cytotoxity of spirastrellolide B has

not been linked to a phosphatase inhibition mechanism. Therefore, the total synthesis of spirastrellolide B will serve not merely as another synthetic campaign but for the identification of the pharmacophore of spirastrellolide A/B, which could, in turn serve, as an excellent biological tool to investigate protein phosphatase-mediated cellular regulation.

4.3.1: Proposed retrosynthetic analysis of the C9–C25 fragment of spirastrellolide B

In a collaborative project in the Hanson lab, we are aiming for the total synthesis of spirastrellolide B, in which my contribution has involved the assembly of the C9–C25 fragment **4.18.1** (Scheme 4.18). In this regard, we designed a synthetic route which utilizes phosphate tether-mediated regioselective oxidation and diastereoselective cuprate displacement of bicyclo[4.3.1]phosphate (*R*,*R*,R_P)-**4.18.5** to access the western C9–C16 subunit **4.18.4**.

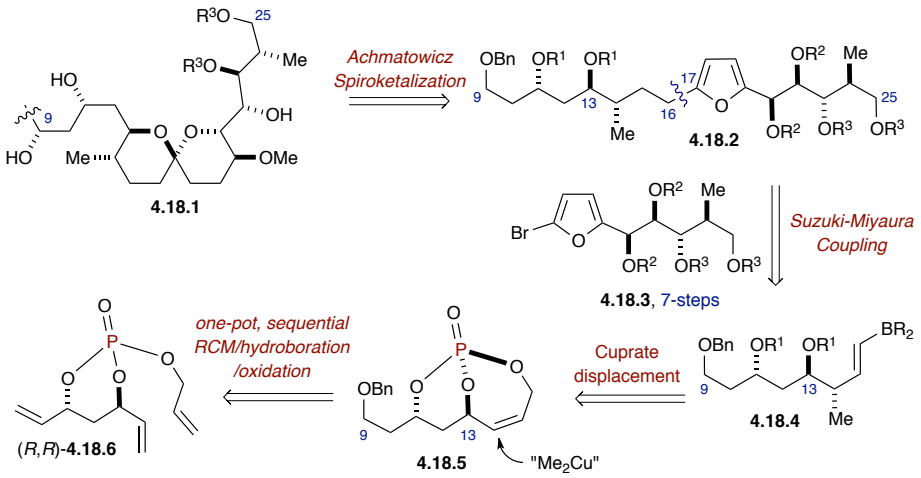

Scheme 4.18. *Our retrosynthetic strategy for C9–C25 fragment of spirastrellolide B.*

Our proposed retrosynthetic route relies on a late-stage Achmatowicz spirocyclization of key precursor containing furan subunit **4.18.2**. The key fragment was

envisioned to be derived via Suzuki-Miyaura coupling of a furan substrate **4.18.3** with the 1,3-diol containing synthon **4.18.4**. Overall, successful implementation of this route would achieve the synthesis of the C9–C25 fragment of spirastrellolide B with a longest linear sequence (LLS) of 14 steps and a total step count (TSC) of 22. In comparison, a brief summary of other elegant synthetic routes towards similar fragments of spirastrellolides to our proposed route towards the C9–C25 fragment of spiratsrellolide B is shown in Figure **4.8**.

Author and References (fragment targeted) *Key Reactions*	*Step count* *(LLS and TSC)*
Paterson *et. al. Org Lett.* **2005** (C1–C25 of spirastrellolide A) *Boron-mediated asymmetric aldol and allylation*	20 LLS, 40 TSC
Fürstner *et. al. Angew. Chem. Int. Ed*. **2009** (C1–C24 of spirastrellolide F) *Mukaiyama aldol and glycolate aldol strategy*	22 LLS, 43 TSC
Fürstner *et. al. Chem. Eur. J.* **2013** (C1–C24 of spirastrellolide A) *Mukaiyama aldol and strategic use of dithiane functionality*	26 LLS, 45 TSC
Phillips *et. al. Org. Lett.* **2008** (C1–C23 of spirastrellolide B) *Use of Kulinkovich-cyclopropanol ring-opening strategy twice*	15 LLS, 30 TSC
Smith et. al. Org. Lett. **2007** (C1–C25 of spirastrellolide A) *Anion relay chemistry (ARC)*	32 LLS, 42 TSC
Smith *et. al. Tetrahedron* **2010** (C1–C25 of spirastrellolide B) *Anion relay chemistry (ARC)*	33 LLS, 43 TSC
Smith *et. al. Tetrahedron Lett.* **2015** (C1–C24 of spirastrellolide E) *Anion relay chemistry (ARC) and gold-catalyzed alkyne functionalization*	19 LLS, 36 TSC
Smith *et. al. Org. Lett.* **2015** (C1–C23 of spirastrellolide E)	19 LLS, 34 TSC

Anion relay chemistry (ARC) and gold-catalyzed alkyne functionalization	
Hsung *et. al. Org. Lett.* **2008** (C1–C23 of spirastrellolide E) *Ketal-tetherd RCM and Mukaiyama aldol*	17 LLS, 29 TSC
Brabander *et. al. Synlett* **2006** (C1–C22 of spirastrellolide A) *Mukaiyama aldol strategy*	13 LLS, 24 TSC
Chandrasekhar *et. al. Org. Lett.* **2008** (C9–C25 of spirastrellolide B) *chiron and asymmetric approaches*	21 LLS, 33 TSC
Yadav *et. al. Org. Biomol. Chem.* **2013** (C9–C25 of spirastrellolide B) *HWE olefination and conjugate reduction*	38 LLS, 56 TSC
Our proposed route (C9–C25 of spirastrellolide B) Achmatowicz spiroketalization, Suzuki-Miyaura coupling and phosphate tether-mediated stereoselective reactions	*14 LLS, 22 TSC*

Figure 4.8: *A brief summary of steps counts and key reaction towards similar fragments targeted by different groups in comparison with our proposed route.*

4.3.2: Model studies towards the synthesis of the C9–C23 fragment of spirastrellolide B

Our initial focus was to check the feasibility of the key reactions in this synthetic route, namely the Suzuki-Miyaura coupling and Achmatowicz cyclization. Therefore, we chose to synthesize a shorter fragment, the C9–C23 containing **4.19.1** fragment, with less complexity but with an appropriate core scaffold consisting of the spiroacetal unit and other required functional groups (Scheme 4.19). Alternatively, we were looking into the same bond formation between C15 and C16 *via* a cross-metathesis and hydrogenation route to produce the key spirocyclization precursor **4.19.2**.

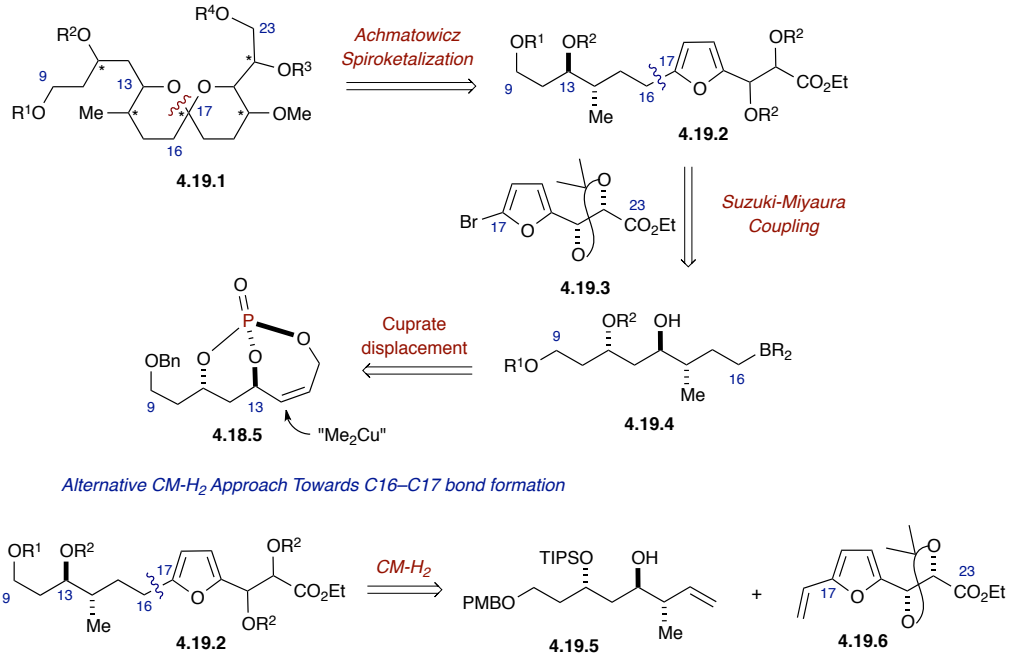

Scheme 4.19. *Retrosynthetic plans for model studies.*

4.3.2.1: Synthesis of the C9–C16 fragment and the C17–C23 fragment: model studies towards the synthesis of C9–C23 fragment of spirastrellolide B

Towards the aforementioned goal, we initiated our synthesis of the C9–C16 polyol containing fragment **4.19.5** (Scheme 4.20). Starting with the bicylo[4.3.1]phosphate **4.20.1**, prepared over 4 steps from 1,5-dichloropentane-2,4-dione, the regioselective hydroboration-oxidation in the presence of 9-BBN[60] followed by a mild work-up protocol developed by Burke and coworkers,[61] provided phosphate intermediate containing a primary alcohol (not shown in the Scheme) in 78% yield. Subsequent PMB ether formation in the presence of *p*-methoxybenzyl trichloroacetimidate and catalytic amount of PPTS delivered PMB ether **4.20.2** in 72% yield.[60] Next, the allylic methyl group at C14 was introduced via a higly diastereselctive

and regioselective allylic cuprate displacement protocol. For this purpose, phosphate **4.20.2** was treated with dimethyl cuprate generated *in situ* by the reaction of dimethyl zinc and copper cyanide. After completion of the reaction, monitored by TLC, the crude phosphoric acid was subjected to Red-Al reduction to generate diol in 80% yield (over 2 steps). Selective monoprotection (as a TIPS-ether) of the less-hindered secondary alcohol produced the C9–C16 fragment, **4.19.5** over 8 total steps.[60]

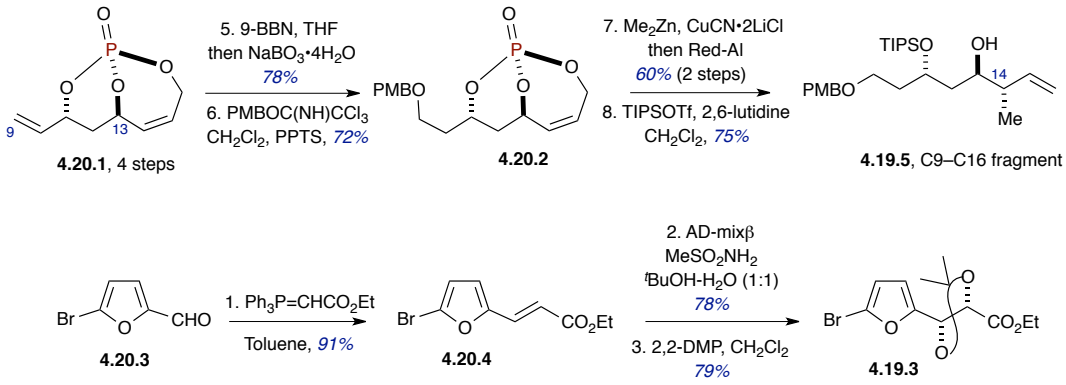

Scheme 4.20. *Synthesis of the C9–C16 fragment and the model C17–C23 furan fragment.*

The synthesis of the C17–C23 fragment **4.19.3** started with the HWE olefination of 5-bromo-2-furaldehyde (**4.20.3**) to generate ester **4.20.4** in excellent yield (Scheme 4.20). Subsequent Sharpless asymmetric dihyroxylation[62] followed by acetonide protection produced the coupling partner **4.19.3**.

Concurrent with the effort outlined above, we also focused on a cross-metathesis route towards the construction of the same fragment **4.21.1** (Scheme 4.21). For that purpose, we began with the synthesis of vinyl furan fragment **4.19.6**. Following Molander's protocol,[63] the Suzuki-Miyaura coupling of furan **4.19.3** was performed with potassium vinyltrifluroborate in the presence of catalytic $PdCl_2$ and $CaCO_3$ in refluxing THF, to generate the vinyl furan intermediate **4.19.6** in satisfactory 65% yield. However,

when the vinyl furan intermediate **4.19.6** was subjected to the CM reaction with olefin **4.19.5** in the presence of the **HG-II** catalyst, the desired CM product **4.21.2** was not observed.

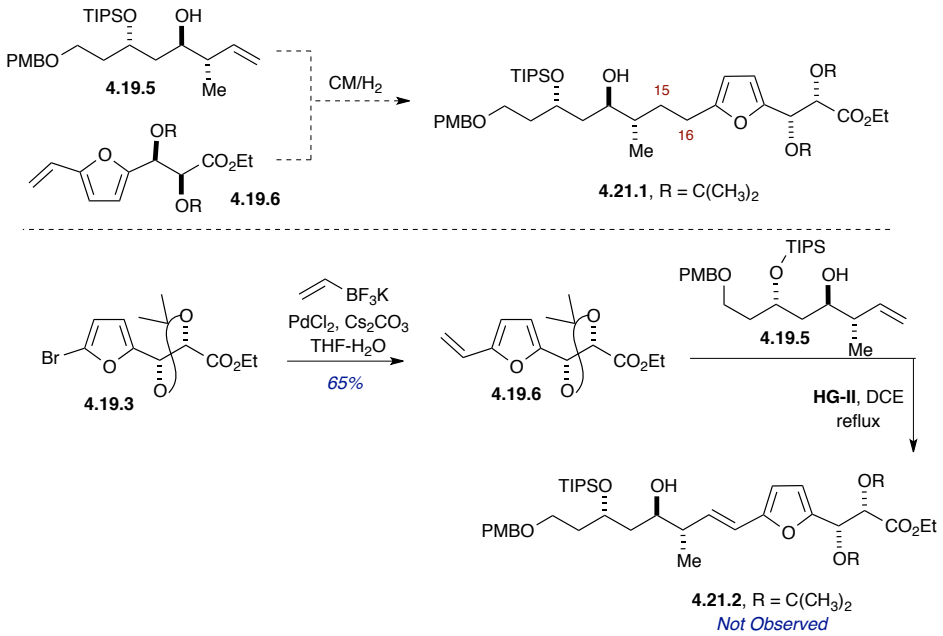

Scheme 4.21. *Cross-metathesis efforts towards C15–C16 bond formation.*

4.3.2.2: Efforts towards the synthesis of the model C9–C23 fragment via Suzuki-Miyuara coupling

We therefore directed our attention towards our previously designed route of Suzuki-Miyuara coupling with bromofuran intermediate **4.19.3** and borate ester **4.19.4** (Scheme 4.19). The corresponding borate ester synthesis started with bicylo[4.3.1]phosphate **4.20.1**, which was converted to alcohol via a hydroboration-oxidation protocol and subsequent benzylation to produce benzylated bicyclo[4.3.1]phosphate **4.18.5** (Scheme 4.22). Allylic cuprate displacement, followed by acetonide protection, generated protected diol **4.22.1** in 87% yield.

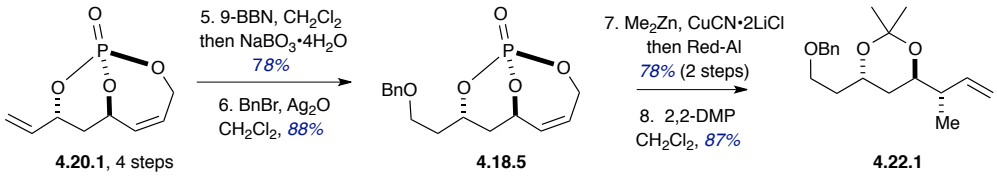

Scheme 4.22. *Synthesis of the C9–C16 fragment.*

The synthesis of borate ester **4.23.2** commenced with the initial attempt of hydroboration of protected diol **4.23.1** in the presence of 9-BBN (Scheme 4.23). However, even with different protecting groups, we were unable to obtain the hydroborated product **4.23.2**. Therefore, we decided to pursue metal-catalyzed hydroboration route.[64] Gratifyingly, we were able to isolate the alkyl pinacolboronates **4.23.3**, albeit in low yield (47%). Our first attempt at the Suzuki-Miyaura coupling of alkyl pinacolboronates **4.23.3** with bromofuran derivative **4.19.3** in the presence of $PdCl_2(dppf)•CH_2Cl_2$, Cs_2CO_3 and $AsPh_3$ in refluxing toluene-water generated the Suzuki-Miyaura product **4.23.4** only in trace amount; mostly unreacted starting materials were observed.

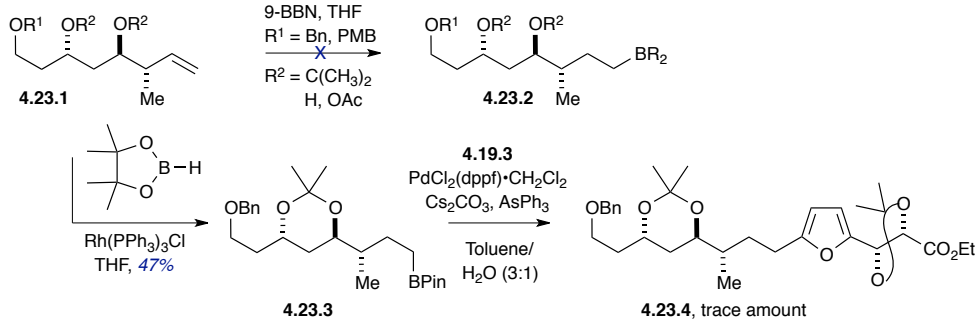

Scheme 4.23. *Trial route for the Suzuki-Miyuara coupling reaction.*

To facilitate the Suzuki-Miyaura coupling reaction, we decided to prepare the boronic ester **4.24.1** *via* a cross-metathesis route. Accordingly, olefin **4.22.1** was subjected to cross-metathesis reaction with vinylpinacolatoborane in the presence of the **HG-II** catalyst, in refluxing toluene, to produce the boronic ester **4.24.1** in excellent yield (Scheme 4.24).[65]

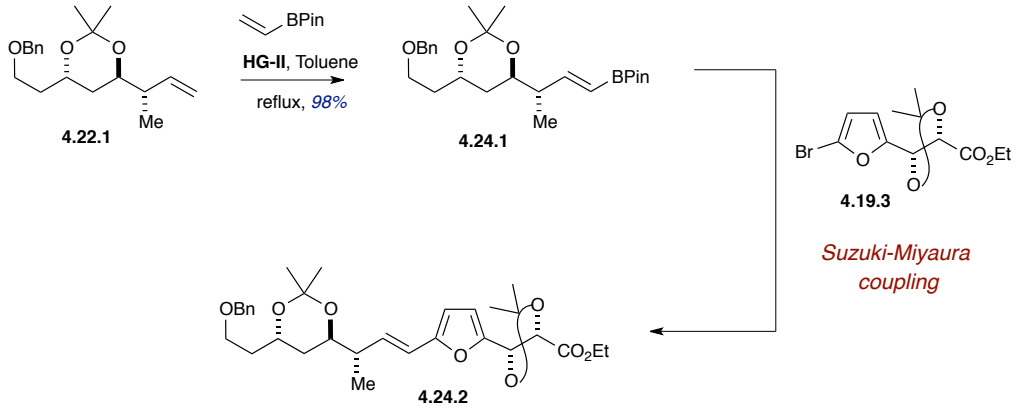

Entry	Reaction Conditions	Yield (%)	Entry	Reaction Conditions	Yield (%)
1	$Pd_2(dba)_3$, K_3PO_4, PCy_3 DME-H_2O (2:1), 85 °C, 19 h	*25*	5	$Pd_2(dba)_3$, K_3PO_4, $AsPh_3$ DME-H_2O (2:1), 85 °C, 19 h	*29*
2	$Pd_2(dba)_3$, K_3PO_4, PCy_3 Dioxane-H_2O (2:1), 100 °C, 19 h	*25*	6	$Pd_2(dba)_3$, Cs_2CO_3, P(2-furyl)$_3$ DME-H_2O (2:1), 85 °C, 19 h	*12*
3	$Pd_2(dba)_3$, K_3PO_4, P(2-furyl)$_3$ Dioxane-H_2O (2:1), 100 °C, 19 h	*18*	7	$Pd_2(dba)_3$, K_3PO_4, S-Phos Toluene-H_2O (10:1), 100 °C, 16 h	*45*
4	$Pd_2(dba)_3$, K_3PO_4, P(2-furyl)$_3$ DME-H_2O (2:1), 85 °C, 19 h	*52*	8	$Pd_2(dba)_3$, K_3PO_4, S-Phos DME-H_2O (10:1), 85 °C, 16 h	*50*
			9	Pd-PEPSI-IPent, THF 5 M KOH, 70 °C, 7 h	***56%***

Scheme 4.24: *Successful Suzuki-Miyaura Coupling studies.*

Next, we performed optimization studies for the Suzuki-Miyaura coupling reaction of boronic ester **4.24.1** and bromofuran **4.19.3**. Our initial attempts of Suzuki-Miyaura coupling in the presence of $Pd_2(dba)_3$, PCy_3 and K_3PO_4 in refluxing DMF-H_2O resulted the formation of product in only 25% yield (entry 1, Scheme 4.24). Change in solvent did not improve the yield (entry 2); however, change of ligand from PCy_3 to P(2-furyl)$_3$ improved the yield to 52% (entry 4).[66] The best result (56%, entry 9) for this coupling reaction was achieved using the Pd-IPent-PEPSI catalyst,[67] developed by Organ and coworkers, in the presence of 5M KOH in refluxing THF.

Subsequent hydrogenation under Lindlar reduction condition provided the saturated furan intermediate **4.25.1**, with which we planned to perform a global deprotection followed by Achmatowicz cyclization (Scheme 4.25). Unfortunately, we were unable to achieve the globally deprotected product **4.25.2,** even after subjecting **4.25.1** to various deprotection conditions. With these unforeseen results in hand, we continued towards the synthesis of different intermediates en route to the synthesis of the C9–C25 fragment of spirastrellolide B.

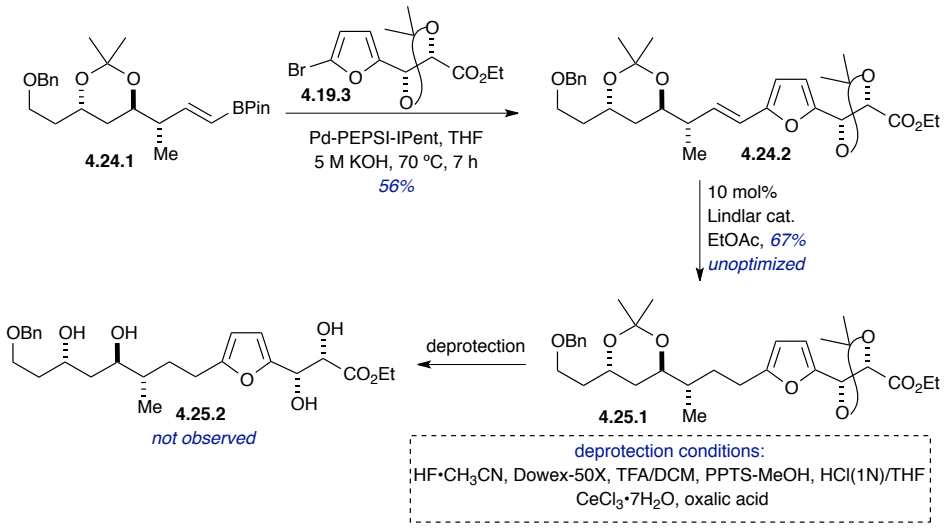

Scheme 4.25. *Model studies towards the synthesis of C9–C23 fragment.*

4.3.3: Synthesis of the C17–C25 fragment

In light of the outcome of model studies, we revisited our synthetic route and decided to prepare the furan containing C17–C25 fragment **4.26.1** without protecting the adjacent diol. Our initial retrosynthetic analysis of the C17–C25 fragment **4.26.1** involved the installation of *cis*-dihydroxyl groups (at C21 and C22) via dihydroxylation. The C23–C24 bond formation of furan intermediate **4.26.2** would be achieved by *anti*-selective aldol reaction between 5-bromofuryl acrylaldehyde **4.26.3** and propanaldehyde (**4.26.4**). However, no aldol product formation was observed after several trials, presumably due to the deactivation of aldehyde by the electron rich furan ring. The alternative strategy towards the construction of the C17–C25 fragment **4.26.1** included a CM protocol uniting the furan-containing fragment **4.26.6** and olefin **4.26.7** to achieve the C21–C22 bond formation. For this purpose, the furan intermediate **4.26.6** was synthesized via a Wittig olefination starting from 5-bromo-2-furaldehyde (**4.20.3**) in 65% yield. [68]

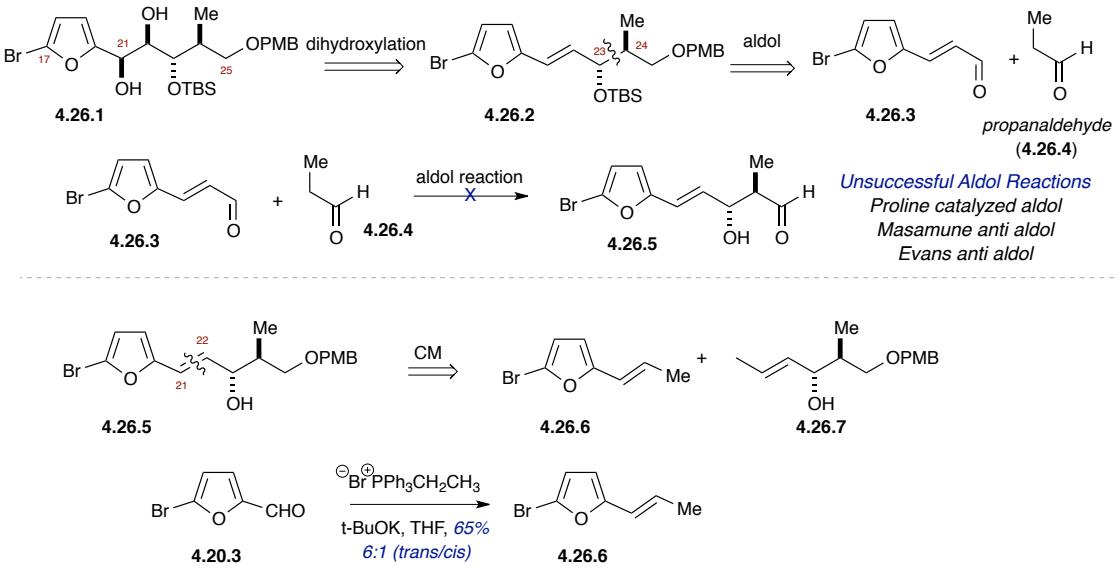

Scheme 4.26. *Retrosynthetic strategy for the synthesis of C17–C25 furan fragment.*

The synthesis of the olefinic CM-partner commenced with the PMB protection of (*S*)-Roche ester (**4.27.1**), followed by the conversion to Weinreb aminde **4.27.2** in the presence of (OMe)NH(Me)HCl and *i*PrMgCl (Scheme 4.27).[69] Subsequent Grignard addition followed by the CBS reduction,[70] generated olefinic cross-partner, substituted allylic alcohol **4.26.7**. Further CM reaction with furan substrate **4.26.6** in the presence of **HG-II** catalyst in refluxing CH_2Cl_2 produced furan substituted allylic alcohol **4.26.5** in 72% yield. Subsequent TBS protection of the hydroxyl group at C23 in the cross-metathesis product and dihydroxylation[35] delivered the coupling partner **4.26.1**, the C17–C25 fragment in 7 overall steps.

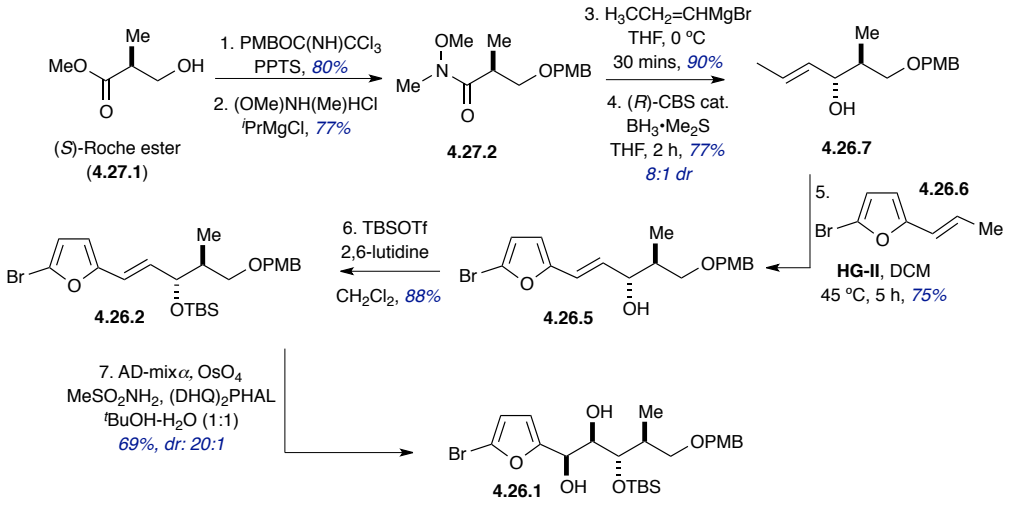

Scheme 4.27. *Synthesis of the C17–C25 furan fragment.*

4.3.4: Progress towards the C9–C23 fragment

Suzuki-Miyaura coupling of the boronic ester C9–C16 fragment **4.24.1** and furan intermediate **4.26.1** in the presence of $Pd(PPh_3)_4$ and K_3PO_4 resulted in the coupling

product **4.28.1** in 50% yield (Scheme 4.28). Subsequent hydrogenation using *o*-NBSH yielded the Achmatowicz precursor **4.28.2** in 84% yield. Next, we performed the Achmatowicz cyclization by subjecting the hydrogenated product **4.28.2** to NBS, $NaHCO_3$ and NaOAc in THF/H_2O (4:1) mixture to produce α,β-unsaturated pyran **4.28.3** in 82% yield.[71] Our next goal was to protect the secondary hydroxyl group at C22 as acetate prior to spirocycliczation in order to prevent the possible formation of bridged product during spirocyclization. However, when subjected to Ac_2O and pyridine in the presence of DMAP, the only product isolated was the ring-opened product **4.28.5**, no diacetate product **4.28.4** was observed.

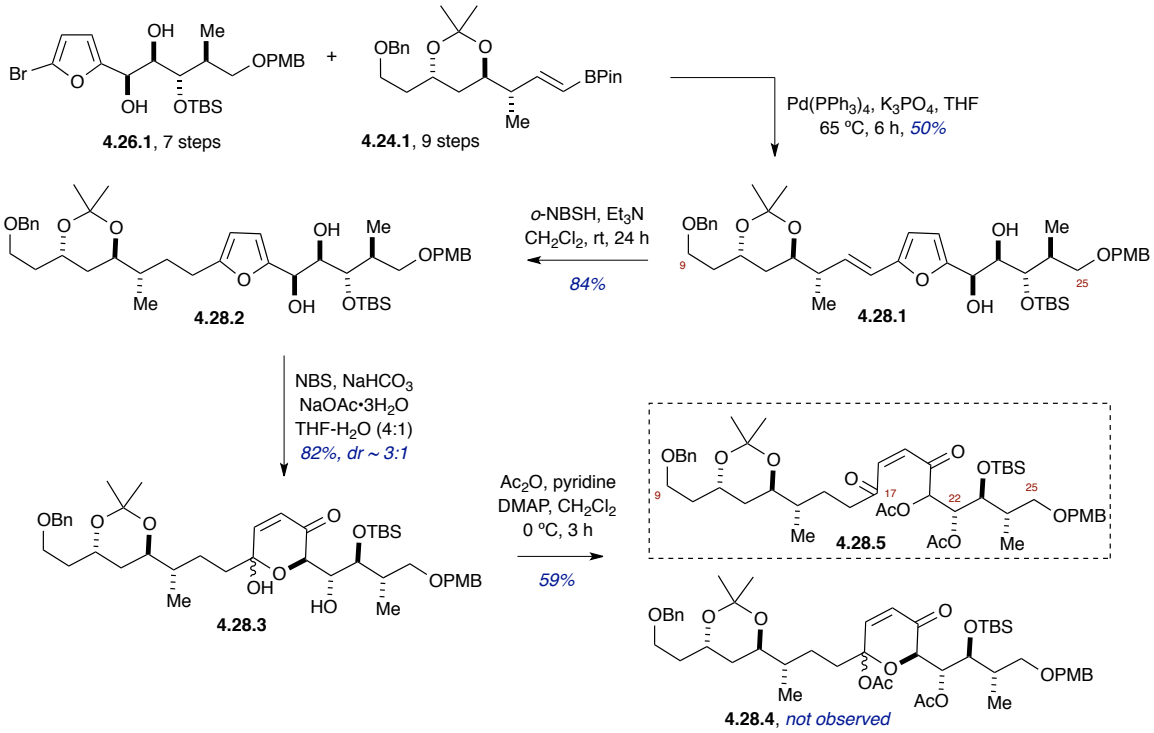

Scheme 4.28. *Progress towards the synthesis of the C9–C25 fragment of spirastrellolide B.*

4.4: Future direction

Future directions towards the synthesis of the C9–C25 fragment involve the selective protection of C22 hydroxyl as TBS ether or Pivaloyl ester (Scheme 4.29). Alternatively, the double bond present in α,β-unsaturated pyran **4.28.3** will be reduced which might prevent the formation of ring-opening product. Our next goal would be to subject the saturated pyran intermediate **4.29.2** to spirocyclization condition without protecting the hydroxyl group at C22. Subsequent reduction of the carbonyl group would generate the C9–C25 fragment **4.29.3**.

In conclusion, we were able to construct the key intermediate **4.28.3** required for spirocyclization by utilizing a late-stage Achmatowicz cyclization. The key intermediates required for the Suzuki-Miyaura coupling were generated over 7 steps (for the furan intermediate) and 9 steps (the boronic ester). Studies will be next directed to facilitate the spirocyclization reaction with or without protecting C22 hydroxyl group. In addition, ongoing efforts are aimed towards developing one-pot sequential RCM/hydroboration and one-pot sequential CM/Suzuki/H_2 to further streamline the synthesis of the C9–C25 fragment. The successful implementation of the one-pot RCM/hydroboration protocol would further reduce the step count of the boronic ester intermediate from 9 steps to 8 steps. In addition, the development of one-pot CM/Suzuki/H_2 protocol would facilitate the synthesis of the C9–C25 fragment of spirastrellolide B over 14 longest linear steps and 22 total steps.

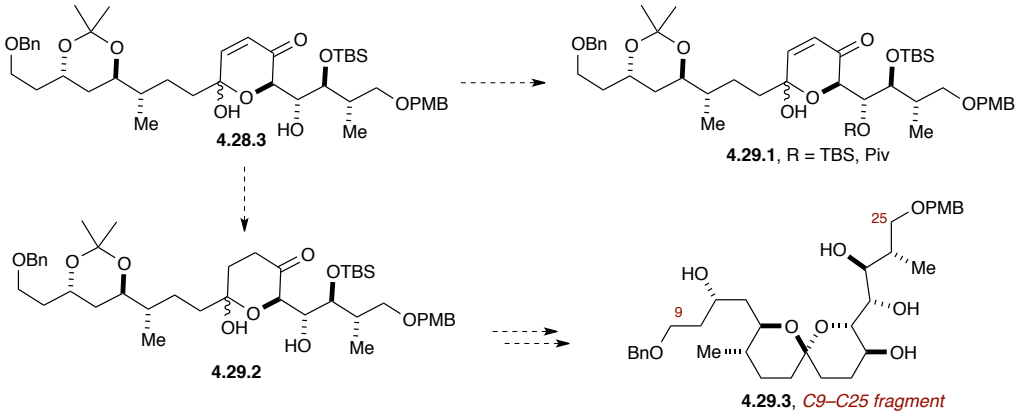

Scheme 4.29. *Future plans towards the synthesis of the C9–C25 fragment of spirastrellolide B.*

4.5: References cited:

[1] (a) Hamel, E. Antimitotic natural products and their interactions with tubulin. *Med. Res. Rev.* **1996**, *16*, 207–231; (b) Hamel, E. Interactions of antimitotic peptides and depsipeptides with tubulin. *Biopolymers* **2002**, *66*, 142–160; (c) Hood, K. A.; West, L. M.; Rouwe, B.; Northcote, P. T.; Berridge, M. V.; Wakefield, S. J.; Miller, J. H. Peloruside A, a novel antimitotic agent with paclitaxel-like microtubule-stabilizing activity. *Cancer Res.* **2002**, *62*, 3356–3360; (d) Mooberry, S. L.; Tien, G.; Hernandez, A. H.; Plubrukarn, A.; Davidson, B. S. Laulimalide and isolaulimalide, new paclitaxel-like microtubule-stabilizing agents. *Cancer Res.* **1999**, *59*, 653–660; (e) Luduena, R. F.; Roach, M. C.; Prasad, V.; Pettit, G. R. Interaction of halichondrin B and homohalichondrin B with bovine brain tubulin. *Biochem. Pharmacol.* **1993**, *45*, 421–427.

[2] (a) Nieman, J. A.; Coleman, J. E.; Wallace, D. J.; Piers, E.; Lim, L. Y.; Roberge, M.; Andersen, R. J. Synthesis and Antimitotic/Cytotoxic Activity of Hemiasterlin Analogues. *J. Nat. Prod.* **2003**, *66*, 183–199; (b) Cinel, B.; Roberge, M.; Behrisch, H.; van Ofwegen, L.; Castro, C. B.; Andersen, R. J. Antimitotic diterpenes from Erythropodium caribaeorum test pharmacophore models for microtubule stabilization. *Org. Lett.* **2000**, *2*, 257–260; (c) Anderson, H. J.; Coleman, J. E.; Andersen, R. J.; Roberge, M. Cytotoxic peptides hemiasterlin, hemiasterlin A, and hemiasterlin B include mitotic arrest and abnormal spindle formation. *Cancer Chemother. Pharmacol.* **1997**, *39*, 223–226.

[3] Roberge, M.; Cinel, B.; Anderson, H. J.; Lim, L.; Jiang, X.; Xu, L.; Bigg, C. M.; Kelly, M. T.; Andersen, R. J. Cell-based screen for antimitotic agents and identification of analogues of rhizoxin, eleutherobin, and paclitaxel in natural extracts. *Cancer Res.* **2000**, *60*, 5052–5058.

[4] Williams, D. E.; Roberge, M.; Van Soest, R.; Andersen, R. J. Spirastrellolide A, an antimitotic macrolide isolated from the Caribbean marine sponge Spirastrella coccinea. *J. Am. Chem. Soc.* **2003**, *125*, 5296–5297.

[5] Jordan, M. A. Mechanism of action of antitumor drugs that interact with

microtubules and tubulin. *Curr. Med. Chem.: Anti-Cancer Agents* **2002**, *2*, 1–17.

[6] Williams, D. E.; Lapawa, M.; Feng, X.; Tarling, T.; Roberge, M.; Andersen, R. J. Spirastrellolide A: Revised Structure, Progress toward the Relative Configuration, and Inhibition of Protein Phosphatase 2A. *Org. Lett.* **2004**, *6*, 2607–2610.

[7] Warabi, K.; Williams, D. E.; Patrick, B. O.; Roberge, M.; Andersen, R. J. Spirastrellolide B Reveals the Absolute Configuration of the Spirastrellolide Macrolide Core. *J. Am. Chem. Soc.* **2007**, *129*, 508–509.

[8] Williams, D. E.; Keyzers, R. A.; Warabi, K.; Desjardine, K.; Riffell, J. L.; Roberge, M.; Andersen, R. J. Spirastrellolides C to G: Macrolides Obtained from the Marine Sponge Spirastrella coccinea. *J. Org. Chem.* **2007**, *72*, 9842–9845.

[9] (a) Cheng, H.-C.; Qi, R. Z.; Paudel, H.; Zhu, H.-J. Regulation and function of protein kinases and phosphatases. *Enzyme Res* **2011**, *2011*, 794089; (b) Holt, L. J.; Tuch, B. B.; Villen, J.; Johnson, A. D.; Gygi, S. P.; Morgan, D. O. Global Analysis of Cdk1 Substrate Phosphorylation Sites Provides Insights into Evolution. *Science (Washington, DC, U. S.)* **2009**, *325*, 1682–1686; (c) Serber, Z.; Ferrell, J. E., Jr. Tuning bulk electrostatics to regulate protein function. *Cell (Cambridge, MA, U. S.)* **2007**, *128*, 441–444.

[10] Mustelin, T. A brief introduction to the protein phosphatase families. *Methods Mol Biol* **2007**, *365*, 9–22.

[11] Hunter, T. Signaling - 2000 and beyond. *Cell (Cambridge, Mass.)* **2000**, *100*, 113–127.

[12] Wipf, P.; Cunningham, A.; Rice, R. L.; Lazo, J. S. Combinatorial synthesis and biological evaluation of library of small-molecule Ser/Thr-protein phosphatase inhibitors. *Bioorg. Med. Chem.* **1997**, *5*, 165–177.

[13] Sheppeck, J. E., II; Gauss, C.-M.; Chamberlin, A. R. Inhibition of the Ser-Thr phosphatases PP1 and PP2A by naturally occurring toxins. *Bioorg. Med. Chem.* **1997**, *5*, 1739–1750.

[14] Tachibana, K.; Scheuer, P. J.; Tsukitani, Y.; Kikuchi, H.; Van Engen, D.; Clardy, J.; Gopichand, Y.; Schmitz, F. J. Okadaic acid, a cytotoxic polyether from two marine sponges of the genus Halichondria. *J. Am. Chem. Soc.* **1981**, *103*, 2469–2471; (b) Schmitz, F. J.; Prasad, R. S.; Gopichand, Y.; Hossain, M. B.; Van der Helm, D.; Schmidt, P. Acanthifolicin, a new episulfide-containing polyether carboxylic acid from extracts of the marine sponge Pandaros acanthifolium. *J. Am. Chem. Soc.* **1981**, *103*, 2467–2469.

[15] Maynes, J. T.; Bateman, K. S.; Cherney, M. M.; Das, A. K.; Luu, H. A.; Holmes, C. F. B.; James, M. N. G. Crystal structure of the tumor-promoter okadaic acid bound to protein phosphatase-1. *J. Biol. Chem.* **2001**, *276*, 44078–44082.

[16] Kennedy, S. M. "Studies Toward the Total Synthesis of Spirastrellolide A". Ph. D. Thesis., University of California, Irvine, 2010.

[17] Warabi, K.; Williams, D. E.; Patrick, B. O.; Roberge, M.; Andersen, R. J. *J. Am. Chem. Soc*. **2007**, *129*, 508–509.

[18] Suzuki, M.; Ueoka, R.; Takada, K.; Okada, S.; Ohtsuka, S.; Ise, Y.; Matsunaga, S. *J. Nat. Prod.* **2012**, *75*, 1192–1195.

[19] Paterson, I.; Dalby, S. M. Synthesis and stereochemical determination of the spirastrellolides. *Nat. Prod. Rep.* **2009**, *26*, 865–873.

[20] (a) Paterson, I.; Anderson, E. A.; Dalby, S. M. Synthesis of the C1-C21 southern hemisphere of the originally proposed structure of spirastrellolide A. *Synthesis* **2005**, 3225–3228; (b) Paterson, I.; Anderson, E. A.; Dalby, S. M.; Loiseleur, O. Toward the Synthesis of Spirastrellolide A: Construction of Two C1-C25 Diastereomers Containing the BC-Spiroacetal. *Org. Lett.* **2005**, *7*, 4125–4128; (c) Paterson, I.; Anderson, E. A.; Dalby, S. M.; Genovino, J.; Lim, J. H.; Moessner, C. Synthesis of two diastereomeric C1-C22 fragments of spirastrellolide A. *Chem. Commun.* **2007**, 1852–1854; (d) Paterson, I.; Anderson, E. A.; Dalby, S. M.; Lim, J. H.; Genovino, J.; Maltas, P.; Moessner, C. Total synthesis of spirastrellolide A methyl ester-part 1: synthesis of an advanced C17-C40 bis-spiroacetal subunit.

Angew. Chem., Int. Ed. **2008**, *47*, 3016–3020; (e) Paterson, I.; Anderson, E. A.; Dalby, S. M.; Lim, J. H.; Genovino, J.; Maltas, P.; Moessner, C. Total synthesis of spirastrellolide A methyl ester-part 2: subunit union and completion of the synthesis. *Angew. Chem., Int. Ed.* **2008**, *47*, 3021–3025; (e) Benson, S.; Collin, M.-P.; O'Neil, G. W.; Ceccon, J.; Fasching, B.; Fenster, M. D. B.; Godbout, C.; Radkowski, K.; Goddard, R.; Fürstner, A. Total Synthesis of Spirastrellolide F Methyl Ester-Part 2: Macrocyclization and Completion of the Synthesis. *Angew. Chem., Int. Ed.* **2009**, *48*, 9946–9950.

[21] (a) Paterson, I.; Anderson, E. A.; Dalby, S. M.; Lim, J. H.; Maltas, P.; Loiseleur, O.; Genovino, J.; Moessner, C. The stereocontrolled total synthesis of spirastrellolide A methyl ester. Expedient construction of the key fragments. *Org. Biomol. Chem.* **2012**, *10*, 5861–5872; (b) Paterson, I.; Maltas, P.; Dalby, S. M.; Lim, J. H.; Anderson, E. A. A Second-Generation Total Synthesis of Spirastrellolide A Methyl Ester. *Angew. Chem., Int. Ed.* **2012**, *51*, 2749–2753.

[22] (a) Arlt, A.; Benson, S.; Schulthoff, S.; Gabor, B.; Fürstner, A. A Total Synthesis of Spirastrellolide A Methyl Ester. *Chem. - Eur. J.* **2013**, *19*, 3596–3608; (b) Benson, S.; Collin, M.-P.; Arlt, A.; Gabor, B.; Goddard, R.; Fürstner, A. Second-Generation Total Synthesis of Spirastrellolide F Methyl Ester: The Alkyne Route. *Angew. Chem., Int. Ed.* **2011**, *50*, 8739–8744; (c) O'Neil, G. W.; Ceccon, J.; Benson, S.; Collin, M.-P.; Fasching, B.; Fürstner, A. Total synthesis of spirastrellolide F methyl ester--part 1: Strategic considerations and revised approach to the southern hemisphere. *Angew. Chem. Int. Ed.* **2009**, *48*, 9940–9945.

[23] (a) Paterson, I.; Goodman, J. M.; Isaka, M. Aldol reactions in polypropionate synthesis: high π-face selectivity of enol borinates from α-chiral methyl and ethyl ketones under substrate control. *Tetrahedron Lett.* **1989**, *30*, 7121–7124; (b) Paterson, I.; Oballa, R. M. Studies in marine macrolide synthesis: synthesis of the C1-C15 subunit of spongistatin 1 (Altohyrtin A) and 15,16-anti aldol coupling reactions. *Tetrahedron Lett.* **1997**, *38*, 8241–8244.

[24] Jadhav, P. K.; Bhat, K. S.; Perumal, P. T.; Brown, H. C. Chiral synthesis via organoboranes. 6. Asymmetric allylboration via chiral allyldialkylboranes. Synthesis of homoallylic alcohols with exceptionally high enantiomeric excess. *J. Org. Chem.* **1986**, *51*, 432–439.

[25] Fürstner, A.; Fenster, M. D. B.; Fasching, B.; Godbout, C.; Radkowski, K. Toward the total synthesis of spirastrellolide A. Part 1: strategic considerations and preparation of the southern domain. *Angew. Chem., Int. Ed.* **2006**, *45*, 5506–5510.

[26] Fürstner, A.; Fasching, B.; O'Neil, G. W.; Fenster, M. D. B.; Godbout, C.; Ceccon, J. Toward the total synthesis of spirastrellolide A. Part 3: Intelligence gathering and preparation of a ring-expanded analog. *Chem. Commun.* **2007**, 3045–3047.

[27] O'Neil, G. W.; Ceccon, J.; Benson, S.; Collin, M.-P.; Fasching, B.; Fuerstner, A. Total Synthesis of Spirastrellolide F Methyl Ester. Part 1: Strategic Considerations and Revised Approach to the Southern Hemisphere. *Angew. Chem., Int. Ed.* **2009**, *48*, 9940–9945.

[28] (a) Evans, D. A.; Dart, M. J.; Duffy, J. L.; Yang, M. G. A Stereochemical Model for Merged 1,2- and 1,3-Asymmetric Induction in Diastereoselective Mukaiyama Aldol Addition Reactions and Related Processes. *J. Am. Chem. Soc.* **1996**, *118*, 4322–4343; (b) for review see: Mukaiyama, T. The directed aldol reaction. *Org. React. (N. Y.)* **1982**, *28*, 203–331.

[29] Evans, D. A.; Hoveyda, A. H. Samarium-catalyzed intramolecular Tishchenko reduction of β-hydroxy ketones. A stereoselective approach to the synthesis of differentiated anti 1,3-diol monoesters. *J. Am. Chem. Soc.* **1990**, *112*, 6447–6449.

[30] Timmer, M. S. M.; Adibekian, A.; Seeberger, P. H. Short de novo synthesis of fully functionalized uronic acid monosaccharides. *Angew. Chem., Int. Ed.* **2005**, *44*, 7605–7607.

[31] Hattori, K.; Yamamoto, H. Highly selective generation and application of (E)- and (Z)-silyl ketene acetals from β-hydroxy esters. *J. Org. Chem.* **1993**, *58*, 5301–

5303.

[32] Arlt, A.; Benson, S.; Schulthoff, S.; Gabor, B.; Fürstner, A. A Total Synthesis of Spirastrellolide A Methyl Ester. *Chem. - Eur. J.* **2013**, *19*, 3596–3608.

[33] (a) Bal, B. S.; Childers, W. E., Jr.; Pinnick, H. W. Oxidation of α,β-unsaturated aldehydes. *Tetrahedron* **1981**, *37*, 2091–2096; (b) Kraus, G. A.; Taschner, M. J. Model studies for the synthesis of quassinoids. 1. Construction of the BCE ring system. *J. Org. Chem.* **1980**, *45*, 1175–1176; (c) Lindgren, B. O.; Nilsson, T. Preparation of carboxylic acids from aldehydes (including hydroxylated benzaldehydes) by oxidation with chlorite. *Acta Chem. Scand.* **1973**, *27*, 888–890.

[34] Keaton, K. A.; Phillips, A. J. A Cyclopropanol-Based Strategy for Subunit Coupling: Total Synthesis of (+)-Spirolaxine Methyl Ether. *Org. Lett.* **2007**, *9*, 2717–2719.

[35] Keaton, K. A.; Phillips, A. J. Toward the Synthesis of Spirastrellolide B: A Synthesis of the C1-C23 Subunit. *Org. Lett.* **2008**, *10*, 1083–1086.

[36] (a) Smith, A. B., III; Kim, D.-S. The Spirastrellolides: Construction of the Southern C(1)-C(25) Fragment Exploiting Anion Relay Chemistry. *Org. Lett.* **2007**, *9*, 3311–3314; (b) Smith, A. B., III; Smits, H.; Kim, D.-S. Spirastrellolide studies. Synthesis of the C(1)-C(25) southern hemispheres of spirastrellolides A and B, exploiting anion relay chemistry. *Tetrahedron* **2010**, *66*, 6597–6605.

[37] (a) Smith, A. B., III; Xian, M. Anion Relay Chemistry: An Effective Tactic for Diversity Oriented Synthesis. *J. Am. Chem. Soc.* **2006**, *128*, 66–67; (b) Smith, A. B., III; Xian, M.; Kim, W.-S.; Kim, D.-S. The [1,5]-Brook Rearrangement: An Initial Application in Anion Relay Chemistry. *J. Am. Chem. Soc.* **2006**, *128*, 12368–12369.

[38] Schlosser, M.; Strunk, S. The super-basic butyllithium/potassium tert-butoxide mixture and other LICKOR reagents. *Tetrahedron Lett.* **1984**, *25*, 741–744.

[39] (a) Honda, Y.; Morita, E.; Ohshiro, K.; Tsuchihashi, G. 1,3-Asymmetric induction

in acyclic systems by practical application of the dithioacetal group. *Chem. Lett.* **1988**, 21-24; (b) Honda, Y.; Tuchihashi, G. 1,3-Anti asymmetric induction in addition of organotitanium reagents to β-substituted aldehydes with a dithioacetal group. *Chem. Lett.* **1988**, 1937–1938.

[40] (a) Hicks, D. R.; Fraser-Reid, B. Selective sulfonylation with N-tosylimidazole. One-step preparation of methyl 2,3-anhydro-4,6-O-benzylidene-α-D-mannopranoside. *Synthesis* **1974**, 203. (b) Cink, R. D.; Forsyth, C. J. Facile One-Pot Epoxidation-Nucleophilic Opening Sequence for Vicinal Diols. *J. Org. Chem.* **1995**, *60*, 8122-8123.

[41] Sokolsky, A.; Wang, X.; Smith, A. B. Spirastrellolide E: synthesis of an advanced C(1)-C(24) southern hemisphere. *Tetrahedron Lett.* **2015**, Ahead of Print.

[42] Nieto-Oberhuber, C.; Munoz, M. P.; Lopez, S.; Jimenez-Nunez, E.; Nevado, C.; Herrero-Gomez, E.; Raducan, M.; Echavarren, A. M. Gold(I)-catalyzed cyclizations of 1,6-enynes: alkoxycyclizations and exo/endo skeletal rearrangements. *Chem. - Eur. J.* **2006**, *12*, 1677–1693.

[43] Sokolsky, A.; Cattoen, M.; Smith, A. B., III Synthesis of a C(1)-C(23) Fragment for Spirastrellolide E: Development of a Mechanistic Rationale for Spiroketalization. *Org. Lett.* **2015**, *17*, 1898–1901.

[44] Liu, J.; Yang, J. H.; Ko, C.; Hsung, R. P. Synthesis of the C1-C16 fragment of spirastrellolide A. *Tetrahedron Lett.* **2006**, *47*, 6121–6123.

[45] Parikh, J. R.; Doering, W. v. E. Sulfur trioxide in the oxidation of alcohols by dimethyl sulfoxide. *J. Am. Chem. Soc.* **1967**, *89*, 5505–5507.

[46] Mukaiyama, T.; Banno, K.; Narasaka, K. New cross-aldol reactions. Reactions of silyl enol ethers with carbonyl compounds activated by titanium tetrachloride. *J. Am. Chem. Soc.* **1974**, *96*, 7503–7509.

[47] Liu, J.; Hsung, R. P. Synthesis of the C11-C23 Fragment of Spirastrellolide A. A Ketal-Tethered RCM Approach to the Construction of Spiroketals. *Org. Lett.*

2005, *7*, 2273–2276.

[48] (a) Yang, J.-H.; Liu, J.; Hsung, R. P. Synthesis of the C1-C23 Fragment of Spirastrellolide A. *Org. Lett.* **2008**, *10*, 2525–2528; (b) Tang, Y.; Yang, J.-H.; Liu, J.; Wang, C.-C.; Lv, M.-C.; Wu, Y.-B.; Yu, X.-L.; Ko, C.; Hsung, R. P. Assembly of the southern macrocyclic half of (+)-spirastrellolide a through cyclic acetal tethered ring-closing metathesis and 1,3-anti-Mukaiyama-aldol. *Heterocycles* **2012**, *86*, 565–598.

[49] Evans, D. A.; Dart, M. J.; Duffy, J. L.; Yang, M. G. A Stereochemical Model for Merged 1,2- and 1,3-Asymmetric Induction in Diastereoselective Mukaiyama Aldol Addition Reactions and Related Processes. *J. Am. Chem. Soc.* **1996**, *118*, 4322–4343.

[50] Pan, Y.; De Brabander, J. K. Synthesis of spirastrellolide A fragments for structure elucidation. *Synlett* **2006**, 853–856.

[51] Evans, D. A.; Chapman, K. T.; Carreira, E. M. Directed reduction of β-hydroxy ketones employing tetramethylammonium triacetoxyborohydride. *J. Am. Chem. Soc.* **1988**, *110*, 3560–3578.

[52] For excellent review on chiron approach; see: Hanessian, S. The Enterprise of Synthesis: From Concept to Practice. *J. Org. Chem.* **2012**, *77*, 6657–6688.

[53] Chandrasekhar, S.; Rambabu, C.; Reddy, A. S. Spirastrellolide B: The Synthesis of Southern (C9-C25) Region. *Org. Lett.* **2008**, *10*, 4355–4357.

[54] (a) Katsuki, T.; Sharpless, K. B. The first practical method for asymmetric epoxidation. *J. Am. Chem. Soc.* **1980**, *102*, 5974–5976; (b) Gao, Y.; Klunder, J. M.; Hanson, R. M.; Masamune, H.; Ko, S. Y.; Sharpless, K. B. Catalytic asymmetric epoxidation and kinetic resolution: modified procedures including in situ derivatization. *J. Am. Chem. Soc.* **1987**, *109*, 5765–5780.

[55] Nagoka, H.; Kishi, Y. Further synthetic studies on rifamycin S. *Tetrahedron* **1981**, *37*, 3873–3888.

[56] (a) Sanchez, C. C.; Keck, G. E. Total Synthesis of (+)-Dactylolide. *Org. Lett.* **2005**, *7*, 3053–3056; (b) Crimmins, M. T.; Shamszad, M.; Mattson, A. E. A Highly Convergent Approach toward (-)-Brevenal. *Org. Lett.* **2010**, *12*, 2614–2617.

[57] Sabitha, G.; Rao, A. S.; Yadav, J. S. Synthesis of the C1-C25 southern domain of spirastrellolides B and F. *Org. Biomol. Chem.* **2013**, *11*, 7218–7231.

[58] Baker, B. A.; Boskovic, Z. V.; Lipshutz, B. H. (BDP)CuH: A "Hot" Stryker's Reagent for Use in Achiral Conjugate Reductions. *Org. Lett.* **2008**, *10*, 289–292.

[59] (a) Venukadasula, P. K. M.; Chegondi, R.; Maitra, S.; Hanson, P. R. A Concise, Phosphate-Mediated Approach to the Total Synthesis of (-)-Tetrahydrolipstatin. *Org. Lett.* **2010**, *12*, 1556–1559; b) Chegondi, R.; Tan, M. M. L.; Hanson, P. R. Phosphate tether-mediated approach to the formal total synthesis of (-)-salicylihalamides A and B. *J. Org. Chem.* **2011**, *76*, 3909–3916; c) Hanson, P. R.; Chegondi, R.; Nguyen, J.; Thomas, C. D.; Waetzig, J. D.; Whitehead, A. Total Synthesis of Dolabelide C: A Phosphate-Mediated Approach. *J. Org. Chem.* **2011**, *76*, 4358 –4370; (d) Jayasinghe, S.; Venukadasula, P. K. M.; Hanson, P. R. An Efficient, Modular Approach for the Synthesis of (+)-Strictifolione and a Related Natural Product. *Org. Lett.* **2014**, *16*, 122–125; (e) Chegondi, R.; Hanson, P. R. Synthetic studies to lyngbouilloside: a phosphate tether-mediated synthesis of the macrolactone core. *Tetrahedron Lett.* **2015**, Ahead of Print.

[60] Whitehead, A.; Waetzig, J. D.; Thomas, C. D.; Hanson, P. R. A Multifaceted Phosphate Tether: Application to the C15-C30 Subunit of Dolabelides A-D. *Org. Lett.* **2008**, *10*, 1421–1424.

[61] Lucas, B. S.; Luther, L. M.; Burke, S. D. Synthesis of the C1-C17 Segment of Phorboxazole B. *Org. Lett.* **2004**, *6*, 2965–2968.

[62] (a) Kolb, H. C.; Andersson, P. G.; Sharpless, K. B. Toward an Understanding of the High Enantioselectivity in the Osmium-Catalyzed Asymmetric Dihydroxylation (AD). 1. Kinetics. *J. Am. Chem. Soc.* **1994**, *116*, 1278–1291; (b)

Norrby, P.-O.; Kolb, H. C.; Sharpless, K. B. Toward an Understanding of the High Enantioselectivity in the Osmium-Catalyzed Asymmetric Dihydroxylation. 2. A Qualitative Molecular Mechanics Approach. *J. Am. Chem. Soc.* **1994**, *116*, 8470–8478.

[63] Molander, G. A.; Brown, A. R. Suzuki-Miyaura cross-coupling reactions of potassium vinyltrifluoroborate with aryl and heteroaryl electrophiles. *J. Org. Chem.* **2006**, *71*, 9681–9686.

[64] Pereira, S.; Srebnik, M. A study of hydroboration of alkenes and alkynes with pinacolborane catalyzed by transition metals. *Tetrahedron Lett.* **1996**, *37*, 3283–3286.

[65] (a) Bolduc, K. L.; Larsen, S. D.; Sherman, D. H. Efficient, divergent synthesis of cryptophycin unit A analogues. *Chem. Commun. (Cambridge, U. K.)* **2012**, *48*, 6414-6416; (b) Ghosh, A. K.; Li, J. A stereoselective synthesis of (+)-herboxidiene/GEX1A. *Org. Lett.* **2011**, *13*, 66–69; (c) Nicolaou, K. C.; Li, A.; Edmonds, D. J.; Tria, G. S.; Ellery, S. P. Total Synthesis of Platensimycin and Related Natural Products. *J. Am. Chem. Soc.* **2009**, *131*, 16905–16918.

[66] For similar rate acceleration in Stille coupling, see: Farina, V.; Krishnan, B. Large rate accelerations in the stille reaction with tri-2-furylphosphine and triphenylarsine as palladium ligands: mechanistic and synthetic implications. *J. Am. Chem. Soc.* **1991**, *113*, 9585–9595.

[67] Organ, M. G.; Calimsiz, S.; Sayah, M.; Hoi, K. H.; Lough, A. J. Pd-PEPPSI-IPent: an active, sterically demanding cross-coupling catalyst and its application in the synthesis of tetra-ortho-substituted biaryls. *Angew. Chem., Int. Ed.* **2009**, *48*, 2383–2387.

[68] Farcet, J.-B.; Himmelbauer, M.; Mulzer, J. Photochemical and Thermal [2+2] Cycloaddition to Generate the Bicyclo[3.2.0]heptane Core of Bielschowskysin. *Eur. J. Org. Chem.* **2013**, *2013*, 4379–4398.

[69] Banwell, M.; McLeod, M.; Premraj, R.; Simpson, G. Total synthesis of

herboxidiene, a complex polyketide from Streptomyces species A7847. *Pure Appl. Chem.* **2000**, *72*, 1631–1634.

[70] Corey, E. J.; Helal, C. J. Reduction of carbonyl compounds with chiral oxazaborolidine catalysts: A new paradigm for enantioselective catalysis and a powerful new synthetic method. *Angew. Chem., Int. Ed.* **1998**, *37*, 1986–2012.

[71] Haukaas, M. H.; O'Doherty, G. A. Enantioselective Synthesis of N-Cbz-Protected 6-Amino-6-deoxymannose, -talose, and -gulose. *Org. Lett.* **2001**, *3*, 3899–3902.

Chapter 5

Experimental data and spectra for chapters 2–4

General Experimental Section

All reactions were carried out in an oven- or flame-dried glassware under argon atmosphere using standard gas-tight syringes, cannulae, and septa. Stirring was achieved with oven-dried magnetic stir bars. The solvents Et_2O, THF and CH_2Cl_2 were purified by passage through a purification system (Solv-Tek) employing activated Al_2O_3 ((Pangborn, A. B.; Giardello, M. A.; Grubbs, R. H.; Rosen, R. K.; Timmers, F. J. *Organometallics* **1996**, *15*, 1518–1520). Et_3N was purified by passage over basic alumina and stored over KOH. Butyllithium was purchased from Aldrich and titrated prior to use. All olefin metathesis catalysts were acquired from Materia and used without further purification. Flash column chromatography was performed with Sorbent Technologies (30930M-25, Silica Gel 60A, 40-63 mm) and thin layer chromatography was performed on silica gel $60F_{254}$ plates (EM-5717, Merck). Deuterated solvents were purchased from Cambridge Isotope laboratories. ^1H and ^{13}C NMR spectra were recorded in $CDCl_3$ (unless otherwise mentioned) on a Bruker DRX-500 spectrometer operating at 500 MHz, and 125 MHz, respectively and calibrated to the solvent peak. ^{31}P NMR spectra was recorded on Bruker DRX-400 spectrometer operating at 162 MHz. High-resolution mass spectrometry (HRMS) was recorded on a LCT Premier Spectrometer (Micromass UK Limited) operating on ESI (MeOH). Observed rotations at 589 nm, were measured using AUTOPOL IV Model automatic polarimeter. IR was recorded on Shimadzu FTIR-8400S instrument.

5.1: Phosphate tether-mediated ring-closing metathesis studies (Chapter 2)

Experimental Section

General procedure for Triene generation: To a solution of alcohol (1.1 mmol) in THF (0.2 M), at -40 ºC under argon, was added *n*BuLi (2.5 M, 0.9 mmol), dropwise. The mixture was allowed to stir for 5 minutes, at which point a solution of phosphate monochloride (1.5 mmol) in THF (1 mL) was slowly added to the reaction vessel via cannulation. The mixture stirred at –40 ºC for 2 hours (monitored by TLC) and was quenched with 5 mL of aqueous NH_4Cl (sat.). The biphasic solution was separated, and the aqueous layer was extracted

EtOAc (3 x 10 mL). The combined organic layers were washed with brine, dried over Na_2SO_4 and concentrated under reduced pressure. Purification via flash chromatography (Hexanes:EtOAc eluent) provided triene-containing monocyclic phosphate triester product. All of the trienes reported here are synthesized following the same procedure.

General procedure for RCM to provide bicyclo[4.3.1] phosphates, bicyclo[5.3.1] phosphates and bicyclo[6.3.1]phosphates: To a flask containing monocyclic phosphate triester (1 mmol) in CH_2Cl_2 (dry, degassed, 0.007 M), equipped with an argon inlet and reflux condenser, was added the **G-II** catalyst (portion-wise), and the reaction mixture was heated to reflux. Upon completion (monitored by TLC), the reaction was cooled to room temperature and concentrated under reduced pressure. Purification via flash chromatography (Hexanes:EtOAc eluent) provided the corresponding bicyclic phosphate.

General procedure for RCM to provide bicyclo[5.3.1]phosphates (generated from homologated diene diol), bicyclo[6.3.1]phosphates (generated from homologated diene diol) and bicyclo[8.3.1]phosphates: To a flask containing monocyclic phosphate triester (1 mmol) in CH_2Cl_2 (dry, degassed, 0.001 M), equipped with an argon inlet and reflux condenser, was added *p*-benzoquinone (10 mol %). Then, **G-I** or **G-II** catalyst [see reaction Schemes, *vide supra*] was added to the reaction [portion-wise over the allotted reaction time], and the reaction mixture was heated to reflux. Upon completion (monitored by TLC), the reaction was cooled to room temperature and concentrated under reduced pressure. Purification via flash chromatography (Hexanes:EtOAc eluent) provided the corresponding bicyclic phosphate.

Experimental data

(4*S*,6*S*)-2-(((2*S*,3*S*,4*S*)-1-((4-methoxybenzyl)oxy)-2,4-dimethylhex-5-en-3-yl)oxy)-4,6-divinyl-1,3,2-dioxaphosphinane 2-oxide (2.1.3):

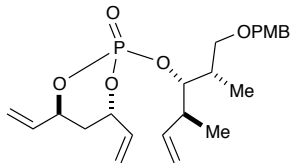

2.1.3

Yield: 82% (172 mg isolated as colorless oil starting from 100 mg of monochlorophosphate);

FTIR (thin film): 2952, 2949, 1615, 1547, 1252, 1234, 1009, 845, 741 cm-1;

Optical Rotation: $[\alpha]_D$ = +23.0 (c = 0.1, $CHCl_3$);

^{1}H NMR (500 MHz, $CDCl_3$) δ 7.28 (d, *J* = 8.0 Hz, 2H), 6.87 (d, *J* = 8.1 Hz, 2H), 6.01 (ddd, *J* = 16.7, 10.8, 5.7 Hz, 1H), 5.96–5.78 (m, 2H), 5.45 (d, *J* = 17.1 Hz, 1H), 5.38 (d, *J* = 17.2 Hz, 1H), 5.29 (d, *J* = 10.6 Hz, 2H), 5.10–5.02 (m, 3H), 4.97–4.90 (m, 1H), 4.60–4.55 (m, 1H), 4.49 (d, *J* = 11.5 Hz, 1H), 4.36 (d, *J* = 11.5 Hz, 1H), 3.81 (s, 3H), 3.41 (dd, *J* = 9.0, 7.1 Hz, 1H), 3.32 (dd, *J* = 8.9, 7.1 Hz, 1H), 2.50 (dq, *J* = 13.8, 6.9 Hz, 1H), 2.18–2.11 (m, 1H), 2.06 (ddd, *J* = 18.5, 14.0, 6.0 Hz, 2H), 1.07 (d, *J* = 6.8 Hz, 3H), 0.99 (d, *J* = 6.8 Hz, 3H);

^{13}C NMR (126 MHz, CDCl3) δ 159.0, 140.0, 135.4 (d, J_{CP} = 4.0 Hz), 135.3 (d, J_{CP} = 7.6 Hz), 130.7, 129.4, 117.7, 117.1, 115.6, 113.7, 85.0 (d, J_{CP} = 7.4 Hz), 77.3 (d, J_{CP} = 6.8 Hz), 75.5 (d, J_{CP} = 6.2 Hz), 72.8 (d, J_{CP} = 6.0 Hz), 72.5, 55.3, 41.2 (d, J_{CP} = 3.5 Hz), 36.1 (d, J_{CP} = 3.9 Hz), 35.2 (d, J_{CP} = 7.3 Hz), 17.5, 11.9;

^{31}P NMR (162 MHz, CDCl3) δ –7.01;

HRMS: cald. for $C_{23}H_{33}O_6PNa$ $(M+Na)^+$ 459.1912; found 459.1902 (TOF MS ES+).

(4*R*,6*R*)-2-(((2*S*,3*S*,4*S*)-1-((4-methoxybenzyl)oxy)-2,4-dimethylhex-5-en-3-yl)oxy)-4,6-divinyl-1,3,2-dioxaphosphinane 2-oxide (2.1.4):

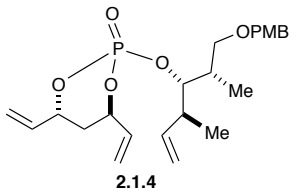

2.1.4

Yield: 75% (55 mg isolated starting from 32 mg of monochlorophosphate);

FTIR (thin film): 2978, 2962, 1610, 1521, 1278, 1249, 1000, 836, 746 cm^{-1};

Optical Rotation: $[\alpha]_D = -26.2$ (c = 1, $CHCl_3$);

^{1}H NMR (500 MHz, $CDCl_3$) δ 7.28 (d, J = 8.6 Hz, 2H), 6.87 (d, J = 8.6 Hz, 2H), 6.00 (dddd, J = 17.1, 10.5, 6.2, 0.8 Hz, 1H), 5.90 (dddd, J = 17.1, 10.7, 5.1, 1.7 Hz, 1H), 5.85–5.79 (m, 1H), 5.44 (ddd, J = 17.1, 1.5, 1.2 Hz, 1H), 5.35 (ddd, J = 17.2, 1.3, 1.0 Hz, 1H), 5.27 (dddd, J = 10.7, 4.8, 1.3, 1.0 Hz, 2H), 5.06–5.00 (m, 3H), 4.96 (ddt, J = 9.6, 7.9, 5.0 Hz, 1H), 4.55 (dddd, J = 9.7, 6.5, 4.3 Hz, 1H), 4.51 (d, J = 11.5 Hz, 1H), 4.38 (d, J = 11.5 Hz, 1H), 3.80 (s, 3H), 3.49 (dd, J = 9.2, 6.2 Hz, 1H), 3.35 (dd, J = 9.2, 6.6 Hz, 1H), 2.53–2.43 (m, 1H), 2.14 (dddd, J = 14.5, 7.9, 4.8, 1.5 Hz, 1H), 2.10–2.05 (m, 1H), 2.02 (dddd, J = 14.6, 5.6, 3.9, 1.7 Hz, 1H), 1.04 (d, J = 6.4 Hz, 3H), 1.00 (d, J = 5.8 Hz, 3H);

^{13}C NMR (126 MHz, $CDCl_3$) δ 159.1, 140.0, 135.4 (d, J_{CP} = 3.9 Hz), 135.3 (d, J_{CP} = 7.6 Hz), 130.7, 129.4, 117.7, 117.1, 115.6, 113.7, 85.0 (d, J_{CP} = 7.4 Hz), 77.4 (d, J_{CP} = 6.7 Hz), 75.5 (d, J_{CP} = 6.2 Hz), 72.8, 72.6, 55.3, 41.2 (d, J_{CP} = 3.5 Hz), 36.2 (d, J_{CP} = 3.9 Hz), 35.2 (d, J_{CP} = 7.3 Hz), 17.5, 11.8;

^{31}P NMR (162 MHz, $CDCl_3$) δ –6.64;

HRMS: cald. for $C_{23}H_{33}O_6PNa$ $(M+Na)^+$ 459.1912; found 459.1895 (TOF MS ES+).

(1*R*,3*S*,4*S*,7*R*,9*R*,*Z*)-3-((S)-1-((4-methoxybenzyl)oxy)propan-2-yl)-4-methyl-9-vinyl-2,10,11-trioxa-1-phosphabicyclo[5.3.1]undec-5-ene 1-oxide (*trans*,*anti*-2.1.6):

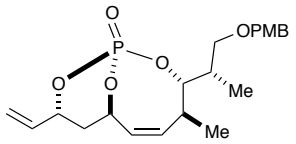

trans,anti-**2.1.6**

Yield: 65% (60 mg isolated as colorless oil starting from 80 mg of triene);

FTIR (thin film): 2982, 2934, 1605, 1507, 1268, 1241, 1003, 831, 741 cm-1;

Optical Rotation: $[\alpha]_D = -7.3$ (c = 0.16, $CHCl_3$);

^{1}H NMR (500 MHz, $CDCl_3$) δ 7.26 (d, *J* = 8.5 Hz, 2H), 6.87 (d, *J* = 8.5 Hz, 2H), 5.87 (dddd, *J* = 17.2, 10.6, 5.4, 2.0 Hz, 1H), 5.49 (ddd, *J* = 11.6, 8.2, 2.8 Hz, 1H), 5.43 (ddd, *J* = 17.2, 1.2, 1.2 Hz, 1H), 5.39 (d, *J* = 11.9 Hz, 1H), 5.27 (ddd, *J* = 10.6, 1.2, 1.1 Hz, 1H), 4.98 (dd, *J* = 11.8, 5.4 Hz, 1H), 4.48 (s, 2H), 4.06 (ddd, *J* = 29.1, 11.5, 3.3 Hz, 1H), 3.80 (s, 3H), 3.71 (t, *J* = 8.9 Hz, 1H), 3.53–3.45 (m, 1H), 3.48 (dd, *J* = 9.1, 5.9 Hz, 2H), 2.24–2.11 (m, 2H), 1.78 (ddd, *J* = 14.5, 3.9, 1.8 Hz, 1H), 1.19 (d, *J* = 7.2 Hz, 3H), 1.01 (d, *J* = 6.6 Hz, 3H);

^{13}C NMR (126 MHz, CDCl3) δ 159.1, 136.0, 135.4 (d, J_{CP} = 10.5 Hz), 130.7, 129.2, 128.1, 117.1 (d, J_{CP} = 1.3 Hz), 113.7, 83.6 (d, J_{CP} = 7.4 Hz), 77.8 (d, J_{CP} = 7.2 Hz), 76.1 (d, J_{CP} = 6.3 Hz), 72.9, 72.2, 55.2, 36.5 (d, J_{CP} = 6.2 Hz), 35.1, 32.6 (d, J_{CP} = 1.3 Hz), 17.4, 9.4;

^{31}P NMR (162 MHz, CDCl3) δ –10.71;

HRMS: cald. for $C_{21}H_{29}O_6PNa$ $(M+Na)^+$ 431.1599; found 431.1575 (TOF MS ES+).

(4*S*,6*S*)-2-((2,4-dimethylpenta-1,4-dien-3-yl)oxy)-4,6-divinyl-1,3,2-dioxaphosphinane 2-oxide (2.3.2):

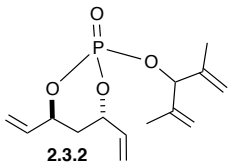

2.3.2

Yield: 35% (53 mg isolated as colorless oil starting from 111 mg of monochlorophosphate);

FTIR (thin film): 2922, 1827, 1649, 1448, 1375, 1281, 1140, 1119, 1003, 928 cm^{-1};

Optical Rotation: $[\alpha]_D$ = +48.40 (*c* = 0.75, $CHCl_3$);

^{1}H NMR (400 MHz, $CDCl_3$) δ 6.02 (ddd, *J* = 16.7, 10.7, 5.5 Hz 1H), 5.90 (dddd, *J* = 17.3, 10.6, 5.1, 1.5 Hz, 1H), 5.45 (d, *J* = 22.0 Hz, 1H), 5.39 (d, *J* = 21.6 Hz, 1H), 5.33–5.27 (m, 2H), 5.20–5.11 (m, 3H), 5.11–5.03 (m, 1H), 5.01 (s, 2H), 4.99–4.92 (m, 1H), 2.17 (dddd, *J* = 12.8, 7.8, 4.8, 1.4 Hz, 1H), 2.07 (dddd, *J* = 14.7, 5.4, 3.7, 1.8 Hz, 1H), 1.66 (s, 6H);

^{13}C NMR (126 MHz, $CDCl_3$) δ 141.3 (d, J_{CP} = 4.3 Hz), 141.1 (d, J_{CP} = 5.3 Hz), 135.2 (d, J_{CP} = 3.2 Hz), 135.1 (d, J_{CP} = 7.5 Hz), 117.7, 117.5, 114.4, 113.5, 84.7 (d, J_{CP} = 5.2 Hz), 77.6 (d, J_{CP} = 6.8 Hz), 76.0 (d, J_{CP} = 6.1 Hz), 35.1 (d, J_{CP} = 7.7 Hz), 18.0, 17.4;

^{31}P NMR (162 MHz, $CDCl_3$) δ –8.58;

HRMS cald for $C_{14}H_{21}O_4PNa$ $(M+Na)^+$ 307.1075; found 307.1067 (TOF MS ES+).

(1*S*,3*R*,6*S*,8*S*)-4-methyl-3-(prop-1-en-2-yl)-8-vinyl-2,9,10-trioxa-1-phosphabicyclo[4.3.1]dec-4-ene 1-oxide (*cis*-2.3.3):

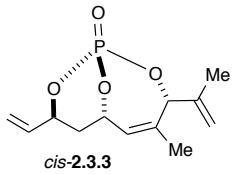

cis-**2.3.3**

Yield: 36% brsm (4.8 mg isolated as colorless oil starting from 20 mg of triene);

FTIR (thin film): 2922, 1726, 1298, 1026, 966, 768 cm^{-1};

Optical Rotation: $[\alpha]_D$ = +103.14(*c* = 0.17, $CHCl_3$);

^{1}H NMR (500 MHz, $CDCl_3$) δ 5.89 (dddd, *J* = 17.2, 10.8, 5.1, 2.1 Hz 1H), 5.59 (d, *J* = 5.3 Hz, 1H), 5.45 (d, *J* = 17.2 Hz, 1H), 5.43–5.39 (m, 1H), 5.28 (d, *J* = 10.7 Hz, 1H), 5.12 (d, *J* = 21.5 Hz, 1H), 5.09–5.03 (m, 3H), 2.19 (ddd, *J* = 14.5, 12.1, 6.2 Hz, 1H), 1.93–1.81 (m, 1H), 1.79 (s, 3H), 1.75 (s, 3H);

^{13}C NMR (126 MHz, $CDCl_3$) δ 141.1 (d, J_{CP} = 10.1 Hz), 138.1, 135.0 (d, J_{CP} = 10.2 Hz), 124.9, 117.1 (d, J_{CP} = 1.0 Hz), 116.6, 80.6 (d, J_{CP} = 5.7 Hz), 76.7 (d, J_{CP} = 6.2 Hz), 76.5 (d, J_{CP} = 6.2 Hz), 35.3 (d, J_{CP} = 6.2 Hz), 22.2, 17.5;

^{31}P NMR (162 MHz, $CDCl_3$) δ (ppm) –5.91;

HRMS cald for $(C_{12}H_{17}O_4P)_2Na(2M+Na)^+$ 535.1627; found 536.1624 (TOF MS ES+).

(4*S*,6*S*)-2-(((*R*)-1-(benzyloxy)-4-methylpent-4-en-2-yl)oxy)-4,6-divinyl-1,3,2-dioxaphosphinane-2-oxide (2.5.2):

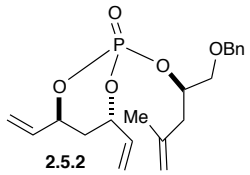

2.5.2

Yield: 69% (105 mg isolated as colorless oil starting from 84 mg of monochlorophosphate);

FTIR (thin film): 2920, 2359,1827, 1649, 1454, 1283, 1121, 1097, 999, 929, 739 cm^{-1};

Optical Rotation: $[\alpha]_D$ = +40.72 (*c* = 1.04, $CHCl_3$);

^{1}H NMR (400 MHz, $CDCl_3$) δ 7.36–7.27 (m, 5H), 6.06 (ddd, *J* = 17.1, 10.6, 6.2 Hz, 1H), 5.89 (dddd, *J* = 17.2, 10.6, 5.2, 1.7 Hz, 1H), 5.43 (ddd, *J* = 17.1, 1.3, 1.1 Hz, 1H), 5.35 (ddd, *J* = 17.2, 1.4, 1.0 Hz, 1H), 5.28 (dd, *J* = 11.7, 1.1 Hz, 1H), 5.23 (dd, *J* = 10.6, 1.1 Hz, 1H), 5.08–4.95 (m, 2H), 4.86–4.80 (m, 2H), 4.80–4.71 (m, 1H), 4.60 (d, *J* = 12.0 Hz, 1H), 4.55 (d, *J* = 12.0 Hz, 1H), 3.71–3.63 (m, 2H), 2.53–2.40 (m, 2H), 2.14 (dddd, *J* = 14.6, 8.1, 4.9, 1.5 Hz, 1H), 2.04 (dddd, *J* = 14.7, 5.4, 3.8, 1.8 Hz, 1H), 1.77 (s, 3H);

^{13}C NMR (126 MHz, $CDCl_3$) δ 141.2, 138.1, 135.3 (d, J_{CP} = 3.0 Hz), 135.2 (d, J_{CP} = 7.8 Hz), 128.3, 127.7, 127.6 (d, J_{CP} = 5.8 Hz), 117.9 117.2, 113.9, 78.1 (d, J_{CP} = 6.9 Hz), 76.1 (d, J_{CP} = 6.3 Hz), 75.8 (d, J_{CP} = 6.2 Hz), 73.3, 71.8 (d, J_{CP} = 3.2 Hz), 40.9 (d, J_{CP} = 5.8 Hz), 35.3 (d, J_{CP} = 7.6 Hz), 22.2;

^{31}P NMR (162 MHz, $CDCl_3$) δ –8.20;

HRMS cald for $C_{20}H_{27}O_5PNa$ $(M+Na)^+$ 401.1494; found 401.1512 (TOF MS ES+).

(1*S*,3*R*,7*S*,9*S*,*Z*)-3-((benzyloxy)methyl)-5-methyl-9-vinyl-2,10,11-trioxa-1-phosphabicyclo[5.3.1]undec-5-ene 1-oxide (*trans*-2.5.4):

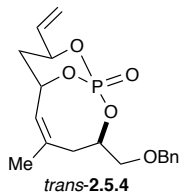

trans-**2.5.4**

Yield: 32% (11.8 mg isolated as colorless oil starting from 40 mg of triene); **FTIR** (thin film): 2918, 2849, 1718, 1582, 1364, 1333, 1283, 1126, 1090, 1001, 901 cm^{-1}; **Optical Rotation**: $[\alpha]_D$ = +24.51(*c* = 0.16, $CHCl_3$);

^{1}H NMR (500 MHz, $CDCl_3$) δ 7.41–7.27 (m, 5H), 5.84 (dddd, *J* = 17.2, 10.6, 5.4, 2.1 Hz, 1H), 5.42 (ddd, *J* = 17.1, 5.8, 4.6 Hz, 1H), 5.34–5.16 (m, 2H), 5.24 (m, ddd, *J* = 10.7, 1.2, 1.1 Hz, 1H), 5.02 (dd, *J* = 11.7, 5.4 Hz, 1H), 4.68 (dd, *J* = 11.9, 4.3 Hz, 1H), 4.60 (dd, *J* = 11.9, 5.1 Hz, 1H), 4.08 (dd, *J* = 10.0, 6.2 Hz, 1H), 3.75 (dd, *J* = 10.0, 6.5 Hz, 1H), 3.38–3.26 (m, 1H), 2.21–2.14 (m, 1H), 2.09 (dd, *J* = 13.9, 3.1 Hz, 1H), 1.92–1.89 (m, 1H), 1.88 (dd, *J* = 2.4, 1.4 Hz, 3H), 1.76 (ddd, *J* = 14.5, 3.9, 1.9 Hz, 1H);

^{13}C NMR (126 MHz, $CDCl_3$) δ 137.9, 135.5, 128.8, 128.4, 127.9, 127.7, 124.6, 117.2, 77.6 (d, J_{CP} = 7.4 Hz), 75.3 (d, J_{CP} = 5.8 Hz), 73.7, 72.3, 36.7 (d, J_{CP} = 6.6 Hz), 34.7, 34.1, 29.7;

^{31}P NMR (162 MHz, $CDCl_3$) δ (ppm) –10.34;

HRMS cald for $C_{18}H_{23}O_5PNa$ $(M+Na)^+$ 373.1181; found 373.1176 (TOF MS ES+).

(4*R*,6*R*)-2-(((*R*)-1-(benzyloxy)-4-methylpent-4-en-2-yl)oxy)-4,6-divinyl-1,3,2-dioxaphosphinane 2-oxide (2.5.3):

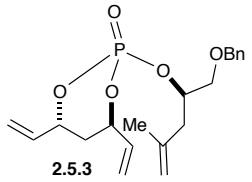

2.5.3

Yield: 45% (85 mg isolated as colorless oil starting from 105 mg of monochlorophosphate); **FTIR** (thin film): 2924, 1827, 1645, 1454, 1285, 1120, 1003, 926 cm^{-1}; **Optical Rotation**: $[\alpha]_D$ = –53.0 (*c* = 2.61, $CHCl_3$);

^{1}H NMR (400 MHz, $CDCl_3$) δ 7.35–7.28 (m, 5H), 6.08 (dddd, *J* = 17.2, 10.6, 6.3, 0.8 Hz, 1H), 5.82 (dddd, *J* = 17.4, 10.6, 5.2, 1.7 Hz, 1H), 5.37(ddd, *J* = 7.4, 1.4, 1.2 Hz, 1H), 5.32 (ddd, *J* = 7.2, 1.4, 1.1 Hz, 1H),), 5.27 (ddd, *J* = 10.5, 1.2, 1.0 Hz, 1H), 5.22 (ddd, *J* = 10.6, 1.3, 1.1 Hz, 1H), 5.06–4.97 (m, 2H), 4.86–4.78 (m, 2H), 4.77–4.71 (m, 1H), 4.58 (d, *J* = 11.9 Hz, 1H), 4.52 (d, *J* = 11.8 Hz, 1H), 3.66 (ddd, *J* = 10.7, 3.5, 1.7 Hz, 1H), 3.58 (dd, *J* = 10.7, 5.8 Hz, 1H), 2.55 (dd, *J* = 14.2, 6.6 Hz, 1H), 2.43 (dd, *J* = 14.1, 7.1 Hz, 1H), 2.10

(dddd, J = 14.4, 8.0, 4.8, 1.6 Hz, 1H), 2.01 (dddd, J = 14.7, 5.5, 3.9, 1.8 Hz, 1H), 1.79 (s, 3H);

^{13}C NMR (126 MHz, $CDCl_3$) δ 140.9, 137.9, 135.3, 135.3 (d, J_{CP} = 3.0 Hz), 128.3, 127.8, 127.7 (d, J_{CP} = 5.4 Hz), 117.8, 117.0, 114.0, 78.1 (d, J_{CP} = 6.8 Hz), 76.1 (d, J_{CP} = 6.1 Hz), 75.71 (d, J_{CP} = 6.0 Hz), 73.3, 71.6 (d, J_{CP} = 4.3 Hz), 40.6 (d, J_{CP} = 4.8 Hz), 35.3 (d, J_{CP} = 7.6 Hz), 22.6;

^{31}P NMR (162 MHz, $CDCl_3$) δ –8.09;

HRMS cald for $C_{20}H_{27}O_5PNa$ $(M+Na)^+$ 401.1494; found 401.1479 (TOF MS ES+).

(4*R*,6*R*)-2-(((1*R*,2*S*)-2-methyl-1-(4-nitrophenyl)but-3-en-1-yl)oxy)-4,6-divinyl-1,3,2-dioxaphosphinane 2-oxide (2.7.2):

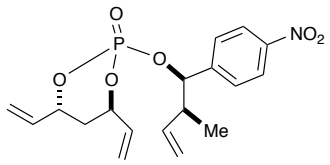

2.7.2

Yield: 57% (95 mg isolated as colorless oil starting from 91 mg of monochlorophosphate);

FTIR (thin film): 3080, 2969, 2913, 1617, 1525, 1339, 1281, 1102, 1019, 921, 879, 751 cm^{-1};

Optical Rotation: $[\alpha]_D$ = –44.8 (c = 0.5, $CHCl_3$);

^{1}H NMR (500 MHz, $CDCl_3$) δ 8.20 (d, J = 8.2 Hz, 2H), 7.47 (d, J = 8.7 Hz, 2H), 6.01 (ddd, J = 16.4, 10.7, 5.4 Hz, 1H), 5.72 (ddd, J = 15.9, 10.6, 5.3 Hz, 1H), 5.61 (ddd, J = 17.8, 9.0, 5.5 Hz, 1H), 5.43–5.31 (m, 3H), 5.18 (ddd, J = 6.0, 2.7, 0.9 Hz, 2H), 5.14–5.06 (m, 1H), 5.02 (d, J = 10.3 Hz, 1H), 4.97 (dd, J = 17.2, 1.0 Hz, 1H), 4.69–4.62 (m, 1H), 2.81–2.73 (m, 1H), 2.17–2.10 (m, 1H), 2.01 (dddd, J = 14.8, 5.3, 3.6, 1.8 Hz, 1H), 1.14 (d, J = 6.8 Hz, 3H);

^{13}C NMR (126 MHz, $CDCl_3$) δ 147.6, 145.9 (d, J_{CP} = 2.3 Hz), 137.3, 134.9 (d, J_{CP} = 3.2 Hz),

134.4 (d, J_{CP} = 7.3 Hz), 127.9, 123.3 (d, J_{CP} = 5.1 Hz), 118.0 (d, J_{CP} = 14.5 Hz), 117.6, 117.2, 82.8 (d, J_{CP} = 6.0 Hz), 77.9 (d, J_{CP} = 6.8 Hz), 75.9 (d, J = 6.1 Hz), 44.2 (d, J_{CP} = 6.7 Hz), 34.9 (d, J_{CP} = 7.7 Hz), 15.6;

^{31}P NMR (162 MHz, $CDCl_3$) δ –7.54;

HRMS: cald. for $C_{18}H_{22}NO_6PNa$ $(M+Na)^+$ 402.1082; found 402.1069 (TOF MS ES+).

(1*R*,3*R*,4*S*,7*R*,9*R*,*Z*)-4-methyl-3-(4-nitrophenyl)-9-vinyl-2,10,11-trioxa-1 phosphabicyclo[5.3.1]undec-5-ene 1-oxide (*cis,syn*-2.7.4):

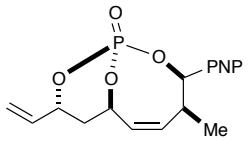

cis,syn-**2.7.4**

Yield: 65% (18 mg isolated as colorless oil starting from 30 mg of triene); **FTIR** (thin film): 2982, 2923, 1613, 1545, 1324, 1295, 1012, 975, 814, 759 cm^{-1};

Optical Rotation: $[\alpha]_D$ = +70.4 (*c* = 1.05, $CHCl_3$);

^{1}H NMR (500 MHz, $CDCl_3$) δ 8.21 (d, *J* = 8.8 Hz, 2H), 7.43 (d, *J* = 8.7 Hz, 2H), 5.91 (dddd, *J* = 17.2, 10.7, 5.1, 2.3 Hz, 1H), 5.67 (d, *J* = 11.7 Hz, 1H), 5.51–5.44 (m, 2H), 5.38 (dd, *J* = 25.2, 4.8 Hz, 1H), 5.32 (ddd, *J* = 10.7, 1.1, 1.0 Hz, 1H), 5.30–5.21 (m, 2H), 4.09–4.01 (m, 1H), 2.31 (ddd, *J* = 14.7, 12.0, 6.1 Hz, 1H), 1.99 (ddd, *J* = 14.7, 3.7, 2.1 Hz, 1H), 0.80 (d, *J* = 6.9 Hz, 3H);

^{13}C NMR (126 MHz, $CDCl_3$) δ 147.9, 143.4 (d, J_{CP} = 13.6 Hz), 134.7 (d, J_{CP} = 10.0 Hz), 131.6, 130.7, 128.2, 123.2, 117.5 (d, J_{CP} = 1.0 Hz), 78.4 (d, J_{CP} = 3.7 Hz), 78.3 (d, J_{CP} = 7.3 Hz), 77.7 (d, J_{CP} = 6.3 Hz), 36.2 (d, J_{CP} = 6.6 Hz), 34.2, 16.8;

^{31}P NMR (162 MHz, $CDCl_3$) δ –9.46;

HRMS: cald. for $2(C_{16}H_{18}NO_6P)Na$ $(2M+Na)^+$ 725.1641; found 725.1623 (TOF MS ES+).

(4*S*,6*S*)-2-(((1*R*,2*S*)-2-methyl-1-(4-nitrophenyl)but-3-en-1-yl)oxy)-4,6-divinyl-1,3,2-dioxaphosphinane 2-oxide (2.7.3):

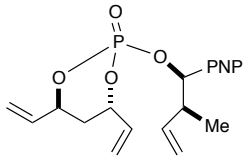

2.7.3

Yield: 57% (90 mg isolated as colorless oil starting from 91 mg of monochlorophosphate); **FTIR** (thin film): 3059, 2952, 2931, 1617, 1501, 1331, 1269, 1139, 1024, 927, 739 cm^{-1};

Optical Rotation: $[\alpha]_D$ = +32.9 (*c* = 0.93, $CHCl_3$);

^{1}H NMR (500 MHz, $CDCl_3$) δ 8.21 (d, *J* = 8.7 Hz, 2H), 7.48 (d, *J* = 8.7 Hz, 2H), 5.96–5.85 (m, 2H), 5.66 (ddd, *J* = 17.5, 8.8, 5.6 Hz, 1H), 5.48 (d, *J* = 17.1 Hz, 1H), 5.42 (dd, *J* = 8.5, 6.0 Hz, 1H), 5.33 (d, *J* = 10.7 Hz, 1H), 5.29 (d, *J* = 17.2 Hz, 1H), 5.25 (d, *J* = 10.6 Hz, 1H), 5.07–4.98 (m, 4H), 2.79–2.71 (m, 1H), 2.18 (dddd, *J* = 14.1, 7.6, 4.7, 1.6 Hz, 1H), 2.08 (dddd, *J* = 14.8, 5.6, 3.8, 1.8 Hz, 1H), 1.07 (d, *J* = 6.8 Hz, 3H);

^{13}C NMR (126 MHz, $CDCl_3$) δ 147.5, 145.9 (d, J_{CP} = 3.1 Hz), 137.7, 134.8 (d, J_{CP} = 3.6 Hz), 134.7 (d, J_{CP} = 7.1 Hz), 127.8, 123.3, 118.0, 117.7, 116.9, 82.8 (d, J_{CP} = 6.0 Hz), 77.6 (d, J_{CP} = 6.8 Hz), 76.4 (d, J_{CP} = 6.3 Hz), 44.0 (d, J_{CP} = 6.1 Hz), 35.0 (d, J_{CP} = 7.9 Hz), 14.8;

^{31}P NMR (162 MHz, $CDCl_3$) δ –7.82;

HRMS: cald. for $C_{18}H_{22}NO_6PNa$ $(M+Na)^+$ 402.1082; found 402.1072 (TOF MS ES+).

(4*R*,6*R*)-2-(((1*R*,2*R*)-2-methyl-1-(4-nitrophenyl)but-3-en-1-yl)oxy)-4,6-divinyl-1,3,2-dioxaphosphinane 2-oxide (2.8.2):

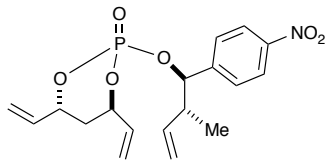

2.8.2

Yield: 55% (100 mg isolated as colorless oil starting from 100 mg of monochlorophosphate);

FTIR (thin film): 2972, 2933, 1610, 1521, 1348, 1282, 1112, 1004, 927, 885, 750 cm^{-1};

Optical Rotation: $[\alpha]_D$ = –32.8 (*c* = 0.6, $CHCl_3$);

^{1}H NMR (500 MHz, $CDCl_3$) δ 8.21 (d, *J* = 8.7 Hz, 2H), 7.47 (d, *J* = 8.7 Hz, 2H), 6.01 (dddd, *J* = 17.0, 10.7, 5.3, 0.7 Hz, 1H), 5.81–5.70 (m, 2H), 5.43–5.38 (m, 2H), 5.36 (d, *J* = 10.9 Hz, 1H), 5.21 (d, *J* = 17.0 Hz, 1H), 5.19 (d, *J* = 10.9 Hz, 1H), 5.11 (d, *J* = 10.3 Hz, 1H), 5.13–5.06 (m, 1H), 5.02 (d, *J* = 17.1 Hz, 1H), 4.76–4.69 (m, 1H), 2.77–2.68 (m, 1H), 2.15 (dddd, *J* = 9.5, 8.0, 4.5, 2.1 Hz, 1H), 2.03 (dddd, *J* = 14.8, 5.4, 3.6, 1.8 Hz, 1H), 1.01 (d, *J* = 6.9 Hz, 3H);

^{13}C NMR (126 MHz, $CDCl_3$) δ 147.6, 146.1 (d, J_{CP} = 2.5 Hz), 137.7, 135.0 (d, J_{CP} = 3.2 Hz), 134.5 (d, J_{CP} = 7.2 Hz), 127.7, 123.5, 117.9, 117.7, 117.1, 82.8 (d, J_{CP} = 6.0 Hz), 77.9 (d, J_{CP} = 6.8 Hz), 76.1 (d, J_{CP} = 6.1 Hz), 44.4 (d, J_{CP} = 6.5 Hz), 34.9 (d, J_{CP} = 7.7 Hz), 15.8;

^{31}P NMR (162 MHz, $CDCl_3$) δ –7.61;

HRMS: cald. for $C_{18}H_{22}NO_6PNa$ $(M+Na)^+$ 402.1082; found 402.1074 (TOF MS ES+).

(4*S*,6*S*)-2-(((1*R*,2*R*)-2-methyl-1-(4-nitrophenyl)but-3-en-1-yl)oxy)-4,6-divinyl-1,3,2-dioxaphosphinane 2-oxide (2.8.3):

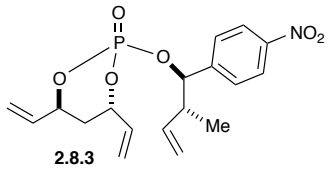

2.8.3

Yield: 61% (110 mg isolated as colorless oil starting from 100 mg of monochlorophosphate);

FTIR (thin film): 2954, 2931, 1608, 1529, 1319, 1289, 1136, 1015, 920, 875, 751 cm^{-1};

Optical Rotation: $[\alpha]_D$ = +41.1 (*c* = 1.24, $CHCl_3$);

^{1}H NMR (500 MHz, $CDCl_3$) δ 8.21 (d, *J* = 8.7 Hz, 2H), 7.48 (d, *J* = 8.7 Hz, 2H), 5.96–5.88 (m, 2H), 5.73 (ddd, *J* = 17.9, 10.3, 7.8Hz, 1H), 5.48 (d, *J* = 17.0 Hz, 1H), 5.39 (dd, *J* = 8.6, 6.2 Hz, 1H), 5.33 (d, *J* = 4.2 Hz, 1H), 5.30 (d, *J* = 11.1 Hz, 1H), 5.27 (d, *J* = 10.6 Hz, 1H), 5.09 (d, *J* = 10.3 Hz, 1H), 5.07–4.99 (m, 3H), 2.75–2.67 (m, 1H), 2.18 (dddd, *J* = 14.1, 7.6, 4.7, 1.5 Hz, 1H), 2.08 (dddd, *J* = 14.8, 5.6, 3.8, 1.8 Hz, 1H), 0.99 (d, *J* = 6.9 Hz, 3H);

^{13}C NMR (126 MHz, $CDCl_3$) δ 147.5, 146.1 (d, J_{CP} = 2.9 Hz), 137.9, 134.7 (d, J_{CP} = 3.4 Hz), 134.7 (d, J_{CP} = 7.2 Hz), 127.6, 123.3, 118.0, 117.7, 117.0, 82.9 (d, J_{CP} = 5.9 Hz), 77.7 (d, J_{CP} = 6.8 Hz), 76.3 (d, J_{CP} = 6.3 Hz), 44.4 (d, J_{CP} = 6.2 Hz), 35.0 (d, J_{CP} = 7.8 Hz), 15.8;

^{31}P NMR (162 MHz, $CDCl_3$) δ –7.82;

HRMS: cald. for $C_{18}H_{22}NO_6PNa$ $(M+Na)^+$ 402.1082; found 402.1064 (TOF MS ES+).

(1*S*,3*R*,4*R*,7*S*,9*S*,*Z*)-4-methyl-3-(4-nitrophenyl)-9-vinyl-2,10,11-trioxa-1-phosphabicyclo[5.3.1]undec-5-ene 1-oxide (*trans,anti*-2.8.5):

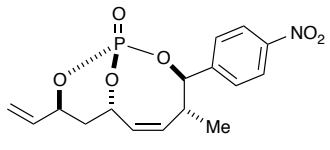

trans,anti-**2.8.5**

Yield: 62% (17 mg isolated starting from 30 mg of triene);

FTIR (thin film): 2984, 2914, 1623, 1523, 1349, 1290, 1004, 970, 852, 750 cm^{-1};

Optical Rotation: $[\alpha]_D$ = +151.2 (*c* = 0.4, $CHCl_3$);

^{1}H NMR (500 MHz, $CDCl_3$) δ 8.27 (d, *J* = 8.8 Hz, 2H), 7.74(d, *J* = 8.8 Hz, 2H), 5.86 (dddd, *J* = 17.1, 10.6, 5.5, 2.0 Hz, 1H), 5.66–5.58 (m, 2H), 5.40 (d, *J* = 17.2 Hz, 1H), 5.38 (dd, *J* = 24.8, 5.6 Hz, 1H), 5.27 (d, *J* = 10.6 Hz, 1H), 5.04 (dd, *J* = 11.8, 5.5 Hz, 1H), 4.59 (dd, *J* = 29.6, 11.7 Hz, 1H), 4.04–3.90 (m, 1H), 2.26 (ddd, *J* = 14.6, 12.0, 5.8 Hz, 1H), 1.87 (ddd, *J* = 14.6, 3.8, 1.8 Hz, 1H), 0.85 (d, *J* = 6.6 Hz, 3H);

^{13}C NMR (126 MHz, $CDCl_3$) δ 148.3, 142.9, 134.9 (d, J_{CP} = 10.3 Hz), 134.6, 130.1, 130.0, 123.8, 117.5 (d, J_{CP} = 1.3 Hz), 83.2 (d, J_{CP} = 6.6 Hz), 78.2 (d, J_{CP} = 7.3 Hz), 77.1 (d, J_{CP} = 6.5 Hz), 36.2 (d, J_{CP} = 6.4 Hz), 34.5, 18.3;

^{31}P NMR (162 MHz, $CDCl_3$) δ –11.71;

HRMS: cald. for $2(C_{16}H_{18}NO_6P)Na$ $(2M+Na)^+$ 725.1641; found 725.1647 (TOF MS ES+).

(4*S*,6*S*)-2-((2-methylbut-3-en-1-yl)oxy)-4,6-divinyl-1,3,2-dioxaphosphinane 2-oxide (2.9.2): *(pair of diastereomers detected by ^{13}C NMR)*

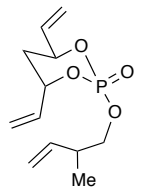

2.9.2

Yield: 67% (84 mg isolated as colorless oil starting from 102 mg of monochlorophosphate);

FTIR (thin film): 2964, 2926, 1647, 1458, 1283, 1140, 1119, 1013, 926 cm^{-1};

Optical Rotation: $[\alpha]_D$ = +62.02(*c* = 1.24, $CHCl_3$);

^{1}H NMR (400 MHz, $CDCl_3$) δ 6.03 (ddd, *J* = 16.6, 10.6, 6.2 Hz, 1H), 5.90 (ddddd, *J* = 17.7, 10.6, 5.2, 1.7, 0.7 Hz, 1H), 5.75 (dddd, *J* = 17.4, 10.2, 7.0, 2.7 Hz, 1H), 5.46 (ddd, *J* = 17.2, 1.1, 1.1 Hz, 1H), 5.37 (ddd, *J* = 17.2, 1.2, 0.9 Hz, 1H), 5.33 – 5.27 (m, 2H), 5.14–5.01 (m, 3H), 5.00–4.93 (m, 1H), 4.03–3.97 (m, 1H), 3.95 (ddd, *J* = 13.3, 6.4, 3.9 Hz, 1H), 2.70–2.47

(m, 1H), 2.17 (dddd, J = 14.6, 8.3, 4.9, 1.5 Hz, 1H), 2.10–1.98 (m, 1H), 1.06 (d, J = 6.8 Hz, 3H);

^{13}C NMR (126 MHz, $CDCl_3$) δ 139.4 (d, J_{CP} = 5.7 Hz), 135.0 (d, J_{CP} = 3.0 Hz), 135.0, 118.1 (d, J_{CP} = 1.6 Hz), 117.4, 115.4 (d, J_{CP} = 7.1 Hz), 77.8 (d, J_{CP} = 6.8 Hz), 76.0 (d, J_{CP} = 1.1 Hz), 75.9 (d, J_{CP} = 1.0 Hz), 71.6 (d, J_{CP} = 6.2 Hz), 38.2 (d, J_{CP} = 7.3 Hz), 38.1 (d, J_{CP} = 7.1 Hz), 35.2 (d, J_{CP} = 1.1 Hz), 35.1 (d, J_{CP} = 1.1 Hz), 16.0 (d, J_{CP} = 6.0 Hz);

^{31}P NMR (162 MHz, $CDCl_3$) δ –7.61;

HRMS cald for $C_{12}H_{19}O_4PNa$ $(M+Na)^+$ 281.0919; found 281.0913 (TOF MS ES+).

(4*S*,6*S*)-2-(((*S*)-2-methylbut-3-en-1-yl)oxy)-4,6-divinyl-1,3,2-dioxaphosphinane 2-oxide (2.9.3):

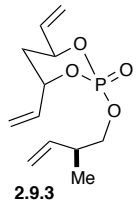

2.9.3

Yield: 27% (8.7 mg isolated starting from 32.7 mg of triene **2.9.2**);

FTIR (thin film): 2968, 2920, 1625, 1456, 1280, 1145, 1016, 925 cm^{-1};

Optical Rotation: $[\alpha]_D$ = +83.91(c = 0.44, $CHCl_3$);

^{1}H NMR (400 MHz, $CDCl_3$) δ 6.04 (ddd, J = 17.0, 10.6, 6.0 Hz, 1H), 5.91 (dddd, J = 17.3, 10.5, 5.1, 1.2 Hz, 1H), 5.76 (ddd, J = 14.1, 10.4, 7.0 Hz, 1H), 5.46 (d, J = 17.1 Hz, 1H), 5.38 (d, J = 17.2 Hz, 1H), 5.31 (ddd, J = 10.6, 1.9, 1.0 Hz, 2H), 5.16–5.06 (m, 2H), 5.06–5.01 (m, 1H), 5.01–4.95 (m, 1H), 4.03–3.95 (m, 2H), 2.57 (dt, J = 13.4, 6.7 Hz, 1H), 2.17 (dddd, J = 14.7, 8.1, 4.7, 1.3 Hz, 1H), 2.08–2.01 (m, 1H), 1.07 (d, J = 6.8 Hz, 3H);

^{13}C NMR (126 MHz, $CDCl_3$) δ 139.5, 135.1 (d, J_{CP} = 2.9 Hz), 135.0, 118.1, 117.4, 115.4, 77.8 (d, J_{CP} = 6.8 Hz), 76.0 (d, J_{CP} = 6.1 Hz), 71.6 (d, J_{CP} = 6.1 Hz), 38.2 (d, J_{CP} = 7.0 Hz), 35.2 (d, J_{CP} = 7.7 Hz), 16.0;

^{31}P NMR (162 MHz, $CDCl_3$) δ –7.61;

HRMS cald for $C_{12}H_{19}O_4PNa$ $(M+Na)^+$ 281.0919; found 281.0914 (TOF MS ES+).

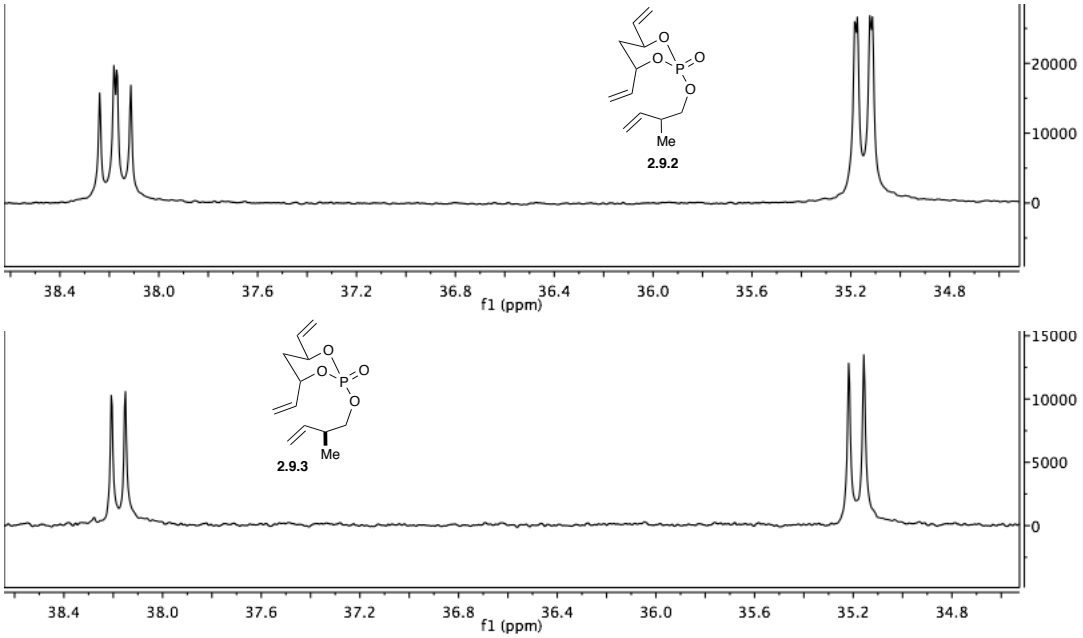

(1*S*,4*R*,7*S*,9*S*,*Z*)-4-methyl-9-vinyl-2,10,11-trioxa-1-phosphabicyclo[5.3.1] undec-5-ene 1-oxide (2.9.4):[1]

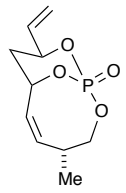

2.9.4

Yield: 39% (11.4 mg isolated starting from 32.7 mg of triene);

FTIR (thin film): 2922, 1827, 1649, 1448, 1375, 1281, 1140, 1119, 1003, 928 cm^{-1};

Optical Rotation: $[\alpha]_D$ = +122.98 (*c* = 0.57, $CHCl_3$);

[1] CCDC 905667 contains the crystallographic data for this compound. This X-ray crystallography data has been published in: Chegondi, R.; Maitra, S.; Markley, J. L.; Hanson, P. R. Phosphate-Tether-Mediated Ring-Closing Metathesis for the Preparation of Complex 1,3-anti-Diol-Containing Subunits. *Chem. - Eur. J.* **2013**, *19*, 8088–8093.

^{1}H NMR (400 MHz, $CDCl_3$) δ 5.85 (dddd, J = 18.0, 10.6, 5.4, 2.1 Hz, 1H), 5.48–5.45 (m, 2H), 5.45–5.39 (m, 1H), 5.33–5.22 (m, 2H), 5.07 (dd, J = 11.7, 5.3 Hz, 1H), 4.33 (ddd, J = 10.8, 6.2, 2.1 Hz, 1H), 3.64–3.52 (m, 1H), 3.34 (ddd, J = 30.9, 12.5, 10.8 Hz, 1H), 2.26–2.15 (m, 1H), 1.82 (ddd, J = 14.5, 3.7, 2.0 Hz, 1H), 1.01 (d, J = 6.6 Hz, 3H);

^{13}C NMR (126 MHz, $CDCl_3$) δ 135.0 (d, J_{CP} = 10.1 Hz), 134.1, 129.3, 117.3 (d, J_{CP} = 1.1 Hz), 77.9 (d, J_{CP} = 7.1 Hz), 77.1 (d, J_{CP} = 6.2 Hz), 68.2 (d, J_{CP} = 5.0 Hz), 36.2 (d, J_{CP} = 6.5 Hz), 31.2, 16.6;

^{31}P NMR (162 MHz, $CDCl_3$) δ –8.05;

HRMS cald for $C_{10}H_{15}O_4PNa$ $(M+Na)^+$ 253.0606; found 253.0617 (TOF MS ES+).

(4*R*,6*R*)-4,6-diallyl-2-(((*R*)-1-(benzyloxy)but-3-en-2-yl)oxy)-1,3,2-dioxaphosphinane 2-oxide (2.10.3):

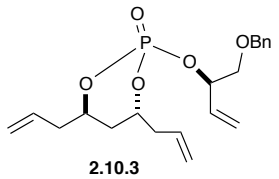

2.10.3

Yield: 73% (139 mg isolated as colorless oil starting from 119 mg of monochlorophosphate);

FTIR (thin film): 2924, 1643, 1431, 1366, 1286, 1095, 1011, 976, 922 cm^{-1};

Optical Rotation: $[\alpha]_D$ = +41.66 (c = 0.71, $CHCl_3$);

^{1}H NMR (400 MHz, $CDCl_3$) δ 7.37–7.28 (m, 5H), 5.94 (ddd, J = 17.2, 10.5, 6.7 Hz, 1H), 5.84 – 5.77 (m, 1H), 5.77–5.70 (m, 1H), 5.44 (ddd, J = 17.2, 1.1,1.1 Hz, 1H), 5.31 (ddd, J = 10.5, 1.1, 1.1 Hz, 1H), 5.18–5.12 (m, 3H), 5.12–5.09 (m, 1H), 5.07–5.00 (m, 1H), 4.67–4.55 (m, 3H), 4.55–4.48 (m, 1H), 3.67 (dd, J = 10.5, 5.6 Hz, 1H), 3.63 (ddd, J = 10.5, 4.7, 1.1 Hz, 1H), 2.66 (dt, J = 13.2, 6.5 Hz, 1H), 2.54 (ddd, J = 7.6, 6.6, 3.3 Hz, 1H), 2.44–2.33 (m, 2H), 2.00 (dddd, J = 13.5, 8.4, 5.0, 1.2 Hz, 1H), 1.89 (dddd, J = 14.6, 5.4, 3.8, 1.8 Hz, 1H);

^{13}C NMR (126 MHz, $CDCl_3$) δ 137.9, 133.9 (d, J_{CP} = 3.9 Hz), 132.6 (d, J_{CP} = 5.7 Hz), 132.3, 128.4 (d, J_{CP} = 9.9 Hz), 127.8 (d, J_{CP} = 2.7 Hz), 127.6, 118.7 (d, J_{CP} = 2.6 Hz), 78.0 (d, J_{CP} = 5.6 Hz), 77.3, 75.3 (d, J_{CP} = 6.7 Hz), 73.3 (d, J_{CP} = 6.1 Hz), 72.2 (d, J_{CP} = 6.0 Hz), 40.0 (d, J_{CP} = 7.7 Hz), 40.0 (d, J_{CP} = 3.5 Hz), 33.0 (d, J_{CP} = 6.8 Hz), 31.0;

^{31}P NMR (162 MHz, $CDCl_3$) δ –7.34;

HRMS cald for $C_{20}H_{27}O_5PNa$ $(M+Na)^+$ 401.1494; found 401.1493 (TOF MS ES+).

(4*S*,6*S*)-4,6-diallyl-2-(((*R*)-1-(benzyloxy)but-3-en-2-yl)oxy)-1,3,2-dioxaphosphinane 2-oxide (2.10.4):

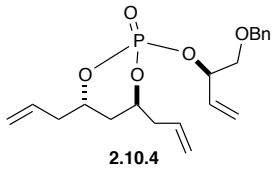

2.10.4

Yield: 64% (206 mg isolated starting from 200 mg of monochlorophosphate);

FTIR (thin film): 2922, 1641, 1364, 1286, 1095, 1119, 1007, 920 cm^{-1};

Optical Rotation: $[\alpha]_D$ = –44.31 (*c* = 0.24, $CHCl_3$);

^{1}H NMR (400 MHz, $CDCl_3$) δ 7.36–7.28 (m, 5H), 5.90 (ddd, *J* = 16.9, 10.6, 6.0 Hz, 1H), 5.81–5.72 (m, 1H), 5.72–5.62 (m, 1H), 5.45 (ddd, *J* = 17.2, 1.2 Hz, 1H), 5.31 (ddd, *J* = 10.6, 1.2 Hz, 1H), 5.15–5.10 (m, 3H), 5.10–5.07 (m, 1H), 5.02 (td, *J* = 11.6, 5.5 Hz, 1H), 4.63 – 4.54 (m, 4H), 3.62 (dd, *J* = 5.5, 0.8 Hz, 2H), 2.70 (dt, *J* = 13.3, 6.7 Hz, 1H), 2.49–2.43 (m, 1H), 2.39 (dd, *J* = 14.5, 7.3 Hz, 1H), 2.34–2.26 (m, 1H), 2.02–1.93 (m, 1H), 1.87–1.79 (m, 1H);

^{13}C NMR (126 MHz, $CDCl_3$) δ 137.7, 133.4 (d, J_{CP} = 3.8 Hz), 132.8, 132.3, 128.4, 127.7 (d, J_{CP} = 7.8 Hz), 118.7 (d, J_{CP} = 8.5 Hz), 118.5, 77.7 (d, J_{CP} = 7.1 Hz), 77.6 (d, J_{CP} = 5.5 Hz), 75.0 (d, J_{CP} = 6.6 Hz), 73.2, 72.4 (d, J_{CP} = 6.0 Hz), 40.0 (d, J_{CP} = 8.0 Hz), 38.8 (d, J_{CP} = 2.8 Hz), 32.9 (d, J_{CP} = 6.9 Hz), 30.9;

^{31}P NMR (162 MHz, $CDCl_3$) δ –7.59;

HRMS cald for $C_{20}H_{27}O_5PNa$ $(M+Na)^+$ 401.1494; found 401.1491 (TOF MS ES+).

(1*S*,3*R*,7*R*,9*R*,*Z*)-9-allyl-3-((benzyloxy)methyl)-2,10,11-trioxa-1-phosphabicyclo[5.3.1]undec-4-ene 1-oxide (*trans*-2.10.5):

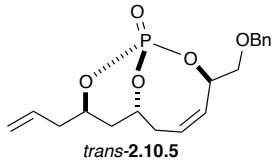

trans-**2.10.5**

Yield: 11% (3 mg isolated starting from 30 mg of triene);

FTIR (thin film): 2920, 1364, 1288, 1113, 1092, 1022, 972, 928 cm^{-1};

Optical Rotation: $[\alpha]_D$ = +61.6 (*c* = 0.38, $CHCl_3$);

^{1}H NMR (400 MHz, $CDCl_3$) δ 7.40–7.28 (m, 5H), 5.89–5.78 (m, 3H), 5.19 (dd, *J* = 4.2, 2.8 Hz, 1H), 5.15 (s, 1H), 5.03 (ddd, *J* = 28.5, 7.1 Hz, 1H), 4.83–4.73 (m, 1H), 4.68 (d, *J* = 11.8 Hz, 1H), 4.59 (d, *J* = 11.8 Hz, 1H), 4.52–4.37 (m, 1H), 4.03 (dd, *J* = 9.8, 6.9 Hz, 1H), 3.79 (dd, *J* = 9.8, 7.2 Hz, 1H), 3.17 (ddd, *J* = 13.6, 10.4, 6.2 Hz, 1H), 2.59 – 2.50 (m, 1H), 2.41 (dt, *J* = 14.3, 6.7 Hz, 1H), 2.27 (ddd, *J* = 14.6, 11.9, 5.2 Hz, 1H), 2.21–2.13 (m, 1H), 1.69 (dd, *J* = 14.6, 1.1 Hz, 1H);

^{13}C NMR (126 MHz, $CDCl_3$) δ 137.8, 132.1, 130.1, 128.4 (d, J_{CP} = 7.3 Hz), 128.0, 127.7 (d, J_{CP} = 12.6 Hz), 126.4, 119.0, 75.8 (d, J_{CP} = 7.4 Hz), 73.6, 73.1 (d, J_{CP} = 6.4 Hz), 71.8 (d, J_{CP} = 2.1 Hz), 40.6 (d, J_{CP} = 8.6 Hz), 33.5 (d, J_{CP} = 6.3 Hz), 31.1 (d, J_{CP} = 32.0 Hz), 29.7;

^{31}P NMR (162 MHz, $CDCl_3$) δ –10.75;

HRMS cald for $C_{18}H_{23}O_5PNa$ $(M+Na)^+$ 373.1181; found 373.1173 (TOF MS ES+).

(1*R*,3*R*,7*S*,9*S*,*Z*)-9-allyl-3-((benzyloxy)methyl)-2,10,11-trioxa-1-phosphabicyclo[5.3.1]undec-4-ene 1-oxide (*cis*-2.10.6):

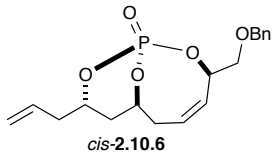

cis-**2.10.6**

Yield: 46% (20.2 mg isolated starting from 48 mg of triene);

FTIR (thin film): 2924, 2363, 1641, 1497, 1452, 1364, 1292, 1103, 978, 928 cm^{-1};

Optical Rotation: $[\alpha]_D$ = +43.30(*c* = 1.03, $CHCl_3$);

^{1}H NMR (400 MHz, $CDCl_3$) δ 7.39–7.27 (m, 5H), 5.89–5.81 (m, 1H), 5.81–5.74 (m, 1H), 5.68 (dd, *J* = 11.9, 3.0 Hz, 1H), 5.25–5.17 (m, 2H), 5.16 (d, *J* = 1.1 Hz, 1H), 4.79 (dddd, *J* = 12.5, 6.2, 6.2, 2.7 Hz, 1H), 4.63 (d, *J* = 12.3 Hz, 1H), 4.59 (d, *J* = 12.2 Hz, 1H), 4.56–4.41 (m, 1H), 3.70–3.61 (m, 2H), 3.31 (td, *J* = 13.1, 8.4 Hz, 1H), 2.53 (ddd, *J* = 12.9, 7.1, 1.3 Hz, 1H), 2.47 – 2.36 (m, 1H), 2.24 (ddd, *J* = 14.6, 12.2, 5.2 Hz, 1H), 2.07 (ddd, *J* = 13.7, 8.4, 5.3 Hz, 1H), 1.65 (d, *J* = 14.7 Hz, 1H);

^{13}C NMR (126 MHz, $CDCl_3$) δ 137.8, 132.0, 130.3, 128.3, 127.6 (d, J_{CP} = 15.2 Hz), 126.2, 124.2, 119.0, 77.2 (d, J_{CP} = 5.5 Hz), 76.0 (d, J_{CP} = 7.3 Hz), 74.3 (d, J_{CP} = 6.4 Hz), 73.1, 71.4 (d, J_{CP} = 12.0 Hz), 40.4 (d, J_{CP} = 9.2 Hz), 33.8 (d, J_{CP} = 6.3 Hz), 30.2 (d, J_{CP} = 10.3 Hz);

^{31}P NMR (162 MHz, $CDCl_3$) δ –7.60;

HRMS cald for $C_{18}H_{23}O_5PNa$ $(M+Na)^+$ 373.1181; found 373.1174 (TOF MS ES+).

(4*R*,6*R*)-2-(((*R*)-1-(benzyloxy)but-3-en-2-yl)oxy)-4,6-bis(2-methylallyl)-1,3,2-dioxaphosphinane 2-oxide (2.11.3):

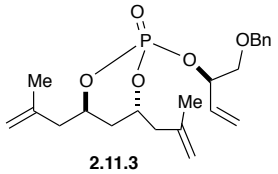

2.11.3

Yield: 67% (83 mg isolated starting from 80 mg of monochlorophosphate);

FTIR (thin film): 3076, 2964, 2926, 2359, 1827, 1649, 1454, 1364, 1288, 1099, 1074, 1007, 982, 739 cm^{-1};

Optical Rotation: $[\alpha]_D$ = +44.04 (*c* = 1.3, $CHCl_3$);

^{1}H NMR (400 MHz, $CDCl_3$) δ 7.34 (d, *J* = 4.4 Hz, 3H), 7.32–7.28 (m, 2H), 5.95 (ddd, *J* = 17.2, 10.5, 6.7 Hz, 1H), 5.44 (ddd, *J* = 17.2, 1.3, 1.3 Hz, 1H), 5.31 (ddd, *J* = 10.6, 1.1, 1.2 Hz, 1H), 5.08–4.99 (m, 1H), 4.85 (ddd, *J* = 7.04, 1.6, 1.6 Hz, 2H), 4.77 (d, *J* = 9.8 Hz, 2H), 4.74–4.59 (m, 3H), 4.56 (d, *J* = 12.0 Hz, 1H), 3.67 (dd, *J* = 10.5, 5.6 Hz, 1H), 3.63 (ddd, *J* = 10.6, 4.9, 1.0 Hz, 1H), 2.62 (dd, *J* = 14.2, 6.7 Hz, 1H), 2.53 (dd, *J* = 14.1, 6.7 Hz, 1H), 2.37 (dd, *J* = 14.1, 7.8 Hz, 1H), 2.32 (dd, *J* = 13.6, 6.5 Hz, 1H), 1.98 (dddd, *J* = 13.0, 8.0, 4.9, 1.2 Hz, 1H), 1.89 (dddd, *J* = 14.6, 5.4, 3.9, 1.9 Hz, 1H), 1.75 (s, 3H), 1.73 (s, 3H);

^{13}C NMR (126 MHz, $CDCl_3$) δ 140.4, 140.2, 139.8, 137.9, 134.0 (d, J_{CP} = 4.1 Hz), 128.3, 127.6, 118.7, 114.6 (d, J_{CP} = 3.7 Hz), 114.2 (d, J_{CP} = 4.8 Hz), 78.0 (d, J_{CP} = 5.6 Hz), 76.1 (d, J_{CP} = 6.9 Hz), 74.4 (d, J_{CP} = 6.6 Hz), 73.2, 72.2 (d, J_{CP} = 5.8 Hz), 43.8 (d, J_{CP} = 7.5 Hz), 42.8 (d, J_{CP} = 3.4 Hz), 33.2 (d, J_{CP} = 6.8 Hz), 22.6, 22.3;

^{31}P NMR (162 MHz, $CDCl_3$) δ –7.09;

HRMS cald for $C_{22}H_{31}O_5PNa$ $(M+Na)^+$ 429.1807; found 429.1802 (TOF MS ES+).

(4*S*,6*S*)-2-(((*R*)-1-(benzyloxy)but-3-en-2-yl)oxy)-4,6-bis(2-methylallyl)-1,3,2-dioxaphosphinane 2-oxide (2.11.4):

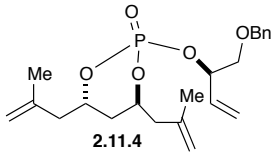

2.11.4

Yield: 60% (110 mg isolated starting from 120 mg of monochlorophosphate);

FTIR (thin film): 2918, 1827, 1649, 1448, 1290, 1092, 1074, 1007, 976 cm^{-1};

Optical Rotation: $[\alpha]_D$ = –40.69 (*c* = 1.4, $CHCl_3$);

^{1}H NMR (400 MHz, $CDCl_3$) δ 7.38–7.28 (m, 5H), 5.90 (ddd, *J* = 16.9, 10.6, 6.1 Hz, 1H), 5.44 (d, *J* = 17.2 Hz, 1H), 5.30 (d, *J* = 10.6 Hz, 1H), 5.01 (dq, *J* = 12.4, 6.1 Hz, 1H), 4.85 (ddd, *J* = 10.6, 1.4, 1.4 Hz, 2H), 4.79–4.68 (m, 4H), 4.61 (d, *J* = 12.1 Hz, 1H), 4.57 (d, *J* = 12.0 Hz, 1H), 3.66–3.57 (m, 2H), 2.65 (dd, *J* = 14.1, 6.9 Hz, 1H), 2.49 (dd, *J* = 14.1, 6.4 Hz, 1H), 2.39 (dd, *J* = 14.2, 7.7 Hz, 1H), 2.29 (dd, *J* = 14.1, 7.3 Hz, 1H), 1.97 (dddd, *J* = 14.7, 8.2, 5.1,1.3 Hz, 1H), 1.87 (dddd, *J* = 14.6, 5.3, 3.7,1.9 Hz, 1H), 1.74 (s, 3H), 1.69 (s, 3H);

^{13}C NMR (126 MHz, $CDCl_3$) δ140.5, 140.3, 137.7, 133.5 (d, J_{CP} = 3.8 Hz), 128.4 (d, J_{CP} = 2.7 Hz), 128.4, 127.8 (d, J_{CP} = 5.0 Hz), 127.7 (d, J_{CP} = 9.0 Hz), 118.5, 114.1 (d, J_{CP} = 2.9 Hz), 77.7 (d, J_{CP} = 5.5 Hz), 76.3 (d, J_{CP} = 7.0 Hz), 74.3 (d, J_{CP} = 6.7 Hz), 73.2, 72.3 (d, J_{CP} = 6.1 Hz), 43.8 (d, J_{CP} = 7.7 Hz), 42.7 (d, J_{CP} = 3.0 Hz), 33.1 (d, J_{CP} = 7.1 Hz), 22.6, 22.3;

^{31}P NMR (162 MHz, $CDCl_3$) δ –7.58;

HRMS cald for $C_{22}H_{31}O_5PNa$ $(M+Na)^+$ 429.1807; found 429.1794 (TOF MS ES+).

(1*S*,3*R*,7*R*,9*R*,*Z*)-3-((benzyloxy)methyl)-5-methyl-9-(2-methylallyl)-2,10,11-trioxa-1-phosphabicyclo[5.3.1]undec-4-ene 1-oxide (*trans*-2.11.5):

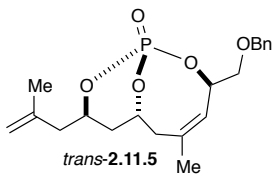

trans-**2.11.5**

Yield: 49% (76% brsm, 14 mg isolated starting from 30 mg of triene);

FTIR (thin film): 2924, 2853, 1718, 1649, 1452, 1246, 1175, 1095, 1013, 899, 818, 748 cm^{-1};

Optical Rotation: $[\alpha]_D$ = +50.10 (*c* = 1.3, $CHCl_3$);

^{1}H NMR (400 MHz, $CDCl_3$) δ 7.39–7.28 (m, 5H), 5.57 (s, 1H), 4.98 (dd, *J* = 25.2, 1.7 Hz, 1H), 4.93–4.84 (m, 2H), 4.82 (s, 1H), 4.67 (d, *J* = 11.9 Hz, 1H), 4.58 (d, *J* = 11.9 Hz, 1H), 4.56–4.45 (m, 1H), 3.94 (dd, *J* = 9.9, 7.0 Hz, 1H), 3.72 (dd, *J* = 9.9, 6.6 Hz, 1H), 3.29 (t, *J* = 12.8 Hz, 1H), 2.57 (dd, *J* = 14.0, 6.6 Hz, 1H), 2.33 (ddd, *J* = 14.0, 6.8, 1.4 Hz, 1H), 2.24 (ddd, *J* = 14.6, 11.7, 5.3 Hz, 1H), 1.97 (dd, *J* = 13.1, 5.2 Hz, 1H), 1.86 (t, *J* = 1.6 Hz, 3H), 1.78 (s, 3H), 1.73 (d, *J* = 14.6 Hz, 1H);

^{13}C NMR (126 MHz, $CDCl_3$) δ 140.1, 137.8, 137.1, 128.4, 127.8 (d, J_{CP} = 26.9 Hz), 123.6, 114.4, 76.1 (d, J_{CP} = 7.7 Hz), 75.2 (d, J_{CP} = 7.4 Hz), 73.6, 72.3 (d, J_{CP} = 6.4 Hz), 72.1 (d, J_{CP} = 3.7 Hz), 44.7 (d, J_{CP} = 7.7 Hz), 36.5, 33.7 (d, J_{CP} = 6.6 Hz), 29.7, 24.3, 22.8;

^{31}P NMR (162 MHz, $CDCl_3$) δ –4.06;

HRMS cald for $C_{20}H_{27}O_5PNa$ $(M+Na)^+$ 401.1494; found 401.1495 (TOF MS ES+).

(4*S*,6*S*)-2-(((*S*)-1-(benzyloxy)hex-5-en-2-yl)oxy)-4,6-divinyl-1,3,2-dioxaphosphinane 2-oxide (2.12.2)

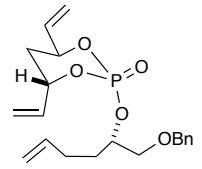

2.12.2

Yield: 60% (97 mg isolated starting from 89 mg of monochlorophosphate);

FTIR (thin film): 2917, 2359, 1641, 1454, 1281, 1119, 991, 926, 750, 698, 667 cm^{-1};

Optical Rotation: $[\alpha]_D$ = +48.94 (*c* = 0.66, $CHCl_3$);

^{1}H NMR (500 MHz, $CDCl_3$) δ 7.31–7.21 (m, 5H, aromatic), 6.01 (dddd, *J* = 17.0, 10.7, 6.2, 0.8 Hz, 1H, H_2C=C<u>H</u>CHO(P)CH_2), 5.82–5.70 (m, 2H, H_2C=C<u>H</u>CHO(P)CH_2, H_2C=C<u>H</u>CH_2CH_2), 5.33–5.30 (m, 1H, <u>H</u>$_2$C=CHCHO(P)CH_2), 5.29–5.27 (m, 1H, <u>H</u>$_2$C=CHCHO(P)CH_2), 5.22 (dt, *J* = 10.6, 1.2 Hz, 1H, <u>H</u>$_2$C=CHCHO(P)CH_2), 5.17 (dt, *J* = 10.6, 1.2 Hz, 1H, <u>H</u>$_2$C=CHCHO(P)CH_2), 5.01–4.89 (m, 4H, <u>H</u>$_2$C=CHCH_2CH_2,

H_2C=CHC<u>H</u>O(P)CH_2), 4.60–4.54 (m, 1H, C<u>H</u>O(P)CH_2OBn), 4.52 (d, *J* = 12.0 Hz, 1H, OC<u>H_2</u>Ph), 4.45 (d, *J* = 12.0 Hz, 1H, OC<u>H_2</u>Ph), 3.56 (ddd, *J* = 10.7, 3.9, 1.3 Hz, 1H, CHO(P)C<u>H_2</u>OBn), 3.52 (dd, *J* = 10.6, 5.6 Hz, 1H, CHO(P)C<u>H_2</u>OBn), 2.18–2.07 (m, 2H, H_2C=CHC<u>H_2</u>CH_2), 2.08–2.02 (m, 1H, H_2C=CHCHO(P)C<u>H_2</u>CHO[P]), 1.96 (dddd, *J* = 14.7, 5.6, 3.8, 1.8 Hz, 1H, H_2C=CHCHO(P)C<u>H_2</u>CHO[P]), 1.86 – 1.76 (m, 1H, CH_2C<u>H_2</u>CHO[P] CH_2OBn), 1.76–1.68 (m, 1H, CH_2C<u>H_2</u>CHO[P] CH_2OBn);

^{13}C NMR (126 MHz, $CDCl_3$) δ 137.9, 137.5, 135.3 (d, J_{CP} = 5.9 Hz), 135.2 (d, J_{CP} = 1.8 Hz), 128.4 (2 C), 127.7 (2 C), 127.68, 117.9, 117.1, 115.2, 77.9 (d, J_{CP} = 6.7 Hz), 77.6 (d, J_{CP} = 6.2 Hz), 75.8 (d, J_{CP} = 6.2 Hz), 73.2, 71.7 (d, J_{CP} = 4.1 Hz), 35.3 (d, J_{CP} = 7.4 Hz), 31.4 (d, J_{CP} = 5.0 Hz), 29.2;

^{31}P NMR (162 MHz, $CDCl_3$) δ –7.9;

HRMS calcd. for $C_{20}H_{27}O_5PNa$ $(M+Na)^+$ 401.1494; found 401.1485 (TOF MS ES+).

(4*R*,6*R*)-2-(((*S*)-1-(benzyloxy)hex-5-en-2-yl)oxy)-4,6-divinyl-1,3,2-dioxaphosphinane 2-oxide(2.12.3)

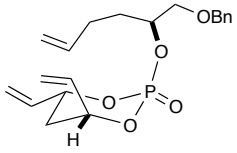

2.12.3

Yield: 38% (94 mg isolated starting from 120 mg of monochlorophosphate);

FTIR (thin film): 2929, 1281, 1099, 995, 960, 739 cm^{-1};

Optical Rotation: $[\alpha]_D$ = –51.0 (*c* = 1.05, $CHCl_3$);

^{1}H NMR (500 MHz, $CDCl_3$) δ 7.34–7.20 (m, 5H, aromatic), 5.96 (dddd, *J* = 17.4, 10.7, 6.0, 0.9 Hz, 1H, H_2C=C<u>H</u>CHO(P)CH_2), 5.85 (dddd, *J* = 17.3, 10.6, 5.2, 1.6 Hz, 1H, H_2C=C<u>H</u>CHO(P)CH_2), 5.74 (ddt, *J* = 16.9, 10.2, 6.6 Hz, 1H, H_2C=C<u>H</u>CH_2CH_2), 5.39 (ddd, *J* = 17.1, 1.6, 0.9 Hz, 1H, <u>H_2</u>C=CHCHO(P)CH_2), 5.29 (dt, *J* = 17.2, 1.2 Hz, 1H, <u>H_2</u>C=CHCHO(P)CH_2), 5.23 (dt, *J* = 10.7, 1.2 Hz, 1H, <u>H_2</u>C=CHCHO(P)CH_2), 5.17 (dt, *J* = 10.6, 1.1 Hz, 1H, <u>H_2</u>C=CHCHO(P)CH_2), 5.02–4.89 (m, 4H, <u>H_2</u>C=CHCH_2CH_2, H_2C=CHC<u>H</u>O(P)CH_2), 4.58 (ddt, *J* = 12.2, 8.4, 4.9 Hz, 1H, C<u>H</u>O(P)CH_2OBn), 4.53 (d, *J* =

12.0 Hz, 1H, OC$\underline{H}_2$Ph), 4.47 (d, J = 12.1 Hz, 1H, OC$\underline{H}_2$Ph), 3.56 (d, J = 4.8 Hz, 2H, CHO(P)C$\underline{H}_2$OBn), 2.20–1.96 (m, 4H, H_2C=CHC$\underline{H}_2CH_2$, H_2C=CHCHO(P)C$\underline{H}_2$CHO[P]), 1.84–1.69 (m, 2H, $CH_2C\underline{H}_2$CHO[P]CH_2OBn);

^{13}C NMR (126 MHz, $CDCl_3$) δ 138.1, 137.5, 135.3 (d, J_{CP} = 3.7 Hz), 135.1 (d, J_{CP} = 7.2 Hz), 128.4 (2C), 127.7 (2C), 127.6, 117.8, 117.5, 115.3, 77.9 (d, J_{CP} = 6.4 Hz), 77.6 (d, J_{CP} = 6.7 Hz), 76.2 (d, J_{CP} = 6.1 Hz), 73.2, 71.6 (d, J_{CP} = 3.9 Hz), 35.3 (d, J_{CP} = 7.5 Hz), 31.4 (d, J_{CP} = 5.1 Hz), 29.2;

^{31}P NMR (162 MHz, $CDCl_3$) δ –8.1;

HRMS calcd. for $C_{20}H_{27}O_5PNa$ $(M+Na)^+$ 401.1494; found 401.1471 (TOF MS ES+).

(1*S*,3*S*,8*S*,10*S*,*Z*)-3-((benzyloxy)methyl)-10-vinyl-2,11,12-trioxa-1-phosphabicyclo [6.3.1]dodec-6-ene 1-oxide (*cis*-2.12.4):

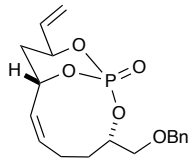

cis-**2.12.4**

Yield: 60% (20 mg isolated starting from 36 mg of triene);

FTIR (thin film): 2924, 2359, 1718, 1452, 1283, 1117, 1092, 989, 852, 565 cm^{-1};

Optical Rotation: $[\alpha]_D$ = –5.03 (c =0.78, $CHCl_3$);

^{1}H NMR (500 MHz, $CDCl_3$) δ 7.31–7.20 (m, 5H, aromatic), 5.83–5.78 (m, 1H, H_2C-HC=C$\underline{H}$CHO(P)CH_2), 5.78–5.72 (m, 1H, $H_2C\underline{H}$C=CHCHO(P)CH_2), 5.39–5.28 (m, 2H, $\underline{H}_2$C=CHCHO[P], HC=CHC$\underline{H}$O(P)CH_2), 5.20 (dt, J = 10.6, 1.2 Hz, 1H, $\underline{H}_2$C=CHCHO[P]), 5.10 (d, J = 11.8 Hz, 1H), 5.02 (ddd, J = 11.8, 5.5, 1.4 Hz, 1H, H_2C=CH-C$\underline{H}$O(P)CH_2), 4.83–4.74 (m, 1H, C$\underline{H}$O(P)CH_2OBn), 4.55 (d, J = 12.1 Hz, 1H, OC$\underline{H}_2$Ph), 4.47 (d, J = 12.1 Hz, 1H, OC$\underline{H}_2$Ph), 3.49 (dd, J = 10.4, 4.5 Hz, 1H, CHO(P)C$\underline{H}_2$OBn), 3.45 (dd, J = 10.4, 5.3 Hz, 1H, CHO(P)C$\underline{H}_2$OBn), 2.92–2.83 (m, 1H, HC=CHC$\underline{H}_2CH_2$), 2.19–2.13 (m, 1H, H_2C=CHCHO(P)C$\underline{H}_2$CHO[P]), 2.13–2.07 (m, 1H, HC=CH-C$\underline{H}_2CH_2$), 1.85–1.77 (m, 1H, $CH_2C\underline{H}_2$CHO[P]CH_2OBn), 1.76–1.65 (m, 2H, HC=CHCHO(P)C$\underline{H}_2$CHO[P], $CH_2C\underline{H}_2$CHO[P]CH_2OBn);

^{13}C NMR (126 MHz, $CDCl_3$) δ 138.0, 137.3, 135.2 (d, J_{CP} = 9.8 Hz), 128.3 (2C), 127.7 (2C), 127.6, 124.2, 117.3 (d, J_{CP} = 1.4 Hz), 79.7 (d, J_{CP} = 5.6 Hz), 77.02 (d, J_{CP} = 7.7 Hz), 76.8 (d, J_{CP} = 6.5 Hz), 73.2, 72.7 (d, J_{CP} = 4.7 Hz), 37.4 (d, J_{CP} = 6.5 Hz), 29.3 (d, J_{CP} = 2.3 Hz), 25.4;

^{31}P NMR (162 MHz, $CDCl_3$) δ –8.4;

HRMS calcd. for $C_{18}H_{23}O_5PNa$ $(M+Na)^+$ 373.1181; found 373.1161(TOF MS ES+).

(1*R*,3*S*,8*R*,10*R*,*Z*)-3-((benzyloxy)methyl)-10-vinyl-2,11,12-trioxa-1-phosphabicyclo[6.3.1]dodec-6-ene 1-oxide (*trans*-2.12.5):

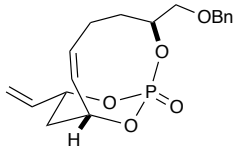

trans-**2.12.5**

Yield: 69% (6 mg isolated starting from 10 mg of triene);

FTIR (thin film): 2924, 1279, 1132, 1109, 1012, 746 cm^{-1};

Optical Rotation: $[\alpha]_D$ = –52.55 (*c* = 0.25, $CHCl_3$);

^{1}H NMR (500 MHz, $CDCl_3$) δ 7.38–7.28 (m, 5H, aromatic), 5.93 (dddd, *J* = 17.1, 10.5, 5.6, 1.8 Hz, 1H, H_2C-HC=C<u>H</u>CHO(P)CH_2), 5.69 (dddd, *J* = 17.5, 11.9, 6.4, 2.8 Hz, 1H, H_2C-<u>H</u>C=CHCHO(P)CH_2), 5.50 (dt, *J* = 12.0, 1.2 Hz, 1H, H_2C=C<u>H</u>CHO[P]), 5.44 (dt, *J* = 17.1, 1.1 Hz, 1H, <u>H</u>$_2$C=CHCHO[P]), 5.41–5.33 (m, 1H, HC=CHC<u>H</u>O(P)CH_2), 5.29 (dt, *J* = 10.5, 1.1 Hz, 1H, <u>H</u>$_2$C=CHCHO[P]), 5.19–5.12 (m, 1H, H_2C=CH-C<u>H</u>O(P)CH_2), 4.59 (d, *J* = 11.8 Hz, 1H, OC<u>H</u>$_2$Ph), 4.56 (d, *J* = 11.8 Hz, 1H, OC<u>H</u>$_2$Ph), 4.38 (ttd, *J* = 11.5, 5.6, 1.9 Hz, 1H, C<u>H</u>O(P)CH_2OBn), 3.66 (dd, *J* = 10.2, 5.8 Hz, 1H, CHO(P)C<u>H</u>$_2$OBn), 3.53 (ddd, *J* = 10.2, 5.4, 1.6 Hz, 1H, CHO(P)C<u>H</u>$_2$OBn), 3.19 (qd, *J* = 13.1, 4.0 Hz, 1H, HC=CHC<u>H</u>$_2$$CH_2$), 2.33 (ddd, *J* = 14.8, 12.0, 4.9 Hz, 1H, H_2C=CH-CHO(P)C<u>H</u>$_2$CHO[P]), 2.10–2.02 (m, 1H, HC=CHC<u>H</u>$_2$$CH_2$), 1.98 (dq, *J* = 14.8, 2.7 Hz, 1H, H_2C=CHCHO(P)C<u>H</u>$_2$CHO[P]), 1.84 (ddt, *J* = 15.3, 11.8, 3.7 Hz, 1H, HC=CHCHO(P)C<u>H</u>$_2$CHO[P]), 1.68–1.59 (m, 1H, HC=CHCHO(P)C<u>H</u>$_2$CHO[P]);

^{13}C NMR (126 MHz, $CDCl_3$) δ 137.9, 135.5 (d, J_{CP} = 4.5 Hz), 132.7, 128.5, 128.3 (2C), 127.63, 127.6 (2C), 117.6, 78.9 (d, J_{CP} = 7.6 Hz), 77.2 (d, J_{CP} = 7.8 Hz), 75.1 (d, J_{CP} = 8.6 Hz), 73.6, 72.9 (d, J_{CP} = 7.9 Hz), 36.6 (d, J_{CP} = 10.9 Hz), 29.5, 23.1;

^{31}P NMR (162 MHz, $CDCl_3$) δ –15.17;

HRMS calcd. for $C_{18}H_{23}O_5PNa$ $(M+Na)^+$ 373.1181; found 373.1173 (TOF MS ES+).

(4*R*,6*R*)-2-(((*R*)-1-(benzyloxy)pent-4-en-2-yl)oxy)-4,6-bis(2-methylallyl)-1,3,2-dioxaphosphinane 2-oxide (2.13.1):

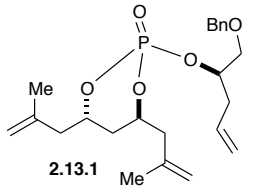

2.13.1

Yield: 47% (89 mg isolated starting from 120 mg of monochlorophosphate);

FTIR (thin film): 2922, 2359, 1290, 1101, 1005, 986 cm^{-1};

Optical Rotation: $[\alpha]_D$ = –53.2 (*c* = 1.04, $CHCl_3$);

^{1}H NMR (400 MHz, $CDCl_3$) δ (ppm) 7.40–7.28 (m, 5H), 5.80 (ddt, *J* = 17.2, 10.2, 7.1 Hz, 1H), 5.17–5.07 (m, 2H), 4.91–4.80 (m, 2H), 4.79–4.73 (m, 2H), 4.73–4.61 (m, 3H), 4.59 (d, *J* = 11.9 Hz, 1H), 4.53 (d, *J* = 12.0 Hz, 1H), 3.63–3.54 (m, 2H), 2.65 (dd, *J* = 14.1, 6.9 Hz, 1H), 2.54 (t, *J* = 6.7 Hz, 2H), 2.49 (dd, *J* = 14.1, 6.4 Hz, 1H), 2.37 (dd, *J* = 14.2, 7.6 Hz, 1H), 2.28 (dd, *J* = 14.1, 7.3 Hz, 1H), 1.96 (dddd, *J* = 13.3, 8.2, 4.9, 1.2 Hz, 1H), 1.86 (dddd, *J* = 14.6, 5.3, 3.7, 1.8 Hz, 1H), 1.75 (s, 3H), 1.68 (s, 3H);

^{13}C NMR (126 MHz, $CDCl_3$) δ 140.5, 140.3, 137.9, 132.7, 128.4 (2C), 127.7, 127.6 (2C), 118.4, 114.2 (d, J_{CP} = 2.5 Hz), 76.8 (d, J_{CP} = 6.0 Hz), 76.3 (d, J_{CP} = 6.9 Hz), 74.3 (d, J_{CP} = 6.6 Hz), 73.3, 71.3 (d, J_{CP} = 5.2 Hz), 43.8 (d, J_{CP} = 7.6 Hz), 42.7 (d, J_{CP} = 3.1 Hz), 36.8 (d, J_{CP} = 4.1 Hz), 33.2 (d, J_{CP} = 6.9 Hz), 29.7, 22.6, 22.4;

^{31}P NMR (162 MHz, $CDCl_3$) δ –7.37;

HRMS cald for $(C_{23}H_{33}O_5P)_2Na$ $(2M+Na)^+$ 863.4029; found 863.3986 (TOF MS ES+).

(1*R*,3*R*,8*S*,10*S*,*Z*)-3-((benzyloxy)methyl)-6-methyl-10-(2-methylallyl)-2,11,12-trioxa-1-phosphabicyclo[6.3.1]dodec-5-ene 1-oxide (2.13.2):[2]

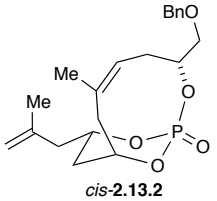

cis-**2.13.2**

Yield: 36% (53% brsm, 9.5 mg isolated starting from 30 mg of triene with 10 mg unreacted starting triene);

FTIR (thin film): 2922, 2853, 2359, 1448, 1294, 1105, 1074, 995, 972, 912, 897, 741, 698 cm^{-1};

Optical Rotation: $[\alpha]_D = -13.9$ ($c = 0.42$, $CHCl_3$);

^{1}H NMR (400 MHz, $CDCl_3$) δ 7.39–7.27 (m, 5H), 5.61 (t, J = 8.2 Hz, 1H), 4.92–4.84 (m, 2H), 4.81 (s, 1H), 4.79–4.68 (m, 1H), 4.60 (d, J = 12.0 Hz, 1H), 4.56 (d, J = 12.0 Hz, 1H), 4.39 (ddd, J = 15.4, 10.5, 5.1 Hz, 1H), 3.61 (dd, J = 10.0, 4.4 Hz, 1H), 3.51 (dd, J = 10.0, 6.4 Hz, 1H), 3.35 (t, J = 13.0 Hz, 1H), 2.52 (dd, J = 14.2, 6.6 Hz, 1H), 2.48–2.39 (m, 1H), 2.36–2.29 (m, 1H), 2.28 (dd, J = 6.1, 2.2 Hz, 1H), 2.26–2.17 (m, 1H), 1.79 (s, 6H), 1.84–1.60 (m, 2H);

^{13}C NMR (126 MHz, $CDCl_3$) δ 140.1, 137.9, 134.6, 128.4 (2C), 127.73 (2C), 127.71, 124.1, 114.2, 77.1 (d, J_{CP} = 6.2 Hz), 74.9 (d, J_{CP} = 6.8 Hz), 74.6 (d, J_{CP} = 7.3 Hz), 73.3, 72.7 (d, J_{CP} = 4.2 Hz), 44.4 (d, J_{CP} = 9.2 Hz), 36.1, 34.4 (d, J_{CP} = 6.3 Hz), 30.3 (d, J_{CP} = 3.1 Hz), 22.8, 22.5;

^{31}P NMR (162 MHz, $CDCl_3$) δ –9.86;

HRMS cald. for $(C_{21}H_{29}O_5P)_2Na$ $(2M+Na)^+$ 807.3403; found 807.3442 (TOF MS ES+).

[2] CCDC 905669 contains the supplementary crystallographic data for this compound. This X-ray crystallography data has been published in: Maitra, S.; Markley, J. L.; Chegondi, R.; Hanson, P. R. Phosphate Tether-Mediated Ring-Closing Metathesis for the Generation of Medium to LargeBicyclo[n.3.1]phosphates *Tetrahedron* **2015**, *ASAP*.

(4*S*,6*S*)-2-(((1*R*,2*R*)-2-methyl-1-(4-nitrophenyl)but-3-en-1-yl)oxy)-4,6-bis(2-methylallyl)-1,3,2-dioxaphosphinane 2-oxide (2.13.3):

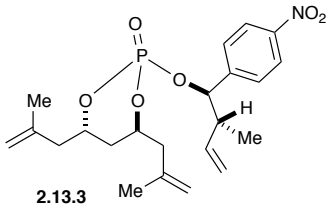

2.13.3

Yield: 46% (91 mg isolated starting from 120 mg of monochlorophosphate);

FTIR (thin film): 2954, 2912, 1617, 1281, 1245, 1040, 100, 758, 712 cm^{-1};

Optical Rotation: $[\alpha]_D = -31.9$ ($c = 0.66$, $CHCl_3$);

^{1}H NMR (400 MHz, $CDCl_3$) δ 8.22 (d, J = 6.9 Hz, 2H), 7.48 (d, J = 8.1 Hz, 2H), 5.80–5.72 (m, 1H), 5.38 (t, J = 7.4 Hz, 1H), 5.09 (d, J = 10.4 Hz, 1H), 5.01 (d, J = 17.2 Hz, 1H), 4.89 (s, 1H), 4.80–4.73 (m, 1H), 4.78 (s, 1H), 4.74 (s, 1H), 4.62 (s, 1H), 4.40–4.33 (m, 1H), 2.76–2.68 (m, 1H), 2.62 (dd, J = 14.1, 6.8 Hz, 1H), 2.38 (dd, J = 14.2, 7.6 Hz, 1H), 2.30 (dd, J = 14.3, 6.8 Hz, 1H), 2.19 (dd, J = 14.2, 6.8 Hz, 1H), 2.01–1.93 (m, 1H), 1.90–1.82 (m, 1H), 1.76 (s, 3H), 1.55 (s, 3H), 1.00 (dd, J = 6.8, 1.5 Hz, 3H);

^{13}C NMR (126 MHz, $CDCl_3$) δ 147.6, 146.2 (d, J_{CP} = 2.6 Hz), 140.2, 139.9, 137.7, 127.7, 123.4, 117.0, 114.4, 114.2, 82.6 (d, J_{CP} = 5.9 Hz), 76.2 (d, J_{CP} = 6.9 Hz), 74.7 (d, J_{CP} = 6.7 Hz), 44.3 (d, J_{CP} = 6.1 Hz), 43.5 (d, J_{CP} = 7.2 Hz), 43.0 (d, J_{CP} = 3.6 Hz), 33.3 (d, J_{CP} = 6.9 Hz), 22.5, 22.4, 15.7;

^{31}P NMR (162 MHz, $CDCl_3$) δ –6.5;

HRMS cald. for $C_{22}H_{30}NO_6PNa$ $(M+Na)^+$ 458.1708; found 429.1714 (TOF MS ES+).

(4*S*,6*S*)-2-(((1*R*,2*S*)-2-methyl-1-(4-nitrophenyl)but-3-en-1-yl)oxy)-4,6-bis(2-methylallyl)-1,3,2-dioxaphosphinane 2-oxide (2.13.4):

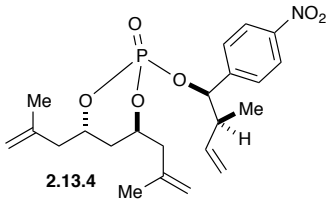

2.13.4

Yield: 81% (160 mg isolated starting from 120 mg of monochlorophosphate);

FTIR (thin film): 2969, 1630, 1535, 1350, 1289, 1259, 1068, 1020, 1008, 758 cm^{-1};

Optical Rotation: $[\alpha]_D$ = –41.4 (*c* = 1.03, $CHCl_3$);

^{1}H NMR (400 MHz, $CDCl_3$) δ (ppm) δ 8.21 (d, *J* = 8.8 Hz, 2H), 7.48 (d, *J* = 8.8 Hz, 2H), 5.59 (ddd, *J* = 17.4, 10.4, 7.0 Hz, 1H), 5.31 (dd, *J* = 8.5, 7.5 Hz, 1H), 5.00 (d, *J* = 10.4 Hz, 1H), 4.95 (ddd, *J* = 17.2, 1.3, 1.3 Hz, 1H), 4.89 (dd, *J* = 1.3, 1.3 Hz, 1H), 4.80–4.72 (m, 1H), 4.78 (s, 1H), 4.73 (dd, *J* = 1.4, 1.4 Hz, 1H), 4.60 (s, 1H), 4.34–4.26 (m, 1H), 2.79–2.72 (m, 1H), 2.63 (dd, *J* = 14.1, 6.9 Hz, 1H), 2.37 (dd, *J* = 14.1, 7.5 Hz, 1H), 2.27 (dd, *J* = 14.2, 6.8 Hz, 1H), 2.17 (ddd, *J* = 14.2, 6.9, 1.0 Hz, 1H), 1.96 (dddd, *J* = 14.7, 8.3, 5.0, 1.1 Hz, 1H), 1.83 (dddd, *J* = 14.7, 5.2, 3.7, 1.8 Hz, 1H), 1.77 (s, 3H), 1.52 (s, 3H), 1.14 (d, *J* = 6.8 Hz, 3H);

^{13}C NMR (126 MHz, $CDCl_3$) δ 147.7, 146.1 (d, J_{CP} = 2.5 Hz), 140.1, 139.9, 137.4, 128.0, 123.4, 117.2, 114.4, 114.2, 82.6 (d, J_{CP} = 5.9 Hz), 76.3 (d, J_{CP} = 6.9 Hz), 74.6 (d, J_{CP} = 6.6 Hz), 44.3 (d, J_{CP} = 6.4 Hz), 43.6 (d, J_{CP} = 7.4 Hz), 43.0 (d, J_{CP} = 3.5 Hz), 33.3 (d, J_{CP} = 6.9 Hz), 22.5, 22.3, 15.7;

^{31}P NMR (162 MHz, $CDCl_3$) δ (ppm) –6.56;

HRMS cald for $C_{22}H_{30}NO_6PNa$ $(M+Na)^+$ 458.1708; found 429.1706 (TOF MS ES+).

(1*R*,3*R*,4*R*,8*S*,10*S*,*Z*)-4,6-dimethyl-10-(2-methylallyl)-3-(4-nitrophenyl)-2,11,12-trioxa-1-phosphabicyclo[6.3.1]dodec-5-ene 1-oxide (*cis*,*anti*-2.13.5):[3]

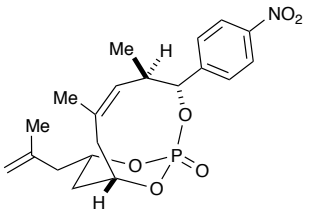

cis,*anti*-**2.13.5**

Yield: 61% (17 mg isolated starting from 30 mg of triene);

FTIR (thin film): 2982, 2916, 1614, 1523, 1351, 1242, 1082, 1042, 962, 750, 732 cm^{-1};

Optical Rotation: $[\alpha]_D$ = –30.0 (*c* = 0.39, $CHCl_3$);

---

[3] CCDC 905670 contains the supplementary crystallographic data for this compound. This X-ray crystallography data has been published in: Maitra, S.; Markley, J. L.; Chegondi, R.; Hanson, P. R. Phosphate Tether-Mediated Ring-Closing Metathesis for the Generation of Medium to LargeBicyclo[n.3.1]phosphates *Tetrahedron* **2015**, *ASAP*.

^{1}H NMR (400 MHz, $CDCl_3$) δ 8.24 (d, *J* = 8.7 Hz, 2H), 7.49 (d, *J* = 8.7 Hz, 2H), 5.33 (d, *J* = 7.4 Hz, 1H), 5.06 (t, *J* = 9.4 Hz, 1H), 5.01–4.94 (m, 1H), 4.89 (s, 1H), 4.89–4.77 (m, 1H), 4.81 (s, 1H), 3.52 (t, *J* = 12.9 Hz, 1H), 2.91–2.82 (m, 1H), 2.51 (dd, *J* = 14.5, 7.1 Hz, 1H), 2.35–2.25 (m, 2H), 1.96 (dd, *J* = 13.0, 4.2 Hz, 1H), 1.84 (s, 3H), 1.80 (s, 3H), 1.76 (d, *J* = 14.6 Hz, 1H), 0.65 (d, *J* = 7.1 Hz, 3H);

^{13}C NMR (126 MHz, $CDCl_3$) δ 147.8, 146.4 (d, J_{CP} = 3.5 Hz), 139.9, 133.6, 131.8, 127.8, 123.8, 114.1, 83.2 (d, J_{CP} = 6.4 Hz), 75.3 (d, J_{CP} = 7.0 Hz), 74.5 (d, J_{CP} = 7.4 Hz), 44.2 (d, J_{CP} = 9.1 Hz), 38.0 (d, J_{CP} = 4.2 Hz), 36.6, 34.1 (d, J_{CP} = 6.3 Hz), 22.8, 22.8, 18.7;

^{31}P NMR (162 MHz, $CDCl_3$) δ –9.73;

HRMS cald for $C_{20}H_{26}NO_6P$ $(M+H)^+$ 408.1576; found 408.1574 (TOF MS ES+).

(4*S*,6*S*)-2-(((2*S*,3*S*,4*S*)-3-hydroxy-2,4-dimethylhex-5-en-1-yl)oxy)-4,6-divinyl-1,3,2-dioxaphosphinane 2-oxide (2.14.2a):

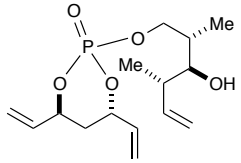

2.14.2a

Yield: 65% (99 mg isolated starting from 100 mg of monochlorophosphate);

FTIR (thin film): 2959, 2910, 1650, 1392, 1272, 1118, 1012, 927, 877 cm^{-1};

Optical Rotation: $[\alpha]_D$ = +56.2 (*c* = 1.5, $CHCl_3$);

^{1}H NMR (500 MHz, $CDCl_3$) δ 5.97 (ddd, *J* = 16.7, 10.6, 6.0 Hz, 1H), 5.85 (dddd, *J* = 17.3, 10.6, 5.2, 1.6 Hz, 1H), 5.71 (ddd, *J* = 17.3, 10.2, 8.4 Hz, 1H), 5.41 (dd, *J* = 17.1, 1.1 Hz, 1H), 5.32 (dd, *J* = 17.2, 1.0 Hz, 1H), 5.25 (ddd, *J* = 10.6, 6.6, 1.0 Hz, 2H), 5.09–5.03 (m, 2H), 5.02–4.91 (m, 2H), 4.11–4.05 (m, 1H), 3.92 (ddd, *J* = 10.0, 7.7, 6.1 Hz, 1H), 3.38 (dd, *J* = 8.8, 2.8 Hz, 1H), 2.25–2.17 (m, 1H), 2.12 (dddd, *J* = 14.6, 8.1, 4.8, 1.5 Hz, 2H), 2.03–1.97 (m, 2H), 0.91 (d, *J* = 6.8 Hz, 3H), 0.84 (d, *J* = 6.9 Hz, 3H);

^{13}C NMR (126 MHz, $CDCl_3$) δ 141.6, 135.0 (d, J_{CP} = 1.8 Hz), 135.0 (d, J_{CP} = 3.1 Hz), 118.2, 117.6, 116.2, 77.6 (d, J_{CP} = 6.7 Hz), 76.4 (d, J_{CP} = 6.0 Hz), 72.6, 70.3 (d, J_{CP} = 6.0 Hz), 41.8, 35.5 (d, J_{CP} = 6.1 Hz), 35.1 (d, J_{CP} = 7.7 Hz), 16.4, 8.8;

^{31}P NMR (162 MHz, $CDCl_3$) δ –6.62;

HRMS: cald. for $C_{15}H_{26}O_5P$ $(M+H)^+$ 317.1518; found 317.1513 (TOF MS ES+).

(1*S*,4*S*,5*S*,6*S*,9*S*,11*S*,*E*)-5-hydroxy-4,6-dimethyl-11-vinyl-2,12,13-trioxa-1-phosphabicyclo[7.3.1]tridec-7-ene 1-oxide (2.14.4a):

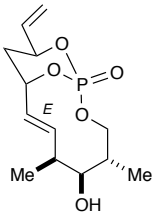

2.14.4a

Yield: 62% (5 mg isolated starting from 9 mg of triene);

FTIR (thin film): 2962, 2958, 1459, 1245, 1012 cm^{-1};

Optical Rotation: $[\alpha]_D$ = +47.6 (*c* = 0.105, $CHCl_3$);

^{1}H NMR (500 MHz, $CDCl_3$) δ 6.21 (ddd, *J* = 16.1, 8.7, 1.8 Hz, 1H), 5.87 (dddd, *J* = 17.9, 9.9, 4.8, 1.7 Hz, 1H), 5.83 (dd, *J* = 15.4, 4.6 Hz, 1H), 5.44 (ddd, *J* = 17.1, 1.1, 1.1 Hz, 1H), 5.29 (ddd, *J* = 10.7, 1.1, 1.0 Hz, 1H), 5.19–5.07 (m, 2H), 4.28 (dd, *J* = 10.9, 5.6 Hz, 1H), 3.95 (dd, *J* = 11.1, 5.0 Hz, 1H), 3.73 (d, *J* = 5.9 Hz, 1H), 2.71–2.61 (m, 1H), 2.24 (ddd, *J* = 14.6, 12.1, 5.2 Hz, 1H), 2.06–1.97 (m, 1H), 1.83 (ddd, *J* = 14.6, 3.7, 2.1 Hz, 1H), 1.69 (s, 1H), 1.16 (d, *J* = 7.1 Hz, 3H), 1.11 (d, *J* = 7.2 Hz, 3H);

^{13}C NMR (126 MHz, $CDCl_3$) δ 139.9, 135.3 (d, J_{CP} = 10.1 Hz), 127.7, 117.1, 79.4, 77.2, 76.3 (d, J_{CP} = 6.4 Hz), 75.1 (d, J_{CP} = 7.0 Hz), 64.2, 39.4, 37.3 (d, J_{CP} = 10.1 Hz), 35.5 (d, J_{CP} = 5.6 Hz), 13.6;

^{31}P NMR (162 MHz, $CDCl_3$) δ –7.10;

HRMS: cald. for $C_{13}H_{21}O_5PNa$ $(M+Na)^+$ 311.1024; found 311.0998 (TOF MS ES+).

(4*S*,6*S*)-2-(((2*S*,3*S*,4*S*)-3-((*tert*-butyldimethylsilyl)oxy)-2,4-dimethylhex-5-en-1-yl)oxy)-4,6-divinyl-1,3,2-dioxaphosphinane 2-oxide (2.14.2b):

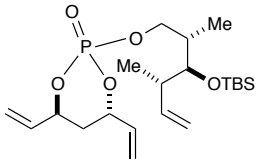

2.14.2b

Yield: 89% (156 mg isolated starting from 80 mg of monochlorophosphate);

FTIR (thin film): 2951, 2919, 1491, 1256, 1231, 1109, 1000, 919, 853, 829 cm^{-1};

Optical Rotation: $[\alpha]_D$ = +37.0 (*c* = 1.1, $CHCl_3$);

^{1}H NMR (500 MHz, $CDCl_3$) δ 6.01 (ddd, *J* = 16.6, 10.6, 5.8 Hz, 1H), 5.92 (dddd, *J* = 15.9, 10.6, 5.2, 1.5 Hz, 1H), 5.82 (ddd, *J* = 17.9, 10.2, 8.0 Hz, 1H), 5.46 (ddd, *J* = 17.2, 1.3, 0.8 Hz, 1H), 5.38 (dd, *J* = 17.2, 0.9 Hz, 1H), 5.30 (dd, *J* = 10.6, 0.9 Hz, 2H), 5.09–5.02 (m, 1H), 5.04–4.97 (m, 2H), 5.01–4.93 (m, 1H), 4.03–3.93 (m, 2H), 3.63 (dd, *J* = 4.5, 3.7 Hz, 1H), 2.37 (dq, *J* = 14.0, 7.0 Hz, 1H), 2.18 (dddd, *J* = 14.5, 8.1, 4.8, 1.5 Hz, 1H), 2.04 (dddd, *J* = 14.3, 5.2, 3.7, 1.7 Hz, 2H), 1.01 (d, *J* = 7.0 Hz, 3H), 0.94 (d, *J* = 6.9 Hz, 3H), 0.90 (s, 9H), 0.06 (s, 6H);

^{13}C NMR (126 MHz, $CDCl_3$) δ 141.2, 135.1 (d, J_{CP} = 3.2 Hz), 135.0 (d, J_{CP} = 7.1 Hz), 117.9, 117.5, 114.6, 77.4 (d, J_{CP} = 6.7 Hz), 76.1 (d, J_{CP} = 6.1 Hz), 75.3, 70.6 (d, J_{CP} = 6.0 Hz), 42.5, 38.0 (d, J_{CP} = 6.7 Hz), 35.1 (d, J_{CP} = 7.6 Hz), 26.0, 18.3, 17.3, 11.8, -3.8, -4.1;

^{31}P NMR (162 MHz, $CDCl_3$) δ –7.05;

HRMS: cald. for $C_{21}H_{39}O_5PSiNa$ $(M+Na)^+$ 453.2202; found 453.2189 (TOF MS ES+).

(1*S*,4*S*,5*S*,6*S*,9*S*,11*S*,*E*)-5-((*tert*-butyldimethylsilyl)oxy)-4,6-dimethyl-11-vinyl-2,12,13-trioxa-1-phosphabicyclo[7.3.1]tridec-7-ene 1-oxide (2.14.4b):

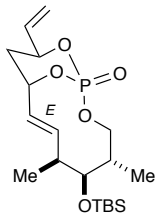

2.14.4b

Yield: 72% (101 mg isolated starting from 150 mg of triene);

FTIR (thin film): 2956, 2929, 1471, 1276, 1257, 1103, 1001, 927, 862, 837 cm^{-1};

Optical Rotation: $[\alpha]_D$ = +36.5 (*c* = 3.75, $CHCl_3$);

^{1}H NMR (500 MHz, $CDCl_3$) δ 6.22 (dd, *J* = 15.5, 9.7 Hz, 1H), 5.87 (dddd, *J* = 17.4, 9.9, 4.8, 1.8 Hz, 1H), 5.75 (dd, *J* = 16.0, 4.7 Hz, 1H), 5.45 (ddd, *J* = 17.0, 1.2, 1.0 Hz, 1H), 5.27 (d, *J* = 10.6 Hz, 1H), 5.18–5.04 (m, 2H), 4.34 (s, 1H), 3.91 (dd, *J* = 11.2, 6.6 Hz, 1H), 3.68

(dd, J = 5.9, 2.1 Hz, 1H), 2.49 (s, 1H), 2.22 (ddd, J = 14.6, 12.2, 5.2 Hz, 1H), 2.10–1.96 (m, 1H), 1.81 (dd, J = 14.5, 1.5 Hz, 1H), 1.09 (d, J = 6.9 Hz, 3H), 1.01 (d, J = 7.4 Hz, 3H), 0.92 (s, 9H), 0.08 (s, 3H), 0.03 (s, 3H);

^{13}C NMR (126 MHz, $CDCl_3$) δ 135.4 (d, J_{CP} = 10.0 Hz), 127.1, 116.9, 80.0, 77.2 (d, J_{CP} = 6.1 Hz), 76.1 (d, J_{CP} = 6.5 Hz), 75.1 (d, J_{CP} = 7.0 Hz), 70.6 (d, J_{CP} = 5.9 Hz), 42.5, 39.5, 35.6 (d, J_{CP} = 5.7 Hz), 29.6, 26.0, 25.9, 18.1, -4.2, -4.8;

^{31}P NMR (162 MHz, $CDCl_3$) δ –7.16;

HRMS: cald. for $C_{19}H_{35}O_5PSiNa$ $(M+Na)^+$ 425.1889; found 425.1885 (TOF MS ES+).

(4*R*,6*R*)-2-(((2*S*,3*S*,4*S*)-3-((4-methoxybenzyl)oxy)-2,4-dimethylhex-5-en-1-yl)oxy)-4,6-divinyl-1,3,2-dioxaphosphinane 2-oxide (2.14.3):

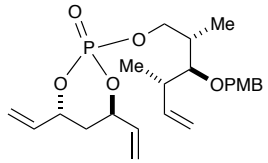

2.14.3

Yield: 68% (150 mg isolated starting from 100 mg of monochlorophosphate);

FTIR (thin film): 2971, 1651, 1521, 1282, 1249, 1112, 1008, 964, 927, 827 cm^{-1};

Optical Rotation: $[\alpha]_D$ = –16.4 (c = 1.8, $CHCl_3$);

^{1}H NMR (500 MHz, $CDCl_3$) δ 7.27 (d, J = 9.0 Hz, 2H), 6.86 (d, J = 8.8 Hz, 2H), 6.05–5.87 (m, 3H), 5.46 (ddd, J = 17.1, 1.5, 0.9 Hz, 1H), 5.37 (ddd, J = 17.1, 1.5 0.9 Hz, 1H), 5.29 (dddd, J = 10.8, 9.1, 1.1, 1.1 Hz, 2H), 5.11 (ddd, J = 17.3, 1.7, 1.4 Hz, 1H), 5.08–5.04 (m, 1H), 5.04 (ddd, J = 10.3, 1.6, 1.1 Hz, 1H), 4.98–4.89 (m, 1H), 4.50 (dd, J = 31.2, 10.5 Hz, 2H), 4.28–4.07 (m, 2H), 3.80 (s, 3H), 3.27 (dd, J = 6.9, 4.9 Hz, 1H), 2.52–2.42 (m, 1H), 2.16 (dddd, J = 14.0, 7.7, 4.7, 1.5 Hz, 1H), 2.10–2.00 (m, 2H), 1.06 (d, J = 7.0 Hz, 3H), 1.05 (d, J = 7.1 Hz, 3H);

^{13}C NMR (126 MHz, $CDCl_3$) δ 159.1, 142.1, 135.1 (d, J_{CP} = 3.5 Hz), 135.0 (d, J_{CP} = 6.8 Hz), 130.74, 129.3, 117.8, 117.5, 114.3, 113.7, 83.8, 77.3 (d, J_{CP} = 4.1 Hz), 76.1 (d, J_{CP} = 6.1 Hz), 74.3, 70.1 (d, J_{CP} = 6.1 Hz), 55.2, 40.1, 37.0 (d, J_{CP} = 7.6 Hz), 35.1 (d, J_{CP} = 7.6 Hz), 14.6, 14.1;

^{31}P NMR (162 MHz, $CDCl_3$) δ –6.81;

HRMS: cald. for $C_{23}H_{33}O_6PNa$ $(M+Na)^+$ 459.1912; found 459.1908 (TOF MS ES+).

(1*R*,4*S*,5*S*,6*S*,9*R*,11*R*,*E*)-5-((4-methoxybenzyl)oxy)-4,6-dimethyl-11-vinyl-2,12,13-trioxa-1-phosphabicyclo[7.3.1]tridec-7-ene 1-oxide (2.14.5):

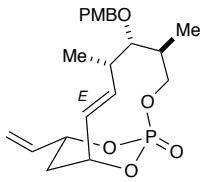

2.14.5

Yield: 75% (28 mg isolated starting from 40 mg of triene);

FTIR (thin film): 2979, 1659, 1515, 1279, 1239, 1111, 1002, 957, 922, 821 cm^{-1};

Optical Rotation: $[\alpha]_D = -18.5$ ($c = 0.26$, $CHCl_3$);

^{1}H NMR (500 MHz, $CDCl_3$) δ 7.26 (d, J = 8.0 Hz, 2H), 6.84 (d, J = 8.7 Hz, 2H), 5.88–5.77 (m, 2H), 5.73 (dd, J = 15.8, 3.9 Hz, 1H), 5.36 (d, J = 17.0 Hz, 1H), 5.24 (d, J = 10.5 Hz, 1H), 5.12 (ddd, J = 24.4, 5.1, 3.8 Hz, 1H), 5.04 (d, J = 7.6 Hz, 1H), 4.51 (d, J = 10.7 Hz, 1H) 4.40 (d, J = 10.7, 1H), 4.18 (dd, J = 10.4, 8.5 Hz, 1H), 3.90 (dd, J = 11.0, 6.6 Hz, 1H), 3.82 (s, 3H), 3.11 (d, J = 7.2, 1H), 2.55 (br.s, 1H), 2.33 (br.s, 1H), 2.20 (ddd, J = 14.5, 12.2, 5.3 Hz, 1H), 1.78 (d, J = 14.4 Hz, 1H), 1.12 (d, J = 6.6 Hz, 3H), 1.07 (d, J = 7.3 Hz, 3H);

^{13}C NMR (126 MHz, $CDCl_3$) δ 159.3, 139.0, 135.3 (d, J_{CP} = 9.9 Hz), 130.2, 129.5, 127.0, 117.0, 113.8, 87.4, 77.2 (d, J_{CP} = 6.1 Hz), 76.4 (d, J_{CP} = 6.4 Hz), 75.3 (d, J_{CP} = 6.0 Hz), 72.0, 65.7, 55.3, 35.6 (d, J_{CP} = 3.2 Hz), 35.5, 34.60 (d, J_{CP} = 8.9 Hz), 17.9;

^{31}P NMR (162 MHz, $CDCl_3$) δ –8.02;

HRMS: cald. for $C_{21}H_{29}O_6PNa$ $(M+Na)^+$ 431.1599; found 431.1605 (TOF MS ES+).

(4*S*,6*S*)-2-(((*S*)-1-(benzyloxy)oct-7-en-2-yl)oxy)-4,6-divinyl-1,3,2-dioxaphosphinane 2-oxide (2.15.2)

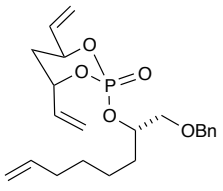

2.15.2

Yield: 30% (68 mg isolated starting from 110 mg of monochlorophosphate);

FTIR (thin film): 2928, 2858, 1639, 1454, 1285, 1119, 999, 926, 737, 698 cm^{-1};

Optical Rotation: $[\alpha]_D$ = +45.54 (*c* = 0.92, $CHCl_3$);

^{1}H NMR (500 MHz, Chloroform-*d*) 7.37–7.27 (m, 5H, aromatic), 6.07 (dddd, *J* = 17.0, 10.6, 6.3, 0.8 Hz, 1H, H_2C=C<u>H</u>-CHO(P)CH_2), 5.87–5.81 (m, 1H, H_2C=C<u>H</u>CHO(P)CH_2), 5.78 (ddt, *J* = 17.1, 10.2, 6.7 Hz, 1H, H_2C=C<u>H</u>CH_2CH_2), 5.37 (dt, *J* = 5.3, 1.3 Hz, 1H, <u>H_2</u>C=CH-CHO(P)CH_2), 5.34 (dt, *J* = 5.3, 1.3 Hz, 1H, <u>H_2</u>C=CHCHO(P)CH_2), 5.28 (dt, *J* = 10.6, 1.2 Hz, 1H, <u>H_2</u>C=CHCHO(P)CH_2), 5.23 (dt, *J* = 10.6, 1.3 Hz, 1H, <u>H_2</u>C=CHCHO(P)CH_2), 5.06–5.00 (m, 2H, H_2C=CHC<u>H</u>O(P)CH_2), 5.00–4.90 (m, 2H, <u>H_2</u>C=CHCH_2CH_2), 4.65–4.58 (m, 1H, C<u>H</u>O(P)CH_2OBn), 4.58 (d, J = 11.9 Hz, 1H, OC<u>H_2</u>Ph), 4.51 (d, J = 11.9 Hz, 1H, OC<u>H_2</u>Ph), 3.61 (ddd, *J* = 10.7, 3.9, 1.5 Hz, 1H, CHO(P)C<u>H_2</u>OBn), 3.57 (dd, *J* = 10.6, 5.8 Hz, 1H, CHO(P)C<u>H_2</u>OBn), 2.11 (dddd, *J* = 14.4, 7.9, 4.8, 1.6 Hz, 1H, H_2C=CHCHO(P)C<u>H_2</u>CHO[P]), 2.08–2.05 (m, 1H, H_2C=HC<u>H_2</u>CH_2CH_2C), 2.02 (dddd, *J* = 14.7, 5.5, 3.9, 1.8 Hz, 2H, H_2C=HC<u>H_2</u>CH_2CH_2C, H_2C=CHCHO(P)C<u>H_2</u>CHO[P]), 1.81–1.65 (m, 2H, H_2C<u>H_2</u>CCHO(P)CH_2OBn), 1.49–1.33 (m, 4H, H_2C=HCH_2C<u>H_2</u>C<u>H_2</u>CH_2CCHO(P)CH_2OBn);

^{13}C NMR (126 MHz, $CDCl_3$) δ 138.7, 137.9, 135.3 (d, J_{CP} = 4.2 Hz), 135.2, 128.3 (2C), 127.7(2C), 127.66, 117.8, 117.1, 114.4, 78.2 (d, J_{CP} = 6.1 Hz), 77.9 (d, J_{CP} = 6.7 Hz), 75.7 (d, J_{CP} = 6.0 Hz), 73.2, 71.8 (d, J_{CP} = 4.4 Hz), 35.3 (d, J_{CP} = 7.6 Hz), 33.5, 32.1 (d, J_{CP} = 4.7 Hz), 28.7, 24.4;

^{31}P NMR (162 MHz, $CDCl_3$) δ –7.90;

HRMS cald for $C_{22}H_{31}O_5PNa$ $(M+Na)^+$ 429.1807; found 429.1801 (TOF MS ES+).

(4*R*,6*R*)-2-(((*S*)-1-(benzyloxy)oct-7-en-2-yl)oxy)-4,6-divinyl-1,3,2-dioxaphosphinane 2-oxide (2.15.3):

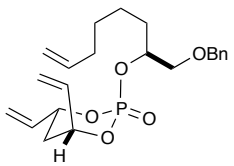

2.15.3

Yield: 30% (65 mg isolated starting from 110 mg of monochlorophosphate);

FTIR (thin film): 2926, 2858, 2391, 1283, 1119, 1082, 1005, 928, 737, 698 cm^{-1};

Optical Rotation: $[\alpha]_D = -57.3$ ($c = 0.55$, $CHCl_3$);

^{1}H NMR (400 MHz, $CDCl_3$) δ 7.38–7.27 (m, 5H, aromatic), 6.02 (dddd, J = 17.3, 10.6, 5.9, 0.7 Hz, 1H, H_2C=C<u>H</u>CHO(P)CH_2), 5.92 (dddd, J = 17.3, 10.6, 5.2, 1.6 Hz, 1H, H_2C=C<u>H</u>-CHO(P)CH_2), 5.79 (ddt, J = 16.9, 10.2, 6.7 Hz, 1H, H_2C=C<u>H</u>CH_2CH_2), 5.46 (dt, J = 17.1, 1.3 Hz, 1H, <u>H_2</u>C=CHCHO(P)CH_2), 5.36 (dt, J = 17.1, 1.2 Hz, 1H, <u>H_2</u>C=CHCHO(P)CH_2), 5.30 (dt, J = 10.7, 1.2 Hz, 1H, <u>H_2</u>C=CHCHO(P)CH_2), 5.23 (dt, J = 10.6, 1.2 Hz, 1H, <u>H_2</u>C=CHCHO(P)CH_2), 5.05 (dddd, J = 12.9, 7.3, 4.4, 1.5 Hz, 1H, H_2C=CHC<u>H</u>O(P)CH_2), 5.02 – 4.95 (m, 2H, H_2C=CHC<u>H</u>O(P)CH_2, <u>H_2</u>C=CHCH_2CH_2), 4.93 (ddt, J = 10.2, 2.3, 1.2 Hz, 1H, <u>H_2</u>C=CHCH_2CH_2), 4.70 – 4.60 (m, 1H, C<u>H</u>O(P)CH_2OBn), 4.60 (d, J = 12.0 Hz, 1H, OC<u>H_2</u>Ph), 4.54 (d, J = 12.0 Hz, 1H, OC<u>H_2</u>Ph), 3.62 (d, J = 1.9 Hz, 1H, CHO(P)C<u>H_2</u>OBn), 3.62 (d, J = 1.6 Hz, 1H, CHO(P)C<u>H_2</u>OBn), 2.14 (dddd, J = 14.1, 7.6, 4.8, 1.6 Hz, 1H, H_2C=CHCHO(P)C<u>H_2</u>CHO[P]), 2.10–2.06 (m, 1H, H_2C=CHCHO(P)C<u>H_2</u>CHO[P]), 2.06–2.01 (m, 2H, H_2C=HC<u>H_2</u>CH_2CH_2C), 1.75–1.70 (m, 2H, H_2C<u>H_2</u>CCHO(P)CH_2OBn), 1.53–1.29 (m, 4H, H_2C=HCH_2C<u>H_2</u>C<u>H_2</u>CH_2CCHO(P)CH_2OBn);

^{13}C NMR (126 MHz, $CDCl_3$) δ 138.7, 138.1, 135.3 (d, J_{CP} = 3.7 Hz), 135.1 (d, J_{CP} = 7.2 Hz), 128.3 (2C), 127.6 (2C), 127.58, 117.7, 117.4, 114.5, 78.5 (d, J_{CP} = 6.4 Hz), 77.5 (d, J_{CP} = 6.7 Hz), 76.1 (d, J_{CP} = 6.2 Hz), 73.2, 71.7 (d, J_{CP} = 4.0 Hz), 35.3 (d, J_{CP} = 7.5 Hz), 33.5, 32.0 (d, J_{CP} = 5.0 Hz), 28.6, 24.4.

^{31}P NMR (162 MHz, $CDCl_3$) δ –8.0;

HRMS cald for $C_{22}H_{31}O_5PNa$ $(M+Na)^+$ 429.1807; found 429.1793 (TOF MS ES+).

(1*S*,3*S*,10*S*,12*S*,*E*)-3-((benzyloxy)methyl)-12-vinyl-2,13,14-trioxa-1-phosphabicyclo[8.3.1]tetradec-8-ene 1-oxide (*cis*-2.15.4):

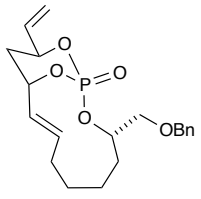

cis-**2.15.4**

Yield: 69% (3.5 mg isolated starting from 5.5 mg of triene); *E/Z*: 20:1)

FTIR (thin film): 2929, 1280, 1099, 995,921, 739 cm^{-1};

Optical Rotation: $[\alpha]_D$ = + 66.25 (*c* = 0.48, $CHCl_3$);

^{1}H NMR (400 MHz, $CDCl_3$) δ 7.38–7.28 (m, 5H, aromatic), 6.02 (ddd, *J* = 15.4, 10.7, 4.6 Hz, 1H, HC=C<u>H</u>CH_2CH_2), 5.94–5.81 (m, 2H, H_2C=C<u>H</u>CHO(P)CH_2, <u>H</u>C=CH-CH_2CH_2), 5.45 (d, *J* = 17.2 Hz, 1H, H_2C=C<u>H</u>CHO(P)CH_2), 5.28 (d, *J* = 10.6 Hz, 1H, H_2C=C<u>H</u>CHO(P)CH_2), 5.19 (dd, *J* = 11.7, 5.0 Hz, 1H,), 5.09 (dt, *J* = 23.9, 6.4 Hz, 1H), 4.68 (q, *J* = 5.9 Hz, 1H, C<u>H</u>O(P)CH_2OBn), 4.59 (d, *J* = 12.1 Hz, 1H, OC<u>H</u>$_2$Ph), 4.54 (d, *J* = 12.1 Hz, 1H, OC<u>H</u>$_2$Ph), 3.65 (dd, *J* = 10.2, 5.4 Hz, 1H, CHO(P)C<u>H</u>$_2$OBn), 3.57 (dd, *J* = 10.2, 6.3 Hz, 1H, CHO(P)C<u>H</u>$_2$OBn), 2.44–2.35 (m, 1H, HC=CHC<u>H</u>$_2CH_2$), 2.31–2.20 (m, 1H, H_2C<u>H</u>$_2$CCHO(P)CH_2OBn), 2.03–1.90 (m, 1H, HC=CHC<u>H</u>$_2CH_2$), 1.84 (d, *J* = 15.0 Hz, 1H, H_2C<u>H</u>$_2$CCHO(P)CH_2OBn), 1.79–1.66(m, 3H, H_2C<u>H</u>$_2$CCHO(P)CH_2OBn, H_2C=HCH_2CH_2C<u>H</u>$_2CH_2$CCHO(P)CH_2OBn), 1.65–1.53 (m, 1H, H_2C=HCH_2CH_2C<u>H</u>$_2CH_2$C CHO(P)CH_2OBn), 1.44–1.36 (m, 1H, H_2C=HCH_2C<u>H</u>$_2CH_2CH_2$CCHO(P)CH_2OBn), 1.25–1.13 (m, 1H, H_2C=HCH_2C<u>H</u>$_2$C<u>H</u>$_2CH_2$CCHO(P)CH_2OBn);

^{13}C NMR (126 MHz, $CDCl_3$) δ 138.8, 138.1, 135.4 (d, J_{CP} = 9.9 Hz), 128.3 (2C), 127.9, 127.7 (2C), 127.6 (d, J_{CP} = 3.7 Hz), 117.1, 76.9, 76.6 (d, J_{CP} = 6.4 Hz), 76.0 (d, J_{CP} = 6.4 Hz), 73.1, 70.8 (d, J_{CP} = 4.9 Hz), 34.9 (d, J_{CP} = 6.1 Hz), 32.3, 30.9 (d, J_{CP} = 4.2 Hz), 24.2, 19.7;

^{31}P NMR (162 MHz, $CDCl_3$) δ –9.17;

HRMS cald for $C_{20}H_{27}O_5PNa$ $(M+Na)^+$ 401.1494; found 401.1501 (TOF MS ES+).

(4*S*,6*S*)-2-(((2*S*,3*S*,4*S*)-1-((4-methoxybenzyl)oxy)-2,4-dimethylhex-5-en-3-yl)oxy)-4,6-divinyl-1,3,2-dioxaphosphinane 2-oxide (2.1.3):

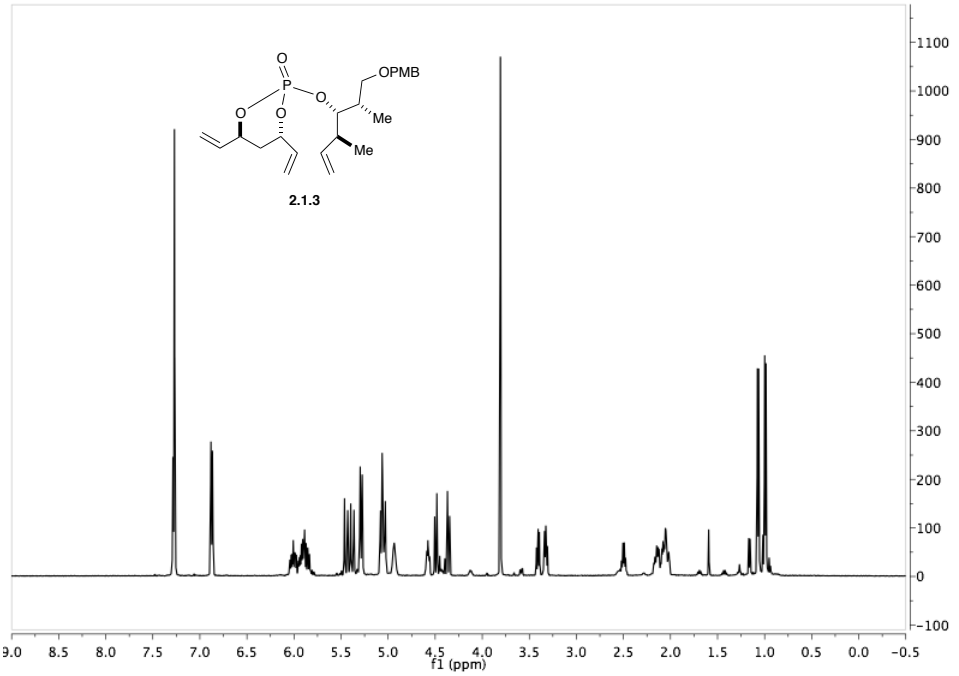

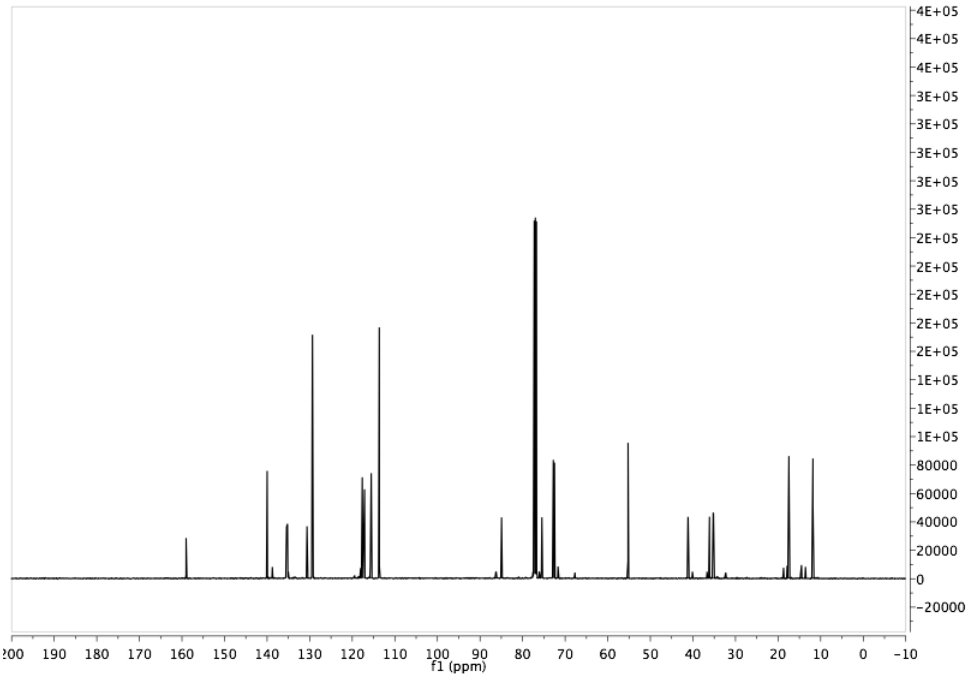

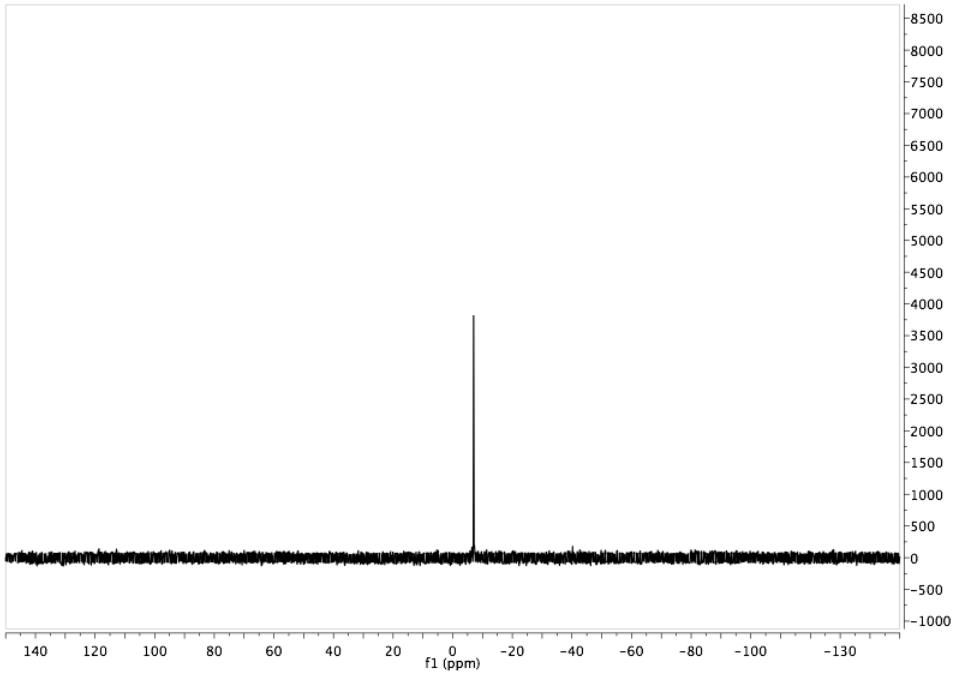

(4*R*,6*R*)-2-(((2*S*,3*S*,4*S*)-1-((4-methoxybenzyl)oxy)-2,4-dimethylhex-5-en-3-yl)oxy)-4,6-divinyl-1,3,2-dioxaphosphinane 2-oxide (2.1.4):

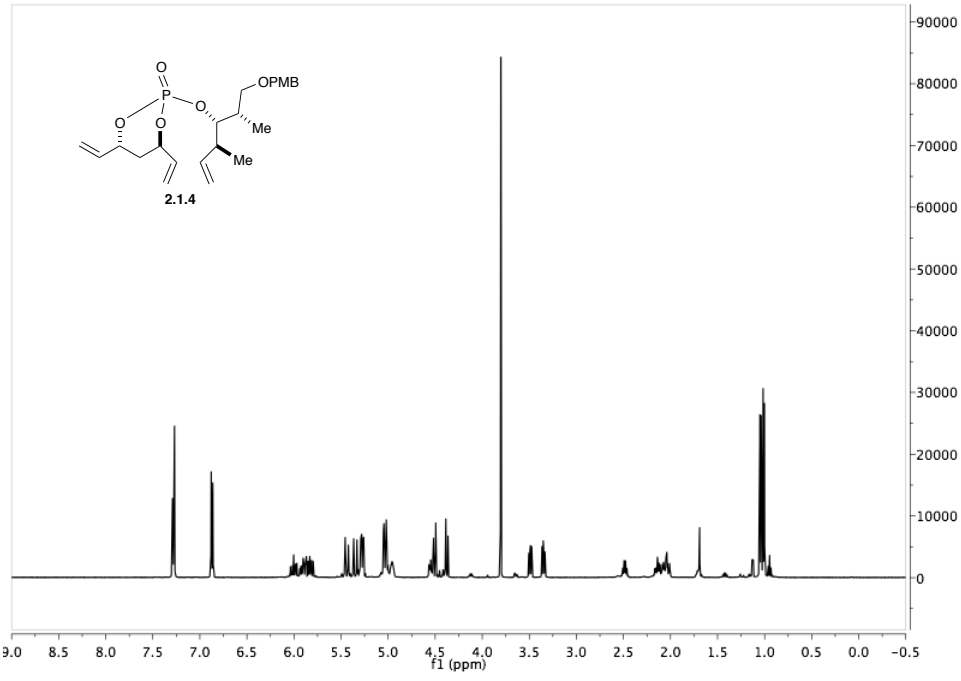

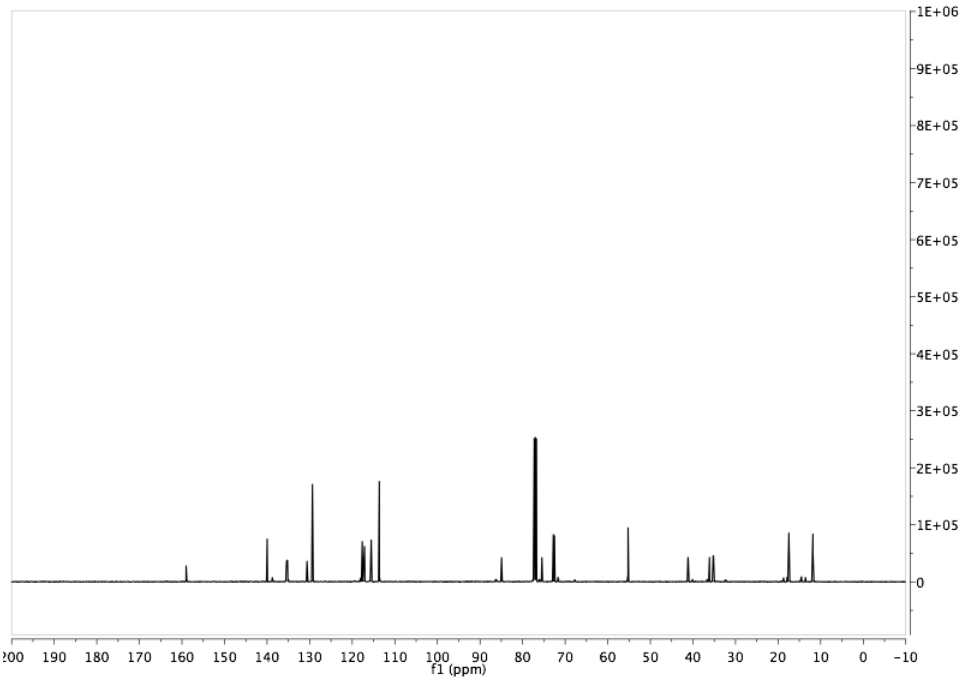
1E+06
9E+05
8E+05
7E+05
6E+05
5E+05
4E+05
3E+05
2E+05
1E+05
0
200 190 180 170 160 150 140 130 120 110 100 90 80 70 60 50 40 30 20 10 0 -10
f1 (ppm)

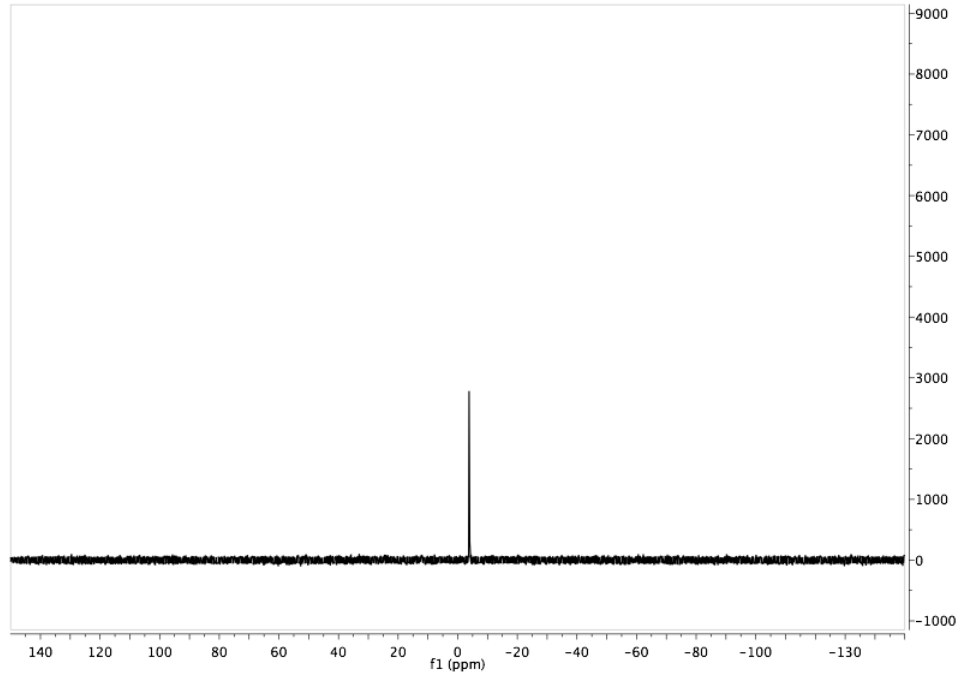
9000
8000
7000
6000
5000
4000
3000
2000
1000
0
-1000
140 120 100 80 60 40 20 0 -20 -40 -60 -80 -100 -130
f1 (ppm)

(1*R*,3*S*,4*S*,7*R*,9*R*,*Z*)-3-((S)-1-((4-methoxybenzyl)oxy)propan-2-yl)-4-methyl-9-vinyl-2,10,11-trioxa-1-phosphabicyclo[5.3.1]undec-5-ene 1-oxide (*trans*,*anti*-2.1.6):

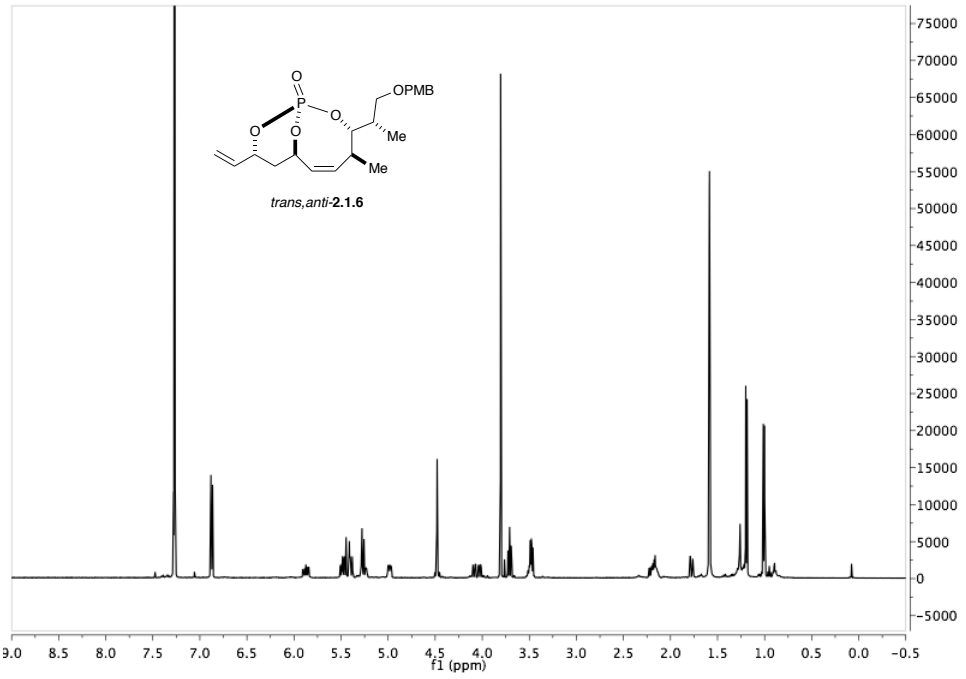

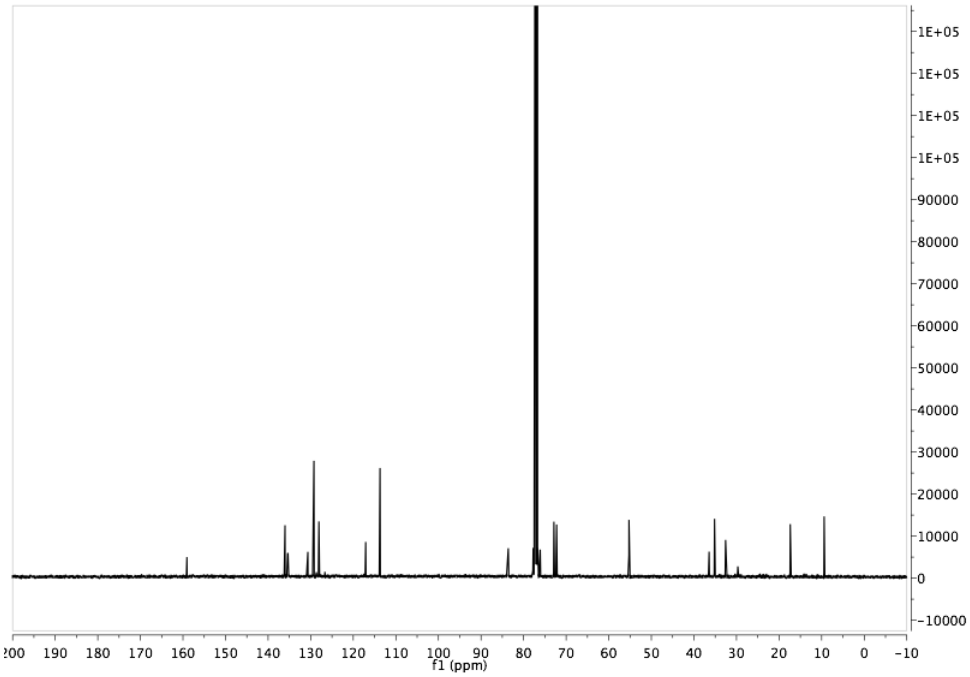

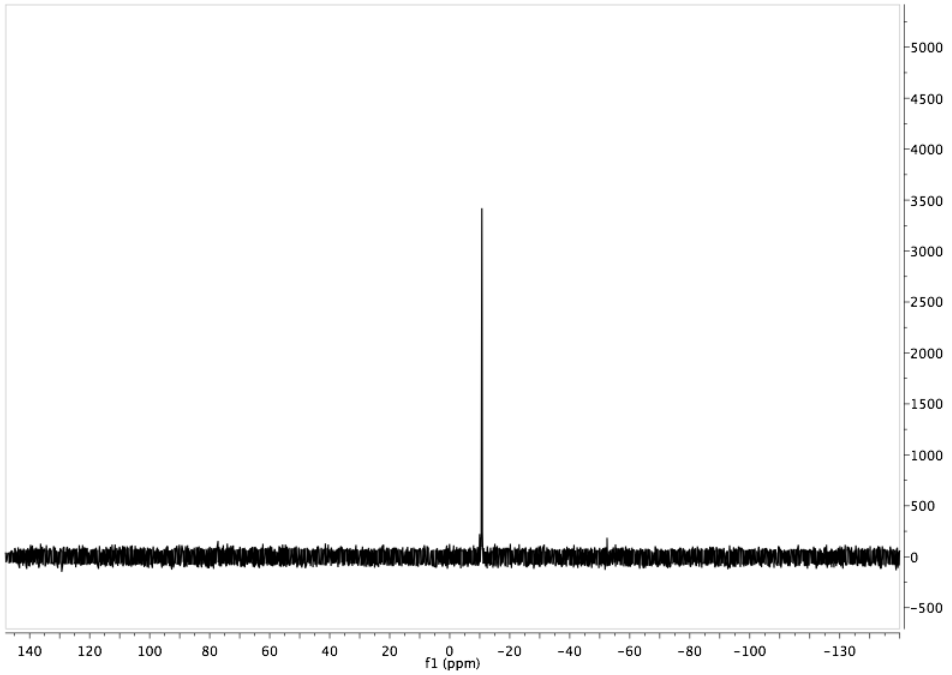

(4*S*,6*S*)-2-((2,4-dimethylpenta-1,4-dien-3-yl)oxy)-4,6-divinyl-1,3,2-dioxaphosphinane 2-oxide (2.3.2):

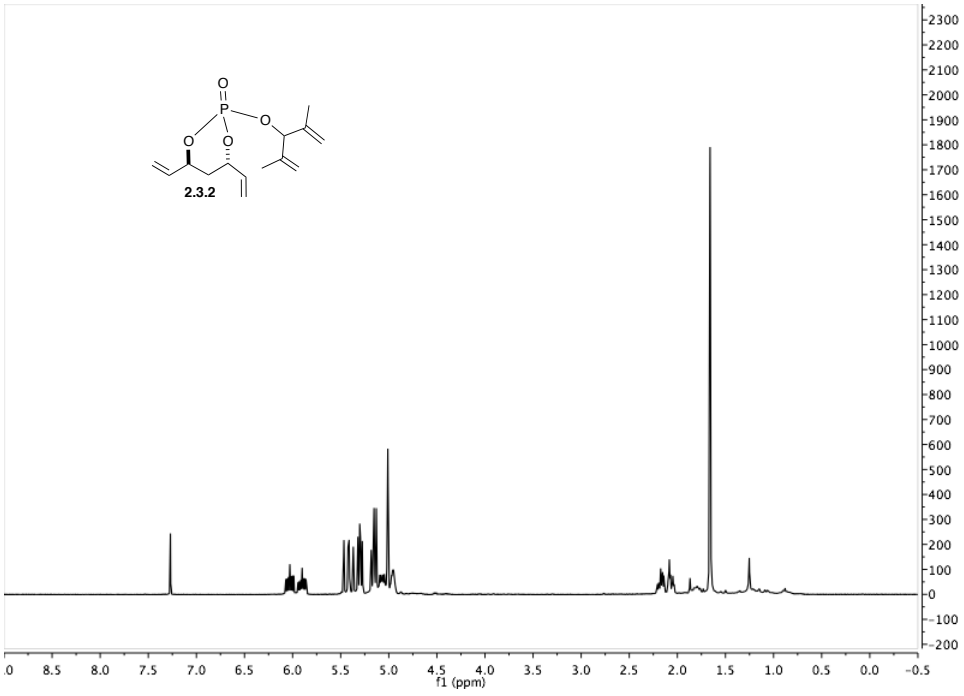

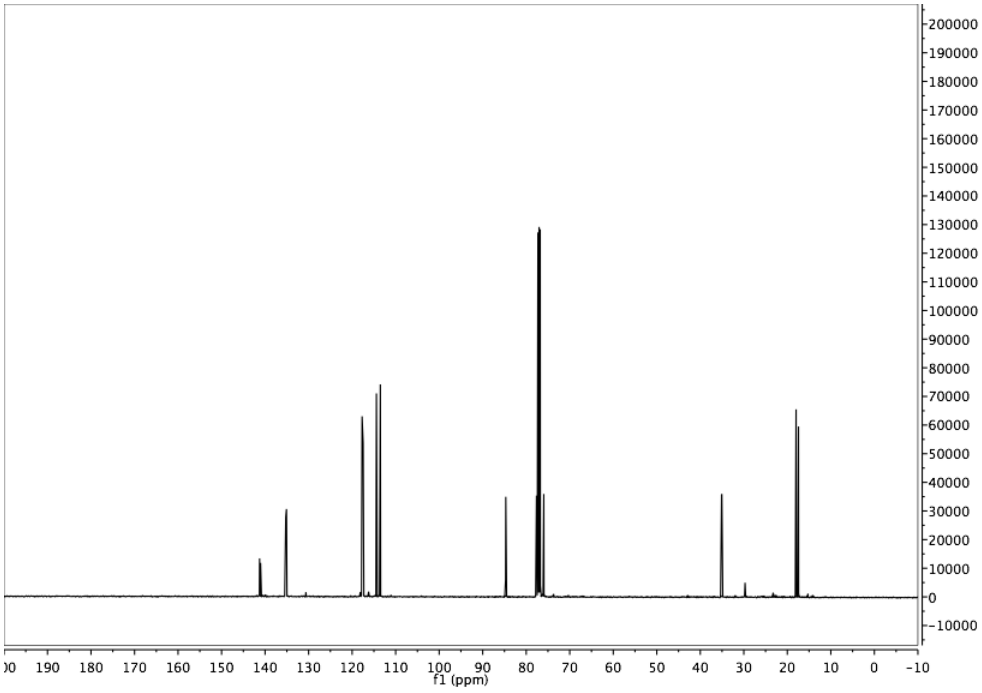
200000
190000
180000
170000
160000
150000
140000
130000
120000
110000
100000
90000
80000
70000
60000
50000
40000
30000
20000
10000
0
-10000
190 180 170 160 150 140 130 120 110 100 90 80 70 60 50 40 30 20 10 0 -10
f1 (ppm)

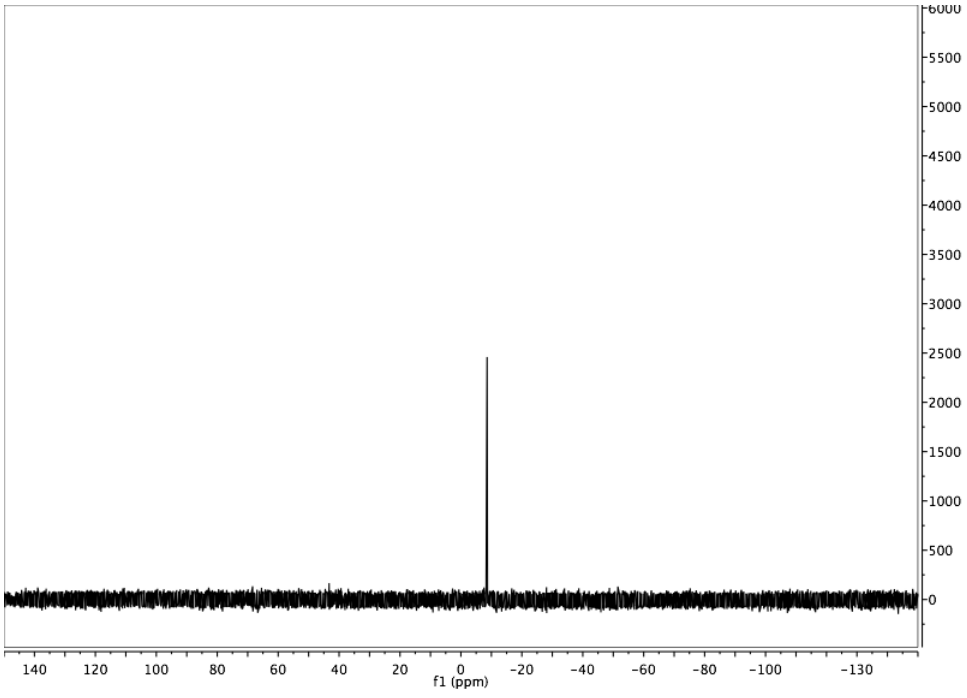
6000
5500
5000
4500
4000
3500
3000
2500
2000
1500
1000
500
0
140 120 100 80 60 40 20 0 -20 -40 -60 -80 -100 -130
f1 (ppm)

(1*S*,3*R*,6*S*,8*S*)-4-methyl-3-(prop-1-en-2-yl)-8-vinyl-2,9,10-trioxa-1-phosphabicyclo[4.3.1]dec-4-ene 1-oxide (*cis*-2.3.3):

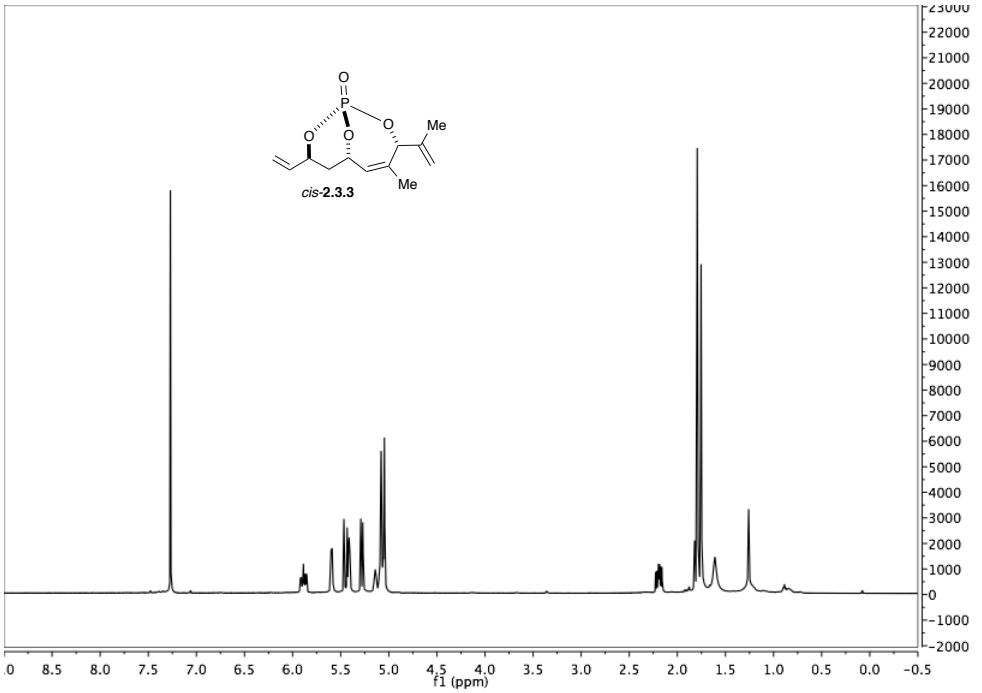

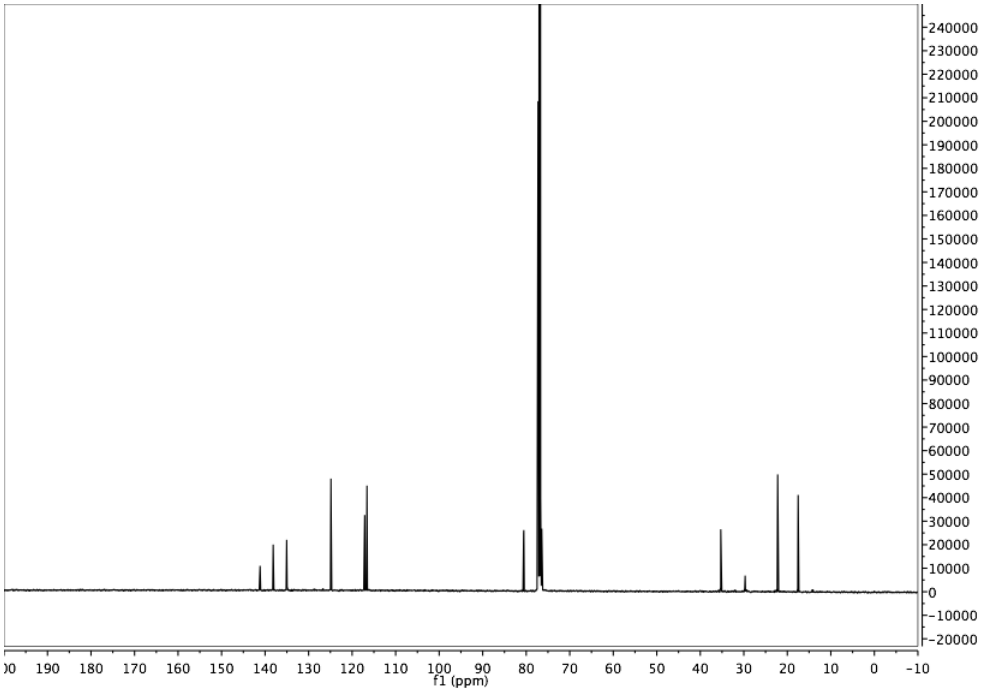

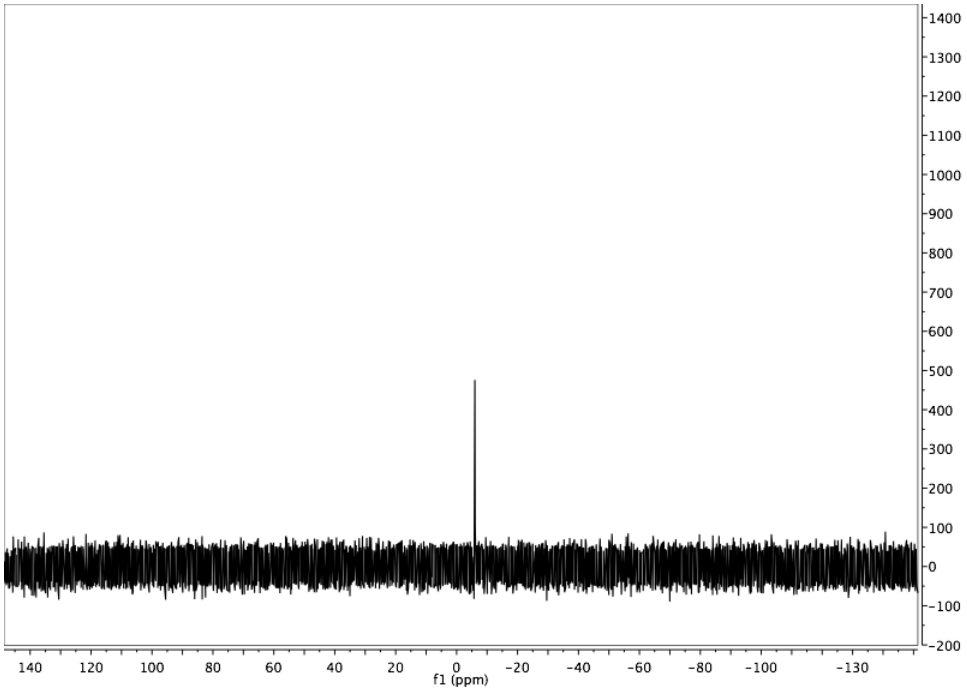

(4*S*,6*S*)-2-(((*R*)-1-(benzyloxy)-4-methylpent-4-en-2-yl)oxy)-4,6-divinyl-1,3,2-dioxaphosphinane-2-oxide (2.5.2):

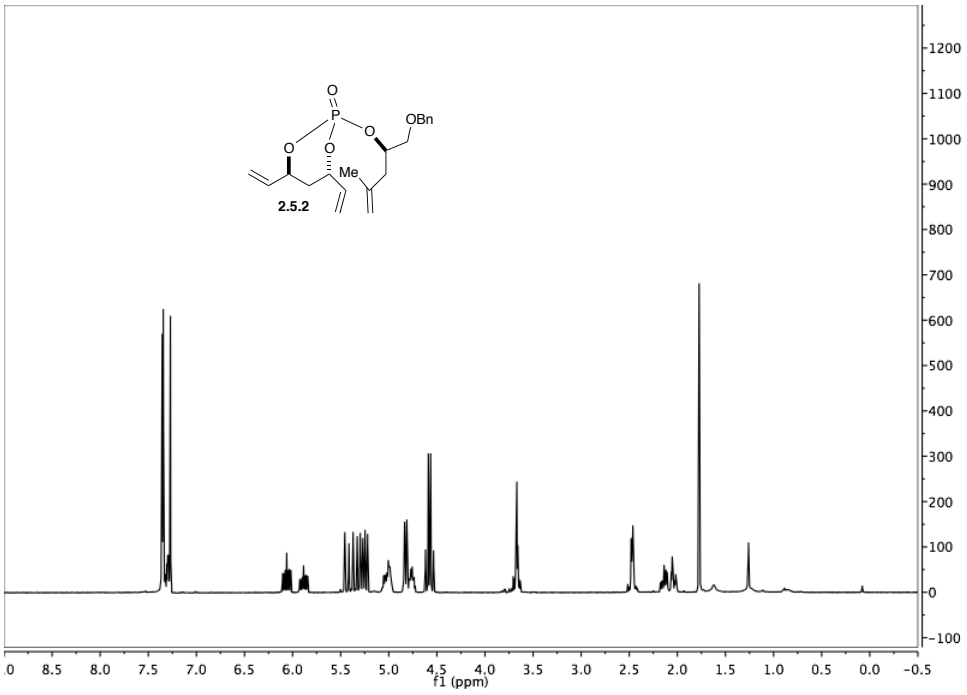

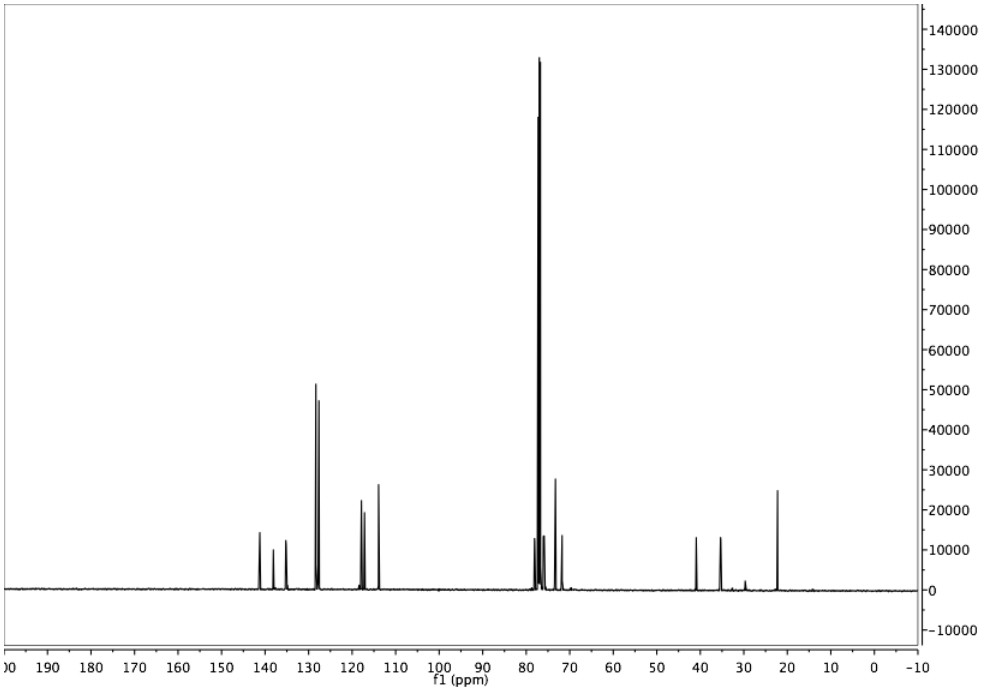
140000
130000
120000
110000
100000
90000
80000
70000
60000
50000
40000
30000
20000
10000
0
−10000
190 180 170 160 150 140 130 120 110 100 90 80 70 60 50 40 30 20 10 0 −10
f1 (ppm)

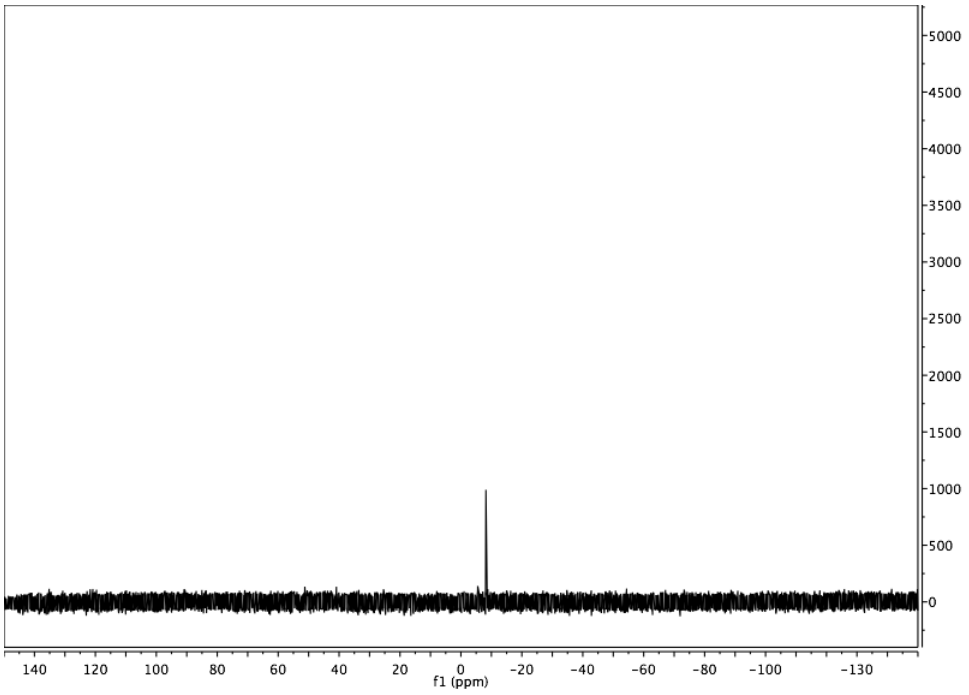
5000
4500
4000
3500
3000
2500
2000
1500
1000
500
0
140 120 100 80 60 40 20 0 −20 −40 −60 −80 −100 −130
f1 (ppm)

(4*R*,6*R*)-2-(((*R*)-1-(benzyloxy)-4-methylpent-4-en-2-yl)oxy)-4,6-divinyl-1,3,2-dioxaphosphinane 2-oxide (2.5.3):

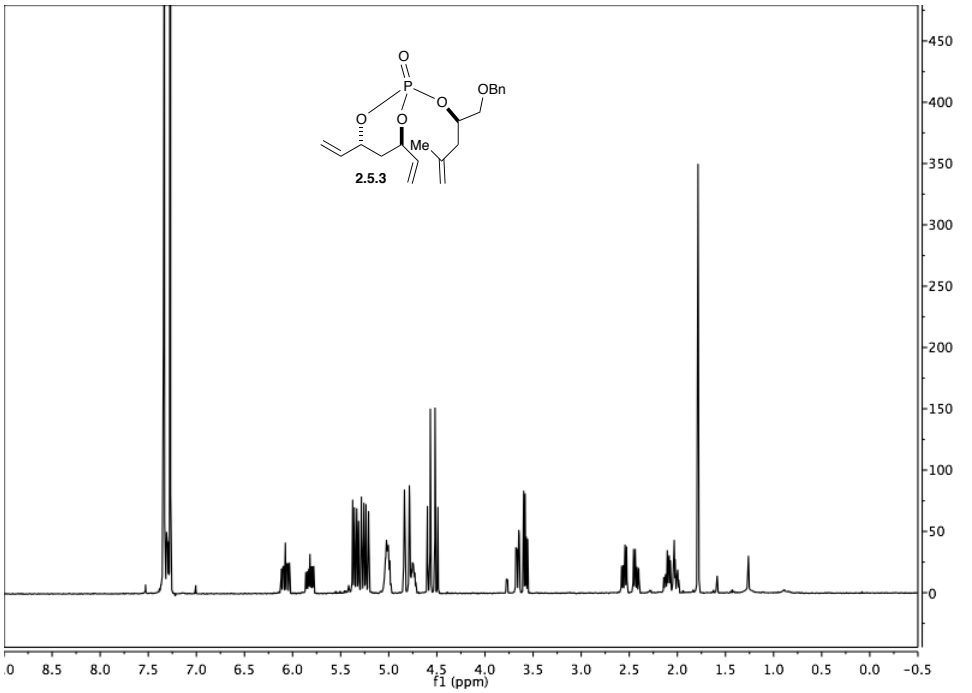

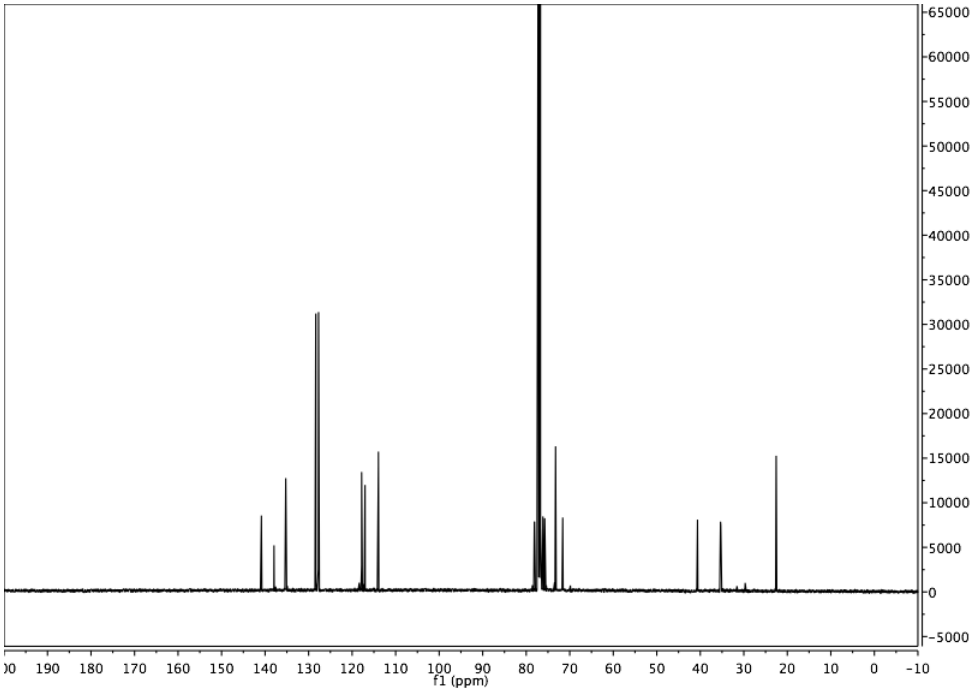

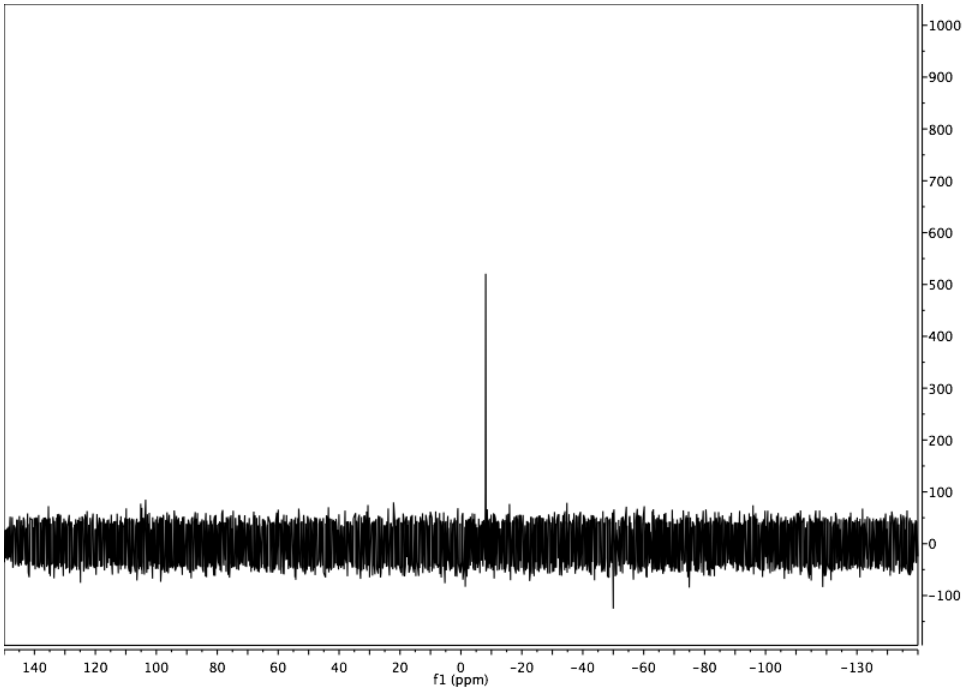

(1*S*,3*R*,7*S*,9*S*,*Z*)-3-((benzyloxy)methyl)-5-methyl-9-vinyl-2,10,11-trioxa-1-phosphabicyclo[5.3.1]undec-5-ene 1-oxide (*trans*-2.5.4):

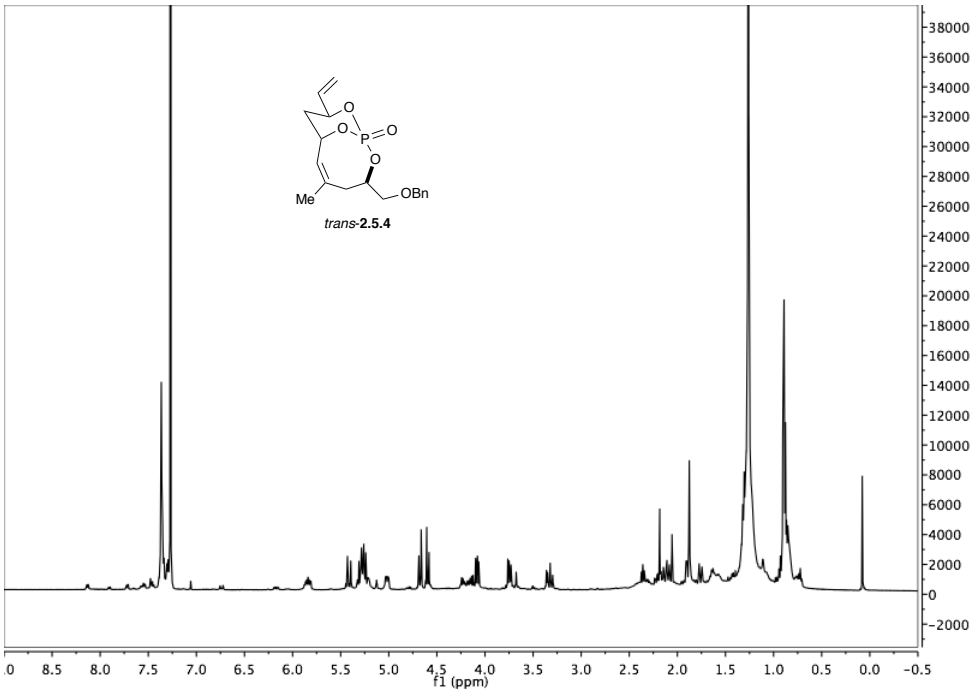

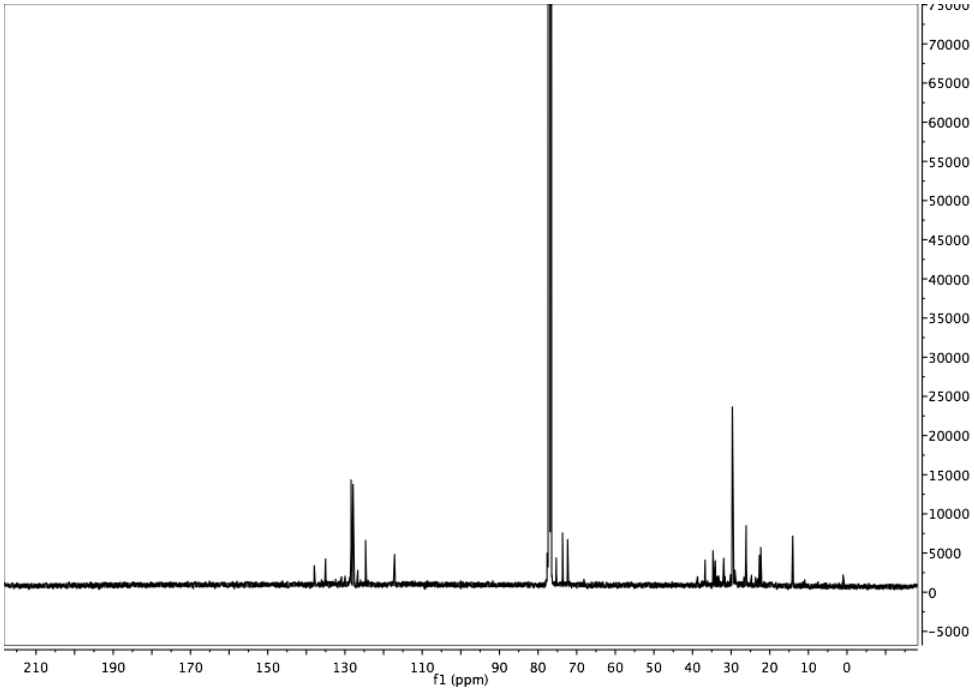
70000
65000
60000
55000
50000
45000
40000
35000
30000
25000
20000
15000
10000
5000
0
-5000
210
190
170
150
130
110
90
80
70
60
50
40
30
20
10
0
f1 (ppm)

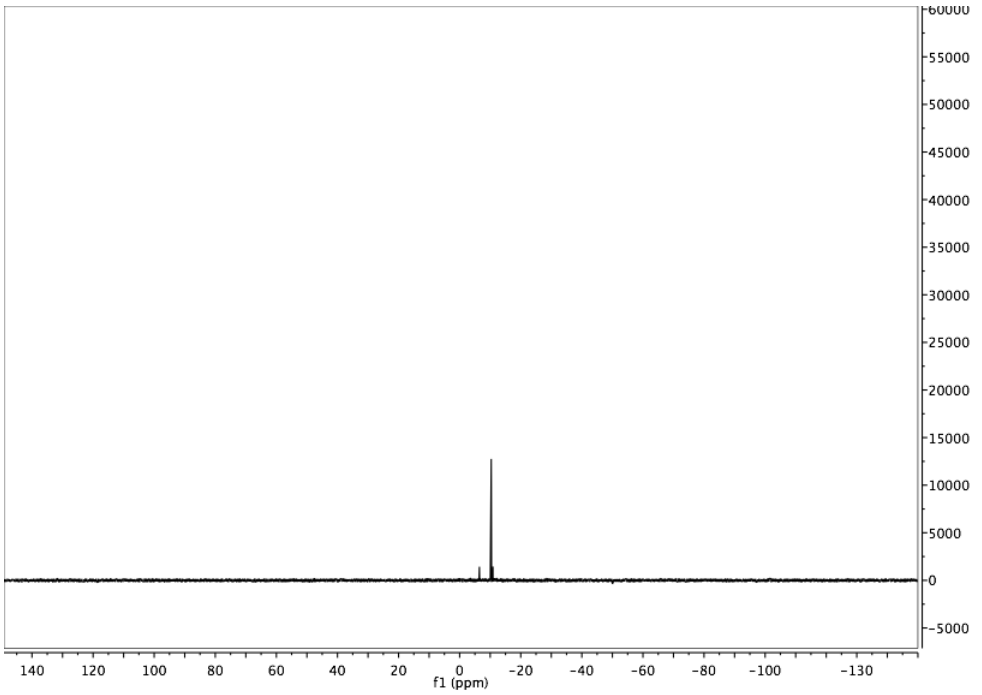
60000
55000
50000
45000
40000
35000
30000
25000
20000
15000
10000
5000
0
-5000
140
120
100
80
60
40
20
0
-20
-40
-60
-80
-100
-130
f1 (ppm)

(4*R*,6*R*)-2-(((1*R*,2*S*)-2-methyl-1-(4-nitrophenyl)but-3-en-1-yl)oxy)-4,6-divinyl-1,3,2-dioxaphosphinane 2-oxide (2.7.2):

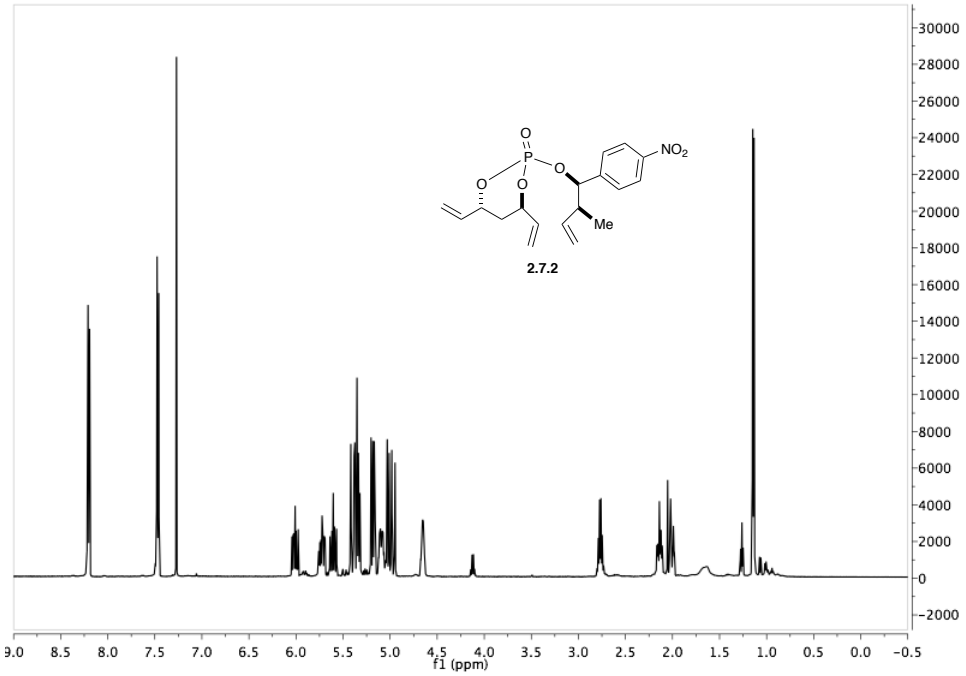

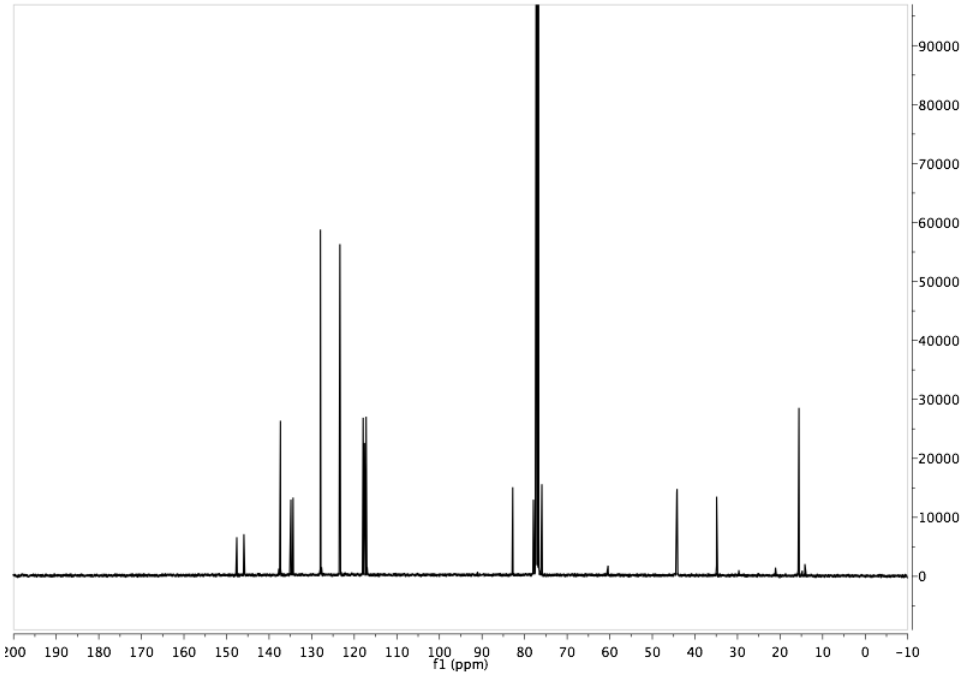

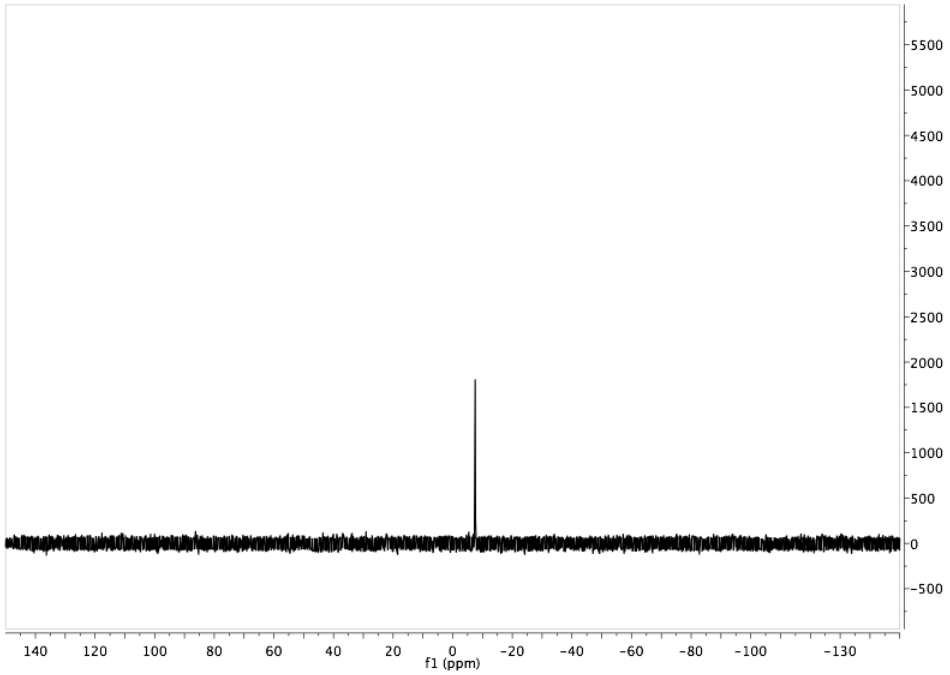

(4*R*,6*R*)-2-(((1*R*,2*R*)-2-methyl-1-(4-nitrophenyl)but-3-en-1-yl)oxy)-4,6-divinyl-1,3,2-dioxaphosphinane 2-oxide (2.8.2):

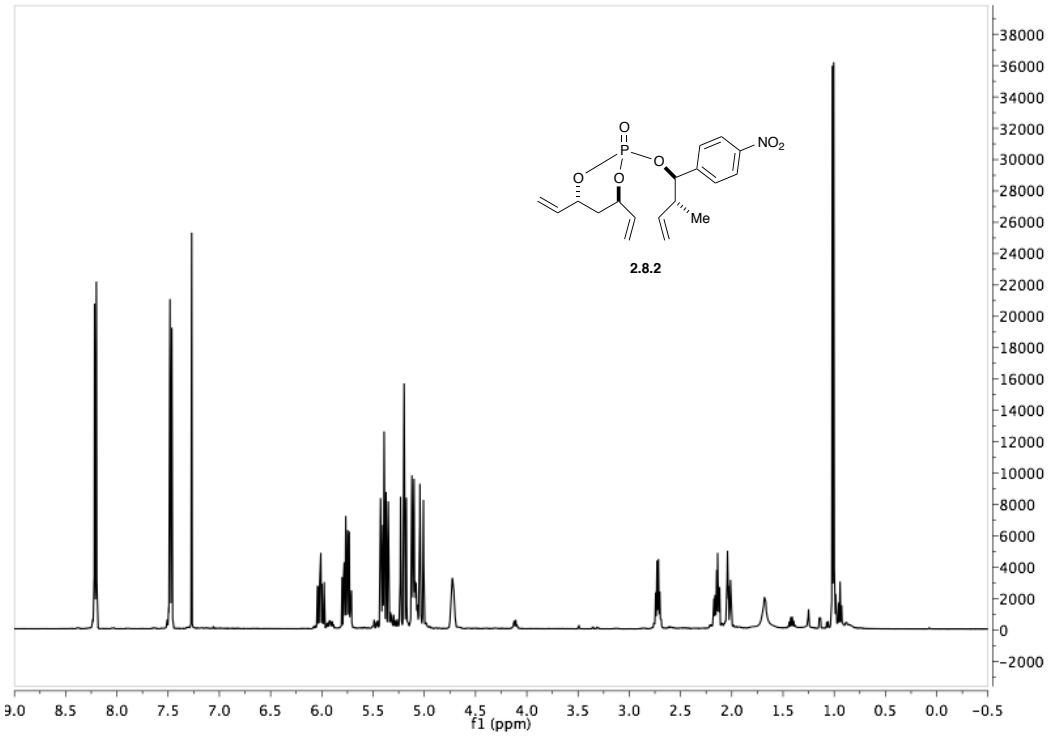

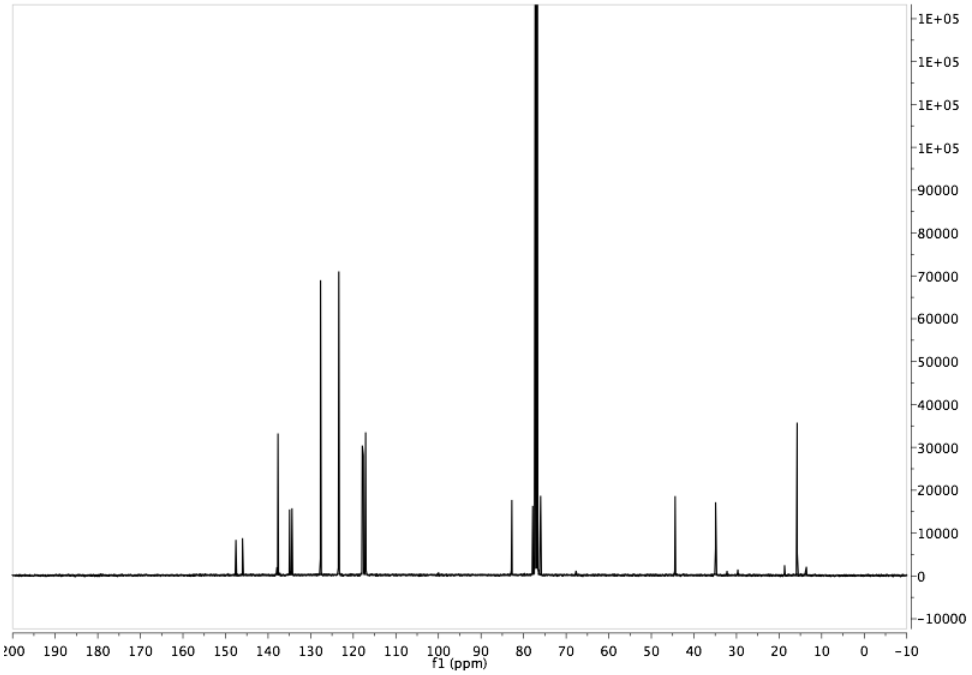
1E+05
1E+05
1E+05
1E+05
90000
80000
70000
60000
50000
40000
30000
20000
10000
0
−10000
200 190 180 170 160 150 140 130 120 110 100 90 80 70 60 50 40 30 20 10 0 −10
f1 (ppm)

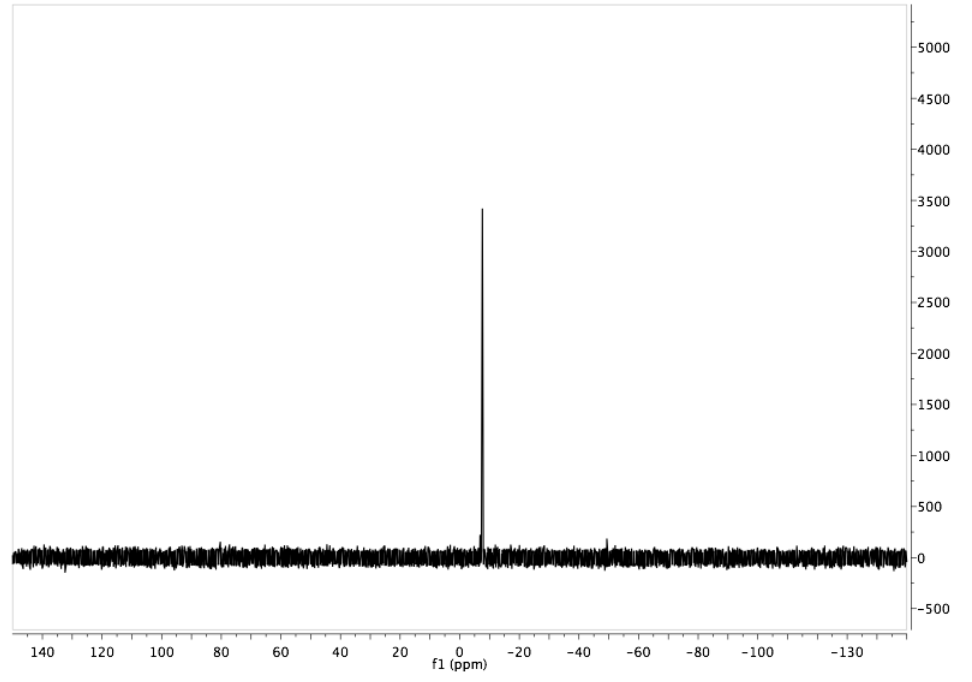
5000
4500
4000
3500
3000
2500
2000
1500
1000
500
0
−500
140 120 100 80 60 40 20 0 −20 −40 −60 −80 −100 −130
f1 (ppm)

(1*R*,3*R*,4*S*,7*R*,9*R*,*Z*)-4-methyl-3-(4-nitrophenyl)-9-vinyl-2,10,11-trioxa-1 phosphabicyclo[5.3.1]undec-5-ene 1-oxide (*cis,syn*-2.7.4):

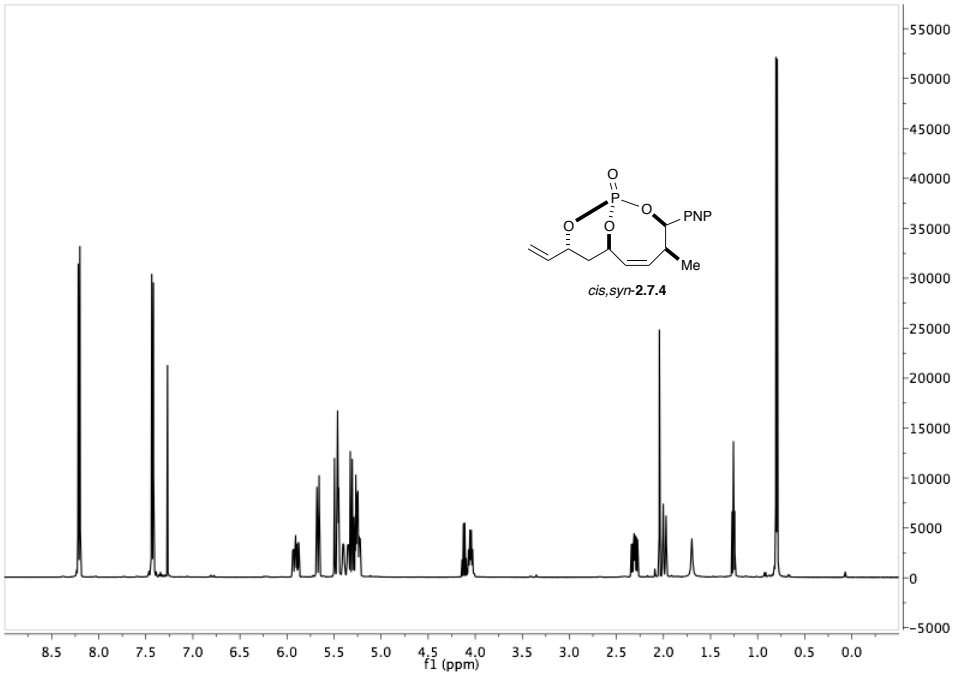

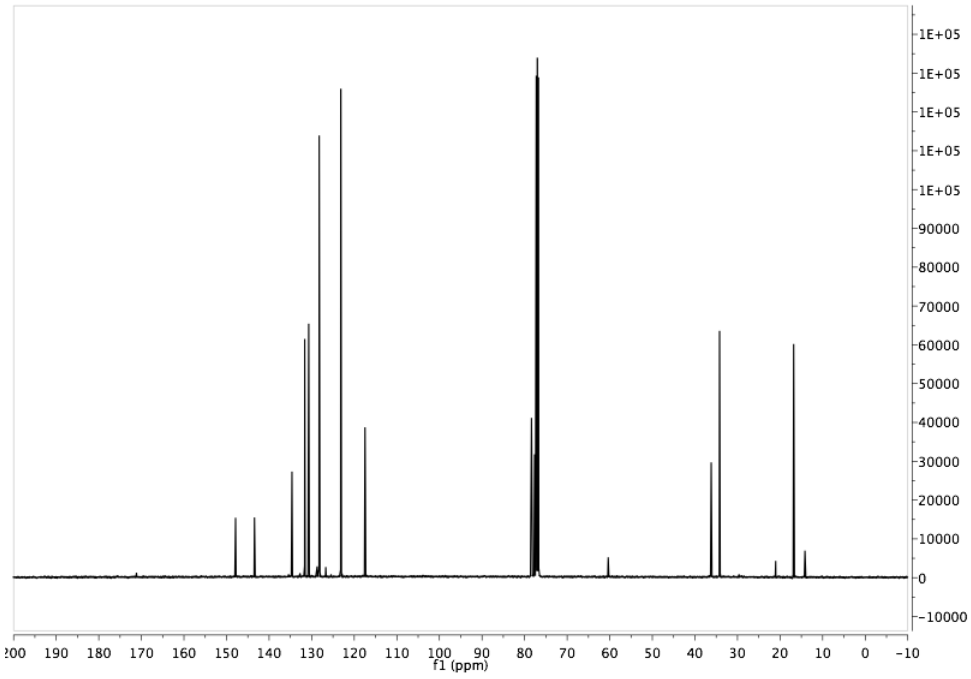

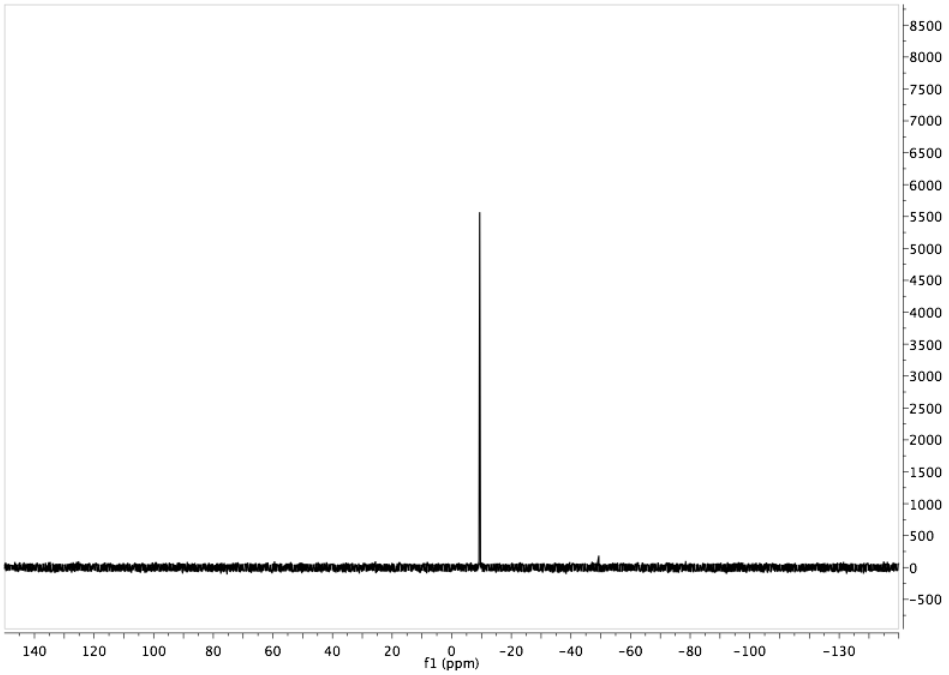

(4*S*,6*S*)-2-(((1*R*,2*S*)-2-methyl-1-(4-nitrophenyl)but-3-en-1-yl)oxy)-4,6-divinyl-1,3,2-dioxaphosphinane 2-oxide (2.7.3):

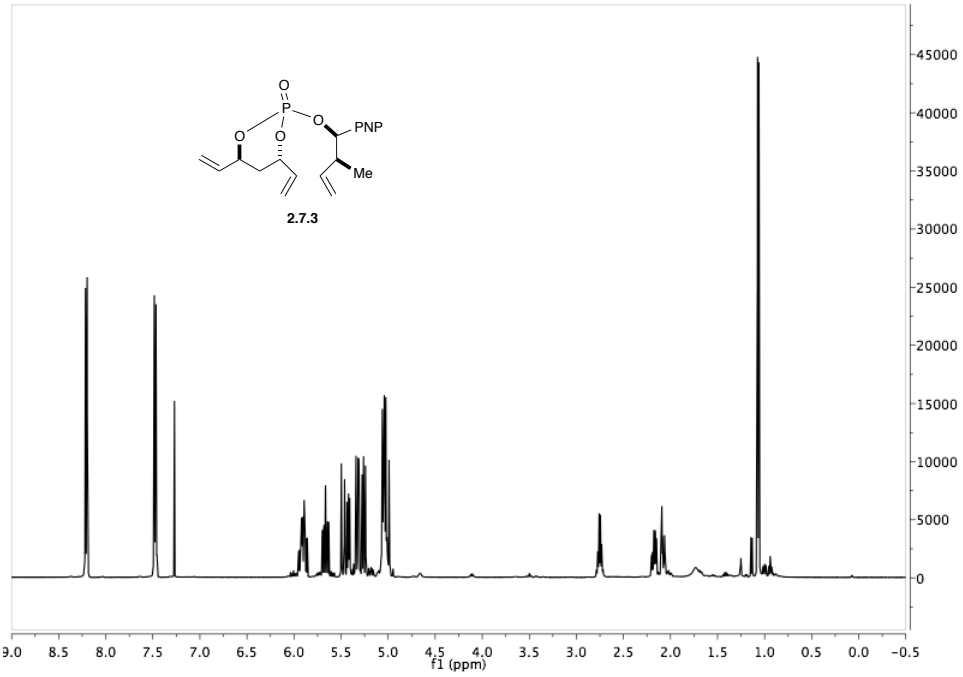

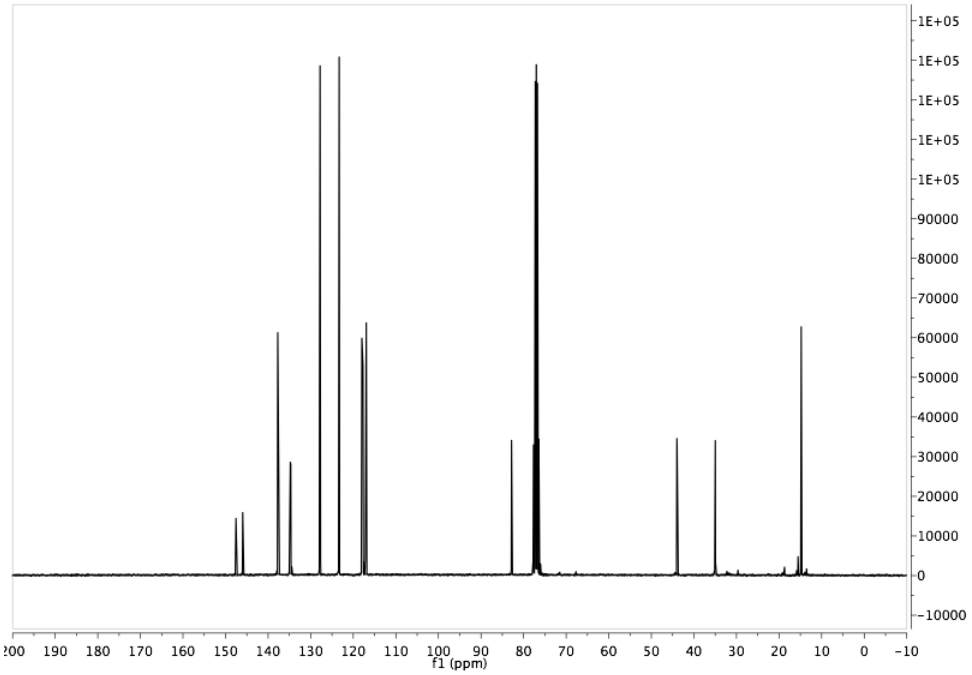
1E+05
1E+05
1E+05
1E+05
1E+05
90000
80000
70000
60000
50000
40000
30000
20000
10000
0
−10000
200 190 180 170 160 150 140 130 120 110 100 90 80 70 60 50 40 30 20 10 0 −10
f1 (ppm)

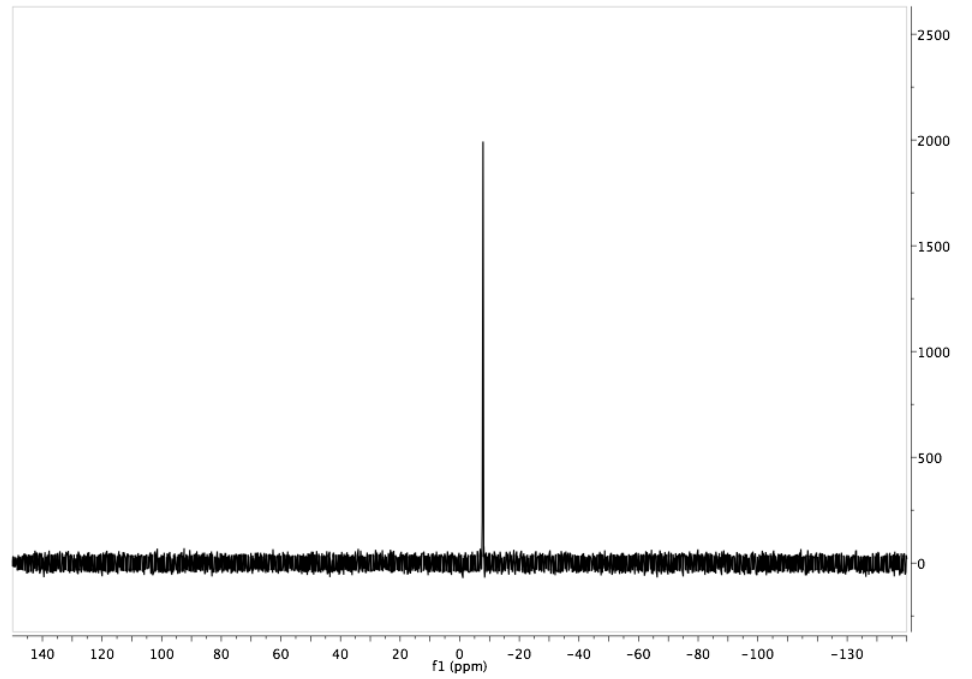
2500
2000
1500
1000
500
0
140 120 100 80 60 40 20 0 −20 −40 −60 −80 −100 −130
f1 (ppm)

(4*S*,6*S*)-2-(((1*R*,2*R*)-2-methyl-1-(4-nitrophenyl)but-3-en-1-yl)oxy)-4,6-divinyl-1,3,2-dioxaphosphinane 2-oxide (2.8.3):

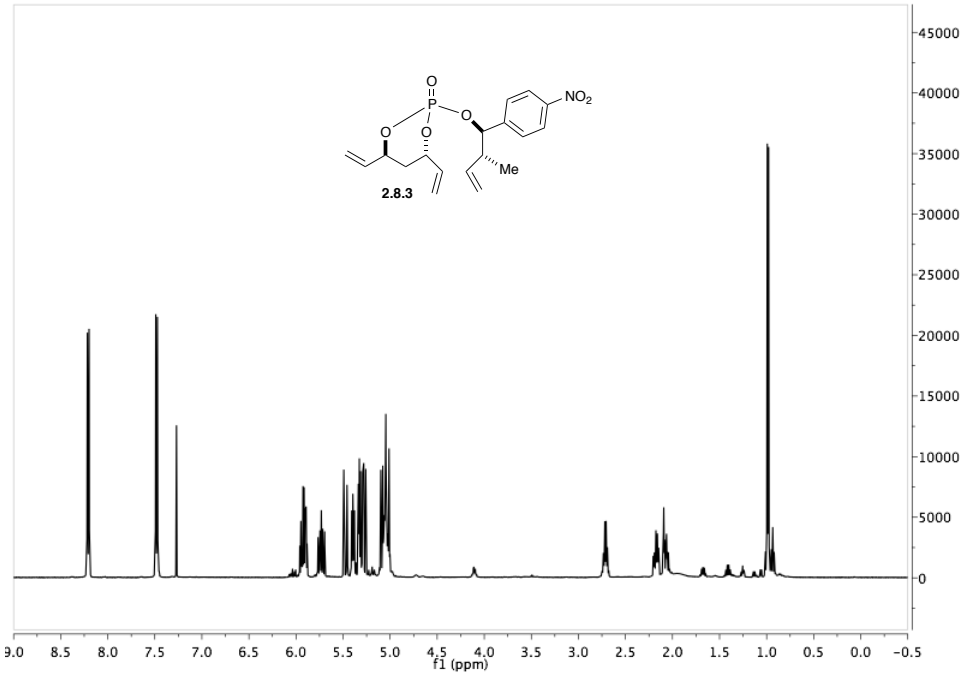

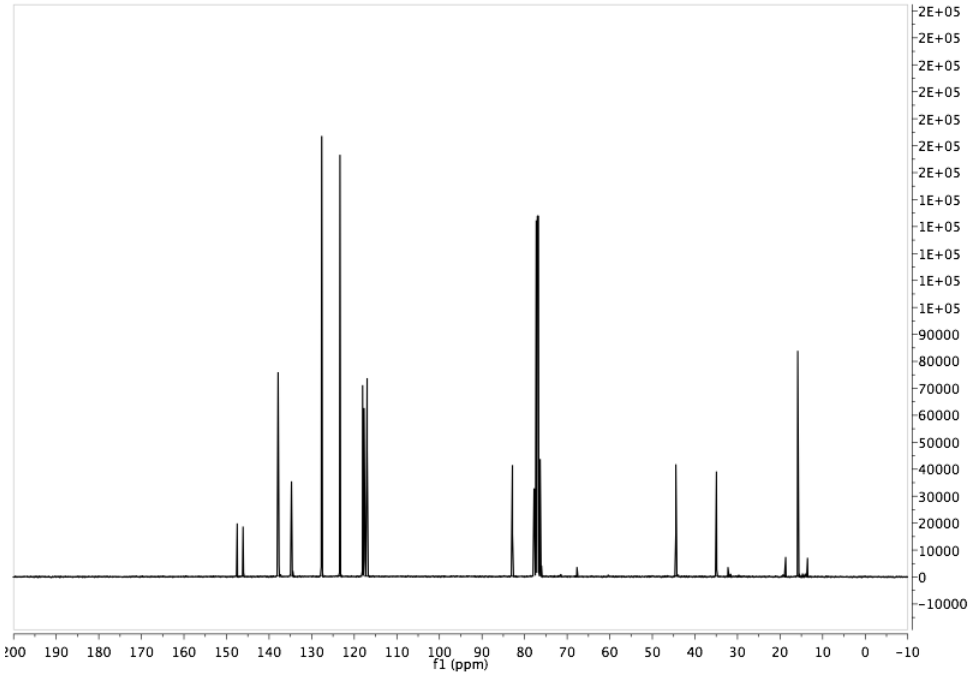

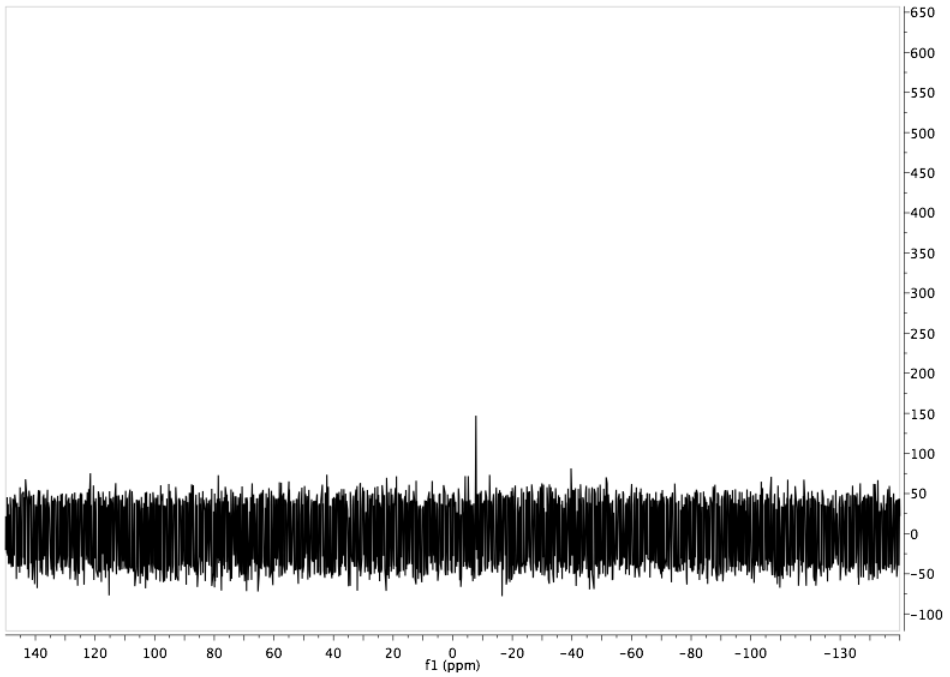

(1*S*,3*R*,4*R*,7*S*,9*S*,*Z*)-4-methyl-3-(4-nitrophenyl)-9-vinyl-2,10,11-trioxa-1-phosphabicyclo[5.3.1]undec-5-ene 1-oxide (*trans,anti*-2.8.5):

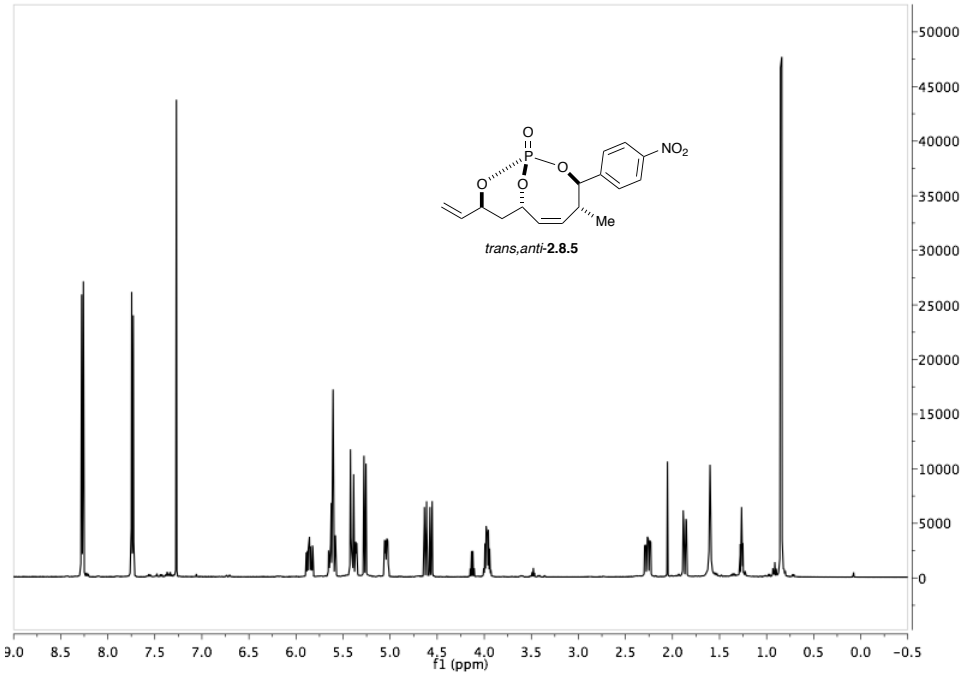

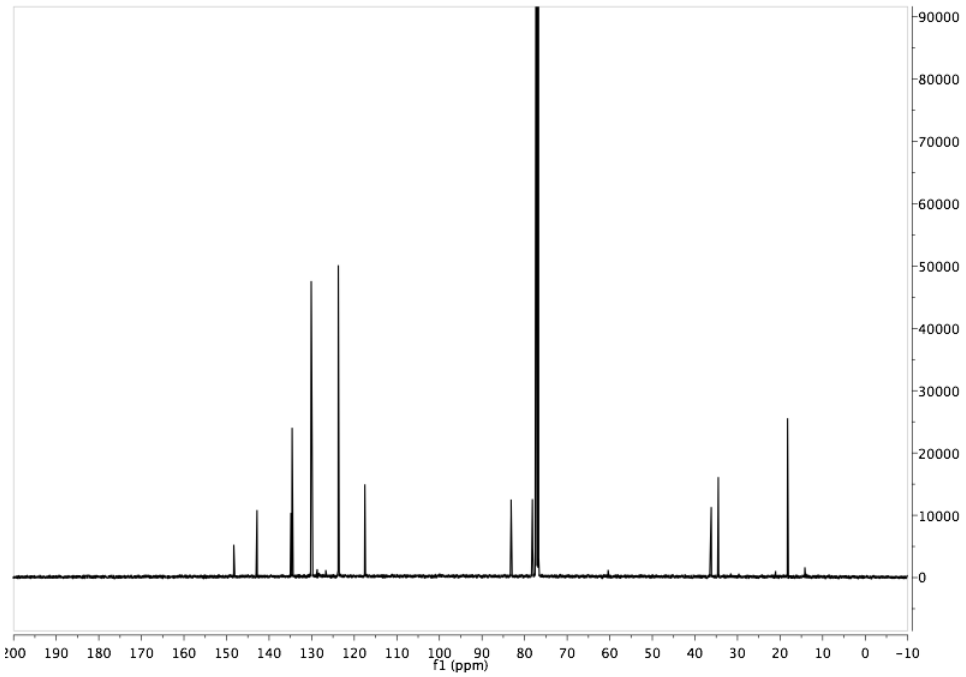
90000
80000
70000
60000
50000
40000
30000
20000
10000
0
200 190 180 170 160 150 140 130 120 110 100 90 80 70 60 50 40 30 20 10 0 −10
f1 (ppm)

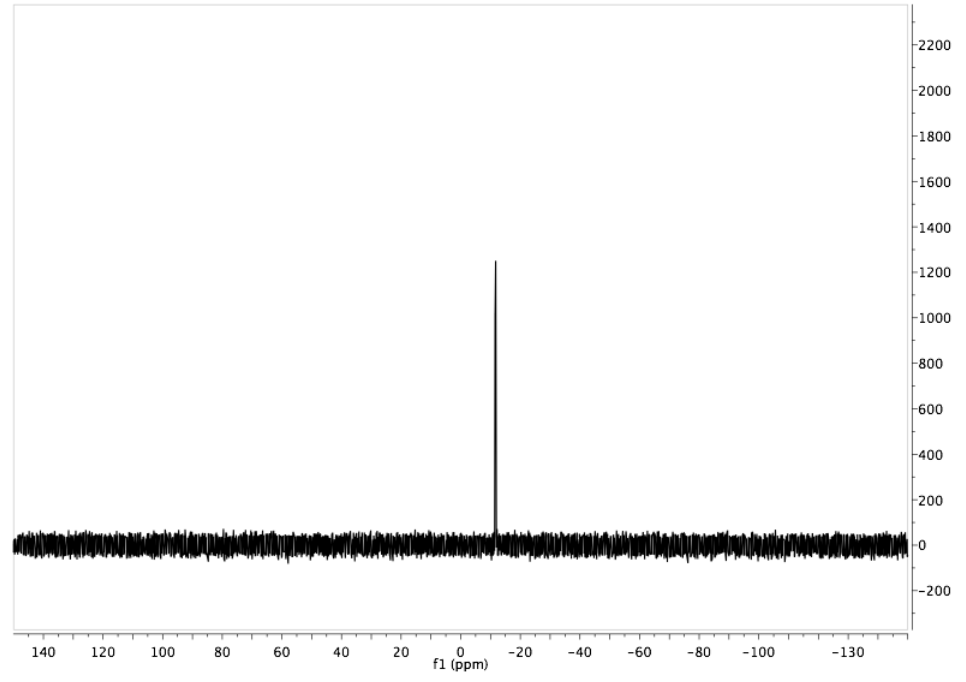
2200
2000
1800
1600
1400
1200
1000
800
600
400
200
0
−200
140 120 100 80 60 40 20 0 −20 −40 −60 −80 −100 −130
f1 (ppm)

(4*S*,6*S*)-2-((2-methylbut-3-en-1-yl)oxy)-4,6-divinyl-1,3,2-dioxaphosphinane 2-oxide (2.9.2):

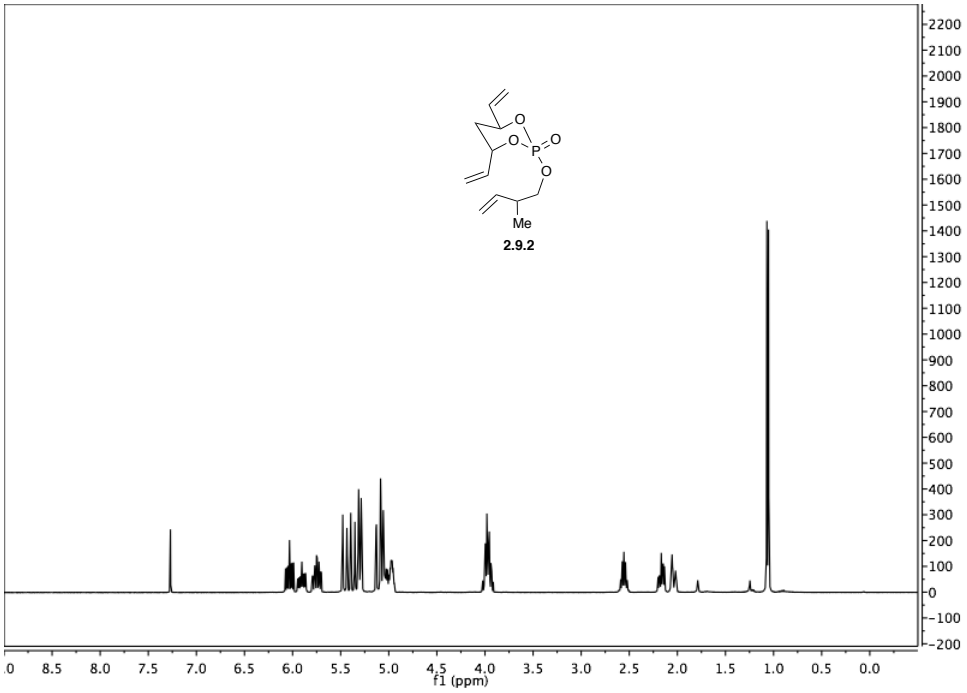

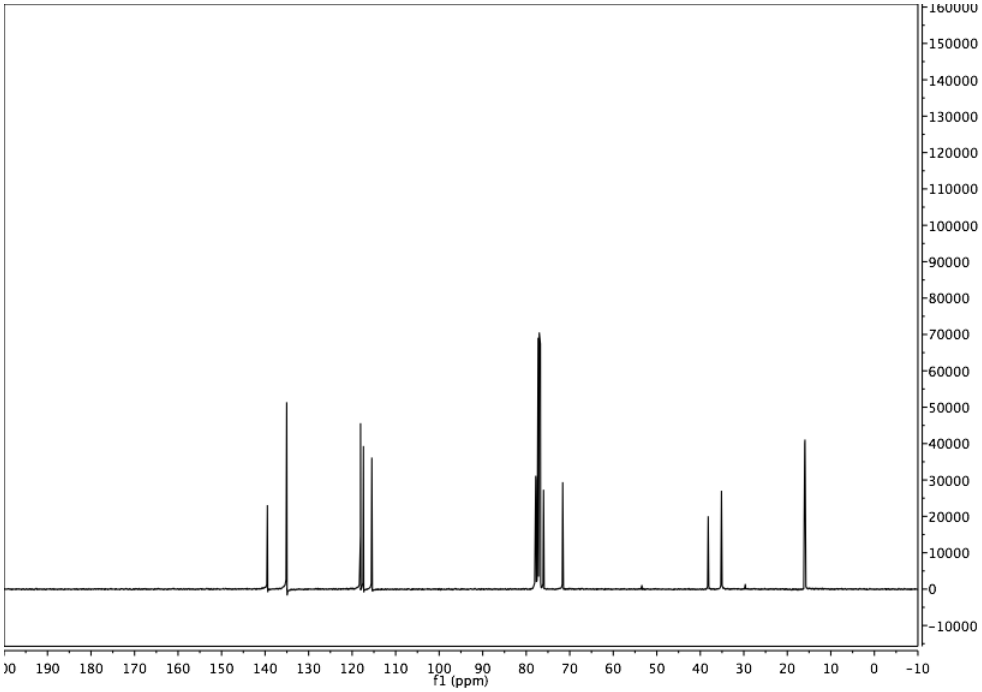

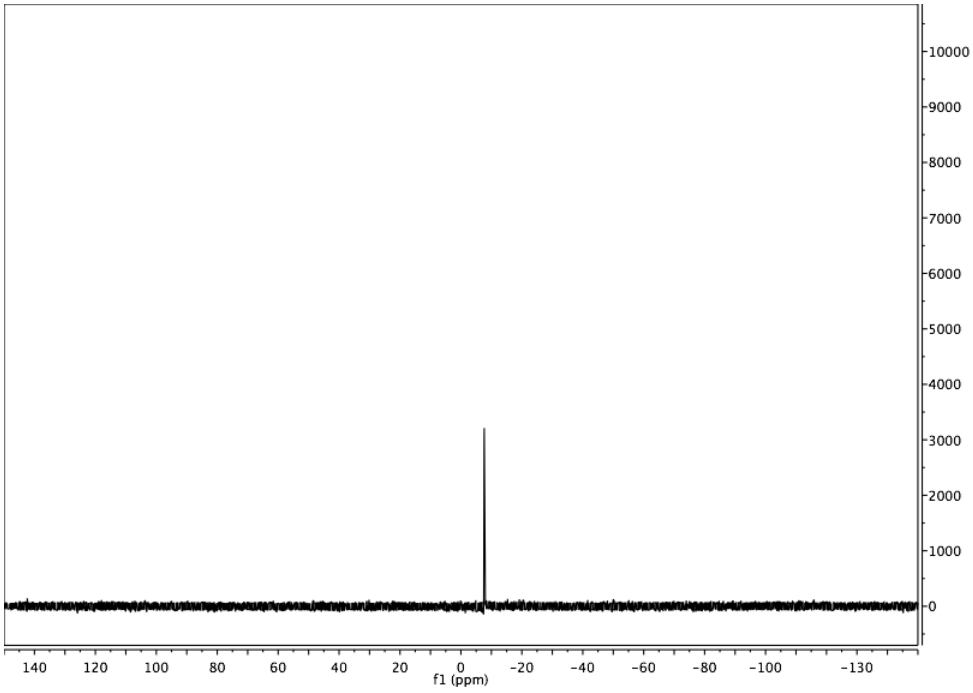

(4*S*,6*S*)-2-(((*S*)-2-methylbut-3-en-1-yl)oxy)-4,6-divinyl-1,3,2-dioxaphosphinane 2-oxide (2.9.3):

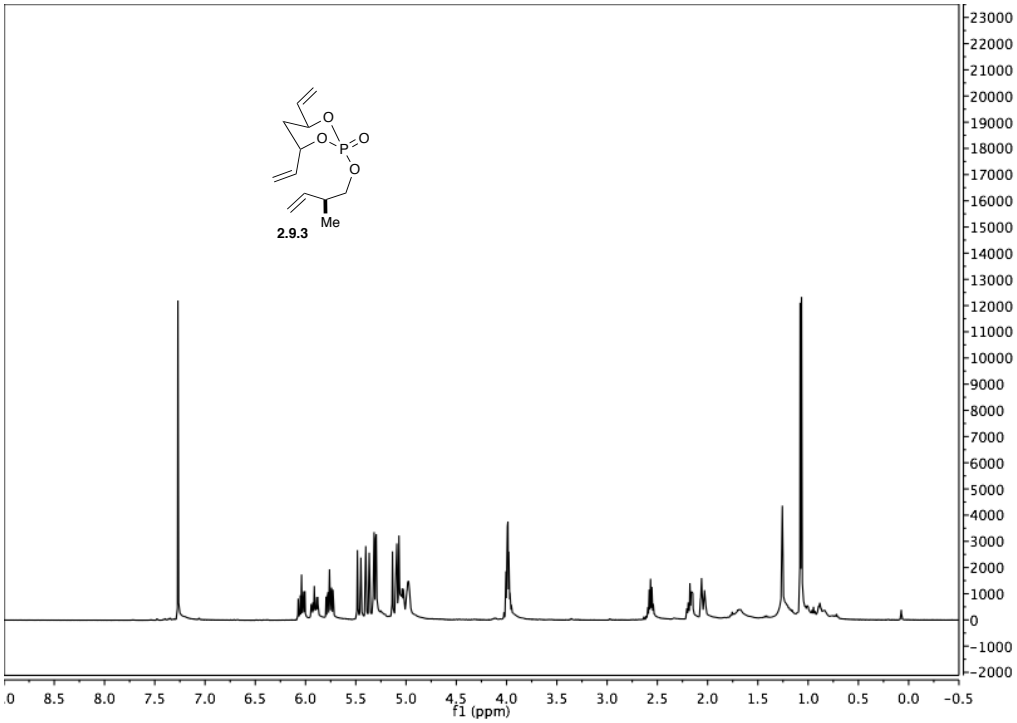

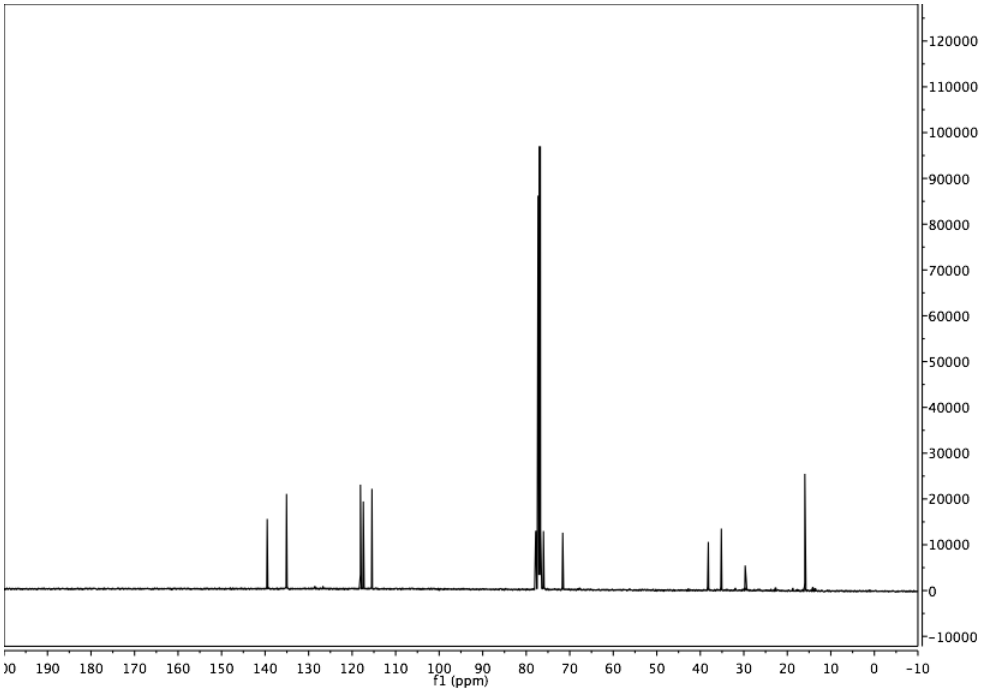
120000
110000
100000
90000
80000
70000
60000
50000
40000
30000
20000
10000
0
−10000
190 180 170 160 150 140 130 120 110 100 90 80 70 60 50 40 30 20 10 0 −10
f1 (ppm)

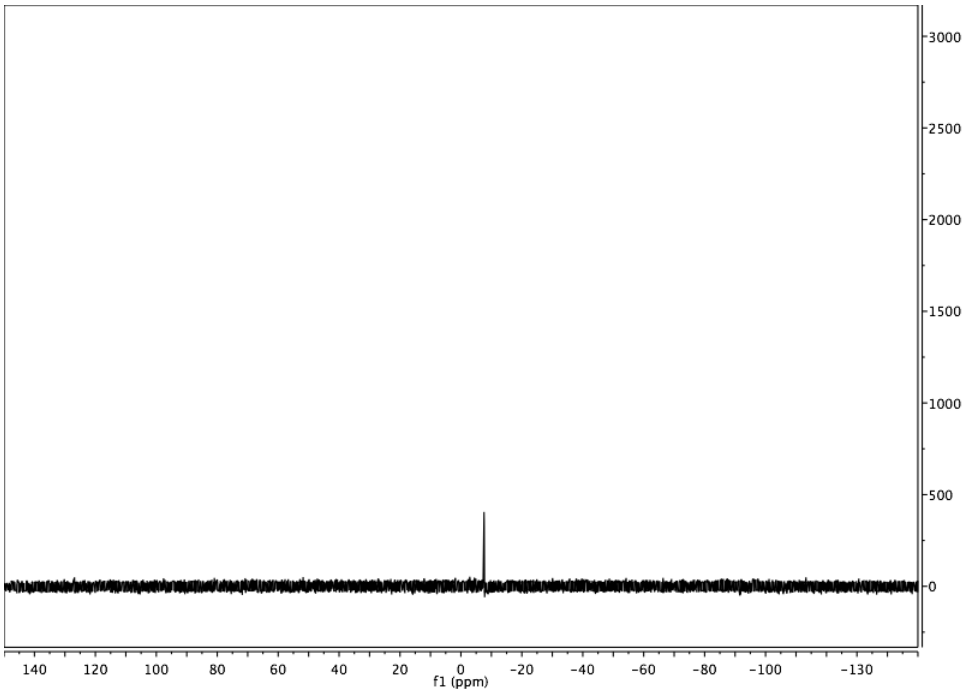
3000
2500
2000
1500
1000
500
0
140 120 100 80 60 40 20 0 −20 −40 −60 −80 −100 −130
f1 (ppm)

(1*S*,4*R*,7*S*,9*S*,*Z*)-4-methyl-9-vinyl-2,10,11-trioxa-1-phosphabicyclo[5.3.1] undec-5-ene 1-oxide (2.9.4):

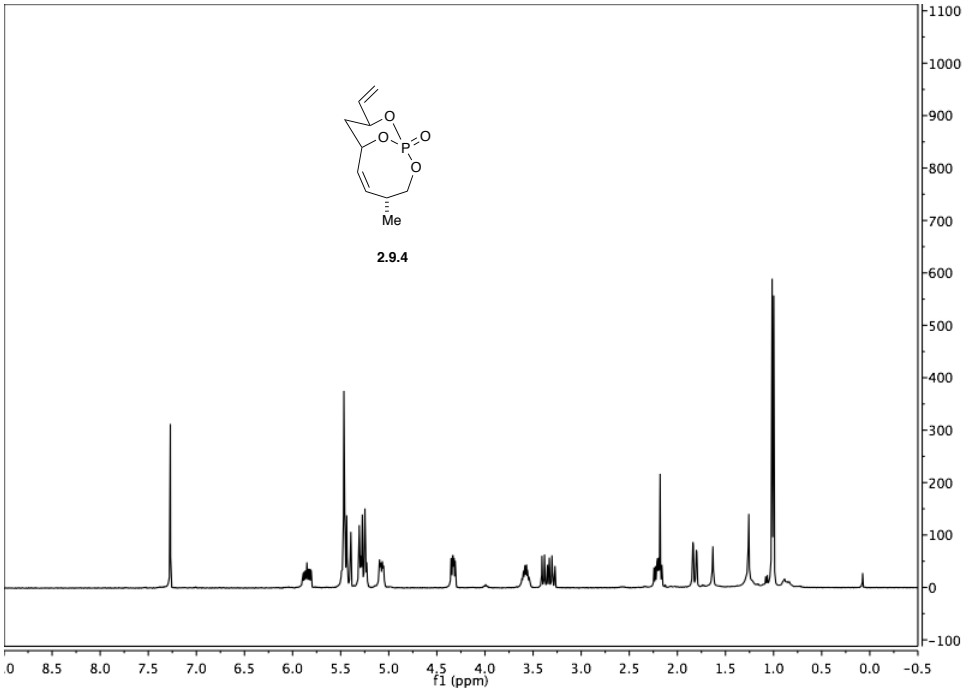

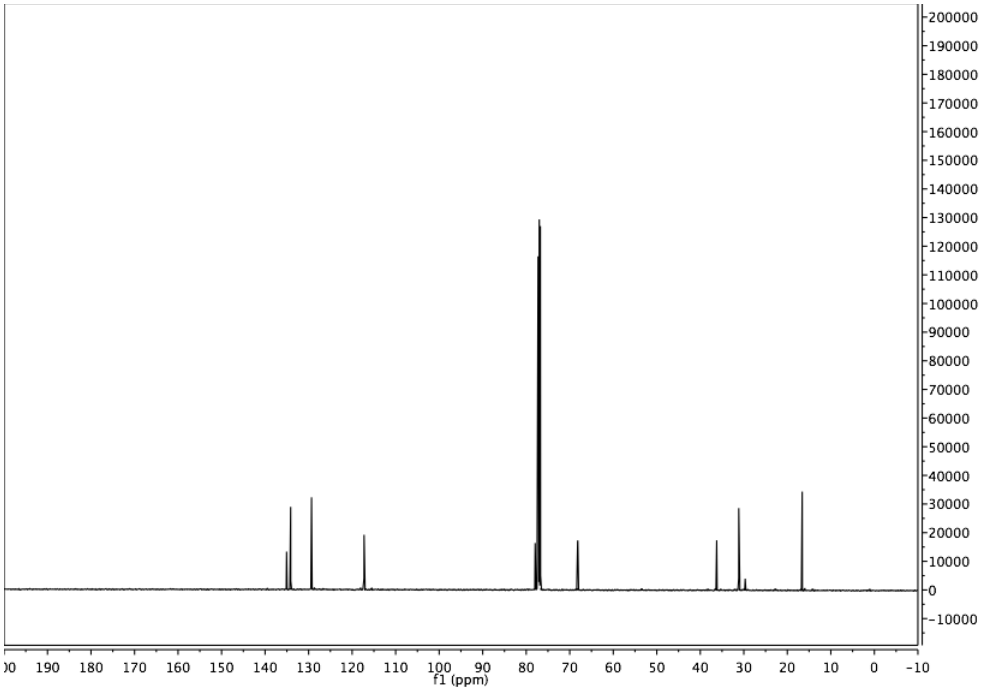

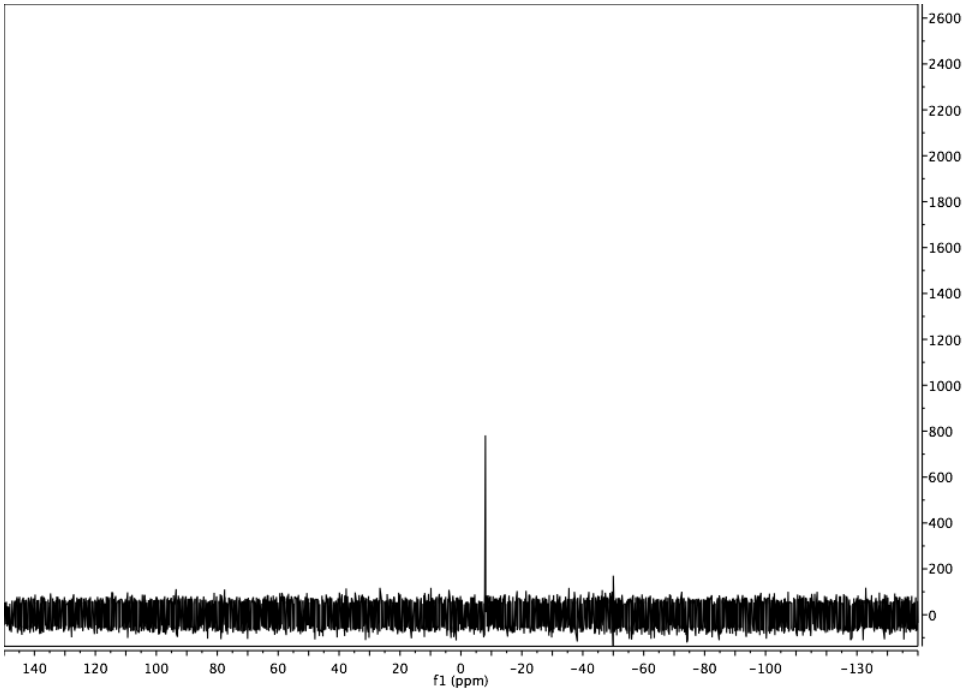

(4*R*,6*R*)-4,6-diallyl-2-(((*R*)-1-(benzyloxy)but-3-en-2-yl)oxy)-1,3,2-dioxaphosphinane 2-oxide (2.10.3):

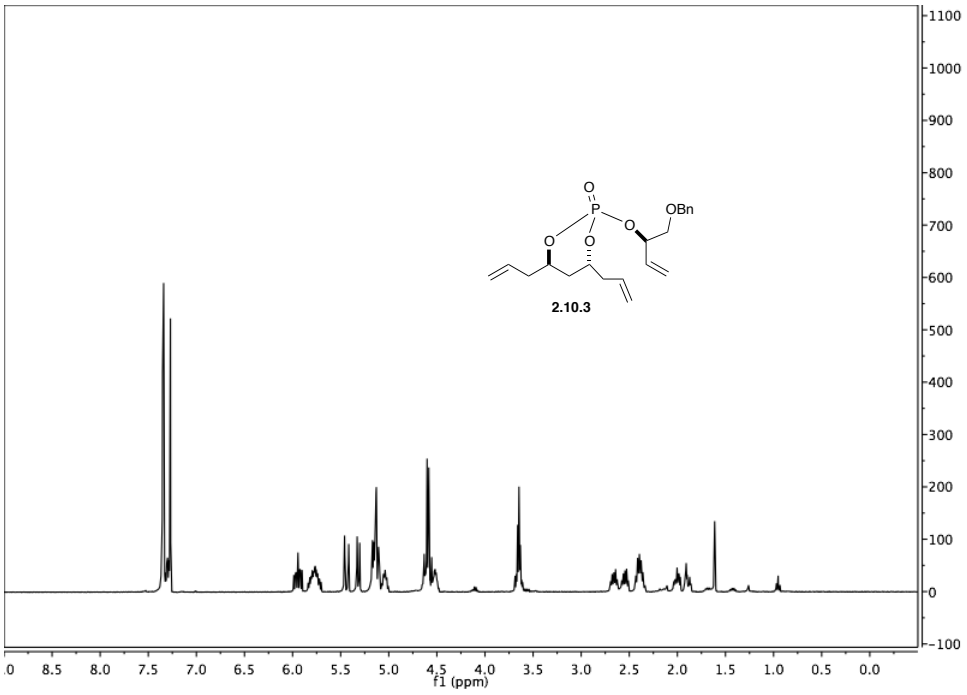

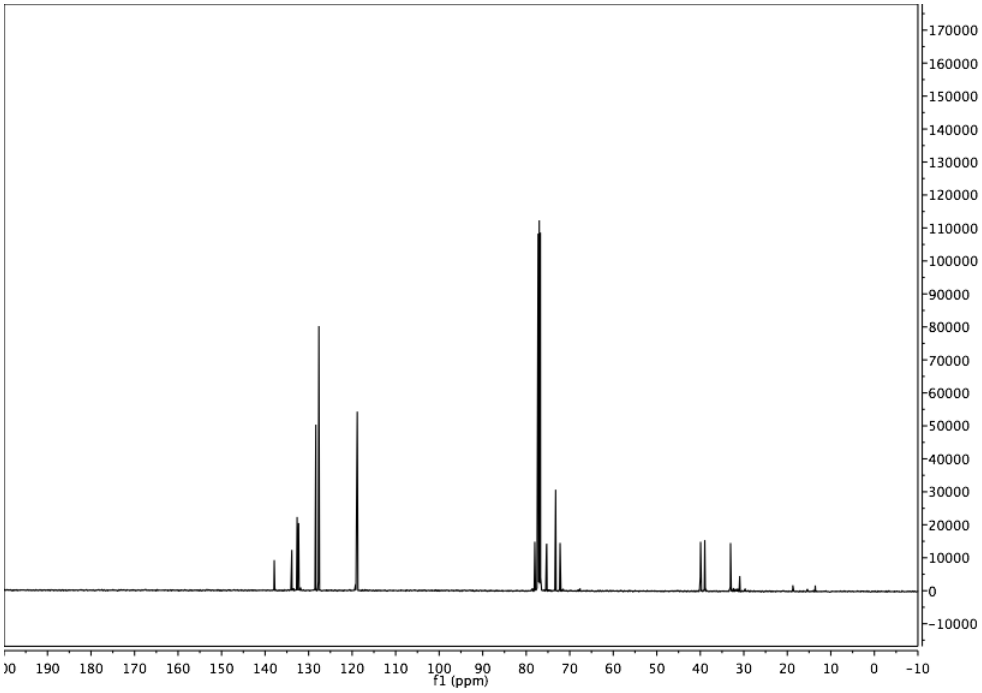
170000
160000
150000
140000
130000
120000
110000
100000
90000
80000
70000
60000
50000
40000
30000
20000
10000
0
−10000
190 180 170 160 150 140 130 120 110 100 90 80 70 60 50 40 30 20 10 0 −10
f1 (ppm)

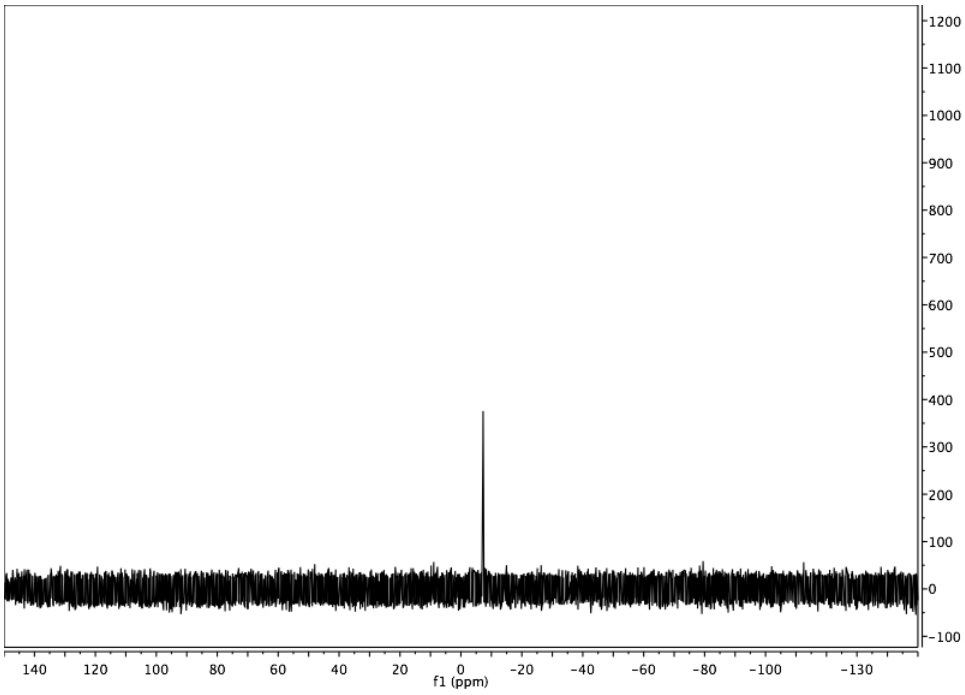
1200
1100
1000
900
800
700
600
500
400
300
200
100
0
−100
140 120 100 80 60 40 20 0 −20 −40 −60 −80 −100 −130
f1 (ppm)

(4*R*,6*R*)-2-(((*R*)-1-(benzyloxy)but-3-en-2-yl)oxy)-4,6-bis(2-methylallyl)-1,3,2-dioxaphosphinane 2-oxide (2.11.3):

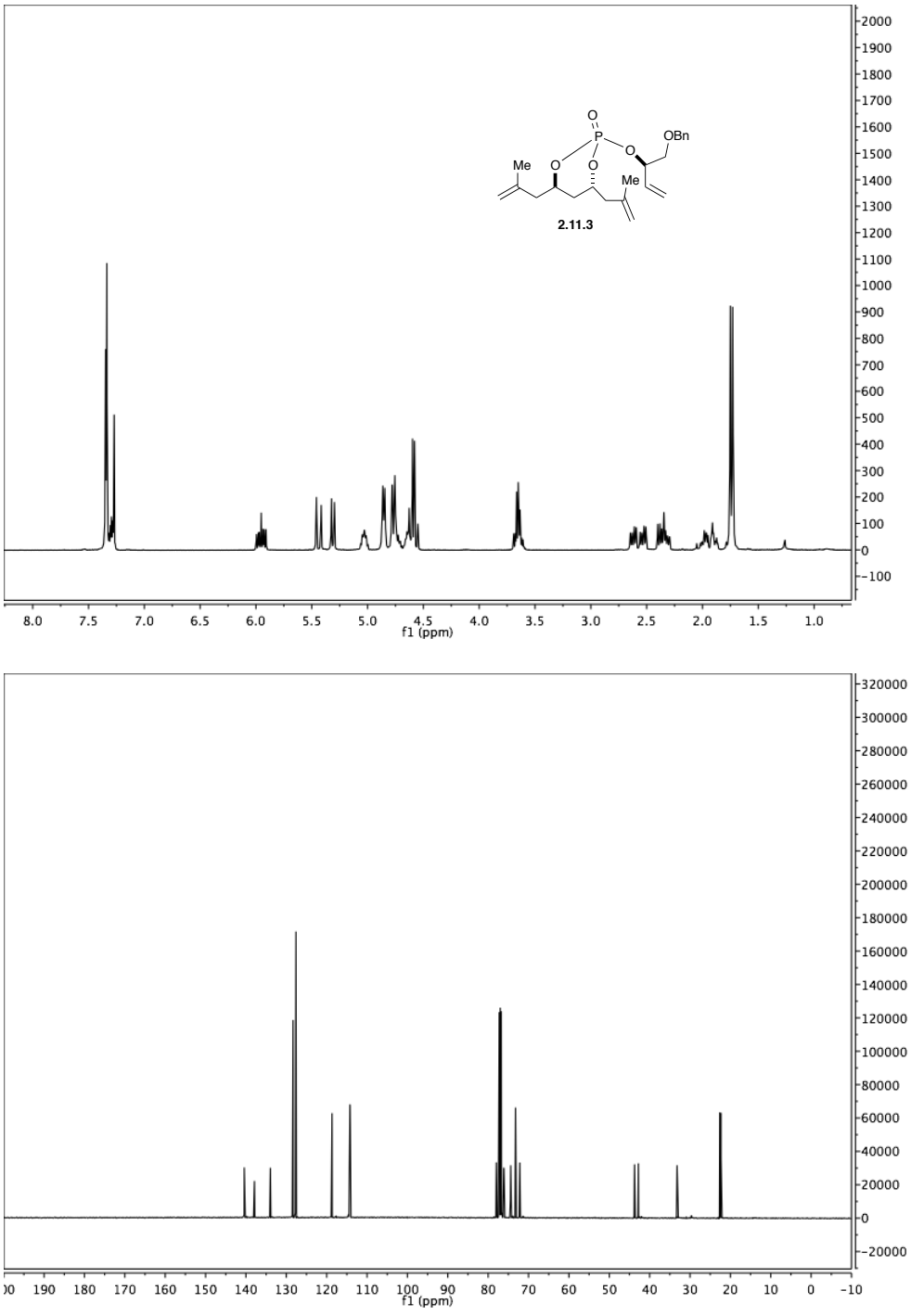

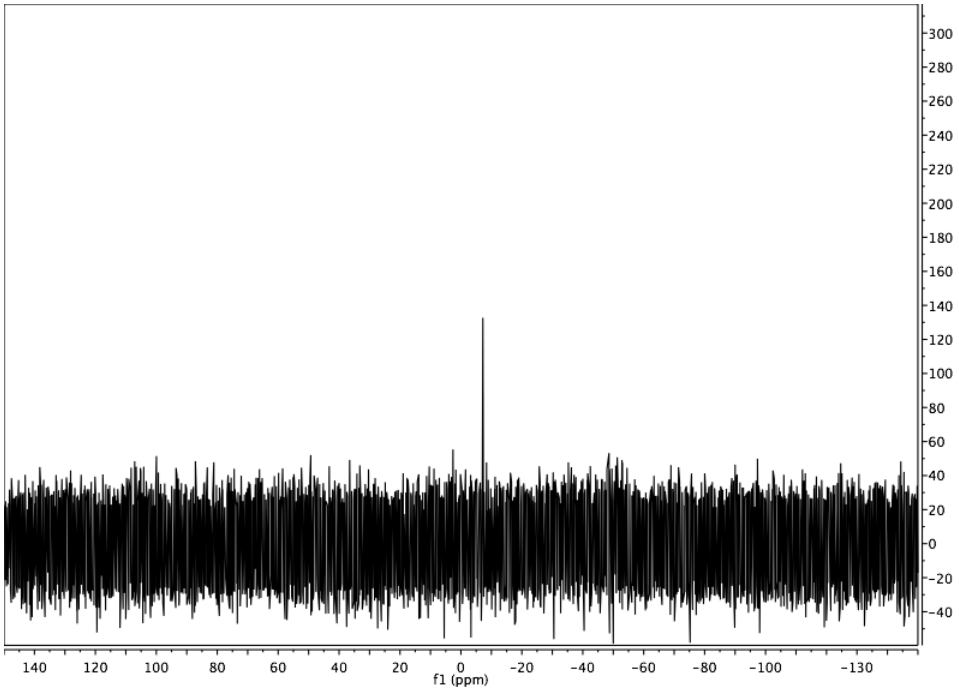

(1*S*,3*R*,7*R*,9*R*,*Z*)-9-allyl-3-((benzyloxy)methyl)-2,10,11-trioxa-1-phosphabicyclo[5.3.1]undec-4-ene 1-oxide (*trans*-2.10.5):

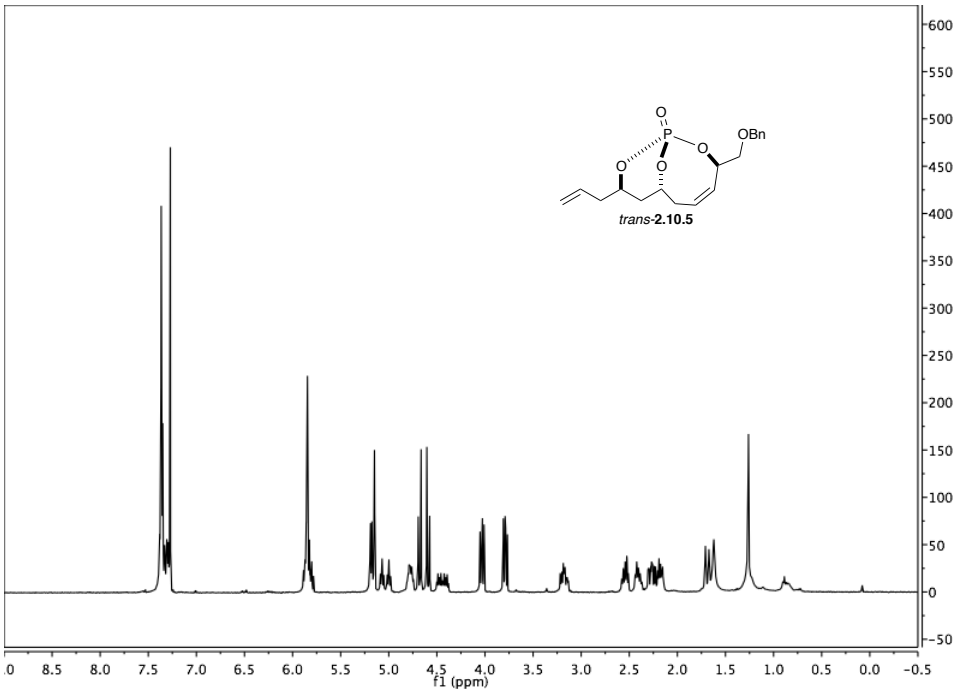

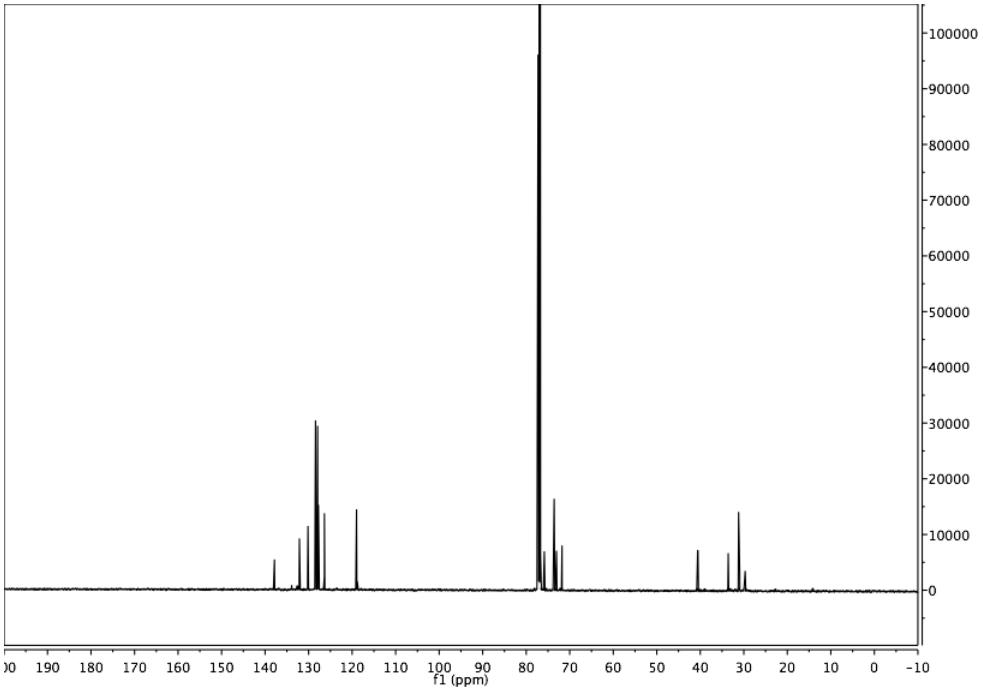
100000
90000
80000
70000
60000
50000
40000
30000
20000
10000
0
190 180 170 160 150 140 130 120 110 100 90 80 70 60 50 40 30 20 10 0 -10
f1 (ppm)

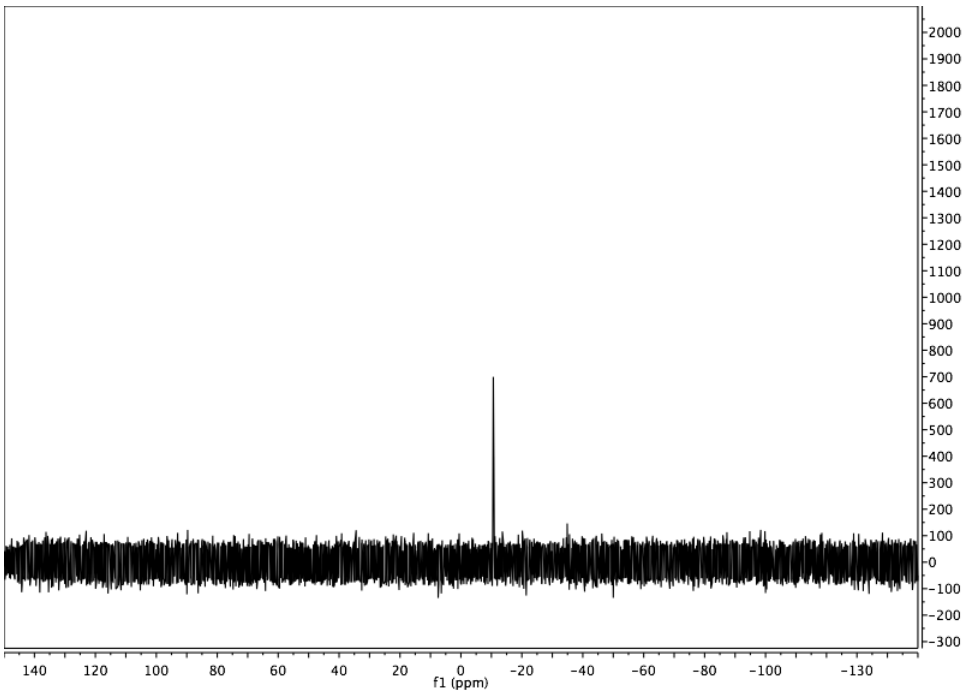
2000
1900
1800
1700
1600
1500
1400
1300
1200
1100
1000
900
800
700
600
500
400
300
200
100
0
-100
-200
-300
140 120 100 80 60 40 20 0 -20 -40 -60 -80 -100 -130
f1 (ppm)

(1*S*,3*R*,7*R*,9*R*,*Z*)-3-((benzyloxy)methyl)-5-methyl-9-(2-methylallyl)-2,10,11-trioxa-1-phosphabicyclo[5.3.1]undec-4-ene 1-oxide (*trans*-2.11.5):

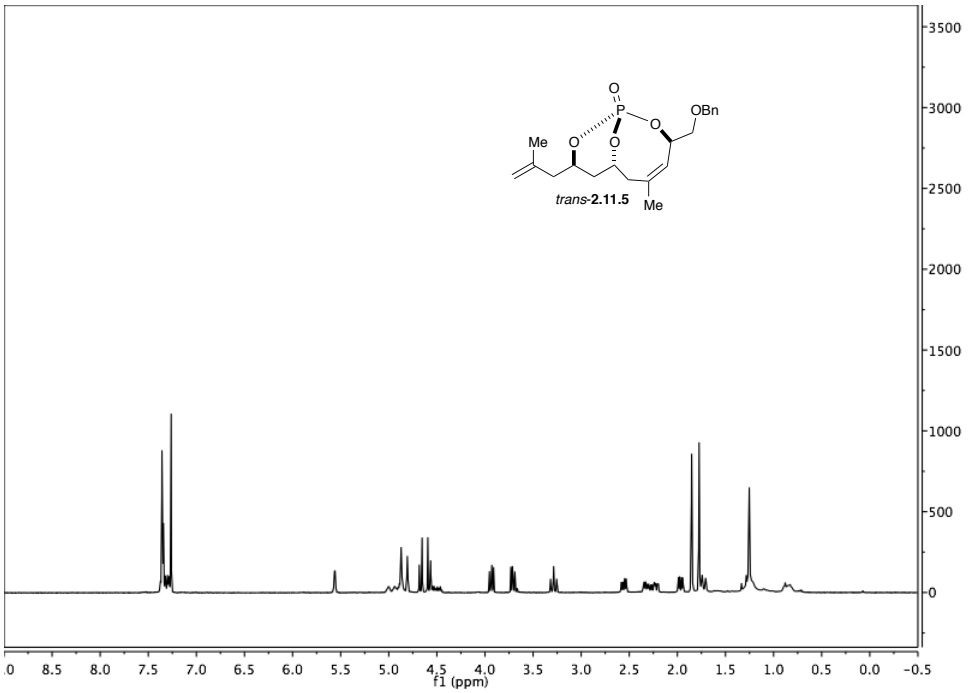

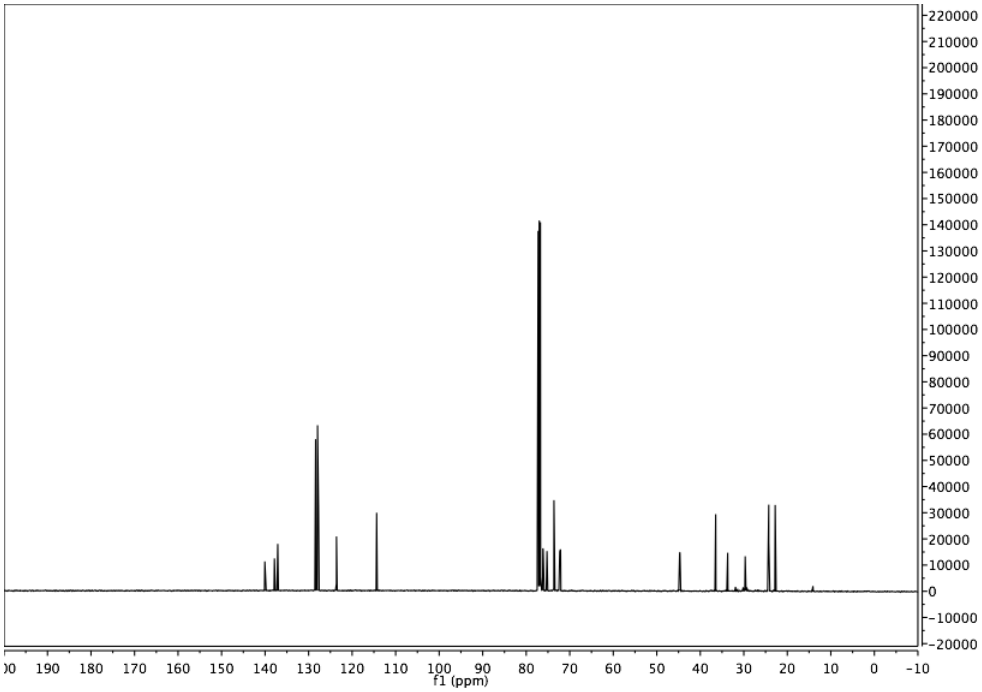

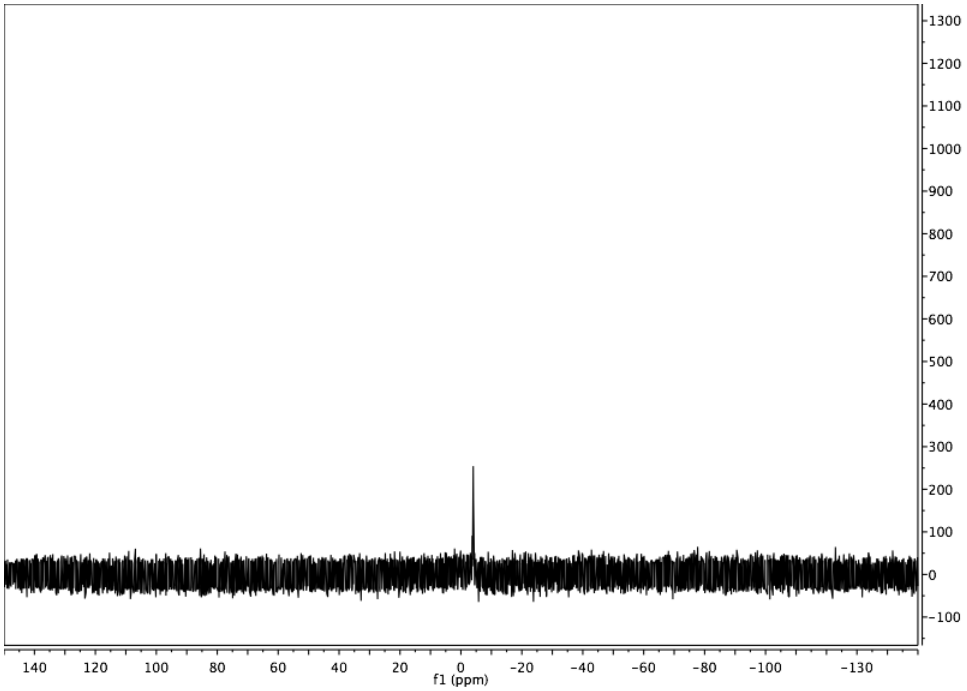

(4*S*,6*S*)-4,6-diallyl-2-(((*R*)-1-(benzyloxy)but-3-en-2-yl)oxy)-1,3,2-dioxaphosphinane 2-oxide (2.10.4):

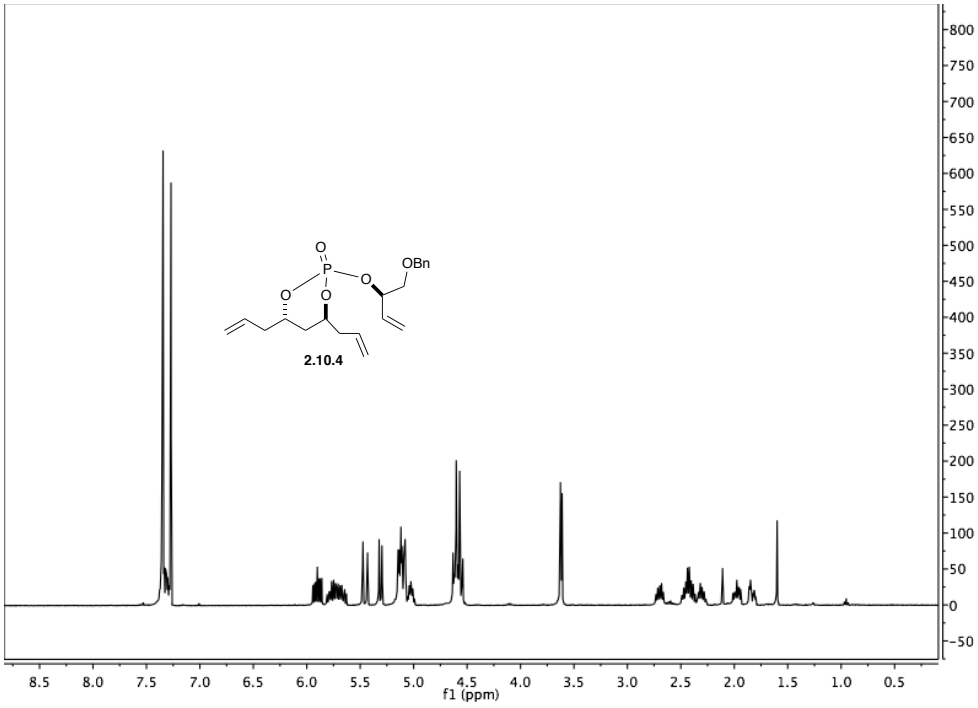

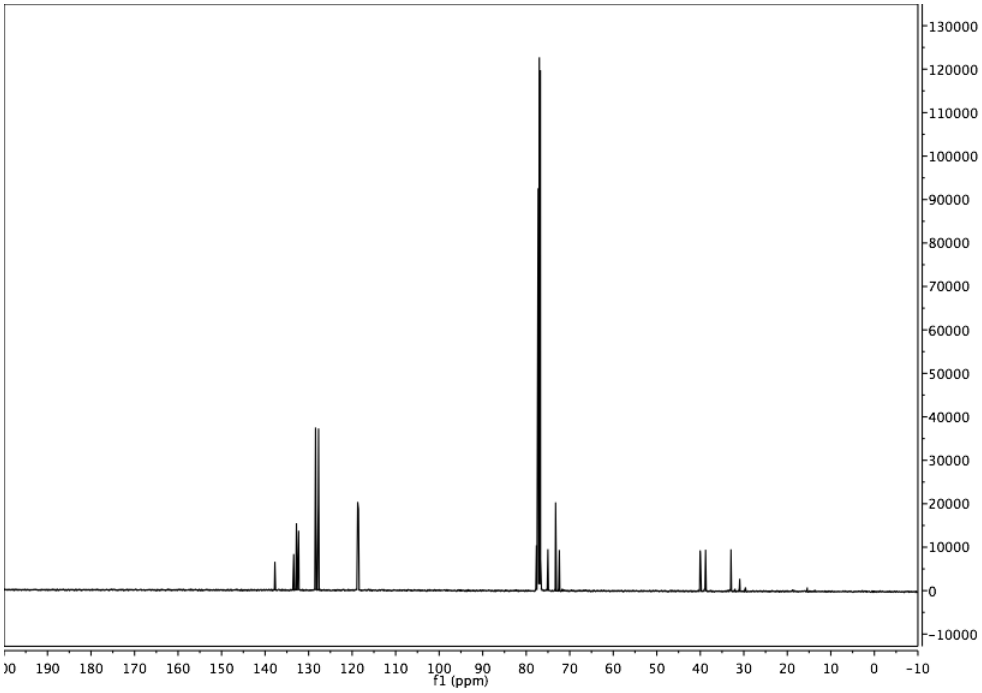
130000
120000
110000
100000
90000
80000
70000
60000
50000
40000
30000
20000
10000
0
−10000
190 180 170 160 150 140 130 120 110 100 90 80 70 60 50 40 30 20 10 0 −10
f1 (ppm)

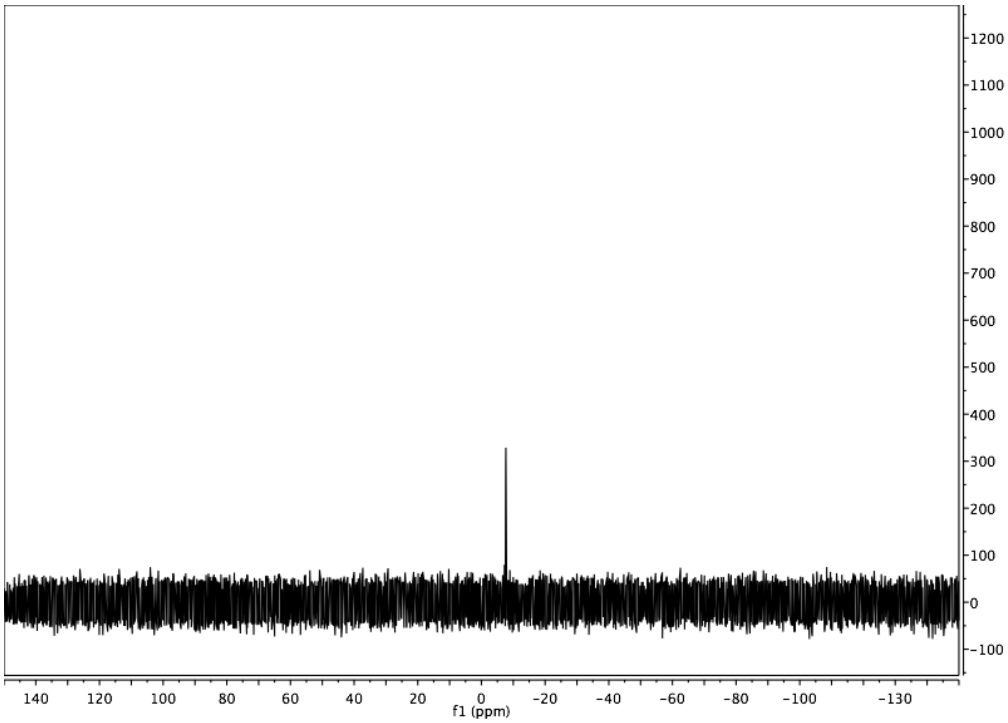
1200
1100
1000
900
800
700
600
500
400
300
200
100
0
−100
140 120 100 80 60 40 20 0 −20 −40 −60 −80 −100 −130
f1 (ppm)

(4*S*,6*S*)-2-(((*R*)-1-(benzyloxy)but-3-en-2-yl)oxy)-4,6-bis(2-methylallyl)-1,3,2-dioxaphosphinane 2-oxide (2.11.4):

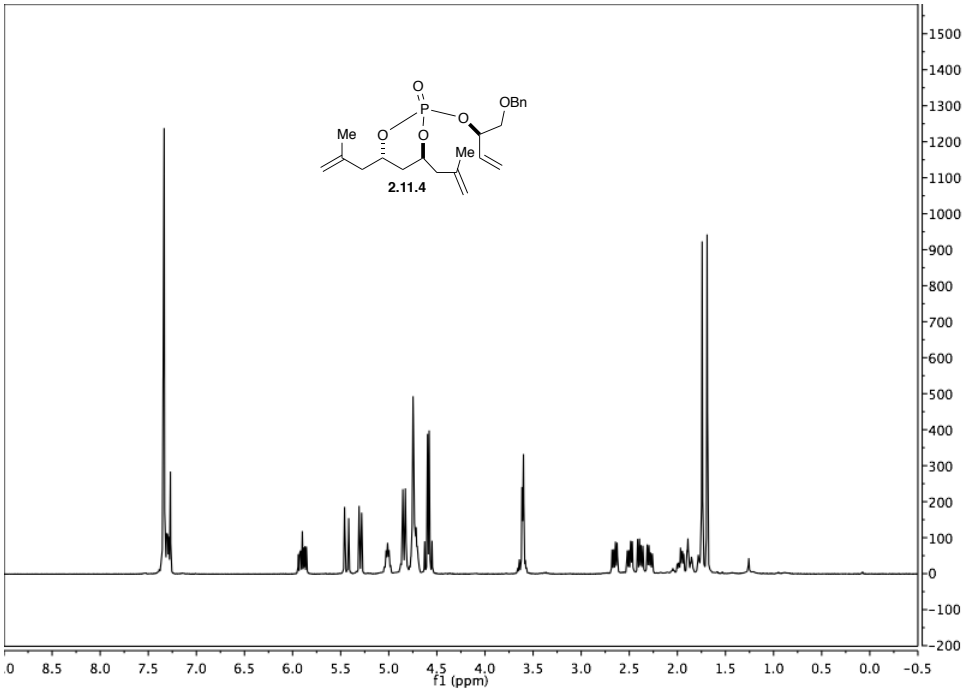

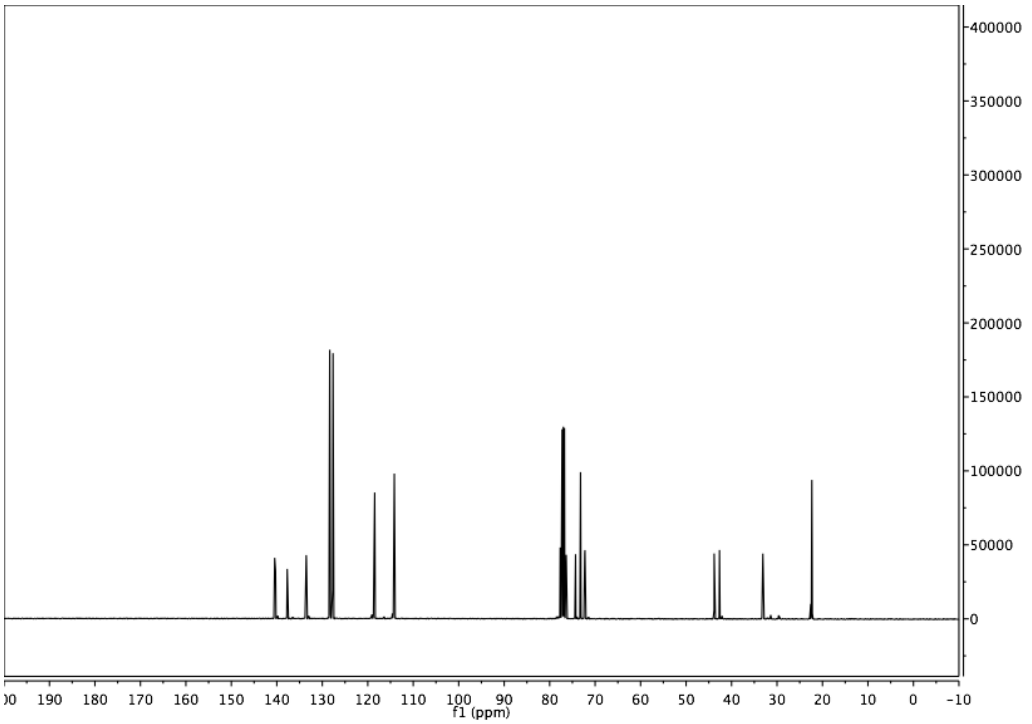

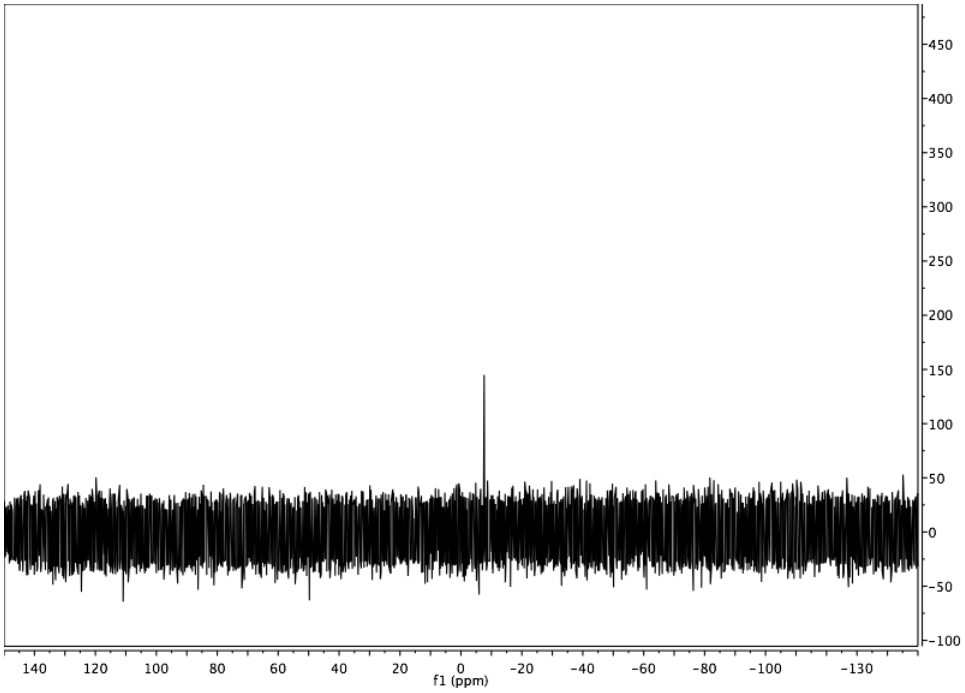

(1*R*,3*R*,7*S*,9*S*,*Z*)-9-allyl-3-((benzyloxy)methyl)-2,10,11-trioxa-1-phosphabicyclo[5.3.1]undec-4-ene 1-oxide (*cis*-2.10.6):

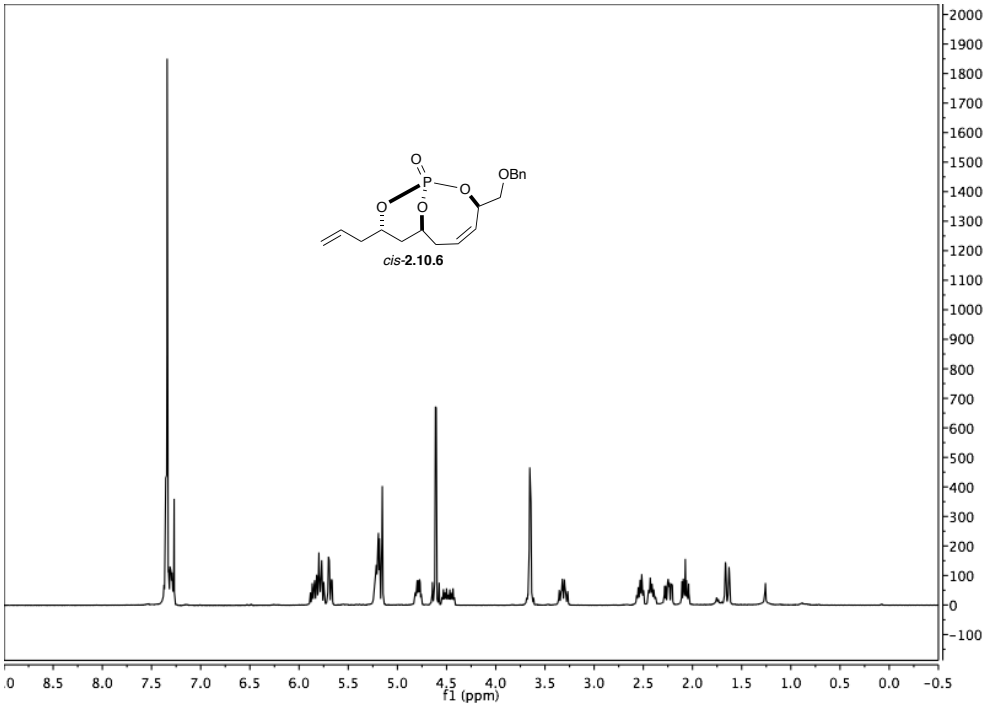

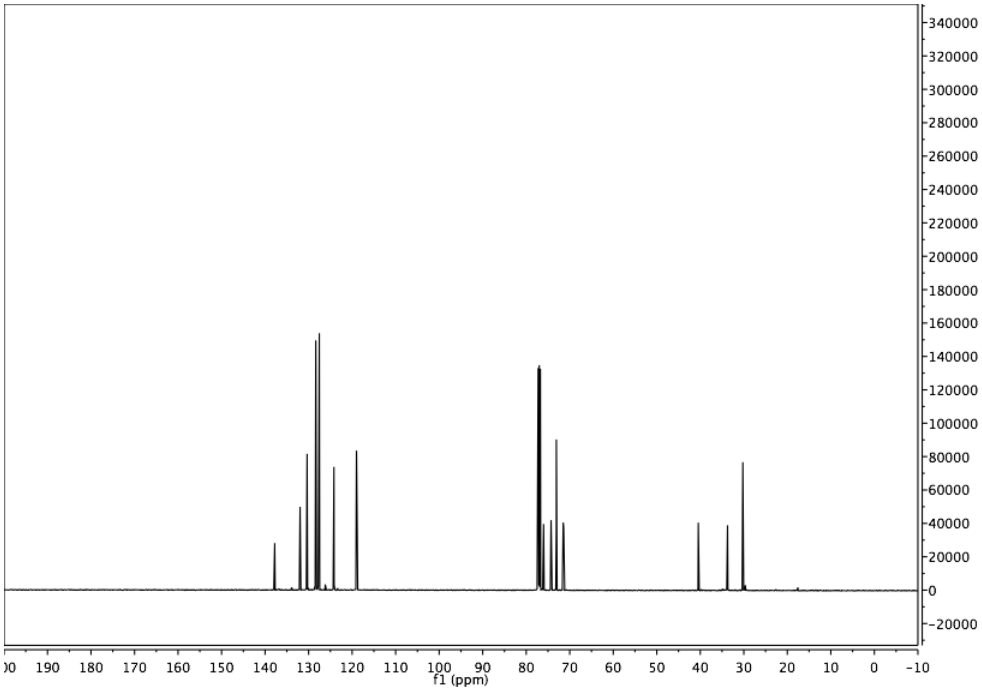
340000
320000
300000
280000
260000
240000
220000
200000
180000
160000
140000
120000
100000
80000
60000
40000
20000
0
-20000
190 180 170 160 150 140 130 120 110 100 90 80 70 60 50 40 30 20 10 0 -10
f1 (ppm)

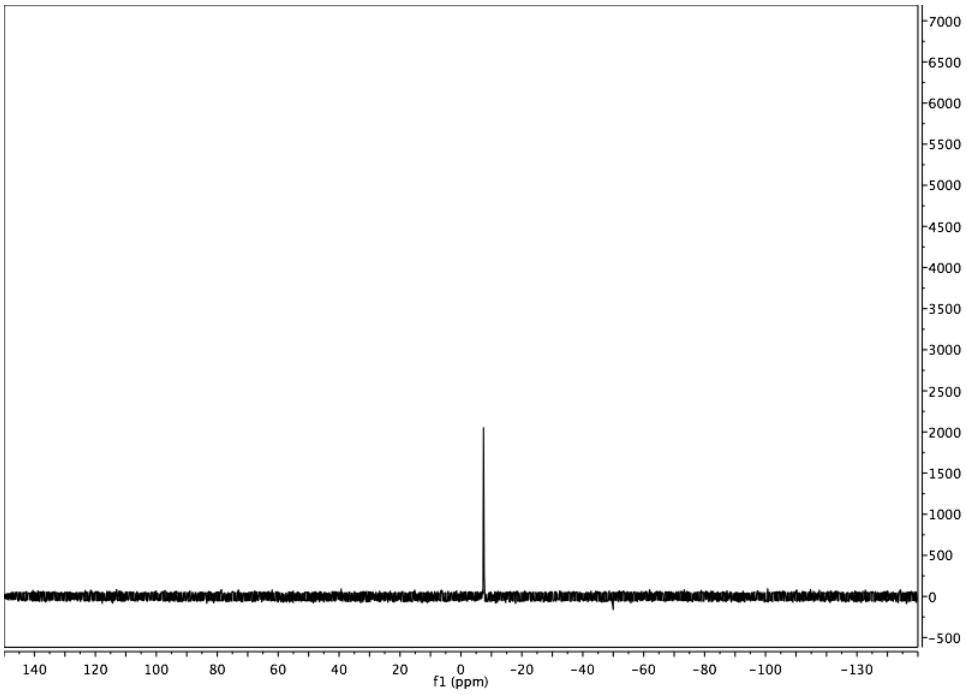
7000
6500
6000
5500
5000
4500
4000
3500
3000
2500
2000
1500
1000
500
0
-500
140 120 100 80 60 40 20 0 -20 -40 -60 -80 -100 -130
f1 (ppm)

(4*S*,6*S*)-2-(((*S*)-1-(benzyloxy)hex-5-en-2-yl)oxy)-4,6-divinyl-1,3,2-dioxaphosphinane 2-oxide (2.12.2)

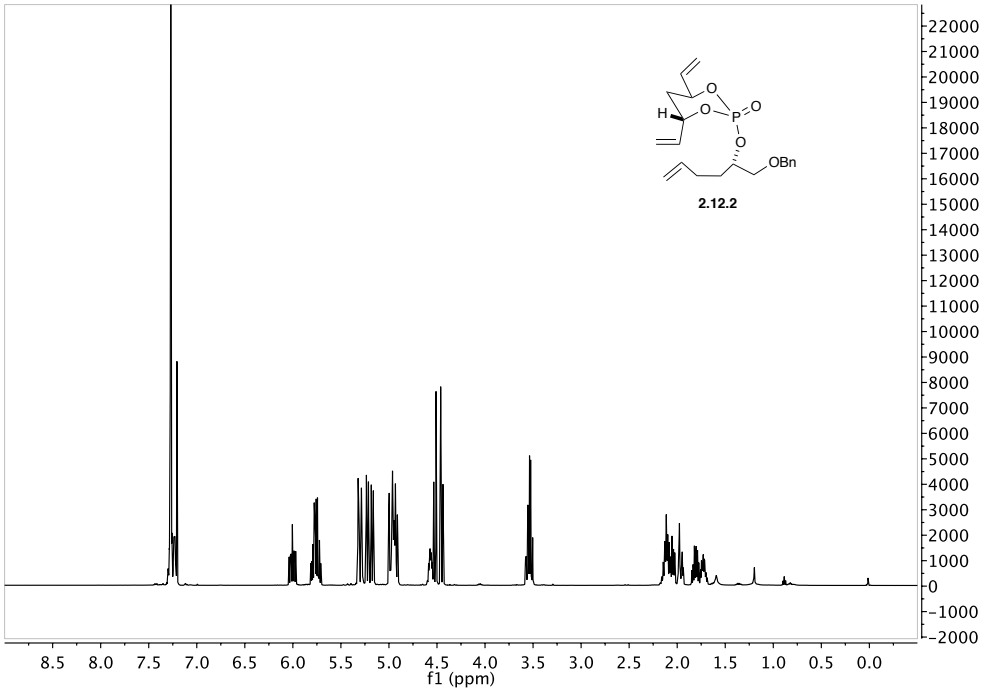

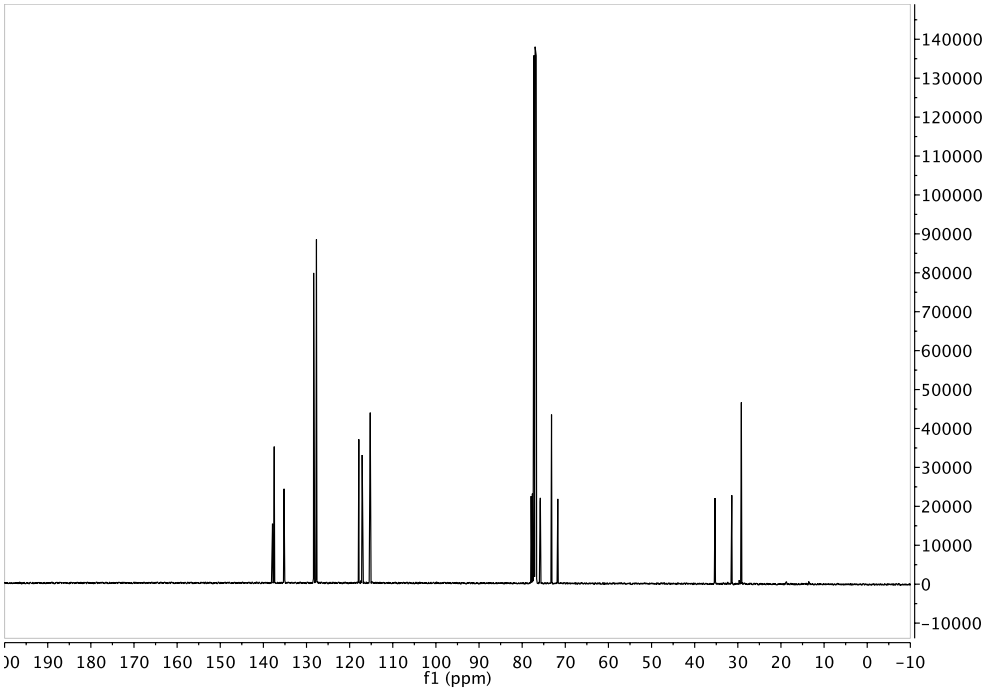

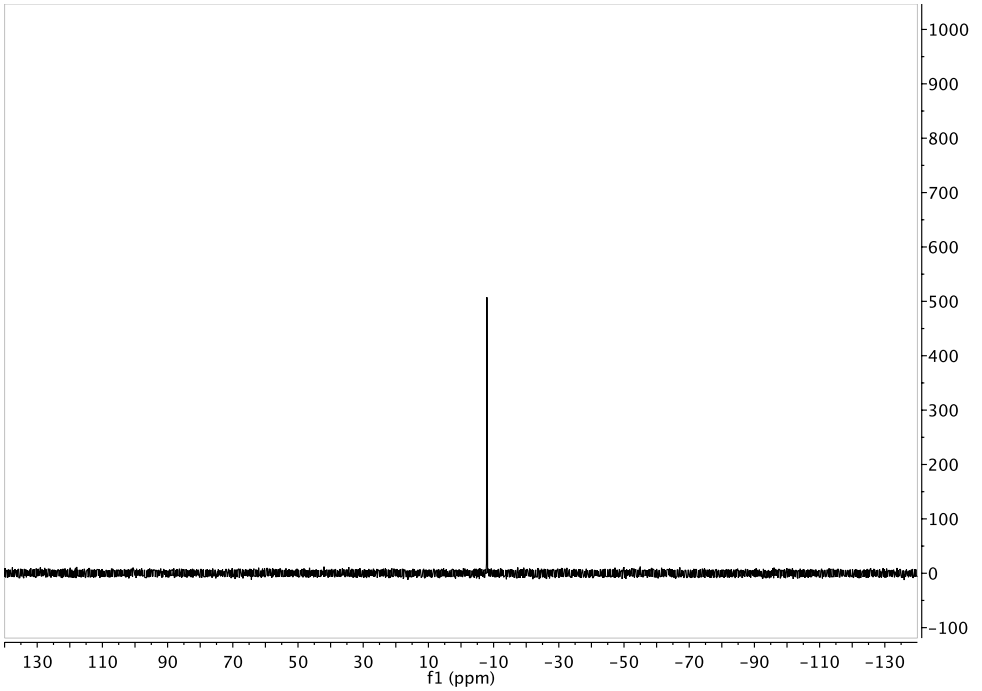

(4*R*,6*R*)-2-(((*S*)-1-(benzyloxy)hex-5-en-2-yl)oxy)-4,6-divinyl-1,3,2-dioxaphosphinane 2-oxide(2.12.3):

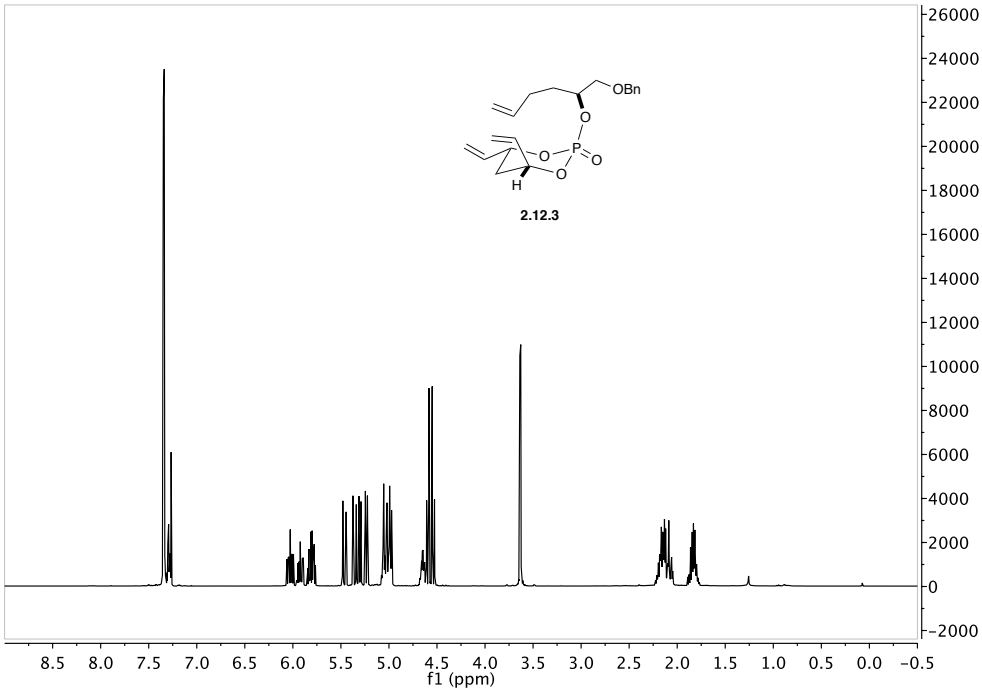

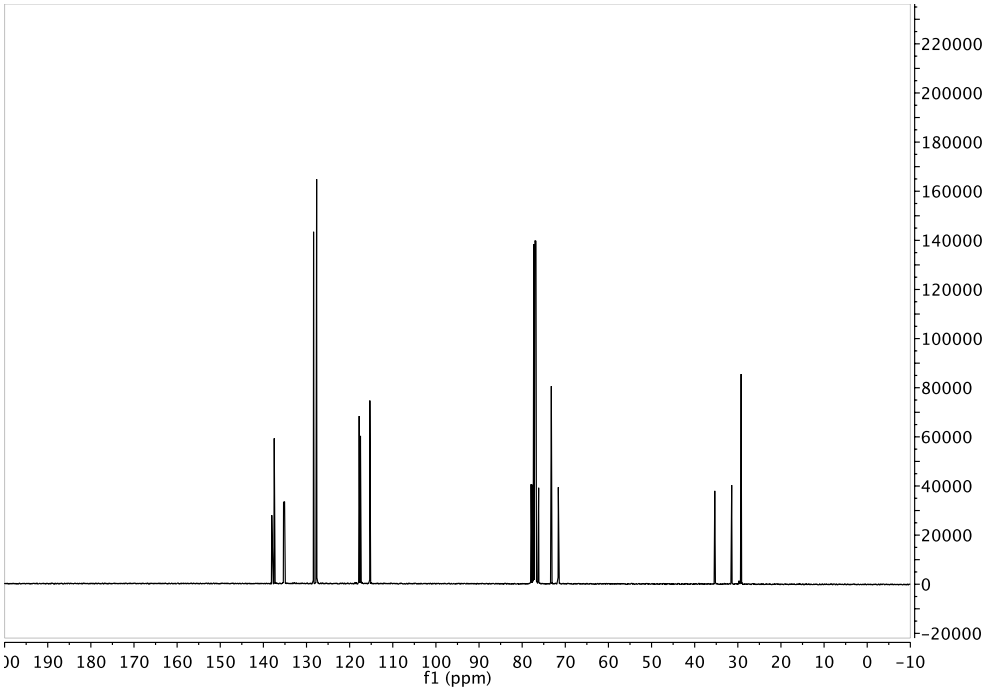
220000
200000
180000
160000
140000
120000
100000
80000
60000
40000
20000
0
-20000
190 180 170 160 150 140 130 120 110 100 90 80 70 60 50 40 30 20 10 0 -10
f1 (ppm)

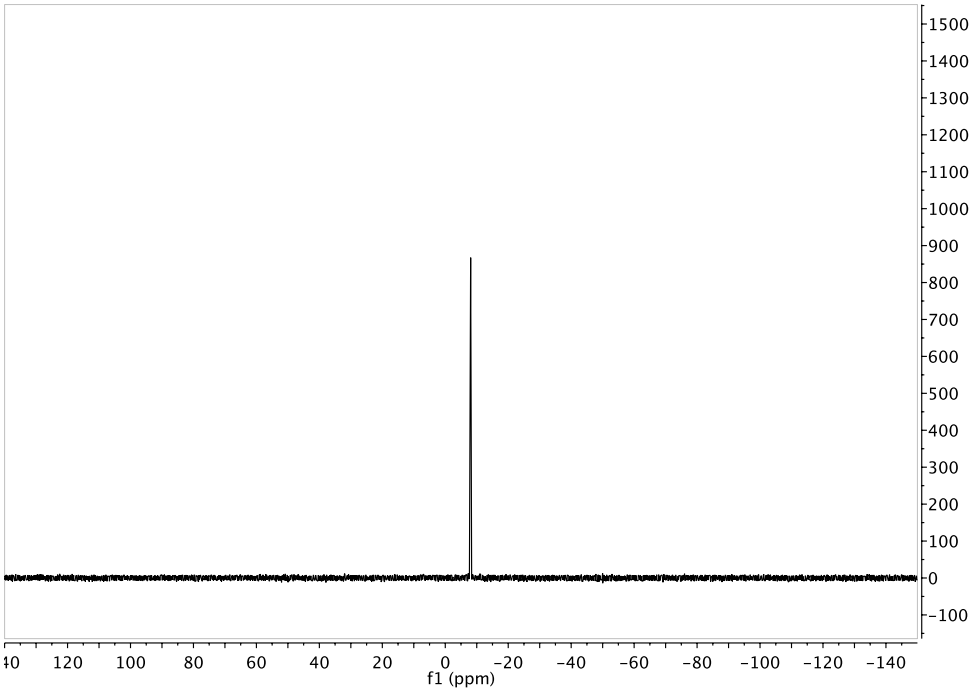
1500
1400
1300
1200
1100
1000
900
800
700
600
500
400
300
200
100
0
-100
120 100 80 60 40 20 0 -20 -40 -60 -80 -100 -120 -140
f1 (ppm)

(1*S*,3*S*,8*S*,10*S*,*Z*)-3-((benzyloxy)methyl)-10-vinyl-2,11,12-trioxa-1-phosphabicyclo [6.3.1]dodec-6-ene 1-oxide (*cis*-2.12.4):

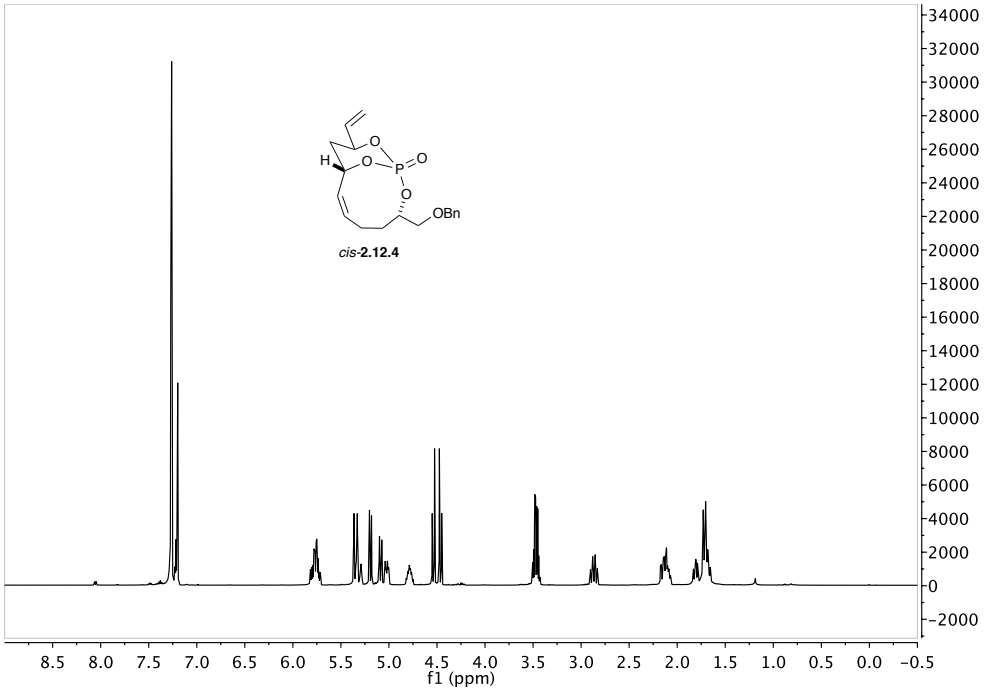

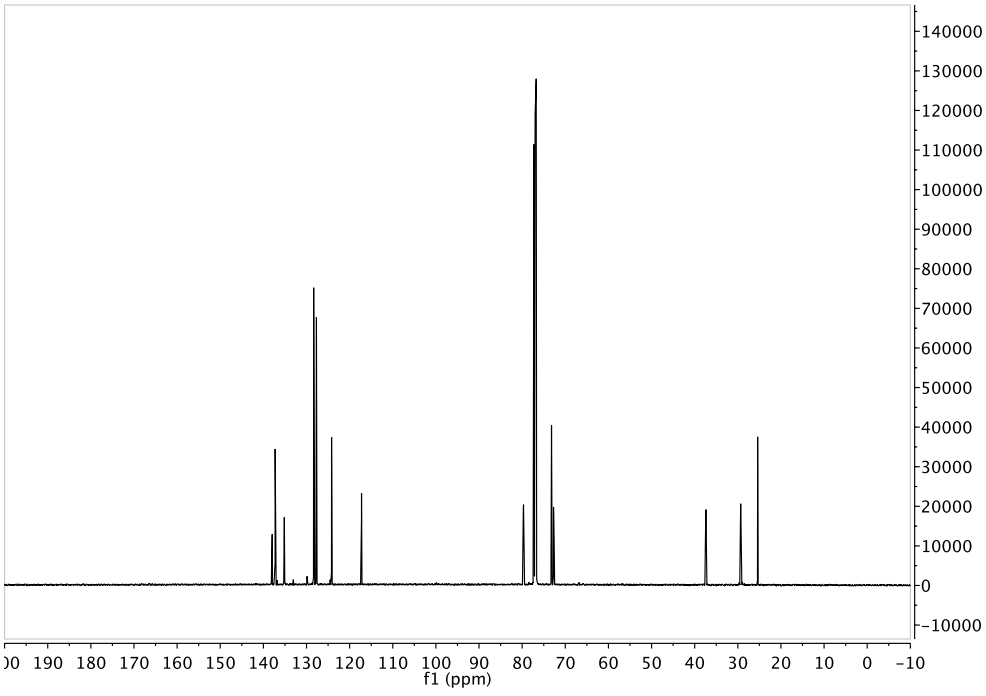

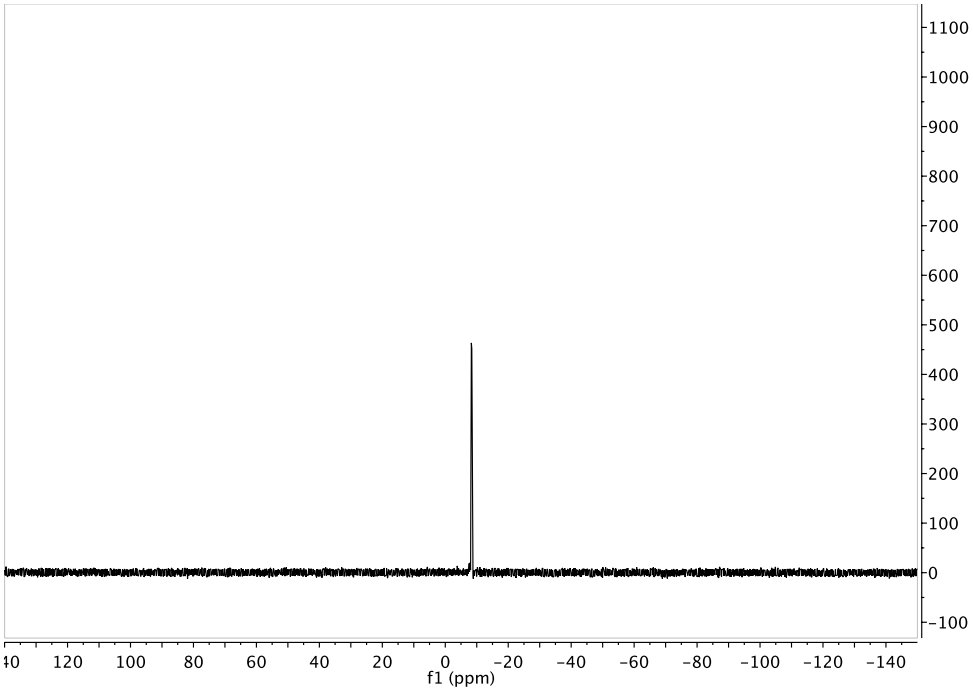

(1*R*,3*S*,8*R*,10*R*,*Z*)-3-((benzyloxy)methyl)-10-vinyl-2,11,12-trioxa-1-phosphabicyclo[6.3.1]dodec-6-ene 1-oxide (*trans*-2.12.5):

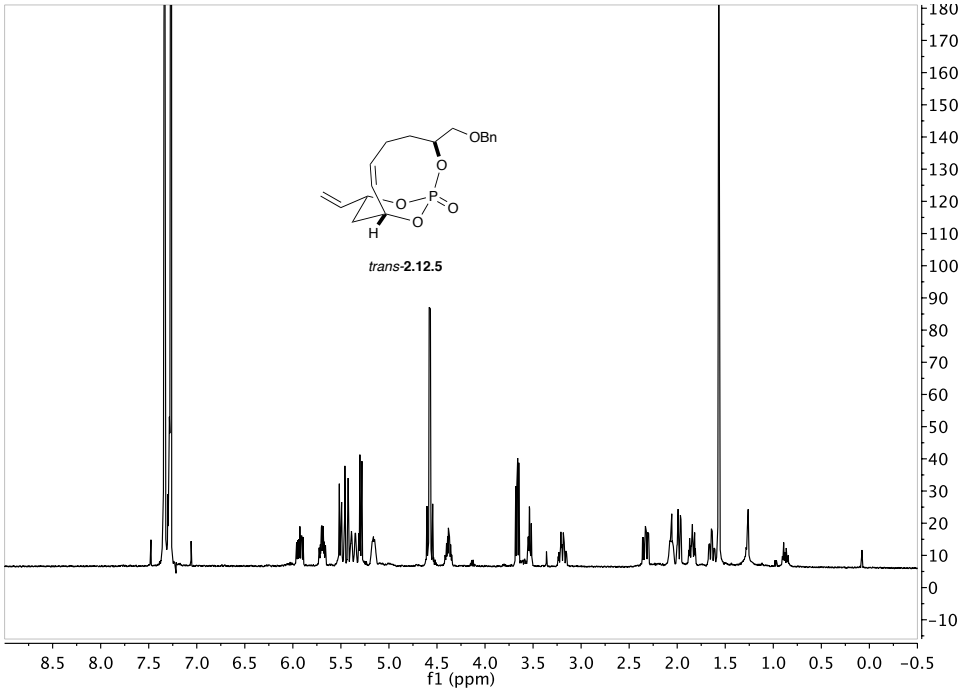

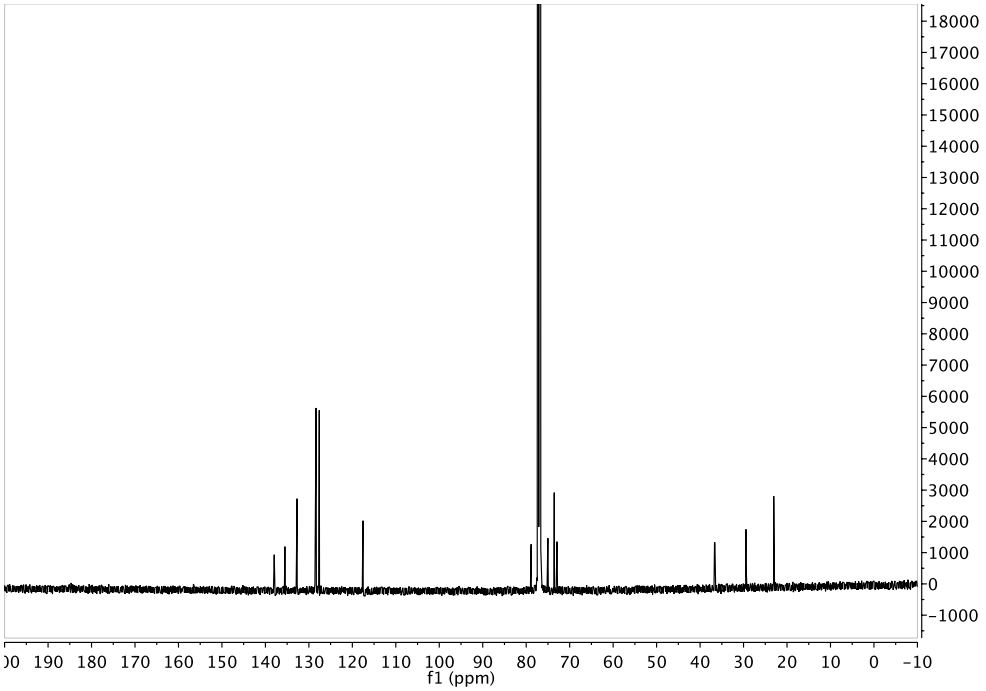
18000
17000
16000
15000
14000
13000
12000
11000
10000
9000
8000
7000
6000
5000
4000
3000
2000
1000
0
−1000
190 180 170 160 150 140 130 120 110 100 90 80 70 60 50 40 30 20 10 0 −10
f1 (ppm)

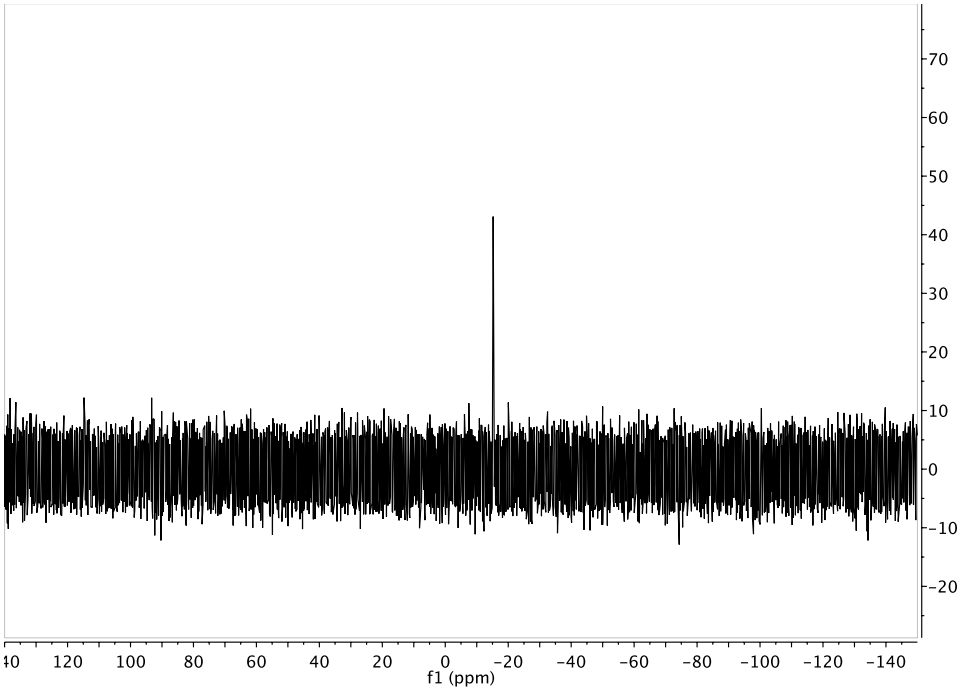
70
60
50
40
30
20
10
0
−10
−20
120 100 80 60 40 20 0 −20 −40 −60 −80 −100 −120 −140
f1 (ppm)

(4*R*,6*R*)-2-(((*R*)-1-(benzyloxy)pent-4-en-2-yl)oxy)-4,6-bis(2-methylallyl)-1,3,2-dioxaphosphinane 2-oxide (2.13.1):

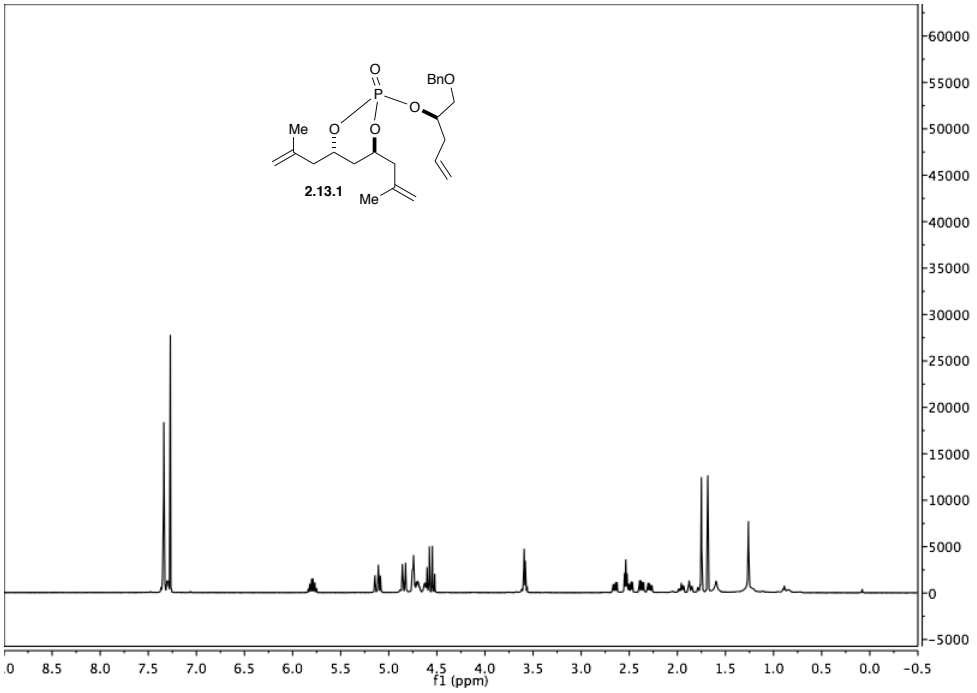

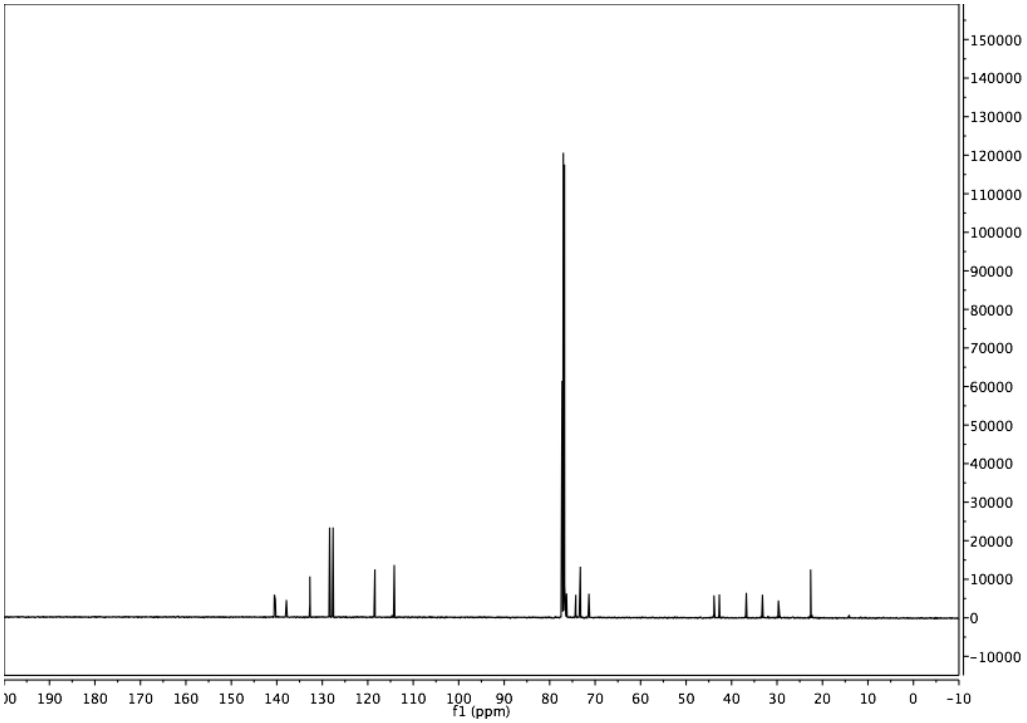

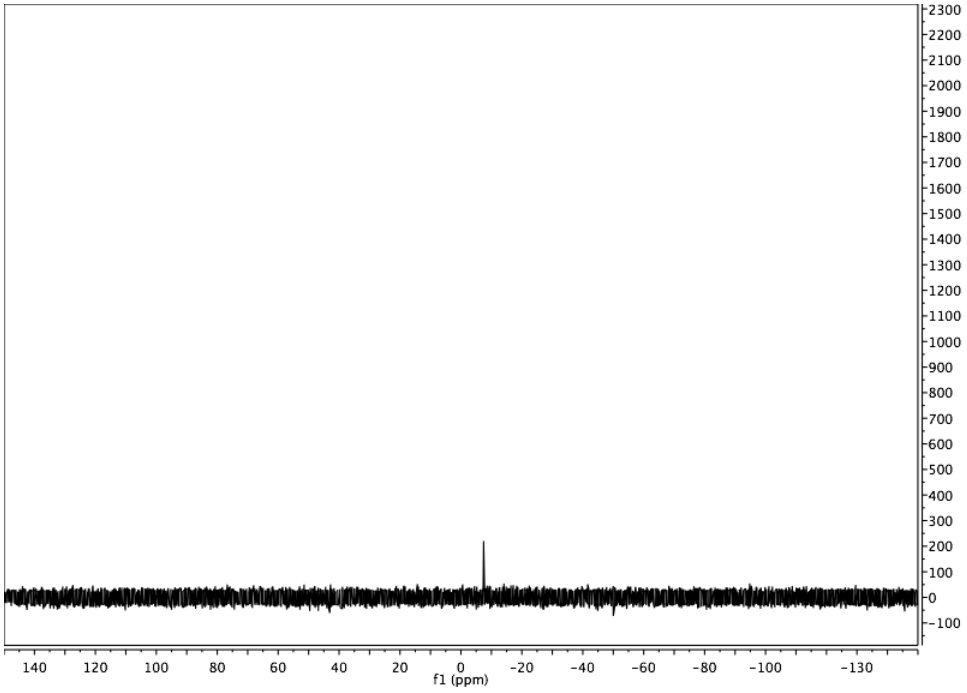

(1*R*,3*R*,8*S*,10*S*,*Z*)-3-((benzyloxy)methyl)-6-methyl-10-(2-methylallyl)-2,11,12-trioxa-1-phosphabicyclo[6.3.1]dodec-5-ene 1-oxide (2.13.2):

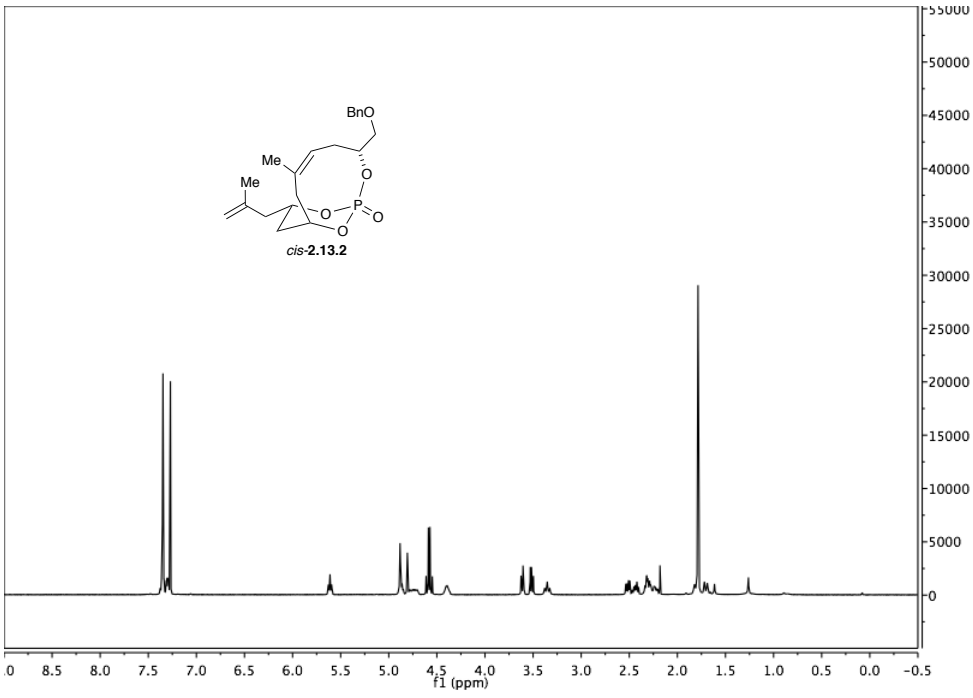

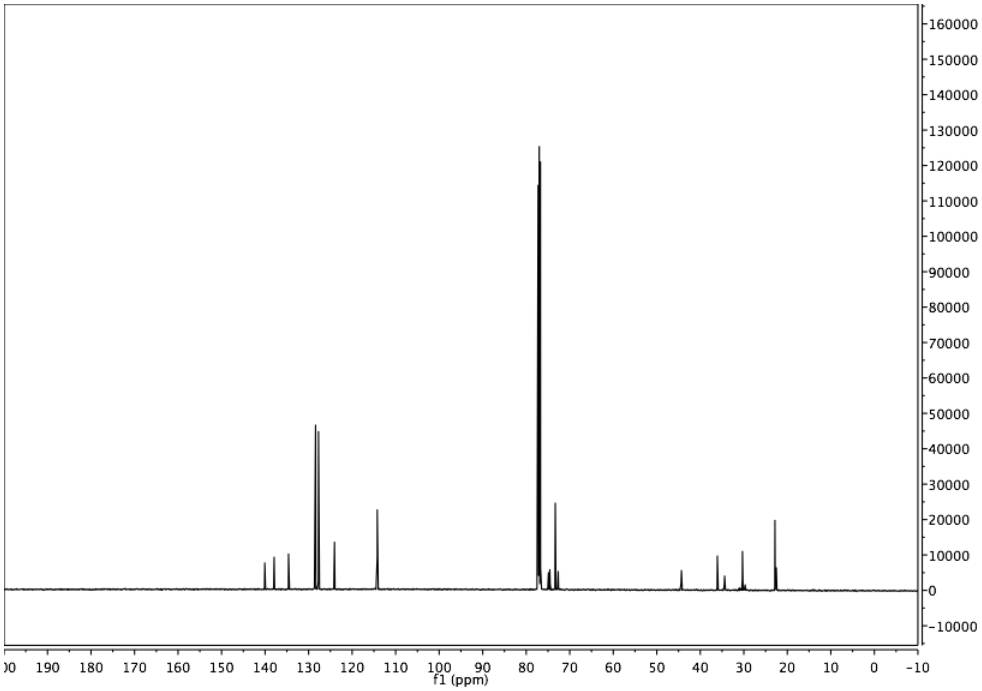
160000
150000
140000
130000
120000
110000
100000
90000
80000
70000
60000
50000
40000
30000
20000
10000
0
−10000
190 180 170 160 150 140 130 120 110 100 90 80 70 60 50 40 30 20 10 0 −10
f1 (ppm)

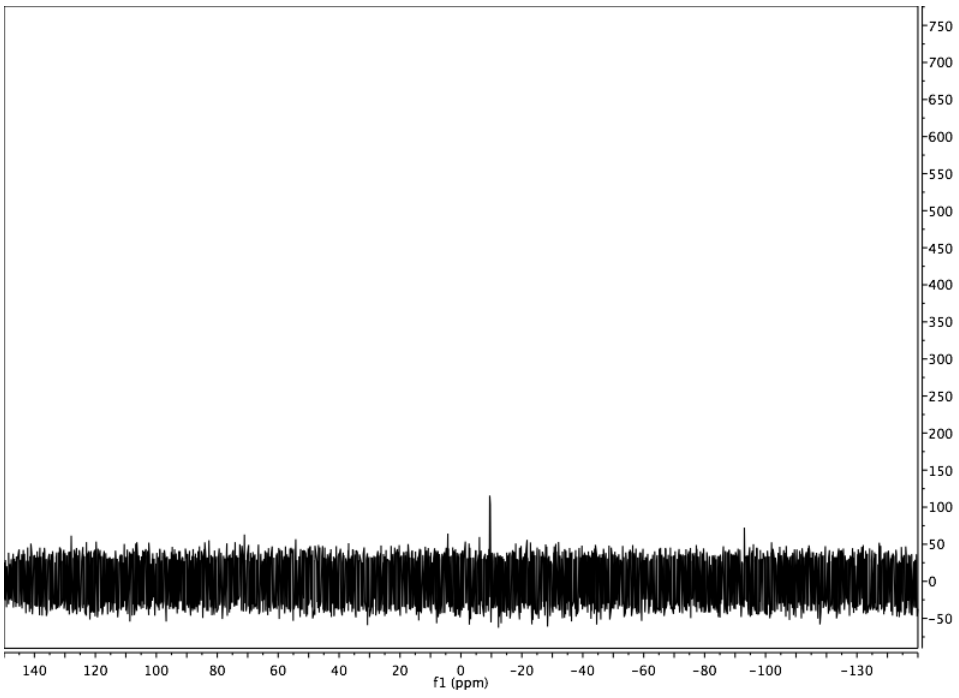
750
700
650
600
550
500
450
400
350
300
250
200
150
100
50
0
−50
140 120 100 80 60 40 20 0 −20 −40 −60 −80 −100 −130
f1 (ppm)

(4*S*,6*S*)-2-(((1*R*,2*R*)-2-methyl-1-(4-nitrophenyl)but-3-en-1-yl)oxy)-4,6-bis(2-methylallyl)-1,3,2-dioxaphosphinane 2-oxide (2.13.3):

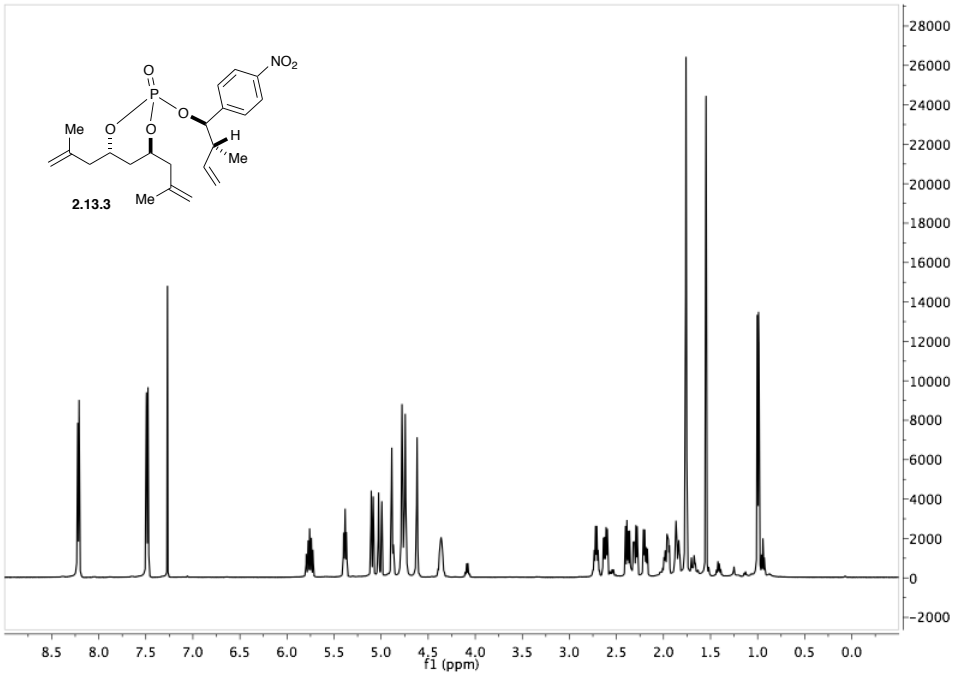

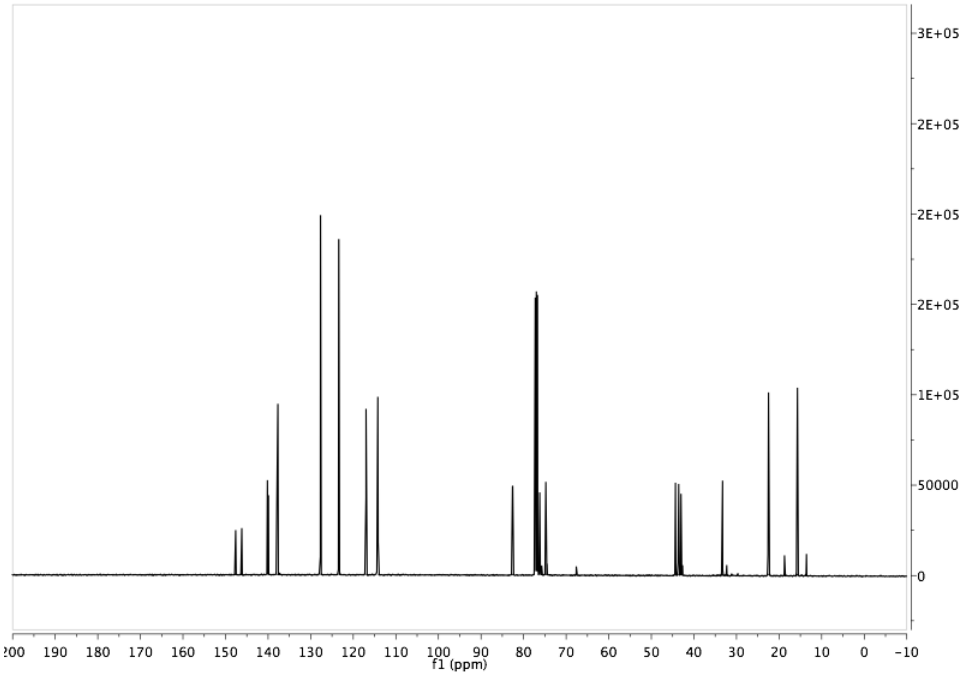

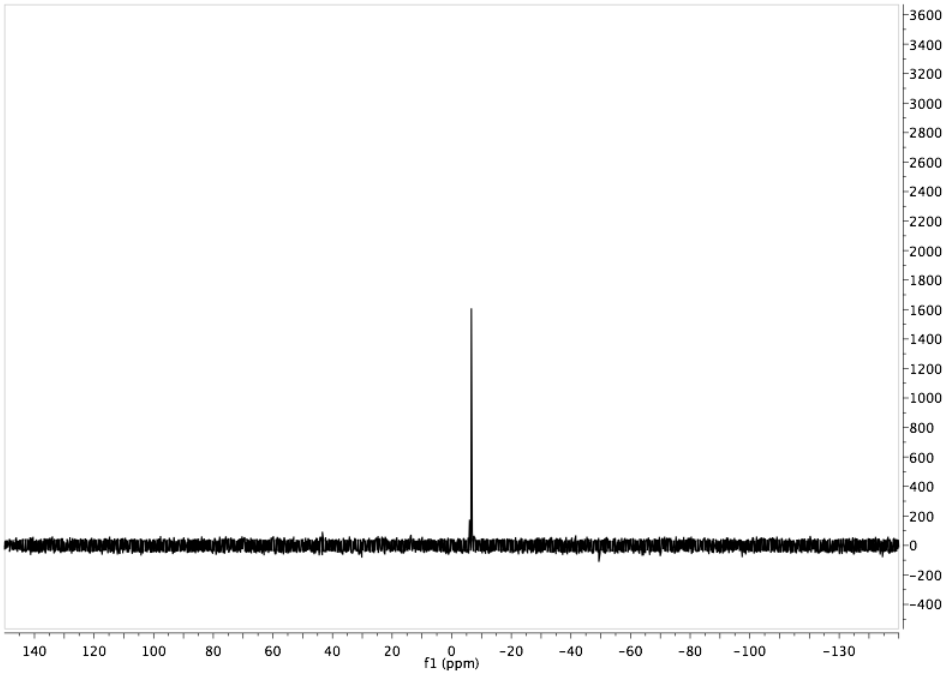

(4*S*,6*S*)-2-(((1*R*,2*S*)-2-methyl-1-(4-nitrophenyl)but-3-en-1-yl)oxy)-4,6-bis(2-methylallyl)-1,3,2-dioxaphosphinane 2-oxide (2.13.4):

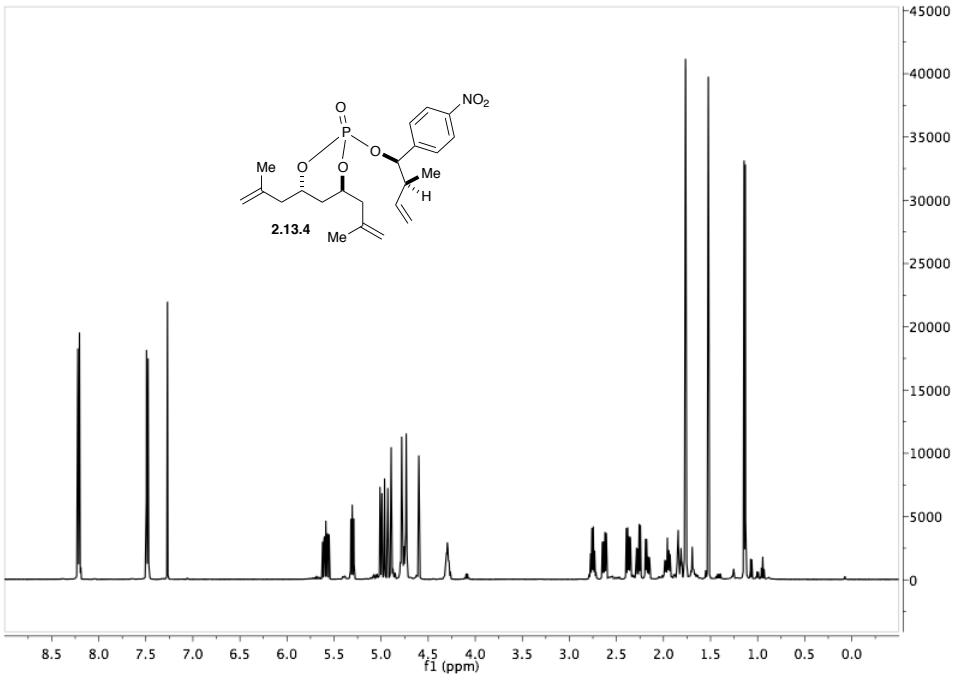

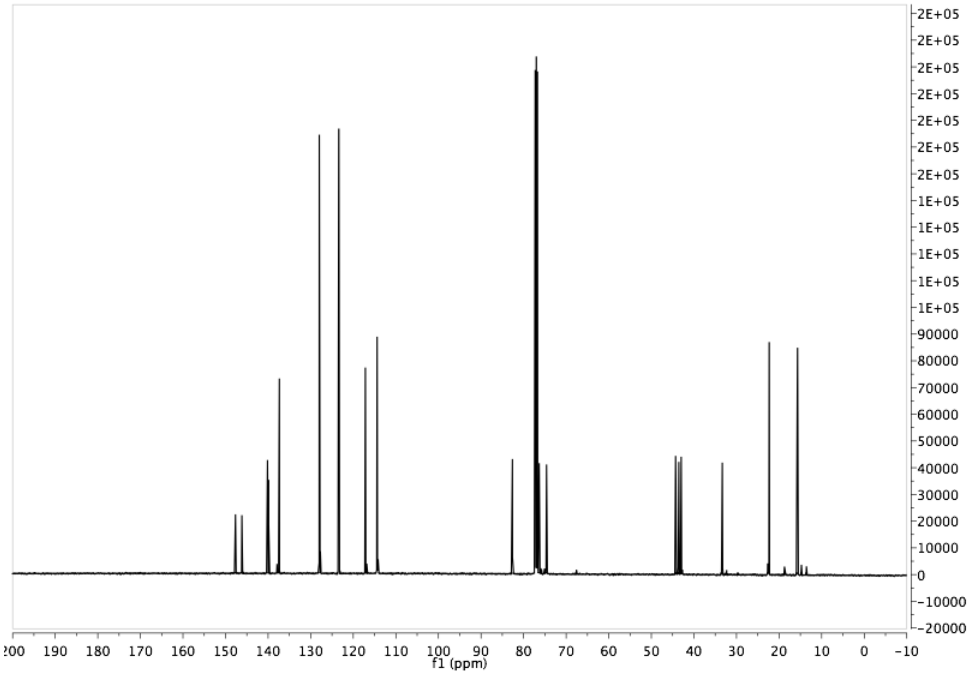
2E+05
2E+05
2E+05
2E+05
2E+05
2E+05
2E+05
1E+05
1E+05
1E+05
1E+05
1E+05
90000
80000
70000
60000
50000
40000
30000
20000
10000
0
−10000
−20000
200 190 180 170 160 150 140 130 120 110 100 90 80 70 60 50 40 30 20 10 0 −10
f1 (ppm)

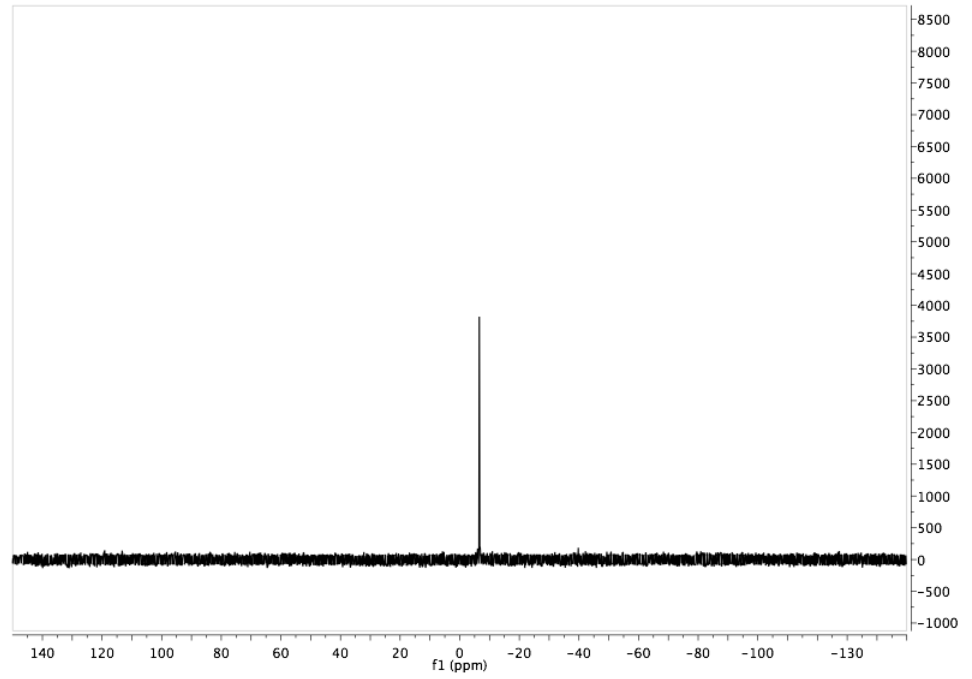
8500
8000
7500
7000
6500
6000
5500
5000
4500
4000
3500
3000
2500
2000
1500
1000
500
0
−500
−1000
140 120 100 80 60 40 20 0 −20 −40 −60 −80 −100 −130
f1 (ppm)

(1*R*,3*R*,4*R*,8*S*,10*S*,*Z*)-4,6-dimethyl-10-(2-methylallyl)-3-(4-nitrophenyl)-2,11,12-trioxa-1-phosphabicyclo[6.3.1]dodec-5-ene 1-oxide (2.13.5):

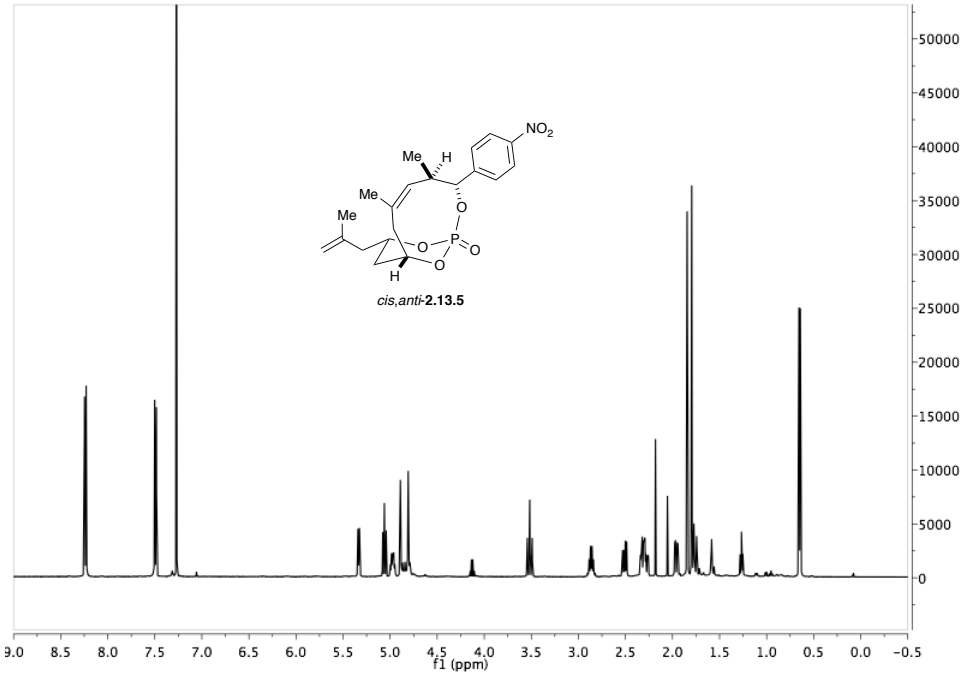

cis,anti-**2.13.5**

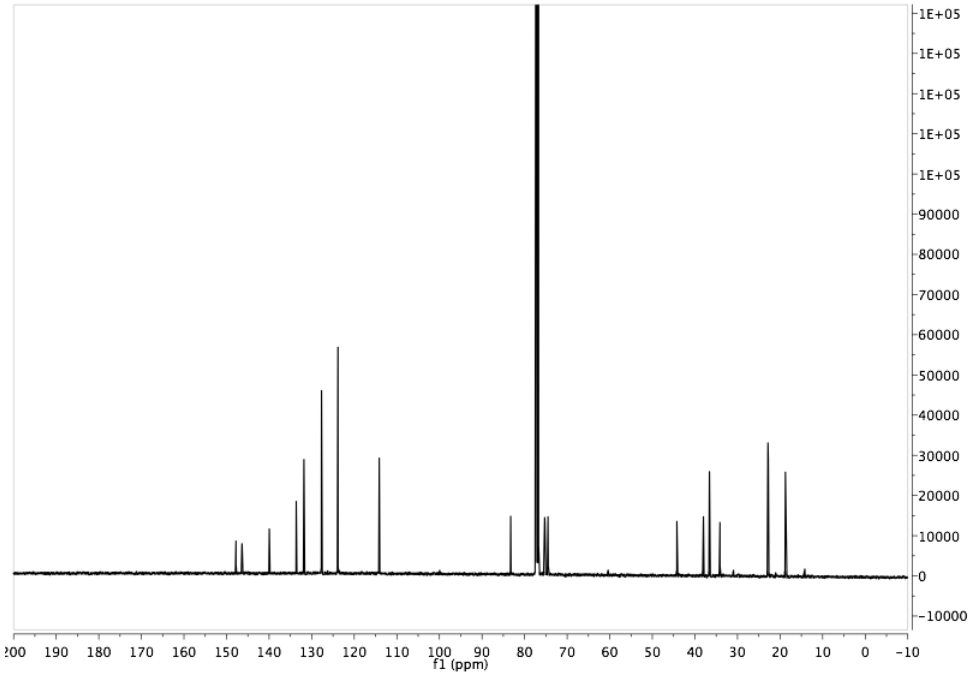

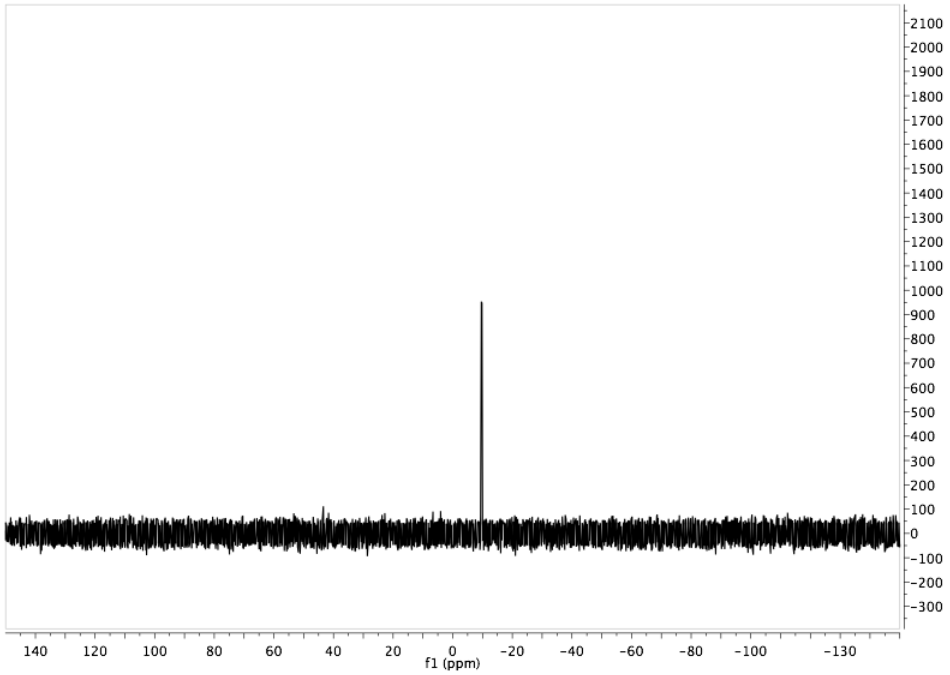

(4*S*,6*S*)-2-(((2*S*,3*S*,4*S*)-3-hydroxy-2,4-dimethylhex-5-en-1-yl)oxy)-4,6-divinyl-1,3,2-dioxaphosphinane 2-oxide (2.14.2a):

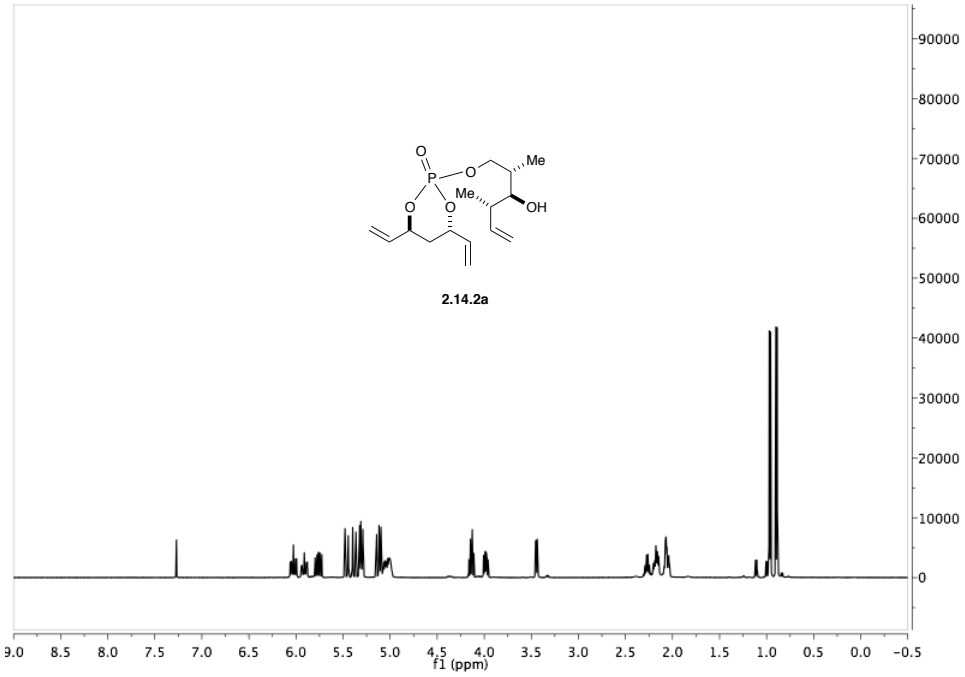

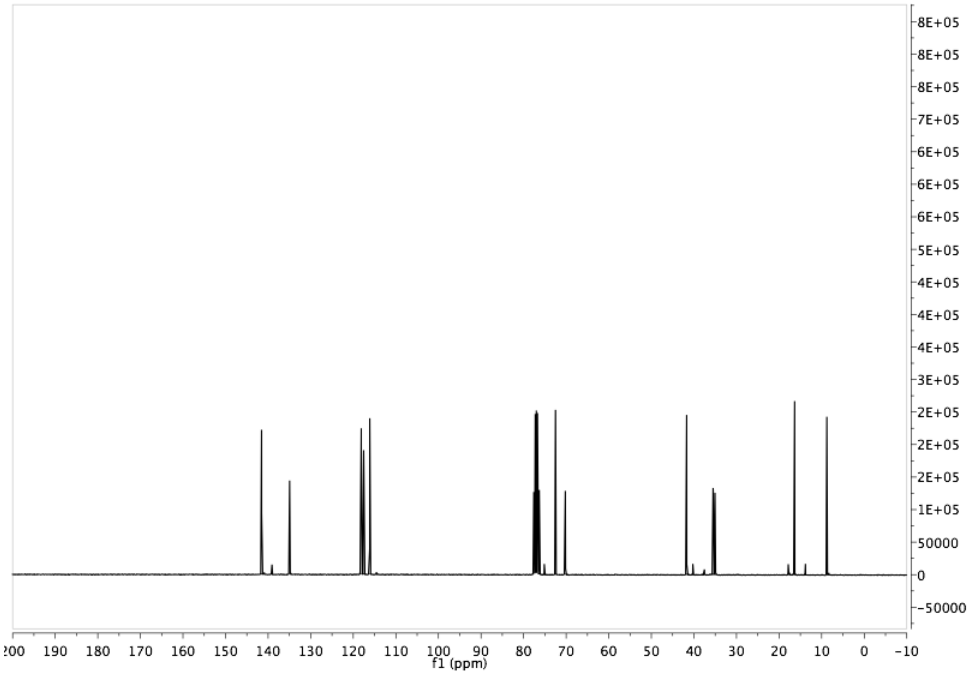
8E+05
8E+05
8E+05
7E+05
6E+05
6E+05
6E+05
6E+05
5E+05
4E+05
4E+05
4E+05
3E+05
2E+05
2E+05
2E+05
1E+05
50000
0
-50000
200 190 180 170 160 150 140 130 120 110 100 90 80 70 60 50 40 30 20 10 0 -10
f1 (ppm)

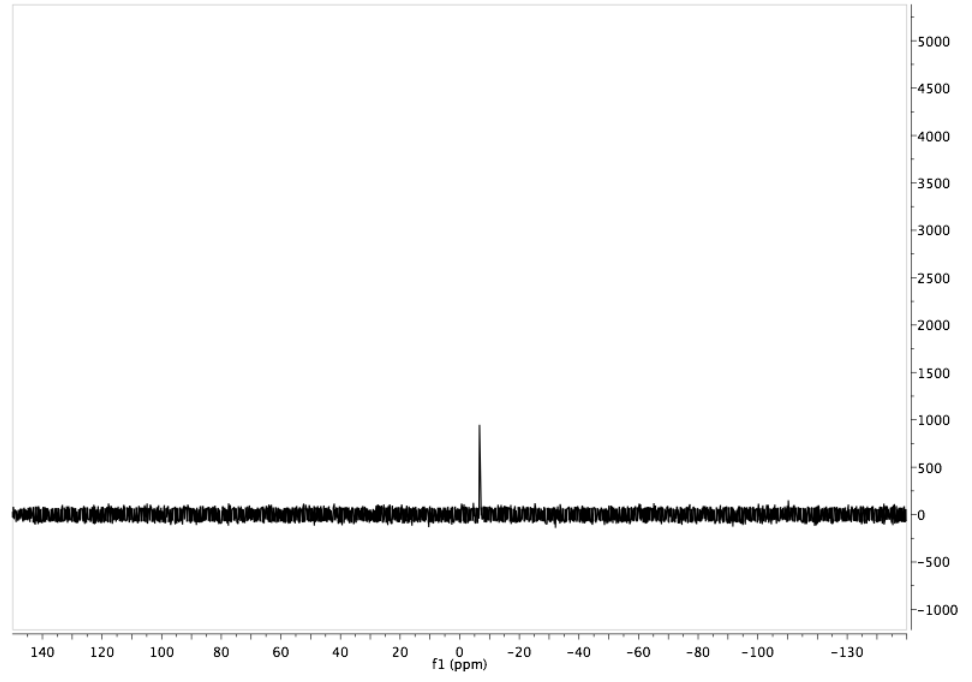
5000
4500
4000
3500
3000
2500
2000
1500
1000
500
0
-500
-1000
140 120 100 80 60 40 20 0 -20 -40 -60 -80 -100 -130
f1 (ppm)

(1*S*,4*S*,5*S*,6*S*,9*S*,11*S*,*E*)-5-hydroxy-4,6-dimethyl-11-vinyl-2,12,13-trioxa-1-phosphabicyclo[7.3.1]tridec-7-ene 1-oxide (2.14.4a):

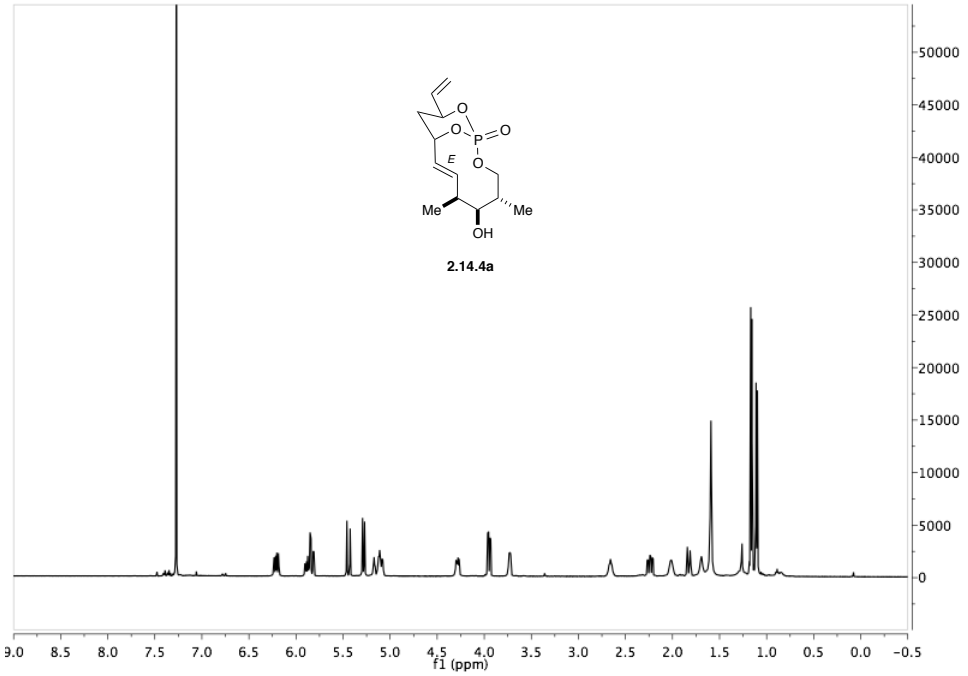

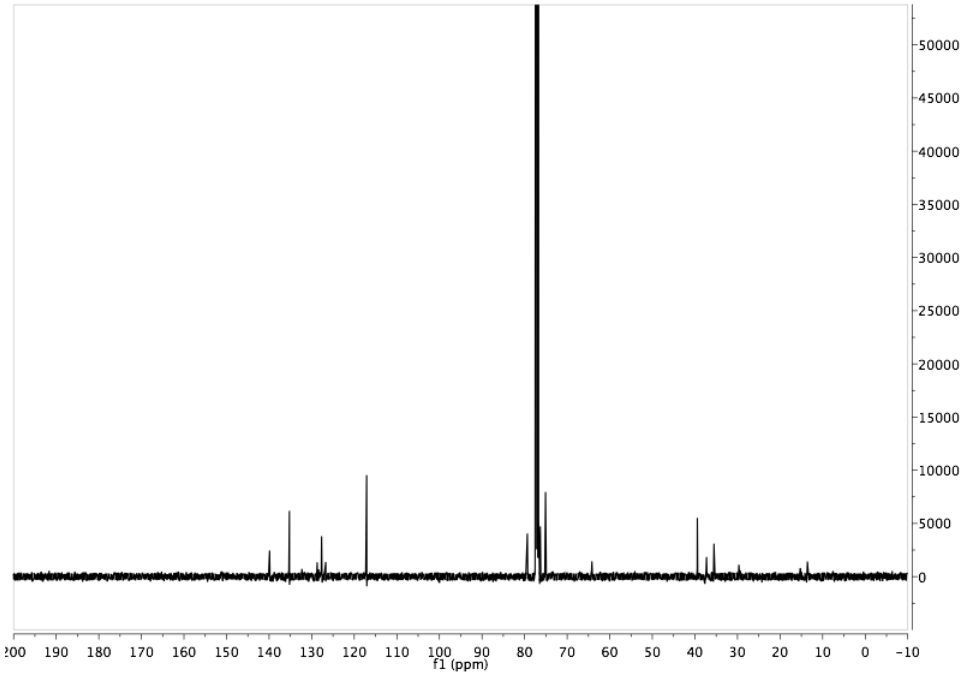

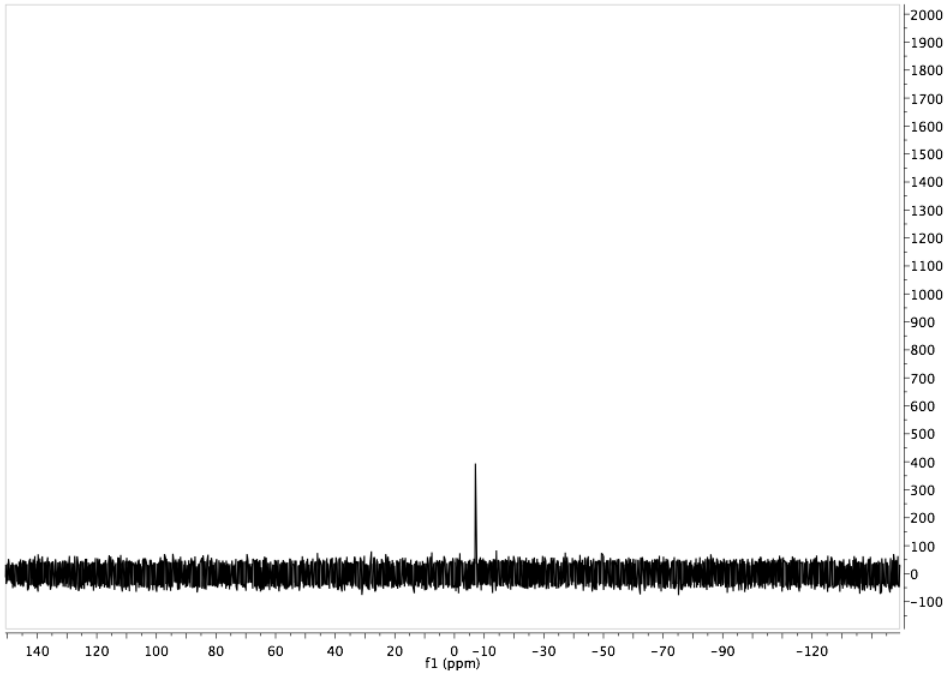

(4*S*,6*S*)-2-(((2*S*,3*S*,4*S*)-3-((*tert*-butyldimethylsilyl)oxy)-2,4-dimethylhex-5-en-1-yl)oxy)-4,6-divinyl-1,3,2-dioxaphosphinane 2-oxide (2.14.2b):

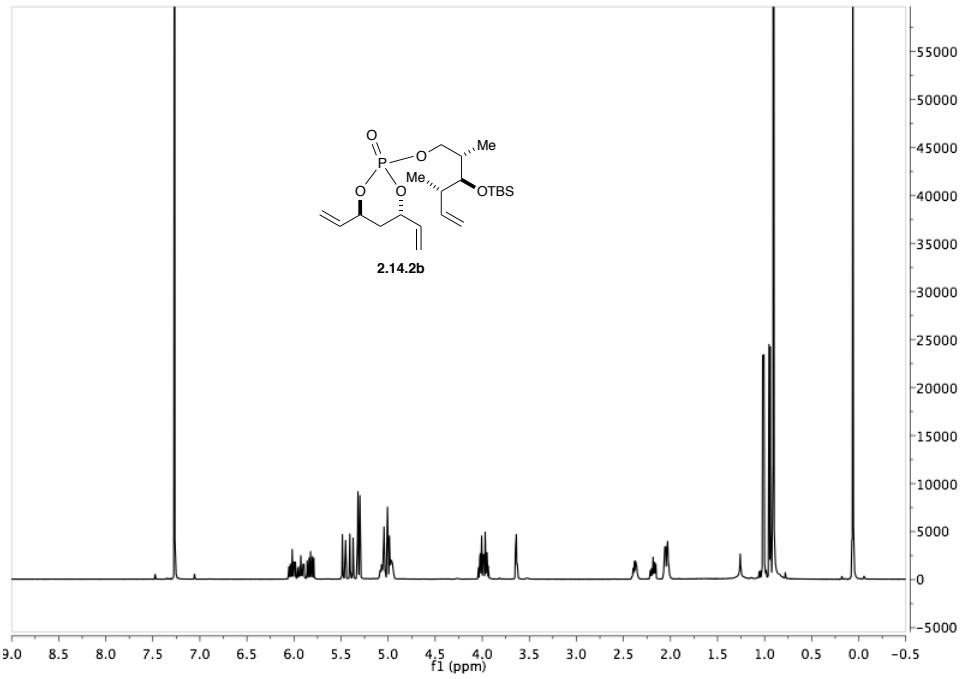

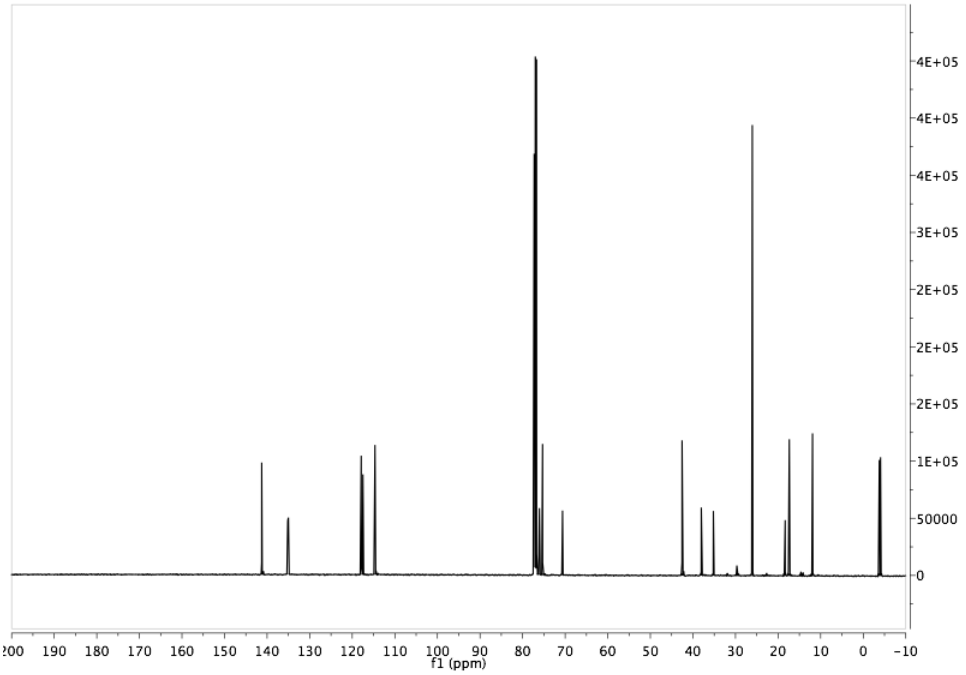
4E+05
4E+05
4E+05
3E+05
2E+05
2E+05
2E+05
1E+05
50000
0
200 190 180 170 160 150 140 130 120 110 100 90 80 70 60 50 40 30 20 10 0 -10
f1 (ppm)

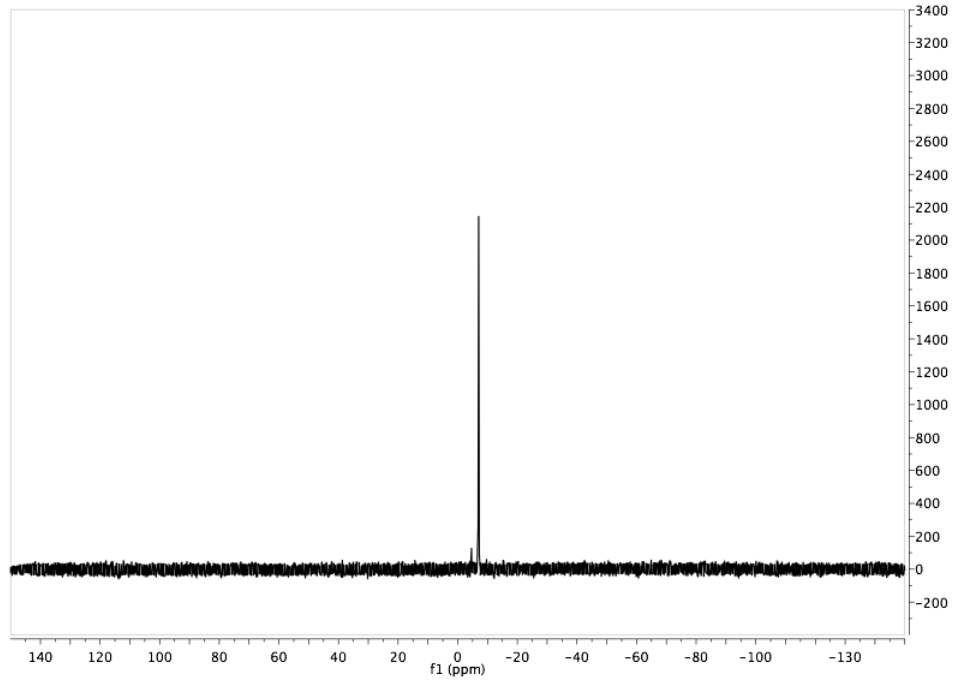
3400
3200
3000
2800
2600
2400
2200
2000
1800
1600
1400
1200
1000
800
600
400
200
0
-200
140 120 100 80 60 40 20 0 -20 -40 -60 -80 -100 -130
f1 (ppm)

(1*S*,4*S*,5*S*,6*S*,9*S*,11*S*,*E*)-5-((*tert*-butyldimethylsilyl)oxy)-4,6-dimethyl-11-vinyl-2,12,13-trioxa-1-phosphabicyclo[7.3.1]tridec-7-ene 1-oxide (2.14.4b):

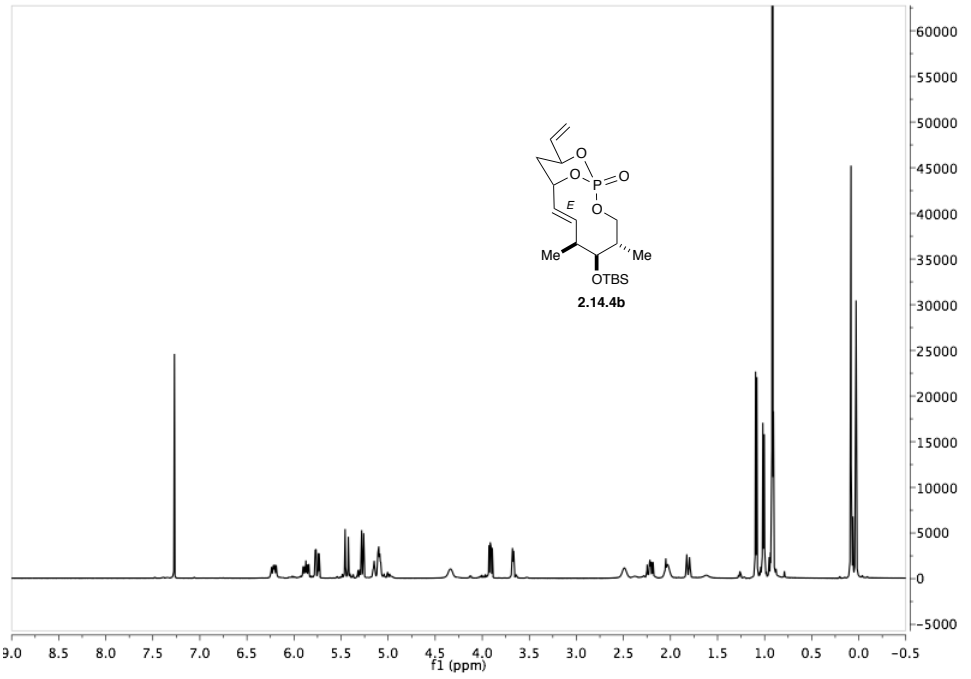

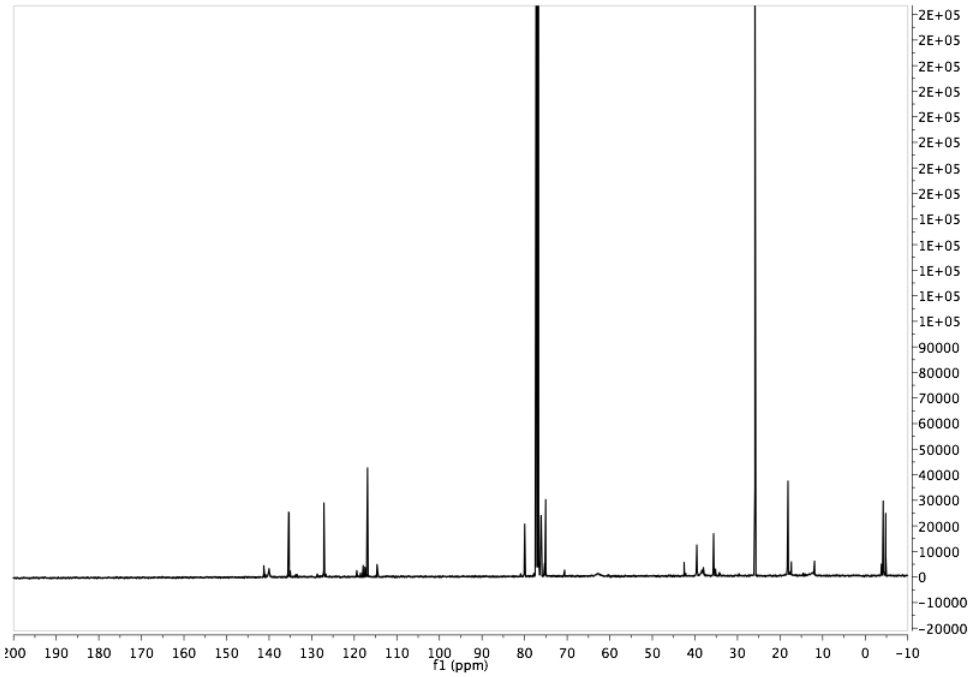

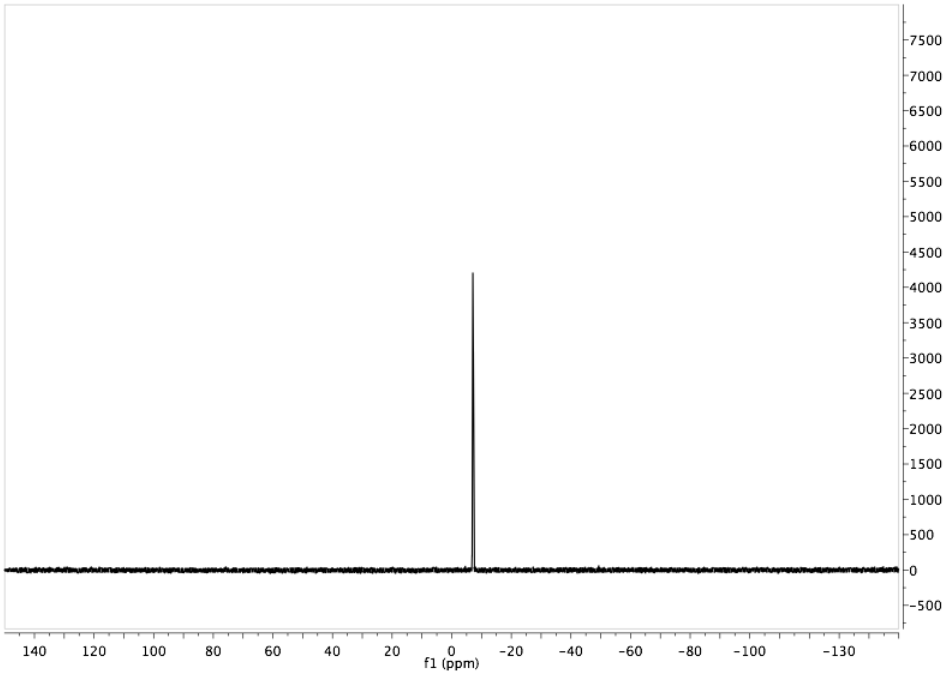

(4*R*,6*R*)-2-(((2*S*,3*S*,4*S*)-3-((4-methoxybenzyl)oxy)-2,4-dimethylhex-5-en-1-yl)oxy) -4,6-divinyl-1,3,2-dioxaphosphinane 2-oxide (2.14.3):

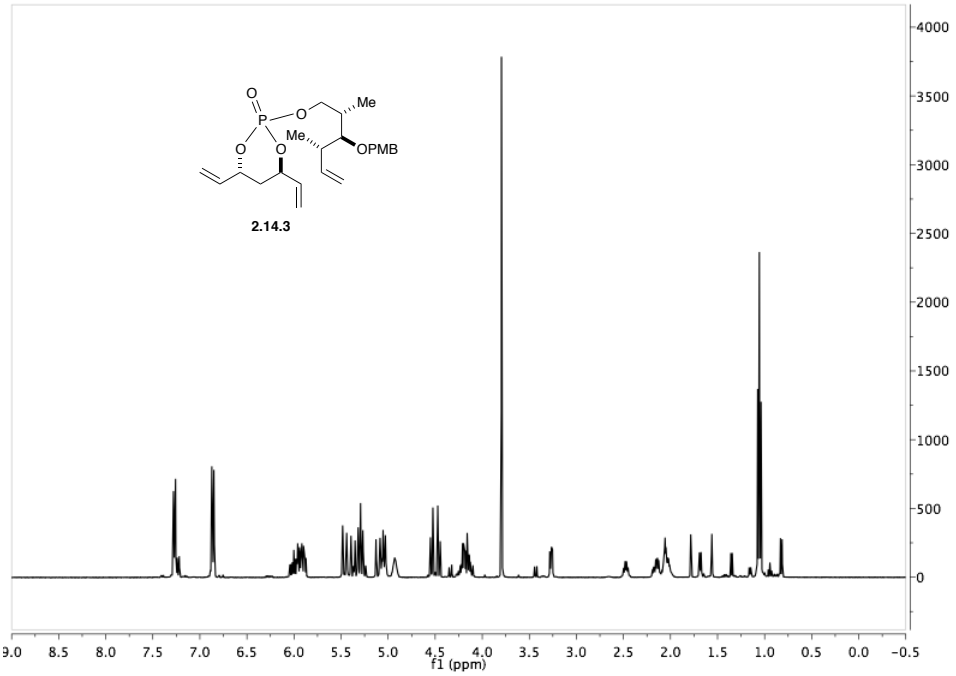

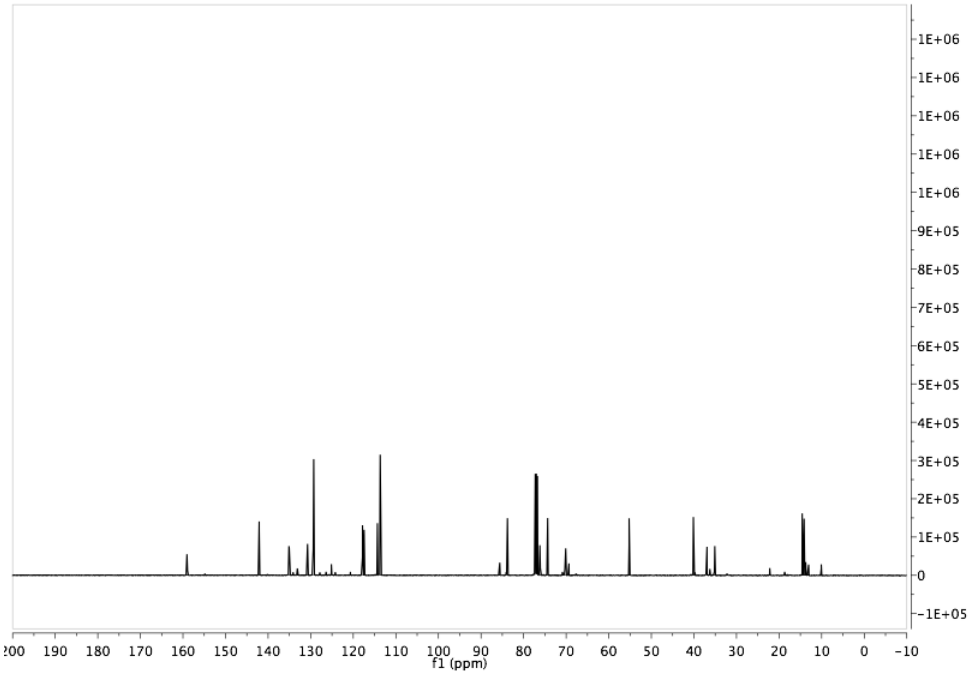
1E+06
1E+06
1E+06
1E+06
1E+06
9E+05
8E+05
7E+05
6E+05
5E+05
4E+05
3E+05
2E+05
1E+05
0
-1E+05
200 190 180 170 160 150 140 130 120 110 100 90 80 70 60 50 40 30 20 10 0 -10
f1 (ppm)

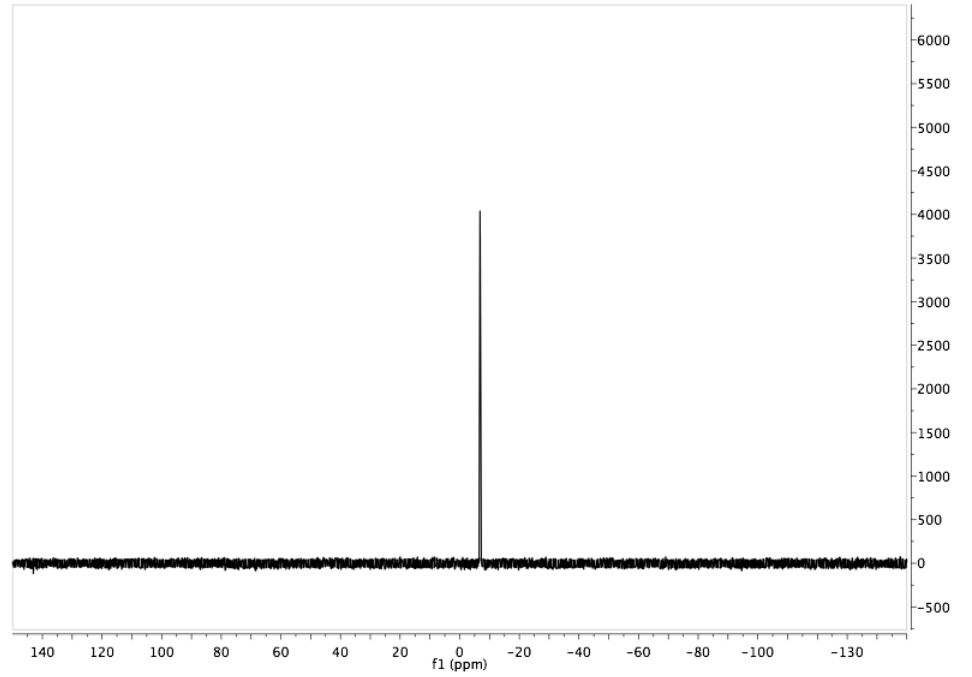
6000
5500
5000
4500
4000
3500
3000
2500
2000
1500
1000
500
0
-500
140 120 100 80 60 40 20 0 -20 -40 -60 -80 -100 -130
f1 (ppm)

(1*R*,4*S*,5*S*,6*S*,9*R*,11*R*,*E*)-5-((4-methoxybenzyl)oxy)-4,6-dimethyl-11-vinyl-2,12,13-trioxa-1-phosphabicyclo[7.3.1]tridec-7-ene 1-oxide (2.14.5):

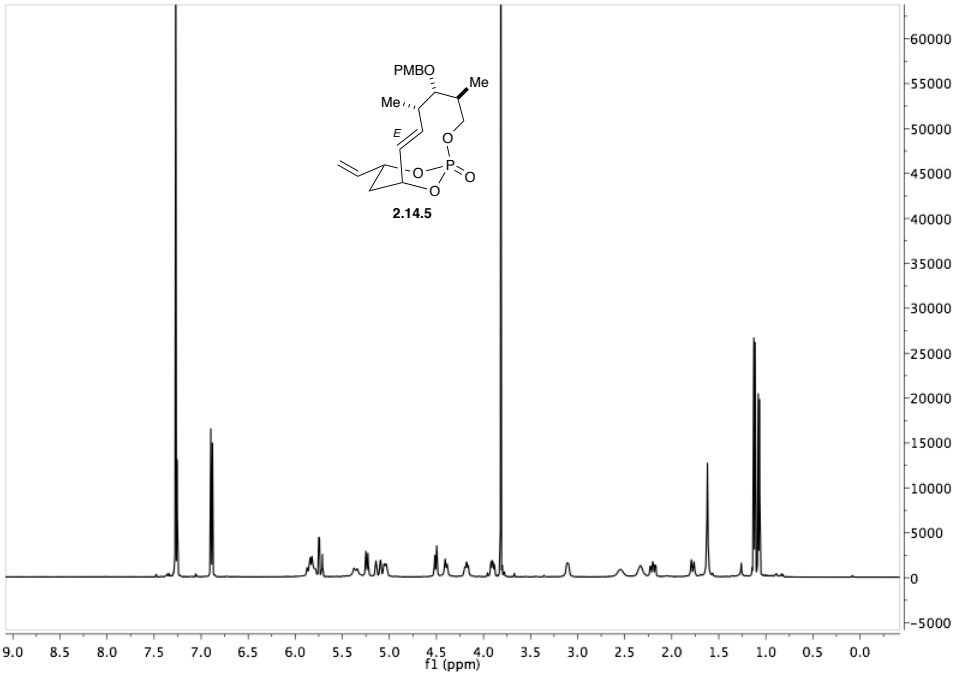

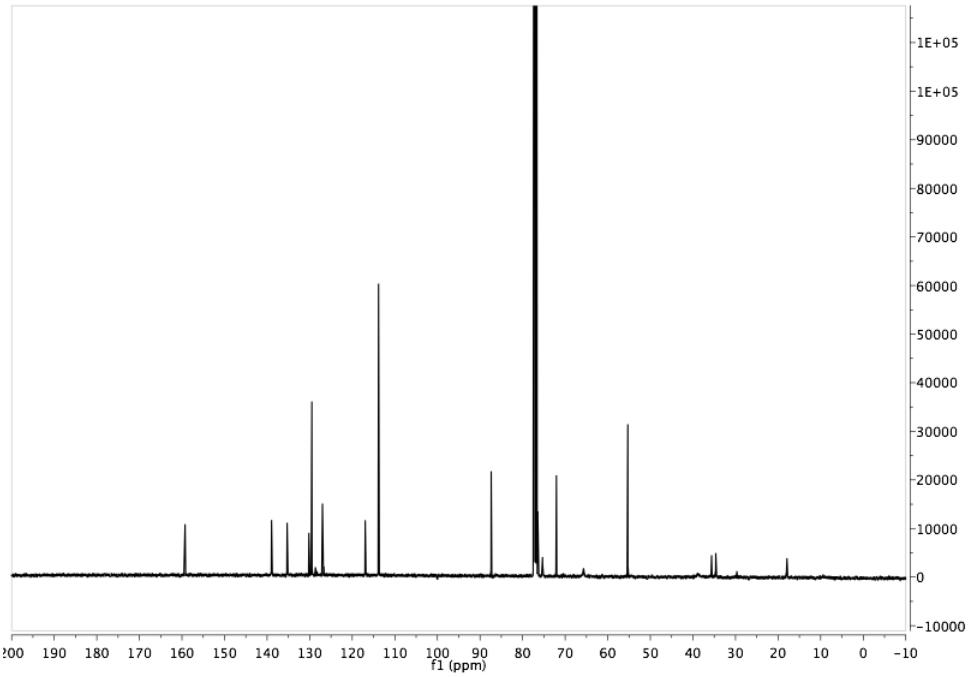

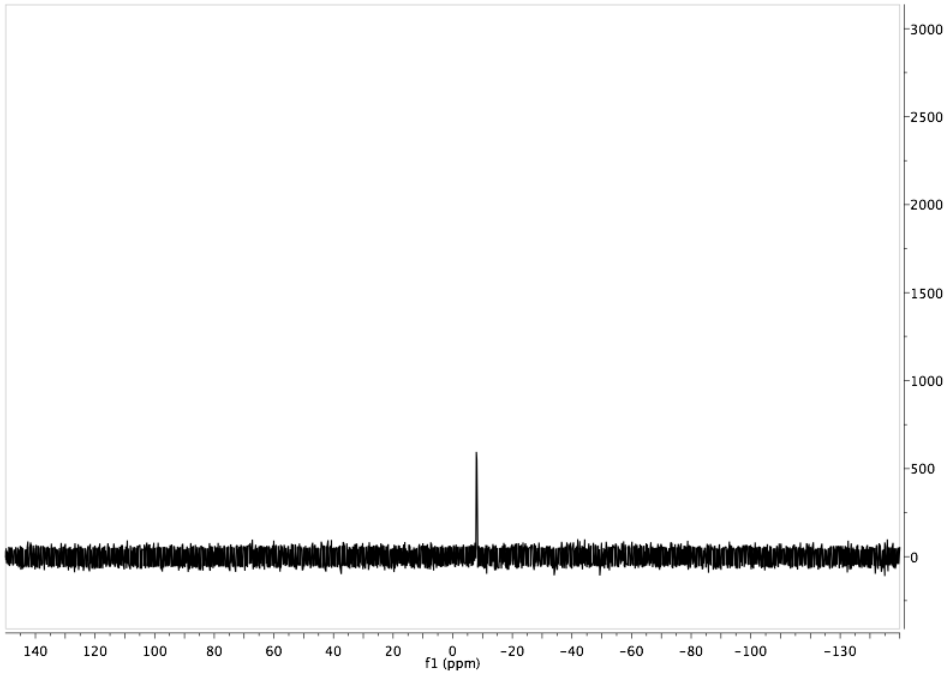

(4*S*,6*S*)-2-(((*S*)-1-(benzyloxy)oct-7-en-2-yl)oxy)-4,6-divinyl-1,3,2-dioxaphosphinane 2-oxide (2.15.2):

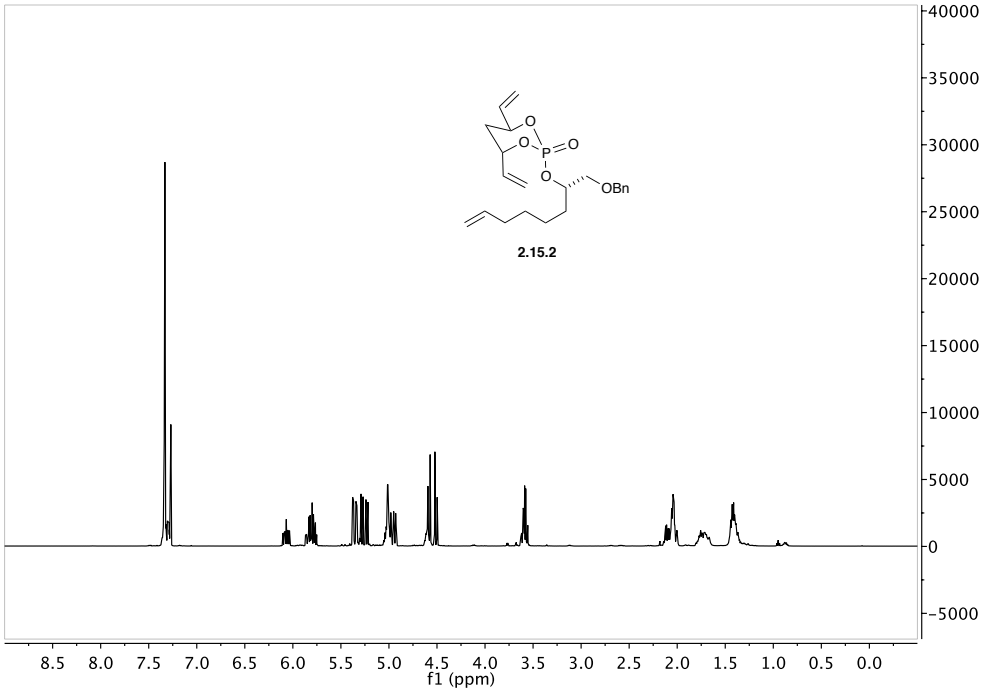

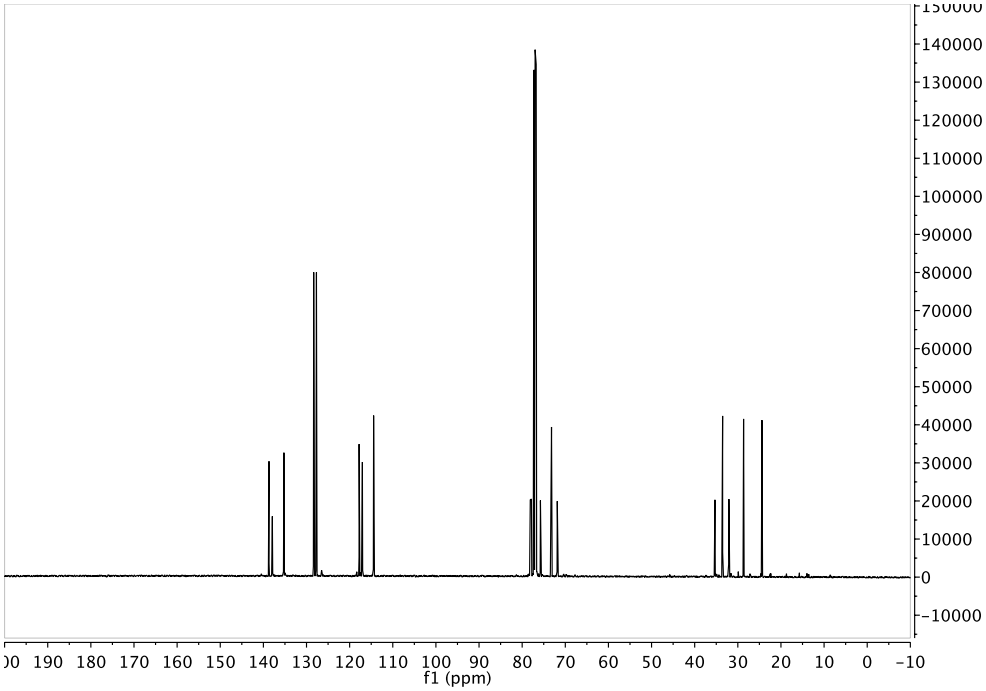
150000
140000
130000
120000
110000
100000
90000
80000
70000
60000
50000
40000
30000
20000
10000
0
−10000
190 180 170 160 150 140 130 120 110 100 90 80 70 60 50 40 30 20 10 0 −10
f1 (ppm)

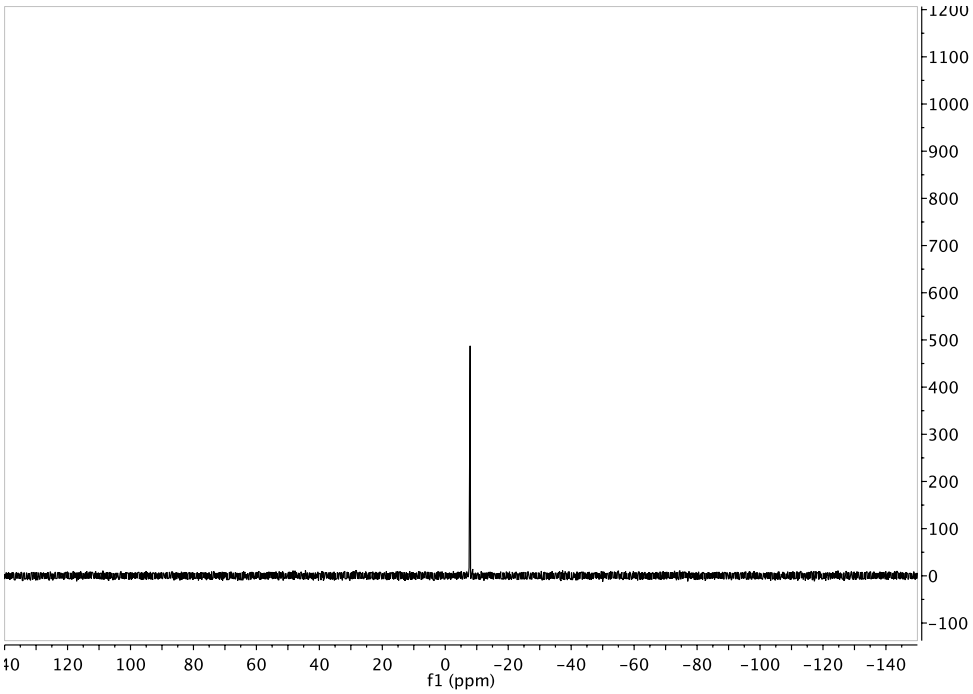
1200
1100
1000
900
800
700
600
500
400
300
200
100
0
−100
120 100 80 60 40 20 0 −20 −40 −60 −80 −100 −120 −140
f1 (ppm)

(4*R*,6*R*)-2-(((*S*)-1-(benzyloxy)oct-7-en-2-yl)oxy)-4,6-divinyl-1,3,2-dioxaphosphinane 2-oxide (2.15.3):

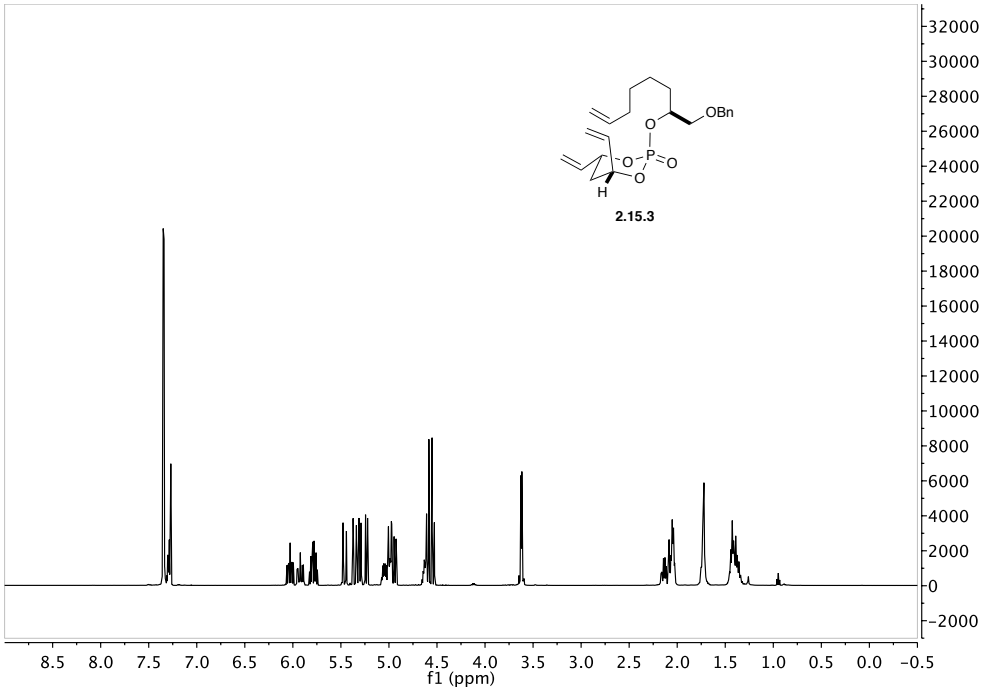

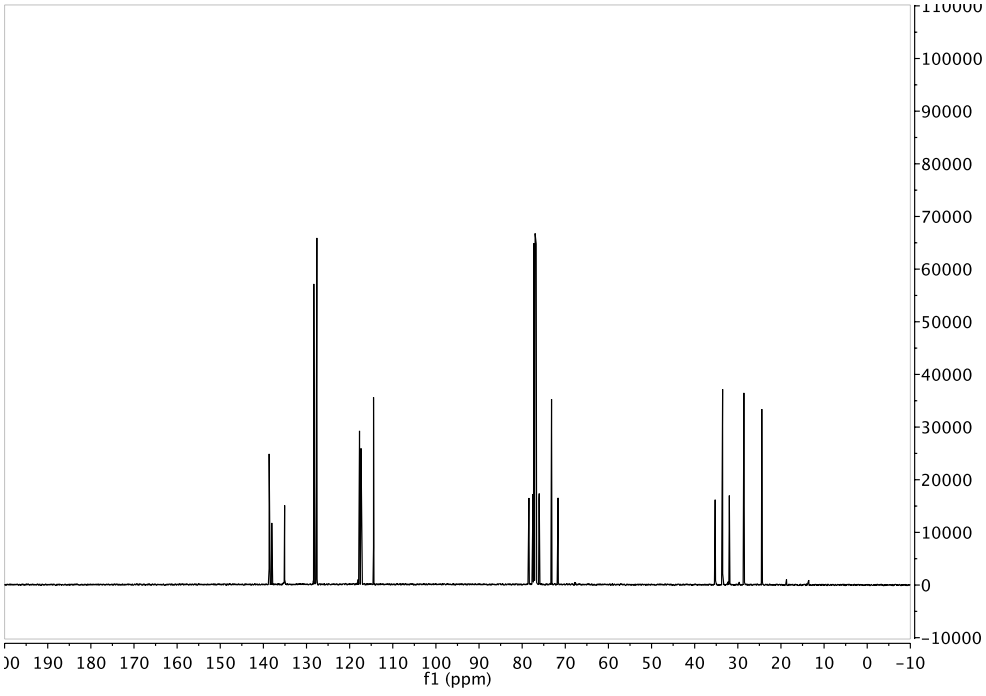

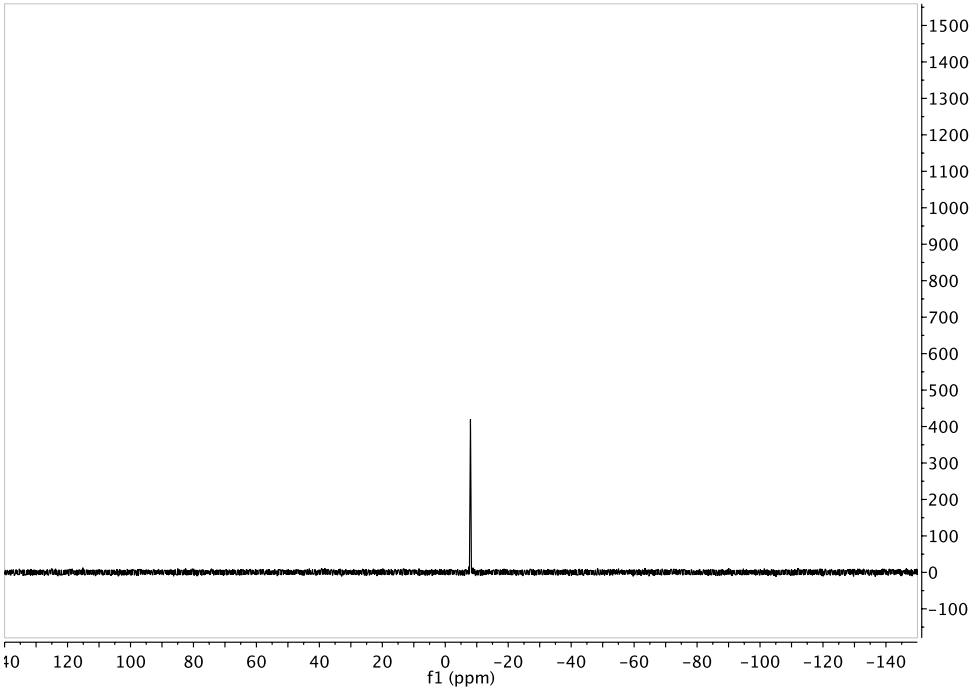

(1*S*,3*S*,10*S*,12*S*,*E*)-3-((benzyloxy)methyl)-12-vinyl-2,13,14-trioxa-1-phosphabicyclo[8.3.1]tetradec-8-ene 1-oxide (2.15.4):

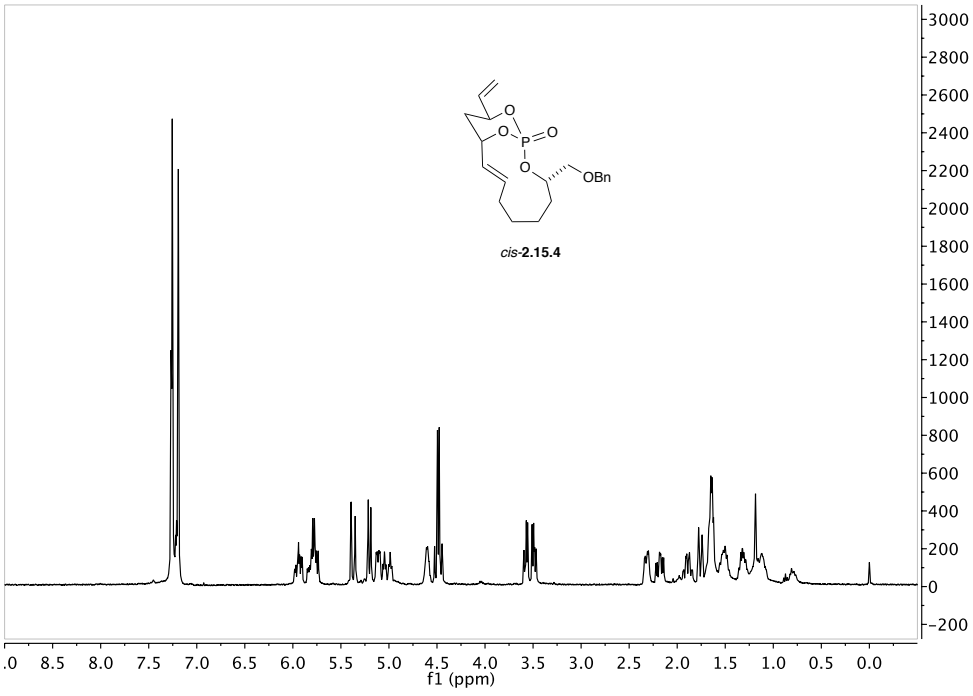

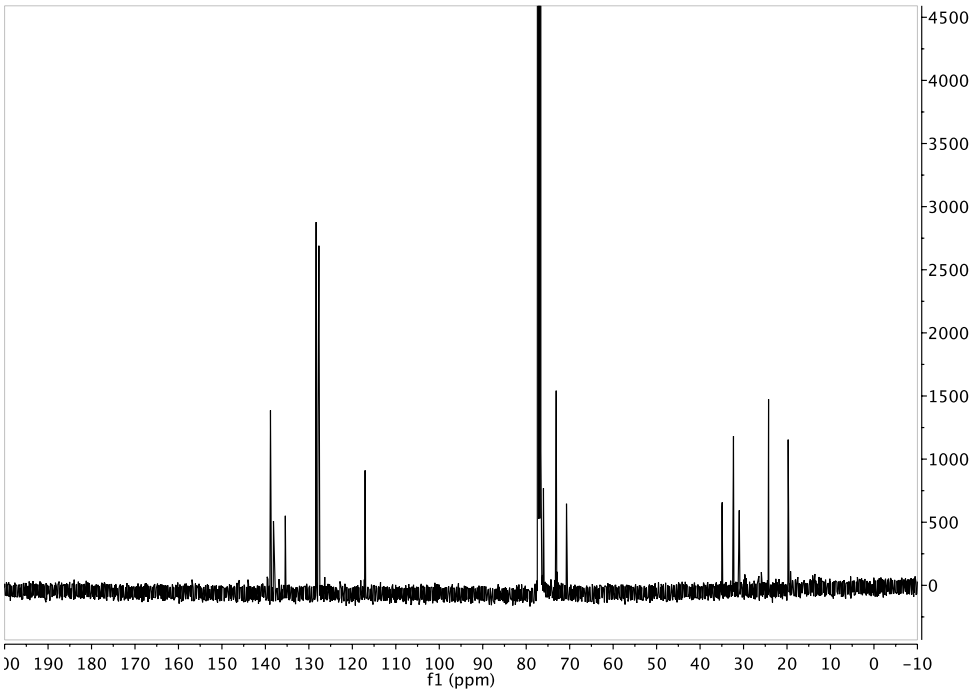
4500
4000
3500
3000
2500
2000
1500
1000
500
0
190 180 170 160 150 140 130 120 110 100 90 80 70 60 50 40 30 20 10 0 −10
f1 (ppm)

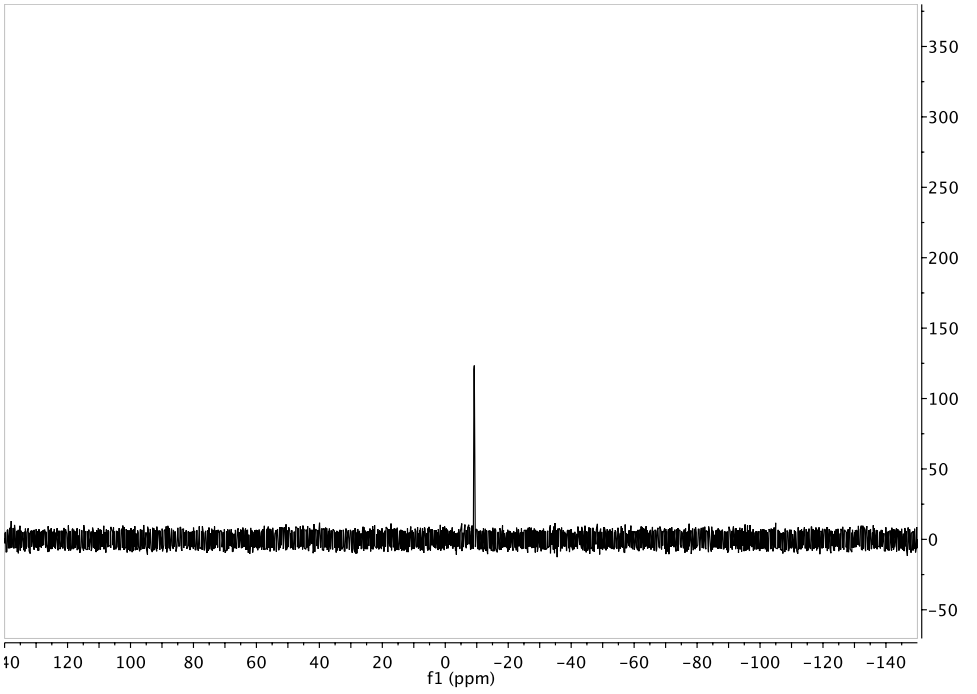
350
300
250
200
150
100
50
0
−50
120 100 80 60 40 20 0 −20 −40 −60 −80 −100 −120 −140
f1 (ppm)

5.2: A Modular Phosphate Tether-Mediated Divergent Strategy to Complex Polyols (Chapter 3)

General procedure for RCM/CM/hydrogenation (Procedure A)

To a stirring solution of triene (*S*,*S*) in freshly distilled, freeze-degas-thawed dichloroethane[4] (0.007 M) was added Hoveyda-Grubbs 2nd Gen. catalyst (HG-II) (3 mol%) and the reaction was refluxed for 2 hours. After completion of RCM (monitored by TLC), the solvent was removed under reduced pressure and olefin cross partner [3–5 equivalent with respect to the triene (*S*,*S*)] dissolved in freeze-degas-thawed CH_2Cl_2 (0.1 M) was introduced, followed by addition of HG-II (3–5 mol%). It should be noted that the use of dichloromethane was critical for successful cross-metathesis reaction in order to avoid the formation of isomerized ketone by-products. Cross-metathesis (CM) reaction in dichloroethane provided the isomerized ketone by-product (confirmed by ^{1}H and ^{13}C spectra) and the cross-metathesis product with 1:1 ratio both at 70 ºC and 90 ºC. The reaction was refluxed for an additional 2–3 hours upon which the reaction showed the CM product formation along with some amounts of RCM starting material (*S*,*S*,S_P). The reaction mixture was cooled to RT and *o*-nitrobenzenesulfonyl hydrazine (*o*-NBSH) (12 equiv.) and Et_3N (2 mL/g of *o*-NBSH) were added, upon which the reaction was stirred at RT overnight. The reaction mixture was quenched with sat. $NaHCO_3$ (1 mL), and diluted with CH_2Cl_2 (10 mL). The aqueous layer was washed with CH_2Cl_2 (3x5 mL) and the combined organic layers were dried (Na_2SO_4), concentrated under reduced pressure and purified using flash column chromatography.

(4) In CH_2Cl_2, the RCM appeared to be slower in the presence of HG-II.

General procedure for RCM/CM/hydrogenation (Procedure B)

To a stirring solution of triene (*S*,*S*) in freshly distilled, freeze-degas-thawed CH_2Cl_2 (0.007 M) was added HG-II (3 mol%) and the reaction was refluxed for 2 hours. After completion of RCM (monitored by TLC), the solvent was removed and olefin cross partner [3 equivalent with respect to the triene (*S*,*S*)] dissolved in freeze-degas-thawed CH_2Cl_2 (0.1 M) was introduced, followed by addition of HG-II (3 mol%). It should be noted that the use of dichloromethane was critical for successful CM reaction in order to avoid the formation of isomerized ketone by-products. Cross-metathesis reaction in dichloroethane provided the isomerized ketone by-product (confirmed by ^{1}H and ^{13}C spectra) and the CM product with 1:1 ratio both at 70 ºC and 90 ºC. The reaction was refluxed for an additional 2–3 hours upon which the reaction showed the CM product formation along with some amounts of RCM starting material (*S*,*S*,S_P). The reaction mixture was cooled to RT and *o*-nitrobenzenesulfonyl hydrazine (*o*-NBSH) (12 equiv.) and Et_3N (2 mL/g of *o*-NBSH) were added, upon which the reaction was stirred at RT overnight. The reaction mixture was quenched with sat. $NaHCO_3$ (1 mL), and diluted with CH_2Cl_2 (10 mL). The aqueous layer was washed with CH_2Cl_2 (3x5 mL) and the combined organic layers were dried (Na_2SO_4), concentrated under reduced pressure and purified using flash column chromatography.

General procedure for RCM/CM/hydrogenation and subsequent reduction with $LiAlH_4$ (Procedure C)

The above-mentioned procedure for one-pot RCM/CM/hydrogenation was followed and the crude product was purified using flash column chromatography.[5] To a stirring solution of the hydrogenated product in dry THF (0.5 M), $LiAlH_4$ (2–4 equiv.) was added portion wise at 0 ºC and the reaction was stirred at 0 ºC for 2 hours. After the completion of reduction, the reaction was quenched via slow sequential addition of H_2O (1 mL/g of $LiAlH_4$), 10% NaOH (1 mL/g of $LiAlH_4$), and H_2O (3 mL/g of $LiAlH_4$) [Feiser workup],[6] and the ice bath was removed and the reaction was stirred for 2 h. The reaction was filtered through Celite® and washed with EtOAc (2x5 mL). The combined organic layers were concentrated under reduced pressure and purified using flash column chromatography.

General procedure for RCM/CM/$LiAlH_4$ reduction (Procedure D)

To a stirring solution of triene (*S*,*S*) in freshly distilled, freeze-degas-thawed dichloroethane (0.007 M) was added HG-II (3 mol%) and the reaction was refluxed for 2 hours. After completion of RCM (monitored by TLC), the solvent was removed and olefin cross partner [3–5 equivalent with respect to the triene (*S*,*S*)] dissolved in freeze-degas-thawed CH_2Cl_2 (0.1 M) was introduced, followed by addition of HG-II (3–6 mol%). The reaction was refluxed for an additional 2–3 hours upon which the reaction showed the CM product formation along with some amounts of RCM starting material (*S*,*S*,S_P). After the

(5) Purification was necessary at this stage for subsequent successful LAH reduction.
(6) Fieser, L.F.; Fieser, M. Reagents for Organic Synthesis Vol. 1, Wiley, New York 1967, pp 581–595.

completion of CM, the solvent was evaporated under reduced pressure. The crude reaction mixture was then dissolved in dry THF (0.5 M) and cooled to 0 ºC. To this solution $LiAlH_4$ (4 equiv.) was added portion wise and the reaction was stirred at 0 ºC for 2 hours. After the completion of reduction, the reaction was quenched via slow sequential addition of H_2O (1 mL/g of $LiAlH_4$), 10% NaOH (1 mL/g of $LiAlH_4$), and H_2O (3 mL/g of $LiAlH_4$) [Feiser workup], and the ice bath was removed and the reaction was stirred for 2 h. The reaction was filtered through Celite® and washed with EtOAc (2x5 mL). The combined organic layers were concentrated under reduced pressure and purified using flash column chromatography.

General procedure for RCM/CM/$LiAlH_4$ reduction (Procedure E)

To a stirring solution of triene (*S*,*S*) in freshly distilled, freeze-degas-thawed CH_2Cl_2 (0.007 M) was added HG-II (3 mol%) and the reaction was refluxed for 2 hours. After completion of RCM (monitored by TLC), the solvent was removed and olefin cross partner [3 equivalent with respect to the triene (*S*,*S*)] dissolved in freeze-degas-thawed CH_2Cl_2 (0.1 M) was introduced, followed by addition of Hoveyda-Grubbs 2nd Gen. catalyst (3 mol%). The reaction was refluxed for an additional 2–3 hours upon which the reaction showed the CM product formation along with some amounts of RCM starting material (*S*,*S*,S_P). After the completion of CM, the solvent was evaporated under reduced pressure. The crude reaction mixture was then dissolved in dry THF (0.5 M) and cooled to 0 ºC. To this solution $LiAlH_4$ (4 equiv.) was added portion wise and the reaction was stirred at 0 ºC for 2 hours. After the completion of reduction, the reaction was quenched via slow sequential addition of H_2O (1 mL/g of $LiAlH_4$), 10% NaOH (1 mL/g of $LiAlH_4$), and H_2O (3 mL/g of $LiAlH_4$)

[Feiser workup], and the ice bath was removed and the reaction was stirred for 2 h. The reaction was filtered through Celite® and washed with EtOAc (2x5 mL). The combined organic layers were concentrated under reduced pressure and purified using flash column chromatography.

General procedure for RCM/CM/ $LiAlH_4$ reduction and subsequent global hydrogenation (Procedure F)

The above-mentioned procedure (D or E) was followed to obtain the reduced product and the crude product was dissolved in CH_2Cl_2 (0.1 M) and *o*-nitrobenzenesulfonyl hydrazine (*o*-NBSH) (20 equiv.) and Et_3N (2 mL/g of *o*-NBSH) were added, upon which the reaction was stirred at RT overnight. The reaction mixture was quenched with sat. $NaHCO_3$ (1 mL) and diluted with CH_2Cl_2 (10 mL). The aqueous layer was washed with CH_2Cl_2 (3x5 mL) and the combined organic layers were dried (Na_2SO_4), concentrated under reduced pressure and purified using flash column chromatography.

(1*S*,3*S*,6*S*,8*R*)-3-((benzyloxy)methyl)-8-((3*R*,4*S*)-4-(4-bromophenyl)-4-hydroxy-3-methylbutyl)-2,9,10-trioxa-1-phosphabicyclo[4.3.1]dec-4-ene 1-oxide (3.6.3):

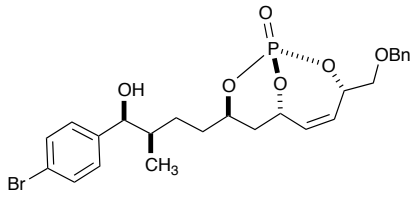

Synthesized by following procedure A

Yield: 40% over 3 reactions (72% avg/rxn, 12.4 mg isolated starting from 20 mg of triene)

FTIR (thin film): 3400, 2974, 2285, 1630, 1288, 1209, 1101, 977, 848 cm^{-1};

Optical Rotation: $[\alpha]_D$ = + 17.34(*c* = 1, $CHCl_3$);

^{1}H NMR (500 MHz, $CDCl_3$) δ 7.50–7.43 (m, 2H, aromatic), 7.40–7.29 (m, 5H, aromatic), 7.21–7.16 (m, 2H, aromatic), 6.01 (ddd, *J* = 11.9, 3.0, 2.1 Hz, 1H, CH=C<u>H</u>CHOPCH$_2$OBn), 5.56 (ddd, *J* = 11.9, 3.9, 2.4 Hz, 1H, C<u>H</u>=CHCHOPCH$_2$OBn), 5.27 (dddd, *J* = 5.3, 5.3, 2.6, 2.6 Hz, 1H, CH=CHC<u>H</u>OPCH$_2$OBn), 5.18 (dddd, $J_{PH,}$ = 24.6, J_{HH} =6.2, 4.1, 1.9 Hz, 1H, CH$_2$C<u>H</u>OPCH=CH), 4.65–4.58 (m, 2H, CH$_2$OC<u>H$_2$</u>Ph), 4.58–4.47 (m, 2H, 4-BrC$_6$H$_4$C<u>H</u>OH, CH$_2$CH$_2$C<u>H</u>OP), 3.71 (ddd, *J* = 10.3, 5.1, 1.2 Hz, 1H, C<u>H$_2$</u>OBn), 3.61 (dd, *J* = 10.2, 6.0 Hz, 1H, C<u>H$_2$</u>OBn), 2.16 (ddd, *J* = 14.7, 12.0, 6.2 Hz, 1H, CHOPC<u>H$_2$</u>CHOP), 1.88 (d, *J* = 3.5 Hz, 1H, OH), 1.87–1.71 (m, 2H, 4-BrC$_6$H$_4$CHOHC<u>H</u>(CH$_3$)CH$_2$, C<u>H$_2$</u>CHOPCH$_2$CHOP), 1.67 (ddd, *J* = 14.6, 3.5, 2.0 Hz, 1H, CHOPC<u>H$_2$</u>CHOP), 1.58–1.48 (m, 1H, C<u>H$_2$</u>CHOPCH$_2$CHOP), 1.48–1.40 (m, 1H, C<u>H$_2$</u>CH$_2$CHOPCH$_2$CHOP), 1.39–1.30 (m, 1H, C<u>H$_2$</u>CH$_2$CHOPCH$_2$CHOP), 0.88 (d, *J* = 6.7 Hz, 3H, 4-BrC$_6$H$_4$CHOHCH(C<u>H$_3$</u>)CH$_2$);

^{13}C NMR (126 MHz, $CDCl_3$) δ 142.4, 137.5, 131.3 (2C), 129.9, 129.6, 128.5 (2C), 128.0 (2C), 127.9, 127.7 (2C), 121.1, 77.3 (d, J_{CP} = 6.8 Hz), 77.0, 76.8 (d, J_{CP} = 7.2 Hz), 73.5, 72.2 (d, J_{CP} = 6.1 Hz), 71.2 (d, J_{CP} = 12.2 Hz), 39.9, 34.8 (d, J_{CP} = 6.0 Hz), 33.5 (d, J_{CP} = 9.3 Hz), 27.9, 14.0;

^{31}P NMR (162 MHz, $CDCl_3$) δ –5.30;

HRMS: cald. for $C_{25}H_{30}BrO_6P$ $(M+Na)^+$ 559.0861; found (TOF MS ES+) 559.0856.

(1*S*,2*R*,5*R*,7*S*,10*S*,*Z*)-11-(benzyloxy)-1-(4-bromophenyl)-2-methylundec-8-ene-1,5,7,10-tetraol (3.6.4)

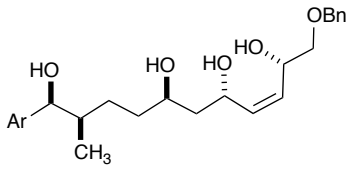

Synthesized by following procedure C

Yield: 26% over 4 reactions (71% avg/rxn, 10 mg isolated starting from 28 mg of triene);

FTIR (thin film): 3365, 3294, 2943, 2872, 2349, 2872, 1631, 1485, 1454, 1070, 1028, 827, 750, 698 cm^{-1};

Optical Rotation: $[\alpha]_D$ = + 5.0 (*c* = 0.12, $CHCl_3$);

^{1}H NMR (500 MHz, $CDCl_3$) δ 7.50–7.44 (m, 2H, aromatic), 7.39–7.28 (m, 5H, aromatic), 7.22–7.17 (m, 2H, aromatic), 5.71 (ddd, *J* = 11.5, 7.3, 1.4 Hz, 1H, CHOHC<u>H</u>=CHCHOHCH$_2$OBn), 5.50 (ddd, *J* = 11.4, 7.3, 1.3 Hz, 1H, CHOHCH=C<u>H</u>CHOHCH$_2$OBn), 4.85–4.77 (m, 1H, C<u>H</u>OHCH=CHCHOHCH$_2$OBn), 4.75–4.69 (m, 1H, CHOHCH=CHC<u>H</u>OHCH$_2$OBn), 4.62–4.54 (m, 3H, 4-BrC$_6$H$_4$C<u>H</u>OHCH(CH$_3$)CH$_2$, CH$_2$OC<u>H</u>$_2$Ph), 3.88 (bs, 1H, OH), 3.76–3.68 (m, 1H, CH$_2$C<u>H</u>OHCH$_2$CHOHCH=CH), 3.50 (dd, J = 9.4, 4.1 Hz, 1H, C<u>H</u>$_2$OBn), 3.45 (dd, J = 9.4, 7.6 Hz, 1H, C<u>H</u>$_2$OBn), 1.84–1.74 (m, 1H, 4-BrC$_6$H$_4$CHOHC<u>H</u>(CH$_3$)CH$_2$), 1.72–1.68 (m, 1H, OH), 1.67–1.62 (m, 2H, CHOHC<u>H</u>$_2$CHOH), 1.46–1.37 (m, 2H, CH$_2$C<u>H</u>$_2$CHOHCH$_2$CHOH), 1.26 (s, 4H, OH, C<u>H</u>$_2$CH$_2$CHOHCH$_2$CHOH), 0.88 (d, *J* = 6.8 Hz, 3H, 4-BrC$_6$H$_4$CHOHCH(C<u>H</u>$_3$)CH$_2$).

^{13}C NMR (126 MHz, $CDCl_3$) δ 142.5, 137.5, 136.5, 131.2 (2C), 129.2, 128.5 (2C), 128.0 (2C), 127.99, 127.9 (2C), 120.9, 76.9, 73.6, 73.5, 67.3, 66.2, 62.9, 42.6, 40.0, 28.9, 28.8, 14.3.

HRMS: cald. for $C_{25}H_{33}BrO_5$ $(M+Na)^+$ 515.1409; found (TOF MS ES+) 515.1398.

(1*S*,2*R*,3*E*,5*S*,7*S*,8*Z*,10*S*)-11-(benzyloxy)-1-(4-bromophenyl)-2-methylundeca-3,8-diene-1,5,7,10-tetraol (3.7.2):

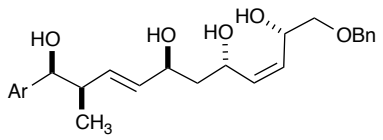

Synthesized by following procedure D

Yield: 35% over 3 reactions (70% avg/rxn, 9.7 mg isolated starting from 20 mg of triene)

FTIR (thin film): 3440, 3417, 3386, 2390, 1643, 1633, 1054, 698, 522 cm^{-1};

Optical Rotation: $[\alpha]_D = -4.81$ ($c = 0.22$, $CHCl_3$)

^{1}H NMR (500 MHz, $CDCl_3$) δ 7.47–7.43 (m, 2H, aromatic), 7.37–7.29 (m, 5H, aromatic), 7.18–7.12 (m, 2H, aromatic), 5.68 (ddd, *J* = 11.4, 7.6, 1.4 Hz, 1H, CHOHC<u>H</u>=CH$_{cis}$CHOHCH$_2$OBn), 5.61 (ddd, *J* = 15.6, 7.0, 1.0 Hz, 1H, C<u>H</u>=CH$_{trans}$CHOHCH$_2$CHOH), 5.53 (d, *J* = 6.2 Hz, 1H, CH=C<u>H</u>$_{trans}$CHOHCH$_2$CHOH), 5.48 (ddd, *J* = 11.4, 7.4, 1.3 Hz, 1H, CH=CH$_{cis}$C<u>H</u>OHCH$_2$CHOH), 4.76 (dd, *J* = 7.9, 2.9 Hz, 1H, C<u>H</u>OHCH=CHCHOHCH$_2$OBn), 4.68 (ddd, *J* = 7.5, 4.1, 1.4 Hz, 1H, CHOHCH=CHC<u>H</u>OHCH$_2$OBn), 4.59 (d, *J* = 5.1 Hz, 1H, 4-BrC$_6$H$_4$C<u>H</u>OHCH(CH$_3$)CH$_2$), 4.56 (bs, 2H, C<u>H</u>$_2$OBn), 4.35 (dd, *J* = 6.6, 10.4 Hz, 1H, CH=CHC<u>H</u>OHCH$_2$CHOH), 3.55 (s, 1H, OH), 3.48 (dd, *J* = 9.5, 4.1 Hz, 1H, C<u>H</u>$_2$OBn), 3.44 (dd, *J* = 9.5, 7.5 Hz, 1H, C<u>H</u>$_2$OBn), 3.16 (s, 1H, OH), 2.90 (s, 1H, OH), 2.52 (dd, *J* = 12.6, 6.7 Hz, 1H, 4-BrC$_6$H$_4$CHOHC<u>H</u>(CH$_3$)CH$_2$), 2.46 (s, 1H, OH), 1.74 (ddd, *J* = 14.4, 8.7, 3.8 Hz, 1H, CHOHC<u>H</u>$_2$CHOH), 1.61 (ddd, *J* = 14.3, 7.5, 3.3 Hz, 1H, CHOHC<u>H</u>$_2$CHOH), 0.96 (d, *J* = 6.8 Hz, 3H, 4-BrC$_6$H$_4$CHOHCH(C<u>H</u>$_3$)CH$_2$);

^{13}C NMR (126 MHz, $CDCl_3$) δ 141.6, 137.5, 136.3, 133.8, 132.5, 131.1 (2C), 129.2, 128.5 (2C), 128.1 (2C), 127.9, 127.9 (2C), 121.0, 76.6, 73.6, 73.5, 70.1, 67.2, 65.7, 43.3, 42.8, 14.0;

HRMS: cald. for $C_{25}H_{31}BrO_5$ $(M+Na)^+$513.1253; found (TOF MS ES+) 513.1237.

(1*S*,3*S*,6*S*,8*R*)-8-((*S*)-5-(benzyloxy)-4-hydroxypentyl)-3-((benzyloxy)methyl)-2,9,10-trioxa-1-phosphabicyclo[4.3.1]dec-4-ene 1-oxide (3.10.3)

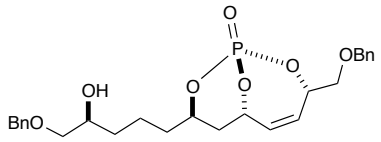

Synthesized by following procedure A

Yield: 35% over 3 reactions (70% avg/rxn, 14.2 mg isolated staring from 30 mg of triene);

FTIR (thin film): 3520, 3444, 2395, 1633, 1286, 1101, 973, 734 cm^{-1};

Optical Rotation: $[\alpha]_D = +21.57$(c = 0.26, $CHCl_3$);

^{1}H NMR (500 MHz, $CDCl_3$) δ 7.42–7.28 (m, 10H, aromatic), 6.02 (ddd, J = 11.9, 3.0, 2.1 Hz, 1H,CH=C<u>H</u>CHOPCH$_2$OBn), 5.57 (ddd, J = 11.9, 3.9, 2.4 Hz, 1H, C<u>H</u>=CHCHOPCH$_2$OBn), 5.28 (ddddd, J = 5.3, 5.3, 2.7, 2.7, 2.7 Hz, 1H, CH=CHC<u>H</u>OPCH$_2$OBn), 5.19 (ddddd, J_{PH} = 24.5, J_{HH} = 6.2, 4.1, 1.8, 1.8 Hz, 1H, CH$_2$C<u>H</u>OPCH=CH), 4.66–4.52 (m, 5H, CH$_2$OC<u>H$_2$</u>Ph, CH$_2$CH$_2$CH$_2$C<u>H</u>OP), 3.84–3.77 (m, 1H, CH$_2$C<u>H</u>OHCH$_2$OBn), 3.72 (ddd, J = 10.2, 5.1, 1.1 Hz, 1H, C<u>H$_2$</u>OBn), 3.61 (dd, J = 10.2, 6.1 Hz, 1H, C<u>H$_2$</u>OBn), 3.50 (dd, J = 9.4, 3.1 Hz, 1H, C<u>H$_2$</u>OBn), 3.32 (dd, J = 9.4, 7.9 Hz, 1H, C<u>H$_2$</u>OBn), 2.34 (d, J = 3.4 Hz, 1H, BnOCH$_2$CHO<u>H</u>CH$_2$CH$_2$CH$_2$CHOP), 2.22–2.12 (m, 2H, CHOPC<u>H$_2$</u>CHOP), 1.83–1.55 (m, 4H, BnOCH$_2$CHOHCH$_2$C<u>H$_2$</u>C<u>H$_2$</u>CHOP), 1.52–1.37 (m, 2H, BnOCH$_2$CHOHC<u>H$_2$</u>CH$_2$CH$_2$CHOP);

^{13}C NMR (126 MHz, $CDCl_3$) δ 137.8, 137.5, 129.9, 129.6, 128.5 (4C), 127.9, 127.8, 127.7 (4C), 77.3 (d, J_{CP} = 6.7 Hz), 76.6 (d, J_{CP} = 6.8 Hz), 74.4, 73.5, 73.4, 72.1 (d, J_{CP} = 6.0 Hz), 71.2 (d, J_{CP} = 12.2 Hz), 70.0, 35.4 (d, J_{CP} = 9.3 Hz), 34.7 (d, J_{CP} = 6.0 Hz), 32.4, 20.5;

^{31}P NMR (162 MHz, $CDCl_3$) δ –5.46;

HRMS: cald. for $C_{26}H_{33}O_7PNa$ $(M+Na)^+$ 511. 1862; found (TOF MS ES+) 511.1847.

(2*S*,5*S*,7*R*,11*S*,*Z*)-1,12-bis(benzyloxy)dodec-3-ene-2,5,7,11-tetraol (3.10.4)

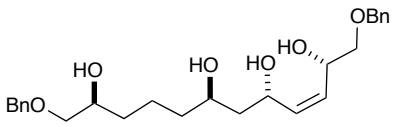

Synthesized by following procedure C

Yield: 23% over 4 reactions (69% avg/rxn, 8 mg isolated starting from 20 mg of triene);

FTIR (thin film): 3400, 3290, 2943, 2350, 1631, 1480, 1070, 750, 698 cm^{-1};

Optical Rotation: $[\alpha]_D$ = + 6.32(*c* = 0.19, $CHCl_3$);

^{1}H NMR (500 MHz, $CDCl_3$) δ 7.40–7.28 (m, 10H, aromatic), 5.70 (ddd, *J* = 11.5, 7.5, 1.4 Hz, 1H, CHOHC<u>H</u>=CHCHOHCH$_2$OBn), 5.48 (ddd, *J* = 11.4, 7.4, 1.4 Hz, 1H, CHOHCH=C<u>H</u>CHOHCH$_2$OBn), 4.80 (ddd, *J* = 10.4, 7.3, 3.4 Hz, 1H, C<u>H</u>OHCH=CHCHOHCH$_2$OBn), 4.75–4.67 (m, 1H, CHOHCH=CHC<u>H</u>OHCH$_2$OBn), 4.59–4.53 (m, 4H, CH$_2$OC<u>H$_2$</u>Ph), 3.97–3.88 (m, 1H, CH$_2$C<u>H</u>OHCH$_2$CHOHCH=CH), 3.88–3.79 (m, 1H, BnOCH$_2$C<u>H</u>OHCH$_2$CH$_2$CH$_2$), 3.56–3.41 (m, 4H, C<u>H$_2$</u>OBn), 3.40–3.29 (m, 2H, BnOC<u>H$_2$</u>CHOHCH$_2$CH$_2$CH$_2$), 1.66 (ddd, *J* = 14.5, 7.5, 2.6 Hz, 1H, CHOHC<u>H$_2$</u>CHOH), 1.63–1.57 (m, 3H, CHOHC<u>H$_2$</u>CHOH, BnOCH$_2$CHOHC<u>H$_2$</u>CH$_2$CH$_2$, O<u>H</u>), 1.53–1.35 (m, 6H, BnOCH$_2$CHOHC<u>H$_2$</u>C<u>H$_2$</u>C<u>H$_2$</u>CHOH);

^{13}C NMR (126 MHz, $CDCl_3$) δ 137.9, 137.6, 136.5, 129.2, 128.5 (2C), 128.46 (2C), 127.9, 127.85 (2C), 127.8, 127.7 (2C), 74.5, 73.6, 73.4, 73.3, 70.23, 68.8, 67.1, 66.1, 42.7, 37.2, 32.8, 21.5;

HRMS: cald. for $C_{26}H_{36}O_6$ $(M+Na)^+$ 467.2410; found (TOF MS ES+) 467.2413.

(2*S*,3*Z*,5*S*,7*S*,8*E*,11*S*)-1,12-bis(benzyloxy)dodeca-3,8-diene-2,5,7,11-tetraol (3.11.2)

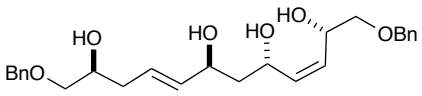

Synthesized by following procedure D

Yield: 40% over 3 reactions (72% avg/rxn, 14 mg isolated starting from 18 mg of triene);

FTIR (thin film): 3408, 3402, 3385, 2918, 2852, 2349, 1637, 1632, 1072, 1027, 972, 737, 698 cm^{-1};

Optical Rotation: $[\alpha]_D$ = +5.92(*c* = 0.14, $CHCl_3$);

^{1}H NMR (500 MHz, $CDCl_3$) δ 7.42–7.28 (m, 10H, aromatic), 5.75–5.64 (m, 2H, CHOHC<u>H</u>=C<u>H</u>CHOHCH$_2$OBn), 5.62–5.53 (m, 1H, BnOCH$_2$CHOHCH$_2$CH=C<u>H</u>CHOH), 5.48 (ddd, *J* = 11.3, 7.4, 1.3 Hz, 1H, BnOCH$_2$CHOHCH$_2$C<u>H</u>=CHCHOH), 4.78 (ddd, *J* = 7.8, 7.8, 3.0 Hz, 1H, C<u>H</u>OHCH=CHCHOHCH$_2$OBn), 4.70 (dddd, *J* = 7.5, 7.5, 4.3, 1.4 Hz, 1H, CHOHCH$_2$CHOHCH=CHC<u>H</u>OHCH$_2$OBn), 4.59–4.52 (m, 4H, CH$_2$OC<u>H$_2$</u>Ph), 4.42–4.35 (m, 1H, CHOHCH$_2$CH=CHC<u>H</u>OH), 3.90–3.82 (m, 1H, BnOCH$_2$C<u>H</u>OHCH$_2$CH=CH), 3.54–3.40 (m, 4H, BnOC<u>H$_2$</u>CHOH, OH), 3.36 (dd, *J* = 9.5, 7.3 Hz, 2H, BnOC<u>H$_2$</u>CHOH), 2.30–2.13 (m, 4H, BnOCH$_2$CHOHC<u>H$_2$</u>CH=CH), 1.77 (ddd, *J* = 14.3, 8.6, 3.6 Hz, 1H, CHOHC<u>H$_2$</u>CHOH), 1.64 (ddd, *J* = 14.4, 7.7, 3.3 Hz, 1H, CHOHC<u>H$_2$</u>CHOH);

^{13}C NMR (126 MHz, $CDCl_3$) δ 137.8, 137.6, 136.3, 135.5, 129.3, 128.5 (2C), 128.4 (2C), 127.9, 127.85 (2C), 127.8, 127.7 (2C), 126.7, 77.2, 73.9, 73.6, 73.4, 73.3, 69.9, 67.1, 65.6, 42.6, 36.2;

HRMS: cald. for $C_{26}H_{34}O_6$ $(M+Na)^+$ 465.2253; found (TOF MS ES+) 465.2236.

(2*S*,5*R*,7*R*,11*S*)-1,12-bis(benzyloxy)dodecane-2,5,7,11-tetraol (3.12.1)

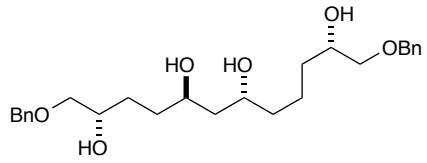

Synthesized by following procedure F

Yield: 34% over 4 reactions (77% avg/rxn, 12 mg isolated starting from 28 mg of triene);

FTIR (thin film): 3283, 2943, 2394, 1454, 1093, 1076, 737 cm^{-1};

Optical Rotation: $[\alpha]_D$ = + 2.80 (*c* = 0.25, $CHCl_3$);

^{1}H NMR (500 MHz, $CDCl_3$) δ 7.40–7.29 (m, 10H, aromatic), 4.60–4.52 (m, 4H, CH$_2$OC<u>H$_2$</u>Ph), 4.04–3.91 (m, 2H, C<u>H</u>OHCH$_2$C<u>H</u>OH), 3.92–3.76 (m, 2H, C<u>H</u>OHCH$_2$OBn), 3.51 (ddd, *J* = 9.5, 4.9, 3.2 Hz, 2H, BnOC<u>H$_2$</u>CHOH), 3.36 (ddd, *J* = 17.2, 9.4, 8.0 Hz, 2H,

BnOC$\underline{H}_2$CHOH), 2.80 (s, 1H, OH), 2.61 (s, 1H, OH), 2.40 (bs, 1H, OH), 1.70–1.37 (m, 13H, aliphatic, OH).

^{13}C NMR (126 MHz, $CDCl_3$) δ 137.9, 137.8, 128.5 (4C), 127.9, 127.8, 127.77 (2C), 127.75 (2C), 74.3, 74.5, 73.3 (2C), 70.4, 70.3, 69.3, 69.0, 42.3, 37.2, 33.5, 32.8, 29.1, 21.6.

HRMS: cald. for $C_{26}H_{38}O_6$ $(M+Na)^+$ 469.2566; found (TOF MS ES+) 469.2567.

(1*S*,3*S*,6*S*,8*R*)-3-((benzyloxy)methyl)-8-((3*R*,4*S*)-4-(4-bromophenyl)-4-hydroxy-3-methylbutyl)-2,9,10-trioxa-1-phosphabicyclo[4.3.1]dec-4-ene 1-oxide (3.6.3):

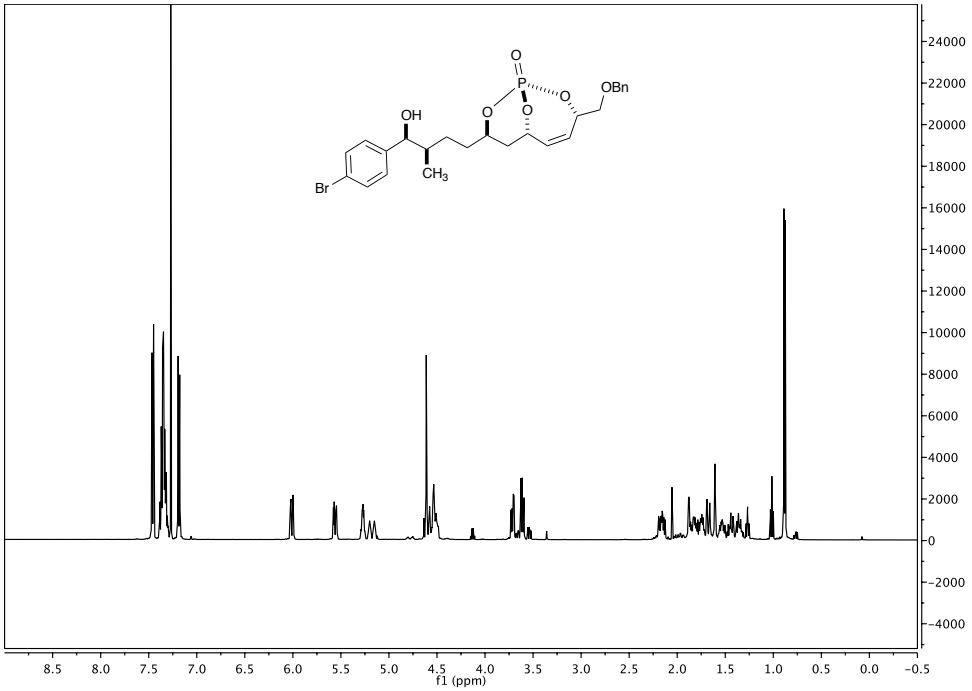

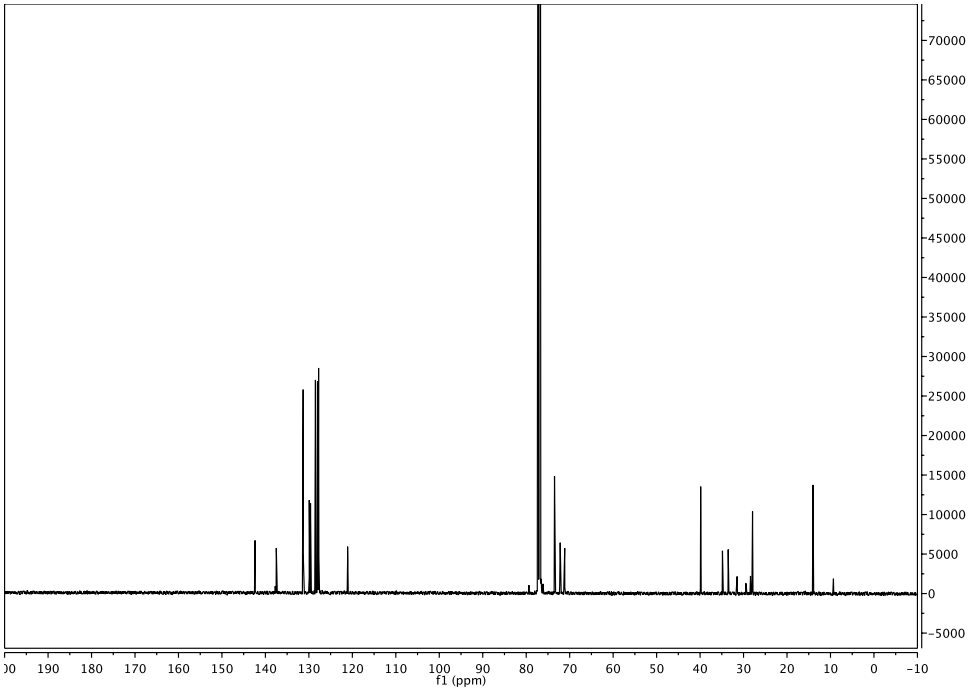

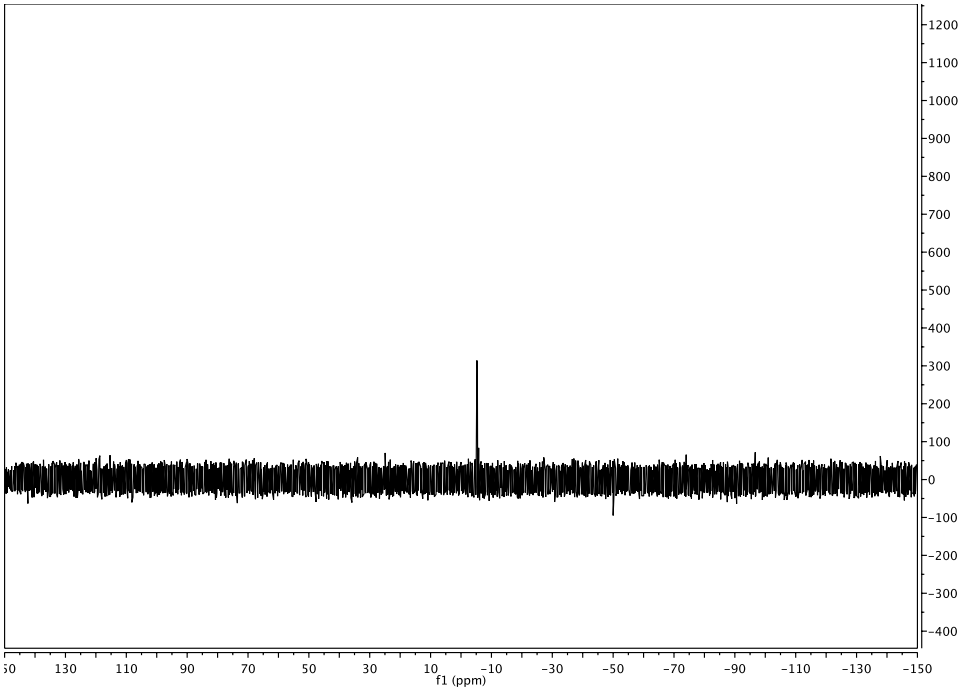

(1*S*,2*R*,5*R*,7*S*,10*S*,*Z*)-11-(benzyloxy)-1-(4-bromophenyl)-2-methylundec-8-ene-1,5,7,10-tetraol (3.6.4):

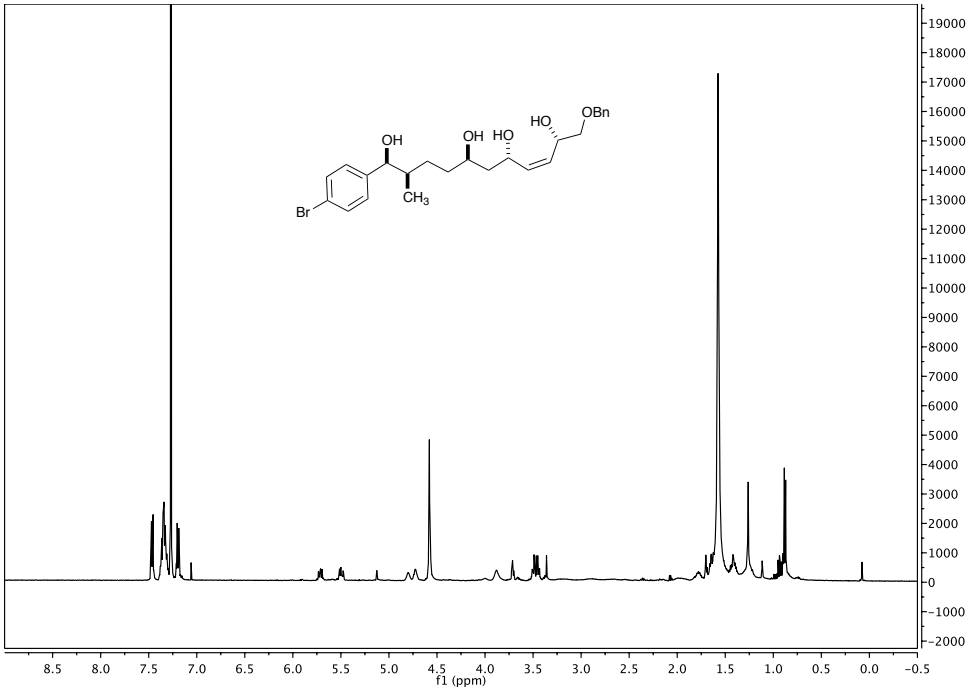

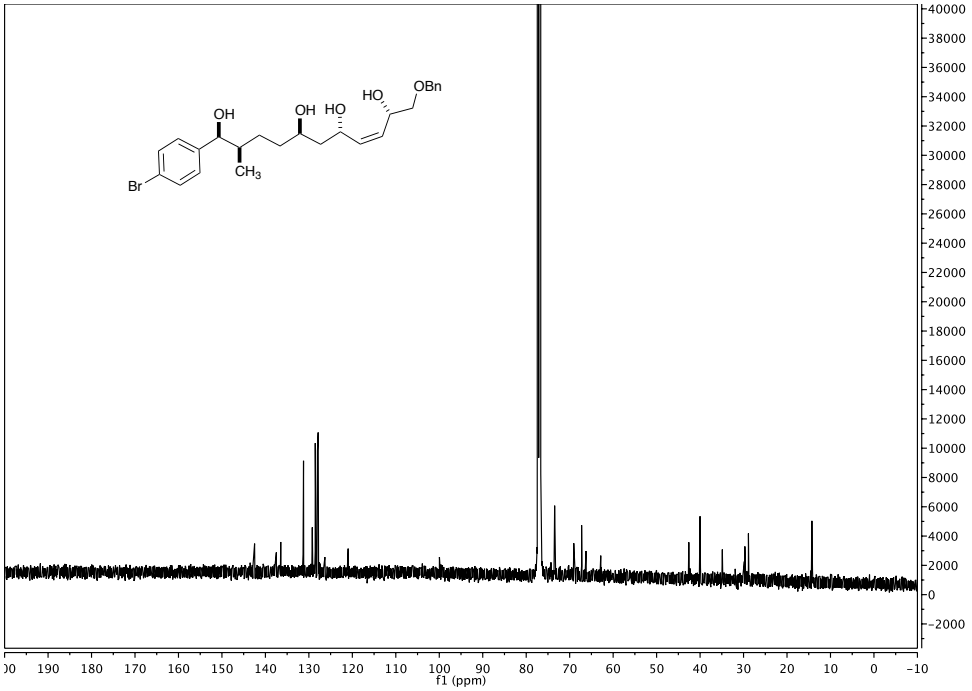

(1*S*,2*R*,3*E*,5*S*,7*S*,8*Z*,10*S*)-11-(benzyloxy)-1-(4-bromophenyl)-2-methylundeca-3,8-diene-1,5,7,10-tetraol (3.7.2):

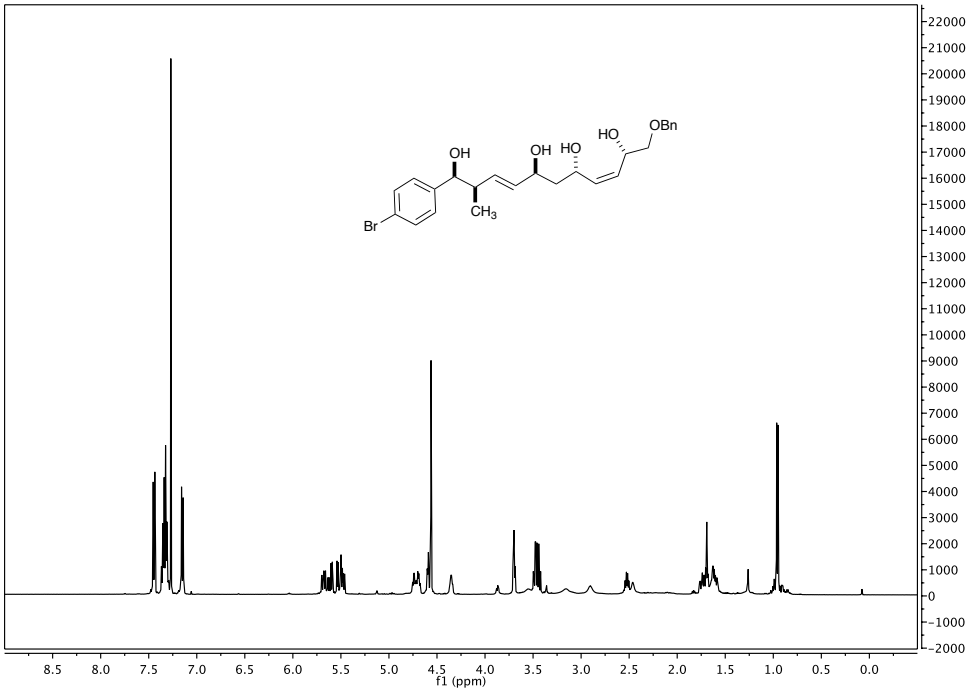

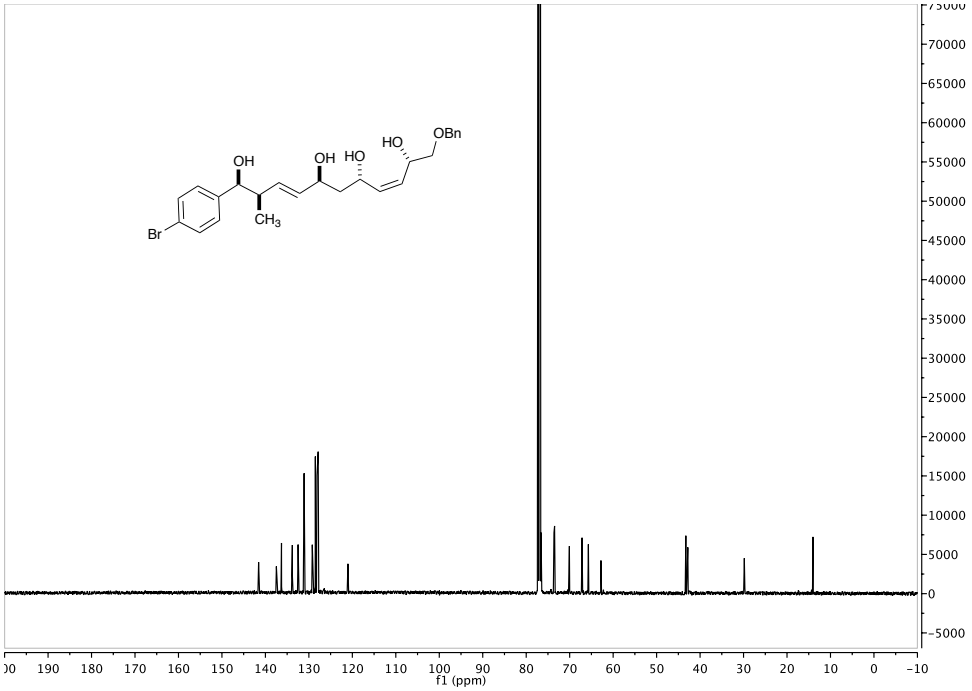

(1*S*,3*S*,6*S*,8*R*)-8-((*S*)-5-(benzyloxy)-4-hydroxypentyl)-3-((benzyloxy)methyl) -2,9,10-trioxa-1-phosphabicyclo[4.3.1]dec-4-ene 1-oxide (3.10.3):

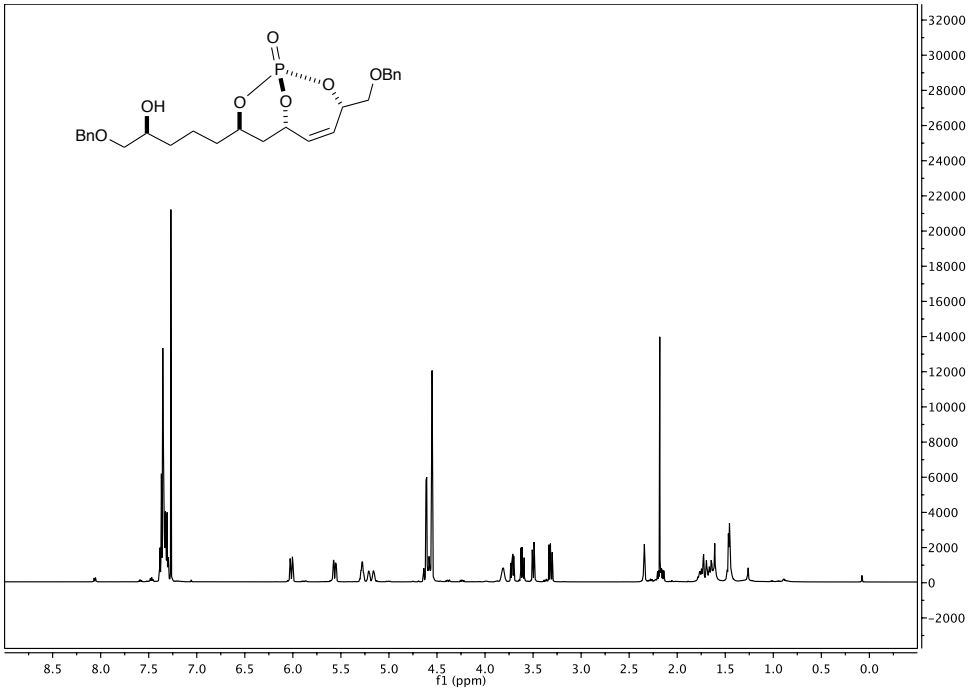

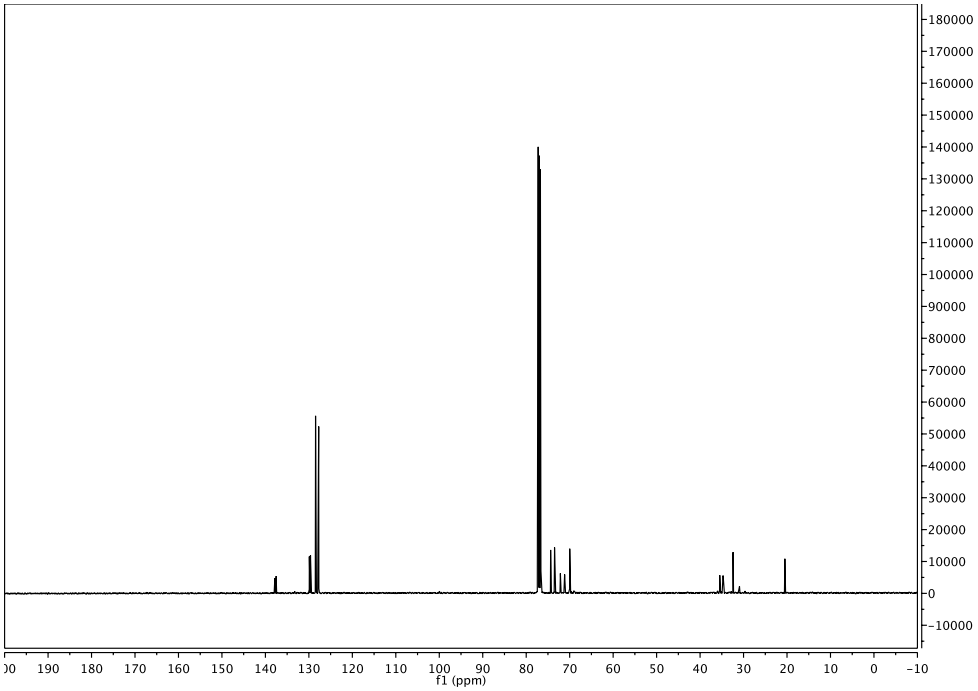
f1 (ppm)

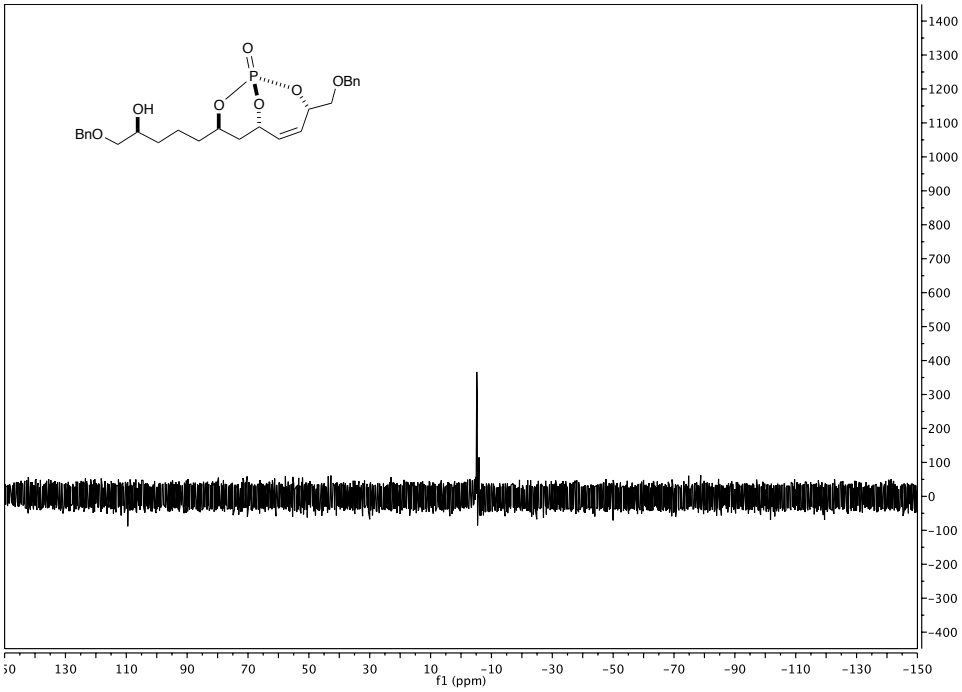
O
P
O
O
O
OBn
OH
BnO
f1 (ppm)

(2*S*,5*S*,7*R*,11*S*,*Z*)-1,12-bis(benzyloxy)dodec-3-ene-2,5,7,11-tetraol (3.10.4):

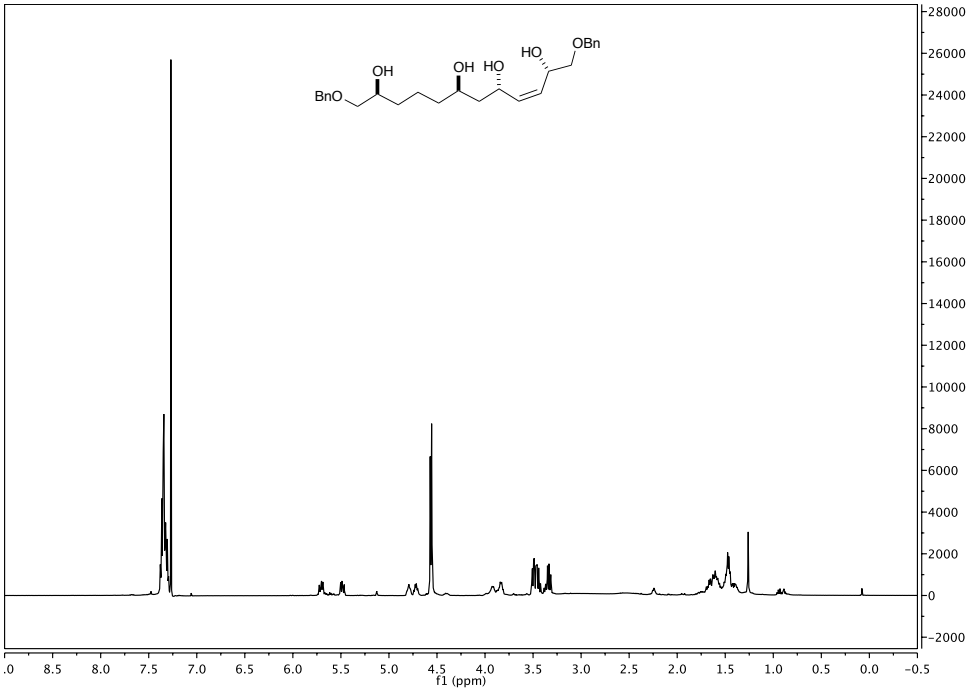

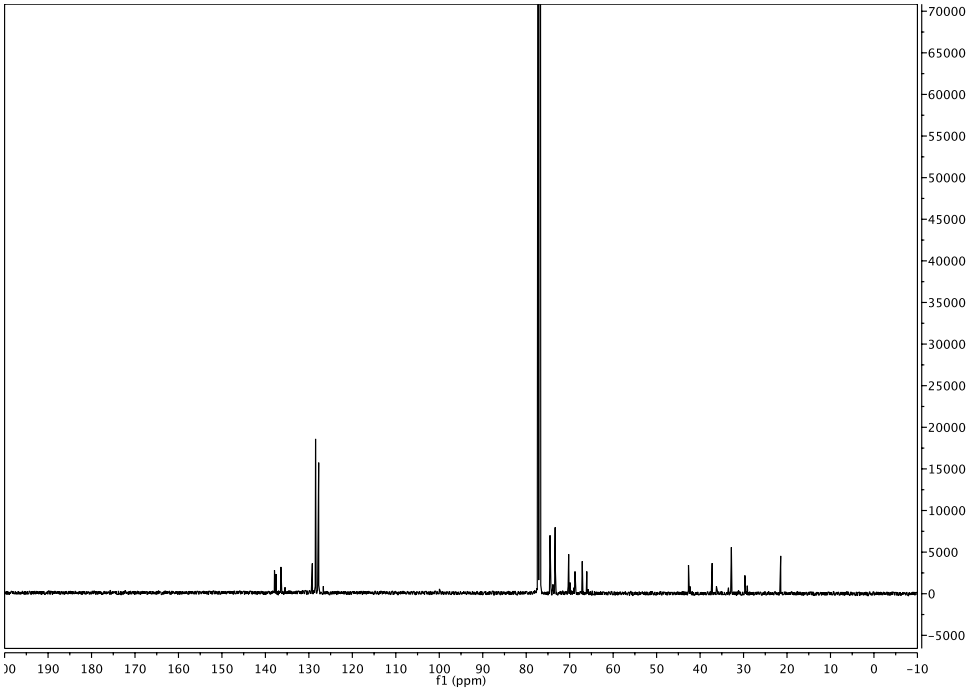

(2*S*,3*Z*,5*S*,7*S*,8*E*,11*S*)-1,12-bis(benzyloxy)dodeca-3,8-diene-2,5,7,11-tetraol (3.11.2):

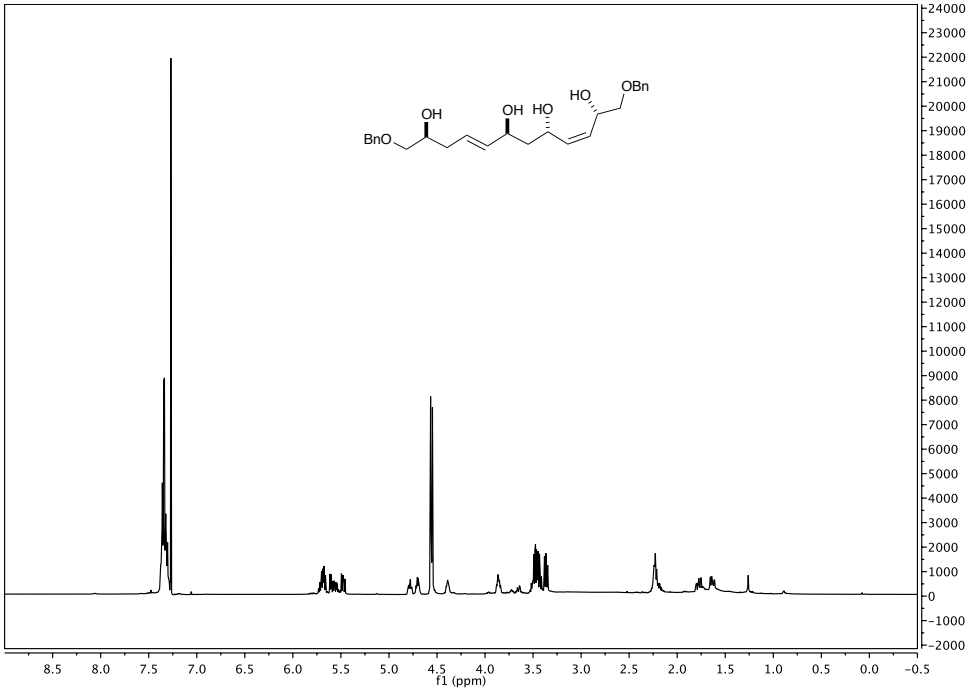

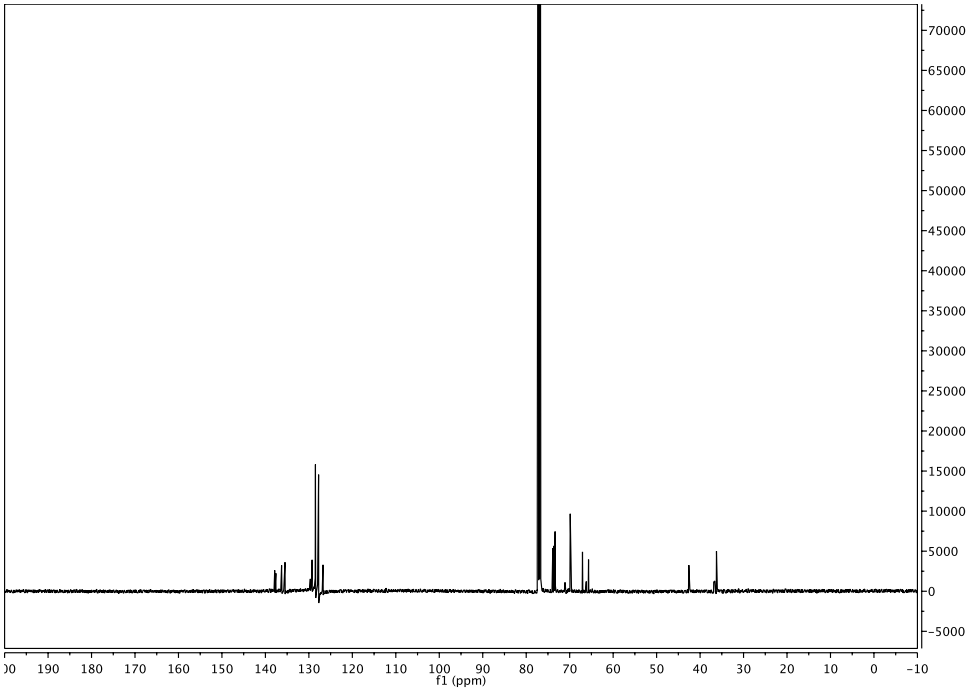

(2*S*,5*R*,7*R*,11*S*)-1,12-bis(benzyloxy)dodecane-2,5,7,11-tetraol (3.12.1):

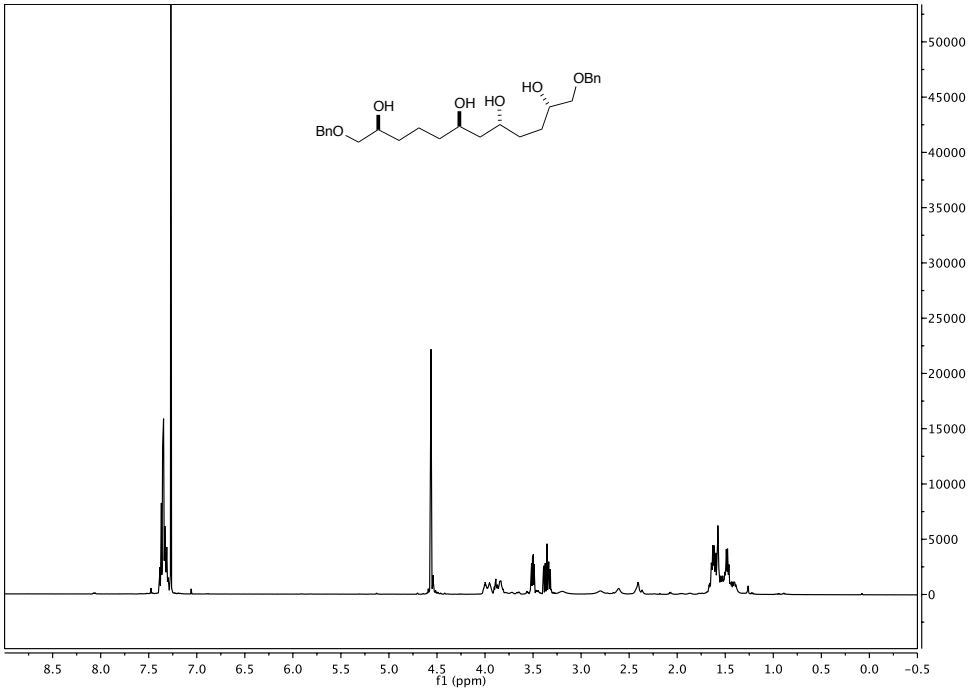

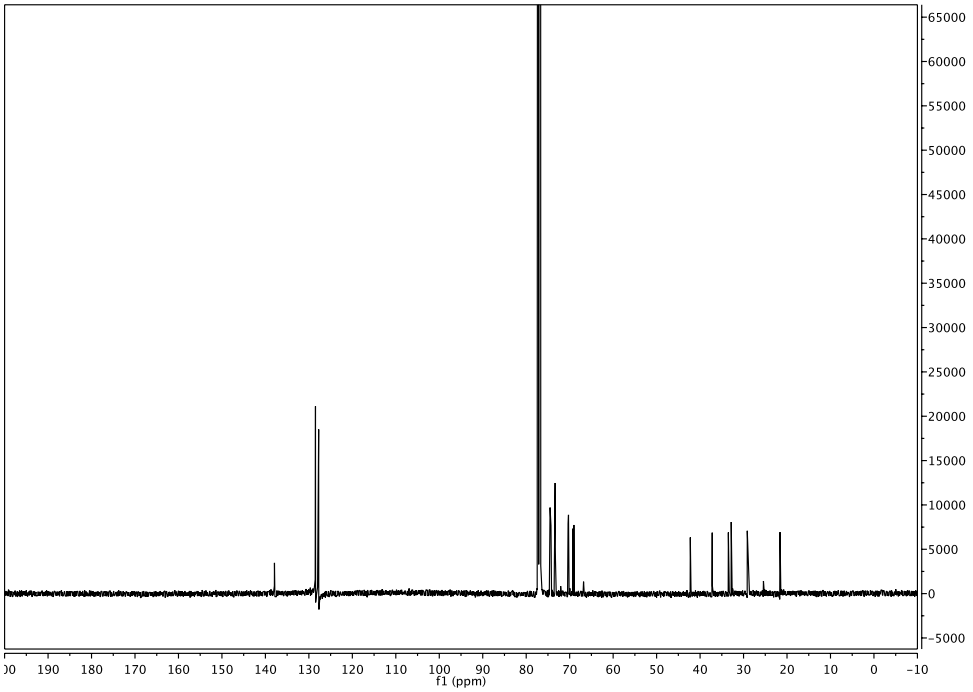

5.3. Phosphate tether-mediated approach towards the synthesis of the C9–C25 fragment of spirastrellolide B (Chapter 3)

Experimental section:

(2*S*,3*S*)-ethyl 3-(5-bromofuran-2-yl)-2,3-dihydroxypropanoate (4.20.4A)

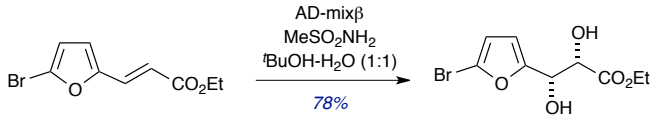

4.20.4 **4.20.4A** (not numbered in the scheme)

To a solution of α,β-unsaturated furan **4.20.4** (1 mmol) dissolved in *t*BuOH-H_2O (1:1, 0.2 M each) were added AD-mix-α (1.4 g/mmol) and $CH_3SO_2NH_2$ (2 mmol) at room temperature. The orange colored reaction mixture was then stirred at room temperature for 24 hours. The reaction mixture was quenched with solid Na_2SO_3 and stirred vigorously for several hours till the disappearance of the yellow color. The reaction mixture was filtered through celite, the aqueous layer was extracted with EtOAc (2 X 20 mL) and evaporated after drying over Na_2SO_4. The crude product was purified via flash chromatography

Yield: 78% (886 mg isolated as a cream colored solid from 1g of α,β-unsaturated furan **4.20.4**);

FTIR (thin film): 3344, 1732, 1497, 1319, 1119, 1014, 795 cm^{-1};

Optical Rotation: $[\alpha]_D$ = +3.13 (*c* = 0.6, $CHCl_3$);

^{1}H NMR (500 MHz, $CDCl_3$) δ 6.40 (dd, *J* = 3.3, 0.9 Hz, 1H), 6.28 (d, *J* = 3.3 Hz, 1H), 4.98 (d, *J* = 2.7 Hz, 1H), 4.49 (d, *J* = 2.7 Hz, 1H), 4.32 (d, *J* = 7.1 Hz, 1H), 4.29 (d, *J* = 7.1 Hz, 1H), 3.10 (s, 1H), 1.32 (t, *J* = 7.1 Hz, 3H), 1.20 (d, *J* = 6.1 Hz, 1H);

^{13}C NMR (126 MHz, $CDCl_3$) δ 172.2, 154.9, 121.6, 112.1, 110.4, 72.2, 68.7, 62.6, 14.1;

HRMS cald for $C_9H_{11}BrO_5Na$ $(M+Na)^+$ 300.9688; found 300.9662, 302.9638 (TOF MS ES+).

(4*S*,5*S*)-ethyl 5-(5-bromofuran-2-yl)-2,2-dimethyl-1,3-dioxolane-4-carboxylate (4.19.3)

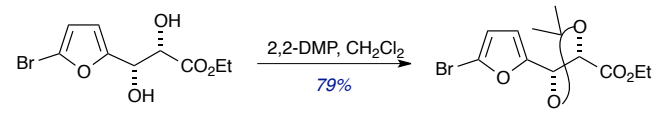

4.20.4A
(not numbered in the scheme)

4.19.3

To a solution of dihydroxyled bromofuran **4.20.4A**(1 mmol) in CH_2Cl_2 (0.02 M) was added 2,2-DMP (0.09M) and PPTS (catalytic amount) at room temperature. The reaction was stirred at room temperature for 24 hours till the TLC showed complete consumption of starting material. The reaction was quenched with solid $NaHCO_3$ and the solvent was evaporated. The crude product was purified via flash chromatography

Yield: 79% (isolated as a colorless oil from 117 mg of dihydroxyled bromofuran **4.20.4A**);

FTIR (thin film): 1952, 1751, 1466, 1381, 1196, 1103, 1018, 756 cm^{-1};

Optical Rotation: $[\alpha]_D$ = +90.4 (*c* = 0.13, $CHCl_3$);

^{1}H NMR (500 MHz, $CDCl_3$) δ 6.43 (d, *J* = 3.4 Hz, 1H), 6.31 (d, *J* = 3.3 Hz, 1H), 5.12 (d, *J* = 7.5 Hz, 1H), 4.72 (d, *J* = 7.5 Hz, 1H), 4.26 (dd, *J* = 7.1, 3.2 Hz, 1H), 4.24 (dd, *J* = 7.1, 3.1 Hz, 1H), 1.56 (s, 3H), 1.53 (s, 3H), 1.28 (t, *J* = 7.1 Hz, 3H);

^{13}C NMR (126 MHz, $CDCl_3$) δ 169.6, 151.8, 123.1, 112.3, 112.2, 112.1, 77.4, 74.0, 61.7, 26.7, 26.1, 14.1;

HRMS cald for $C_{12}H_{15}BrO_5Na$ $(M+Na)^+$ 341.0001; found 341.0005, 342.9976 (TOF MS ES+).

(1*R*,6*R*,8*S*)-8-(2-hydroxyethyl)-2,9,10-trioxa-1-phosphabicyclo[4.3.1]dec-4-ene 1-oxide (4.20.1A):

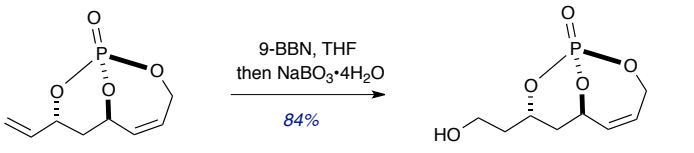

4.20.1 **4.20.1A**
(not numbered in the scheme)

To a solution of bicyclo[4.3.1]phosphate **4.20.1** dissolved in THF (0.12 M) was added 9-BBN (3 mmol, dissolved in THF, 0.5M) dropwise. The resulting mixture was left stirring at room temperature for 3 h till the disappearance of the starting material monitored by TLC. Reaction mixture was quenched by the addition of $NaBO_3$•$4H_2O$ (9 mmol) and H_2O (1.8 M) at 0 ºC. After removing the ice-bath the reaction was stirred at room temperature and additional H_2O (0.9 M) was added. After completion of the oxidation as monitored by TLC, the crude solution was dried over Na_2SO_4 and filtered through celite. The crude product was purified via flash chromatography.

Yield: 84% (1.6 g isolated as white solid starting from 1.78g of bicyclic phosphate);

FTIR (thin film): 3418, 1360, 1286, 1059, 910, 771 cm^{-1};

Optical Rotation: $[\alpha]_D$ = –94.5 (*c* = 1.75, $CHCl_3$);

^{1}H NMR (500 MHz, $CDCl_3$) δ 5.97 (dddd, *J* = 12.0, 6.8, 3.2, 2.1 Hz, 1H), 5.54 (ddd, *J* = 11.9, 4.0, 2.6 Hz, 1H), 5.15 (dqd, J_{PH}= 24.6, 4.0, 1.9 Hz, 1H), 4.93 (ddq, *J* = 14.3, 5.6, 2.8 Hz, 1H), 4.77 (dddt, *J* = 11.9, 8.5, 3.5, 1.6 Hz, 1H), 4.32 (ddd, *J* = 27.8, 14.7, 6.7 Hz, 1H), 3.75 (td, *J* = 9.6, 8.4, 4.5 Hz, 1H), 3.69 (dt, *J* = 10.8, 5.3 Hz, 1H), 2.53 (s, 1H), 2.18 (ddd, *J* = 14.7, 11.9, 6.2 Hz, 1H), 1.90 (ddt, *J* = 13.7, 9.2, 4.9 Hz, 1H), 1.82–1.77 (m, 1H), 1.74 (dq, *J* = 14.8, 1.9 Hz, 1H);

^{13}C NMR (126 MHz, $CDCl_3$) δ 129.8, 127.8, 77.4 (d, J_{CP} = 6.5 Hz), 74.4 (d, J_{CP} = 6.5 Hz), 63.0 (d, J_{CP} = 6.5 Hz), 57.6, 38.1 (d, J_{CP} = 9.1 Hz), 34.9 (d, J_{CP} = 6.0 Hz);

^{31}P NMR (162 MHz, $CDCl_3$) δ –3.77;

HRMS cald for $C_8H_{13}O_5PNa$ $(M+Na)^+$243.0398; found 243.0386 (TOF MS ES+).

(1*R*,6*R*,8*S*)-8-(2-(benzyloxy)ethyl)-2,9,10-trioxa-1-phosphabicyclo[4.3.1]dec-4-ene 1-oxide (4.18.5)

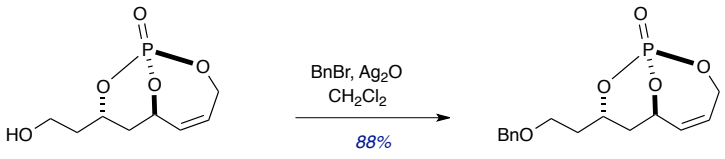

4.20.1A
(not numbered in the scheme)

4.18.5

To a solution of alcohol **4.20.1A** (1 mmol) dissolved in CH_2Cl_2 (0.1 M) were added Ag_2O (4.5 mmol) and BnBr (3.3 mmol) at room temperature. The reaction was stirred for 15 hours at room temperature after which the TLC showed 80% consumption of starting material. An additional batch of Ag_2O (3 mmol) and BnBr (2.2 mmol) were added to the reaction mixture and stirred for 5 hours after which the TLC showed complete consumption of starting material. The reaction was filtered through celite and evaporated. The crude product was purified via flash chromatography.

Yield: 88% (2.05 g isolated as colorless oil from 1.7 g);

FTIR (thin film): 2928, 2359, 1298, 1261, 1094, 1067, 972, 741 cm^{-1};

Optical Rotation: $[\alpha]_D = -83.47$(*c* = 0.54, $CHCl_3$);

^{1}H NMR (500 MHz, $CDCl_3$) δ 7.41–7.28 (m, 5H), 6.04 (dddd, *J* = 12.0, 6.8, 3.2, 2.1 Hz, 1H), 5.58 (ddd, *J* = 11.8, 4.0, 2.5 Hz, 1H), 5.26–5.13 (m, 1H), 5.02 (ddq, *J* = 14.8, 5.7, 2.7 Hz, 1H), 4.84 (dddd, *J* = 11.9, 8.2, 3.9, 1.8 Hz, 1H), 4.51 (d, *J* = 2.0 Hz, 2H), 4.39 (ddd, *J* = 27.7, 14.8, 6.7 Hz, 1H), 3.66 (ddd, *J* = 9.6, 8.8, 4.5 Hz, 1H), 3.60 (dt, *J* = 9.8, 5.1 Hz, 1H), 2.22 (ddd, *J* = 14.6, 12.0, 6.2 Hz, 1H), 2.05–1.96 (m, 1H), 1.91 (dddt, *J* = 14.2, 8.6, 5.3, 4.2 Hz, 1H), 1.76 (dtd, *J* = 14.6, 2.3, 1.4 Hz, 1H);

^{13}C NMR (126 MHz, $CDCl_3$) δ 138.1, 129.8, 128.4 (2C), 127.9, 127.7, 127.67 (2C), 77.2, 74.0 (d, J_{CP} = 6.7 Hz), 73.2, 65.0, 63.0 (d, J_{CP} = 6.4 Hz), 36.0 (d, J_{CP} = 9.5 Hz), 35.0 (d, J_{CP} = 6.1 Hz);

^{31}P NMR (162 MHz, $CDCl_3$) δ –3.83;

HRMS cald for $C_{15}H_{19}O_5PNa$ $(M+Na)^+$ 333.0868; found 333.0856 (TOF MS ES+).

(3*S*,5*R*,6*S*)-1-(benzyloxy)-6-methyloct-7-ene-3,5-diol (4.18.5A)

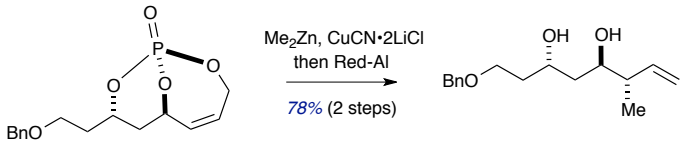

4.18.5 **4.18.5A** (not numbered in the scheme)

To a flask containing CuCN (3 mmol) and LiCl (7 mmol), weighted inside the glove box, was added THF (0.1 M) and stirred at room temperature for 15 minutes. A pale green coloration was observed. The reaction was cooled to –30 ºC followed by slow addition of a 2.0M solution of Me_2Zn in THF (3 mmol). The reaction mixture turned colorless. The reaction was stirred for 35-40 minutes at –30 ºC at which point a solution of bicyclic phosphate **4.18.5** in THF (0.1 M) was cannulated into the flask with the cuprate. The reaction was removed from the dry ice bath and allowed to warm to room temperature. Upon completion after 2.5 hours, the reaction is acidified to a pH of 1 with 10% aq. HCl (0.16 M). The reaction was stirred for 15 minutes and the aqueous layer was extracted with CH2Cl2 (4x 20) and the combined organic layers washed with H_2O (1x 3). The reaction was concentrated under reduced pressure and then filtered through a celite pad again to get rid of the salt particles. The celite layer was washed with EtOAc and evaporated again to afford as yellowish colored clear oil that was carried on without further purification.

To a flask containing the crude acid was added THF (0.08 M). The reaction mixture was cooled to 0 ºC followed by the addition of a 65% solution of Red-Al in toluene (6 mmol). The reaction was brought to rt and stirred for 12 hours. The reaction was quenched with NH_4Cl (sat'd aq.) and extracted with CH_2Cl_2 (6x). The organic layer was dried over anhydrous Na_2SO_4 and the solvent was evaporated. The crude product was purified via flash chromatography.

Yield: 78% (over 2 Steps; 500 mg isolated as colorless oil from 749 mg of bicyclic phosphate **4.18.5**);

FTIR (thin film): 3408, 2939, 2868, 2359, 2341, 1637, 1454, 1094, 912, 735, 696, 667 cm^{-1};

Optical Rotation: $[\alpha]_D$ = +12.39 (*c* = 1.34, $CHCl_3$);

^{1}H NMR (500 MHz, $CDCl_3$) δ 7.32–7.18 (m, 5H), 5.76–5.68 (m, 1H), 5.08–5.01 (m, 2H), 4.47 (s, 2H), 4.15–4.04 (m, 1H), 3.72–3.65 (m, 2H), 3.62 (ddd, *J* = 9.4, 8.5, 4.2 Hz, 1H), 3.49–3.42 (m, 1H), 2.56 (s, 1H), 2.21–2.13 (m, 1H), 1.89–1.81 (m, 1H), 1.66 (dddd, *J* = 14.5, 5.5, 4.3, 2.8 Hz, 1H), 1.57–1.54 (m, 2H), 0.96 (d, *J* = 6.8 Hz, 3H);

^{13}C NMR (126 MHz, $CDCl_3$) δ 140.5, 137.8, 128.4 (2C), 127.7, 127.6 (2C), 116.0, 73.3, 71.6, 69.2, 69.0, 44.3, 39.9, 36.3, 16.0;

HRMS cald for $C_{16}H_{24}O_3Na$ $(M+Na)^+$ 287.1623; found 287.1614 (TOF MS ES+).

(4*S*,6*R*)-4-(2-(benzyloxy)ethyl)-6-((*S*)-but-3-en-2-yl)-2,2-dimethyl-1,3-dioxane (4.22.1):

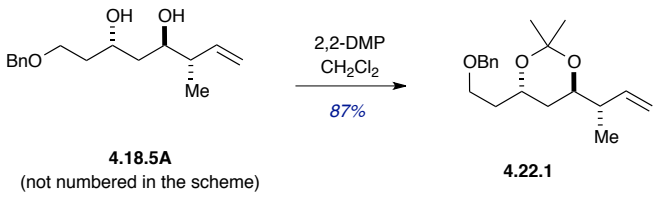

4.18.5A
(not numbered in the scheme)

4.22.1

To a solution containing diol **4.18.5A** (1 mmol) dissolved in CH_2Cl_2 (0.27 M), was added 2,2-DMP (0.27 M) and PPTS (0.05 mmol) and the reaction was stirred for 1 hour at room temperature. Upon completion of the reaction, (<10% starting material remaining after 1 hour), the reaction was first diluted with CH_2Cl_2 and quenched with $NaHCO_3$ (satd.), dried over Na_2SO_4. The solvent was evaporated and purified via flash chromatography.

Yield: 87% (445 mg isolated as colorless oil from 444 mg of diol **4.18.5A**);

FTIR (thin film): 2984, 2937, 2870, 2341, 1454, 1379, 1225, 1099, 989, 912, 735, 696 cm^{-1};

Optical Rotation: $[\alpha]_D$ = +23.8 (*c* = 0.4, $CHCl_3$);

^{1}H NMR (500 MHz, $CDCl_3$) δ 7.39–7.27 (m, 5H), 5.84 (ddd, *J* = 17.7, 10.5, 7.2 Hz, 1H), 5.06–5.03 (m, 1H), 5.03–5.01 (m, 1H), 4.54–4.46 (m, 2H), 3.95 (dq, *J* = 9.8, 6.4 Hz, 1H), 3.65 (dt, *J* = 9.6, 6.3 Hz, 1H), 3.60–3.52 (m, 2H), 2.29–2.20 (m, 1H), 1.78 (q, *J* = 6.4 Hz,

2H), 1.71 (ddd, *J* = 12.7, 9.6, 5.9 Hz, 1H), 1.51 (ddd, *J* = 12.7, 9.8, 6.2 Hz, 1H), 1.33 (s, 3H), 1.32 (s, 3H), 1.00 (d, *J* = 6.9 Hz, 3H);

^{13}C NMR (126 MHz, $CDCl_3$) δ 140.8, 138.5, 128.4 (2C), 127.7 (2C), 127.5, 114.4, 100.3, 73.1, 69.9, 66.7, 63.9, 42.0, 36.1, 36.0, 24.7, 24.3, 15.2;

HRMS cald for $C_{19}H_{28}O_3Na$ $(M+Na)^+$ 327.1936; found 327.1924 (TOF MS ES+).

2-((*S*,*E*)-3-((4*R*,6*S*)-6-(2-(benzyloxy)ethyl)-2,2-dimethyl-1,3-dioxan-4-yl) but-1-en-1-yl)-4,4,5,5-tetramethyl-1,3,2-dioxaborolane (4.24.1):

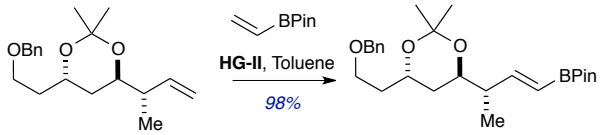

4.22.1 **4.24.1**

The boronic ester was synthesized following similar literature reports.[1] To a solution of protected diol **4.22.1** (1 mmol) and vinylboronic acid pinacol ester (1.6 mmol) dissolved in degassed toluene (0.2 M) at 80 ºC was added dropwise a solution of the **HG-II** cat (10 mol%) dissolved in toluene (0.02M). A second batch of vinylboronic acid pinacol ester (1.6 mmol) was added to the reaction mixture after 20 minutes (TLC showed complete consumption of vinylboronic acid pinacol ester), followed by dropwise addition of second batch of the **HG-II** cat (10 mol%) in toluene (0.02 M). The reaction mixture was heated for 1 hour at 80 ºC after which the TLC showed complete consumption of protected diol. The reaction mixture was cooled to room temperature and the solvent was evaporated and purified via flash chromatography.

Yield: 98% (137mg isolated as yellow colored oil from 99 mg of protected diol **4.22.1**);

FTIR (thin film): 2980, 2363, 1722, 1637, 1371, 1223, 1146, 851, 771 cm^{-1};

Optical Rotation: $[\alpha]_D$ = +14.1 (*c* = 1.02, $CHCl_3$);

^{1}H NMR (500 MHz, $CDCl_3$) δ 7.37–7.27 (m, 5H), 6.60 (dd, *J* = 18.2, 6.9 Hz, 1H), 5.47 (dd, *J* = 18.2, 1.3 Hz, 1H), 4.50 (d, *J* = 1.4 Hz, 2H), 3.94 (dq, *J* = 9.8, 6.3 Hz, 1H), 3.73 (dt, *J* = 9.6, 6.2 Hz, 1H), 3.59–3.51 (m, 2H), 2.40–2.31 (m, 1H), 1.80–1.74 (m, 2H), 1.70 (ddd, *J* =

12.8, 9.6, 5.9 Hz, 1H), 1.49 (ddd, *J* = 12.8, 9.8, 6.3 Hz, 1H), 1.32 (s, 3H), 1.32 (s, 3H), 1.28 (s, 12H), 1.00 (d, *J* = 6.9 Hz, 3H).

^{13}C NMR (126 MHz, $CDCl_3$) δ 155.7, 138.4, 128.3 (2C), 127.7 (2C), 127.5, 118.7, 100.3, 83.0 (2C), 73.1, 69.4, 66.6, 63.8, 43.6, 36.0, 35.6, 24.8 (2C), 24.76 (2C), 24.7, 24.4, 14.6;

HRMS cald for $C_{25}H_{39}BO_5Na$ $(M+Na)^+$ 453.2788; found 453.2764 (TOF MS ES+).

(5*R*)-ethyl 5-(5-((*S*,*E*)-3-((4*R*,6*S*)-6-(2-(benzyloxy)ethyl)-2,2-dimethyl-1,3-dioxan-4-yl)but-1-en-1-yl)furan-2-yl)-2,2-dimethyl-1,3-dioxolane-4-carboxylate (4.24.2):

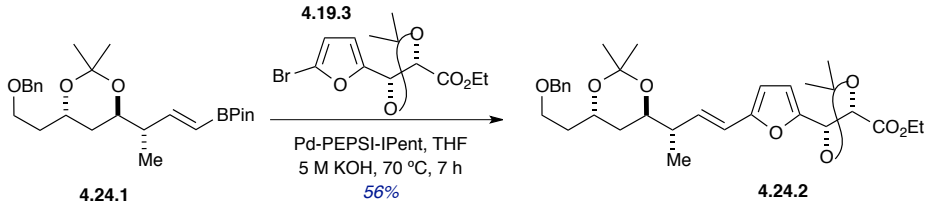

The Suzuki-Miyaura coupling was performed following the literature procedure reported by Organ and coworkers.[2] To a stirred solution of boronic ester **4.24.1**(1.5 mmol) dissolved in degassed THF (0.25 M) was added Pd-PEPSI-IPent catalyst (2 mol%). The reaction flask/vial was then purged with Argon (3X). Bromo-furan compound **4.19.3** (1 mmol) was added to the solution followed by the addition of 5M KOH (4 mmol). The reaction mixture was heated at 70 ºC for 7 hours after which TLC showed complete consumption of starting material. The reaction mixture was cooled to room temperature and extracted with EtOAc (3x). The combined organic layer was dried over Na_2SO_4 and the solvent was evaporated. The solvent was evaporated and purified via flash chromatography.

Yield: 56% (9.5 mg isolated as pale yellow colored oil starting from 10 mg of bromofuran compound **4.19.3**);

FTIR (thin film): 2955, 1751, 1373, 1227, 1103, 702 cm^{-1};

Optical Rotation: $[\alpha]_D$ = +54.4 (*c* = 0.16, $CHCl_3$);

^{1}H NMR (500 MHz, $CDCl_3$) δ 7.50–7.03 (m, 5H), 6.40 (d, *J* = 3.3 Hz, 1H), 6.22–6.19 (m, 2H), 6.14 (d, *J* = 3.2 Hz, 1H), 5.17 (d, *J* = 7.4 Hz, 1H), 4.76 (d, *J* = 7.4 Hz, 1H), 4.50 (d, *J* = 1.4 Hz, 2H), 4.26 (dd, *J* = 7.2, 2.2 Hz, 1H), 4.23 (dd, *J* = 7.1, 2.1 Hz, 1H), 3.96 (dq, *J* = 9.7,

6.3 Hz, 1H), 3.71 (dt, *J* = 9.6, 6.3 Hz, 1H), 3.61–3.50 (m, 2H), 2.43–2.32 (m, 1H), 1.78 (q, *J* = 6.4 Hz, 2H), 1.76–1.70 (m, 1H), 1.57(s, 3H), 1.55 (s, 3H), 1.54–1.49 (m, 1H), 1.33 (s, 6H), 1.27 (t, *J* = 7.2 Hz, 3H), 1.06 (d, *J* = 6.8 Hz, 3H);

^{13}C NMR (126 MHz, $CDCl_3$) δ 169.9, 154.2, 148.5, 138.4, 132.6, 128.4 (2C), 127.7 (2C), 127.5, 118.3, 112.0, 111.2, 107.0, 100.4, 77.6, 74.4, 73.1, 70.0, 66.6, 63.9, 61.6, 41.2, 36.1, 36.0, 26.7, 26.2, 24.6, 24.4, 15.3, 14.1;

HRMS cald for $C_{31}H_{42}O_8Na$ $(M+Na)^+$ 565.2777; found 565.2750 (TOF MS ES+).

(*E*)-2-bromo-5-(prop-1-en-1-yl)furan (4.26.6):

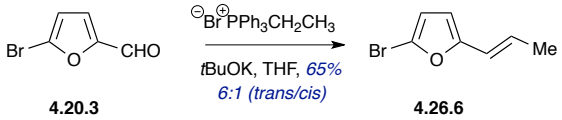

4.20.3 4.26.6

To a solution of phosphonium ylide (1.9 mmol) dissolved in THF (0.28 M) was added *t*BuOK (1.8 mmol) in one portion at 0 ºC. An orange coloration was observed upon the addition of *t*BuOK. A solution of 5-bromo-2-furaldehyde (**4.20.3**) in THF (0.57 M) was added immediately to this mixture at 0 ºC producing a color change from orange to yellow. The reaction was stirred at 0 ºC for 30 minutes after which the TLC showed complete consumption of the starting material. The reaction mixture was quenched with the addition of H_2O (11 mL). The layers were separated and extracted with Et_2O (3X 20 mL) and the combined layer was washed with, brine and dried over Na_2SO_4. The solvent was evaporated under continuous Argon flow and purified via flash chromatography using pentane.[7]

Yield: 65% (70 mg isolated as colorless oil that turned pale yellow after few days of storing in Et_2O under Argon at –20 ºC from 100 mg of 5-bromo-2-furaldehyde); *trans*/*cis*: 6:1;

---

[7] The Wittig product was found to be very unstable at room temperature (rapid color change from pale yellow to black was observed within 24 hours when stored at bench top and decomposition occurred). But the product was relatively stable when stored in ether under Argon at 0 ºC for few days. For this purpose, the product was used in next reaction immediately after purification.

FTIR (thin film): 3026, 1784, 1686, 1489, 1207, 1192, 1124, 1011, 951, 779 cm^{-1};

^{1}H NMR (500 MHz, $CDCl_3$) δ 6.32 (d, *J* = 3.3 Hz, 1H), 6.22 (d, *J* = 3.4 Hz, 1H), 6.15 (dq, *J* = 11.7, 1.8 Hz, 1H), 5.68 (dq, *J* = 11.7, 7.3 Hz, 1H), 1.97 (dd, *J* = 7.3, 1.7 Hz, 3H);

^{13}C NMR (126 MHz, $CDCl_3$) δ 155.3, 126.0, 120.5, 117.7, 112.7, 111.1, 15.1.

(*S*,*E*)-1-((4-methoxybenzyl)oxy)-2-methylhex-4-en-3-one (4.27.3):

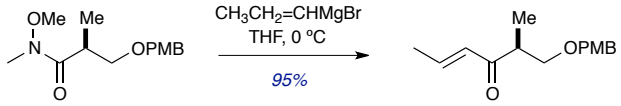

4.27.2 **4.27.3**

To a solution of Weinreb amide **4.27.2** (1 mmol) dissolved in THF (0.3 M) was added a solution of propenylmagnesium bromide (0.5 M in THF, 2 mmol) at 0 ºC. After 30 minutes of stirring at 0 ºC, the reaction was quenched with NH_4Cl (5 mL) at 0 ºC and stirred at ambient temperature till the effervescence ceased. The layers were separated and extracted with Et_2O (3X 20 mL) and the combined layer was washed with H_2O, brine and dried over Na_2SO_4. The solvent was evaporated and purified via flash chromatography.

Yield: 95% (1.77 g isolated as colorless oil from 2 g of Weinreb amide **4.27.2**);

FTIR (neat): 2916, 1690, 1620, 1512, 1250, 1095, 818 cm^{-1};

Optical Rotation: $[\alpha]_D$ = +9.4 (*c* = 0.16, $CHCl_3$);

^{1}H NMR (500 MHz, $CDCl_3$) δ 7.25–7.21 (m, 2H), 6.92 (dt, *J* = 15.7, 6.9 Hz, 1H), 6.88–6.85 (m, 2H), 6.21 (dq, *J* = 15.6, 1.7 Hz, 1H), 4.45 (d, *J* = 11.7 Hz, 1H), 4.41 (d, *J* = 11.7 Hz, 1H), 3.81 (s, 3H), 3.67 (dd, *J* = 9.2, 7.3 Hz, 1H), 3.42 (dd, *J* = 9.2, 6.0 Hz, 1H), 3.15–3.05 (m, 1H), 1.90 (dd, *J* = 6.9, 1.7 Hz, 3H), 1.10 (d, *J* = 7.0 Hz, 3H);

^{13}C NMR (126 MHz, $CDCl_3$) δ 202.1, 159.1, 143.0, 130.9, 130.3, 129.2 (2C), 113.7 (2C), 72.9, 71.8, 55.3, 44.0, 18.3, 14.1;

HRMS cald for $C_{15}H_{20}O_3Na$ $(M+Na)^+$ 273.1310; found 271.1301(TOF MS ES+).

(2*S*,3*R*,*E*)-1-((4-methoxybenzyl)oxy)-2-methylhex-4-en-3-ol (4.26.7):

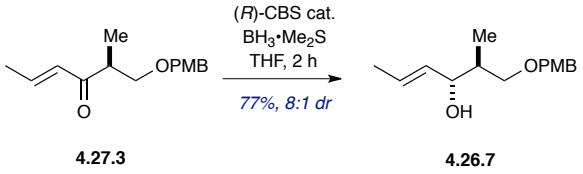

4.27.3 **4.26.7**

The substituted allylic alcohol was prepared following the literature procedure reported by Chandrasekhar and coworkers.[3] To a solution of enone **4.27.3** (1 mmol) dissolved in THF (0.33 M) was added a solution of (*R*)-2-methyl-CBS-oxazaborolidine (1M in Toluene, 2 mmol) at –40 ºC. After 10 minutes of stirring at –40 ºC, BH_3•DMS (5 mmol) was added and the reaction was stirred at – 40 ºC for 2 additional hours. Upon completion of the reaction, monitored by TLC, the reaction was quenched with EtOH (4 mL) at -40 ºC and stirred at ambient temperature. The layers were separated and extracted with Et_2O (3X 30 mL) and the combined layer was washed with H_2O, brine and dried over Na_2SO_4. The solvent was evaporated and purified via flash chromatography.

Yield: 77%(931 mg isolated as colorless oil starting from 1.2 g of enone); dr: 8:1;

FTIR (thin film): 3421, 2959, 2914, 2854, 1610, 1512, 1248, 1090, 966, 771 cm^{-1};

Optical Rotation: $[\alpha]_D$ = +26.0 (*c* = 0.21, $CHCl_3$);

^{1}H NMR (500 MHz, $CDCl_3$) δ 7.29–7.23 (m, 2H), 6.91–6.87 (m, 2H), 5.66 (dqd, *J* = 15.3, 6.5, 0.9 Hz, 1H), 5.45 (ddd, *J* = 15.2, 7.5, 1.6 Hz, 1H), 4.46 (s, 2H), 3.93 (t, *J* = 7.5 Hz, 1H), 3.82 (s, 3H), 3.57 (dd, *J* = 9.2, 4.3 Hz, 1H), 3.43 (dd, *J* = 9.2, 7.6 Hz, 1H), 3.33 (s, 1H), 1.87 (qd, *J* = 7.3, 4.3 Hz, 1H), 1.71 (dd, *J* = 6.4, 1.6 Hz, 3H), 0.85 (d, *J* = 7.0 Hz, 3H);

^{13}C NMR (126 MHz, $CDCl_3$) δ 159.2, 132.5, 129.9, 129.3 (2C), 127.7, 113.8 (2C), 77.7, 74.6, 73.0, 55.3, 38.7, 17.7, 13.7;

HRMS cald for $C_{15}H_{22}O_3Na$ $(M+Na)^+$ 273.1467; found 273.1449 (TOF MS ES+).

(3*R*,4*S*,*E*)-1-(5-bromofuran-2-yl)-5-((4-methoxybenzyl)oxy)-4-methylpent-1-en-3-ol (4.26.5):

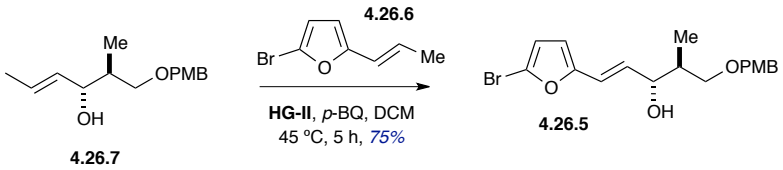

To a solution of allylic alcohol **4.26.7** (1 mmol) dissolved in degassed CH_2Cl_2 (0.1 M) was added propenyl bromofuran **4.26.6** (3 mmol) followed by the **HG-II** catalyst (6 mol%) and *para*-benzoquinone (10 mol%). The reaction mixture was refluxed for 3 hours after which the TLC showed significant consumption of allylic alcohol (< 20% starting material remained).[8] The reaction mixture was cooled to room temperature and the solvent was evaporated. The crude product was purified via flash chromatography.

Yield: 75% (57.3 mg isolated as green colored oil from 50 mg of allylic alcohol **4.26.7**);

FTIR (thin film): 3431, 2905, 2359, 1612, 1514, 1248, 820 cm^{-1};

Optical Rotation: $[\alpha]_D = -9.8$ ($c = 0.5$, $CHCl_3$);

^{1}H NMR (500 MHz, $CDCl_3$) δ 7.29–7.22 (m, 2H), 6.90–6.86 (m, 2H), 6.35 (dd, J = 15.8, 1.4 Hz, 1H), 6.28 (d, J = 3.4 Hz, 1H), 6.20–6.14 (m, 2H), 4.46 (s, 2H), 4.21–4.13 (m, 1H), 3.81 (s, 3H), 3.63 (dd, J = 9.2, 3.9 Hz, 1H), 3.55 (d, J = 3.8 Hz, 1H), 3.45 (dd, J = 9.3, 7.2 Hz, 1H), 1.95 (ddt, J = 10.9, 7.0, 3.9 Hz, 1H), 0.97 (d, J = 7.0 Hz, 3H);

^{13}C NMR (126 MHz, $CDCl_3$) δ 159.3, 154.6, 130.5, 129.7, 129.4 (2C), 121.2, 118, 113.8 (2C), 112.9, 110, 76.6, 74.2, 73.1, 55.3, 38.9, 13.9;

HRMS cald for $C_{18}H_{21}BrO_4SiNa$ $(M+Na)^+$ 403.0521; found: 403.0505, 405.0489 (TOF MS ES+).

[8] It is important to note here that the reaction produced lesser yield if run for more that 3 hours. In addition, the reaction yield was dependent on the purity of both of the starting material.

(((3*R*,4*S*,*E*)-1-(5-bromofuran-2-yl)-5-((4-methoxybenzyl)oxy)-4-methylpent-1-en-3-yl)oxy)(*tert*-butyl)dimethylsilane (4.26.2):

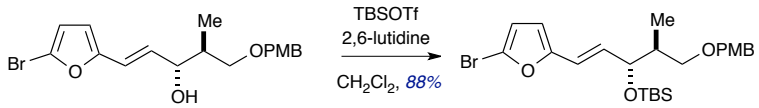

4.26.5 **4.26.2**

To a flask containing alcohol **4.26.5** (1 mmol) dissolved in CH_2Cl_2 (0.1 M) was added 2,6-lutidine (4 mmol). The reaction mixture was cooled to -78 ºC and TBSOTf (2 mmol) was added drop wise. The reaction mixture was stirred for 1 hour at -78 ºC till the complete consumption of starting material, monitored by TLC. The reaction was quenched with NH_4Cl (5 mL). The layers were separated and extracted with CH_2Cl_2 (2X 20 mL). The combined organic layer was dried over Na_2SO_4, the solvent was evaporated and purified via flash chromatography.

Yield: 88% (66.5 mg isolated as colorless oil that turned pale yellow color after few days of storing it under Argon atmosphere at – 20 ºC starting from 57 mg of alcohol **4.26.5**);

FTIR (thin film): 2928, 2855, 2359, 1612, 1512, 1248, 835, 775 cm^{-1};

Optical Rotation: $[\alpha]_D$ = +2.4 (*c* = 0.38, $CHCl_3$);

^{1}H NMR (500 MHz, $CDCl_3$) δ 7.28–7.24 (m, 2H), 6.91–6.84 (m, 2H), 6.28 (d, *J* = 3.3 Hz, 1H), 6.20 (dd, *J* = 15.8, 1.1 Hz, 1H), 6.13 (d, *J* = 3.3 Hz, 1H), 6.10 (dd, *J* = 15.8, 6.2 Hz, 1H), 4.46 (d, *J* = 11.6 Hz, 1H), 4.39 (d, *J* = 11.6 Hz, 1H), 4.30 (ddd, *J* = 6.4, 5.5, 1.2 Hz, 1H), 3.82 (s, 3H), 3.44 (dd, *J* = 9.3, 6.4 Hz, 1H), 3.34 (dd, *J* = 9.3, 6.2 Hz, 1H), 2.05–1.96 (m, 1H), 0.93–0.86 (m, 12H), 0.06 (s, 3H), 0.02 (s, 3H);

^{13}C NMR (126 MHz, $CDCl_3$) δ 159.0, 154.8, 130.7, 130.5, 129.2 (2C), 121.0, 117.7, 113.7 (2C), 112.9, 109.5, 74.0, 72.6, 71.9, 55.3, 40.5, 25.9 (3C), 18.2, 12.7, –4.3, –4.9;

HRMS cald for $C_{24}H_{35}BrO_4SiNa$ $(M+Na)^+$ 517.1386; found 517.1406, 519.1403 (TOF MS ES+).

(1*R*,2*R*,3*S*,4*S*)-1-(5-bromofuran-2-yl)-3-((*tert*-butyldimethylsilyl)oxy)-5-((4-methoxybenzyl)oxy)-4-methylpentane-1,2-diol (4.26.1):

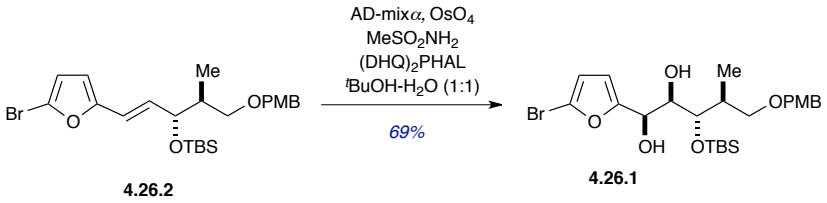

The dihydroxylation of furan was achieved by following the literature procedure reported by Phillips and coworkers.[4] To a flask containing compound **4.26.2** (1 mmol) dissolved in *t*BuOH-H_2O (1:1, 0.2 M each) were added OsO_4 (2 mol%), $CH_3SO_2NH_2$ (2 mmol), AD-mix-α (1.4 g/mmol) and $(DHQ)_2PHAL$ (4 mol%) at 0 ºC. The orange colored reaction mixture was then stirred at 0 ºC for 2 days in dark. The reaction mixture was quenched with solid Na_2SO_3 and stirred vigorously for several hours till the disappearance of the yellow color. The reaction mixture was filtered through celite, the aqueous layer was extracted with EtOAc (2 X 20 mL) and evaporated after drying over Na_2SO_4. The crude product was purified via flash chromatography.

Yield: 69% (17 mg isolated as colorless oil starting from 23 mg of **4.26.2**); ds: 20:1;

FTIR (thin film): 3369, 2953, 2928, 2856, 2359, 1612, 1512, 1250, 1038, 835 cm^{-1};

Optical Rotation: $[\alpha]_D$ = +13.0 (*c* = 0.28, $CHCl_3$);

^{1}H NMR (500 MHz, $CDCl_3$) δ 7.26–7.22 (m, 2H), 6.91–6.87 (m, 2H), 6.31 (dd, *J* = 3.3, 0.8 Hz, 1H), 6.27 (d, *J* = 3.3 Hz, 1H), 4.71 (dd, *J* = 6.8, 3.6 Hz, 1H), 4.55 (d, *J* = 5.3 Hz, 1H), 4.50 (d, *J* = 11.4 Hz, 1H), 4.44 (d, *J* = 11.4 Hz, 1H), 3.82 (s, 3H), 3.81–3.79 (m, 1H), 3.72 (dd, *J* = 6.3, 2.4 Hz, 1H), 3.59 (dd, *J* = 9.2, 7.7 Hz, 1H), 3.32 (dd, *J* = 9.1, 3.2 Hz, 1H), 3.00 (d, *J* = 6.8 Hz, 1H), 2.11 (tdd, *J* = 10.0, 4.9, 3.3 Hz, 1H), 0.96 (d, *J* = 7.2 Hz, 3H), 0.90 (s, 9H), 0.13 (s, 3H), 0.05 (s, 3H);

^{13}C NMR (126 MHz, $CDCl_3$) δ 159.4, 157.3 129.6 (2C), 129.1, 120.9, 113.9 (2C), 111.9, 109.6, 74.8, 73.7, 73.1, 70.7, 67.7, 55.3, 36.7, 25.9 (3C), 18.2, 14.2, –4.47, –4.5;

HRMS cald for $C_{24}H_{37}BrO_6Si$ Na $(M+Na)^+$ 551.1440; found 551.1469, 553.1449 (TOF MS ES+).

(1*R*,2*R*,3*S*,4*S*)-1-(5-((*S*,*E*)-3-((4*R*,6*S*)-6-(2-(benzyloxy)ethyl)-2,2-dimethyl-1,3-dioxan-4-yl)but-1-en-1-yl)furan-2-yl)-3-((*tert*-butyldimethylsilyl)oxy)-5-((4-methoxybenzyl)oxy)-4-methylpentane-1,2-diol (4.28.1):

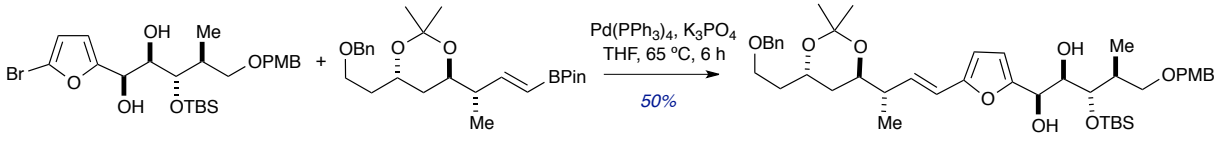

To a stirred solution of boronic ester **4.24.1** (1.5 mmol) and furan **4.26.1** (1 mmol) dissolved in degassed THF (0.1 M) were added $Pd(PPh_3)_4$ (20 mol%) and K_3PO_4 (4 mmol) under argon atmosphere. The reaction mixture was then purged with Argon (3x) and was refluxed for 6 hours after which the TLC showed significant consumption of starting material (<10% of furan remained unreacted). The reaction mixture was cooled to room temperature and quenched with H_2O (2 mL). The organic layer was extracted with EtOAc (3 X 20 mL) and purified via flash chromatography.

Yield: 50% (65 mg isolated starting from 92 mg of furan **4.26.1**);

FTIR (thin film): 3416, 2930, 2359, 1715, 1614, 1514, 1454, 1379, 1250, 1097, 837 cm^{-1};

Optical Rotation: $[\alpha]_D$ = +20.6 (*c* = 0.11, $CHCl_3$);

^{1}H NMR (500 MHz, Chloroform-*d*) δ 7.38–7.27 (m, 5H), 7.26–7.22 (m, 2H), 6.91–6.85 (m, 2H), 6.29 (d, *J* = 3.3 Hz, 1H), 6.19 (d, *J* = 16.2 Hz, 1H), 6.15–6.09 (m, 2H), 4.70 (t, *J* = 4.9 Hz, 1H), 4.51 (d, *J* = 8.5 Hz, 1H), 4.50 (d, *J* = 2.0 Hz, 2H), 4.48–4.40 (m, 2H), 3.94 (dq, *J* = 9.9, 6.5 Hz, 1H), 3.88–3.83 (m, 1H), 3.81 (s, 3H), 3.76 – 3.70 (m, 1H), 3.69–3.66 (m, 1H), 3.61 (dd, *J* = 9.1, 8.0 Hz, 1H), 3.54 (td, *J* = 6.3, 2.9 Hz, 2H), 3.28 (dd, *J* = 9.1, 3.7 Hz, 1H), 3.06 (d, *J* = 5.4 Hz, 1H), 2.37 (q, *J* = 6.8 Hz, 1H), 2.17–2.07 (m, 1H), 1.77 (q, *J* = 6.4 Hz, 2H), 1.75–1.69 (m, 1H), 1.52 (ddd, *J* = 12.7, 9.8, 6.2 Hz, 1H), 1.32 (s, 3H), 1.31 (s, 3H), 1.05 (d, *J* = 6.9 Hz, 3H), 0.93 (d, *J* = 7.1 Hz, 3H), 0.90 (s, 9H), 0.12 (s, 3H), 0.02 (s, 3H);

^{13}C NMR (126 MHz, $CDCl_3$) δ 159.4, 153.5, 152.8, 138.5, 131.4, 129.5 (2C), 129.2, 128.3 (2C), 127.7 (2C), 127.5, 118.6, 113.9 (2C), 108.7, 107.1, 100.4, 75.0, 74.8, 73.1, 73.06, 70.6, 69.9, 68.1, 66.7, 63.9, 55.2, 41.3, 36.2, 36.0, 35.9, 25.9 (3C), 24.6, 24.4, 18.2, 15.5, 15.0, –4.4, –4.6;

HRMS cald for $C_{43}H_{64}O_9SiNa$ $(M+Na)^+$775.4217; found 775.4214 (TOF MS ES+).

(1*R*,2*R*,3*S*,4*S*)-1-(5-((*S*)-3-((4*R*,6*S*)-6-(2-(benzyloxy)ethyl)-2,2-dimethyl-1,3-dioxan-4-yl)butyl)furan-2-yl)-3-((*tert*-butyldimethylsilyl)oxy)-5-((4-methoxybenzyl)oxy)-4-methylpentane-1,2-diol (4.28.2):

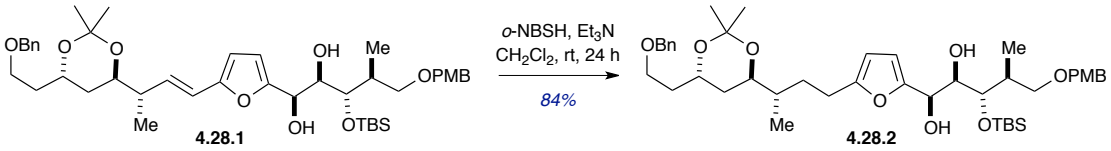

To a stirred solution of compound **4.28.1** (1mmol) dissolved in CH_2Cl_2 (0.06 M) were added *o*-NBSH (15 mmol) and Et_3N (2 ml/g) under argon atmosphere at room temperature producing an orange-colored heterogeneous reaction mixture. The reaction mixture was then stirred for 15 hours at room temperature after which the reaction mixture became clear and a dark orange coloration was observed. A second batch of *o*-NBSH (15 mmol) and Et_3N (2 ml/g) were added and the reaction was stirred for additional 15 hours. The reaction was diluted with EtOAc (10 mL), extracted with saturated aqueous $NaHCO_3$ (7 mL) followed by washing with EtOAc (2 x 20 mL). The combined organic layers were dried (Na_2SO_4) and concentrated under reduced pressure. The crude product was purified via flash chromatography.

Yield: 84% (33 mg isolated as yellow colored sticky liquid from 40 mg of Suzuki-Miyaura product);

FTIR (thin film): 3400, 2930, 2856, 1512, 1458, 1377, 1248, 1095, 1038, 835, 775 cm^{-1};

Optical Rotation: $[\alpha]_D$ = +9.2 (*c* = 0.3, $CHCl_3$);

^{1}H NMR (500 MHz, Chloroform-*d*) δ 7.38–7.28 (m, 5H), 7.26–7.22 (m, 2H), 6.92–6.85 (m, 2H), 6.20 (d, *J* = 3.1 Hz, 1H), 5.94 (d, *J* = 3.0 Hz, 1H), 4.66 (t, *J* = 5.0 Hz, 1H), 4.50 (d, *J* =

2.0 Hz, 2H), 4.47 (d, *J* = 4.1 Hz, 2H), 4.45 – 4.43 (m, 1H), 4.03–3.89 (m, 1H), 3.86–3.82 (m, 1H), 3.81 (s, 3H), 3.65 (dd, *J* = 5.3, 2.4 Hz, 1H), 3.61 (dd, *J* = 9.1, 7.9 Hz, 1H), 3.58–3.51 (m, 3H), 3.28 (dd, *J* = 9.1, 3.8 Hz, 1H), 3.06 (d, *J* = 5.1 Hz, 1H), 2.69 (ddd, *J* = 15.7, 10.7, 5.2 Hz, 1H), 2.56 (ddd, *J* = 15.8, 10.5, 6.0 Hz, 1H), 2.16–2.01 (m, 1H), 1.97–1.86 (m, 1H), 1.78 (q, *J* = 6.3 Hz, 2H), 1.65 (ddd, *J* = 12.6, 9.6, 6.0 Hz, 1H), 1.54 (ddd, *J* = 12.7, 9.9, 6.3 Hz, 2H), 1.40 (dddd, *J* = 13.7, 10.5, 8.8, 5.3 Hz, 1H), 1.32 (s, 3H), 1.32 (s, 3H), 0.92 (d, *J* = 7.2 Hz, 3H), 0.89 (s, 9H), 0.88 (d, *J* = 6.8 Hz, 3H), 0.11 (s, 3H), 0.02 (s, 3H);

^{13}C NMR (126 MHz, $CDCl_3$) δ 159.3, 156.2, 152.5, 138.5, 129.5 (2C), 129.3, 128.4 (2C), 127.7 (2C), 127.5, 113.9 (2C), 107.8, 105.2, 100.3, 75.0, 74.7, 73.1, 73.0, 70.6, 70.3, 68.0, 66.7, 63.9, 55.3, 37.5, 36.4, 36.2, 36.0, 30.9, 25.9 (3C), 25.5, 24.6, 24.3, 18.2, 15.0, 14.3, –4.4, –4.7;

HRMS cald for $C_{43}H_{66}O_9SiNa$ $(M+Na)^+$ 777.4374; found 777.4367 (TOF MS ES+).

(2*R*)-6-((*S*)-3-((4*R*,6*S*)-6-(2-(benzyloxy)ethyl)-2,2-dimethyl-1,3-dioxan-4-yl)butyl)-2-((1*R*,2*S*,3*S*)-2-((*tert*-butyldimethylsilyl)oxy)-1-hydroxy-4-((4-methoxybenzyl)oxy)-3-methylbutyl)-6-hydroxy-2*H*-pyran-3(6*H*)-one (4.28.3):

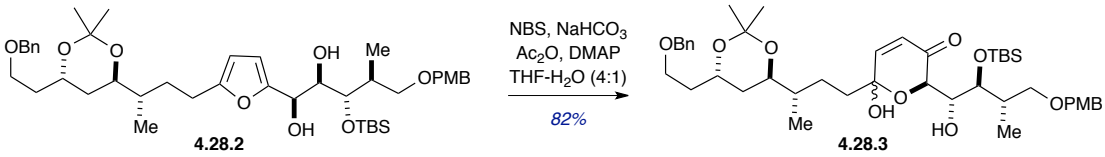

The synthesis of α,β-unsaturated hydroxypyranone **4.28.3** was performed by following the modified literature procedure reported by O'Doherty and coworkers.[5] To a solution of furan **4.28.2** (1 mmol) dissolved in THF (1.3 M) and H_2O (5.8 M) was added $NaHCO_3$ (2 mmol) and $NaOAc.3H_2O$ (1 mmol). The solution was cooled to 0 ºC and NBS (1 mmol) was added. The reaction mixture was stirred for 1–2 hours at 0 ºC until the disappearance of the starting material, monitored by TLC. Upon completion, the reaction mixture was diluted[9] and filtered over celite, evaporated and purified via flash chromatography.

[9]. The literature reports for similar but less complex substrates mentioned quenching with saturated $NaHCO_3$ solution however inconsistent results were obtained while optimizing the

Yield: 82% (8 mg isolated as colorless sticky liquid starting from 10 mg of hydrogenated Suzuki-Miyaura product);

FTIR (thin film): 3373, 2955, 2932, 2856, 1688, 1610, 1458, 1377, 1250, 1223, 1105, 1038, 835, 775, 698 cm^{-1};

Optical Rotation: $[\alpha]_D$ = +27.14 (*c* = 0.14, $CHCl_3$);

^{1}H NMR (500 MHz, Chloroform-*d*) δ 7.38–7.28 (m, 5H), 7.19–7.15 (m, 2H), 6.90–6.86 (m, 2H), 6.78 (d, *J* = 10.4 Hz, 1H), 6.13 (d, *J* = 10.5 Hz, 1H), 6.08 (s, 1H), 5.61 (s, 1H), 4.58 (t, *J* = 2.0 Hz, 1H), 4.50 (d, *J* = 2.2 Hz, 2H), 4.45 (d, *J* = 11.4 Hz, 1H), 4.40 (d, *J* = 11.3 Hz, 1H), 4.01 (dd, *J* = 9.2, 2.4 Hz, 1H), 3.95 (dt, *J* = 12.6, 6.2 Hz, 1H), 3.87 (dt, *J* = 9.2, 2.4 Hz, 1H), 3.81 (s, 3H), 3.60–3.50 (m, 4H), 3.40 (dd, *J* = 9.4, 1.6 Hz, 1H), 2.08 (dd, *J* = 9.9, 4.8 Hz, 1H), 1.93 (td, *J* = 13.1, 4.4 Hz, 2H), 1.78 (q, *J* = 6.2 Hz, 2H), 1.72 (dd, *J* = 13.0, 4.4 Hz, 1H), 1.69–1.60 (m, 2H), 1.56–1.49 (m, 2H), 1.32 (s, 3H), 1.32 (s, 3H), 0.99 (d, *J* = 7.3 Hz, 3H), 0.88 (s, 9H), 0.86 (d, *J* = 6.7 Hz, 3H), 0.11 (s, 3H), 0.07 (s, 3H);

^{13}C NMR (126 MHz, $CDCl_3$) δ 196.7, 159.5, 149.5, 138.5, 129.7 (2C), 128.5, 128.4 (2C), 127.7 (2C), 127.6, 126.5, 114.0 (2C), 100.3, 92.3, 78.0, 73.3, 73.1, 73.07, 72.9, 70.7, 70.3, 66.7, 63.8, 55.3, 37.9, 37.8, 37.6, 36.2, 36.0, 26.4, 26.0 (3C), 24.6, 24.4, 18.2, 14.3, 12.3, –4.3, –4.6;

HRMS cald for $C_{43}H_{66}O_{10}SiNa$ $(M+Na)^+$ 793.4323; found 793.4359 (TOF MS ES+).

---

amount of $NaHCO_3$ required for quenching, therefore we preferred to purify the crude product without quenching.

(6*R*)-6-((1*R*,2*S*,3*S*)-1-acetoxy-2-((*tert*-butyldimethylsilyl)oxy)-4-((4-methoxybenzyl)oxy)-3-methylbutyl)-2-((*S*)-3-((4*R*,6*S*)-6-(2-(benzyloxy)ethyl)-2,2-dimethyl-1,3-dioxan-4-yl)butyl)-5-oxo-5,6-dihydro-2*H*-pyran-2-yl acetate (4.28.5):

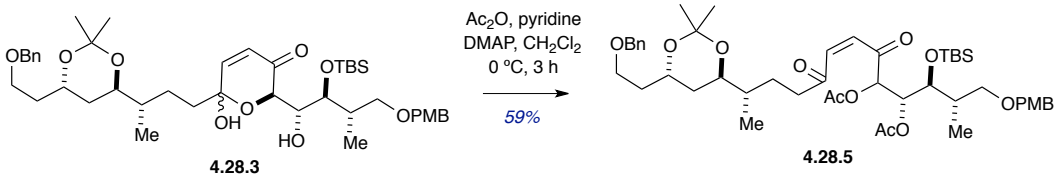

To a solution of containing α,β-unsaturated hydroxypyranone **4.28.3** (1 mmol) dissolved in CH_2Cl_2 (0.5 M) were added pyridine (4 mmol), Ac_2O (4 mmol) and DMAP (0.1 mmol) at 0 ºC. The reaction mixture was stirred for 3 hours at 0 ºC until the disappearance of the starting material, monitored by TLC. Upon completion, the reaction mixture was diluted and quenched with H_2O. The layers were separated and extracted with CH_2Cl_2 (3X 20 mL) and the combined layer was washed with H_2O, brine and dried over Na_2SO_4. The solvent was evaporated and purified via flash chromatography.

Yield: 59% (5.7 mg isolated starting from 8.6 mg of α,β-unsaturated hydroxypyranone **4.28.3**);

FTIR (thin film): 2930, 1747, 1514, 1373, 1248, 1092, 837 cm^{-1};

Optical Rotation: $[\alpha]_D = -14.0$ ($c = 0.05$, $CHCl_3$);

^{1}H NMR (500 MHz, $CDCl_3$) δ 7.39–7.28 (m, 5H), 7.26–7.23 (m, 2H), 7.03 (d, J = 15.9 Hz, 1H), 6.96 (d, J = 15.9 Hz, 1H), 6.91–6.85 (m, 2H), 5.45 (d, J = 1.6 Hz, 1H), 5.26 (dd, J = 8.6, 1.6 Hz, 1H), 4.50 (d, J = 1.9 Hz, 2H), 4.41 (s, 2H), 4.10 (dd, J = 8.5, 2.7 Hz, 1H), 3.95 (dq, J = 9.7, 6.3 Hz, 1H), 3.81 (s, 3H), 3.62 – 3.47 (m, 3H), 3.44 (dd, J = 9.2, 6.4 Hz, 1H), 3.17 (dd, J = 9.2, 7.0 Hz, 1H), 2.75–2.67 (m, 1H), 2.63 (ddd, J = 17.1, 9.7, 5.6 Hz, 1H), 2.34–2.28 (m, 1H), 2.20 (s, 3H), 2.18–1.95 (m, 2H), 1.91 (s, 3H), 1.78 (q, J = 6.3 Hz, 2H), 1.69–1.58 (m, 2H), 1.49–1.41 (m, 1H), 1.32 (s, 3H), 1.31 (s, 3H), 0.97 (d, J = 7.1 Hz, 3H), 0.90 (s, 9H), 0.85 (d, J = 6.7 Hz, 3H), 0.16– -0.03 (m, 6H);

^{13}C NMR (126 MHz, $CDCl_3$) δ 199.7, 193.9, 170.1, 169.6, 159.1, 138.5, 136.7, 132.5, 130.4, 129.2 (2C), 128.4 (2C), 127.7 (2C), 127.5, 113.7 (2C), 100.3, 76.2, 73.1, 72.6, 71.4,

71.1, 70.7, 70.4, 66.6, 63.8, 55.3, 40.1, 38.1, 37.5, 36.7, 35.9, 26.6, 25.9 (3C), 24.6, 24.3, 20.7, 20.6, 18.1, 14.6, 12.9, –3.9, –4.9;

HRMS cald for $C_{47}H_{70}O_{12}SiNa$ $(M+Na)^+$: 877.4534; found (TOF MS ES+): 877.4562.

(2*S*,3*S*)-ethyl 3-(5-bromofuran-2-yl)-2,3-dihydroxypropanoate (4.20.4A):

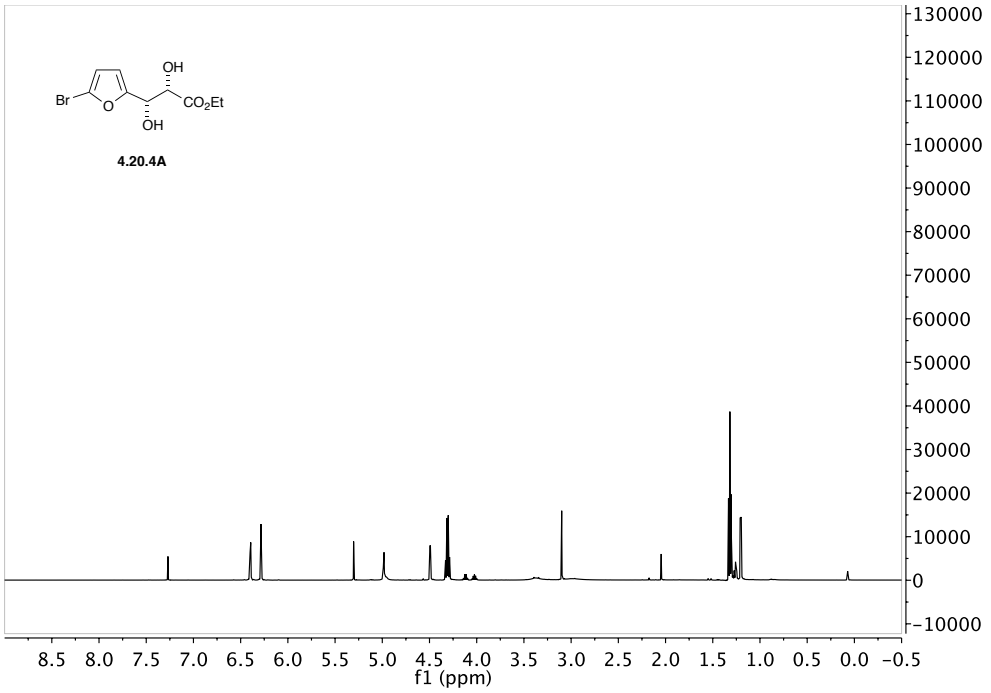

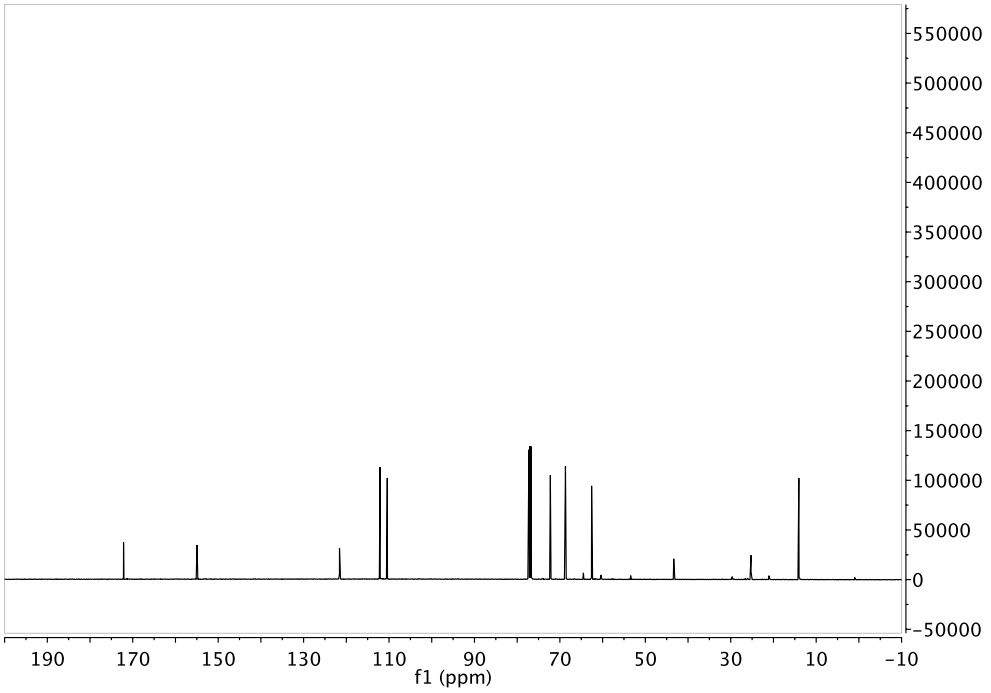

(4*S*,5*S*)-ethyl 5-(5-bromofuran-2-yl)-2,2-dimethyl-1,3-dioxolane -4-carboxylate (4.19.3):

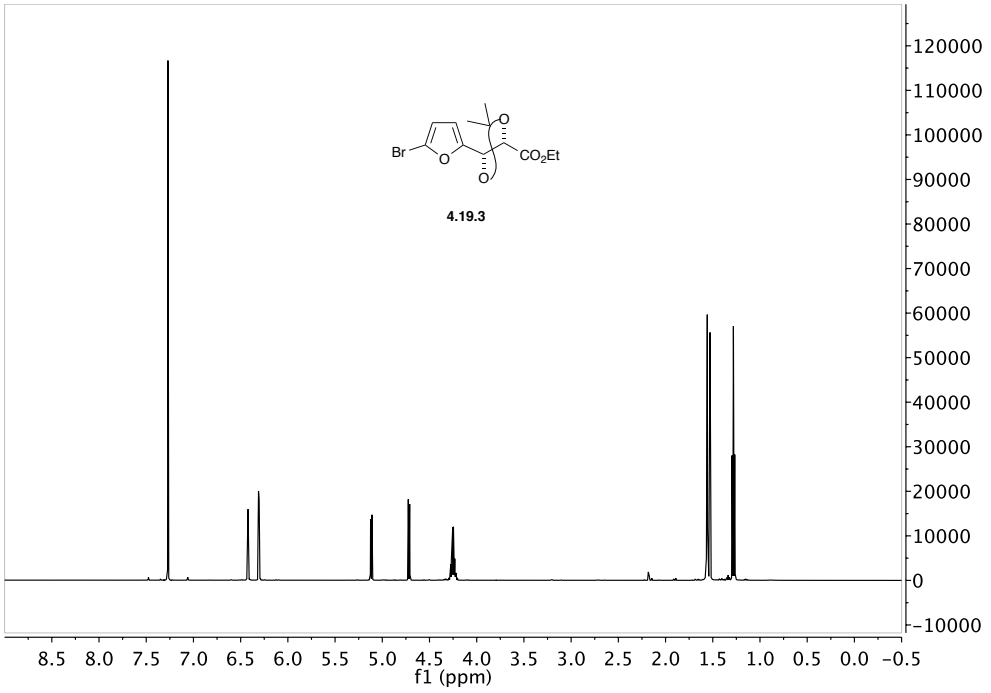

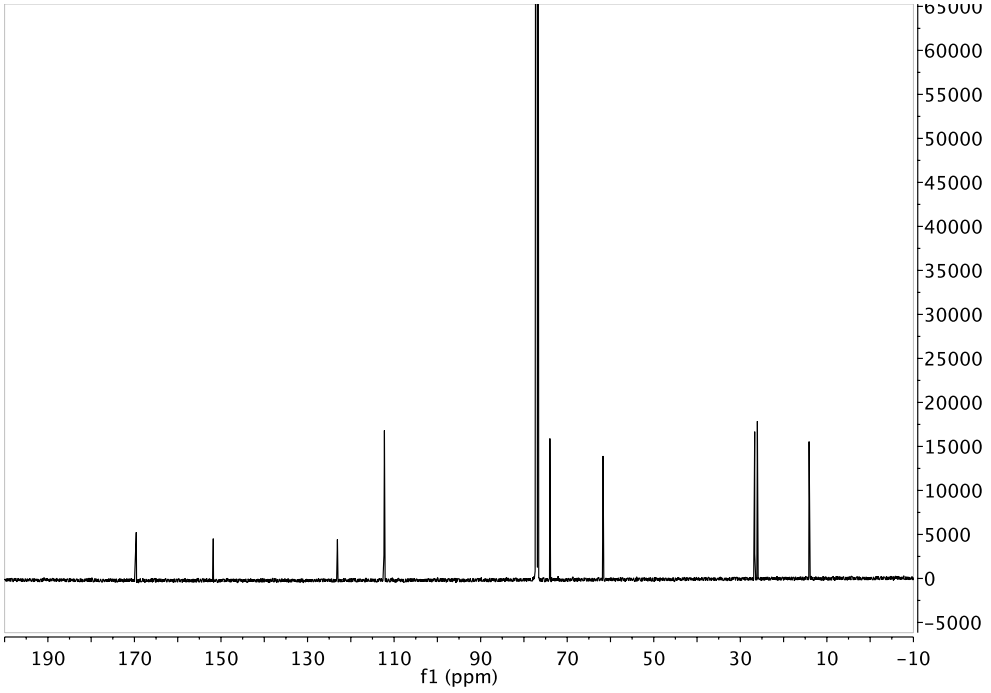

(1*R*,6*R*,8*S*)-8-(2-hydroxyethyl)-2,9,10-trioxa-1-phosphabicyclo[4.3.1]dec-4-ene 1-oxide (4.20.1A):

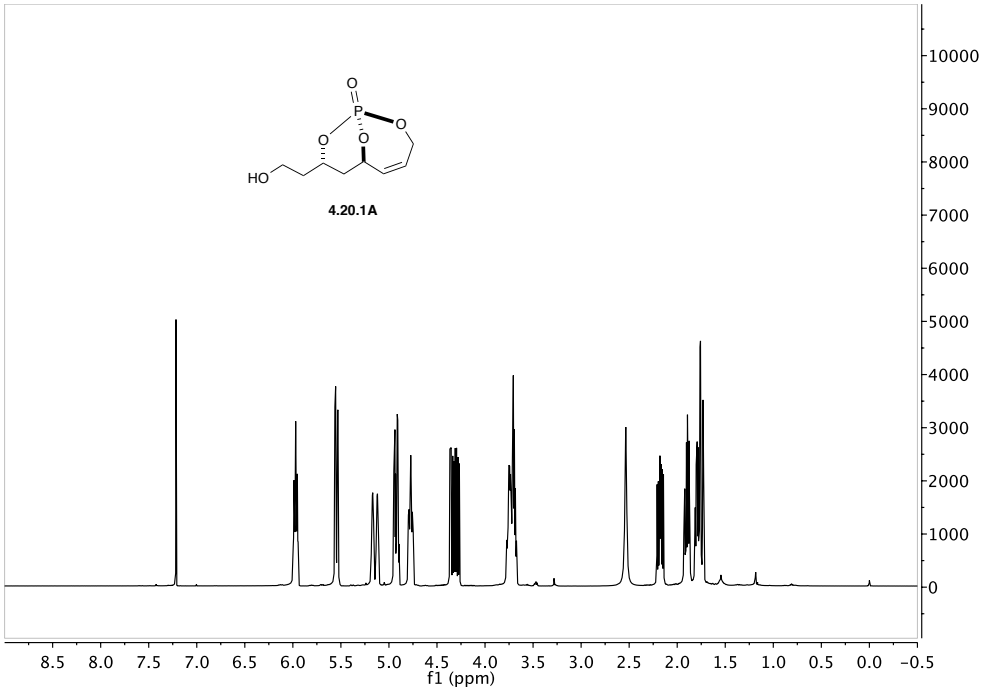

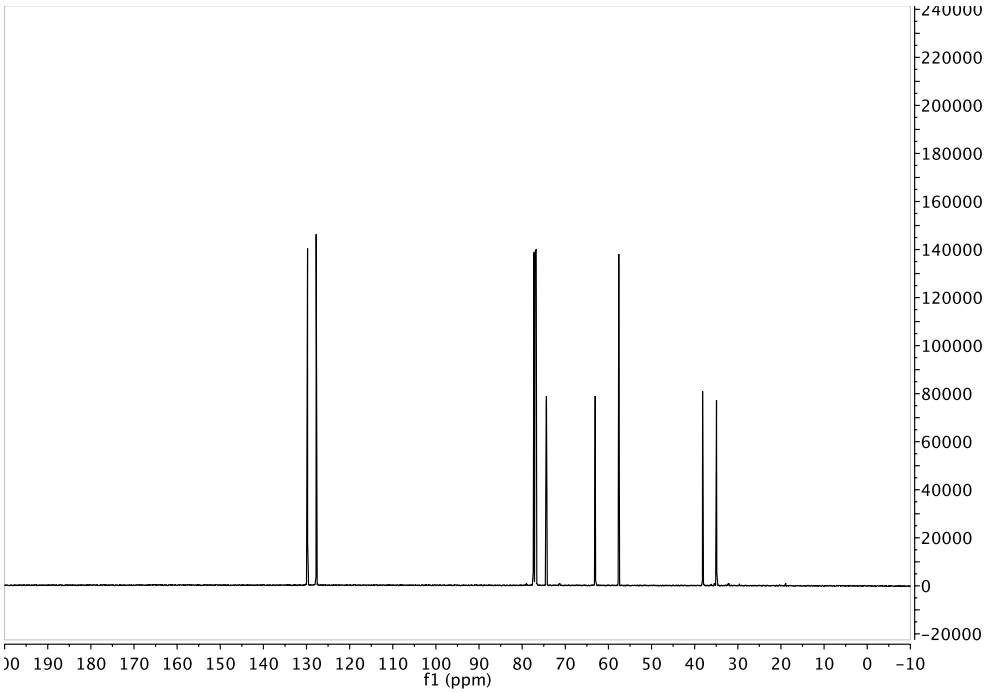

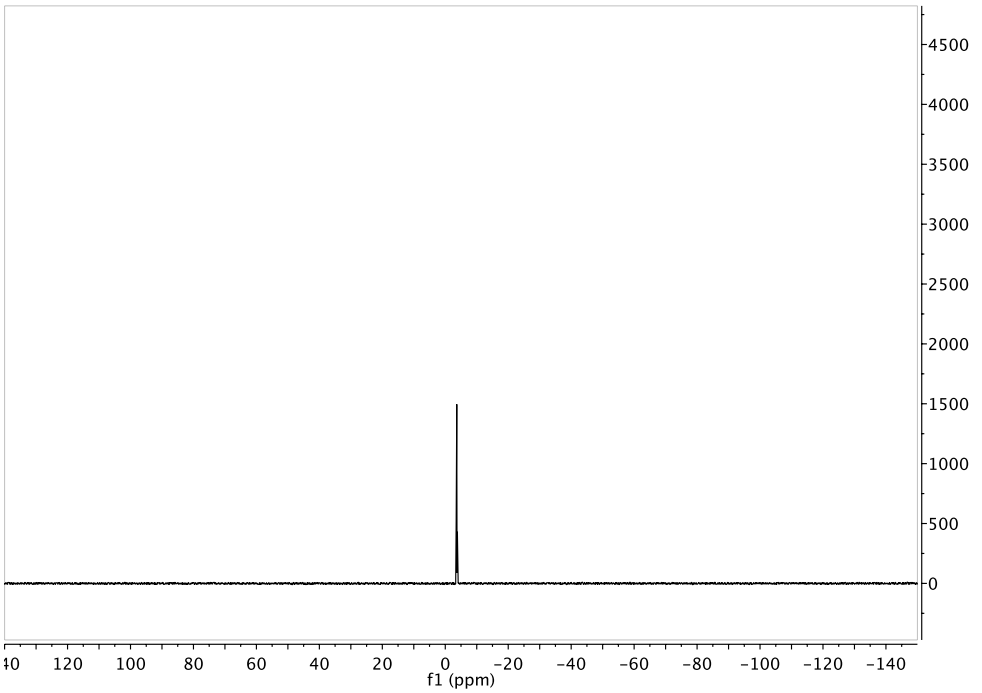

(1*R*,6*R*,8*S*)-8-(2-(benzyloxy)ethyl)-2,9,10-trioxa-1-phosphabicyclo [4.3.1]dec-4-ene 1-oxide (4.18.5):

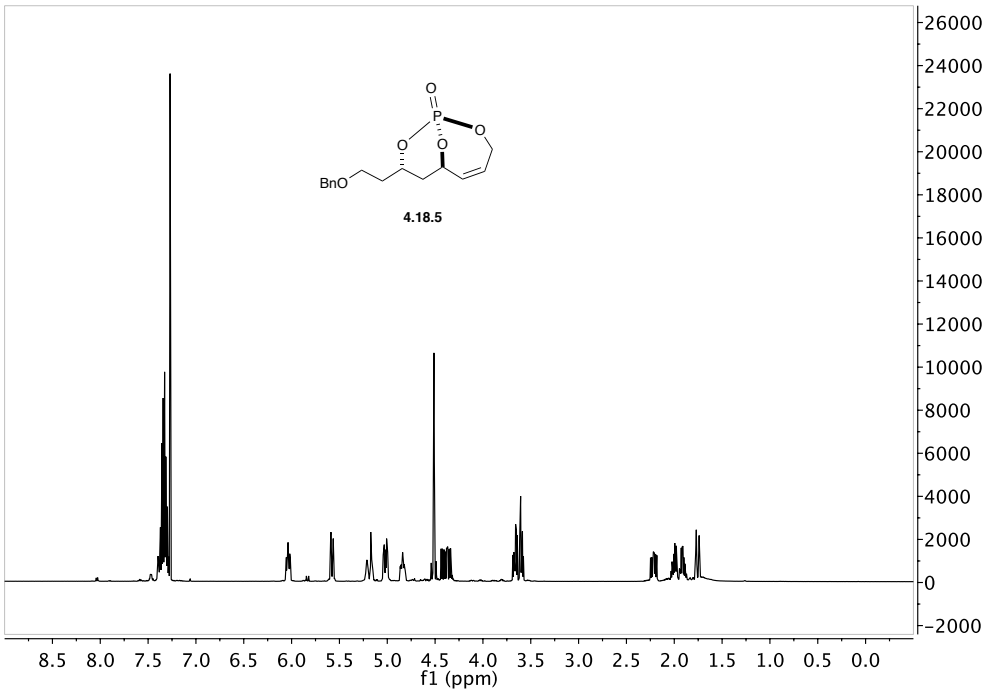

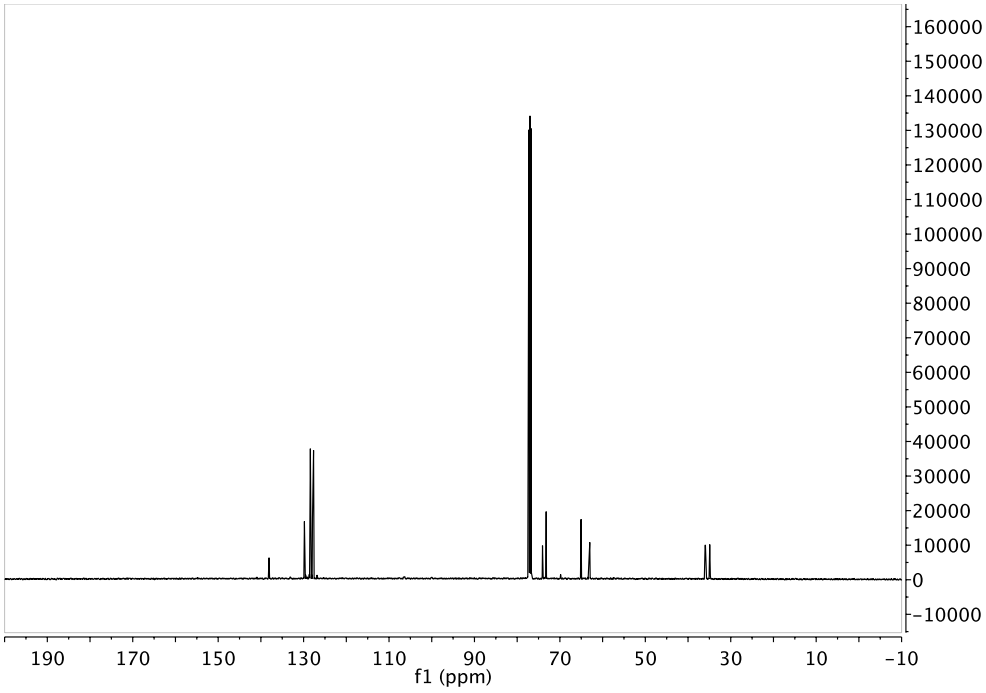
160000
150000
140000
130000
120000
110000
100000
90000
80000
70000
60000
50000
40000
30000
20000
10000
0
−10000
190
170
150
130
110
90
70
50
30
10
−10
f1 (ppm)

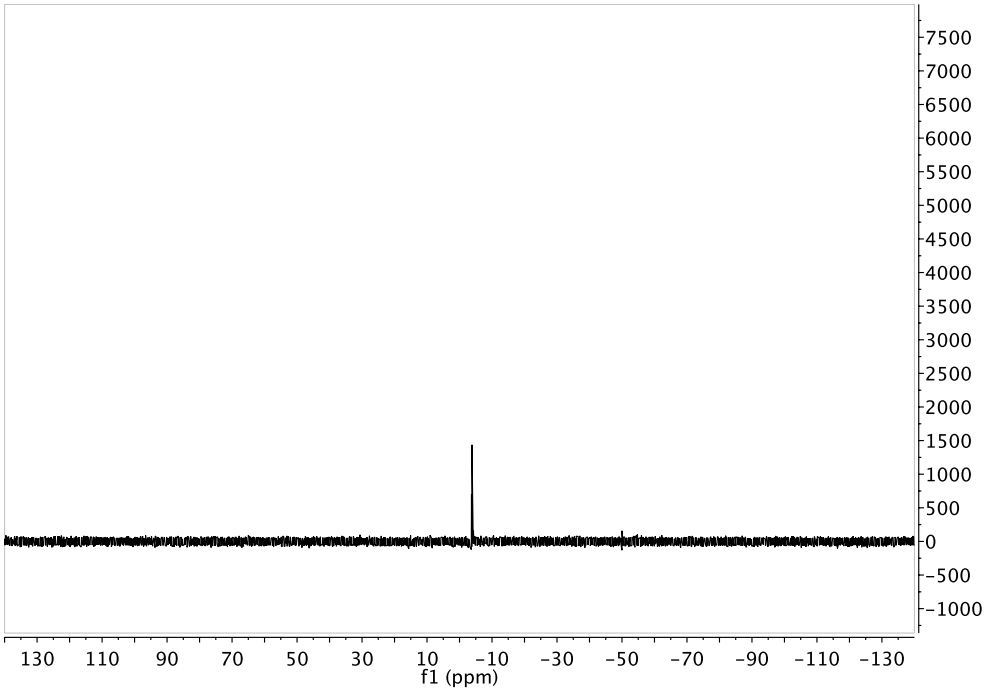
7500
7000
6500
6000
5500
5000
4500
4000
3500
3000
2500
2000
1500
1000
500
0
−500
−1000
130
110
90
70
50
30
10
−10
−30
−50
−70
−90
−110
−130
f1 (ppm)

(3*S*,5*R*,6*S*)-1-(benzyloxy)-6-methyloct-7-ene-3,5-diol (4.18.5A):

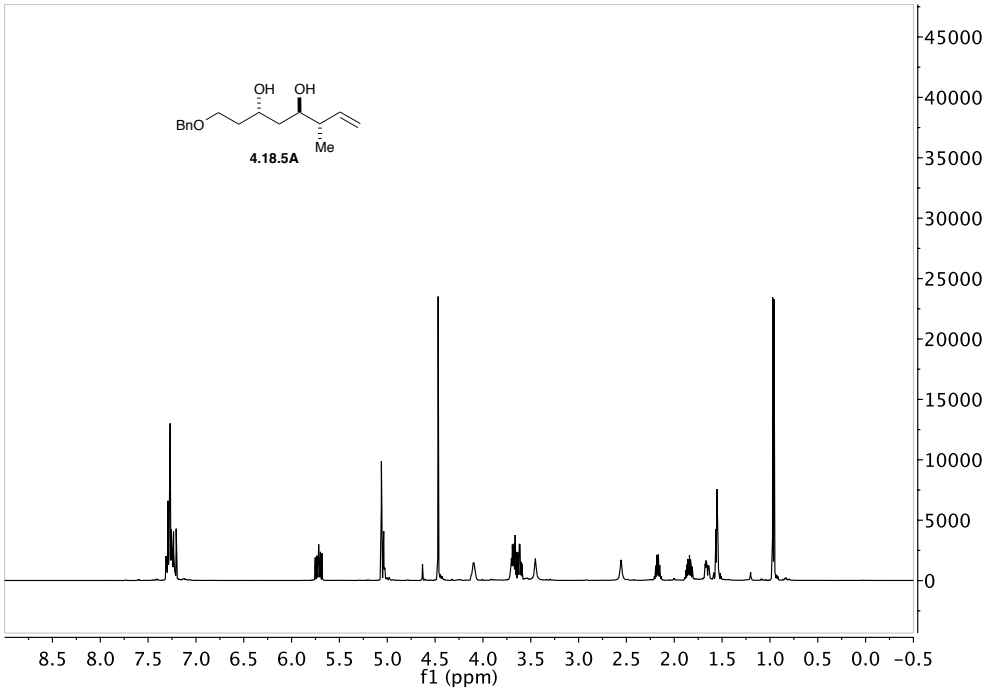

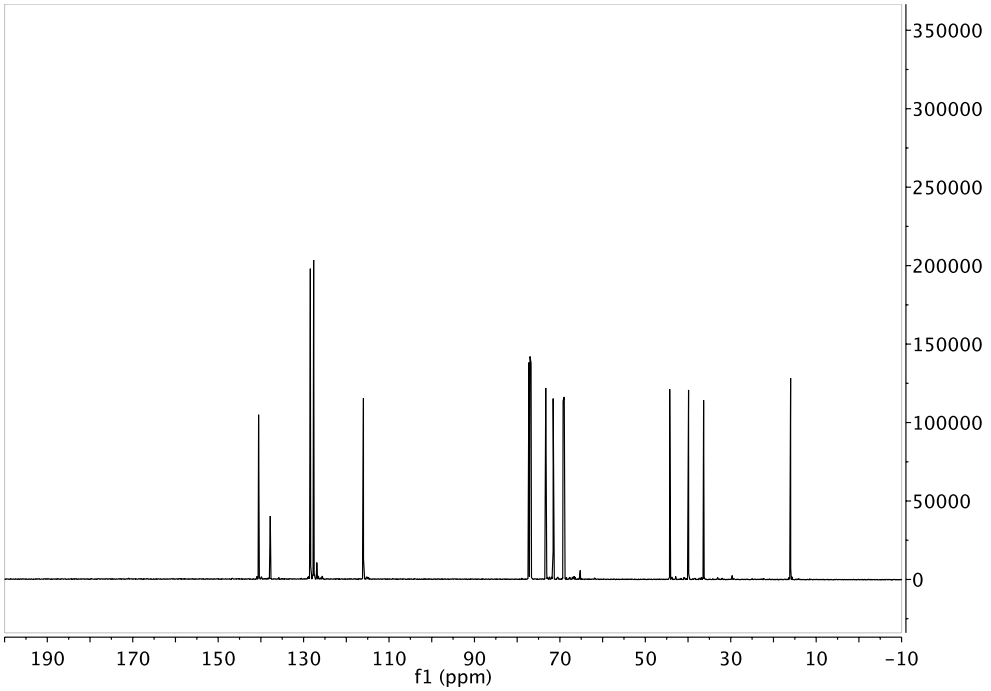

(4*S*,6*R*)-4-(2-(benzyloxy)ethyl)-6-((*S*)-but-3-en-2-yl)-2,2-dimethyl-1,3-dioxane (4.22.1):

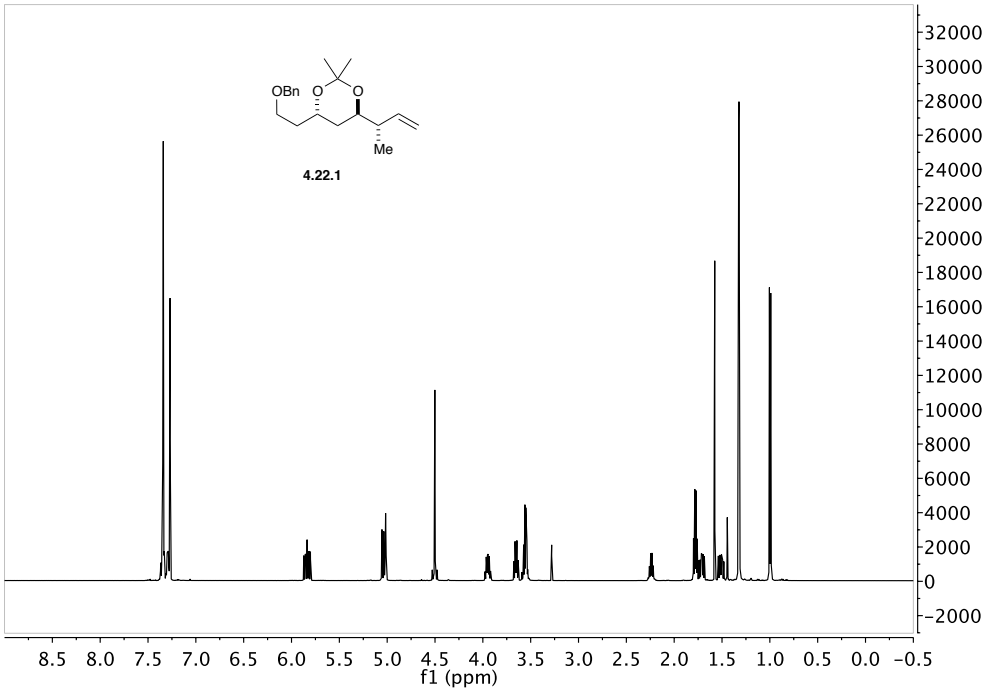

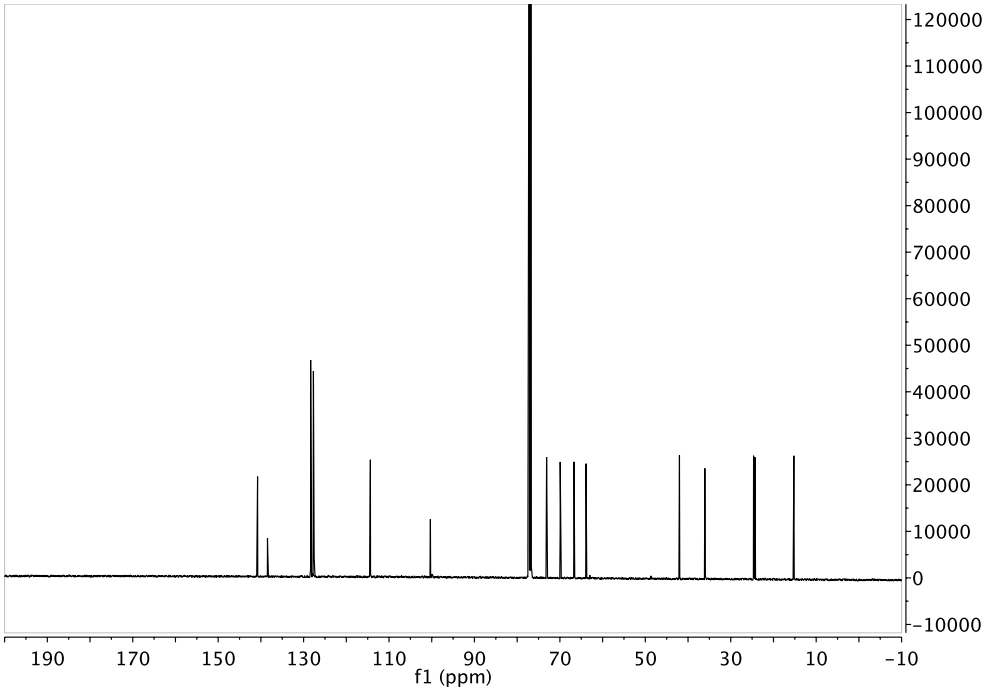

2-((*S*,*E*)-3-((4*R*,6*S*)-6-(2-(benzyloxy)ethyl)-2,2-dimethyl-1,3-dioxan-4-yl) but-1-en-1-yl)-4,4,5,5-tetramethyl-1,3,2-dioxaborolane (4.24.1):

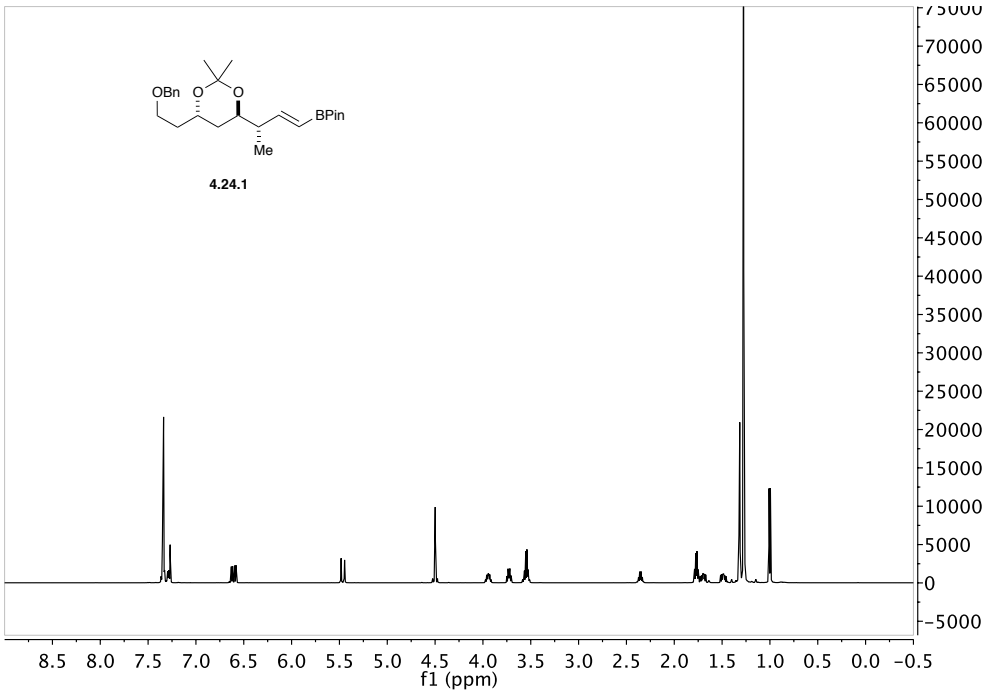

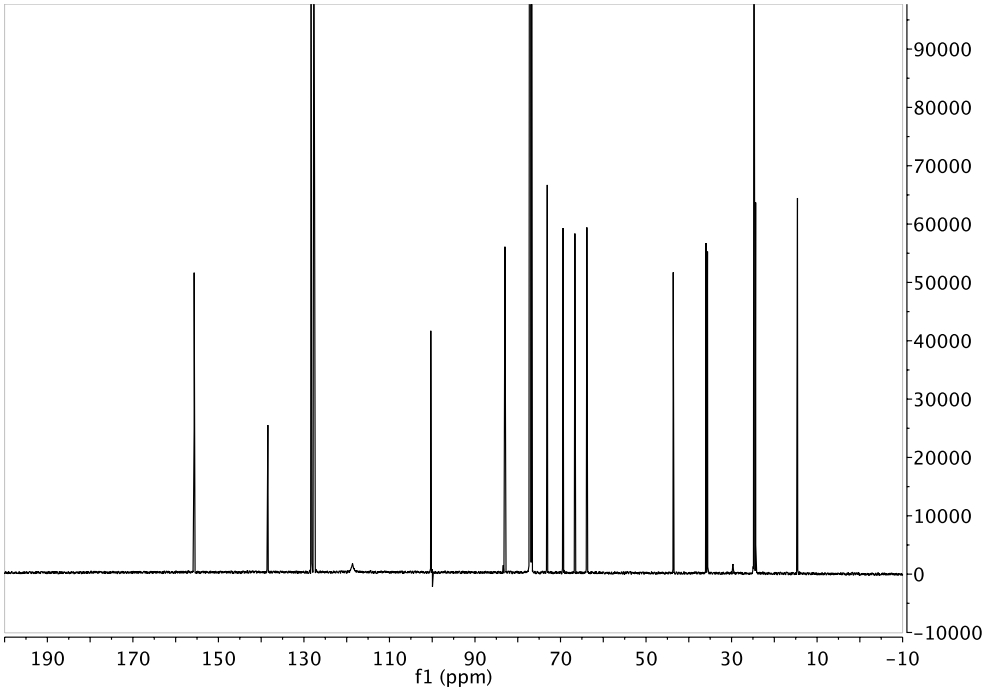

(5*R*)-ethyl 5-(5-((*S*,*E*)-3-((4*R*,6*S*)-6-(2-(benzyloxy)ethyl)-2,2-dimethyl-1,3-dioxan-4-yl)but-1-en-1-yl)furan-2-yl)-2,2-dimethyl-1,3-dioxolane-4-carboxylate (4.24.2):

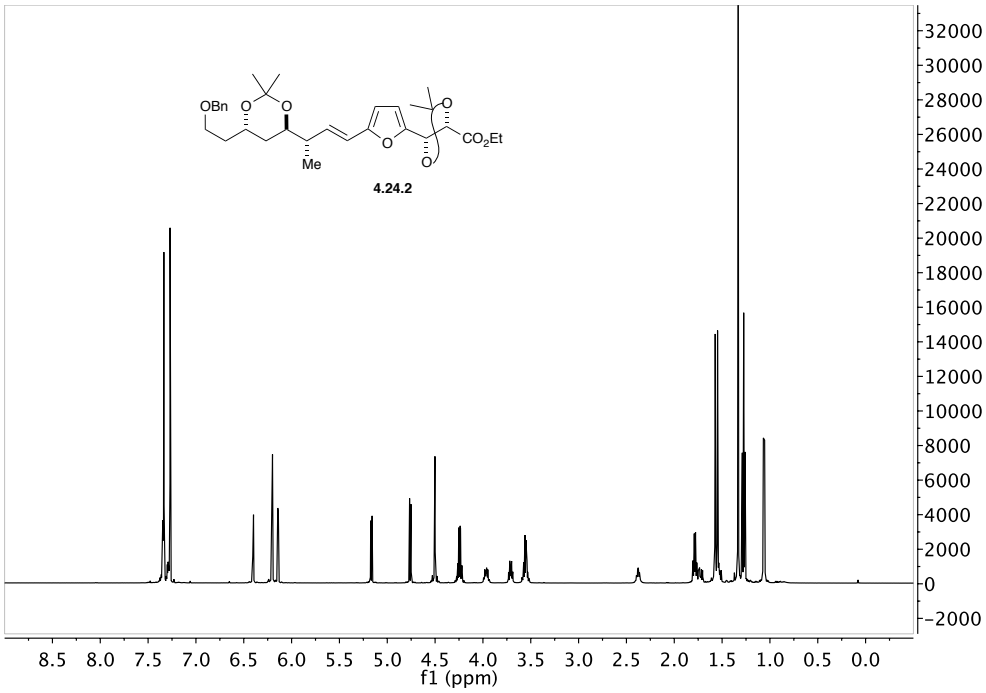

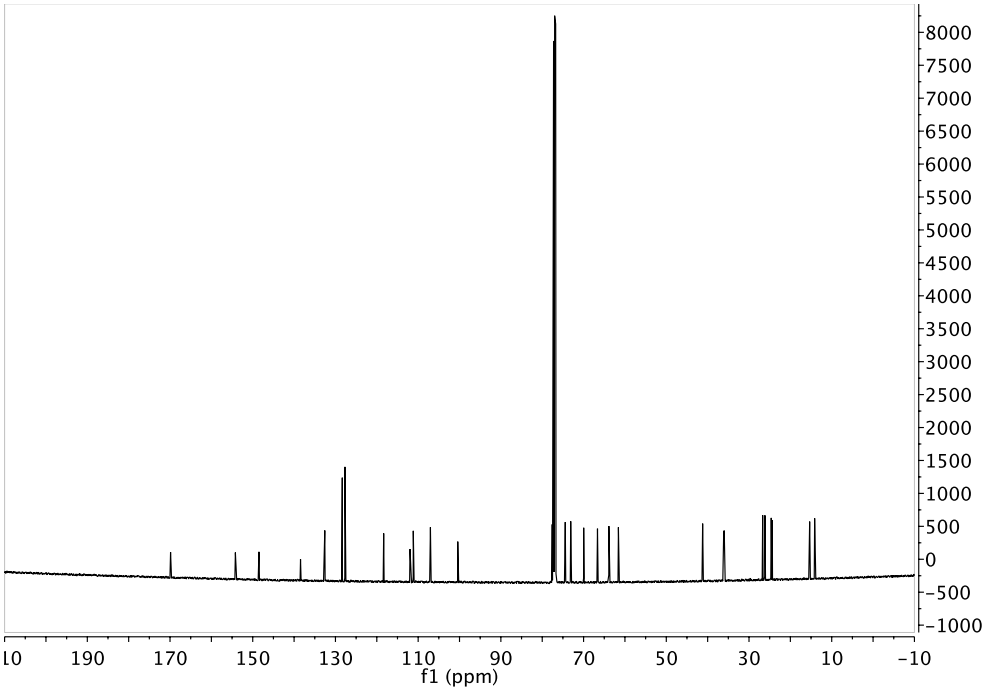

(*E*)-2-bromo-5-(prop-1-en-1-yl)furan (4.26.6):

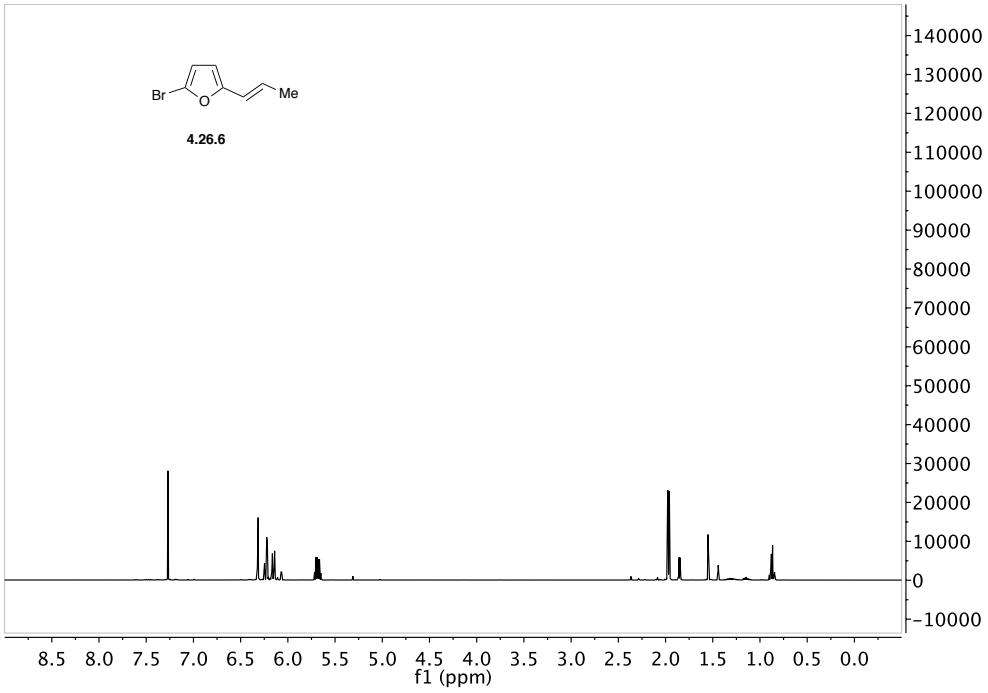

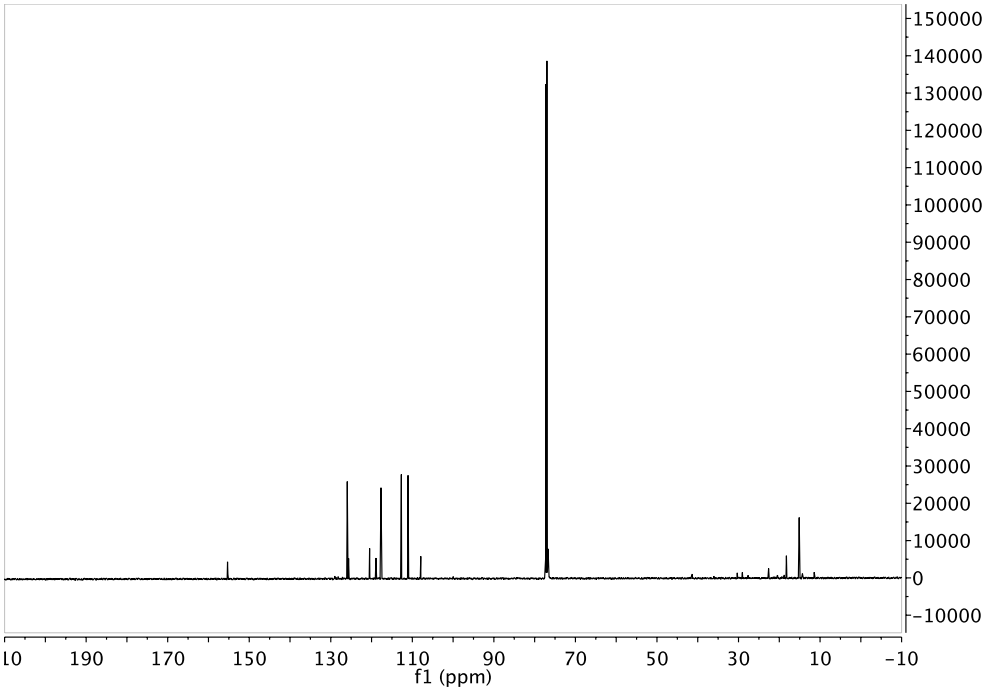

(*S*,*E*)-1-((4-methoxybenzyl)oxy)-2-methylhex-4-en-3-one (4.27.3):

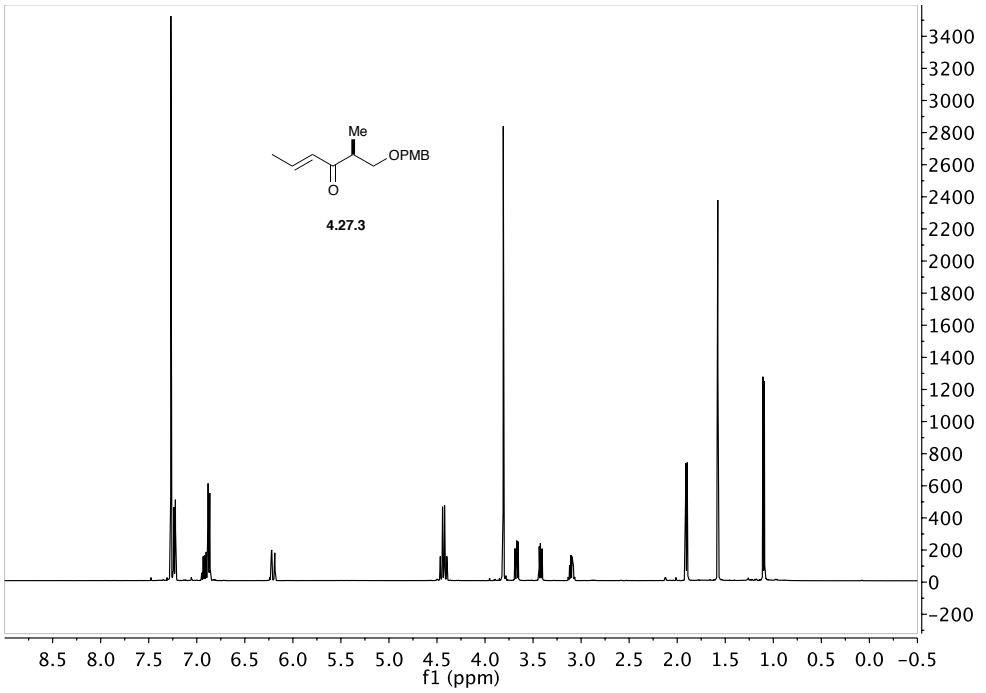

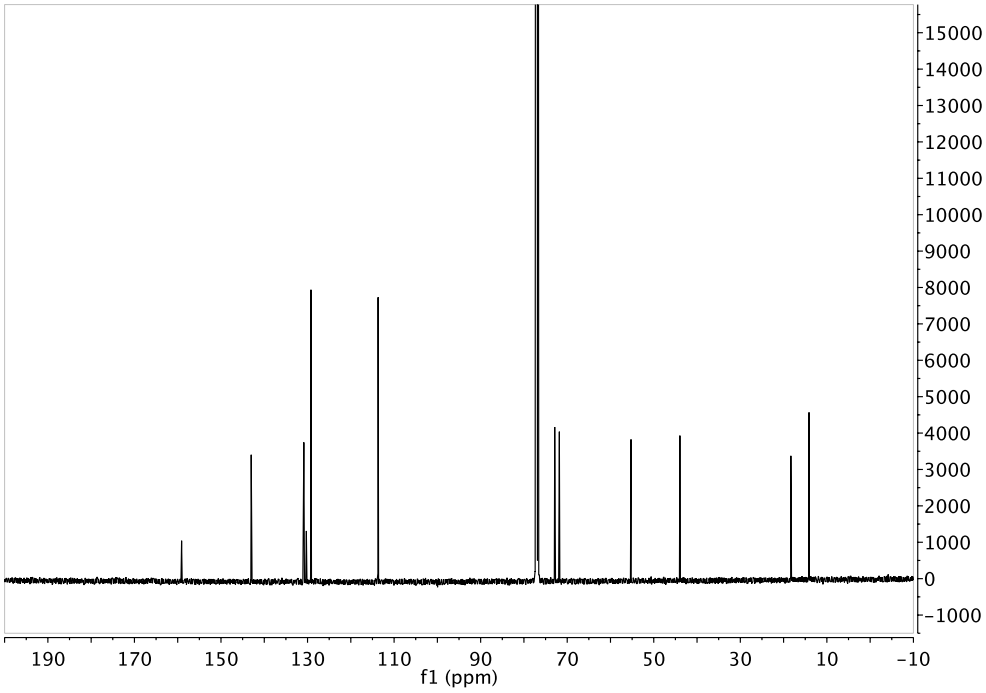

(2*S*,3*R*,*E*)-1-((4-methoxybenzyl)oxy)-2-methylhex-4-en-3-ol (4.26.7):

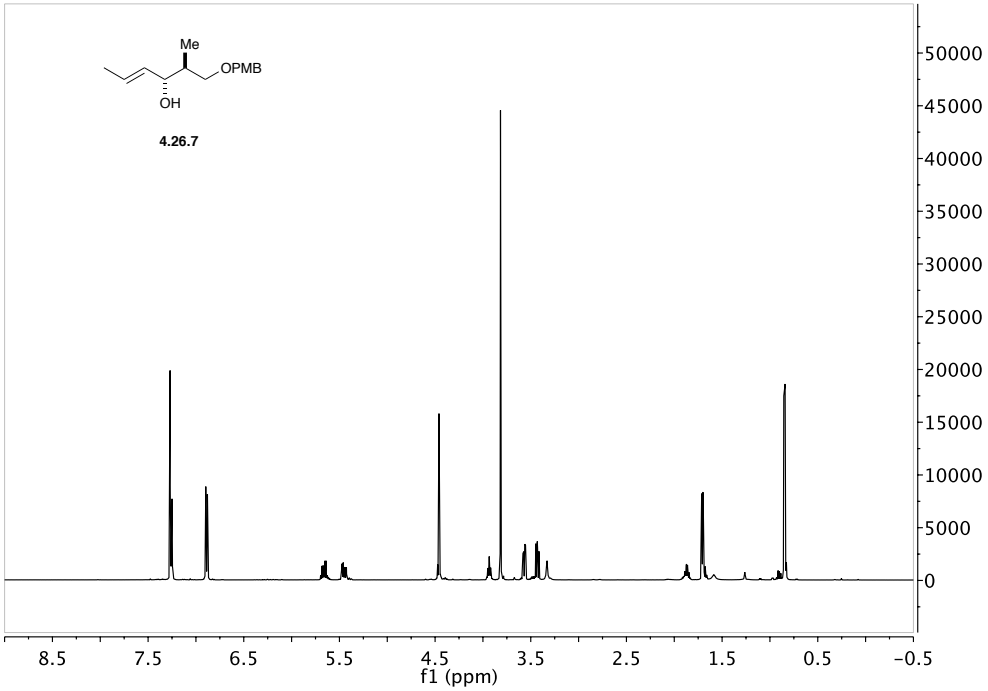
Me
OPMB
OH
4.26.7
50000
45000
40000
35000
30000
25000
20000
15000
10000
5000
0
8.5
7.5
6.5
5.5
4.5
3.5
2.5
1.5
0.5
-0.5
f1 (ppm)

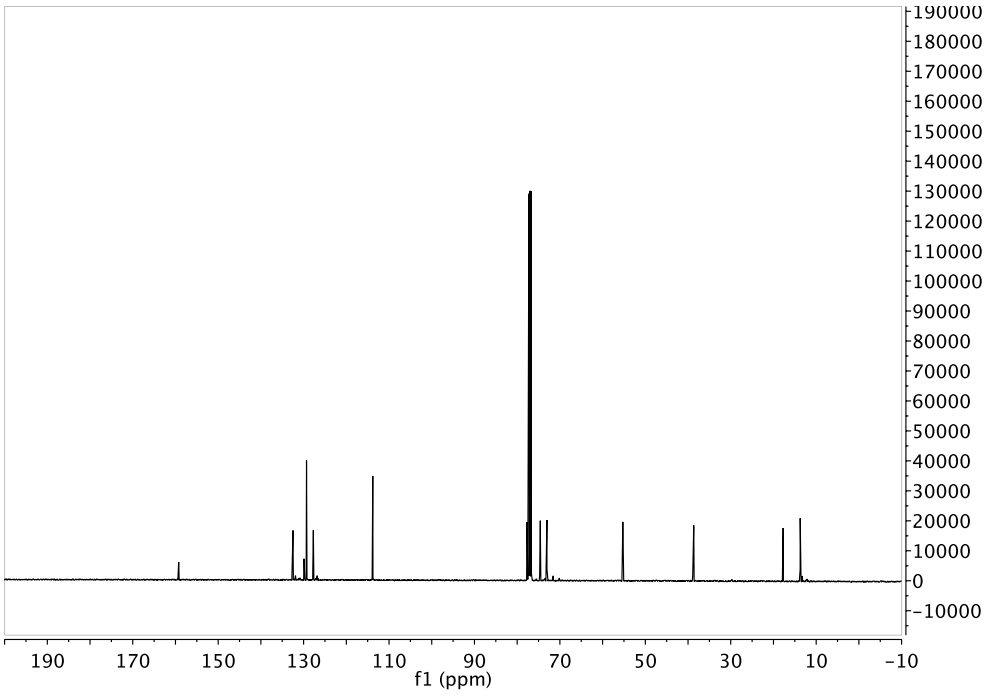
190000
180000
170000
160000
150000
140000
130000
120000
110000
100000
90000
80000
70000
60000
50000
40000
30000
20000
10000
0
-10000
190
170
150
130
110
90
70
50
30
10
-10
f1 (ppm)

(3*R*,4*S*,*E*)-1-(5-bromofuran-2-yl)-5-((4-methoxybenzyl)oxy)-4-methylpent-1-en-3-ol (4.26.5):

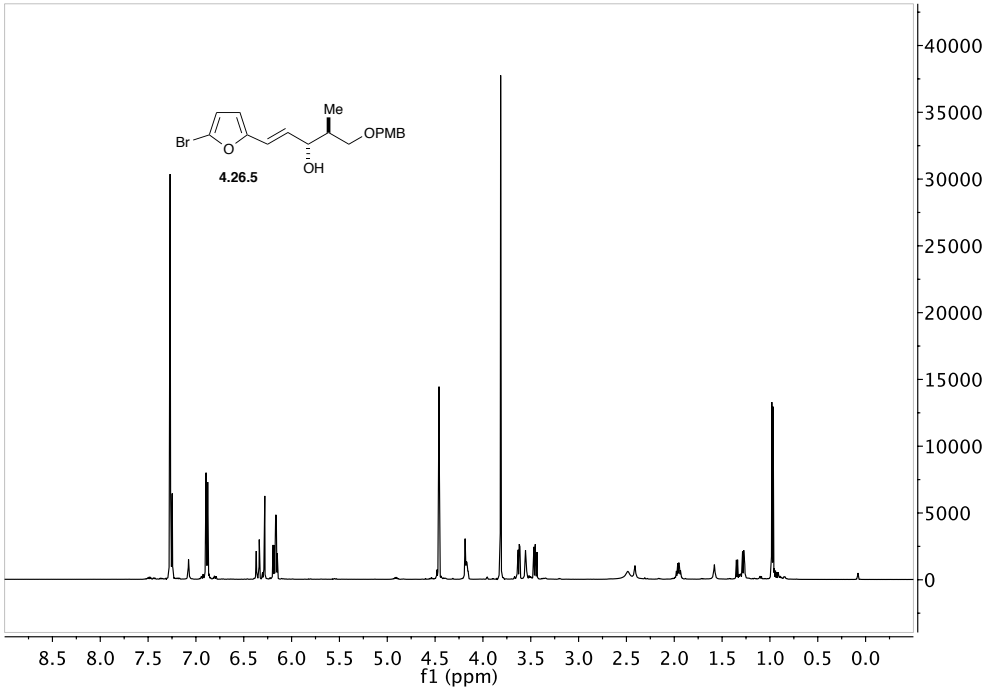

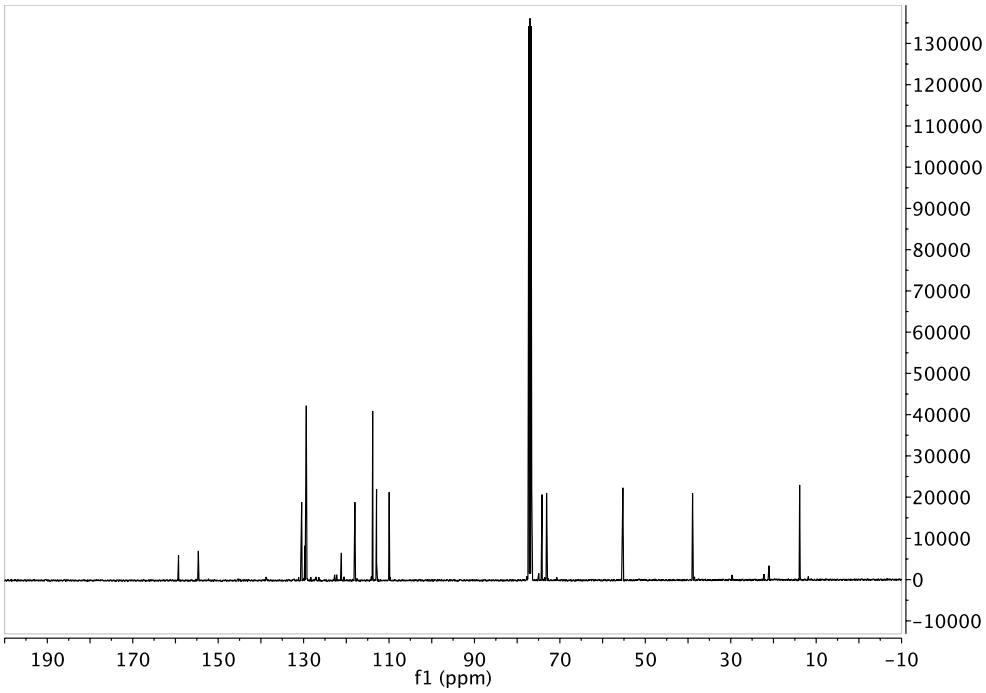

(((3*R*,4*S*,*E*)-1-(5-bromofuran-2-yl)-5-((4-methoxybenzyl)oxy)-4-methylpent-1-en-3-yl)oxy)(*tert*-butyl)dimethylsilane (4.26.2):

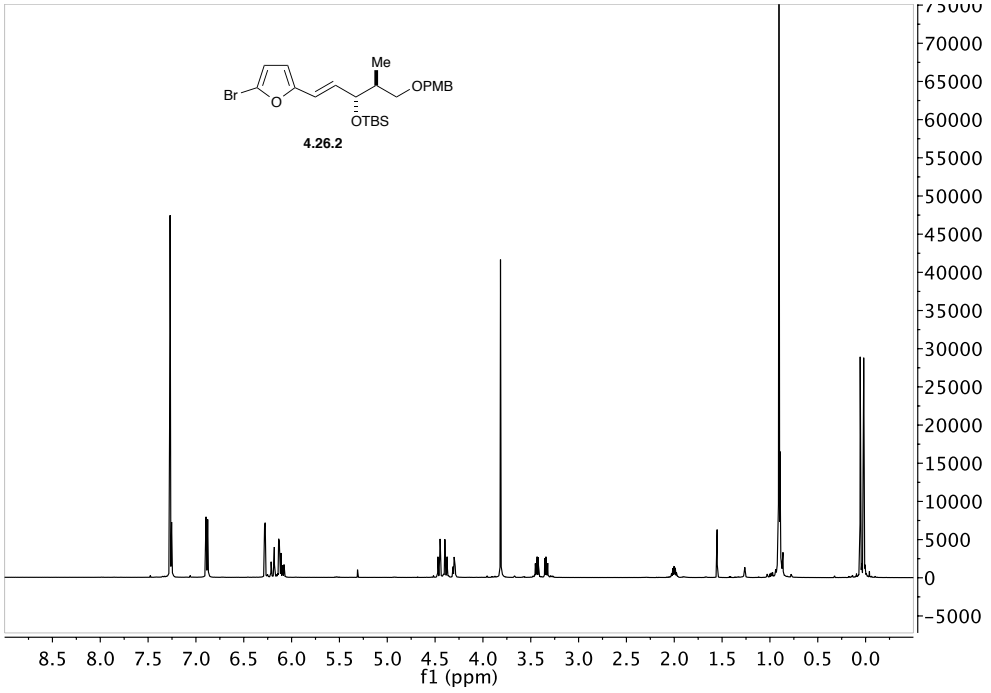

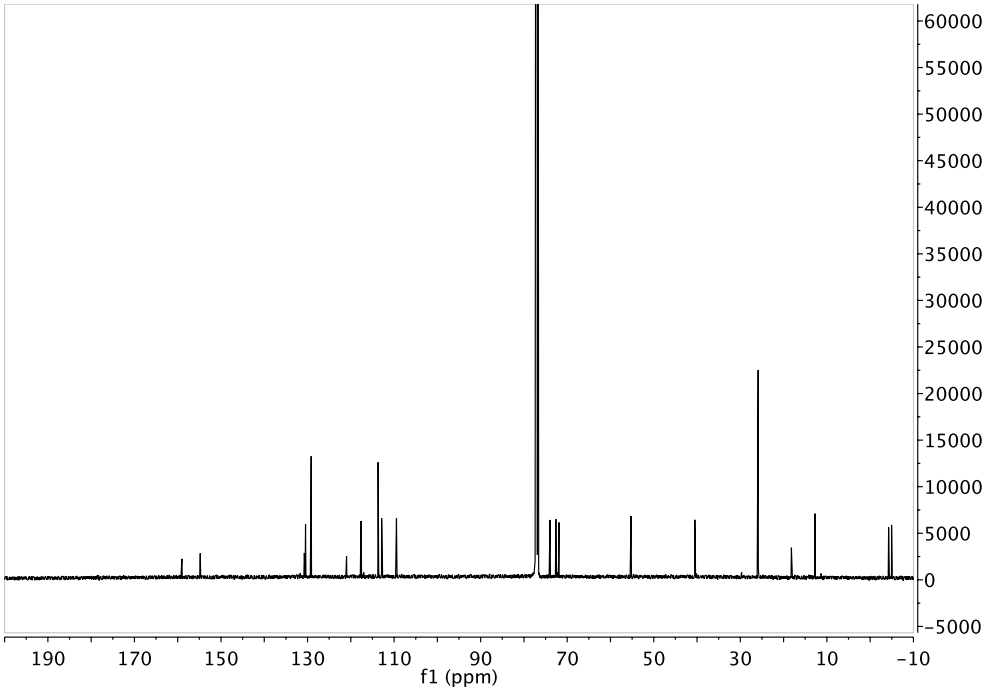

(1*R*,2*R*,3*S*,4*S*)-1-(5-bromofuran-2-yl)-3-((*tert*-butyldimethylsilyl)oxy)-5-((4-methoxybenzyl)oxy)-4-methylpentane-1,2-diol (4.26.1):

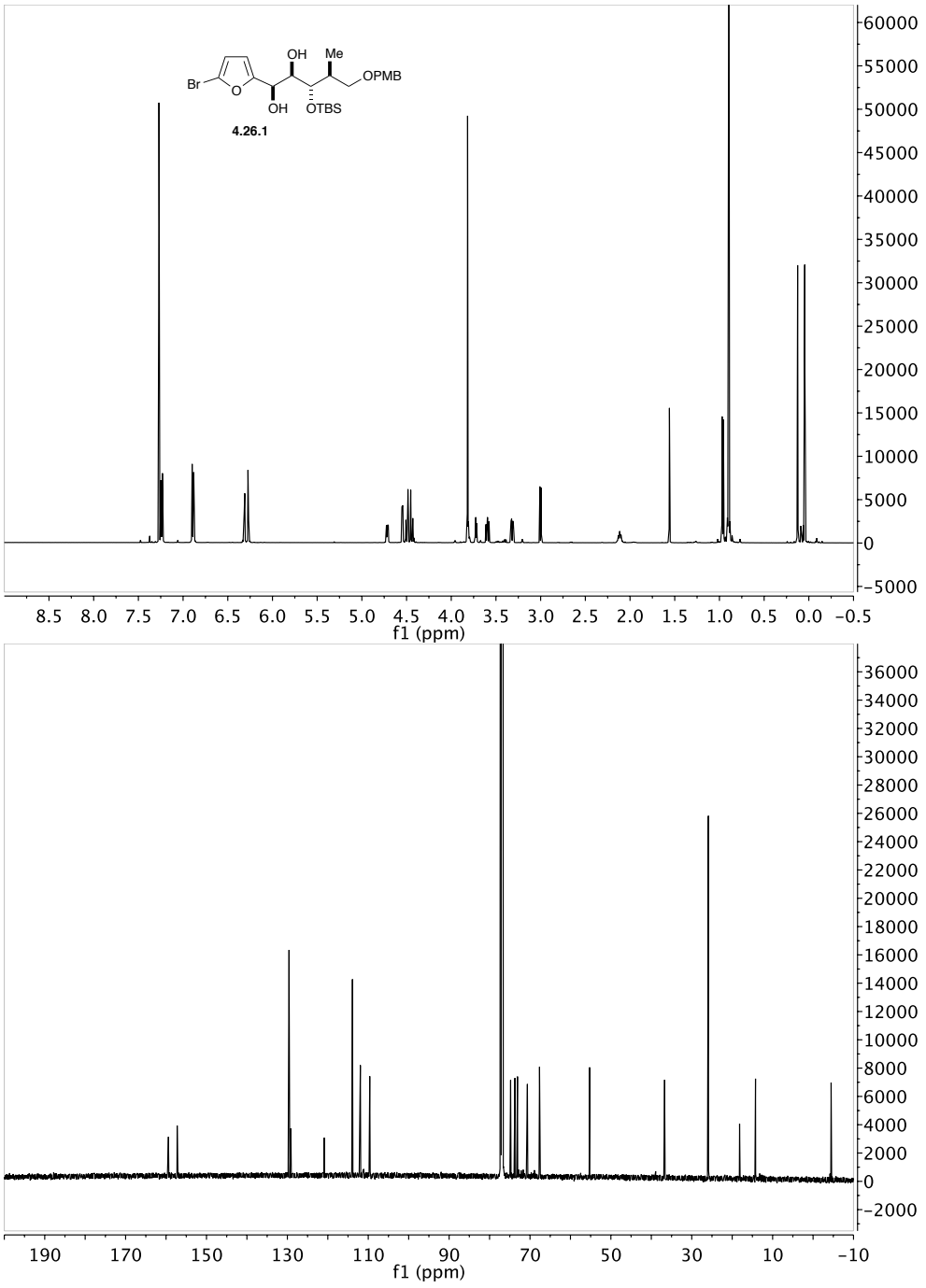

(1*R*,2*R*,3*S*,4*S*)-1-(5-((*S*,*E*)-3-((4*R*,6*S*)-6-(2-(benzyloxy)ethyl)-2,2-dimethyl-1,3-dioxan-4-yl)but-1-en-1-yl)furan-2-yl)-3-((*tert*-butyldimethylsilyl)oxy)-5-((4-methoxybenzyl)oxy)-4-methylpentane-1,2-diol (4.28.1):

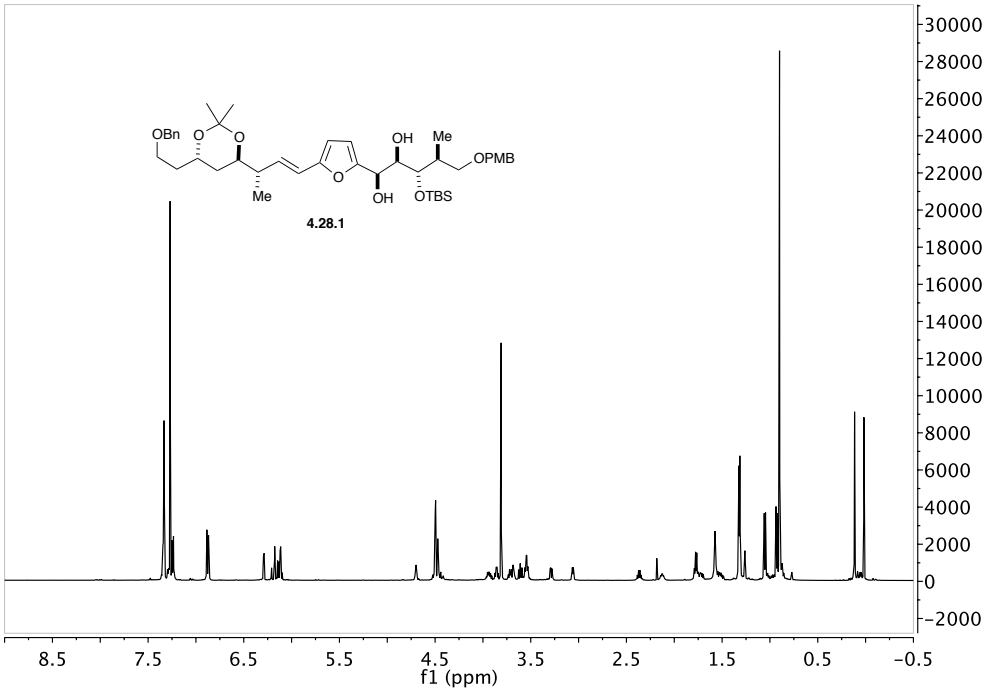

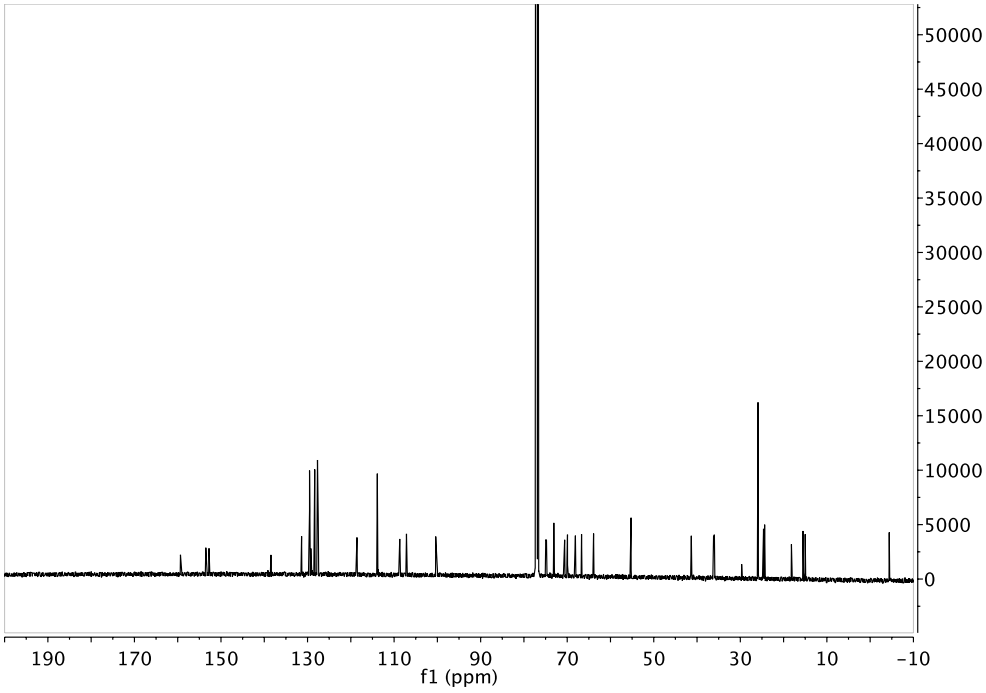

(1*R*,2*R*,3*S*,4*S*)-1-(5-((*S*)-3-((4*R*,6*S*)-6-(2-(benzyloxy)ethyl)-2,2-dimethyl-1,3-dioxan-4-yl)butyl)furan-2-yl)-3-((*tert*-butyldimethylsilyl)oxy)-5-((4-methoxybenzyl)oxy)-4-methylpentane-1,2-diol (4.28.2):

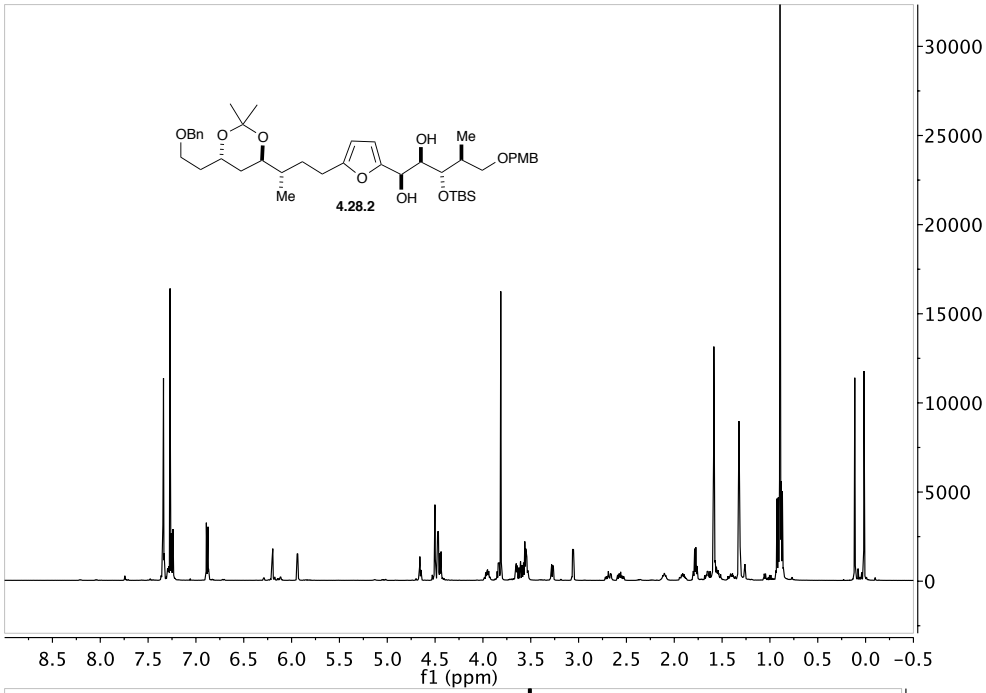

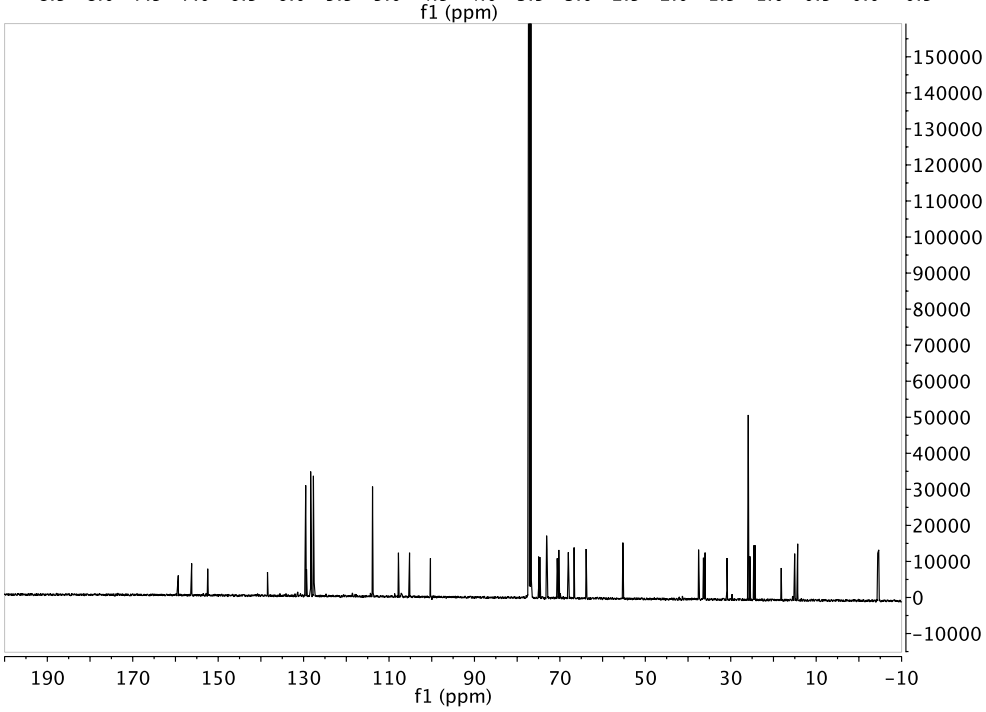

(2*R*)-6-((*S*)-3-((4*R*,6*S*)-6-(2-(benzyloxy)ethyl)-2,2-dimethyl-1,3-dioxan-4-yl)butyl)-2-((1*R*,2*S*,3*S*)-2-((*tert*-butyldimethylsilyl)oxy)-1-hydroxy-4-((4-methoxybenzyl)oxy)-3-methylbutyl)-6-hydroxy-2*H*-pyran-3(6*H*)-one (4.28.3):

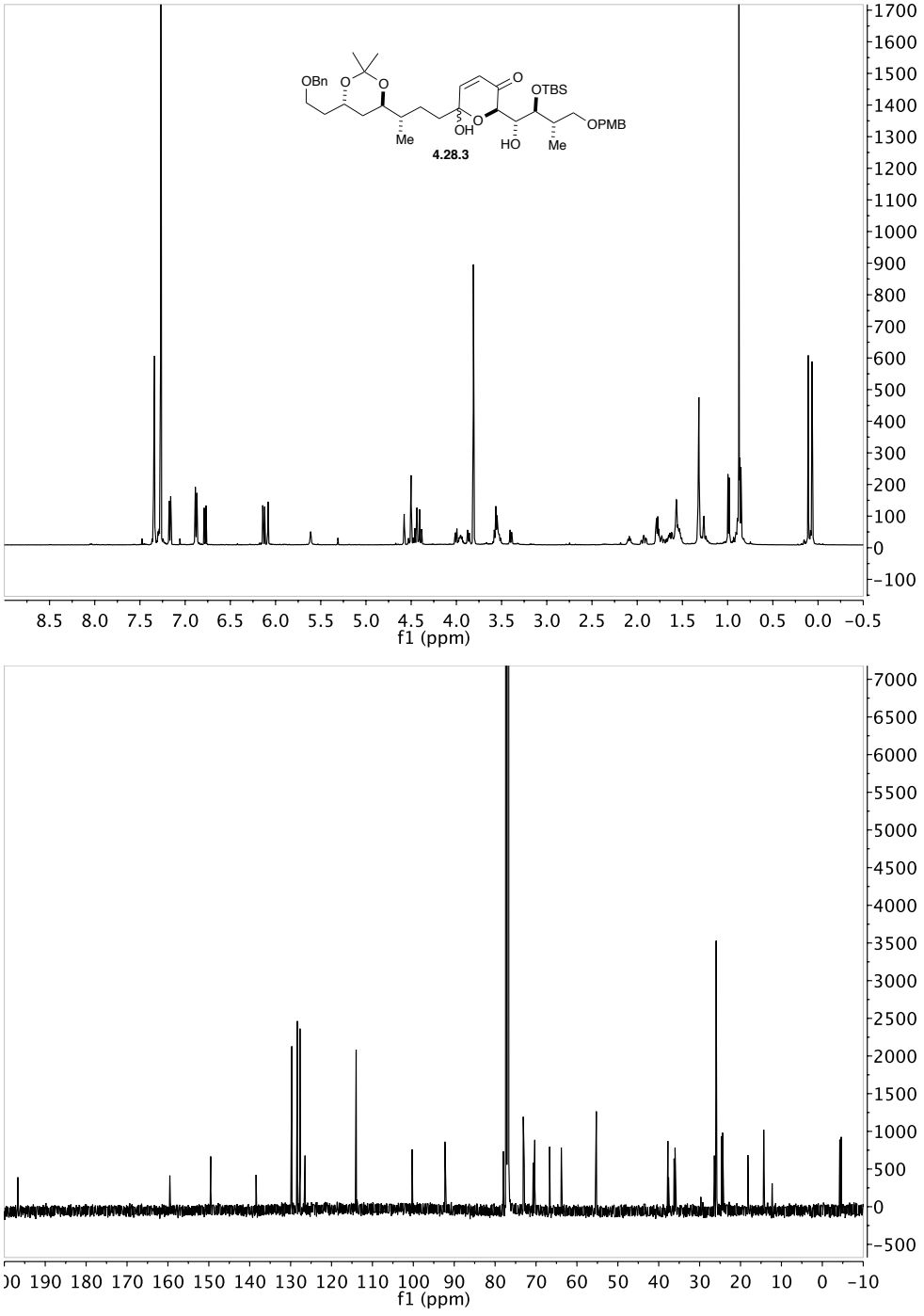

(6*R*)-6-((1*R*,2*S*,3*S*)-1-acetoxy-2-((*tert*-butyldimethylsilyl)oxy)-4-((4-methoxybenzyl)oxy)-3-methylbutyl)-2-((*S*)-3-((4*R*,6*S*)-6-(2-(benzyloxy)ethyl)-2,2-dimethyl-1,3-dioxan-4-yl)butyl)-5-oxo-5,6-dihydro-2*H*-pyran-2-yl acetate (4.28.5):

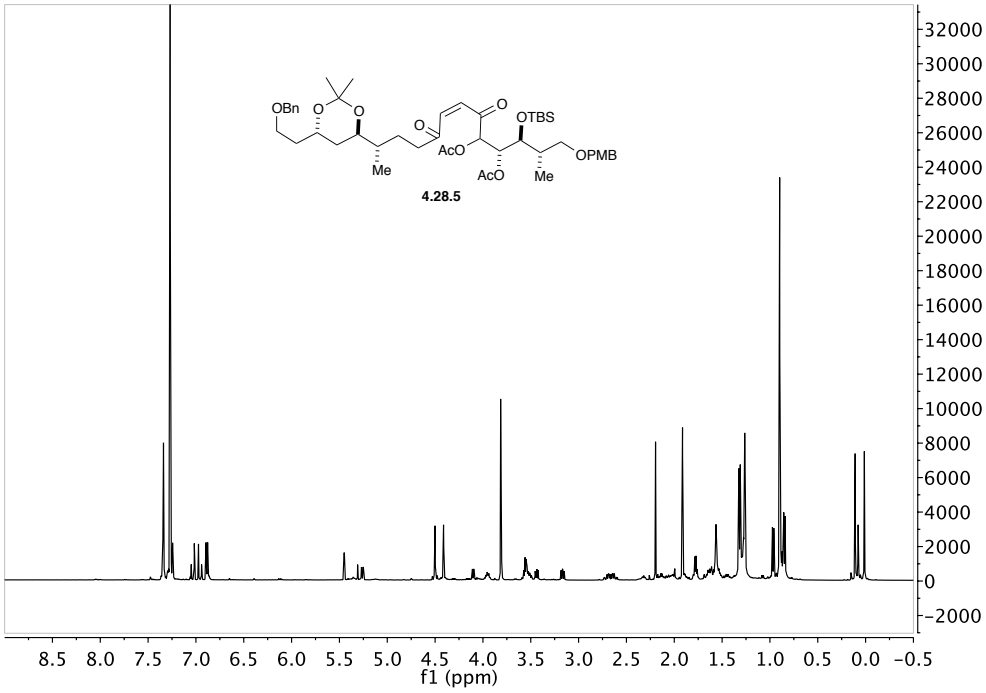

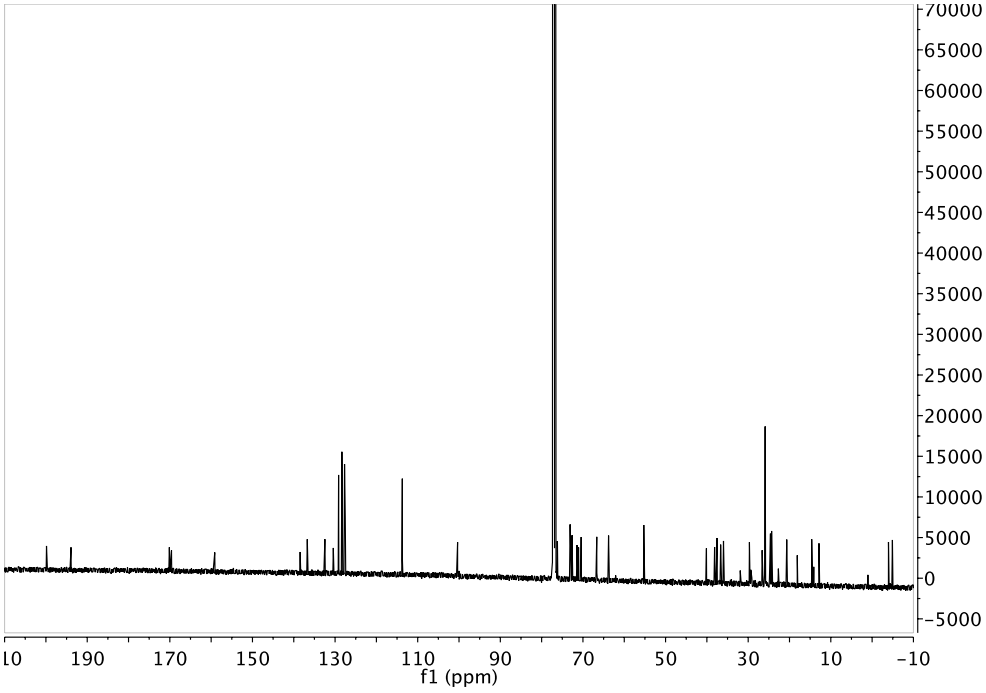

Reference cited:

[1] Chen, L.; Riaz Ahmed, K. B.; Huang, P.; Jin, Z. Design, Synthesis, and Biological Evaluation of Truncated Superstolide A. *Angew. Chem., Int. Ed.* **2013**, *52*, 3446–3449.

[2] Farmer, J. L.; Hunter, H. N.; Organ, M. G. Regioselective Cross-Coupling of Allylboronic Acid Pinacol Ester Derivatives with Aryl Halides via Pd-PEPPSI-IPent. *J. Am. Chem. Soc.* **2012**, *134*, 17470–17473.

[3] Kumar, V. P.; Chandrasekhar, S. Enantioselective Synthesis of Pladienolide B and Truncated Analogues as New Anticancer Agents. *Org. Lett.* **2013**, *15*, 3610–3613.

[4] Keaton, K. A.; Phillips, A. J. A Cyclopropanol-Based Strategy for Subunit Coupling: Total Synthesis of (+)-Spirolaxine Methyl Ether. *Org. Lett.* **2007**, *9*, 2717–2719.

[5] Haukaas, M. H.; O'Doherty, G. A. Enantioselective Synthesis of N-Cbz-Protected 6-Amino-6-deoxymannose, -talose, and -gulose. *Org. Lett.* **2001**, *3*, 3899–3902.